

JAERI-Tech 2000-071  
(ORNL/TR-2001/01)



## Translation of

# TECHNICAL DEVELOPMENT ON BURN-UP CREDIT FOR SPENT LWR FUELS

Edited by  
Yoshinori Nakahara, Kenya Suyama, and  
Takenori Suzuki

January 2002

This report has been reproduced from the best available copy.

Reports are available to the public from the following source.

National Technical Information Service  
5285 Port Royal Road  
Springfield, VA 22161  
**Telephone** 703-605-6000 (1-800-553-6847)  
**TDD** 703-487-4639  
**Fax** 703-605-6900  
**E-mail** [orders@ntis.fedworld.gov](mailto:orders@ntis.fedworld.gov)  
**Web site** <http://www.ntis.gov/ordering.htm>

Reports are available to U.S. Department of Energy (DOE) employees, DOE contractors, Energy Technology Data Exchange (ETDE) representatives, and International Nuclear Information System (INIS) representatives from the following source.

Office of Scientific and Technical Information  
P.O. Box 62  
Oak Ridge, TN 37831  
**Telephone** 423-576-8401  
**Fax** 423-576-5728  
**E-mail** [reports@adonis.osti.gov](mailto:reports@adonis.osti.gov)  
**Web site** <http://www.osti.gov/products/sources.html>

Reports produced after January 1, 1996, are generally available via the DOE Information Bridge.  
**Web site** <http://www.doe.gov/bridge>

This report was prepared as an account of work sponsored by an agency of the United States government. Neither the United States government nor any agency thereof, nor any of their employees, makes any warranty, express or implied, or assumes any legal liability or responsibility for the accuracy, completeness, or usefulness of any information, apparatus, product, or process disclosed, or represents that its use would not infringe privately owned rights. Reference herein to any specific commercial product, process, or service by trade name, trademark, manufacturer, or otherwise, does not necessarily constitute or imply its endorsement, recommendation, or favoring by the United States government or any agency thereof. The views and opinions of authors expressed herein do not necessarily state or reflect those of the United States government or any agency thereof.

本レポートは、日本原子力研究所が不定期に公刊している研究報告書です。

入手の問合せは、日本原子力研究所研究情報部研究情報課（〒319-1195 茨城県那珂郡東海村）あて、お申し越し下さい。なお、このほかに財団法人原子力弘済会資料センター（〒319-1195 茨城県那珂郡東海村日本原子力研究所内）で複写による実費頒布を行っております。

This report is issued irregularly.

Inquiries about availability of the reports should be addressed to Research Information Division, Department of Intellectual Resources, Japan Atomic Energy Research Institute, Tokai-mura, Naka-gun, Ibaraki-ken 〒319-1195, Japan.

© Japan Atomic Energy Research Institute, 2000  
編集兼発行 日本原子力研究所

**Translation of**  
**TECHNICAL DEVELOPMENT ON BURN-UP CREDIT**  
**FOR SPENT LWR FUELS**

Edited by  
Yoshinori Nakahara, Kenya Suyama,  
and Takenori Suzuki

Department of Environmental Sciences  
Tokai Research Establishment  
Japan Atomic Energy Research Institute  
Tokai-mura, Naka-gun, Ibaraki-ken, 319-1995, Japan

**October 2000**

Translation by  
JLS Language Corporation,  
Menlo Park, CA 94025

Translation coordination by  
I. C. Gauld  
Oak Ridge National Laboratory

Prepared by  
OAK RIDGE NATIONAL LABORATORY  
PO Box 2008  
Oak Ridge, Tennessee 37831  
managed by UT-Battelle, LLC  
for the  
U.S. DEPARTMENT OF ENERGY  
under contract DE-AC-00OR22725



# **Technical Development on Burn-up Credit for Spent LWR Fuels**

(Eds.) Yoshinori Nakahara, Kenya Suyama<sup>+</sup> and Takenori Suzuki<sup>++</sup>

Department of Environmental Sciences  
Tokai Research Establishment  
Japan Atomic Energy Research Institute  
Tokai-mura, Naka-gun, Ibaraki-ken

(Received September 21, 2000)

Technical development on burn-up credit for spent LWR fuels had been performed at JAERI since 1990 under the contract with Science and Technology Agency of Japan entitled ‘Technical Development on Criticality Safety Management for Spent LWR Fuels.’ Main purposes of this work are to obtain the experimental data on criticality properties and isotopic compositions of spent LWR fuels and to verify burn-up and criticality calculation codes. In this work three major experiments of exponential experiments for spent fuel assemblies to obtain criticality data, non-destructive gamma-ray measurement of spent fuel rods for evaluating axial burn-up profiles, and destructive analyses of spent fuel samples for determining precise burn-up and isotopic compositions were carried out. The measured data obtained were used for validating calculation codes as well as an examination of criticality safety analyses. Details of the work are described in this report.

Keywords: spent LWR fuels, destructive analysis, gamma scanning, non-destructive analysis, burn-up codes, criticality calculation codes, criticality safety analysis, burn-up credit

---

<sup>+</sup> Department of Fuel Cycle Safety Research

<sup>++</sup> Department of Nuclear Energy System

Contributors to this work;

Department of Environmental Sciences: Y. Nakahara, J. Inagawa, R. Nagaishi, N. Kohno, S. Kurosawa, M. Ohnuki, K. Watanabe, T. Adacht and T. Muromura

Department of Fuel Cycle Safety Research: Y. Nomura, K. Suyama and H. Mochizuki

Department of Nuclear Energy System: T. Suzuki and M. Kurosawa



# CONTENTS

	<u>Page</u>
ABSTRACT .....	iii
LIST OF FIGURES.....	ix
LIST OF TABLES .....	xv
1. GENERAL .....	1
1.1. Introduction.....	1
1.2. Outline of the Work.....	1
1.3. Outline of the Features.....	2
1.3.1. Acquisition of Experimental Data .....	2
1.3.2. Validation of Burnup Calculation Codes .....	3
1.3.3. Validation of the Criticality Calculation Codes.....	4
1.3.4. Examination of the Burnup Estimation Methods.....	4
1.3.5. Examination of the Safety Margin.....	5
References.....	5
2. EXPERIMENTS.....	17
2.1 Gamma-Ray Scanning Measurements of Spent Fuel Rods .....	17
2.1.1 General .....	17
2.1.2 Gamma-Ray Measurement System for Spent Fuels .....	17
2.1.3 Measurement .....	19
2.1.4 Results and the Corresponding Errors.....	19
2.1.5 Axial Distribution Characteristics of FP Activity Ratios .....	21
References.....	23
2.2 Radiochemical Analyses of Spent Fuel Samples .....	102
2.2.1 Samples and Analytical Items .....	102
2.2.2 Samples Dissolution Method.....	102
2.2.3 Chemical Separation Method .....	107
2.2.4 Isotopic Ratio Measurement and Radioactivity Measurement Methods.....	110
2.2.5 Burn-up Rate (Degree) Calculation Method.....	120
2.2.6 Analytical Results and Errors .....	120
References.....	121
2.3 Exponential Experiments of Spent Fuel Assemblies.....	132
2.3.1 Principle of an Exponential Experiment .....	132
2.3.2 Spent Fuel Assemblies .....	133
2.3.3 Experimental Method.....	133
2.3.4 Experimental Results .....	134
References.....	134
3. VALIDATION OF BURN-UP CODES .....	145
3.1 General .....	145
3.2 Equation for Accuracy Evaluation .....	145
3.3 SWAT Analyses .....	147
3.3.1 Cell Configuration .....	147
3.3.2 Temperature.....	148
3.3.3 Void Rate.....	150
3.3.4 Power Histories.....	151
3.3.5 Analytical Results by SWAT .....	151

## CONTENTS (continued)

	<u>Page</u>
3.3.6 Analytical Results Without Considering Power Histories .....	152
3.3.7 Analysis with the Effect of Temperature Change Taken Into Consideration.....	163
3.4 Analysis by ORIGEN2 .....	170
3.4.1 Analytical Results for the SF95 Samples .....	171
3.4.2 Analytical Results for the SF96 Samples .....	171
3.4.3 Analytical Results for the SF97 Samples .....	181
3.4.4 Analytical Results for the SF98 Samples .....	187
3.4.5 Analytical Results for the SF99 Samples .....	192
3.5 Comparison of the Calculated Results for the Isotopes Important for Burn-up Credit .....	197
3.6 Conclusions.....	199
References .....	201
 4. VALIDATION OF CRITICALITY CALCULATION CODES .....	203
4.1 General .....	203
4.2 Analyses of the P14 and P17 Fuel Assemblies .....	205
4.3 Analysis of a B8 Fuel Assembly .....	206
4.3.1 Evaluation of the Neutron Multiplication Factor Based on the Fixed Neutron Source Calculation .....	208
4.3.2 Evaluation of the Neutron Multiplication Factor Based on Buckling Search Calculation .....	209
4.3.3 Neutron Flux Decay Factor .....	210
4.4 Analysis of an HP17 Fuel Assembly .....	212
4.5 Conclusions.....	214
References .....	215
 5. EXAMINATION OF THE BURNUP ESTIMATION METHOD.....	217
5.1 Evaluation of Axial Burnup Profiles Based on the Measured Data .....	217
5.1.1 General .....	217
5.1.2 Data Measurement .....	217
5.1.3 Correlation Between Burnup and FP Activity Ratios in PWR Fuels.....	218
5.1.4 Correlation Between Burnup and FP Activity Ratios in BWR Fuels .....	218
5.1.5 Axial Burnup Distribution of Spent Fuel Rods .....	220
Reference .....	220
5.2 Sensitivity Analysis of Irradiation Parameters Affecting the Correlation Between Burnup and FP Activity Ratios .....	231
5.2.1 Sensitivity Analysis on PWR Fuels .....	231
5.2.2 Sensitivity Analysis on BWR Fuels .....	233
5.2.3 Summary .....	234
 6. EXAMINATION OF THE SAFETY MARGIN .....	295
6.1 Examination of the Criticality Safety Margin for a Spent Fuel Transport Cask Model .....	295
6.1.1 General .....	295
6.1.2 Objective, Conditions, and Modeling for Analysis.....	296
6.1.3 Calculation Codes Used and Their Calculation Conditions .....	297
6.1.4 Results and Discussion.....	298

## CONTENTS (continued)

	<u>Page</u>
6.2 Examination of Safety Margin for a Concrete Storage Model.....	318
6.2.1 General .....	318
6.2.2 Objective, Conditions, and Modeling for Analysis.....	318
6.2.3 Calculation Codes Used and the Associated Calculation.....	319
6.2.4 Results and Discussion.....	320
6.3 Examination of the Source Terms for the Safety Analysis of Shielding and Heating.....	346
6.3.1 General .....	346
6.3.2 Analysis Objective .....	346
6.3.3 Results .....	347
References.....	348
7. CONCLUSION .....	355
ACKNOWLEDGMENTS .....	356
APPENDIX .....	357
A.1 Regulatory Status on Burn-up Credit .....	357
A.1.1 Worldwide Status on Burn-up Credit Uses .....	357
A.1.2 Authorization Status of Burn-up Credit Uses in Each Country.....	358
A.2 Characteristics of Irradiated Fuels.....	359
A.3 Results of Destructive Analysis .....	387
References .....	393



# LIST OF FIGURES

<u>Figure</u>		<u>Page</u>
1-1	Outline of contents for carrying out technical development on criticality safety management for light-water-reactor spent fuels .....	15
1-2	Annual plans for technical development on criticality safety management for light-water-reactor spent fuels.....	16
2.1.1	Composition of burnup measurement system .....	63
2.1.2	Successive approximation of relative efficiency curve .....	64
2.1.3	The geometry of gamma scanning measurement .....	65
2.1.4	A diagram of collimator arrangement.....	66
2.1.5	An example of $\gamma$ -scanning measurement steps in PWR spent fuel rod (NT3G24-C7, burnup 44,300 MWd/t).....	67
2.1.6	An example of $\gamma$ -scanning measurement steps in BWR spent fuel rod (2F2DN23-07, burnup 27,900 MWd/t).....	67
2.1.7	Fuel rod pieces used for $\gamma$ -scanning measurement in BWR (2F2DN23-01, 02).....	68
2.1.8	Arrangement of BWR rod pieces in Al-case.....	69
2.1.9	An example of $\gamma$ -spectrum (NT3G24-C7, 1444 mm from top).....	70
2.1.10	Axial profiles of activity ratios measured in NT3G23-C3 (KD01).....	71
2.1.11	Axial profiles of activity ratios measured in NT3G23-A4 (KC03).....	72
2.1.12	Axial profiles of activity ratios measured in NT3G23-C5 (KD02).....	73
2.1.13	Axial profiles of activity ratios measured in NT3G23-A6 (KD03).....	74
2.1.14	Axial profiles of activity ratios measured in NT3G23-C7 (KD05).....	75
2.1.15	Axial profiles of activity ratios measured in NT3G23-A8 (KD06).....	76
2.1.16	Axial profiles of activity ratios measured in NT3G23-B10 (KC04) .....	77
2.1.17	Axial profiles of activity ratios measured in NT3G23-D11 (KD04).....	78
2.1.18	Axial profiles of activity ratios measured in NT3G23-B12 (KD07) .....	79
2.1.19	Axial profiles of activity ratios measured in NT3G24-C3 (KH11).....	80
2.1.20	Axial profiles of activity ratios measured in NT3G24-A4 (KH06).....	81
2.1.21	Axial profiles of activity ratios measured in NT3G24-C5 (KH09).....	82
2.1.22	Axial profiles of activity ratios measured in NT3G24-A6 (KH07).....	83
2.1.23	Axial profiles of activity ratios measured in NT3G24-C7 (KF02).....	84
2.1.24	Axial profiles of activity ratios measured in NT3G24-A8 (KH12).....	85
2.1.25	Axial profiles of activity ratios measured in NT3G24-B10 (KH08) .....	86
2.1.26	Axial profiles of activity ratios measured in NT3G24-D11 (KH10).....	87
2.1.27	Axial profiles of activity ratios measured in NT3G24-B12 (KH05) .....	88
2.1.28	Axial profiles of activity ratios measured in 2F2DN23-01.....	89
2.1.29	Axial profiles of activity ratios measured in 2F2DN23-02.....	90
2.1.30	Axial profiles of activity ratios measured in 2F2DN23-04 (KE13) .....	91
2.1.31	Axial profiles of activity ratios measured in 2F2DN23-05 (KE08) .....	92
2.1.32	Axial profiles of activity ratios measured in 2F2DN23-06 (KE06) .....	93
2.1.33	Axial profiles of activity ratios measured in 2F2DN23-07 (KE07) .....	94
2.1.34	Axial profiles of activity ratios measured in 2F2DN23-08 (KE05) .....	95
2.1.35	Axial profiles of activity ratios measured in 2F2DN23-09 (KE09) .....	96
2.1.36	Axial profiles of activity ratios measured in 2F2DN23-10 (KE12) .....	97
2.1.37	Axial profiles of activity ratios measured in 2F2DN23-11 (KE04) .....	98
2.1.38	Axial profiles of activity ratios measured in 2F2DN23-12 (KE03) .....	99
2.1.39	Axial profiles of activity ratios measured in 2F2DN23-13 (KE14) .....	100
2.1.40	Axial profiles of activity ratios measured in 2F2DN23-14 (KE02) .....	101

## LIST OF FIGURES (continued)

<u>Figure</u>		<u>Page</u>
2.2.1	Cutting position of samples for the destructive analysis.....	105
2.2.2	Dissolution of apparatus for spent fuel sample .....	106
2.2.3	Flow diagram for analysis of the spent fuel sample .....	112
2.2.4	Schematic diagram for the separation of dissolved solution (1/2) .....	113
2.2.4	Schematic diagram for the separation of dissolved solution (2/2) .....	114
2.2.5	Ion optical system and variable multiple detector configuration for mass-spectrometer .....	115
2.2.6	$\alpha$ -ray spectrum of dissolved solution before chemical separation .....	116
2.2.7	$\alpha$ -ray spectrum of Neptunium fraction .....	116
2.2.8	$\alpha$ -ray spectrum of Plutonium fraction .....	117
2.2.9	$\alpha$ -ray spectrum of FP fraction .....	117
2.2.10	Allocation of sample/standard source and Ge-detector for $\gamma$ -ray measurement .....	118
2.2.11	An example of $\gamma$ -ray spectrum profile for dissolved solution .....	119
2.3.1	Principle of exponential experiment .....	137
2.3.2	Example of calculated variations in $k_{eff}$ , $\gamma$ and K with burnup .....	138
2.3.3	Relation between DS- and SS-methods .....	139
2.3.4	Comparison of measured results between DS- and SS-methods .....	140
2.3.5	Experimental setup at the fuel receiving pool of the Reactor Fuel Examination Facility .....	141
2.3.6	Axial distribution of neutron count rate in spent fuel assembly (without $^{252}Cf$ source) .....	142
3.3.1	Temperature distribution in (SF95) .....	164
3.3.2	Temperature distribution in (SF97) .....	165
3.3.3	Temperature history of SF95 samples .....	166
3.3.4	Temperature history of SF97 samples .....	167
4.1.1	Schematic figure of subcritical experiment of spent fuel (for C33, P17 and HP17) .....	204
4.1.2	Schematic figure of subcritical experiment of spent fuel (for H8) .....	205
4.3.3	B8 subcritical experiment : Position for $\gamma$ evaluation (90 deg. rotation) .....	211
4.4.4	Burnup distribution of HP17 .....	212
4.4.5	HP17 subcritical experiment : Position of source and detector .....	213
5.1.1	Relation of $^{137}Cs$ with burnup .....	223
5.1.2	Examples of axial profiles on FP activity ratios in both PWR and BWR spent fuel rods .....	224
5.1.3	Relation of burnup with single ratio in PWR .....	225
5.1.4	Relation of burnup with multiple ratio in PWR .....	225
5.1.5	Relation of burnup with single ratio .....	226
5.1.6	Relation of burnup with multiple ratio .....	226
5.1.7	Relation of void factor with void rate .....	227
5.1.8	Relation of position factor with rod position .....	227
5.1.9	Axial burnup profile estimated by Vf and Pf .....	228
5.1.10	Relation between activity ratios and burnup based on measured data.....	229
5.1.11	Relation between activity ratios and burnup with different spent fuel rods.....	230
5.1.12	Relation between Dolphin profile and measurement positions .....	230
5.2.1	Cs activity ratio (Cs-134/Cs-137) vs. burnup (Initial enrichment dependency, PWR) .....	258
5.2.2	Eu activity ratio (Eu-154/Cs-137) vs. burnup (Initial enrichment dependency, PWR).....	259
5.2.3	Ru activity ratio ((Cs-134/Cs-137) <sup>2</sup> / (Ru-106/Cs-137)) vs. burnup (Initial enrichment dependency, PWR) .....	260
5.2.4	Relative activity ratio (Cs-134/Cs-137) (Initial enrichment dependency, PWR).....	261

## LIST OF FIGURES (continued)

<u>Figure</u>		<u>Page</u>
5.2.5	Relative activity ratio (Eu-154/Cs-137) (Initial enrichment dependency, PWR).....	262
5.2.6	Relative activity ratio ( $(\text{Cs-134/Cs-137})^2 / (\text{Ru-106/Cs-137})$ ) (Initial enrichment dependency, PWR) .....	263
5.2.7	Cs activity ratio (Cs-134/Cs-137) vs. burnup (Power history dependency, PWR) .....	264
5.2.8	Eu activity ratio (Eu-154/Cs-137) vs. burnup (Power history dependency, PWR) .....	265
5.2.9	Ru activity ratio ( $(\text{Cs-134/Cs-137})^2 / (\text{Ru-106/Cs-137})$ ) vs. burnup (Power history dependency, PWR) .....	266
5.2.10	Relative activity ratio (Cs-134/Cs-137) (Power history dependency, PWR).....	267
5.2.11	Relative activity ratio (Eu-154/Cs-137) (Power history dependency, PWR).....	268
5.2.12	Relative activity ratio ( $(\text{Cs-134/Cs-137})^2 / (\text{Ru-106/Cs-137})$ ) vs. burnup (Power history dependency, PWR) .....	269
5.2.13	Cs activity ratio (Cs-134/Cs-137) vs. burnup (Boron content dependency, PWR).....	270
5.2.14	Eu activity ratio (Eu-154/Cs-137) vs. burnup (Boron content dependency, PWR).....	271
5.2.15	Ru activity ratio ( $(\text{Cs-134/Cs-137})^2 / (\text{Ru-106/Cs-137})$ ) (Boron content dependency, PWR) .....	272
5.2.16	Relative activity ratio (Cs-134/Cs-137) (Boron content dependency, PWR) .....	273
5.2.17	Relative activity ratio (Eu-154/Cs-137) (Boron content dependency, PWR) .....	274
5.2.18	Relative activity ratio ( $(\text{Cs-134/Cs-137})^2 / (\text{Ru-106/Cs-137})$ ) vs. burnup (Boron content dependency, PWR) .....	275
5.2.19	Cs activity ratio (Cs-134/Cs-137) vs. burnup (Initial enrichment dependency, BWR).....	276
5.2.20	Eu activity ratio (Eu-154/Cs-137) vs. burnup (Initial enrichment dependency, BWR).....	277
5.2.21	Ru activity ratio ( $(\text{Cs-134/Cs-137})^2 / (\text{Ru-106/Cs-137})$ ) vs. burnup (Initial enrichment dependency, BWR) .....	278
5.2.22	Relative activity ratio (Cs-134/Cs-137) (Initial enrichment dependency, BWR) .....	279
5.2.23	Relative activity ratio (Eu-154/Cs-137) (Initial enrichment dependency, BWR) .....	280
5.2.24	Relative activity ratio ( $(\text{Cs-134/Cs-137})^2 / (\text{Ru-106/Cs-137})$ ) (Initial enrichment dependency, BWR) .....	281
5.2.25	Cs activity ratio (Cs-134/Cs-137) vs. burnup (Power history dependency, BWR).....	282
5.2.26	Eu activity ratio (Eu-154/Cs-137) vs. burnup (Power history dependency, BWR) .....	283
5.2.27	Ru activity ratio ( $(\text{Cs-134/Cs-137})^2 / (\text{Ru-106/Cs-137})$ ) vs. burnup (Power history dependency, PWR) .....	284
5.2.28	Relative activity ratio (Cs-134/Cs-137) (Power history dependency, BWR) .....	285
5.2.29	Relative activity ratio (Eu-154/Cs-137) (Power history dependency, BWR) .....	286
5.2.30	Relative activity ratio ( $(\text{Cs-134/Cs-137})^2 / (\text{Ru-106/Cs-137})$ ) vs. burnup (Power history dependency, BWR) .....	287
5.2.31	Cs activity ratio (Cs-134/Cs-137) vs. burnup (Void ratio dependency, BWR).....	288
5.2.32	Eu activity ratio (Eu-154/Cs-137) vs. burnup (Void ratio dependency, BWR) .....	289
5.2.33	Ru activity ratio ( $(\text{Cs-134/Cs-137})^2 / (\text{Ru-106/Cs-137})$ ) vs. burnup (Void ratio dependency, BWR).....	290
5.2.34	Relative activity ratio (Cs-134/Cs-137) (Void ratio dependency, BWR) .....	291
5.2.35	Relative activity ratio (Eu-154/Cs-137) (Void ratio dependency, BWR) .....	292
5.2.36	Relative activity ratio ( $(\text{Cs-134/Cs-137})^2 / (\text{Ru-106/Cs-137})$ ) vs. burnup (Void ratio dependency, BWR).....	293
6.1.1	Criticality calculation model for MCNP-4A/KENO-V.a (Longitudinal cross section of transport cask) .....	306
6.1.2	Criticality calculation model for MCNP-4A/KENO-V.a (Horizontal cross section of transport cask).....	307

## LIST OF FIGURES (continued)

<u>Figure</u>	<u>Page</u>
6.1.3 Criticality calculation model for MCNP-4A/KENO-V.a (Horizontal cross section of fuel assembly) .....	308
6.1.4 Axial burnup distribution profile in PWR fuel pin.....	309
6.1.5 Horizontal burnup distribution of spent fuel assemblies .....	310
6.1.6 ( $k_{\text{eff}} + 3\sigma$ ) changing curve with burnup of spent fuel in transport cask (considering Ac and FP to compare its measured and calculated values in effect of criticality) ..	311
6.1.6-1 ( $k_{\text{eff}} + 3\sigma$ ) changing curve with burnup of spent fuel in transport cask (considering only actinide, basket material is SUS304 stainless steel) .....	312
6.1.6-2 ( $k_{\text{eff}} + 3\sigma$ ) changing curve with burnup of spent fuel in transport cask (considering only actinide, basket material is borated SUS304 stainless steel).....	313
6.1.7 ( $k_{\text{eff}} + 3\sigma$ ) changing curve with burnup of spent fuel in transport cask (to compare $k_{\text{eff}}$ considering Ac and FP obtained by ORIGEN2 with $k_{\text{eff}}$ considering Ac only) ..	314
6.1.8 ( $k_{\text{eff}} + 3\sigma$ ) changing curve with burnup of spent fuel in transport cask (considering Ac and FP calculated by ORIGEN2.1).....	315
6.1.9 Criticality analysis results obtained by KENO-V.a (considering burnup distribution with Ac and FP of spent fuel inside transport cask).....	316
6.1.10 Criticality analysis results obtained by KENO-V.a (considering burnup distribution with only Ac of spent fuel inside transport cask).....	317
6.2.1 Construction diagram for spent fuel concrete storage cask .....	332
6.2.2 Calculation model for horizontal cross section .....	333
6.2.3 Calculation model for longitudinal cross section .....	334
6.2.4 Calculation model for fuel assembly configuration inside canister.....	335
6.2.5 Calculation model for canister (horizontal cross section).....	336
6.2.6 Calculation model for axial burnup distribution profile in PWR fuel pin .....	337
6.2.7 ( $k_{\text{eff}} + 3\sigma$ ) changing curve with burnup for spent fuel storage cask model .....	338
6.2.8 ( $k_{\text{eff}} + 3\sigma$ ) changing curve with cooling time for case 6 (SWAT) spent fuel storage cask model .	339
6.2.9 ( $k_{\text{eff}} + 3\sigma$ ) changing curve with cooling time for case 7 (ORIGEN2.1) spent fuel storage cask model .....	340
6.2.10 ( $k_{\text{eff}} + 3\sigma$ ) changing curve with moisture density around canister calculated by KENO-V.a .....	341
6.2.11 ( $k_{\text{eff}} + 3\sigma$ ) changing curve with moisture density inside canister calculated by KENO-V.a.....	342
6.2.12 ( $k_{\text{eff}} + 3\sigma$ ) changing curve with moisture density outside canister calculated by KENO-V.a as canister thickness parameter change .....	343
6.2.13 ( $k_{\text{eff}} + 3\sigma$ ) changing curve with burnup profile consideration with all isotopic nuclides calculated by ORIGEN2.1 and KENO-V.a for spent fuel storage concrete cask.....	344
6.2.14 ( $k_{\text{eff}} + 3\sigma$ ) changing curve with burnup profile consideration with U, Pu, Am, Np isotopic nuclides calculated by ORIGEN2.1 and KENO-V.a for spent fuel storage concrete cask.....	345
6.3.1 Primary neutron source strength change with cooling time for the low and high burnup fuel specimen .....	351
6.3.2 Primary neutron source strength change with cooling time (SF97-1-1, 17950 MWd/MTU) .....	352
6.3.3 Primary neutron source strength change with cooling time (SF97-1-5, 48220 MWd/MTU) .....	353
A.2.1 Position of fuel rod in NT3G23 assembly for SF95 destructive analysis .....	366
A.2.2 Position of fuel rod in NT3G23 assembly for SF96 destructive analysis .....	367
A.2.3 Position of fuel rod in NT3G24 assembly for SF97 destructive analysis .....	368
A.2.4 Position of fuel rod in 2F2DN23 assembly for SF98 destructive analysis .....	369
A.2.5 Position of fuel rod in 2F2DN23 assembly for SF99 destructive analysis .....	370

## LIST OF FIGURES (continued)

<u>Figure</u>		<u>Page</u>
A.2.6	Radial distribution of $^{235}\text{U}$ enrichment in 2F2DN23 assembly .....	371
A.2.7	Axial distribution of $^{235}\text{U}$ enrichment in 2F2DN23 assembly.....	372
A.2.8	Axial distribution of burnup, void ratio (%), $^{235}\text{U}$ enrichment of 2F2DN23 assembly .....	373
A.2.9	NT3G23 $\gamma$ scan position .....	374
A.2.10	NT3G24 $\gamma$ scan position .....	375
A.2.11	2F2DN23 $\gamma$ scan position.....	376



# LIST OF TABLES

<u>Table</u>		<u>Page</u>
1-1	List of names of members of the Specialized Sectional Committee on Technical Development on Criticality Safety Management for Light-Water-Reactor Spent Fuels 1996–1999 .....	6
1-2	List of names of members of the Overall Evaluation Working Group on Technical Development on Criticality Safety Management for Light-Water-Reactor Spent Fuels .....	12
2.1.1	Decay data of fission products $\gamma$ -emitters in spent fuel .....	24
2.1.2	Decay data for internal standard method .....	25
2.1.3	PWR spent fuel rods used in $\gamma$ -scanning measurement .....	26
2.1.4	BWR spent fuel rods used in $\gamma$ -scanning measurement .....	27
2.1.5	Measured data of NT3G23-C3(KD01) .....	28
2.1.6	Measured data of NT3G23-A4(KC03).....	29
2.1.7	Measured data of NT3G23-C5(KD02).....	30
2.1.8	Measured data of NT3G23-A6(KD03).....	31
2.1.9	Measured data of NT3G23-C7(KD05).....	32
2.1.10	Measured data of NT3G23-A8(KD06).....	33
2.1.11	Measured data of NT3G23-B10(KC04).....	34
2.1.12	Measured data of NT3G23-D11(KD04).....	35
2.1.13	Measured data of NT3G23-B12(KD07).....	36
2.1.14	Measured data of NT3G24-C3(KH11).....	37
2.1.15	Measured data of NT3G24-A4(KH06).....	38
2.1.16	Measured data of NT3G24-C5(KH09).....	39
2.1.17	Measured data of NT3G24-A6(KH07).....	40
2.1.18	Measured data of NT3G24-C7(KF02).....	41
2.1.19	Measured data of NT3G24-A8(KH12).....	42
2.1.20	Measured data of NT3G24-B10(KH08).....	43
2.1.21	Measured data of NT3G24-D11(KH10).....	44
2.1.22	Measured data of NT3G24-B12(KH05).....	45
2.1.23	Measured data of 2F2DN23-01.....	46
2.1.24	Measured data of 2F2DN23-02.....	47
2.1.25	Measured data of 2F2DN23-04(KE13) .....	48
2.1.26	Measured data of 2F2DN23-05(KE08) .....	49
2.1.27	Measured data of 2F2DN23-06(KE06) .....	50
2.1.28	Measured data of 2F2DN23-07(KE07) .....	51
2.1.29	Measured data of 2F2DN23-08(KE05) .....	52
2.1.30	Measured data of 2F2DN23-09(KE09) .....	53
2.1.31	Measured data of 2F2DN23-10(KE12) .....	54
2.1.32	Measured data of 2F2DN23-11(KE04) .....	55
2.1.33	Measured data of 2F2DN23-12(KE03) .....	56
2.1.34	Measured data of 2F2DN23-13(KE14) .....	57
2.1.35	Measured data of 2F2DN23-14(KE02) .....	58
2.1.36	Example of relative errors (%) on FP nuclides in the process of non-destructive $\gamma$ -spectrum analysis .....	59
2.1.37	Fission yield data and the relative values to U-235T .....	60
2.1.38	Comparison of $\gamma$ -scanning activity ratio (NDA) with those of destructive analysis (DA) at the end of irradiation in PWR .....	61

## LIST OF TABLES (continued)

<u>Table</u>		<u>Page</u>
2.1.39 Comparison of $\gamma$ -scanning activity ratio (NDA) with those of destructive analysis (DA) data at the end of irradiation in BWR.....		62
2.2.1 Dissolution behavior of spent fuel sample.....		103
2.2.2 Surface equivalent dose rate of sample .....		104
2.2.3 SF95: Destructive analytical results of actinide nuclides for PWR spent fuel ( $\text{UO}_2$ ) sample, normalized in zero cooling.....		122
2.2.4 SF95: Destructive analytical results of FP nuclides for PWR spent fuel ( $\text{UO}_2$ ) sample, normalized in zero cooling.....		123
2.2.5 SF96: Destructive analytical results of actinide nuclides for PWR spent fuel ( $\text{UO}_2\text{-Gd}_2\text{O}_3$ ) sample, normalized in zero cooling.....		124
2.2.6 SF96: Destructive analytical results of FP nuclides for PWR spent fuel ( $\text{UO}_2\text{-Gd}_2\text{O}_3$ ) sample, normalized in zero cooling.....		125
2.2.7 SF97: Destructive analytical results of actinide nuclides for PWR high burnup spent fuel ( $\text{UO}_2$ ) sample, normalized in zero cooling.....		126
2.2.8 SF97: Destructive analytical results of FP nuclides for PWR high burnup spent fuel ( $\text{UO}_2$ ) sample, normalized in zero cooling.....		127
2.2.9 SF98: Destructive analytical results of actinide nuclides for BWR spent fuel ( $\text{UO}_2$ ) sample, normalized in zero cooling.....		128
2.2.10 SF98: Destructive analytical results of FP nuclides for BWR spent fuel ( $\text{UO}_2$ ) sample, normalized in zero cooling.....		129
2.2.11 SF99: Destructive analytical results of actinide nuclides for BWR spent fuel ( $\text{UO}_2\text{-Gd}_2\text{O}_3$ ) sample, normalized in zero cooling.....		130
2.2.12 SF99: Destructive analytical results of FP nuclides for BWR spent fuel ( $\text{UO}_2\text{-Gd}_2\text{O}_3$ ) sample, normalized in zero cooling .....		131
2.3.1 Results of exponential experiments and analyses .....		135
3.1.1 List of destructive analyses samples.....		146
3.3.1 Cell geometry for SF95 and SF97 .....		147
3.3.2 Cell geometry for SF96 .....		147
3.3.3 Cell geometry for SF98 .....		148
3.3.4 Cell geometry for SF99 .....		148
3.3.5 SF95: Temperature of coolant (K) .....		149
3.3.6 SF96: Temperature of coolant (K) .....		149
3.3.7 SF97: Temperature of coolant (K) .....		149
3.3.8 SF98: Temperature of coolant (K) .....		150
3.3.9 SF99: Temperature of coolant (K) .....		150
3.3.10 SF98: Void ratio.....		151
3.3.11 SF99: Void ratio.....		151
3.3.12 SF95: Results (C/E by SWAT) .....		153
3.3.13 SF96: Results (C/E by SWAT) .....		154
3.3.14 SF97: Results (C/E by SWAT) .....		155
3.3.15 SF98: Results (C/E by SWAT) .....		156
3.3.16 SF99: Results (C/E by SWAT) .....		157
3.3.17 SF95: Results (C/E by SWAT : Constant power) .....		158
3.3.18 SF96: Results (C/E by SWAT : Constant power) .....		159
3.3.19 SF97: Results (C/E by SWAT : Constant power) .....		160

## LIST OF TABLES (continued)

<u>Table</u>	<u>Page</u>
3.3.20 SF98: Results (C/E by SWAT : Constant power) .....	161
3.3.21 SF99: Results (C/E by SWAT : Constant power) .....	162
3.3.22 Data for FEMAXI-V calculation.....	163
3.3.23 SF95: Results (C/E by SWAT : Considering pellet temp. history) .....	168
3.3.24 SF97: Results (C/E by SWAT : Considering pellet temp. history) .....	169
3.4.1 Libraries in ORIGEN2.1.....	170
3.4.2 SF95: Results (C/E by ORIGEN2.1 : PWR41J32).....	172
3.4.3 SF95: Results (C/E by ORIGEN2.1 : PWR-UE) .....	173
3.4.4 SF95: Results (C/E by ORIGEN2.1 : PWR-US) .....	174
3.4.5 SF95: Results (C/E by ORIGEN2.1 : PWR-U).....	175
3.4.6 SF95: Results (C/E by ORIGEN2.1 : PUD50) .....	176
3.4.7 SF96: Results (C/E by ORIGEN2.1 : PWR41J32).....	177
3.4.8 SF96: Results (C/E by ORIGEN2.1 : PWR-UE) .....	178
3.4.9 SF96: Results (C/E by ORIGEN2.1 : PWR-US) .....	179
3.4.10 SF96: Results (C/E by ORIGEN2.1 : PWR-U).....	180
3.4.11 SF97: Results (C/E by ORIGEN2.1 : PWR41J32).....	182
3.4.12 SF97: Results (C/E by ORIGEN2.1 : PWR-UE) .....	183
3.4.13 SF97: Results (C/E by ORIGEN2.1 : PWR-US) .....	184
3.4.14 SF97: Results (C/E by ORIGEN2.1 : PWR-U).....	185
3.4.15 SF97: Results (C/E by ORIGEN2.1 : PUD50) .....	186
3.4.16 SF98: Results (C/E by ORIGEN2.1 : BS1XXJ2) .....	188
3.4.17 SF98: Results (C/E by ORIGEN2.1 : BWR-UE).....	189
3.4.18 SF98: Results (C/E by ORIGEN2.1 : BWR-US) .....	190
3.4.19 SF98: Results (C/E by ORIGEN2.1 : BWR-U) .....	191
3.4.20 SF99: Results (C/E by ORIGEN2.1 : BS1XXJ32).....	193
3.4.21 SF99: Results (C/E by ORIGEN2.1 : BWR-UE).....	194
3.4.22 SF99: Results (C/E by ORIGEN2.1 : BWR-US) .....	195
3.4.23 SF99: Results (C/E by ORIGEN2.1 : BWR-U) .....	196
3.5.24 Comparison between several results (SF95).....	197
3.5.25 Comparison between several results (SF97).....	198
3.5.26 Comparison between several results (SF98).....	198
4.1.1 List of subcritical experiment of spent fuel .....	203
4.2.2 Results of subcritical experiment of spent fuel assemblies (P14 and P17).....	206
4.3.3 Burnup and void distribution for 2F2DN23.....	207
4.3.4 Results of subcritical experiment of spent fuel assemblies (B8).....	208
4.3.5 Evaluated $k_{eff}$ of spent fuel assemblies (B8) (Fixed source).....	209
4.3.6 Evaluated $k_{eff}$ of spent fuel assemblies (B8) (Buckling source) .....	209
4.3.7 Difference of $\gamma$ : Effect of distance between source and detector .....	210
4.3.8 Difference of $\gamma$ : 90 deg. revolution.....	211
4.4.9 Evaluated $\gamma$ (Exp. : 0.1256 (1/cm)).....	214
5.1.1 Measured data on burnup and activity ratios .....	221
5.1.2 Estimated burnup by Vf and Pf fitting curve .....	222
5.2.1 PWR fuel rod specification.....	236
5.2.2 Number densities (PWR fuel cell).....	237
5.2.3 Power history .....	238
5.2.4 Initial enrichment .....	236

## LIST OF TABLES (continued)

<u>Table</u>	<u>Page</u>
5.2.5 Power history .....	236
5.2.6 Boron content.....	236
5.2.7 Activity and activity ratio (Enrichment 3.0 wt %, power constant, boron content 500 ppm)....	241
5.2.8 Activity and activity ratio (Enrichment 4.0 wt %, power constant, boron content 500 ppm)....	241
5.2.9 Activity and activity ratio (Enrichment 5.0 wt %, power constant, boron content 500 ppm)....	241
5.2.10 Cs-134/Cs-137 activity ratio enrichment dependency (power constant, boron content 500 ppm).....	242
5.2.11 Eu-154/Cs-137 activity ratio enrichment dependency (power constant, boron content 500 ppm).....	242
5.2.12 (Cs-134/Cs-137) <sup>2</sup> / (Ru-106/Cs-137) Activity ratio enrichment dependency (power constant, boron content 500 ppm) .....	242
5.2.13 Activity and activity ratio (Enrichment 4.0 wt %, power CASE:A, boron content 500 ppm)...	243
5.2.14 Activity and activity ratio (Enrichment 4.0 wt %, power CASE:B, boron content 500 ppm) ...	243
5.2.15 Activity and activity ratio (Enrichment 4.0 wt %, power CASE:C, boron content 500 ppm) ...	243
5.2.16 Activity ratio (Enrichment 4.0 wt %, boron content 500 ppm).....	244
5.2.17 Activity ratio (Enrichment 4.0 wt %, boron content 500 ppm).....	244
5.2.18 Activity ratio (Enrichment 4.0 wt %, boron content 500 ppm).....	244
5.2.19 Activity and activity ratio (Enrichment 4.0 wt %, power constant, boron content 500 ppm)....	245
5.2.20 Activity and activity ratio (Enrichment 4.0 wt %, power constant, boron content 0 ppm).....	245
5.2.21 Activity and activity ratio (Enrichment 4.0 wt %, power constant, boron content 1000 ppm) ..	245
5.2.22 Activity and activity ratio (Enrichment 4.0 wt %, power constant, boron content 1000-0 ppm linear change) .....	245
5.2.23 Cs-134/Cs-137 activity ratio boron content dependency (Enrichment 4 wt %, power constant) .....	246
5.2.24 Eu-154/Cs-137 activity ratio boron content dependency (Enrichment 4 wt %, power constant) .....	246
5.2.25 (Cs-134/Cs-137) <sup>2</sup> / (Ru-106/Cs-137) activity ratio boron content dependency (Enrichment 4 wt %, power constant) .....	246
5.2.26 BWR fuel rod specification .....	247
5.2.27 Number densities (BWR fuel cell) .....	247
5.2.28 Power history .....	248
5.2.29 Dancoff factor .....	251
5.2.30 Initial enrichment .....	251
5.2.31 Initial enrichment .....	251
5.2.32 Void ratio .....	251
5.2.33 Activity and activity ratio (Enrichment 3.0 wt %, power constant, void ratio 40%).....	252
5.2.34 Activity and activity ratio (Enrichment 4.0 wt %, power constant, void ratio 40%).....	252
5.2.35 Activity and activity ratio (Enrichment 5.0 wt %, power constant, void ratio 40%).....	252
5.2.36 Cs-134/Cs-137 activity ratio enrichment dependency (Power constant, void ratio 40%) .....	253
5.2.37 Eu-154/Cs-137 activity ratio enrichment dependency (Power constant, void ratio 40%) .....	253
5.2.38 (Cs-134/Cs-137) <sup>2</sup> / (Ru-106/Cs-137) activity ratio enrichment dependency (Power constant, void ratio 40%) .....	253
5.2.39 Activity and activity ratio (Enrichment 4.0 wt %, power CASE:A, void 40%).....	254
5.2.40 Activity and activity ratio (Enrichment 4.0 wt %, power CASE:B, void 40%).....	254
5.2.41 Activity and activity ratio (Enrichment 4.0 wt %, power CASE:C, void 40%).....	254

## LIST OF TABLES (continued)

<u>Table</u>		<u>Page</u>
5.2.42 Cs-134/Cs-137 activity ratio power history dependency (Enrichment 4.0 wt %, void ratio 40%).....		255
5.2.43 Eu-154/Cs-137 activity ratio power history dependency (Enrichment 4.0 wt %, void ratio 40%).....		255
5.2.44 (Cs-134/Cs-137) <sup>2</sup> / (Ru-106/Cs-137) activity ratio power history dependency (Enrichment 4.0 wt %, void ratio 40%).....		255
5.2.45 Activity and activity ratio (Enrichment 4.0 wt %, power constant, void ratio 0%) .....		256
5.2.46 Activity and activity ratio (Enrichment 4.0 wt %, power constant, void ratio 40%).....		256
5.2.47 Activity and activity ratio (Enrichment 4.0 wt %, power constant, void ratio 70%).....		256
5.2.48 Cs-134/Cs-137 activity ratio void ratio dependency (Power constant, enrichment 4 wt %) ....		257
5.2.49 Eu-154/Cs-137 activity ratio void ratio dependency (Power constant, enrichment 4 wt %) ....		257
5.2.50 (Cs-134/Cs-137) <sup>2</sup> / (Ru-106/Cs-137) activity ratio void ratio dependency (Power constant, enrichment 4 wt %).....		257
6.1.1 Main feature of fuel assembly for criticality analysis .....		299
6.1.2 Spent fuel irradiation conditions .....		299
6.1.3 Atomic number density of actinide and fission product .....		300
6.1.4 Averaged burnup for each fuel region in the assumed PWR ( $\text{UO}_2$ ) fuel rods by considering axial and horizontal burnup distribution .....		305
6.2.1 Main feature of fuel assembly for criticality analysis .....		323
6.2.2 Spent fuel irradiation conditions .....		323
6.2.3 Combination of criticality analysis cases.....		324
6.2.4 Atomic number density of actinide and fission product .....		325
6.2.5 Weight percent and atomic number density for each isotope in an unirradiated $\text{UO}_2$ fuel .....		331
6.3.1 Object nuclides for criticality safety analysis .....		349
6.3.2 Primary neutron source strength .....		349
6.3.3 Primary neutron source strength SF97-1-1 17950 MWd/MTU .....		350
6.3.4 Primary neutron source strength SF97-1-5 48220 MWd/MTU .....		350
A.2.1 Data of Takahama 3 .....		361
A.2.2 Data of Fukushima Daini-2.....		361
A.2.3 Data of Genkai 1 .....		362
A.2.4 Data of Ohi 2.....		362
A.2.5 Data of fuel assembly : NT3G23 and NT3G24 from Takahama 3 .....		363
A.2.6 Data of fuel assembly : 2F2DN23 from Fukushima Daini-2 .....		364
A.2.7 Data of fuel assembly : C33 from Genkai 1.....		365
A.2.8 Data of fuel assembly : J2R from Ohi 2 .....		365
A.2.9 SF95 and SF97 : Initial isotopic composition (Weight (%)).....		377
A.2.10 SF96 : Initial isotopic composition (Weight (%)) .....		377
A.2.11 SF98 : Initial isotopic composition (Weight (%)) .....		377
A.2.12 SF99 : Initial isotopic composition (Weight (%)) .....		377
A.2.13 Operation history of Takahama 3 (SF95 and SF96).....		378
A.2.14 Operation history of Takahama 3 (SF97) .....		378
A.2.15 Operation history of Fukushima Daini-2 (SF98 and SF99 and sub-critical experiment) .....		378
A.2.16 SF95 : Sampling position.....		379
A.2.17 SF96 : Sampling position.....		379
A.2.18 SF97 : Sampling position.....		379
A.2.19 SF98 : Sampling position.....		380

## LIST OF TABLES (continued)

<u>Table</u>		<u>Page</u>
A.2.20	SF99 : Sampling position.....	380
A.2.21	Irradiation history SF95 samples.....	381
A.2.22	Irradiation history SF96 samples.....	382
A.2.23	Irradiation history SF97 samples (1/2) .....	383
A.2.24	Irradiation history SF97 samples (2/2) .....	384
A.2.25	Irradiation history SF98 samples.....	385
A.2.26	Irradiation history SF99 samples.....	386
A.3.27	Results of destructive analysis (End of irradiation) : SF95 .....	388
A.3.28	Results of destructive analysis (End of irradiation) : SF96 .....	389
A.3.39	Results of destructive analysis (End of irradiation) : SF97 .....	390
A.3.30	Results of destructive analysis (End of irradiation) : SF98 .....	391
A.3.31	Results of destructive analysis (End of irradiation) : SF99 .....	392

# **1. GENERAL**

## **1.1. Introduction**

Spent fuel management is costly work for all nuclear power plant operators. Spent fuels must be managed, whatever policy is selected for the back end of a nuclear fuel cycle. Up to the present, 135,000 tHM or more of 210,000 tHM of spent fuels carried away from nuclear power plants are stored in nuclear reactor pools and wet- and dry-mode storage facilities outside the nuclear reactor sites throughout the world. In general, there is a need to cut the cost of power generation. One conceivable possibility of cutting down nuclear fuel costs is to bring burnup credit into spent fuel management systems, and in fact burnup credit is already authorized in many countries and applied to transport systems, dry/wet-mode storage facilities, and reprocessing plant facilities. The introduction of burnup credit is also thought to be needed for final spent fuel disposal sites.<sup>1</sup>

The introduction of burnup credit into the storage and transport of spent fuels is needed for various reasons that differ from country to country, such as to make it possible to handle fuels with higher enrichments than in the past in current storage, transport, or reprocessing plants, to increase storage capacity by decreasing the interval between the fuels in a spent fuel storage system, or to decrease the number of shipments by making a new cask with larger capacity than that of the current casks in spent fuel transport systems.<sup>2</sup>

For burnup credit to be applied to spent fuel management systems, the precision of criticality calculation must be grasped with accuracy, which can be maintained satisfactorily in practical use, on nuclides with large contributions to the reactivity of spent fuels into which burnup credit is introduced. Accordingly, when compared with the case of a new fuel which has been employed so far, various new problems that must be considered in criticality safety analysis arose for implementing burnup credit, such as (1) establishment of appropriate isotopic sets, (2) assessment of adequacy of the burnup calculation codes used, (3) assessment of adequacy of criticality calculation codes, (4) determination of irradiation history related to the assessment of the effect of reactivity in the axial/radial directions, (5) determination of required minimum burnup (usually a function of initial enrichment), and (6) validation of the burnup of an assembly before being conveyed into a spent fuel management system. The effect of burnup credit application increases or decreases, depending on the degree of accuracy of these parameters.

## **1.2. Outline of the Work**

Nuclear power generation by the present mainstream light-water reactors now involves higher burnups and higher enrichments, and their operation is expected to continue for some time into the future. These advancements involving the fuel greatly change the nuclide compositions of the TRUs and FPs in a spent fuel. Since these changes largely affect criticality, shielding, and heat assessments, a burnup calculation code for evaluating the nuclide compositions in a spent fuel with high accuracy needs to be established. Furthermore, a criticality calculation code of high accuracy is also needed to evaluate the reactivity of light-water-reactor spent fuels.

However, measured data on spent fuels necessary for the evaluation of the accuracy of these calculation codes are extremely scarce, thus there is a pressing need to obtain measured data by experiments using actual spent fuels.

It is critical to enhance the economy and safety of spent fuel management in the future by evaluating and improving the accuracy of burnup calculation codes and criticality calculation codes, enabling criticality

safety design with consideration of the burnup in transport and storage facilities, and ensuring a safety margin related to shielding and heat.

The present "technical development on criticality safety management for light-water-reactor spent fuels" carried out the following projects over 10 years from 1990 to 1999 with the goal of developing safety management techniques concerning criticality, shielding, and the heat of spent fuels with the burnup taken into consideration in order to enhance the safety and economics in the storage and transport of spent fuels, and in more concrete terms, with the focus on obtaining measured data of high accuracy on the nuclide compositions and criticality of spent fuels, which are indispensable for the research/development of burnup credit.

1. Experimental Data Acquisition
  - (1) Acquisition of axial  $\gamma$ -ray radioactivity ratio data from spent fuel rods
  - (2) Acquisition of nuclide composition data from spent fuel samples
  - (3) Acquisition of criticality data from spent fuel assemblies
2. Evaluation of the Accuracy of Burnup Calculation Codes
3. Validation of Criticality Calculation Codes
4. Examination of Burnup Estimation Methods
5. Examination of Safety Margin

An outline of the contents of the work is shown in Fig. 1-1, and annual plans in Fig. 1-2. The contents of the work were carried out each year after having been examined and assessed at the "specialized sectional committee on technical development on criticality safety management for light-water-reactor spent fuels," which is made up of people of experience or academic standing. A list of names of members of the specialized sectional committee and the "overall evaluation working group" is shown in Tables 1-1 and 1-2.

The present overall evaluation report is a summary of the main features of the above-mentioned work.

## 1.3. Outline of the Features

### 1.3.1. Acquisition of Experimental Data

#### (1) Gamma Scanning Measurement of Spent Fuel Rods

At the JAERI fuel examination facility, axial  $\gamma$ -ray scanning measurement was carried out on PWR spent fuel rods (18 rods : 2 assemblies) and BWR spent fuel rods (13 rods : one assembly). The instruments used for these measurements included a Ge-BGO detector with high counting rate (300 kcps) characteristics and a pulse-height analyzer, and a spent fuel  $\gamma$ -ray measuring system made up of a computer for monitoring the automatic measurements and for analysis of the  $\gamma$ -ray spectra (software: AUGASS-SF [Automatic Gamma Spectrometry System for Spent Fuel]). For the analysis of  $\gamma$ -ray spectra, the BOB code was used which calculates radioactivity ratios ( $Bq/Bq$ ) by preparing relative detection efficiencies by the internal standard method. Scanning measurements of the spent fuel rod were carried out at intervals of 4–40 mm over the entire length of the fuel rod (stepwise measurement), and the ratio of radioactivity ( $Bq/Bq$ ) of various nuclides, e.g.,  $^{134}\text{Cs}$ ,  $^{106}\text{Ru}$ ,  $^{154}\text{Eu}$ ,  $^{125}\text{Sb}$ , and  $^{144}\text{Ce}$ , to  $^{137}\text{Cs}$  at respective measurement locations was determined. These results were used for evaluating the characteristics of radioactivity ratio profiles of spent

fuel rods, evaluating axial burnup profiles, and moreover evaluating the burnup and composition of spent fuel assemblies to be used for criticality calculation.

## (2) Radiochemical Analysis of Spent Fuel Samples

With the object of measuring the nuclide composition and burnup of light-water-reactor spent fuels, the elements of collected samples were separated by the anion exchange separation process;  $\alpha$ -ray and  $\gamma$ -ray spectra were measured; and analysis by mass spectrometry was carried out. Destructive analysis started in 1995 and a total of 34 samples were analyzed by 1999. These samples were cut out of spent fuel elements (NT3G23, NT3G24) from the Kansai Electric (Ltd.) Reactor No. 3, Takahama Nuclear Power Station, and from a fuel element (DN23) used in Tokyo Electric (Ltd.) Reactor No. 2, Fukushima No. 2 Nuclear Power Station.

The analysis target elements were U, Np, Pu, Am, Cm, and some FP elements starting with Nd. Furthermore, we thought that Sm elements are also important from the standpoint of evaluating criticality safety because they account for about 25% of the proportion of neutron absorption by all FP nuclides, and so we began the analysis of their compositions in 1997.

The results obtained by destructive analysis are summarized as the nuclide composition (number of atoms/initial heavy element) at the end of irradiation of the fuel for each sample together with the calculated results of the burnup rate (degree) by the Nd-148 method.

## (3) Exponential Experiments on Spent Fuel Assemblies

Exponential experiments were conducted on three PWR fuel assemblies and one BWR fuel assembly in the pool of the JAERI fuel examination facility, and the axial exponential decay constant  $\gamma$  was measured. This  $\gamma$  is a quantity that gives the criticality characteristics of a fuel assembly, and it can be used for the validation of criticality calculation codes through the reproducibility of the  $\gamma$  of analytical calculation. Furthermore, if the  $\gamma$  related to the fundamental mode is measured, the effective neutron multiplication factor  $k_{\text{eff}}$  of an infinite-length assembly having a configuration and a composition in the  $\gamma$  measurement region can be estimated by  $1 - 1/k_{\text{eff}} = -K\gamma^2$ . However, the buckling coefficient  $K$  of reactivity is difficult to measure in the subcritical state, so its calculated value must be used.

Experimental values of  $\gamma$  are values in a region where the burnup in the axial direction of an assembly is nearly constant. The value of  $\gamma$  differs with the radial size, initial enrichment, and burnup of an assembly. Moreover,  $\gamma$  increases from the top to the bottom in the BWR assembly, and this result is thought to be due to the difference in the accumulated amount of plutonium due to a void profile. These measured values of  $\gamma$  are compared with the results of criticality analysis calculation shown in Sect. 5.

### 1.3.2. Validation of Burnup Calculation Codes

The destructive test data obtained at the present special committee were analyzed to examine ORIGEN2 and SWAT.

In analyses using ORIGEN2, the incorporated library which has been used in the past and a library based on JENDL-3.2 were used. As a result, it was ascertained that the calculated values of U and Pu were better by analyses using the new library based on JENDL-3.2 than by analyses using the former incorporated library (PWR-UEPWR-U50) thought to be suitable for the analysis of PWR-UO<sub>2</sub> fuel destructive test data, and it was shown that the difference between the experimental values and calculated values is within 5%. In the case of BWR fuel also, the accuracy of analysis was similarly better with the library based on JENDL-3.2, and it was shown that the difference between the experimental values and calculated values is

within 10% with respect to the amounts of major U and Pu. However, it was shown that, with regard to Pu-238 and Cm-244, the calculated values are about 20% smaller than the experimental values when using the library based on JENDL-3.2.

Analyses using SWAT showed that the difference between the calculated values and experimental values is 5% in the PWR-UO<sub>2</sub> fuel, and 10% in the BWR-UO<sub>2</sub> fuel with regard to major U and Pu. Furthermore, the dispersion of the C/E for each sample was smaller than in analyses with ORIGEN2, and the dispersion of the ratios of the calculated values to the experimental values was 3% or less except for Pu-238. This is because calculation by SWAT can take the axial distribution of void ratios into consideration. The changes in the calculations with the fuel temperature history and the power history as parameters were small, and in particular the effect of the former was 2% at maximum. This fact indicates that the established values for the fuel temperature and power history used in the present analyses were appropriate.

### 1.3.3. Validation of the Criticality Calculation Codes

The criticality calculation codes were validated by analyzing the exponential experiments using the four spent fuel assemblies shown in Sect. 2.3. The fuel composition necessary for validating the criticality calculation codes was determined by combining the  $\gamma$ -ray scanning measurement results of Sect. 2.1, the nuclide composition analysis results of Sect. 2.2, and the burnup calculation results of Sect. 3. In the analysis, JENDL-3.2 was used as the nuclear data library; group constants were prepared by SRAC; and the diffusion calculations were done using CITATION. The calculated results agreed with the measured values of the exponential decay constant  $\gamma$  with differences within 3%, and the criticality calculation codes were found to have adequate accuracy.

### 1.3.4. Examination of the Burnup Estimation Methods

#### (1) Evaluation of the Axial Burnup Profiles of Spent Fuel Rods Based on Measured Data

The relationships between two radioactivity ratios, i.e.,  $^{134}\text{Cs}/^{137}\text{Cs}$  and  $(^{134}\text{Cs}/^{137}\text{Cs})^2/(^{106}\text{Ru}/^{137}\text{Cs})$ , and burnup were examined based on the measured data of FP radioactivity ratios and burnup obtained by the nondestructive  $\gamma$ -ray scanning measurement of PWR/BWR spent fuel rods and the destructive analysis of cut samples. As a result, it was found that the relationship between  $^{134}\text{Cs}/^{137}\text{Cs}$  and burnup is nearly linear, and is affected very little by the type of fuel (UO<sub>2</sub> fuel and UO<sub>2</sub>—Gd<sub>2</sub>O<sub>3</sub> fuel), but instead depends on the initial enrichment and irradiation cycle. On the other hand, the relationship between  $(^{134}\text{Cs}/^{137}\text{Cs})^2/(^{106}\text{Ru}/^{137}\text{Cs})$  and burnup is practically unaffected by the initial enrichment and irradiation cycle, and this ratio was found to have excellent properties as an FP radioactivity ratio for the evaluation of burnup. However, both radioactivity ratios depend on the neutron spectrum and are affected strongly by spectral changes due to differences in the void ratios, especially in BWR fuel. In the present evaluation, the relationship between the radioactivity ratio and burnup with consideration of the void ratio (fuel rod position) was determined, and a burnup evaluation method from only measured radioactivity ratios including  $^{154}\text{Eu}/^{137}\text{Cs}$  was also examined. Furthermore, the axial burnup profiles of both PWR and BWR spent fuel rods were evaluated by using burnup evaluation equations (empirical equations) for PWR/BWR that were constructed on the basis of experimental data.

#### (2) Effect of Irradiation Parameters on the Relationship Between Burnup and Radioactivity Ratio

Burnup calculation by SWAT was carried out for PWR and BWR, and the sensitivity of the relationships between burnup and three radioactivity ratios, i.e.,  $^{134}\text{Cs}/^{137}\text{Cs}$ ,  $^{154}\text{Eu}/^{137}\text{Cs}$ , and  $(^{134}\text{Cs}/^{137}\text{Cs})^2/(^{106}\text{Ru}/^{137}\text{Cs})$ , to parameters such as initial enrichment, power history, moderator boron concentration (PWR), and moderator void ratio (BWR), was examined.

### **1.3.5. Examination of the Safety Margin**

In Sect. 6, the safety margin for changes in burnup was compared and examined for models of spent fuel transport and middle storage casks which are close to those actually used, by comparing the criticality analysis results from the measured nuclide compositions obtained by the present special committee by destructive analysis of spent fuels actually irradiated in PWRs and BWRs, and the criticality analysis results from the calculated nuclide compositions obtained by the ORIGEN2.1 burnup calculation code which is usually used and the SWAT calculation code which enables detailed burnup analysis including changes in environmental conditions during irradiation. The source terms for shielding and heat analysis were evaluated by comparing and evaluating the changes in source strength calculated by ORIGEN2 with cooling time as a parameter, based on the neutron strengths determined from measured nuclide compositions immediately after cooling and the values of burnup calculated by ORIGEN2.1 or SWAT.

## **REFERENCES**

1. International Atomic Energy Agency, Overview on the Burnup Credit Activities at the IAEA, Proceedings of ICNC'99 held in Versailles, 20–24 September 1999, Vol. II, 576–585.
2. International Atomic Energy Agency, Implementation of Burnup Credit in Spent Fuel Management Systems, Proceedings of an Advisory Group Meeting held in Vienna, 20–24 October 1997, IAEA-TECDOC-1013 (1998).

TABLE 1-1. List of Names of Members of the Specialized Sectional Committee on Technical Development on Criticality Safety Management for Light-Water-Reactor Spent Fuels 1996–1999

KEY:

- (a) job name;
- (b) name;
- (c) member's workplace;
- (d) committee chairman;
- (e) member;
- (f) S. Daitani;
- (g) Professor, Research Reactor Institute, Kyoto University;
- (h) Tokyo Electric (Ltd.);
- (i) H. Anekawa;
- (j) Manager of the Reactor Core and Fuel Group, Atomic Power Technology Department (1998–1999);
- (k) T. Hattori;
- (l) Manager of the Atomic Power Technology Section, Atomic Power Generation Department (1996–1997);
- (m) H. Ikehata;
- (n) Manager of Materials Technology Development, Nuclear Development (Ltd.);
- (o) T. Iwasaki;
- (p) Research Associated, Faculty of Engineering, Tohoku University;
- (q) A. Ouchi;
- (r) Chief Research Fellow, No. 2 Research Department, Nihon Kakunenryo Kaihatsu (Ltd.);
- (s) Atomic Power Generation Technology Organization (foundation);
- (t) S. Uemura;
- (u) Manager of the Fuel Department (1998–1999);
- (v) T. Aoki;
- (w) same as above (1996-1997);
- (x) Gen-nen Yuso Co., Ltd.;
- (y) K. Onishi;
- (z) Manager of the Technology Department (1999);
- (A) Y. Kitagawa;
- (B) same as above (1997–1998);
- (C) M. Oyama;
- (D) Deputy Manager of the Assurance Measures Department, Nihon Gen-nen (Ltd.);

- (E) Kansai Electric (Ltd.);
- (F) T. Goto;
- (G) Manager of the Nuclear Fuel Technology Section, Atomic Power Thermal Power Headquarters (1997–1999);
- (H) I. Kokaji;
- (I) Deputy Manager of the Nuclear Fuel Department, Atomic Power Thermal Power Headquarters (1999);
- (J) Electric Industries Association;
- (K) T. Wakabayashi;
- (L) Deputy Manager of the Atomic Power Department (1999);
- (M) T. Sato;
- (N) same as above (1997-1998);
- (O) S. Tanuma;
- (P) same as above (1996);
- (Q) Nuclear Fuel Cycle Development Organization;
- (R) A. Kozue;
- (S) Technical Chief, Reprocessing Facility Safety Measures Group (working also as) Manager of the Technical Development Section, Reprocessing Center Technology Department, Tokai Works (1999);
- (T) T. Sugiyama;
- (U) Manager of the Reprocessing Plant Management Section (1996–1998);
- (V) T. Tanzawa;
- (W) Department Manager in Charge of Nuclear Reactor Technology, Toshiba Atomic Power Technology Institute (Ltd.);
- (X) T. Matsumura;
- (Y) Atomic Power Systems Department, Central Research Institute of the Electric Power Industry (foundation);
- (Z) Y. Yamane;
- (aa) Professor, Department of Engineering Research, Nagoya University;
- (bb) T. Yamamoto;
- (cc) Professor Emeritus, Osaka University; and
- (dd) 1999 members listed in Japanese alphabetical order.

(a) 職名	(b) 氏名	(c) 所 属
(d) 部会長	f伏 谷 誠治	<u>京都大学原子炉実験所 教授</u> (g)
(e) 委員		<u>東京電力(株)</u> (h)
//	(i) 鮎川 尚史	原子力技術部炉心・燃料グループマネージャー(10-11年度)(j)
//	(k) 眼部 年逸	原子力発電部原子力技術課長(8-9年度)(l)
//	(m) 池畠 久	<u>ニクライアント・オフィス(株)</u> 材料技術開発主任(n)
//	(o) 岩崎 智彦	<u>東北大学工学部 助手</u> (p)
//	(q) 大内淳弘	<u>日本核燃料開発(株)</u> 第2研究部主幹研究員(r) <u>(財) 原子力発電技術機構</u> (s)
//	(t) 上村勝一郎	燃料部 部長(10-11年度)(u)
//	(v) 齋木 利昌	同上 (8-9年度)(w) <u>原燃輸送株式会社</u> (x)
//	(y) 大西一成	技術部長(11年度)(z)
//	(A) 北河 潤	同上 (9-10年度)(B)
//	(C) 小山 真弘	<u>日本原燃(株)</u> 保障措置部副部長(D) <u>関西電力(株)</u> (E)
//	(F) 後藤 健	原子力火力本部原子燃料技術課長(9-11年度)(G)
//	(H) 小糸治市造	原子力火力本部原子燃料副部長(8年度)(I) <u>電気事業連合会</u> (J)
//	(K) 若林 利明	原子力部副部長(11年度)(L)
//	(M) 佐藤 敏秀	同上 (9-10年度)(N)
//	(O) 田沼 進	同上 (8年度)(P) <u>核燃料サイクル開発機構</u> (Q)
//	(R) 漢 彰	<u>東海事業所再処理施設安全対策班技術主幹(兼)再処理センター技術部技術開発課長</u> (11年度)(S)
//	(T) 杉山 俊英	再処理工場管理課長(8-10年度)(U)
//	(V) 丹沢 寛雄	<u>(株) 東芝原子力技術研究所原子炉技術担当部長</u> (W)
//	(X) 松村 哲夫	<u>(財) 電力中央研究所原子力システム部</u> (Y)
//	(Z) 仙根 義宏	<u>名古屋大学工学研究科 教授</u> (aa)
//	(bb) 仙本 忠史	<u>大阪大学 名誉教授</u> (cc)
		(dd)(以上11年度委員50名)

TABLE 1-1. List of Names of Members of the Specialized Sectional Committee on Technical Development  
on Criticality Safety Management for Light-Water-Reactor Spent Fuels (continued) 1996–1999

KEY:

- (a) job name;
- (b) name;
- (c) member's workplace;
- (d) member;
- (e) secretary;
- (f) Japan Atomic Energy Research Institute;
- (g) T. Muromura;
- (h) Head of the Department of Environmental Sciences (person in charge of the work in 1999);
- (i) H. Katsuta;
- (j) Head of the Department of Material Sciences (person in charge of the work in 1998);
- (k) M. Hoshi;
- (l) Head of the Department of Fuel Research (person in charge of the work in 1996–1997);
- (m) Y. Fujine;
- (n) Head of the Department of Fuel Cycle Safety Research (1998–1999);
- (o) M. Maeda;
- (p) Director of the Safety Test Research Center (working also as)  
Head of the Department of Fuel Cycle Safety Research (1997);
- (q) Y. Naito;
- (r) Head of the Department of Fuel Cycle Safety Research (1996);
- (s) H. Takano;
- (t) Vice-Director of the Neutron Science Research Center (1996–1998);
- (u) T. Adachi;
- (v) Deputy Head of the Department of Environmental Sciences;
- (w) T. Yamahara;
- (x) Head of the Hot Testing Technology Section, Hot Testing Laboratory (1996–1997);
- (y) H. Amano;
- (z) same as above (1998–1999);
- (A) K. Okumura;
- (B) Deputy Chief Research Fellow, Reactor Characteristics Research Laboratory,  
Department of Nuclear Energy Systems (1999);
- (C) H. Nanba;

- (D) Examining Official, Planning Department (1999);
- (E) M. Iwamura;
- (F) same as above (1998);
- (G) S. Dojiri;
- (H) same as above (1996–1997);
- (I) Y. Nomura;
- (J) Head and Deputy Head of the Fuel Cycle Safety Evaluation Laboratory,  
Department of Fuel Cycle Safety Research;
- (K) K. Watanabe;
- (L) Group Leader, Analytical Science Research Group, Department of Environmental Sciences (1999);
- (M) T. Suzuki;
- (N) Deputy Chief Research Fellow, Reactor Physics Research Group, Department  
of Nuclear Energy Systems;
- (O) Y. Nakahara;
- (P) Analytical Science Research Group, Department of Environmental Sciences;
- (Q) M. Kurosawa;
- (R) Reactor Physics Research Group, Department of Nuclear Energy Systems;
- (S) K. Suyama;
- (T) Fuel Cycle Safety Evaluation Laboratory, Department of Fuel Cycle Safety Research;
- (U) K. Ohmori;
- (V) Office Manager, Department of Environmental Sciences (1999);
- (W) M. Nakayama;
- (X) Office Manager, Department of Fuel Cycle Safety Research (1997–1999);
- (Y) S. Takemori;
- (Z) Office Manager, Department of Material Sciences (1998);
- (aa) I. Kurokawa;
- (bb) Office Manager, Department of Fuel Research (1998);
- (cc) K. Ouchi;
- (dd) Office Manager, Department of Fuel Research (1997);
- (ee) S. Idenuma; and
- (ff) Office Manager, Department of Fuel Cycle Safety Research (1997).

職名 (a)	氏名 (b)	所属 (c)
(d) 委員		日本原子力研究所 (f)
// (g) 室村忠純		環境科学研究部長(11年度:事業担当責任者)(h)
// (i) 勝田博司		物質科学研究部長(10年度:事業担当責任者)(j)
// (k) 星三千男		燃料研究部長(8-9年度:事業担当責任者)(l)
// (m) 藤根幸雄		燃料サイクル安全工学部長(10-11年度)(n)
// (o) 前田允		安全性試験研究センター長(兼)(p)
// (q) 内藤淑季		燃料サイクル安全工学部長(9年度)(r)
// (s) 高野秀機		中性子科学研究センター次長(8-10年度)(t)
// (u) 安達武雄		環境科学研究部次長(v)
// (w) 山原 武		ホット試験室ホット試験技術課長(8-9年度)(x)
// (y) 天野英俊		同上(z)(10-11年度)
// (A) 奥村啓介		エネルギーシステム研究部(B)
// (C) 南波秀樹		炉特性研究室 副主任研究員(11年度)
// (E) 岩村公道		企画室調査役(11年度)(D)
// (G) 土尻 滋		同上(10年度)(v)
// (I) 野村 靖		同上(8-9年度)(H)
// (K) 渡部和男		燃料サイクル安全工学部燃料サイクル(J)
// (M) 須崎武則		安全評価研究室長・次長
// (O) 中原嘉則		環境科学研究部分析科学研究グループリーダー(11年度)(L)
// (Q) 黒澤正義		エネルギーシステム研究部(N)
// (S) 須山賢也		炉物理研究グループ 副主任研究員
(e) 幹事	(t) 大森和之	環境科学研究部分析科学研究グループ(p)
// (W) 中山政廣		エネルギーシステム研究部 炉物理研究グループ(R)
// (Y) 竹森聰司		燃料サイクル安全工学部燃料サイクル安全評価研究室(T)
(aa) 黒川勇		環境科学研究部事務長(V)(11年度)
(cc) 大内克美		燃料サイクル安全工学部事務長(9-11年度)(X)
(ee) 出沼節男		物質科学研究部事務長(10年度)(Z)
		燃料研究部事務長(bb)(10年度)
		燃料研究部事務長(dd)(9年度)
		燃料サイクル安全工学部事務長(9年度)(ff)

TABLE 1-2. List of Names of Members of the Overall Evaluation Working Group on Technical Development on Criticality Safety Management for Light-Water-Reactor Spent Fuels

KEY:

- (a) job name;
- (b) name;
- (c) member's workplace;
- (d) leader;
- (e) member;
- (f) S. Daitani;
- (g) Professor, Research Reactor Institute, Kyoto University;
- (h) H. Anekawa;
- (i) Manager of the Reactor Core and Fuel Group, Atomic Power Technology Department, Tokyo Electric (Ltd.);
- (j) T. Iwasaki;
- (k) Research Associate, Faculty of Engineering, Tohoku University;
- (l) T. Tanzawa;
- (m) Department Manager In Charge of Nuclear Reactor Technology, Toshiba Atomic Power Technology Institute (Ltd.);
- (n) T. Matsumura;
- (o) Atomic Power Systems Department, Central Research Institute of the Electric Power Industry (foundation);
- (p) Y. Yamane;
- (q) Professor, Department of Engineering Research, Nagoya University;
- (r) T. Yamamoto;
- (s) Professor Emeritus, Osaka University;
- (t) listed in Japanese alphabetical order;
- (u) Y. Nomura;
- (v) Head and Deputy Head of the Fuel Cycle Safety Evaluation Laboratory, Department of Fuel Cycle Safety Research, Japan Atomic Energy Research Institute;
- (w) K. Watanabe;
- (x) Group Leader, Analytical Science Research Group, Department of Environmental Sciences;
- (y) T. Suzuki;

- (z) Deputy Chief Research Fellow, Reactor Physics Research Group, Department of Nuclear Energy Systems;
- (A) K. Okumura;
- (B) Deputy Chief Research Fellow, Reactor Characteristics Research Laboratory, Department of Nuclear Energy Systems;
- (C) Y. Nakahara;
- (D) Analytical Science Research Group, Department of Environmental Sciences;
- (E) M. Kurosawa;
- (F) Reactor Physics Research Group, Department of Nuclear Energy Systems;
- (G) K. Suyama; and
- (H) Fuel Cycle Safety Evaluation Laboratory, Department of Fuel Cycle Safety Research.

団名 (a)	氏名 (b)	所属 (c)
(d) リーダー(f) 代谷 誠治		京都大学原子炉実験所 教授(g)
(e) 委員(h) 姉川 尚史		東京電力(株) 原子力技術部炉心・燃料グループマネージャ(i)
// (j) 岩崎 智彦		東北大学工学部 助手(k)
// (l) 丹沢 富雄		(株) 東芝原子力技術研究所原子炉技術担当部長(m)
// (n) 松村 哲夫		(財) 電力中央研究所原子力システム部(o)
// (p) 山根 義宏		名古屋大学工学研究科 教授(q)
// (r) 山本 忠史		大阪大学名誉教授(s)
		(t) (以上50音)
// (u) 野村 靖		日本原子力研究所 燃料サイクル安全工学部燃料サイクル(v)
// (w) 渡部 和男		// 安全評価研究室長・次長(x) 環境科学研究部
// (y) 須崎 武則		// 分析科学研究グループリーダー エネルギーシステム研究部
// (A) 奥村 啓介		// エネルギーシステム研究部 (B) 炉特性研究室 副主任研究員
// (C) 中原 嘉則		// 環境科学研究部分析科学研究グループ(D)
// (E) 黒澤 正義		// エネルギーシステム研究部 (F) 炉物理研究グループ
// (G) 須山 賢也		// 燃料サイクル安全工学部 (H) 燃料サイクル安全評価研究室

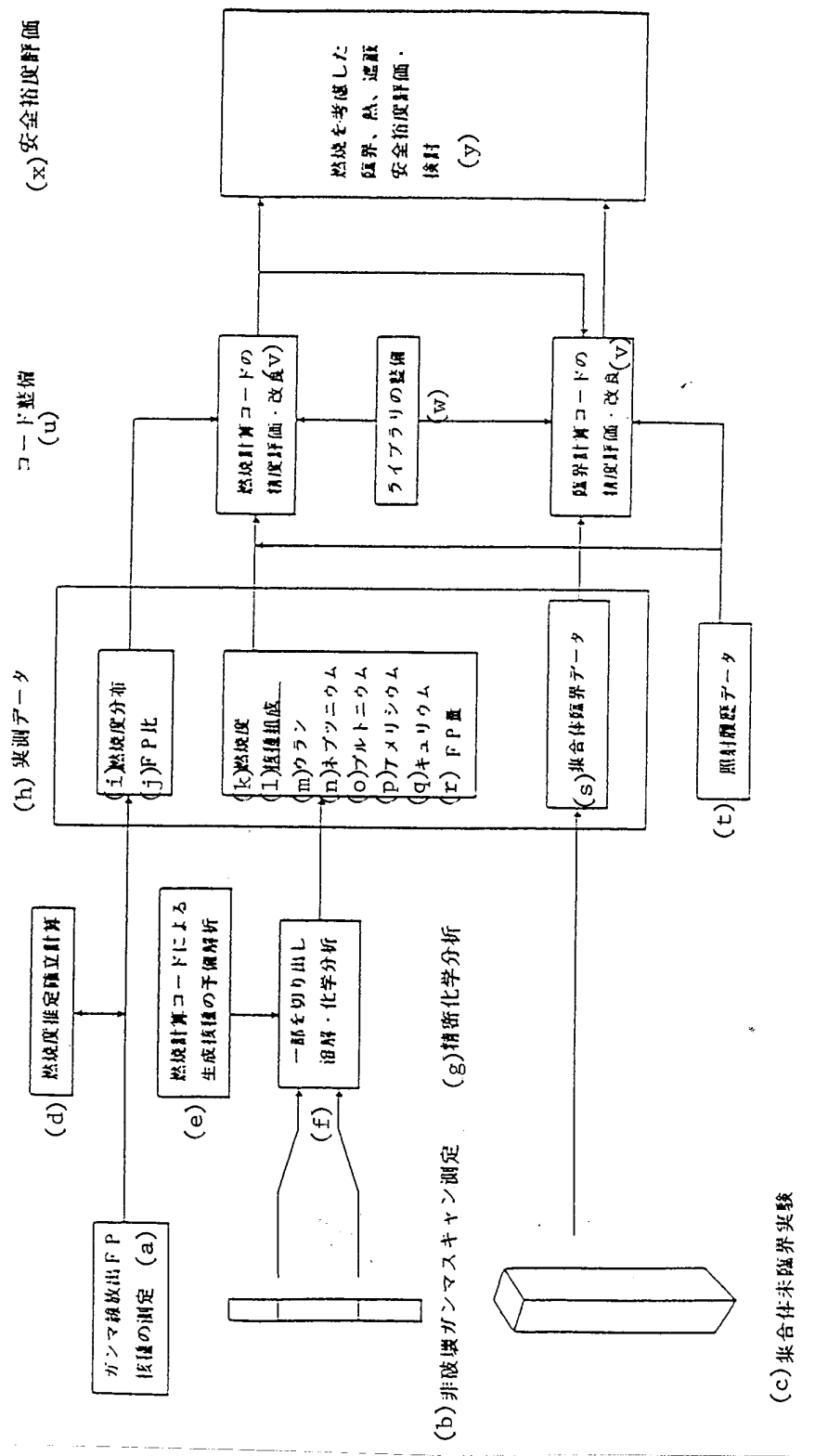


Figure 1-1. Outline of contents for carrying out technical development on criticality safety management for light-water-reactor spent fuels. KEY: (a) measurement of gamma-ray emitting FP nuclides; (b) nondestructive gamma scanning measurement; (c) preliminary experiments on assemblies for estimation and establishment of burnup; (e) preliminary analysis of formed nuclides by burnup calculation codes; (f) cutting of some sections, dissolution, and chemical analysis; (g) precision chemical analysis; (h) measured data; (i) burnup profile; (j) FP ratio; (k) burnup; (l) nuclide composition; (m) uranium; (n) neptunium; (o) plutonium; (p) americium; (q) curium; (r) FP quantity; (s) assembly criticality data; (t) irradiation history data; (u) code preparation; (v) evaluation and improvement of accuracy of burnup calculation codes; (w) preparation of library; (x) evaluation of safety margin; and (y) evaluation and examination of criticality, heat, and shielding safety margin with consideration of burnup.

Figure 1-2. Annual plans for technical development on criticality safety management for light-water-reactor spent fuels. KEY: (a) 1990; (b) 1991; (c) 1992; (d) 1993; (e) 1994; (f) 1995; (g) 1996; (h) 1997; (i) 1998; (j) 1999; (k) obtaining criticality data, preparation of experimental instruments, etc.; (l) subcritical experiments; (m) obtaining nuclide composition data, preparation of experimental instruments, etc.; (n) burnup measurements; (o) nondestructive  $\gamma$ -ray scanning measurements; (p) precision chemical analysis; (q) calculation code preparation and analysis; (r) technical examination and data collection; (s) holding a specialized sectional meeting; (t) overall evaluation; (u) . . . piece(s); (v) (for analysis); and (w) . . . samples.

## 2. EXPERIMENTS

### 2.1. Gamma-Ray Scanning Measurements of Spent Fuel Rods

#### 2.1.1. General

At the JAERI fuel examination facility, axial  $\gamma$ -ray scanning measurements were made of PWR spent fuel rods (18 rods: 2 assemblies) and BWR spent fuel rods (13 rods: one assembly). The measurements were made with measuring instruments such as a Ge-BGO detector with high counting rate (300 kcps) characteristics and a pulse-height analyzer, and a spent fuel  $\gamma$ -ray measurement system made up of a computer (analytical section) for monitoring the automatic measurements and the analysis of the  $\gamma$ -ray spectra. The analysis of  $\gamma$ -ray spectra used BOB code that calculates the radioactivity ratio (Bq/Bq) by establishing the relative detection efficiency by the internal standard method. The scanning measurements of spent fuel rods were carried out at intervals of 4–40 mm over the entire length of the fuel rod (stepwise measurement), and the radioactivity ratio (Bq/Bq) of various nuclides, e.g.,  $^{134}\text{Cs}$ ,  $^{106}\text{Ru}$ ,  $^{154}\text{Eu}$ ,  $^{125}\text{Sb}$ , and  $^{144}\text{Ce}$ , to  $^{137}\text{Cs}$  was determined at respective measurement locations. These results were used to evaluate the characteristics of the radioactivity ratio profiles of spent fuel rods, to evaluate the axial burnup profiles, and, moreover, to evaluate the burnup and composition of spent fuel assemblies to be used for criticality calculation.

#### 2.1.2. Gamma-Ray Measurement System for Spent Fuels

##### (1) System Configuration

Figure 2.1.1 shows the hardware configuration of the system. The measuring section consists of a Ge detector, a Compton suppression device using a BGO ( $\text{Bi}_4\text{Ge}_3\text{O}_{12}$ ) detector, amplifiers, a simultaneous counting circuit, and a pulse-height analyzer. Furthermore, the analytical section consists of a computer (DEC 3000, model 300) for carrying out scanning measurement control, data collection, and spectral analysis, and its related peripheral devices. The measuring section is installed in the service area at the rear of the  $\beta\gamma$  No. 1 cell at the JAERI fuel examination facility, and the analytical section is installed in an operations room at the front of the cell; both are connected to the existing  $\gamma$ -ray scanning system (fuel rod driving system); and the axial profiles of the radioactivity ratios of a spent fuel rod are measured automatically according to a predetermined sequence.

##### (2) Functions of the System

(1) A special feature of the measuring section is that it can make measurements at high counting rates (about 300 kcps) with the use of a preamplifier and a main amplifier. Also, the Compton portion of a spectrum can be decreased to about 1/8 by Compton suppression with the BGO detector. These measures reduce spectral analysis error.

(2) The analytical section carries out the measurements of  $\gamma$ -ray spectra, the collection of spectral data, and the analysis of the spectra by an automatic  $\gamma$ -ray spectrometry system for spent fuels (AUGASS-SF, Automatic Gamma Spectrometry System for Spent Fuel),<sup>1,2</sup> by moving the fuel rod stepwise (in 4- or 8-mm steps) in response to a signal from the fuel rod driving system. In this way, analytical results are obtained for the radioactivity ratio (Bq/Bq, e.g.,  $^{134}\text{Cs}/^{137}\text{Cs}$ ) of a  $\gamma$ -ray emitting nuclide at every measurement point of the approximately 1,000 points per fuel rod length (which is about 4 m).

The nuclides that can be measured and analyzed by this measurement system are  $^{54}\text{Mn}$ ,  $^{60}\text{Co}$ ,  $^{95}\text{Zr}$ ,  $^{95}\text{Nb}$ ,  $^{106}\text{Ru}$ ,  $^{106}\text{Rh}$ ,  $^{125}\text{Sb}$ ,  $^{134}\text{Cs}$ ,  $^{137}\text{Cs}$ ,  $^{144}\text{Ce}$ ,  $^{154}\text{Eu}$ ,  $^{160}\text{Tb}$ , and  $^{110\text{m}}\text{Ag}$ . Table 2.1.1 shows the decay data for these  $\gamma$ -ray emitters included in the AUGASS-SF.

### (3) The BOB spectral analysis code

The BOB<sup>3</sup> analysis code was used for  $\gamma$ -ray spectral analysis. This code calculates the area (counts) of each photoelectric peak and the peak position (channel) with respect to the measured spectra and plots an energy calibration curve and a detection efficiency curve. In the present  $\gamma$ -ray scanning measurement, the internal standard method based on FP nuclides emitted from the fuel being measured was employed for both energy calibration and counting efficiency (relative). Table 2.1.2 shows the decay data for the 4 FP nuclides used in the internal standard method.

### (4) Preparation of the relative detection efficiency curve based on the internal standard method

The detection efficiency by the internal standard method was calculated by the following procedure:

- (a) First, the initial radioactivity strength values for the 4 nuclides shown in Table 2.1.2 are given. For all the nuclides, these same values were used.
- (b) The relative detection efficiency by energy of each nuclide is calculated from the initial radioactivity strength value and the counts by energy of each nuclide (area of each peak divided by its emission probability).
- (c) A relative detection efficiency curve is plotted by fitting the above-mentioned detection efficiencies versus the  $\gamma$ -ray energy values of the respective nuclides using a 4th degree polynomial on a logarithm versus logarithm scale by the method of least squares.
- (d) The relative radioactivity strength of each nuclide is then calculated by using the efficiency curve obtained.
- (e) The initial value of (b) is replaced by the relative radioactivity strength obtained by (d), then (b)-(d) are repeated.

Figure 2.1.2 shows the changes in the relative detection efficiency curve in the process (A → E) of the above-mentioned successive approximation. A converged result can be obtained by 5 iterations, but a 10-iteration scheme was used for the present measurements. This internal standard method is performed for each measured spectrum, and the radioactivity ratio can then be obtained for that particular spectrum. Accordingly, the radioactivity ratio by spectrum (measurement point or measurement sample) can be calculated as long as the object nuclides are present uniformly in the radial direction in the fuel, or this can at least be assumed, even if the form and weight of a spent fuel differ within the field of vision during spectrum measurement.

### (3) Measurement Geometry and Collimator Visual Field

Figure 2.1.3 shows the geometry of a fuel rod, the collimators, and the measurement system involved in the  $\gamma$ -ray scanning measurements, and Fig. 2.1.4 shows the arrangement and visual field of the collimators. The  $\gamma$ -rays from the spent fuel rod being measured in the  $\beta\gamma$  No. 1 cell of the JAERI fuel examination facility reach the Ge detector behind the cell through 3 stages of collimators placed in shielding concrete behind the cell. A second collimator (4 mm × 18 mm × 512 mm) located between a front lead collimator (18 mm  $\phi$  × 375 mm) and a lead collimator (18 mm  $\phi$  × 200 mm) just before the detector is an effective collimator

(Fig. 2.1.4). The distance from the fuel rod to the detector is 1.64 m. The height of the second collimator located in nearly the middle is 4 mm (main visual field), but  $\gamma$ -rays corresponding to a height of 12 mm enter the detector if obliquely incident rays are included. Furthermore, the total visual field in the width direction is 18 mm or more, and a fuel 10-mm thick enters the visual field. Of the  $\gamma$ -rays emitted from within this range, those which have never undergone scattering while traveling from the fuel rod to the detector form photoelectric peaks. Accordingly, the spreads of  $\gamma$ -ray profiles other than these become Compton lines that do not form  $\gamma$ -ray peaks.

### 2.1.3. Measurement

The spectra were measured by moving the fuel rod at 4-mm or 8-mm intervals and scanning for 200–2,750 seconds (real time) at each measurement point. Furthermore, the gain in the measurement was given by the channel number = gamma-ray energy (keV).

Tables 2.1.3 and 2.1.4 show the element name of the PWR and BWR spent fuel rods used in the nondestructive measurements, the date of measurement, the average burnup of the fuel rod, the number of points measured, and the measurement time per point (real time). Figures 2.1.5 and 2.1.6 show examples of measurement positions in the PWR and BWR fuel rods. Furthermore, the measurement start point is the grip edge part, because a portion of the fuel rod is taken in the grip for clamping the fuel rod. In PWR fuel rods, the grip edge is located at 20–25 mm from the top of the fuel rod. In BWR fuel rods, the grip edge is at -10 mm from the top of the fuel rod, because a 10-mm adapter is attached. Furthermore, two of the rods (2F2DN23-01,02) from the BWR fuel rods have been cut off at several points for other PIE tests, and are thus missing some portions. To deal with this, the remaining fuel rod pieces were placed in an aluminum case in the present  $\gamma$ -ray scanning measurement process and then measured. Figures 2.1.7 and 2.1.8 show the measured locations on the fuel rod, and the arrangement of rod pieces in the Al case.

### 2.1.4. Results and the Corresponding Errors

#### (1) Results (Radioactivity Ratio)

Figure 2.1.9 shows an example of a  $\gamma$ -ray spectrum profile and the peak identification results. Figures 2.1.10–2.1.40 show axial profiles of the activity ratios of  $^{134}\text{Cs}$ ,  $^{144}\text{Ce}$ ,  $^{152}\text{Eu}$ , and  $^{106}\text{Ru}$  to  $^{137}\text{Cs}$  for various fuel rods. Here, the value of each activity ratio is exactly the result of analysis of the  $\gamma$ -ray spectra obtained, and the effect on the activity ratio of migration in the pellet radial direction of cesium and the emission of gases such as xenon are not taken into consideration.

Of the measured radioactivity ratios of the above-mentioned 4 nuclides and the  $^{125}\text{Sb}$  to  $^{137}\text{Cs}$  of each fuel rod, the radioactivity ratio data for these nuclides at about 20 points extracted over the entire length of the fuel rod are shown in Tables 2.1.5–2.1.35. For some fuel rods, the data on  $^{144}\text{Ce}$  with a short half life and  $^{125}\text{Sb}$  with a small fission yield were omitted in the tables because of large analysis errors.

Furthermore, all axial profile data of the radioactivity ratios were normalized at the end of irradiation. Therefore, no correction was made for the decay in the reactor during the reactor operation.

#### (2) Radioactivity Ratio Error

The  $\gamma$ -ray spectral data obtained at each measurement point were analyzed by BOB code, and peak counts corresponding to the  $\gamma$ -ray energy and its related error were obtained. This error includes a statistical error in peak counts and a fitting error. The nuclides of the measured peaks were then identified on the basis of the decay data for the 4 nuclides, i.e.,  $^{134}\text{Cs}$ ,  $^{144}\text{Ce}$ ,  $^{152}\text{Eu}$ , and  $^{106}\text{Ru}$ , given in Table 2.1.2, then a relative efficiency curve and its related error were determined from the identified peaks. By using this relative

efficiency curve, the quantity of radioactivity by the energy of each peak was calculated, and all FP nuclides were identified on the basis of the decay data in Table 2.1.1. The error for each peak involved was calculated by the following equation:

$$(\sigma_3)_{\text{Relative}} = \sqrt{(\sigma_1)_{\text{Relative}}^2 + (\sigma_2)_{\text{Relative}}^2} \quad (2.1.1)$$

$(\sigma_1)_{\text{Relative}}$ : relative value of statistical error in peak counts and fitting error (%)

$(\sigma_2)_{\text{Relative}}$ : relative value of error in relative detection efficiency (%)

$(\sigma_3)_{\text{Relative}}$ : relative value of error in the radioactivity of each peak (%)

With regard to  $^{137}\text{Cs}$  with one peak, this error was given as the error in radioactivity of the nuclide. Emission rate errors were not taken into consideration for any of the peaks.

With regard to nuclides with more than one peak, the radioactivity obtained by dividing the peak counts by the emission rate was averaged by weighting over all peaks belonging to the nuclide under consideration, and statistical processing, which discards peaks with more than 3 times the dispersion of the mean value, was performed, and the final relative radioactivity of the nuclide was calculated. The error for each nuclide associated with weighted averaging was calculated by the following equation:

$$\sigma_4 = \sqrt{\frac{\sum_{i=1}^n (x_i - \bar{x})w_i}{(n-1) \sum_{i=1}^n w_i}} \quad (2.1.2)$$

$x_i$ : radioactivity of the  $i$ -th peak

$\bar{x}$ : weighted mean of all peaks picked up

$w_i$ : weight ( $1/\sigma_i^2$ )

$\sigma_i$ : error for the  $i$ -th peak

$n$ : number of peaks picked up

$\sigma_4$ : error in radioactivity for each nuclide

The error in the ratio of the radioactivity of each nuclide thus calculated to the radioactivity of  $^{137}\text{Cs}$  was calculated by the following equation:

$$(\sigma_5)_{\text{Relative}} = \sqrt{(\sigma_4)_{\text{Relative}}^2 + (\sigma_{^{137}\text{Cs}})_{\text{Relative}}^2} \quad (2.1.3)$$

$(\sigma_4)_{\text{Relative}}$ : relative value of error for nuclide  $i$  (%)

$(\sigma_{^{137}\text{Cs}})_{\text{Relative}}$ : relative value of error for  $^{137}\text{Cs}$  (%)

$(\sigma_5)_{\text{Relative}}$ : relative value of error for the (nuclide  $i$ )/( $^{137}\text{Cs}$ ) radioactivity ratio

Table 2.1.36 shows examples of the various error components from  $(\sigma_1)_{\text{Relative}}$  to  $(\sigma_5)_{\text{Relative}}$  in Eqs. (2.1.2)–(2.1.3).

### (3) Comparison of Destructive Analysis Results and Nondestructive Analysis Results

5-10 samples consisting of about 0.5 mm slices were collected from each fuel rod, namely, NT3G23-04, 10, NT3G24-07, and 2F2DN23-01, 02, and subjected to precision chemical analysis. Tables 2.1.37 and 2.1.38 [sic; should be "Tables 2.1.38 and 2.1.39" -- Tr. Ed.] show a comparison of the activity ratios determined from the quantity of FP (absolute quantity of each nuclide determined by determining the efficiency with a standard source) in a sample dissolved in nitric acid, and the activity ratio obtained by  $\gamma$ -ray scanning measurement for NT3G23-04 and NT3G24-10. Here,  $^{106}\text{Ru}$  did not dissolve and was left as a major component of the insoluble residue, and  $^{125}\text{Sb}$  was adsorbed on this insoluble residue and on the dissolving flask, and about 10% stayed in the covering tube; so these were excluded from the comparison.

Furthermore, the  $\gamma$ -ray scanning position (measurement position) is not always the same as the sampling position for destructive analysis; thus,  $\gamma$ -ray scanning data at measurement positions closest to the sampling positions for destructive analysis were used.

$^{134}\text{Cs}/^{137}\text{Cs}$ ,  $^{154}\text{Eu}/^{137}\text{Cs}$ , and  $^{144}\text{Ce}/^{137}\text{Cs}$  by destructive analysis and by nondestructive analysis are in agreement within the margin of error at most points, but the destructive analysis values of  $^{134}\text{Cs}/^{137}\text{Cs}$ ,  $^{154}\text{Eu}/^{137}\text{Cs}$  for NT3G23-04 are 7–8% larger in No. 03 (201 mm). This seems to be due to the difference between the nondestructive measurement position and the sampling position for destructive analysis, the former being shifted about 8 mm to the top side with respect to the latter, and being an area with a large slope of burnup distribution.

#### 2.1.5. Axial Distribution Characteristics of FP Activity Ratios

##### (1) $^{134}\text{Cs}/^{137}\text{Cs}$

$^{137}\text{Cs}$  and  $^{133}\text{Cs}$  do not differ much in fission yield, as shown in Table 2.1.39 [sic; "Table 2.1.37" -- Tr. Ed.]. Because of this, the formed amount of these nuclides is proportional to the neutral fluence (burnup). Accordingly, the ratio of formed  $^{134}\text{Cs}$  (proportional to the square of the neutron fluence) by the neutron capture of  $^{133}\text{Cs}$  to  $^{137}\text{Cs}$ , i.e.,  $^{134}\text{Cs}/^{137}\text{Cs}$ , exhibits a linear relationship to the burnup in PWR fuels. However, this relationship is affected by the initial enrichment and the power history, so corrections have to be made for these parameters.

In BWR fuel rods, this ratio has a large value on the upper side with a higher void ratio and a lower burnup (left-hand side in the figure), as shown in Fig. 2.1.40. Furthermore, a small step can be seen at the boundary with the natural uranium region where the initial enrichment changes, as shown in Fig. 2.1.38.

Furthermore,  $^{134}\text{Cs}/^{137}\text{Cs}$  increases near the boundary between the pellet and plenum in both the PWR and BWR fuel rods, as shown in Figs. 2.1.10 and 2.1.30. The reason for this may be as follows. Whereas the half life of the precursor nuclide  $^{137}\text{Xe}$  of  $^{137}\text{Cs}$  is 3.82 minutes, the half life of the precursor nuclide  $^{133}\text{Xe}$  of the nuclide  $^{133}\text{Cs}$ , which becomes the source of  $^{134}\text{Cs}$ , is long, i.e., 5.25 days, and because of this, its diffusion takes place more easily. Hence, the ratio increases in the plenum where xenon gas diffuses more easily. In the AUGASS-SF analysis results, this increase in  $^{134}\text{Cs}/^{137}\text{Cs}$  has appeared at both ends (particularly the upper end) of the fuel rod, but it can usually be disregarded. In this case, there is no proportionality of  $^{134}\text{Cs}/^{137}\text{Cs}$  to burnup, and thus attention must be paid to the measured values at both ends.

## (2) $^{154}\text{Eu}/^{137}\text{Cs}$

$^{154}\text{Eu}$  is formed by neutron capture from  $^{153}\text{Eu}$ . The fission yield of these nuclides by the fission of the prior nuclide plutonium can be more than twice that by  $^{235}\text{U-T}$  (fission yield by the fission of  $^{235}\text{U}$  by thermal neutrons), as shown in Table 2.1.36 [sic; "Table 2.1.37" -- Tr. Ed.]. Since  $^{154}\text{Eu}$  is proportional to the square of neutron fluence in much the same way as  $^{134}\text{Cs}$ , it can be imagined that  $^{154}\text{Eu}/^{137}\text{Cs}$  may be proportional to burnup. However,  $^{154}\text{Eu}$  has a large neutron capture area, and its outflow due to the  $(n, \gamma)$  reaction during burning is large; thus, there are more problems with this nuclide than with  $^{134}\text{Cs}$ .

As shown in Fig. 2.1.18, the profile of  $^{154}\text{Eu}/^{137}\text{Cs}$  in the PWR fuel has projections without the indentations in the grid parts as seen in  $^{134}\text{Cs}/^{137}\text{Cs}$ . This seems to be related to the large capture area of  $^{154}\text{Eu}$  in the thermal region. In short, in the grid parts, burnup is lower (thermal neutron flux decreases) and  $^{137}\text{Cs}$  has lower values, but  $^{154}\text{Eu}$  has relatively higher values because the outflow due to  $(n, \gamma)$  reaction during burning is controlled (thermal neutron flux decreases).

In the BWR fuel, the profile of  $^{154}\text{Eu}/^{137}\text{Cs}$  has larger values in the upper part of the fuel rod with higher void ratios in much the same way as the profile of  $^{134}\text{Cs}/^{137}\text{Cs}$ , but the changes are greater over the entire fuel rod, as shown in Fig. 2.1.32. This can also be explained by the relationship between thermal neutron flux and the capture reaction of  $^{154}\text{Eu}$ . In other words, the thermal neutron flux is relatively higher (the value of  $^{137}\text{Cs}$  is also higher) in the part (lower part) with higher burnups of the BWR fuel than in the upper part, and on the other hand, the capture reaction of  $^{154}\text{Eu}$  progresses further in this part. Therefore, the  $^{154}\text{Eu}/^{137}\text{Cs}$  ratio is thought to decrease.

## (3) $^{106}\text{Ru}/^{137}\text{Cs}$

This fission yield of  $^{106}\text{Ru}$  to plutonium is more than 10 times larger than that to  $^{235}\text{U-T}$  (Table 2.1.36) [sic; "Table 2.1.37" -- Tr. Ed.]. The  $^{106}\text{Ru}/^{137}\text{Cs}$  ratio increases in proportion to burnup in much the same way as  $^{134}\text{Cs}/^{137}\text{Cs}$ , and shows a convex profile, which is because the proportion of burning of plutonium increases as the burnup increases. In the BWR fuel, a large step can be seen in the radioactivity ratio in the natural uranium regions at both ends, as shown in Fig. 2.1.32. In a fuel with low enrichment, the burning of plutonium increases relatively, and  $^{106}\text{Ru}/^{137}\text{Cs}$  also increases. This is thought to affect the evaluation of the burnup of fuels with different enrichments. In Gd-containing fuel, the radioactivity ratio is higher, in spite of lower burnup than in uranium fuel, as shown in Figs. 2.1.16–2.1.18. This is because the burning of plutonium is more extensive.

## (4) $^{144}\text{Ce}/^{137}\text{Cs}$

$^{144}\text{Ce}$  forms by fission in much the same way as  $^{137}\text{Cs}$ ; thus, if there are no major changes in fission yield, their ratio should be approximately 1 and the profile of the radioactivity ratio should be one horizontal line. However,  $^{144}\text{Ce}$  shows the largest fission yield to  $^{235}\text{U-T}$ , and smaller fission yield values, i.e., roughly 0.7, to those other than  $^{235}\text{U-t}$  (Table 2.1.36) [sic; "Table 2.1.37" -- Tr. Ed.]. It can be seen that  $^{144}\text{Ce}/^{137}\text{Cs}$  is slightly concave-shaped at high burnup at the center of the fuel rod, as shown in Figs. 2.1.17 and 2.1.32.

This indicates that the contribution of plutonium burning is larger at higher burnup. In the PWR fuel, this concavity is more pronounced. In Gd-containing fuel, the concavity is larger and the flat part lower than in uranium fuel, as shown in Figs. 2.1.16 and 2.1.31, which indicates that the contribution of plutonium burning is greater.

## (5) $^{125}\text{Sb}/^{137}\text{Cs}$

The measured value of  $^{125}\text{Sb}$  includes about 10% of the contribution from the Sn of the covering tube. The  $^{125}\text{Sb}$  of the FP existing in a little over 80% shows a large fission yield to plutonium, though not to the extent of  $^{106}\text{Ru}$ . The profile is an approximately horizontal line and flat, but is slightly lower in uranium fuel and slightly higher in Gd-containing fuel. Furthermore, in the BWR fuel, large steps can be seen in the radioactivity ratio in the natural uranium regions at both ends, as seen in  $^{106}\text{Ru}/^{137}\text{Cs}$ . In a fuel with lower enrichment, plutonium burning increases relatively, and  $^{125}\text{Sb}/^{137}\text{Cs}$  also increases. This also is thought to affect the evaluation of the burnup of fuels with different enrichments.

## REFERENCES

1. T. Suzuki, M. Magara, and H. Okashita, Abstracts of Papers, 1987 Meeting of the Atomic Energy Society of Japan, 1986; Abstract F16.
2. T. Suzuki, M. Magara, and H. Okashita, Proceedings of the 8th Annual Meeting on Nuclear Materials Management, 1987; Presentation 20.
3. Hiroshi BABA, Toshiaki SEKINE, Sumiko BABA, Hiroshi OKASHITA, JAERI 1227 (1973).
4. B. F. Rider NEDO-1215 (C), ENDF-322 (1981).
5. A. S. Chesterman and P. A. Clark, Spent Fuel and Residue Measurement Instrumentation at the Shellafield Nuclear Fuel Reprocessing Facility, BNFL Instruments Ltd., Pelham House, Calderbridge, Seascale, Cumbria, CA20 1PG, UK, Oct. (1995).

Table 2.1.1. Decay data of fission products  $\gamma$ -emitters in spent fuel

(Decay data of fission products in AUGASS-SF)

Nuclide	Half life	E $\gamma$ , keV	P $\gamma$	Nuclide	Half life	E $\gamma$ , keV	P $\gamma$		
Cs-137	30.07	y	661.66	0.8521	Ru-106	373.59	d	1988.44	0.000264
					Ru-106	373.59	d	2112.54	0.000348
Cs-134	2.0648	y	475.36	0.01520	Ru-106	373.59	d	2366.04	0.000235
Cs-134	2.0648	y	563.27	0.08360	Ru-106	373.59	d	2405.96	0.000146
Cs-134	2.0648	y	569.30	0.15400					
Cs-134	2.0648	y	604.68	0.97630	Sb-125	2.7582	y	176.33	0.06750
Cs-134	2.0648	y	795.78	0.85500	Sb-125	2.7582	y	380.44	0.01504
Cs-134	2.0648	y	801.86	0.08670	Sb-125	2.7582	y	427.90	0.29600
Cs-134	2.0648	y	1038.53	0.00987	Sb-125	2.7582	y	463.38	0.10420
Cs-134	2.0648	y	1167.89	0.01788	Sb-125	2.7582	y	600.56	0.17610
Cs-134	2.0648	y	1365.17	0.03005	Sb-125	2.7582	y	606.64	0.05020
					Sb-125	2.7582	y	635.90	0.11230
Eu-154	8.593	y	123.14	0.41000	Sb-125	2.7582	y	671.41	0.01788
Eu-154	8.593	y	248.04	0.06950					
Eu-154	8.593	y	591.75	0.05000	Co-60	5.2714	y	1173.24	0.99890
Eu-154	8.593	y	692.42	0.01810	Co-60	5.2714	y	1332.50	0.99982
Eu-154	8.593	y	723.30	0.20280					
Eu-154	8.593	y	756.88	0.04600	Ag-110m	249.79	d	446.81	0.03720
Eu-154	8.593	y	815.57	0.00528	Ag-110m	249.79	d	620.36	0.02802
Eu-154	8.593	y	845.41	0.00589	Ag-110m	249.79	d	657.76	0.94510
Eu-154	8.593	y	873.21	0.12270	Ag-110m	249.79	d	677.62	0.10480
Eu-154	8.593	y	892.75	0.00523	Ag-110m	249.79	d	687.02	0.06430
Eu-154	8.593	y	904.07	0.00915	Ag-110m	249.79	d	706.68	0.16660
Eu-154	8.593	y	996.35	0.10500	Ag-110m	249.79	d	744.28	0.04730
Eu-154	8.593	y	1004.79	0.18170	Ag-110m	249.79	d	763.94	0.22290
Eu-154	8.593	y	1246.63	0.00870	Ag-110m	249.79	d	818.03	0.07330
Eu-154	8.593	y	1274.42	0.34900	Ag-110m	249.79	d	884.69	0.72700
Eu-154	8.593	y	1596.52	0.01820	Ag-110m	249.79	d	937.49	0.34380
					Ag-110m	249.79	d	1384.30	0.24340
Ce-144	284.983	d	133.52	0.11100	Ag-110m	249.79	d	1475.79	0.03990
Ce-144	284.983	d	696.51	0.01342	Ag-110m	249.79	d	1505.04	0.13050
Ce-144	284.983	d	1489.16	0.00278	Ag-110m	249.79	d	1562.30	0.01027
Ce-144	284.983	d	2185.66	0.00694					
					Zr-95	64.02	d	724.20	0.44150
Ru-106	373.59	d	511.86	0.20600	Zr-95	64.02	d	756.73	0.54510
Ru-106	373.59	d	616.22	0.00762	Zr-95	64.02	d	765.80	2.20000
Ru-106	373.59	d	621.93	0.10030					
Ru-106	373.59	d	873.49	0.00443	Tb-160	72.3	d	298.58	0.26640
Ru-106	373.59	d	1050.41	0.01574	Tb-160	72.3	d	879.38	0.30350
Ru-106	373.59	d	1062.14	0.000323	Tb-160	72.3	d	962.32	0.09720
Ru-106	373.59	d	1128.07	0.00408	Tb-160	72.3	d	966.17	0.25060
Ru-106	373.59	d	1194.54	0.000579	Tb-160	72.3	d	1177.95	0.14970
Ru-106	373.59	d	1496.33	0.000225	Tb-160	72.3	d	1199.89	0.02379
Ru-106	373.59	d	1562.25	0.00165	Tb-160	72.3	d	1271.88	0.07505
Ru-106	373.59	d	1766.25	0.000346	Tb-160	72.3	d	1312.12	0.02838
Ru-106	373.59	d	1796.94	0.000280					
Ru-106	373.59	d	1988.44	0.000264	Mn-54	312.3	d	834.84	0.9975

E  $\gamma$ : Gamma-ray Energy (keV), P  $\gamma$ : Gamma-ray Emission Probability ( $\gamma$ /Disintegration)

Table 2.1.2. Decay data for internal standard method

Nuclide	Half life	$\gamma$ -ray energy (keV)	Emission probability (%)
Cs-134	2.065 y	569.30	15.40
		604.68	97.63
		795.78	85.50
		1167.89	1.788
		1365.17	3.005
Eu-154	8.593 y	123.14	41.00
		723.31	20.28
		996.35	10.50
		1004.79	18.17
		1274.42	34.90
Ce-144	284.89 d	133.52	11.10
		696.51	1.342
		1489.16	0.278
		2185.66	0.694
Ru-106	373.59 d	511.86	20.60
		621.93	10.03
		1050.41	1.574

Table 2.1.3. PWR spent fuel rods used in  $\gamma$ -scanning measurement

No.	Rod name	Date ID	Meas. date	End of irrad.	Burnup (MWd/t)	Numbers of meas.	Meas. time of each point (Real time/sec.)
1	NT3G23-C3	KD01	1996/07/16	1992/06/19	32900	193	400
2	NT3G23-A4	KC03	1995/10/27	1992/06/19	33500	94	200
3	NT3G23-C5	KD02	1996/07/17	1992/06/19	31600	192	250
4	NT3G23-A6	KD03	1996/07/18	1992/06/19	31000	192	250
5	NT3G23-C7	KD05	1996/07/22	1992/06/19	33200	192	700
6	NT3G23-A8	KD06	1996/07/24	1992/06/19	34200	192	750
7	NT3G23-B10	Gd	KC04	1995/10/30	1992/06/19	26400	95
8	NT3G23-D11	Gd	KD04	1996/07/19	1992/06/19	24700	192
9	NT3G23-B12	Gd	KD07	1996/07/26	1992/06/19	24500	192
1	NT3G24-C3	KH11	1998/09/21	1993/09/30	40900	266	190
2	NT3G24-A4	KH06	1998/09/07	1993/09/30	43800	266	475
3	NT3G24-C5	KH09	1998/09/16	1993/09/30	39100	266	475
4	NT3G24-A6	KH07	1998/09/09	1993/09/30	41700	266	475
5	NT3G24-C7	KF02	1997/04/18	1993/09/30	44300	263	820
6	NT3G24-A8	KH12	1998/09/22	1993/09/30	43300	266	825
7	NT3G24-B10	Gd	KH08	1998/09/11	1993/09/30	36300	266
8	NT3G24-D11	Gd	KH10	1998/09/18	1993/09/30	34300	266
9	NT3G24-B12	Gd	KH05	1998/09/04	1993/09/30	34500	266

Table 2.1.4. BWR spent fuel rods used in  $\gamma$ -scanning measurement

No.	Rod name	Position	Data ID	Meas. date	End of irradi.	Burnup (MWdt)	Numbers of meas.	Meas. time of each point (Real time/sec.)
1	2F2DN23-01-1	b2	KG01	1997/11/21	1992/11/16	36300	147	2100
	2F2DN23-01-2	b2	KG03	1997/11/27	1992/11/16	36300	153	1950
2	2F2DN23-02-1	Gd	c2	KG04	1997/12/01	1992/11/16	29200	84
	2F2DN23-02-2	Gd	c2	KG05	1997/12/04	1992/11/16	29200	137
	2F2DN23-02-3	Gd	c2	KG02	1997/11/25	1992/11/16	29200	109
3	2F2DN23-04	h1	KE13	1997/03/19	1992/11/16	34300	188	640
4	2F2DN23-05	Gd	b3	KE08	1997/03/07	1992/11/16	29200	263
5	2F2DN23-06	d3	KE06	1997/03/04	1992/11/16	27900	188	690
6	2F2DN23-07	c4	KE07	1997/03/06	1992/11/16	27900	188	310
7	2F2DN23-08	h4	KE05	1997/03/03	1992/11/16	35800	188	310
8	2F2DN23-09	e5	KE09	1997/03/10	1992/11/16	31300	188	760
9	2F2DN23-10	g5	KE12	1997/03/14	1992/11/16	31400	263	810
10	2F2DN23-11	Gd	f7	KE04	1997/02/28	1992/11/16	29300	263
11	2F2DN23-12	g7	KE03	1997/02/25	1992/11/16	38300	263	800
12	2F2DN23-13	d8	KE14	1997/03/21	1992/11/16	35800	263	1190
13	2F2DN23-14	h8	KE02	1997/02/19	1992/11/16	34300	181	325

Table 2.1.5. Measured data of NT3G23-C3(KD01) (Decay corrected for zero cooling)

Position from top (mm)	Spacer	Activity ratio /Cs-137 (): error(%)				
		Cs-134	Eu-154	Ce-144	Ru-106	Sb-125
164		4.94E-01 (2.14)	1.73E-02 (1.95)	1.35E+01 (2.64)	2.72E+00 (2.01)	6.02E-02 (1.62)
364		1.04E+00 (1.14)	4.17E-02 (1.03)	1.24E+01 (1.82)	3.91E+00 (1.52)	7.00E-02 (4.88)
564		1.29E+00 (1.06)	5.32E-02 (0.76)	1.21E+01 (1.10)	4.56E+00 (1.08)	7.00E-02 (2.75)
764		1.49E+00 (1.02)	5.65E-02 (0.81)	1.27E+01 (1.30)	4.91E+00 (1.70)	7.14E-02 (3.97)
964		1.54E+00 (1.14)	5.89E-02 (0.91)	1.26E+01 (1.77)	4.99E+00 (1.35)	6.79E-02 (2.62)
1164		1.56E+00 (1.33)	5.98E-02 (1.15)	1.23E+01 (2.50)	4.90E+00 (1.23)	7.22E-02 (3.90)
1364		1.56E+00 (0.00)	6.08E-02 (0.00)	1.30E+01 (0.00)	4.93E+00 (0.00)	7.37E-02 (0.00)
1564	*	1.54E+00 (0.86)	5.85E-02 (0.79)	1.22E+01 (0.74)	4.83E+00 (0.81)	6.52E-02 (0.84)
1764		1.56E+00 (0.00)	5.78E-02 (0.00)	1.18E+01 (0.00)	4.92E+00 (0.00)	7.01E-02 (0.00)
1964	*	1.48E+00 (1.32)	6.01E-02 (1.13)	1.24E+01 (1.69)	4.89E+00 (1.08)	7.05E-02 (1.10)
2164		1.55E+00 (0.92)	5.89E-02 (0.89)	1.19E+01 (1.70)	4.93E+00 (0.90)	6.91E-02 (2.93)
2364		1.56E+00 (2.13)	5.91E-02 (2.16)	1.29E+01 (1.93)	4.80E+00 (2.15)	6.73E-02 (1.86)
2564		1.56E+00 (1.22)	5.79E-02 (1.06)	1.19E+01 (1.47)	4.98E+00 (1.56)	6.76E-02 (1.96)
2764		1.56E+00 (1.17)	5.85E-02 (0.94)	1.29E+01 (2.46)	4.96E+00 (0.96)	7.09E-02 (0.93)
2964		1.56E+00 (1.74)	5.95E-02 (1.45)	1.25E+01 (3.88)	4.93E+00 (1.45)	6.75E-02 (2.37)
3164		1.54E+00 (1.22)	5.60E-02 (0.98)	1.22E+01 (1.18)	4.94E+00 (1.39)	6.82E-02 (4.39)
3364	*	1.45E+00 (0.00)	5.59E-02 (0.00)	1.27E+01 (0.00)	4.81E+00 (0.00)	6.72E-02 (0.00)
3564		1.30E+00 (1.36)	4.92E-02 (1.06)	1.30E+01 (2.10)	4.54E+00 (1.61)	6.96E-02 (4.65)
3764		7.48E-01 (1.12)	2.80E-02 (1.02)	1.40E+01 (1.09)	3.50E+00 (1.01)	6.46E-02 (1.09)

File ID KD01  
 Comment G23-3, 8mmStep, 4mmColli.  
 Measurement date 1996/7/16  
 Decay correct date 1992/6/19

Table 2.1.6. Measured data of NT3G23-A4(KC03) (Decay corrected for zero cooling)

Position from top (mm)	Spacer	Activity ratio /Cs-137 (): error(%)				
		Cs-134	Eu-154	Ce-144	Ru-106	Sb-125
233	*	7.59E-01 (0.78)	2.87E-02 (0.60)	1.34E+01 (0.97)	3.53E+00 (0.62)	6.81E-02 (0.98)
433		1.26E+00 (0.93)	4.87E-02 (0.64)	1.29E+01 (0.64)	4.53E+00 (1.35)	6.83E-02 (3.17)
633		1.42E+00 (0.96)	5.41E-02 (0.81)	1.24E+01 (1.16)	4.74E+00 (0.84)	6.32E-02 (3.84)
833		1.54E+00 (0.86)	5.81E-02 (0.66)	1.25E+01 (0.98)	4.96E+00 (0.95)	6.36E-02 (3.44)
1033		1.52E+00 (0.87)	5.90E-02 (0.67)	1.22E+01 (1.47)	4.86E+00 (0.67)	6.49E-02 (0.69)
1233		1.59E+00 (0.73)	5.92E-02 (0.61)	1.23E+01 (0.95)	4.97E+00 (0.62)	6.44E-02 (2.57)
1433		1.59E+00 (1.19)	5.89E-02 (0.87)	1.21E+01 (1.15)	5.00E+00 (1.54)	6.58E-02 (1.60)
1633		1.53E+00 (0.82)	5.67E-02 (0.81)	1.17E+01 (1.46)	4.79E+00 (0.84)	6.46E-02 (5.21)
1833		1.56E+00 (1.07)	5.79E-02 (1.01)	1.20E+01 (1.06)	4.98E+00 (1.99)	6.71E-02 (4.64)
2033		1.59E+00 (1.28)	5.84E-02 (1.02)	1.18E+01 (1.10)	4.99E+00 (1.71)	6.64E-02 (1.34)
2233		1.57E+00 (0.77)	5.77E-02 (0.62)	1.19E+01 (0.65)	4.88E+00 (0.83)	6.23E-02 (3.40)
2433		1.50E+00 (0.74)	5.90E-02 (0.63)	1.21E+01 (1.02)	4.85E+00 (1.24)	6.74E-02 (2.15)
2633		1.58E+00 (0.93)	5.80E-02 (0.70)	1.17E+01 (1.42)	4.93E+00 (1.18)	6.40E-02 (3.66)
2833		1.54E+00 (0.87)	5.66E-02 (0.67)	1.18E+01 (0.81)	4.85E+00 (0.68)	6.44E-02 (3.03)
3033		1.55E+00 (0.75)	5.65E-02 (0.75)	1.21E+01 (0.90)	5.00E+00 (0.77)	6.59E-02 (0.75)
3233		1.52E+00 (0.71)	5.52E-02 (0.57)	1.22E+01 (0.78)	4.88E+00 (1.20)	6.50E-02 (1.95)
3433		1.43E+00 (0.77)	5.20E-02 (0.67)	1.22E+01 (0.69)	4.77E+00 (0.67)	6.68E-02 (4.37)
3633		1.19E+00 (0.95)	4.46E-02 (0.69)	1.28E+01 (0.87)	4.34E+00 (1.64)	6.84E-02 (2.49)

File ID	KC03
Comment	G23-4 8mmStep, 40mm test
Measurement date	1995/10/27
Decay correct date	1992/6/19

Table 2.1.7. Measured data of NT3G23-C5(KD02) (Decay corrected for zero cooling)

Position from top (mm)	Spacer	Activity ratio /Cs-137 (): error(%)				
		Cs-134	Eu-154	Ce-144	Ru-106	Sb-125
164	*	5.31E-01 (1.54)	1.81E-02 (1.47)	1.43E+01 (2.59)	2.84E+00 (1.84)	6.15E-02 (3.59)
364		1.08E+00 (1.18)	4.12E-02 (1.07)	1.35E+01 (1.55)	4.26E+00 (1.05)	7.06E-02 (3.48)
564		1.30E+00 (0.95)	5.11E-02 (0.78)	1.31E+01 (1.31)	4.75E+00 (1.09)	7.30E-02 (0.84)
764		1.45E+00 (0.81)	5.30E-02 (0.58)	1.20E+01 (0.81)	4.94E+00 (0.58)	7.21E-02 (4.11)
964		1.47E+00 (1.85)	5.61E-02 (1.95)	1.28E+01 (3.82)	5.00E+00 (1.80)	6.92E-02 (1.75)
1204		1.46E+00 (0.81)	5.36E-02 (0.58)	1.20E+01 (0.73)	4.88E+00 (1.16)	7.06E-02 (3.29)
1364		1.46E+00 (1.14)	5.41E-02 (0.85)	1.19E+01 (1.20)	4.88E+00 (1.78)	6.91E-02 (2.28)
1564		1.47E+00 (0.96)	5.49E-02 (0.97)	1.28E+01 (0.94)	4.86E+00 (0.90)	6.79E-02 (1.37)
1764		1.49E+00 (1.68)	5.48E-02 (1.32)	1.18E+01 (3.41)	4.84E+00 (1.78)	6.78E-02 (1.55)
1964		1.40E+00 (1.48)	5.60E-02 (1.28)	1.21E+01 (3.13)	4.71E+00 (1.60)	6.67E-02 (5.46)
2164		1.48E+00 (1.39)	5.52E-02 (1.18)	1.22E+01 (2.66)	4.82E+00 (1.59)	7.14E-02 (1.64)
2364		1.47E+00 (1.44)	5.55E-02 (1.20)	1.26E+01 (3.09)	4.77E+00 (1.18)	6.50E-02 (3.75)
2564		1.46E+00 (1.22)	5.23E-02 (1.17)	1.20E+01 (1.68)	4.86E+00 (1.17)	7.10E-02 (3.08)
2764		1.47E+00 (0.00)	5.40E-02 (0.00)	1.30E+01 (0.00)	4.86E+00 (0.00)	7.24E-02 (0.00)
2964		1.48E+00 (1.49)	5.50E-02 (1.16)	1.27E+01 (2.01)	4.74E+00 (1.10)	6.58E-02 (5.14)
3164		1.47E+00 (1.12)	5.40E-02 (0.86)	1.26E+01 (1.72)	4.79E+00 (1.62)	6.14E-02 (3.80)
3364		1.38E+00 (0.98)	5.15E-02 (0.71)	1.26E+01 (0.80)	4.75E+00 (1.33)	6.77E-02 (0.71)
3564		1.23E+00 (0.86)	4.58E-02 (0.76)	1.27E+01 (0.75)	4.37E+00 (1.31)	6.94E-02 (2.02)
3764		6.85E-01 (1.54)	2.47E-02 (2.21)	1.40E+01 (1.53)	3.29E+00 (3.10)	6.14E-02 (1.75)

File ID KD02  
 Comment G23-5, 8mmStep, 4mmColli.  
 Measurement date 1996/7/17  
 Decay correct date 1992/6/19

Table 2.1.8. Measured data of NT3G23-A6(KD03) (Decay corrected for zero cooling)

Position from top (mm)	Spacer	Activity ratio /Cs-137 (): error(%)				
		Cs-134	Eu-154	Ce-144	Ru-106	Sb-125
164	*	4.97E-01 (1.95)	1.57E-02 (1.65)	1.51E+01 (3.26)	2.81E+00 (2.58)	5.95E-02 (4.99)
364		1.05E+00 (1.39)	4.08E-02 (1.50)	1.40E+01 (2.56)	4.27E+00 (1.27)	7.53E-02 (1.20)
564		1.26E+00 (1.10)	5.00E-02 (0.82)	1.32E+01 (1.41)	4.64E+00 (0.82)	7.41E-02 (3.55)
764		1.42E+00 (1.42)	5.42E-02 (1.32)	1.32E+01 (2.52)	4.96E+00 (1.71)	7.55E-02 (4.49)
964		1.44E+00 (1.19)	5.36E-02 (0.94)	1.28E+01 (1.12)	4.86E+00 (0.98)	6.73E-02 (6.24)
1164		1.45E+00 (0.79)	5.50E-02 (0.69)	1.31E+01 (0.68)	4.79E+00 (1.09)	6.90E-02 (4.90)
1364		1.45E+00 (1.21)	5.48E-02 (0.99)	1.35E+01 (1.25)	4.90E+00 (1.05)	7.19E-02 (1.66)
1564		1.44E+00 (1.13)	5.56E-02 (0.80)	1.35E+01 (0.81)	4.84E+00 (1.15)	7.28E-02 (1.20)
1764		1.45E+00 (1.25)	5.48E-02 (0.95)	1.27E+01 (1.10)	4.76E+00 (1.08)	
1964		1.37E+00 (1.35)	5.46E-02 (1.08)	1.25E+01 (1.23)	4.73E+00 (1.52)	7.55E-02 (0.97)
2164		1.45E+00 (1.34)	5.52E-02 (1.11)	1.29E+01 (1.78)	4.83E+00 (1.05)	7.46E-02 (5.05)
2364		1.43E+00 (1.08)	5.29E-02 (0.75)	1.22E+01 (1.31)	4.75E+00 (0.81)	7.18E-02 (3.30)
2564		1.46E+00 (0.89)	5.36E-02 (0.67)	1.23E+01 (0.73)	4.91E+00 (0.97)	6.92E-02 (3.14)
2764		1.46E+00 (0.86)	5.38E-02 (0.57)	1.29E+01 (0.57)	4.76E+00 (1.08)	6.87E-02 (2.29)
2964		1.47E+00 (2.11)	5.63E-02 (1.65)	1.36E+01 (4.13)	4.79E+00 (1.82)	6.98E-02 (1.90)
3164		1.44E+00 (0.00)	5.37E-02 (0.00)	1.34E+01 (0.00)	4.83E+00 (0.00)	7.10E-02 (0.00)
3364		1.36E+00 (1.31)	5.12E-02 (1.10)	1.30E+01 (1.74)	4.82E+00 (1.60)	7.35E-02 (7.20)
3564		1.21E+00 (1.48)	4.49E-02 (1.13)	1.31E+01 (1.33)	4.46E+00 (1.12)	7.04E-02 (1.12)
3764		6.74E-01 (1.58)	2.29E-02 (1.54)	1.43E+01 (1.69)	3.31E+00 (2.24)	6.65E-02 (3.35)

File ID KD03  
 Comment G23-6, 8mmStep, 4mmColli.  
 Measurement date 1996/7/18  
 Decay correct date 1992/6/19

Table 2.1.9. Measured data of NT3G23-C7(KD05) (Decay corrected for zero cooling)

Position from top (mm)	Spacer	Activity ratio /Cs-137 (): error(%)				
		Cs-134	Eu-154	Ce-144	Ru-106	Sb-125
204	*	6.69E-01 (0.99)	2.52E-02 (1.15)	1.37E+01 (1.28)	3.36E+00 (0.82)	6.74E-02 (1.54)
404		1.19E+00 (1.15)	4.64E-02 (0.92)	1.32E+01 (1.48)	4.43E+00 (0.95)	6.70E-02 (1.54)
604		1.41E+00 (0.66)	5.31E-02 (0.45)	1.22E+01 (0.65)	4.70E+00 (0.77)	7.05E-02 (2.70)
804		1.50E+00 (0.62)	5.44E-02 (0.54)	1.24E+01 (0.67)	4.90E+00 (0.74)	6.80E-02 (3.60)
1004		1.51E+00 (1.30)	5.49E-02 (1.07)	1.25E+01 (1.23)	5.00E+00 (1.66)	6.85E-02 (1.46)
1204		1.53E+00 (0.00)	5.54E-02 (0.00)	1.21E+01 (0.00)	4.87E+00 (0.00)	6.74E-02 (0.00)
1404		1.54E+00 (1.08)	5.55E-02 (0.71)	1.25E+01 (1.25)	4.81E+00 (1.26)	6.85E-02 (0.77)
1604		1.53E+00 (1.41)	5.73E-02 (1.09)	1.23E+01 (2.25)	4.92E+00 (1.84)	6.79E-02 (1.59)
1804		1.53E+00 (1.22)	5.60E-02 (0.96)	1.26E+01 (1.90)	4.83E+00 (0.96)	6.86E-02 (2.48)
2004		1.52E+00 (0.84)	5.62E-02 (0.43)	1.21E+01 (0.70)	4.81E+00 (0.82)	6.84E-02 (1.33)
2204		1.54E+00 (1.30)	5.67E-02 (1.01)	1.20E+01 (2.05)	4.94E+00 (1.76)	6.85E-02 (1.05)
2404		1.47E+00 (1.09)	5.71E-02 (0.82)	1.21E+01 (1.48)	4.72E+00 (1.09)	7.02E-02 (0.86)
2604		1.54E+00 (1.48)	5.69E-02 (1.15)	1.21E+01 (2.86)	4.91E+00 (1.28)	6.80E-02 (1.59)
2804		1.52E+00 (1.16)	5.57E-02 (0.83)	1.23E+01 (1.15)	4.85E+00 (0.99)	6.67E-02 (1.38)
3004		1.53E+00 (1.12)	5.49E-02 (0.87)	1.19E+01 (1.56)	4.90E+00 (1.34)	6.79E-02 (1.08)
3204		1.50E+00 (1.01)	5.38E-02 (0.68)	1.24E+01 (0.97)	4.74E+00 (1.19)	6.81E-02 (0.72)
3404		1.42E+00 (0.67)	5.17E-02 (0.64)	1.23E+01 (0.62)	4.68E+00 (0.62)	6.91E-02 (5.00)
3604		1.21E+00 (0.82)	4.51E-02 (0.61)	1.29E+01 (0.72)	4.40E+00 (0.66)	6.99E-02 (1.22)
3804		5.83E-01 (0.82)	2.04E-02 (0.67)	1.42E+01 (0.75)	2.91E+00 (0.78)	6.15E-02 (5.77)

File ID KD05  
 Comment G23-7, 8mmStep, 4mmColli.  
 Measurement date 1996/7/22  
 Decay correct date 1992/6/19

Table 2.1.10. Measured data of NT3G23-A8(KD06) (Decay corrected for zero cooling)

Position from top (mm)	Spacer	Activity ratio /Cs-137 (): error(%)				
		Cs-134	Eu-154	Ce-144	Ru-106	Sb-125
204	*	6.53E-01 (0.00)	2.42E-02 (0.00)	1.35E+01 (0.00)	3.22E+00 (0.00)	6.65E-02 (0.00)
404		1.19E+00 (1.11)	4.67E-02 (0.92)	1.31E+01 (2.10)	4.28E+00 (1.18)	6.92E-02 (2.11)
604		1.44E+00 (0.84)	5.53E-02 (0.58)	1.23E+01 (0.94)	4.82E+00 (0.72)	7.17E-02 (2.19)
804		1.56E+00 (1.36)	5.94E-02 (1.02)	1.26E+01 (1.96)	4.99E+00 (1.40)	7.16E-02 (2.06)
1004		1.58E+00 (1.09)	5.93E-02 (0.85)	1.27E+01 (1.86)	4.92E+00 (1.13)	6.74E-02 (3.37)
1204		1.58E+00 (0.83)	5.91E-02 (0.70)	1.25E+01 (0.88)	4.94E+00 (0.88)	7.17E-02 (1.31)
1404		1.60E+00 (1.28)	6.04E-02 (0.95)	1.28E+01 (2.22)	4.92E+00 (1.19)	7.01E-02 (1.24)
1604		1.57E+00 (1.26)	5.94E-02 (0.99)	1.26E+01 (2.27)	4.83E+00 (1.83)	6.88E-02 (1.08)
1804		1.59E+00 (1.23)	5.86E-02 (1.05)	1.18E+01 (1.23)	5.01E+00 (1.14)	7.18E-02 (1.81)
2004		1.57E+00 (1.13)	5.90E-02 (0.85)	1.22E+01 (1.94)	4.97E+00 (0.83)	7.11E-02 (2.92)
2204		1.58E+00 (0.98)	5.77E-02 (0.85)	1.26E+01 (1.37)	4.99E+00 (1.03)	6.87E-02 (1.76)
2404		1.53E+00 (1.41)	6.07E-02 (1.05)	1.29E+01 (2.85)	4.80E+00 (1.09)	6.88E-02 (4.84)
2604		1.58E+00 (0.91)	5.66E-02 (0.75)	1.24E+01 (0.78)	4.84E+00 (1.28)	6.68E-02 (1.57)
2804		1.56E+00 (0.75)	5.63E-02 (0.64)	1.24E+01 (0.78)	4.86E+00 (0.74)	6.80E-02 (2.34)
3004		1.59E+00 (0.86)	5.72E-02 (0.66)	1.28E+01 (1.41)	4.91E+00 (1.01)	6.91E-02 (0.85)
3204		1.55E+00 (0.68)	5.50E-02 (0.66)	1.28E+01 (0.66)	4.87E+00 (1.05)	7.17E-02 (0.85)
3404		1.47E+00 (1.04)	5.27E-02 (0.89)	1.26E+01 (0.87)	4.83E+00 (0.88)	7.00E-02 (3.16)
3604		1.25E+00 (1.18)	4.65E-02 (0.94)	1.32E+01 (1.58)	4.47E+00 (0.99)	7.12E-02 (2.90)
3804		5.75E-01 (1.00)	1.99E-02 (1.11)	1.45E+01 (0.88)	3.02E+00 (1.40)	5.96E-02 (2.13)

File ID: KD06  
 Comment: G23-8, 8mmStep, 4mmColli.  
 Measurement date: 1996/7/24  
 Decay correct date: 1992/6/19

Table 2.1.11. Measured data of NT3G23-B10(KC04) (Decay corrected for zero cooling)

Position from top (mm)	Spacer	Activity ratio /Cs-137 (): error(%)				
		Cs-134	Eu-154	Ce-144	Ru-106	Sb-125
202	*	5.12E-01 (1.20)	2.98E-02 (1.12)	1.58E+01 (1.56)	4.86E+00 (1.39)	9.34E-02 (1.28)
402		1.08E+00 (0.85)	5.00E-02 (0.71)	1.38E+01 (0.83)	6.06E+00 (0.82)	8.84E-02 (1.50)
602		1.32E+00 (1.10)	5.72E-02 (1.03)	1.30E+01 (1.10)	6.42E+00 (1.44)	8.57E-02 (1.14)
802		1.46E+00 (1.05)	5.97E-02 (0.78)	1.30E+01 (0.93)	6.61E+00 (1.13)	8.34E-02 (0.78)
1002		1.48E+00 (1.11)	6.08E-02 (1.02)	1.25E+01 (1.70)	6.69E+00 (1.12)	8.59E-02 (2.40)
1202		1.51E+00 (1.01)	6.16E-02 (0.94)	1.25E+01 (0.95)	6.55E+00 (1.66)	8.25E-02 (2.71)
1402		1.48E+00 (1.01)	6.07E-02 (0.96)	1.26E+01 (1.14)	6.58E+00 (1.40)	8.64E-02 (1.66)
1602		1.49E+00 (1.02)	6.11E-02 (0.72)	1.23E+01 (0.92)	6.55E+00 (1.35)	8.37E-02 (3.51)
1802		1.50E+00 (0.98)	6.10E-02 (0.76)	1.29E+01 (0.85)	6.51E+00 (1.24)	8.30E-02 (0.89)
2002		1.46E+00 (1.01)	6.08E-02 (0.81)	1.27E+01 (0.83)	6.43E+00 (1.38)	8.32E-02 (0.93)
2202		1.50E+00 (0.99)	5.89E-02 (0.85)	1.28E+01 (0.98)	6.55E+00 (1.52)	8.39E-02 (0.86)
2402		1.46E+00 (0.91)	6.15E-02 (0.73)	1.27E+01 (0.70)	6.37E+00 (1.15)	8.08E-02 (3.68)
2602		1.49E+00 (0.87)	5.90E-02 (0.78)	1.24E+01 (0.86)	6.52E+00 (1.20)	8.09E-02 (3.12)
2802		1.49E+00 (1.11)	5.99E-02 (0.83)	1.28E+01 (1.21)	6.53E+00 (1.60)	8.17E-02 (2.88)
3002		1.46E+00 (1.04)	5.77E-02 (0.95)	1.25E+01 (1.04)	6.57E+00 (1.09)	7.99E-02 (1.21)
3202		1.47E+00 (1.04)	5.85E-02 (0.69)	1.24E+01 (0.82)	6.53E+00 (1.29)	7.67E-02 (0.76)
3402		1.38E+00 (0.90)	5.57E-02 (0.86)	1.30E+01 (0.88)	6.44E+00 (1.68)	8.49E-02 (1.66)
3602		1.15E+00 (0.85)	4.92E-02 (0.63)	1.36E+01 (1.09)	5.98E+00 (1.36)	8.42E-02 (4.31)
3802		5.02E-01 (0.97)	2.76E-02 (0.90)	1.66E+01 (0.90)	4.67E+00 (0.91)	9.13E-02 (4.34)

File ID KC04  
 Comment G23-10, 8mmStep, 40mm  
 Measurement date 1995/10/30  
 Decay correct date 1992/6/19

Table 2.1.12. Measured data of NT3G23-D11(KD04) (Decay corrected for zero cooling)

Position from top (mm)	Spacer	Activity ratio /Cs-137 (): error(%)				
		Cs-134	Eu-154	Ce-144	Ru-106	Sb-125
204	*	5.18E-01 (0.73)	3.17E-02 (0.75)	1.69E+01 (1.22)	4.90E+00 (0.78)	8.55E-02 (1.38)
		1.04E+00 (0.89)	4.83E-02 (0.75)	1.43E+01 (0.80)	5.91E+00 (0.82)	8.58E-02 (2.33)
		1.27E+00 (0.69)	5.63E-02 (0.55)	1.37E+01 (0.54)	6.22E+00 (1.41)	8.22E-02 (0.56)
		1.39E+00 (0.86)	5.88E-02 (0.70)	1.32E+01 (0.81)	6.49E+00 (1.07)	8.43E-02 (0.91)
		1.41E+00 (1.15)	6.01E-02 (1.03)	1.31E+01 (1.12)	6.54E+00 (1.83)	8.44E-02 (1.17)
		1.42E+00 (0.63)	5.98E-02 (0.68)	1.30E+01 (0.90)	6.42E+00 (0.58)	8.19E-02 (1.00)
		1.42E+00 (1.09)	5.85E-02 (0.79)	1.31E+01 (0.84)	6.41E+00 (0.79)	8.53E-02 (1.08)
		1.41E+00 (1.12)	5.82E-02 (0.87)	1.27E+01 (1.20)	6.43E+00 (1.60)	8.14E-02 (1.92)
		1.42E+00 (0.86)	5.94E-02 (0.74)	1.27E+01 (1.21)	6.31E+00 (1.37)	8.30E-02 (1.20)
		1.40E+00 (1.10)	5.86E-02 (0.97)	1.28E+01 (1.14)	6.41E+00 (2.15)	8.22E-02 (1.77)
		1.41E+00 (0.78)	5.81E-02 (0.67)	1.29E+01 (0.68)	6.32E+00 (0.70)	8.19E-02 (1.00)
		1.37E+00 (1.04)	6.03E-02 (0.88)	1.32E+01 (1.39)	6.33E+00 (0.87)	8.50E-02 (1.28)
		1.42E+00 (0.85)	5.80E-02 (0.61)	1.28E+01 (0.69)	6.31E+00 (0.85)	8.52E-02 (4.08)
		1.41E+00 (0.62)	5.81E-02 (0.62)	1.30E+01 (0.74)	6.34E+00 (1.07)	8.15E-02 (2.74)
		1.41E+00 (0.93)	5.74E-02 (0.75)	1.31E+01 (0.80)	6.38E+00 (1.46)	8.17E-02 (2.46)
		1.39E+00 (0.87)	5.64E-02 (0.63)	1.27E+01 (0.75)	6.38E+00 (1.61)	8.17E-02 (1.77)
		1.30E+00 (0.94)	5.45E-02 (0.73)	1.33E+01 (0.78)	6.27E+00 (1.21)	8.12E-02 (1.25)
		1.07E+00 (1.02)	4.78E-02 (0.84)	1.46E+01 (0.87)	5.93E+00 (1.12)	8.21E-02 (1.78)
		4.56E-01 (1.34)	2.50E-02 (1.48)	1.78E+01 (1.28)	4.50E+00 (1.31)	8.81E-02 (1.58)

File ID KD04  
 Comment G23-11, 8mmStep, 4mmColli.  
 Measurement date 1996/7/19  
 Decay correct date 1992/6/19

Table 2.1.13. Measured data of NT3G23-B12(KD07) (Decay corrected for zero cooling)

Position from top (mm)	Spacer	Activity ratio /Cs-137 (): error(%)				
		Cs-134	Eu-154	Ce-144	Ru-106	Sb-125
204	*	5.05E-01 (0.68)	3.03E-02 (0.64)	1.63E+01 (0.78)	4.85E+00 (0.90)	8.84E-02 (1.41)
404		1.03E+00 (0.77)	4.79E-02 (0.60)	1.44E+01 (0.65)	6.00E+00 (0.61)	8.74E-02 (3.35)
604		1.26E+00 (0.80)	5.61E-02 (0.70)	1.37E+01 (1.15)	6.24E+00 (0.69)	8.63E-02 (1.40)
804		1.37E+00 (0.86)	5.78E-02 (0.67)	1.30E+01 (0.75)	6.44E+00 (0.72)	8.79E-02 (1.27)
1004		1.39E+00 (1.17)	5.98E-02 (0.89)	1.37E+01 (1.73)	6.42E+00 (0.90)	8.74E-02 (1.28)
1204		1.40E+00 (0.96)	5.84E-02 (0.75)	1.29E+01 (0.79)	6.47E+00 (1.37)	8.61E-02 (2.11)
1404		1.40E+00 (0.94)	5.89E-02 (0.85)	1.29E+01 (1.01)	6.50E+00 (0.79)	8.71E-02 (1.11)
1604		1.40E+00 (0.97)	5.83E-02 (0.76)	1.29E+01 (1.08)	6.36E+00 (0.83)	8.57E-02 (1.42)
1804		1.40E+00 (1.04)	5.87E-02 (0.87)	1.30E+01 (1.41)	6.33E+00 (0.79)	8.44E-02 (1.01)
2004		1.37E+00 (0.89)	5.84E-02 (0.75)	1.30E+01 (0.80)	6.36E+00 (0.75)	8.51E-02 (2.79)
2204		1.40E+00 (0.94)	5.76E-02 (0.74)	1.28E+01 (0.77)	6.40E+00 (1.84)	8.59E-02 (0.81)
2404		1.35E+00 (1.02)	6.00E-02 (0.79)	1.32E+01 (1.38)	6.34E+00 (1.87)	8.60E-02 (1.09)
2604		1.39E+00 (0.89)	5.70E-02 (0.77)	1.31E+01 (0.75)	6.36E+00 (0.76)	8.43E-02 (1.17)
2804		1.38E+00 (0.90)	5.84E-02 (0.92)	1.35E+01 (1.24)	6.34E+00 (0.80)	8.15E-02 (1.20)
3004		1.39E+00 (0.63)	5.72E-02 (0.57)	1.30E+01 (0.57)	6.32E+00 (0.55)	8.37E-02 (1.80)
3204		1.36E+00 (1.01)	5.54E-02 (0.74)	1.31E+01 (1.02)	6.35E+00 (1.43)	8.59E-02 (2.35)
3404		1.28E+00 (0.84)	5.35E-02 (0.62)	1.34E+01 (0.59)	6.19E+00 (1.19)	8.32E-02 (2.40)
3604		1.06E+00 (0.70)	4.63E-02 (0.71)	1.44E+01 (0.68)	5.86E+00 (0.69)	8.65E-02 (2.95)
3804		4.53E-01 (1.05)	2.53E-02 (1.20)	1.73E+01 (0.81)	4.45E+00 (0.80)	8.73E-02 (1.99)

File ID KD07  
 Comment G23-12, 8mmStep, 4mmColli.  
 Measurement date 1996/7/26  
 Decay correct date 1992/6/19

Table 2.1.14. Measured data of NT3G24-C3(KH11) (Decay corrected for zero cooling)

Position from top (mm)	Spacer	Activity ratio /Cs-137 (): error(%)				
		Cs-134	Eu-154	Ce-144	Ru-106	Sb-125
163	*	6.47E-01 (0.80)	2.29E-02 (0.91)		2.83E+00 (0.98)	5.96E-02 (4.49)
363		1.35E+00 (1.49)	5.21E-02 (1.51)		4.13E+00 (1.96)	5.71E-02 (5.09)
563		1.56E+00 (2.33)	6.04E-02 (2.39)		4.56E+00 (3.14)	5.90E-02 (3.08)
763		1.77E+00 (2.23)	6.27E-02 (0.07)		4.67E+00 (3.55)	5.42E-02 (5.76)
963		1.79E+00 (1.29)	6.64E-02 (1.05)		4.95E+00 (1.93)	6.09E-02 (6.69)
1163		1.75E+00 (2.55)	6.22E-02 (1.96)		4.62E+00 (1.81)	
1363		1.80E+00 (2.03)	6.30E-02 (1.65)		4.54E+00 (2.13)	7.29E-02 (4.66)
1563		1.75E+00 (1.82)	6.24E-02 (1.10)		4.58E+00 (1.10)	5.69E-02 (1.23)
1763		1.78E+00 (1.81)	6.17E-02 (1.65)		4.74E+00 (3.06)	6.46E-02 (9.52)
1963		1.69E+00 (1.87)	6.32E-02 (1.76)		4.52E+00 (1.44)	6.45E-02 (8.10)
2163		1.76E+00 (1.84)	5.82E-02 (0.60)		4.55E+00 (3.67)	
2363		1.74E+00 (2.26)	5.94E-02 (1.40)		4.62E+00 (4.15)	4.95E-02 (3.89)
2563		1.78E+00 (1.24)	6.04E-02 (0.96)		4.58E+00 (1.31)	5.14E-02 (7.73)
2763		1.77E+00 (2.11)	5.82E-02 (1.75)		4.60E+00 (2.93)	6.36E-02 (7.02)
2963		1.78E+00 (2.66)	5.92E-02 (1.10)		4.46E+00 (2.18)	5.06E-02 (9.24)
3163		1.78E+00 (2.82)	5.77E-02 (2.45)		4.75E+00 (4.98)	
3363		1.70E+00 (1.39)	6.09E-02 (0.96)		4.65E+00 (2.52)	6.98E-02 (3.79)
3567		1.49E+00 (1.56)	5.40E-02 (1.36)		4.33E+00 (2.26)	
3767		9.02E-01 (0.69)	3.48E-02 (1.22)		3.30E+00 (0.72)	4.87E-02 (2.32)

File ID KH11  
 Comment G24-3, 4mmStep, 4mmColli.  
 Measurement date 1998/9/21  
 Decay correct date 1993/9/30

Table 2.1.15. Measured data of NT3G24-A4(KH06) (Decay corrected for zero cooling)

Position from top (mm)	Spacer	Activity ratio /Cs-137 (): error(%)				
		Cs-134	Eu-154	Ce-144	Ru-106	Sb-125
161.5	*	6.79E-01 (1.04)	2.34E-02 (1.00)		3.03E+00 (1.40)	
361.5		1.39E+00 (1.47)	5.49E-02 (1.30)			
561.5		1.62E+00 (1.20)	6.48E-02 (0.84)		4.21E+00 (4.37)	
761.5		1.75E+00 (2.25)	6.26E-02 (2.32)		4.27E+00 (2.61)	
961.5		1.83E+00 (1.71)	6.35E-02 (2.53)		4.33E+00 (3.93)	
1161.5		1.81E+00 (3.12)	6.62E-02 (2.46)		4.23E+00 (3.49)	
1361.5		1.85E+00 (2.47)	6.37E-02 (2.82)		4.33E+00 (2.79)	
1561.5		1.76E+00 (3.05)	6.35E-02 (2.25)			
1761.5		1.82E+00 (1.15)	6.26E-02 (1.04)		4.19E+00 (2.20)	
1961.5		1.70E+00 (2.67)	6.80E-02 (2.07)		4.46E+00 (3.00)	
2161.5		1.77E+00 (4.17)	6.37E-02 (3.64)		4.37E+00 (6.02)	
2361.5			6.64E-02 (1.25)		4.41E+00 (2.45)	
2561.5		1.78E+00 (2.85)	6.25E-02 (0.85)		4.22E+00 (4.02)	
2761.5		1.81E+00 (1.65)	6.26E-02 (1.41)		4.16E+00 (3.94)	
2961.5		1.79E+00 (2.63)	6.07E-02 (2.96)		4.29E+00 (4.72)	
3161.5		1.83E+00 (0.67)	6.25E-02 (0.56)		4.29E+00 (0.93)	
3361.5		1.70E+00 (2.40)	6.34E-02 (2.23)		4.23E+00 (3.11)	
3565.5		1.57E+00 (3.14)			3.94E+00 (3.52)	
3765.5		9.80E-01 (1.80)	4.04E-02 (1.60)		3.44E+00 (1.26)	

File ID: KH06  
 Comment: G24-4, 4mmStep, 4mmColli.  
 Measurement date: 1998/9/7  
 Decay correct date: 1993/9/30

Table 2.1.16. Measured data of NT3G24-C5(KH09) (Decay corrected for zero cooling)

Position from top (mm)	Spacer	Activity ratio /Cs-137 (): error(%)				
		Cs-134	Eu-154	Ce-144	Ru-106	Sb-125
162		6.45E-01 (0.75)	2.28E-02 (1.69)		2.87E+00 (0.84)	2.87E+00 (0.85)
362		1.34E+00 (0.53)	5.21E-02 (0.51)		4.39E+00 (1.15)	4.39E+00 (4.93)
562	*	1.51E+00 (1.97)	5.82E-02 (1.60)		4.48E+00 (2.66)	4.48E+00 (2.01)
762		1.69E+00 (1.33)	5.82E-02 (2.52)		4.49E+00 (2.84)	
962		1.67E+00 (2.29)	6.08E-02 (2.42)		4.40E+00 (2.42)	
1162		1.68E+00 (1.57)	5.93E-02 (1.27)		4.26E+00 (2.73)	4.26E+00 (4.45)
1362		1.68E+00 (1.57)	5.94E-02 (1.66)		4.31E+00 (2.40)	4.31E+00 (6.10)
1562	*	1.66E+00 (1.44)	6.06E-02 (1.07)		4.23E+00 (2.18)	4.23E+00 (3.55)
1762		1.69E+00 (0.60)	6.04E-02 (0.95)		4.38E+00 (1.88)	4.38E+00 (6.36)
1962	*	1.60E+00 (0.68)	6.42E-02 (0.60)		4.28E+00 (2.27)	4.28E+00 (9.92)
2162		1.67E+00 (0.74)	5.97E-02 (0.72)		4.16E+00 (1.68)	4.16E+00 (4.82)
2362		1.67E+00 (1.73)	6.01E-02 (1.21)			4.17E+00 (2.12) (3.76)
2562			5.83E-02 (1.18)		4.27E+00 (1.73)	4.27E+00 (7.86)
2762		1.65E+00 (1.56)			4.18E+00 (3.02)	4.18E+00 (7.52)
2962		1.65E+00 (1.10)	5.74E-02 (0.91)		4.29E+00 (1.48)	4.29E+00 (6.16)
3162		1.66E+00 (0.77)	5.89E-02 (0.61)		4.41E+00 (1.68)	4.41E+00 (7.64)
3362	*	1.59E+00 (1.34)	5.87E-02 (1.68)		4.19E+00 (2.85)	4.19E+00 (1.95)
3566		1.49E+00 (0.91)	5.56E-02 (0.84)		4.43E+00 (0.88)	4.43E+00 (5.70)
3766		8.91E-01 (1.31)	3.50E-02 (1.19)		3.33E+00 (1.99)	3.33E+00 (2.61)

File ID KH09  
 Comment G24-5, 4mmStep, 4mmColli.  
 Measurement date 1998/9/16  
 Decay correct date 1993/9/30

Table 2.1.17. Measured data of NT3G24-A6(KH07) (Decay corrected for zero cooling)

Position from top (mm)	Spacer	Activity ratio /Cs-137 (): error(%)				
		Cs-134	Eu-154	Ce-144	Ru-106	Sb-125
163.5	*	6.43E-01 (0.84)	2.32E-02 (0.99)		2.86E+00 (0.69)	5.53E-02 (5.79)
363.5		1.30E+00 (0.59)	4.99E-02 (0.58)		4.11E+00 (1.46)	6.41E-02 (4.51)
563.5		1.55E+00 (0.81)	6.07E-02 (0.68)		4.68E+00 (0.74)	6.23E-02 (3.92)
763.5		1.72E+00 (0.77)	5.87E-02 (0.58)		4.73E+00 (2.41)	7.29E-02 (6.09)
963.5		1.73E+00 (0.80)	5.93E-02 (0.76)		4.64E+00 (1.47)	6.56E-02 (7.72)
1163.5		1.71E+00 (1.99)	5.83E-02 (2.28)		4.44E+00 (2.45)	6.33E-02 (4.15)
1363.5		1.73E+00 (1.30)	5.90E-02 (0.98)		4.56E+00 (1.35)	5.56E-02 (8.97)
1563.5			6.01E-02 (0.72)		4.74E+00 (1.35)	6.73E-02 (4.00)
1763.5		1.71E+00 (0.76)	5.73E-02 (1.00)		4.41E+00 (0.96)	5.84E-02 (3.87)
1963.5		1.63E+00 (0.78)	6.06E-02 (0.64)		4.45E+00 (1.15)	5.97E-02 (4.22)
2163.5		1.67E+00 (1.12)	5.49E-02 (1.02)		4.30E+00 (4.21)	
2363.5		1.72E+00 (1.41)	5.86E-02 (1.09)		4.62E+00 (0.75)	6.06E-02 (4.09)
2563.5		1.71E+00 (1.55)	5.81E-02 (1.30)		4.40E+00 (1.96)	6.33E-02 (5.85)
2763.5		1.71E+00 (1.05)	5.74E-02 (1.02)		4.47E+00 (1.92)	5.69E-02 (2.21)
2963.5		1.70E+00 (1.79)	5.97E-02 (1.33)		4.33E+00 (2.84)	5.82E-02 (1.65)
3163.5		1.70E+00 (0.91)	5.81E-02 (0.84)		4.60E+00 (0.91)	
3363.5		1.60E+00 (1.44)	6.06E-02 (2.40)		4.32E+00 (3.86)	
3567.5		1.51E+00 (1.81)	5.27E-02 (1.87)		4.21E+00 (2.61)	6.48E-02 (4.24)
3767.5		9.24E-01 (0.84)	3.78E-02 (0.62)		3.19E+00 (1.23)	5.54E-02 (5.89)

File ID KH07  
 Comment G24-6, 4mmStep, 4mmColli.  
 Measurement date 1998/9/9  
 Decay correct date 1993/9/30

Table 2.1.18. Measured data of NT3G24-C7(KF02) (Decay corrected for zero cooling)

Position from top (mm)	Spacer	Activity ratio /Cs-137 (): error(%)				
		Cs-134	Eu-154	Ce-144	Ru-106	Sb-125
204	*	8.32E-01 (0.89)	3.28E-02 (1.02)	1.13E+01 (0.76)	3.29E+00 (1.48)	6.08E-02 (4.44)
404		1.46E+00 (0.90)	5.82E-02 (0.73)	1.02E+01 (1.43)	4.37E+00 (0.74)	6.64E-02 (1.56)
604		1.72E+00 (1.50)	6.60E-02 (1.23)	9.93E+00 (3.36)	4.54E+00 (1.67)	6.52E-02 (4.63)
804		1.81E+00 (1.14)	6.68E-02 (0.93)	9.05E+00 (1.25)	4.82E+00 (1.33)	6.35E-02 (0.96)
1004		1.82E+00 (1.17)	6.72E-02 (0.99)	9.20E+00 (2.04)	4.60E+00 (1.28)	6.10E-02 (1.10)
1204		1.84E+00 (1.28)	6.73E-02 (1.10)	8.91E+00 (1.94)	4.71E+00 (1.41)	6.25E-02 (2.36)
1404		1.85E+00 (1.21)	6.69E-02 (0.94)	8.73E+00 (2.38)	4.51E+00 (1.43)	5.90E-02 (3.43)
1604		1.84E+00 (0.94)	6.61E-02 (0.84)	8.80E+00 (1.38)	4.49E+00 (1.18)	6.11E-02 (3.04)
1804		1.83E+00 (0.00)	6.42E-02 (0.00)	8.47E+00 (0.00)	4.44E+00 (0.00)	6.20E-02 (0.00)
2004		1.82E+00 (0.63)	6.57E-02 (0.55)	8.80E+00 (0.83)	4.40E+00 (0.94)	5.99E-02 (0.96)
2204		1.85E+00 (2.12)	6.74E-02 (1.76)	9.27E+00 (1.75)	4.58E+00 (2.19)	6.30E-02 (2.02)
2404		1.78E+00 (1.14)	6.85E-02 (0.84)	8.96E+00 (1.52)	4.43E+00 (1.03)	6.55E-02 (1.38)
2604		1.84E+00 (1.11)	6.47E-02 (0.93)	8.50E+00 (1.89)	4.47E+00 (1.48)	6.16E-02 (1.13)
2804		1.85E+00 (1.26)	6.55E-02 (1.06)	9.31E+00 (2.69)	4.49E+00 (1.65)	6.36E-02 (3.36)
3004		1.84E+00 (1.68)	6.67E-02 (1.37)	9.19E+00 (1.44)	4.48E+00 (1.73)	6.54E-02 (1.47)
3204		1.81E+00 (1.08)	6.37E-02 (0.90)	8.30E+00 (1.33)	4.54E+00 (0.95)	5.90E-02 (1.04)
3404		1.75E+00 (1.04)	6.22E-02 (0.77)	9.20E+00 (1.71)	4.46E+00 (1.18)	6.10E-02 (2.36)
3600		1.53E+00 (0.93)	5.69E-02 (0.76)	9.62E+00 (1.34)	4.29E+00 (1.02)	6.26E-02 (2.75)
3804		7.55E-01 (1.09)	2.84E-02 (0.92)	1.10E+01 (0.88)	3.03E+00 (1.38)	5.87E-02 (1.60)

File ID KF02  
 Comment G24-07, 4mmStep, 4mmColli.  
 Measurement date 1997/4/18  
 Decay correct date 1993/9/30

Table 2.1.19. Measured data of NT3G24-A8(KH12) (Decay corrected for zero cooling)

Position from top (mm)	Spacer	Activity ratio /Cs-137 (): error(%)				
		Cs-134	Eu-154	Ce-144	Ru-106	Sb-125
161	*	6.59E-01 (1.78)	2.33E-02 (1.57)		3.09E+00 (1.86)	1.97E-02 (4.07)
361		1.35E+00 (0.78)	5.13E-02 (0.70)		4.33E+00 (2.72)	2.13E-02 (4.33)
561		1.66E+00 (1.21)	6.02E-02 (0.77)		4.36E+00 (1.80)	1.86E-02 (2.65)
761		1.75E+00 (1.43)	5.90E-02 (1.51)		4.45E+00 (2.30)	1.84E-02 (6.67)
961		1.75E+00 (1.76)	5.70E-02 (1.42)		4.49E+00 (1.95)	1.88E-02 (3.04)
1161		1.79E+00 (1.95)	5.94E-02 (1.32)			1.92E-02 (6.04)
1361		1.75E+00 (1.19)	5.93E-02 (1.24)		4.37E+00 (2.31)	2.02E-02 (4.23)
1561		1.76E+00 (1.12)	6.21E-02 (1.14)		4.33E+00 (2.11)	2.16E-02 (3.87)
1761		1.77E+00 (1.17)	5.82E-02 (1.35)		4.36E+00 (2.27)	1.80E-02 (6.94)
1961		1.72E+00 (1.68)	6.29E-02 (1.29)		4.23E+00 (1.85)	1.78E-02 (7.62)
2161		1.77E+00 (1.27)	5.73E-02 (1.25)		4.29E+00 (2.55)	2.05E-02 (1.05)
2361		1.75E+00 (1.15)	6.00E-02 (1.13)		4.23E+00 (1.54)	1.75E-02 (6.38)
2561		1.77E+00 (1.39)	5.90E-02 (1.30)		4.38E+00 (2.15)	1.85E-02 (5.33)
2761		1.74E+00 (1.10)	5.76E-02 (1.37)		4.22E+00 (1.53)	1.80E-02 (7.70)
2961		1.75E+00 (1.53)	5.78E-02 (1.67)		4.27E+00 (3.09)	2.07E-02 (4.06)
3161					4.39E+00 (2.75)	1.92E-02 (0.86)
3361		1.68E+00 (1.44)	5.83E-02 (1.14)		4.28E+00 (1.71)	1.85E-02 (5.71)
3565		1.53E+00 (1.48)	5.49E-02 (2.19)		4.15E+00 (2.11)	1.74E-02 (1.48)
3765		9.43E-01 (0.51)	3.63E-02 (0.43)		3.40E+00 (0.49)	1.83E-02 (0.30)
3773		9.14E-01 (0.90)	3.48E-02 (0.70)		3.37E+00 (1.73)	1.82E-02 (1.32)

File ID: KH12  
 Comment: G24-8, 4mmStep, 4mmColli.  
 Measurement date: 1998/9/22  
 Decay correct date: 1993/9/30

Table 2.1.20. Measured data of NT3G24-B10(KH08) (Decay corrected for zero cooling)

Position from top (mm)	Spacer	Activity ratio /Cs-137 (): error(%)				
		Cs-134	Eu-154	Ce-144	Ru-106	Sb-125
159	*	5.92E-01 (0.90)	3.08E-02 (1.05)		4.35E+00 (0.89)	7.73E-02 (3.48)
359		1.29E+00 (0.55)	5.68E-02 (0.58)		5.83E+00 (0.94)	8.16E-02 (3.79)
559		1.53E+00 (0.68)	6.51E-02 (0.58)		6.01E+00 (0.43)	7.90E-02 (1.64)
759		1.72E+00 (0.65)	6.55E-02 (0.90)		6.04E+00 (1.56)	7.61E-02 (3.22)
959		1.76E+00 (0.64)	6.55E-02 (0.78)		6.08E+00 (1.52)	7.07E-02 (1.25)
1159		1.76E+00 (0.36)	6.52E-02 (0.48)		5.91E+00 (0.86)	7.17E-02 (1.54)
1359		1.76E+00 (0.30)	6.46E-02 (0.00)		5.93E+00 (0.68)	8.03E-02 (3.80)
1559		1.73E+00 (0.66)	6.53E-02 (0.61)		5.92E+00 (1.36)	7.51E-02 (0.58)
1759		1.75E+00 (0.66)	6.50E-02 (0.85)		5.85E+00 (1.09)	7.81E-02 (3.95)
1959		1.70E+00 (1.06)	7.04E-02 (0.79)		5.67E+00 (2.34)	7.23E-02 (2.86)
2159		1.75E+00 (0.69)	6.35E-02 (0.48)		5.57E+00 (0.88)	7.33E-02 (1.71)
2359		1.74E+00 (1.13)	6.53E-02 (0.58)		5.48E+00 (1.56)	6.90E-02 (1.93)
2559		1.74E+00 (0.55)	6.31E-02 (0.53)		5.79E+00 (0.40)	7.65E-02 (3.08)
2759		1.74E+00 (0.67)	6.39E-02 (2.88)		5.82E+00 (0.61)	7.51E-02 (3.21)
2959		1.75E+00 (0.87)	6.45E-02 (0.58)		5.80E+00 (0.66)	7.36E-02 (1.40)
3159		1.73E+00 (0.49)	6.25E-02 (0.50)		5.92E+00 (0.49)	7.73E-02 (2.22)
3359		1.66E+00 (1.16)	6.40E-02 (0.51)		5.85E+00 (1.30)	7.15E-02 (1.01)
3563		1.50E+00 (0.69)	6.02E-02 (0.77)		5.70E+00 (0.53)	7.85E-02 (2.62)
3763		8.44E-01 (0.68)	4.24E-02 (0.60)		4.74E+00 (0.86)	7.62E-02 (1.01)

File ID KH08  
 Comment G24-10, 4mmStep, 4mmColli.  
 Measurement date 1998/9/11  
 Decay correct date 1993/9/30

Table 2.1.21. Measured data of NT3G24-D11(KH10) (Decay corrected for zero cooling)

Position from top (mm)	Spacer	Activity ratio /Cs-137 (): error(%)				
		Cs-134	Eu-154	Ce-144	Ru-106	Sb-125
163.5		5.70E-01 (1.43)	2.87E-02 (1.14)		4.17E+00 (1.83)	7.21E-02 (4.70)
363.5		1.25E+00 (1.01)	5.70E-02 (0.82)		5.57E+00 (1.43)	7.07E-02 (2.48)
563.5	*	1.50E+00 (0.49)	6.62E-02 (0.37)		5.86E+00 (1.03)	7.59E-02 (5.83)
763.5		1.66E+00 (0.55)	6.50E-02 (0.54)		5.89E+00 (0.55)	7.05E-02 (4.75)
963.5		1.68E+00 (0.67)	6.66E-02 (0.55)		5.73E+00 (0.59)	6.80E-02 (0.64)
1163.5		1.68E+00 (0.65)	6.54E-02 (0.58)		5.78E+00 (0.85)	6.82E-02 (3.75)
1363.5		1.66E+00 (1.30)	6.45E-02 (0.86)		5.41E+00 (1.84)	6.55E-02 (0.92)
1563.5	*	1.65E+00 (0.91)	6.60E-02 (0.61)		5.62E+00 (0.75)	7.05E-02 (5.50)
1763.5		1.66E+00 (1.03)	6.60E-02 (0.72)		5.71E+00 (0.88)	7.10E-02 (4.96)
1963.5	*	1.61E+00 (0.70)	6.85E-02 (0.58)		5.66E+00 (0.59)	6.88E-02 (0.68)
2163.5		1.66E+00 (0.85)	6.49E-02 (0.90)		5.63E+00 (1.40)	7.23E-02 (3.60)
2363.5		1.65E+00 (0.81)	6.23E-02 (0.36)		5.50E+00 (0.36)	7.01E-02 (3.38)
2563.5		1.66E+00 (1.20)	6.17E-02 (0.91)		5.63E+00 (0.96)	6.45E-02 (3.27)
2763.5		1.66E+00 (0.65)	6.21E-02 (0.54)		5.71E+00 (0.54)	6.97E-02 (9.27)
2963.5		1.65E+00 (0.57)	6.16E-02 (0.58)		5.59E+00 (1.58)	7.00E-02 (2.94)
3163.5		1.63E+00 (0.85)	6.19E-02 (0.78)		5.79E+00 (0.76)	7.07E-02 (4.18)
3363.5		1.57E+00 (0.71)	6.48E-02 (0.57)		5.59E+00 (0.69)	7.46E-02 (3.44)
3567.5		1.39E+00 (1.33)	5.66E-02 (1.13)		5.57E+00 (0.96)	7.05E-02 (1.56)
3767.5		8.30E-01 (0.85)	4.37E-02 (0.78)		4.76E+00 (0.78)	7.34E-02 (3.45)

File ID KH10  
 Comment G24-11, 4mmStep, 4mmColli.  
 Measurement date 1998/9/18  
 Decay correct date 1993/9/30

Table 2.1.22. Measured data of NT3G24-B12(KH05) (Decay corrected for zero cooling)

Position from top (mm)	Spacer	Activity ratio /Cs-137 (): error(%)				
		Cs-134	Eu-154	Ce-144	Ru-106	Sb-125
203		7.02E-01 (0.94)	3.96E-02 (0.77)		4.84E+00 (1.06)	8.81E-02 (6.51)
403		1.33E+00 (1.22)	5.84E-02 (0.95)		5.79E+00 (0.96)	7.62E-02 (6.00)
603		1.58E+00 (1.49)	6.25E-02 (1.25)		6.04E+00 (1.32)	7.60E-02 (1.59)
803		1.67E+00 (1.14)	6.43E-02 (0.96)		5.77E+00 (1.42)	7.55E-02 (7.32)
1003		1.64E+00 (0.62)			5.79E+00 (0.82)	7.13E-02 (0.42)
1203		1.69E+00 (1.18)	6.46E-02 (0.95)		5.80E+00 (1.35)	7.44E-02 (2.94)
1403		1.68E+00 (0.55)	6.37E-02 (0.94)		5.73E+00 (2.17)	7.66E-02 (5.82)
1603		1.67E+00 (1.20)	6.36E-02 (1.11)		5.73E+00 (2.00)	7.41E-02 (6.02)
1803		1.67E+00 (1.20)	6.39E-02 (0.92)		5.74E+00 (1.00)	7.18E-02 (3.14)
2003		1.66E+00 (1.01)	6.60E-02 (1.05)		5.43E+00 (1.25)	7.26E-02 (1.13)
2203		1.67E+00 (0.78)	6.44E-02 (0.36)		5.80E+00 (0.55)	7.41E-02 (0.40)
2403		1.64E+00 (0.53)	6.65E-02 (0.76)		5.70E+00 (1.05)	7.26E-02 (4.82)
2603		1.68E+00 (0.75)	6.35E-02 (0.56)		5.69E+00 (1.25)	7.64E-02 (1.72)
2803		1.67E+00 (1.18)	6.41E-02 (0.82)		5.63E+00 (1.59)	7.15E-02 (5.78)
3003			6.28E-02 (0.53)		5.67E+00 (0.91)	7.92E-02 (4.24)
3203		1.66E+00 (0.88)	6.27E-02 (0.54)		5.62E+00 (0.79)	7.56E-02 (4.09)
3403		1.59E+00 (0.81)	6.16E-02 (0.47)		5.64E+00 (0.61)	7.32E-02 (3.23)
3599		1.39E+00 (0.82)	5.76E-02 (0.62)		5.50E+00 (1.01)	7.81E-02 (2.05)
3803		6.54E-01 (0.85)	3.46E-02 (1.02)		4.39E+00 (1.36)	7.81E-02 (3.26)

File ID KH05  
 Comment G24-12, 4mmStep, 4mmColli.  
 Measurement date 1998/9/4  
 Decay correct date 1993/9/30

Table 2.1.23. Measured data of 2F2DN23-01 (Decay corrected for zero cooling)

Position from top (mm)	Spacer	Activity ratio /Cs-137 (): error(%)				
		Cs-134	Eu-154	Ce-144	Ru-106	Sb-125
392		6.86E-01 (1.01)	2.93E-02 (1.23)		4.88E+00 (1.10)	
		8.01E-01 (0.92)	3.83E-02 (1.29)		4.35E+00 (0.93)	
		9.66E-01 (1.26)	4.48E-02 (0.91)		3.34E+00 (1.01)	
		1.11E+00 (7.70)	4.96E-02 (2.33)		3.28E+00 (7.55)	
		1.35E+00 (4.66)	5.53E-02 (4.56)		3.74E+00 (5.45)	
		1.38E+00 (1.16)	5.51E-02 (1.06)			
		1.46E+00 (1.26)	5.79E-02 (1.08)		3.78E+00 (1.65)	
		1.46E+00 (1.39)	6.03E-02 (1.43)			
		1.51E+00 (5.39)	5.70E-02 (1.64)		3.76E+00 (6.45)	
		1.47E+00 (2.12)	6.27E-02 (3.99)		3.81E+00 (1.72)	
		1.47E+00 (8.98)	6.04E-02 (9.06)		4.06E+00 (8.82)	
		1.50E+00 (2.42)	5.55E-02 (2.41)		3.82E+00 (1.26)	
		1.47E+00 (1.86)	5.92E-02 (8.80)		3.67E+00 (1.95)	
		1.49E+00 (4.90)	5.12E-02 (4.80)		3.54E+00 (4.98)	
		1.43E+00 (8.87)	4.61E-02 (8.75)		3.49E+00 (9.48)	
		1.43E+00 (0.66)	4.67E-02 (1.42)		3.60E+00 (1.47)	
		1.43E+00 (0.78)	4.60E-02 (0.70)		3.55E+00 (0.77)	
		1.34E+00 (2.23)	4.27E-02 (1.75)		3.36E+00 (3.44)	
		1.25E+00 (5.71)	4.07E-02 (5.70)		3.38E+00 (6.12)	
		1.17E+00 (1.29)	3.82E-02 (1.29)		3.09E+00 (1.66)	
		1.08E+00 (2.40)	3.71E-02 (2.51)		2.86E+00 (2.60)	
		8.47E-01 (1.16)	3.26E-02 (1.44)		2.65E+00 (1.85)	
		6.13E-01 (1.73)	2.88E-02 (1.67)		5.11E+00 (1.69)	
		3.56E-01 (1.23)	1.88E-02 (1.59)		3.96E+00 (1.01)	

Table 2.1.24. Measured data of 2F2DN23-02 (Decay corrected for zero cooling)

Position from top (mm)	Spacer	Activity ratio /Cs-137 (): error(%)				
		Cs-134	Eu-154	Ce-144	Ru-106	Sb-125
376		5.66E-01 (0.76)	2.84E-02 (0.88)		5.01E+00 (0.78)	8.40E-02 (2.13)
		7.24E-01 (1.14)	4.11E-02 (1.22)		5.66E+00 (1.64)	9.22E-02 (2.36)
		8.37E-01 (1.26)	4.39E-02 (1.18)		3.61E+00 (1.08)	6.18E-02 (1.11)
		1.02E+00 (0.88)	5.21E-02 (0.79)		3.78E+00 (1.75)	6.52E-02 (2.79)
		1.24E+00 (0.87)	6.08E-02 (1.22)		4.22E+00 (1.71)	6.45E-02 (4.96)
		1.26E+00 (8.15)	5.40E-02 (9.05)		4.21E+00 (8.84)	0.00E+00 (0.00)
		1.32E+00 (9.21)	7.04E-02 (9.79)		4.46E+00 (2.11)	6.97E-02 (12.97)
		1.35E+00 (9.18)	6.73E-02 (4.11)		4.54E+00 (9.19)	7.19E-02 (6.64)
		1.37E+00 (9.27)	6.74E-02 (4.11)		4.79E+00 (4.66)	6.94E-02 (4.26)
		1.36E+00 (9.42)	6.99E-02 (4.27)		4.66E+00 (2.12)	6.56E-02 (4.14)
		1.34E+00 (9.45)	7.13E-02 (9.59)		4.68E+00 (9.45)	6.64E-02 (4.54)
		1.36E+00 (9.23)	6.61E-02 (10.03)		4.65E+00 (10.41)	7.34E-02 (5.18)
		1.39E+00 (9.39)	6.21E-02 (9.41)		4.68E+00 (9.50)	6.90E-02 (6.75)
		1.33E+00 (5.31)	6.31E-02 (7.01)		4.34E+00 (5.30)	6.31E-02 (4.39)
		1.37E+00 (9.36)	5.62E-02 (10.60)		4.23E+00 (0.79)	6.25E-02 (4.19)
		1.36E+00 (8.77)	5.07E-02 (4.11)		4.06E+00 (9.04)	6.13E-02 (8.01)
		1.32E+00 (5.62)	5.33E-02 (5.64)		4.08E+00 (5.74)	5.96E-02 (5.33)
		1.28E+00 (3.61)	4.63E-02 (5.29)		4.00E+00 (3.59)	5.69E-02 (7.56)
		1.25E+00 (2.59)	4.06E-02 (6.64)		3.98E+00 (5.53)	6.40E-02 (7.46)
		1.18E+00 (1.66)	4.32E-02 (1.58)		3.79E+00 (2.67)	6.05E-02 (1.86)
		1.08E+00 (2.04)	4.34E-02 (1.97)		3.86E+00 (2.14)	5.86E-02 (1.90)
		9.56E-01 (1.49)	3.88E-02 (1.44)		3.65E+00 (2.83)	5.87E-02 (4.26)
		7.00E-01 (1.53)	3.43E-02 (1.45)		3.22E+00 (1.74)	5.80E-02 (2.16)
		5.79E-01 (3.68)	3.17E-02 (4.61)		4.87E+00 (4.39)	8.60E-02 (4.45)

Table 2.1.25. Measured data of 2F2DN23-04(KE13) (Decay corrected for zero cooling)

Position from top (mm)	Spacer	Activity ratio /Cs-137 (): error(%)				
		Cs-134	Eu-154	Ce-144	Ru-106	Sb-125
382	*	7.49E-01 (1.31)	3.15E-02 (1.19)	8.32E+00 1.73	5.84E+00 (1.20)	9.44E-02 (3.66)
582		1.15E+00 (0.97)	4.69E-02 (0.74)	8.41E+00 (1.39)	4.66E+00 (1.12)	6.89E-02 (1.83)
782		1.50E+00 (1.05)	5.62E-02 (0.92)	8.04E+00 (2.18)	5.32E+00 (0.92)	7.05E-02 (1.72)
982		1.65E+00 (0.67)	5.77E-02 (0.57)	8.37E+00 (0.68)	5.39E+00 (0.82)	6.68E-02 (2.36)
1182		1.75E+00 (0.79)	6.06E-02 (0.67)	8.08E+00 (0.75)	6.01E+00 (1.54)	7.27E-02 (2.21)
1382		1.80E+00 (1.54)	6.10E-02 (1.37)	8.27E+00 (3.92)	5.81E+00 (1.91)	6.81E-02 (2.29)
1582		1.80E+00 (1.01)	5.77E-02 (0.78)	7.79E+00 (1.18)	5.61E+00 (1.12)	6.44E-02 (0.80)
1782		1.80E+00 (0.90)	5.67E-02 (0.75)	8.38E+00 (1.86)	5.58E+00 (0.75)	6.61E-02 (5.41)
1982		1.76E+00 (0.91)	5.91E-02 (0.72)	8.68E+00 (2.02)	5.70E+00 (0.70)	7.03E-02 (0.70)
2182		1.78E+00 (3.34)	5.80E-02 (3.32)		5.47E+00 (3.33)	7.23E-02 (5.43)
2382		1.75E+00 (1.30)	5.75E-02 (1.08)	8.48E+00 (3.45)	5.66E+00 (1.32)	6.91E-02 (3.69)
2582		1.75E+00 (1.46)	5.19E-02 (1.30)	8.00E+00 (4.20)	5.21E+00 (1.30)	6.31E-02 (1.48)
2782		1.69E+00 (0.86)	4.74E-02 (0.73)	7.28E+00 (1.22)	5.08E+00 (0.73)	6.17E-02 (1.95)
2982		1.63E+00 (0.79)	4.94E-02 (0.67)	7.62E+00 (1.24)	5.26E+00 (1.17)	6.59E-02 (2.57)
3182		1.59E+00 (1.47)	4.85E-02 (1.29)	6.80E+00 (2.56)	5.23E+00 (2.23)	6.56E-02 (2.78)
3382		1.52E+00 (0.51)	4.59E-02 (0.51)	7.11E+00 (0.75)	5.23E+00 (0.73)	6.96E-02 (0.69)
3582		1.39E+00 (0.92)	4.38E-02 (0.81)	7.26E+00 (1.19)	4.84E+00 (1.16)	6.69E-02 (1.90)
3782		1.13E+00 (1.14)	4.08E-02 (0.74)	7.25E+00 (0.93)	4.52E+00 (0.74)	6.83E-02 (4.48)
3982		5.51E-01 (1.89)	2.68E-02 (1.50)	7.56E+00 (3.14)	4.81E+00 (2.10)	7.91E-02 (2.86)

File ID KE13  
 Comment DN23-04, 4mmSTP, 4mmColli.  
 Measurement date 1997/ 3/19  
 Decay correct date 1992/11/16

Table 2.1.26. Measured data of 2F2DN23-05(KE08) (Decay corrected for zero cooling)

Position from top (mm)	Spacer	Activity ratio /Cs-137 (): error(%)				
		Cs-134	Eu-154	Ce-144	Ru-106	Sb-125
346	*	6.54E-01 (4.61)	2.97E-02 (7.16)	6.85E+00 (4.06)	5.08E+00 (4.92)	1.19E-01 (18.15)
542		7.73E-01 (1.40)	4.00E-02 (1.24)	1.06E+01 (1.74)	3.49E+00 (1.24)	7.10E-02 (2.24)
742		1.12E+00 (1.24)	5.56E-02 (0.92)	9.97E+00 (1.61)	4.05E+00 (0.93)	6.77E-02 (2.77)
942		1.28E+00 (0.79)	6.14E-02 (0.59)	9.20E+00 (0.57)	4.23E+00 (0.57)	6.66E-02 (0.58)
1142		1.37E+00 (0.68)	6.33E-02 (0.57)	9.60E+00 (0.59)	4.54E+00 (0.68)	6.78E-02 (1.01)
1342		1.42E+00 (1.76)	6.72E-02 (1.35)	9.23E+00 (3.62)	4.63E+00 (2.17)	6.72E-02 (3.49)
1542		1.41E+00 (0.56)	6.23E-02 (0.51)	9.48E+00 (1.00)	4.51E+00 (1.15)	6.68E-02 (1.90)
1562		1.40E+00 (0.00)	6.26E-02 (0.00)	9.53E+00 (0.00)	4.58E+00 (0.00)	6.69E-02 (0.00)
1742		1.42E+00 (1.24)	6.16E-02 (0.97)	9.38E+00 (1.40)	4.52E+00 (1.49)	6.86E-02 (1.91)
1942		1.39E+00 (4.51)	6.14E-02 (4.43)	8.99E+00 (4.50)	4.51E+00 (4.43)	6.84E-02 (5.67)
2142		1.43E+00 (1.03)	5.98E-02 (0.81)	9.20E+00 (1.79)	4.41E+00 (1.35)	6.51E-02 (3.78)
2342		1.42E+00 (0.75)	5.73E-02 (0.54)	8.86E+00 (1.29)	4.42E+00 (0.66)	6.22E-02 (1.23)
2542		1.36E+00 (0.76)	5.72E-02 (0.63)		4.41E+00 (1.18)	6.48E-02 (0.99)
2742		1.38E+00 (0.99)	5.31E-02 (0.85)	8.87E+00 (0.85)	4.30E+00 (1.50)	6.48E-02 (2.35)
2942		1.35E+00 (1.18)	5.09E-02 (0.98)	8.37E+00 (1.22)	4.25E+00 (1.75)	6.12E-02 (2.63)
3142		1.31E+00 (0.86)	4.84E-02 (0.73)	8.52E+00 (1.05)	4.11E+00 (0.89)	6.35E-02 (0.77)
3342		1.27E+00 (1.14)	4.72E-02 (1.03)	7.99E+00 (0.99)	4.02E+00 (1.00)	6.10E-02 (2.08)
3542		1.17E+00 (0.86)	4.40E-02 (0.80)	9.57E+00 (1.19)	3.87E+00 (1.08)	6.20E-02 (0.99)
3742		9.28E-01 (0.81)	3.80E-02 (0.82)	9.46E+00 (1.10)	3.52E+00 (0.81)	6.29E-02 (2.90)
3942		5.56E-01 (0.94)	2.94E-02 (0.88)	8.55E+00 (1.08)	4.92E+00 (1.55)	8.58E-02 (2.61)

File ID KE08  
 Comment DN23-05, 4mmSTP, 4mmColli.  
 Measurement date 1997/ 3/ 7  
 Decay correct date 1992/11/16

Table 2.1.27. Measured data of 2F2DN23-06(KE06) (Decay corrected for zero cooling)

Position from top (mm)	Spacer	Activity ratio /Cs-137 (): error(%)				
		Cs-134	Eu-154	Ce-144	Ru-106	Sb-125
382	*	5.49E-01 (1.52)	2.92E-02 (1.31)	8.56E+00 (3.78)	5.09E+00 (1.46)	8.72E-02 (5.97)
582		8.83E-01 (0.57)	4.38E-02 (0.56)	9.89E+00 (0.82)	3.72E+00 (0.58)	6.87E-02 (1.51)
782		1.19E+00 (0.99)	5.90E-02 (0.70)	9.18E+00 (1.33)	4.28E+00 (1.14)	7.38E-02 (2.21)
982		1.29E+00 (1.11)	6.42E-02 (0.69)	8.79E+00 (0.98)	4.56E+00 (1.23)	7.22E-02 (1.64)
1182		1.42E+00 (1.03)	6.64E-02 (0.88)	8.73E+00 (2.18)	4.71E+00 (1.50)	7.25E-02 (0.91)
1382		1.43E+00 (0.98)	6.72E-02 (0.89)	9.05E+00 (1.51)	4.83E+00 (0.86)	7.52E-02 (1.00)
1582		1.45E+00 (0.73)	6.55E-02 (0.58)	8.77E+00 (0.93)	4.76E+00 (0.78)	6.89E-02 (2.10)
1782		1.47E+00 (1.21)	6.55E-02 (0.73)	8.16E+00 (1.14)	4.67E+00 (1.49)	7.02E-02 (3.81)
1982		1.42E+00 (0.71)	6.46E-02 (0.61)	9.36E+00 (1.29)	4.65E+00 (0.62)	6.97E-02 (1.45)
2182		1.45E+00 (0.79)	6.11E-02 (0.71)	8.60E+00 (1.08)	4.70E+00 (0.98)	6.84E-02 (0.71)
2382		1.45E+00 (1.00)	6.17E-02 (0.84)	8.45E+00 (1.48)	4.78E+00 (0.91)	7.08E-02 (1.74)
2582		1.41E+00 (0.81)	5.92E-02 (0.67)	8.33E+00 (0.86)	4.68E+00 (1.25)	6.77E-02 (1.04)
2782		1.42E+00 (0.74)	5.57E-02 (0.68)	7.99E+00 (0.84)	4.58E+00 (0.97)	6.96E-02 (1.63)
2982		1.38E+00 (1.04)	5.25E-02 (0.91)	8.54E+00 (1.93)	4.43E+00 (1.01)	6.62E-02 (2.33)
3182		1.34E+00 (1.68)	5.05E-02 (1.55)	8.20E+00 (1.62)	4.50E+00 (2.24)	6.51E-02 (1.89)
3382		1.29E+00 (1.04)	4.74E-02 (0.89)	7.70E+00 (1.32)	4.21E+00 (1.45)	6.62E-02 (2.53)
3582		1.15E+00 (1.13)	4.43E-02 (0.97)	7.93E+00 (1.59)	4.01E+00 (1.01)	6.38E-02 (1.28)
3782		9.17E-01 (0.99)	3.79E-02 (0.73)	8.55E+00 (0.92)	3.55E+00 (0.94)	6.32E-02 (5.26)
3982		4.67E-01 (1.40)	2.41E-02 (1.27)	8.07E+00 (1.47)	4.43E+00 (2.30)	8.13E-02 (3.94)

File ID KE06  
 Comment DN23-06, 4mmSTP, 4mmColli.  
 Measurement date 1997/ 3/ 4  
 Decay correct date 1992/11/16

Table 2.1.28. Measured data of 2F2DN23-07(KE07) (Decay corrected for zero cooling)

Position from top (mm)	Spacer	Activity ratio /Cs-137 (): error(%)				
		Cs-134	Eu-154	Ce-144	Ru-106	Sb-125
382	*	5.52E-01 (1.88)	2.95E-02 (1.72)	8.91E+00 (1.76)	5.15E+00 (1.83)	8.83E-02 (1.96)
582		8.83E-01 (0.67)	4.30E-02 (0.58)	9.00E+00 (0.89)	3.69E+00 (0.97)	7.03E-02 (5.36)
782		1.19E+00 (1.29)	5.88E-02 (1.02)	8.94E+00 (1.24)	4.35E+00 (1.02)	7.18E-02 (4.39)
982		1.29E+00 (1.08)	6.47E-02 (0.88)	9.53E+00 (2.02)	4.57E+00 (0.98)	7.87E-02 (3.54)
1182		1.41E+00 (1.67)	6.41E-02 (1.28)	9.23E+00 (1.34)	4.78E+00 (1.33)	7.10E-02 (4.70)
1382		1.45E+00 (1.72)	6.75E-02 (1.29)	9.14E+00 (3.61)	4.71E+00 (1.46)	7.27E-02 (1.35)
1582		1.45E+0 (1.53)	6.72E-02 (1.02)	9.33E+0 (2.63)	4.75E+0 (1.53)	6.91E-02 (2.41)
1782		1.46E+00 (0.96)	6.44E-02 (0.79)	8.29E+00 (1.03)	4.75E+00 (0.95)	6.64E-02 (0.81)
1982		1.42E+00 (0.90)	6.32E-02 (0.83)	8.58E+00 (1.21)	4.69E+00 (1.56)	6.98E-02 (1.46)
2182		1.45E+00 (1.59)	6.26E-02 (1.35)	8.99E+00 (3.06)	4.62E+00 (2.02)	6.62E-02 (2.92)
2382		1.45E+00 (1.61)	6.21E-02 (1.40)	8.66E+00 (4.10)	4.60E+00 (1.67)	6.66E-02 (1.44)
2582		1.41E+00 (0.94)	5.97E-02 (0.95)	7.86E+00 (1.84)	4.61E+00 (1.53)	6.96E-02 (4.23)
2782		1.40E+00 (1.24)	5.53E-02 (1.15)	8.26E+00 (1.29)	4.61E+00 (1.28)	7.06E-02 (4.43)
2982		1.37E+00 (1.34)	5.30E-02 (1.14)	8.21E+00 (2.10)	4.40E+00 (1.50)	6.56E-02 (2.71)
3182		1.33E+00 (0.96)	4.98E-02 (0.85)	8.53E+00 (1.13)	4.39E+00 (0.85)	6.73E-02 (1.41)
3382		1.29E+00 (0.00)	4.76E-02 (0.00)	8.03E+00 (0.00)	4.13E+00 (0.00)	6.69E-02 (0.00)
3582		1.16E+00 (1.05)	4.49E-02 (0.92)	8.41E+00 (1.52)	4.02E+00 (1.36)	6.77E-02 (1.62)
3782		9.15E-01 (1.13)	3.77E-02 (0.92)	8.83E+00 (1.85)	3.53E+00 (1.26)	6.59E-02 (2.18)
3982		4.60E-01 (1.50)	2.28E-02 (1.35)	7.98E+00 (2.19)	4.58E+00 (1.63)	8.71E-02 (2.19)

File ID KE07  
 Comment DN23-07, 4mmSTP, 4mmColli.  
 Measurement date 1997/ 3/ 6  
 Decay correct date 1992/11/16

Table 2.1.29. Measured data of 2F2DN23-08(KE05) (Decay corrected for zero cooling)

Position from top (mm)	Spacer	Activity ratio /Cs-137 (): error(%)				
		Cs-134	Eu-154	Ce-144	Ru-106	Sb-125
382	*	6.44E-01 (1.19)	3.02E-02 (1.00)	8.60E+00 (1.38)	5.43E+00 (1.62)	8.39E-02 (1.55)
582		1.01E+00 (1.12)	4.53E-02 (0.82)	9.15E+00 (1.86)	3.64E+00 (1.37)	6.12E-02 (0.89)
782		1.33E+00 (0.76)	5.39E-02 (0.66)	8.27E+00 (1.66)	4.09E+00 (1.38)	6.30E-02 (5.17)
982		1.46E+00 (1.08)	5.48E-02 (0.90)	8.29E+00 (1.59)	4.03E+00 (1.66)	5.82E-02 (3.51)
1382		1.62E+00 (1.13)	5.78E-02 (0.99)	8.19E+00 (1.36)	4.41E+00 (1.48)	5.94E-02 (5.70)
1582		1.60E+00 (0.98)	5.83E-02 (0.83)	9.83E+00 (1.79)	4.30E+00 (1.08)	5.59E-02 (1.45)
1782		1.62E+00 (0.72)	5.78E-02 (0.67)	8.04E+00 (1.05)	4.27E+00 (1.15)	5.95E-02 (5.83)
1982		1.57E+00 (0.51)	5.87E-02 (0.37)	8.23E+00 (0.43)	4.48E+00 (0.64)	6.17E-02 (1.59)
2182		1.58E+00 (0.75)	5.40E-02 (0.60)	9.29E+00 (0.79)	4.31E+00 (0.98)	5.88E-02 (5.11)
2382		1.61E+00 (2.85)	5.78E-02 (2.48)	8.02E+00 (3.88)	4.25E+00 (2.71)	6.44E-02 (8.05)
2582		1.54E+00 (1.31)	5.34E-02 (1.09)	8.71E+00 (2.61)	4.35E+00 (1.23)	5.94E-02 (4.26)
2782		1.53E+00 (0.90)	4.91E-02 (0.77)	7.87E+00 (1.17)	4.12E+00 (1.18)	6.18E-02 (0.79)
2982		1.46E+00 (0.89)	4.82E-02 (0.77)	8.19E+00 (1.76)	4.10E+00 (0.78)	5.73E-02 (4.75)
3182		1.43E+00 (0.65)	4.53E-02 (0.51)	8.15E+00 (0.53)	3.94E+00 (0.72)	5.76E-02 (1.36)
3382		1.38E+00 (1.70)	4.51E-02 (1.53)	7.58E+00 (5.13)	3.95E+00 (2.02)	6.00E-02 (2.08)
3582		1.23E+00 (0.74)	4.13E-02 (0.61)	7.36E+00 (2.86)	3.75E+00 (1.25)	5.67E-02 (2.89)
3782		9.83E-01 (1.70)	3.71E-02 (1.60)	7.95E+00 (1.87)	3.25E+00 (1.97)	5.49E-02 (1.85)
3982		5.13E-01 (1.64)	2.52E-02 (1.40)	8.13E+00 (1.58)	4.68E+00 (2.03)	8.40E-02 (5.22)

File ID	KE05
Comment	DN23-08, 4mmSTP, 4mmColli.
Measurement date	1997/ 3/ 3
Decay correct date	1992/11/16

Table 2.1.30. Measured data of 2F2DN23-09(KE09) (Decay corrected for zero cooling)

Position from top (mm)	Spacer	Activity ratio /Cs-137 (): error(%)				
		Cs-134	Eu-154	Ce-144	Ru-106	Sb-125
382	*	5.68E-01 (1.25)	2.96E-02 (1.05)	8.65E+00 (1.12)	5.22E+00 (1.28)	9.34E-02 (1.93)
582		9.20E-01 (1.14)	4.32E-02 (0.88)	9.61E+00 (1.02)	3.59E+00 (0.88)	6.70E-02 (2.99)
782		1.22E+00 (0.88)	5.76E-02 (0.77)	9.43E+00 (0.78)	4.04E+00 (0.77)	6.83E-02 (2.78)
982		1.36E+00 (0.76)	6.31E-02 (0.70)	9.00E+00 (1.23)	4.21E+00 (0.73)	6.85E-02 (1.45)
1182		1.48E+00 (0.88)	6.62E-02 (0.77)	9.01E+00 (1.11)	4.48E+00 (1.14)	6.71E-02 (3.65)
1382		1.50E+00 (0.67)	6.28E-02 (1.16)	8.40E+00 (0.74)	4.24E+00 (1.13)	6.29E-02 (3.24)
1582		1.51E+00 (0.78)	6.37E-02 (0.64)	8.80E+00 (0.65)	4.40E+00 (0.93)	6.42E-02 (2.75)
1782		1.52E+00 (0.63)	6.36E-02 (0.57)	8.27E+00 (0.76)	4.47E+00 (0.80)	6.76E-02 (2.69)
1982		1.47E+00 (0.86)	6.26E-02 (0.72)	8.63E+00 (0.74)	4.28E+00 (1.22)	6.63E-02 (2.49)
2182		1.50E+00 (0.83)	6.17E-02 (0.68)	8.81E+00 (1.34)	4.41E+00 (1.09)	6.48E-02 (2.62)
2382		1.49E+00 (0.86)	5.88E-02 (0.65)	8.15E+00 (0.92)	4.32E+00 (0.80)	6.47E-02 (4.92)
2582		1.45E+00 (1.09)	5.81E-02 (0.96)	8.54E+00 (1.01)	4.34E+00 (1.06)	6.36E-02 (1.53)
2782		1.47E+00 (1.28)	5.57E-02 (1.06)	8.39E+00 (2.53)	4.30E+00 (1.64)	6.03E-02 (1.12)
2982		1.42E+00 (0.92)	5.05E-02 (0.83)	8.08E+00 (0.88)	4.15E+00 (1.40)	5.93E-02 (4.38)
3182		1.39E+00 (0.74)	4.89E-02 (0.67)	7.92E+00 (0.71)	4.00E+00 (1.14)	6.11E-02 (4.42)
3382		1.32E+00 (0.95)	4.57E-02 (0.82)	7.60E+00 (1.38)	3.81E+00 (1.16)	6.00E-02 (1.51)
3582		1.81E+00 (1.23)	4.47E-02 (1.08)	7.67E+00 (1.86)	3.66E+00 (1.96)	5.88E-02 (2.30)
3782		9.45E-01 (1.03)	3.74E-02 (0.91)	8.54E+00 (1.76)	3.28E+00 (0.92)	5.82E-02 (1.77)
3982		4.83E-01 (1.77)	2.54E-02 (1.51)	7.79E+00 (2.28)	4.69E+00 (1.66)	8.31E-02 (1.55)

File ID KE09  
 Comment DN23-09, 4mmSTP, 4mmColli.  
 Measurement date 1997/ 3/10  
 Decay correct date 1992/11/16

Table 2.1.31. Measured data of 2F2DN23-10(KE12) (Decay corrected for zero cooling)

Position from top (mm)	Spacer	Activity ratio /Cs-137 (): error(%)				
		Cs-134	Eu-154	Ce-144	Ru-106	Sb-125
422	*	6.15E-01 (1.09)	3.28E-02 (1.28)	8.27E+00 (1.96)	5.34E+00 (1.01)	9.04E-02 (3.50)
622		9.66E-01 (0.93)	4.61E-01 (0.74)	8.99E+00 (1.65)	3.93E+00 (1.43)	6.68E-02 (6.39)
1022		1.33E+00 (1.00)	6.05E-02 (0.85)	8.94E+00 (2.55)	3.99E+00 (1.79)	6.11E-02 (5.02)
1222		1.43E+00 (1.04)	6.12E-02 (0.89)	8.97E+00 (2.64)	3.97E+00 (1.37)	5.71E-02 (5.59)
1422		1.43E+00 (1.51)	6.08E-02 (1.31)	7.70E+00 (2.39)	4.23E+00 (1.39)	6.60E-02 (8.70)
1622		1.45E+00 (1.03)	6.02E-02 (0.95)	9.09E+00 (1.88)	4.12E+00 (1.26)	5.85E-02 (9.54)
1822		1.44E+00 (1.24)	5.60E-02 (1.15)	8.01E+00 (1.17)	3.71E+00 (1.53)	4.63E-02 (6.66)
2022		1.38E+00 (0.90)	5.84E-02 (0.73)	8.33E+00 (1.53)	3.90E+00 (0.78)	5.40E-02 (4.84)
2222		1.43E+00 (0.97)	5.59E-02 (0.87)	8.57E+00 (2.99)	4.02E+00 (1.16)	5.58E-02 (6.14)
2422		1.41E+00 (0.83)	5.37E-02 (0.72)	8.32E+00 (1.18)	3.91E+00 (0.85)	5.34E-02 (5.48)
2622		1.38E+00 (1.42)	5.10E-02 (1.27)	7.84E+00 (3.24)	3.77E+00 (1.78)	5.23E-02 (6.89)
2822		1.37E+00 (1.05)	4.91E-02 (0.94)	7.95E+00 (3.37)	3.71E+00 (1.68)	5.51E-02 (2.36)
3022		1.33E+00 (1.70)	5.03E-02 (1.39)	8.15E+00 (1.41)	4.49E+00 (2.01)	6.78E-02 (1.45)
3222		1.28E+00 (1.26)	4.78E-02 (1.12)	7.25E+00 (1.30)	4.25E+00 (1.51)	6.42E-02 (5.37)
3422		1.23E+00 (1.64)	4.59E-02 (1.50)	7.60E+00 (2.78)	4.22E+00 (1.85)	5.88E-02 (2.01)
3622		1.10E+00 (0.97)	4.27E-02 (1.19)	7.24E+00 (1.20)	3.99E+00 (1.30)	5.97E-02 (0.89)
3822		8.31E-01 (1.44)	3.45E-02 (1.43)	7.74E+00 (1.57)	3.37E+00 (1.43)	6.29E-02 (1.54)
4030		3.63E-01 (1.23)	1.92E-02 (1.29)	7.44E+00 (1.18)	3.98E+00 (1.17)	7.65E-02 (1.80)

File ID KE12  
 Comment DN23-10, 4mmSTP, 4mmColli.  
 Measurement date 1997/ 3/14  
 Decay correct date 1992/11/16

Table 2.1.32. Measured data of 2F2DN23-11(KE04) (Decay corrected for zero cooling)

Position from top (mm)	Spacer	Activity ratio /Cs-137 (): error(%)				
		Cs-134	Eu-154	Ce-144	Ru-106	Sb-125
362	*	5.60E-01 (1.21)	2.86E-02 (1.00)	8.51E+00 (1.20)	5.17E+00 (1.76)	8.71E-02 (2.56)
558		8.15E-01 (1.25)	4.21E-02 (1.03)	1.03E+01 (1.60)	3.55E+00 (1.77)	6.65E-02 (3.69)
762		1.15E+00 (1.05)	5.63E-02 (0.70)	1.02E+01 (0.70)	4.10E+00 (1.71)	7.16E-02 (3.10)
962		1.30E+00 (0.00)	6.27E-02 (0.00)	9.35E+00 (0.00)	4.34E+00 (0.00)	6.94E-02 (0.00)
1162		1.39E+00 (0.60)	6.43E-02 (0.58)	9.41E+00 (1.40)	4.58E+00 (0.58)	7.10E-02 (1.10)
1362		1.40E+00 (0.82)	6.41E-02 (0.75)	9.40E+00 (0.72)	4.56E+00 (0.77)	6.86E-02 (1.55)
1562		1.39E+00 (0.80)	6.34E-02 (0.71)	9.53E+00 (0.84)	4.71E+00 (1.10)	7.37E-02 (2.16)
1762		1.41E+00 (0.93)	6.06E-02 (0.74)	8.66E+00 (0.74)	4.45E+00 (1.36)	6.65E-02 (1.38)
1962		1.37E+00 (0.95)	6.19E-02 (0.81)	9.39E+00 (1.03)	4.54E+00 (1.69)	6.64E-02 (4.79)
2162		1.39E+00 (0.54)	5.89E-02 (0.52)	9.74E+00 (0.57)	4.46E+00 (0.86)	6.85E-02 (1.04)
2362		1.37E+00 (1.05)	5.60E-02 (0.92)	8.88E+00 (1.83)	4.35E+00 (1.52)	6.45E-02 (0.92)
2562		1.33E+00 (0.81)	5.58E-02 (0.72)	8.79E+00 (0.91)	4.33E+00 (0.74)	6.71E-02 (4.79)
2762		1.33E+00 (0.74)	5.26E-02 (0.60)	8.64E+00 (0.61)	4.24E+00 (0.68)	6.18E-02 (3.30)
2962		1.31E+00 (0.87)	5.00E-02 (0.72)	8.82E+00 (1.32)	4.18E+00 (1.20)	6.28E-02 (0.72)
3162		1.26E+00 (0.81)	4.72E-02 (0.70)	8.45E+00 (0.86)	3.99E+00 (1.29)	6.30E-02 (0.94)
3362		1.21E+00 (0.71)	4.40E-02 (0.68)	8.40E+00 (0.77)	3.78E+00 (0.96)	5.93E-02 (1.29)
3562		1.10E+00 (1.29)	4.36E-02 (0.98)	8.78E+00 (1.88)	3.82E+00 (1.07)	6.30E-02 (1.31)
3758		8.66E-01 (0.66)	3.76E-02 (0.64)	9.71E+00 (1.62)	3.40E+00 (0.68)	6.13E-02 (0.63)
3958		5.40E-01 (1.18)	2.83E-02 (1.02)	8.03E+00 (1.22)	4.78E+00 (1.63)	8.76E-02 (1.74)
4062		2.85E-01 (1.58)	1.50E-02 (1.54)	8.09E+00 (1.99)	3.51E+00 (2.40)	7.04E-02 (5.23)

File ID KE04  
 Comment DN23-11, 4mmStep, 4mmColli.  
 Measurement date 1997/ 2/28  
 Decay correct date 1992/11/16

Table 2.1.33. Measured data of 2F2DN23-12(KE03) (Decay corrected for zero cooling)

Position from top (mm)	Spacer	Activity ratio /Cs-137 (): error(%)				
		Cs-134	Eu-154	Ce-144	Ru-106	Sb-125
382	*	6.38E-01 (1.27)	2.97E-02 (1.16)	8.67E+00 (1.17)	5.34E+00 (1.15)	9.72E-02 (5.09)
582		9.62E-01 (1.04)	4.04E-02 (0.82)	9.29E+00 (0.87)	3.08E+00 (0.81)	5.53E-02 (1.96)
782		1.29E+00 (0.69)	5.05E-02 (0.60)	8.53E+00 (0.80)	3.43E+00 (1.68)	5.97E-02 (1.88)
982		1.40E+00 (0.52)	5.61E-02 (0.43)	9.35E+00 (0.52)	3.81E+00 (0.52)	6.08E-02 (2.18)
1182		1.52E+00 (1.08)	5.75E-02 (0.91)	8.63E+00 (2.08)	3.83E+00 (1.21)	5.58E-02 (0.93)
1382		1.51E+00 (0.92)	5.98E-02 (0.80)	9.71E+00 (0.86)	4.19E+00 (0.80)	6.07E-02 (0.82)
1582		1.53E+00 (0.82)	5.64E-02 (0.64)	8.06E+00 (0.67)	3.95E+00 (0.65)	5.80E-02 (0.64)
1782		1.52E+00 (0.78)	5.58E-02 (0.57)	8.44E+00 (0.82)	4.05E+00 (0.61)	6.13E-02 (0.96)
1982		1.48E+00 (0.78)	5.81E-02 (0.79)	8.30E+00 (2.05)	3.99E+00 (0.75)	6.17E-02 (4.13)
2182		1.52E+00 (0.91)	5.37E-02 (0.81)	8.08E+00 (2.01)	3.80E+00 (0.84)	5.54E-02 (1.76)
2382		1.50E+00 (0.97)	5.07E-02 (0.84)	7.41E+00 (1.19)	3.76E+00 (1.35)	5.56E-02 (2.37)
2582		1.46E+00 (0.55)	5.13E-02 (0.52)	8.17E+00 (0.52)	3.83E+00 (0.92)	5.88E-02 (1.95)
2782		1.43E+00 (0.68)	4.68E-02 (0.64)	7.65E+00 (1.41)	3.58E+00 (0.82)	5.48E-02 (0.66)
2982		1.39E+00 (0.73)	4.56E-02 (0.55)	7.79E+00 (0.71)	3.60E+00 (1.00)	5.51E-02 (2.15)
3182		1.35E+00 (1.24)	4.45E-02 (1.05)	7.30E+00 (2.76)	3.55E+00 (1.08)	5.85E-02 (3.88)
3382		1.29E+00 (0.77)	4.08E-02 (0.68)	7.35E+00 (0.74)	3.34E+00 (0.86)	5.61E-02 (2.64)
3582		1.14E+00 (0.81)	4.01E-02 (0.64)	7.56E+00 (0.99)	3.33E+00 (0.65)	5.62E-02 (4.66)
3782		9.04E-01 (0.78)	3.44E-02 (0.61)	8.25E+00 (0.61)	2.89E+00 (1.41)	5.41E-02 (0.62)
3982		4.91E-01 (1.53)	2.40E-02 (1.32)	7.63E+00 (2.90)	4.41E+00 (1.82)	7.53E-02 (1.29)

File ID KE03  
 Comment DN23-12, 4mmStep, 4mmColli.  
 Measurement date 1997/ 2/25  
 Decay correct date 1992/11/16

Table 2.1.34. Measured data of 2F2DN23-13(KE14) (Decay corrected for zero cooling)

Position from top (mm)	Spacer	Activity ratio /Cs-137 (): error(%)				
		Cs-134	Eu-154	Ce-144	Ru-106	Sb-125
382		6.63E-01 (1.17)	3.18E-02 (1.08)	8.55E+00 (1.48)	5.55E+00 (1.08)	9.11E-02 (1.95)
582		1.04E+00 (0.70)	4.84E-02 (0.66)	9.73E+00 (0.98)	3.76E+00 (1.34)	6.55E-02 (1.97)
782		1.38E+00 (0.73)	5.59E-02 (0.63)	8.26E+00 (0.73)	4.04E+00 (1.30)	6.32E-02 (0.84)
982	*	1.50E+00 (0.60)	5.99E-02 (0.49)	8.95E+00 (0.49)	4.20E+00 (0.77)	6.36E-02 (2.12)
1182		1.63E+00 (0.98)	6.04E-02 (0.90)	8.77E+00 (1.83)	4.33E+00 (1.33)	6.02E-02 (0.92)
1382		1.66E+00 (0.60)	6.01E-02 (0.52)	8.15E+00 (0.71)	4.41E+00 (0.52)	6.34E-02 (2.00)
1582		1.65E+00 (1.03)	5.88E-02 (0.92)	8.96E+00 (2.58)	4.34E+00 (0.92)	6.03E-02 (1.41)
1782		1.64E+00 (1.06)	5.87E-02 (0.90)	8.59E+00 (2.73)	4.46E+00 (1.17)	6.27E-02 (4.40)
1982	*	1.60E+00 (1.28)	6.02E-02 (1.17)	8.68E+00 (2.95)	4.52E+00 (1.82)	6.47E-02 (1.24)
2182		1.63E+00 (0.76)	5.65E-02 (0.62)	8.16E+00 (1.18)	4.30E+00 (1.75)	6.01E-02 (0.61)
2382		1.60E+00 (1.04)	5.25E-02 (0.89)	8.43E+00 (2.34)	4.38E+00 (0.98)	6.24E-02 (2.39)
2562	*	1.58E+00 (1.01)	5.28E-02 (0.91)	7.62E+00 (2.25)	4.14E+00 (0.94)	6.26E-02 (5.29)
2982		1.51E+00 (0.95)	4.95E-02 (0.84)	8.28E+00 (2.60)	4.13E+00 (0.97)	6.10E-02 (1.78)
3082	*	1.43E+00 (0.90)	4.72E-02 (0.64)	7.67E+00 (1.05)	3.90E+00 (0.97)	5.70E-02 (2.85)
3382		1.39E+00 (0.62)	4.28E-02 (0.53)	7.19E+00 (0.66)	3.72E+00 (0.96)	5.44E-02 (1.78)
3582	*	1.24E+00 (0.70)	4.30E-02 (0.63)	8.13E+00 (1.69)	3.60E+00 (0.88)	5.90E-02 (2.79)
3782		9.73E-01 (1.27)	3.71E-02 (0.91)	8.31E+00 (2.69)	3.19E+00 (0.96)	5.60E-02 (0.89)
3982		5.03E-01 (1.30)	2.41E-02 (1.21)	7.89E+00 (1.60)	4.70E+00 (1.76)	8.69E-02 (2.17)

File ID KE14  
 Comment DN23-13, 4mmStep, 4mmColli.  
 Measurement date 1997/ 3/21  
 Decay correct date 1992/11/16

Table 2.1.35. Measured data of 2F2DN23-14(KE02) (Decay corrected for zero cooling)

Position from top (mm)	Spacer	Activity ratio /Cs-137 (): error(%)				
		Cs-134	Eu-154	Ce-144	Ru-106	Sb-125
422	*	7.77E-01 (1.15)	3.90E-02 (p.83)	9.28E+00 (0.83)	5.94E+00 (1.14)	8.41E-02 (4.52)
622		1.29E+00 (0.92)	4.77E-02 (0.71)	7.86E+00 (1.61)	4.71E+00 (1.24)	6.21E-02 (2.17)
822		1.56E+00 (1.02)	5.58E-02 (0.89)	9.23E+00 (2.18)	5.43E+00 (1.26)	6.52E-02 (1.90)
1022		1.71E+00 (0.96)	5.83E-02 (0.78)	8.32E+00 (1.62)	5.56E+00 (1.40)	6.35E-02 (2.30)
1222		1.78E+00 (0.00)	5.61E-02 (0.00)	7.26E+00 (0.00)	5.60E+00 (0.00)	7.05E-02 (0.00)
1422		1.79E+00 (0.75)	5.89E-02 (0.58)	8.42E+00 (0.79)	5.65E+00 (0.88)	6.68E-02 (0.59)
1622		1.72E+00 (0.86)	5.92E-02 (0.62)	8.82E+00 (1.05)	5.83E+00 (0.80)	6.72E-02 (2.17)
1822		1.73E+00 (0.82)	5.65E-02 (0.70)	8.23E+00 (0.92)	5.78E+00 (0.70)	6.78E-02 (0.98)
2022		1.69E+00 (2.21)	5.27E-02 (2.09)	7.53E+00 (3.64)	5.53E+00 (2.08)	5.98E-02 (2.87)
2222		1.72E+00 (0.00)	5.20E-02 (0.00)	7.20E+00 (0.00)	5.21E+00 (0.00)	6.26E-02 (0.00)
2422		1.70E+00 (1.10)	5.32E-02 (0.94)	8.32E+00 (2.44)	5.34E+00 (1.34)	6.10E-02 (5.37)
2622		1.65E+00 (1.26)	5.01E-02 (1.01)	6.39E+00 (1.31)	5.23E+00 (1.02)	6.40E-02 (3.53)
2822		1.63E+00 (1.15)	4.74E-02 (1.03)	7.38E+00 (2.29)	4.89E+00 (1.38)	6.18E-02 (6.90)
3022		1.55E+00 (1.05)	4.71E-02 (0.96)	6.66E+00 (1.00)	5.03E+00 (1.02)	6.02E-02 (5.24)
3222		1.51E+00 (0.62)	4.60E-02 (0.48)	6.80E+00 (0.85)	5.06E+00 (1.06)	6.96E-02 (3.33)
3422		1.44E+00 (1.49)	4.54E-02 (1.29)	6.51E+00 (3.29)	4.99E+00 (2.05)	6.56E-02 (1.28)
3622		1.29E+00 (1.28)	4.40E-02 (1.12)	7.25E+00 (1.51)	4.70E+00 (1.67)	6.35E-02 (1.20)
3822		9.79E-01 (0.87)	3.68E-02 (0.71)	7.29E+00 (1.06)	4.11E+00 (0.99)	7.01E-02 (2.72)
4022		4.16E-01 (1.91)	2.16E-02 (1.51)	7.25E+00 (1.93)	4.18E+00 (1.86)	7.43E-02 (1.63)

File ID KE02  
 Comment DN23-14, 4mmStep, 4mmColli.  
 Measurement date 1997/ 2/19  
 Decay correct date 1992/11/16

Table 2.1.36. Example of relative errors (%) on FP nuclides in the process of non-destructive  $\gamma$ -spectrum analysis  
(NT3G24-C7 1444 mm position from top)

	$^{134}\text{Cs}$	$^{137}\text{Cs}$						$^{144}\text{Ce}$			$^{154}\text{Eu}$				
Energy (keV)	661.66	563.27	569.30	604.30	795.78	801.86	1038.53	1167.89	1365.17	696.51	1489.16	2185.66	123.14	996.35	1274.42
$\sigma_1$	0.07	0.37	0.28	0.09	0.09	0.26	1.33	0.81	0.55	2.53	3.67	1.60	3.36	1.25	0.58
$\sigma_2$	1.04	1.27	1.21	1.04	1.21	1.21	1.06	1.14	1.51	1.10	1.74	3.66	5.54	1.08	1.32
$\sigma_3$	1.04	1.32	1.24	1.04	1.21	1.24	1.70	1.40	1.61	2.76	4.06	3.99	6.48	1.65	1.44
$\sigma_4$	1.04					0.62				0.93			0.06		
$\sigma_5$						1.21				1.40			1.04		

	$^{106}\text{Ru}$						$^{125}\text{Sb}$					
Energy (keV)	511.86	621.93	1128.07	1562.25	1796.94	1988.44	2112.54	2366.04	2405.97	427.90	463.38	635.90
$\sigma_1$	0.27	0.33	3.08	4.40	13.65	13.91	9.33	12.88	14.98	2.13	5.42	4.66
$\sigma_2$	1.93	1.01	1.10	1.84	2.10	2.60	3.19	5.20	5.62	3.94	2.95	1.02
$\sigma_3$	1.95	1.06	3.27	4.77	13.81	14.15	9.86	13.89	16.00	4.48	6.17	4.77
$\sigma_4$					0.55		1.18			3.51		
$\sigma_5$										3.66		

Table 2.1.37. Fission yield data and the relative values to U-235T

Fission yield (Atom/100 fissions)		B. F. Rider NEDO-12154(C), ENDF-322.(1981)		
Nuclide( $T_{1/2}$ )	U-235T <sup>#1</sup>	U-238F <sup>#2</sup>	Pu-239T <sup>#1</sup>	Pu-241T <sup>#1</sup>
Cs-132 (30.07 y) Relative	6.186 1.00	6.014 0.97	6.715 1.09	6.707 1.08
Cs-133 (Stable) Cs-134 (2.065 y) Relative	6.700 1.00	6.757 1.01	7.005 1.05	6.321 0.94
Eu-153 (Stable) Eu-154 (8.593 y) Relative	0.1580 1.00	0.4003 2.53	0.3582 2.27	0.5393 3.41
Ce-144 (0.780 y) Relative	5.495 1.00	4.553 0.83	3.739 0.68	4.214 0.77
Ru-106 (1.023 y) Relative	0.4014 1.00	2.484 6.2	4.302 10.7	6.125 15.3
Ag-109 (Stable) Ag-110m (0.684 y) Relative	0.03019 1.00	0.2482 8.2	1.661 55	2.257 75
Sn-124 (Stable) Relative	0.02381 1.00	0.04424 1.86	0.07902 3.32	0.03201 1.34
Sb-125 (2.758 y) Relative	0.02904 1.00	0.04637 1.60	0.1151 4.00	0.04862 1.67

#1: Thermal neutron

#2: Fission spectrum neutron

Table 2.1.38. Comparison of  $\gamma$ -scanning activity ratio (NDA) with those of destructive analysis (DA) at the end of irradiation in PWR

NT3G23-04 (KC03), UO<sub>2</sub> (U235 : 4.1%)

KC03 No.	03	07	20	52	87
Meas. position from grip (mm)	168	328	848	2128	3528
from top (mm)	193	353	873	2153	3553
Sampling position from top (mm)	201	361	881	2161	3561
SF-95 No.	1-1	1-2	1-3	1-4	1-5
Meas. date	96.1.17	96.1.19	96.1.25	96.1.29	96.1.22
Burnup (GWd/t)	14.7	25.2	36.7	38.1	38.4
<sup>134</sup> Cs/ <sup>137</sup> Cs					
DA	0.646	1.11	1.55	1.56	1.31
NDA	0.596	1.10	1.57	1.57	1.31
Difference (%)	+8.3 <sup>#1</sup>	+1.5	-1.3	-0.6	-0.2
<sup>154</sup> Eu/ <sup>137</sup> Cs					
DA	2.37E-2	4.38E-2	5.87E-2	5.94E-2	4.95E-2
NDA	2.21E-2	4.29E-2	6.00E-2	5.99E-2	4.95E-2
Difference (%)	+7.2 <sup>#1</sup>	+2.3	-2.2	-0.9	+0.2
<sup>144</sup> Ce/ <sup>137</sup> Cs					
DA	13.2	12.4	12.4	11.2	12.3
NDA	13.7	12.7	12.3	11.9	12.4
Difference (%)	-4.0 <sup>#1</sup>	-2.3	+0.2	-5.5	-0.9

#1: Caused by large difference of measurement position between NDA and DA.

Table 2.1.39. Comparison of  $\gamma$ -scanning activity ratio (NDA) with those of destructive analysis (DA) data at the end of irradiation in BWR

NT3G23-10 (KC04, 05), UO<sub>2</sub> (U235 : 2.6%), Gd<sub>2</sub>O<sub>3</sub>(6.0%)fuel

Decay corrected at the end of irradiation (1992.06.19)

Sampling position from top(mm)	176	336	856	2136	3536
SF-96 No.	1–1	1–2	1–3	1–4	1–5
Burnup (GWd/t)	8.0	16.8	28.9	29.6	24.7
<sup>134</sup> Cs/ <sup>137</sup> Cs					
DA	0.456	0.935	1.47	1.48	1.24
NDA	0.449	0.947	1.47	1.49	1.25
Difference (%)	+1.5	−1.2	−0.6	−0.7	−0.6
<sup>154</sup> Eu/ <sup>137</sup> Cs					
DA	2.56E–2	4.44E–2	6.03E–2	5.89E–2	5.17E–2
NDA	2.68E–2	4.56E–2	6.09E–2	5.97E–2	5.33E–2
Difference (%)	−4.6	−2.6	−1.0	−1.4	−3.0
<sup>144</sup> Ce/ <sup>137</sup> Cs					
DA	15.4	13.8	12.1	12.0	13.5
NDA	16.4	14.3	12.8	12.4	13.5
Difference (%)	−6.2	−3.4	−5.4	−3.0	−0.0

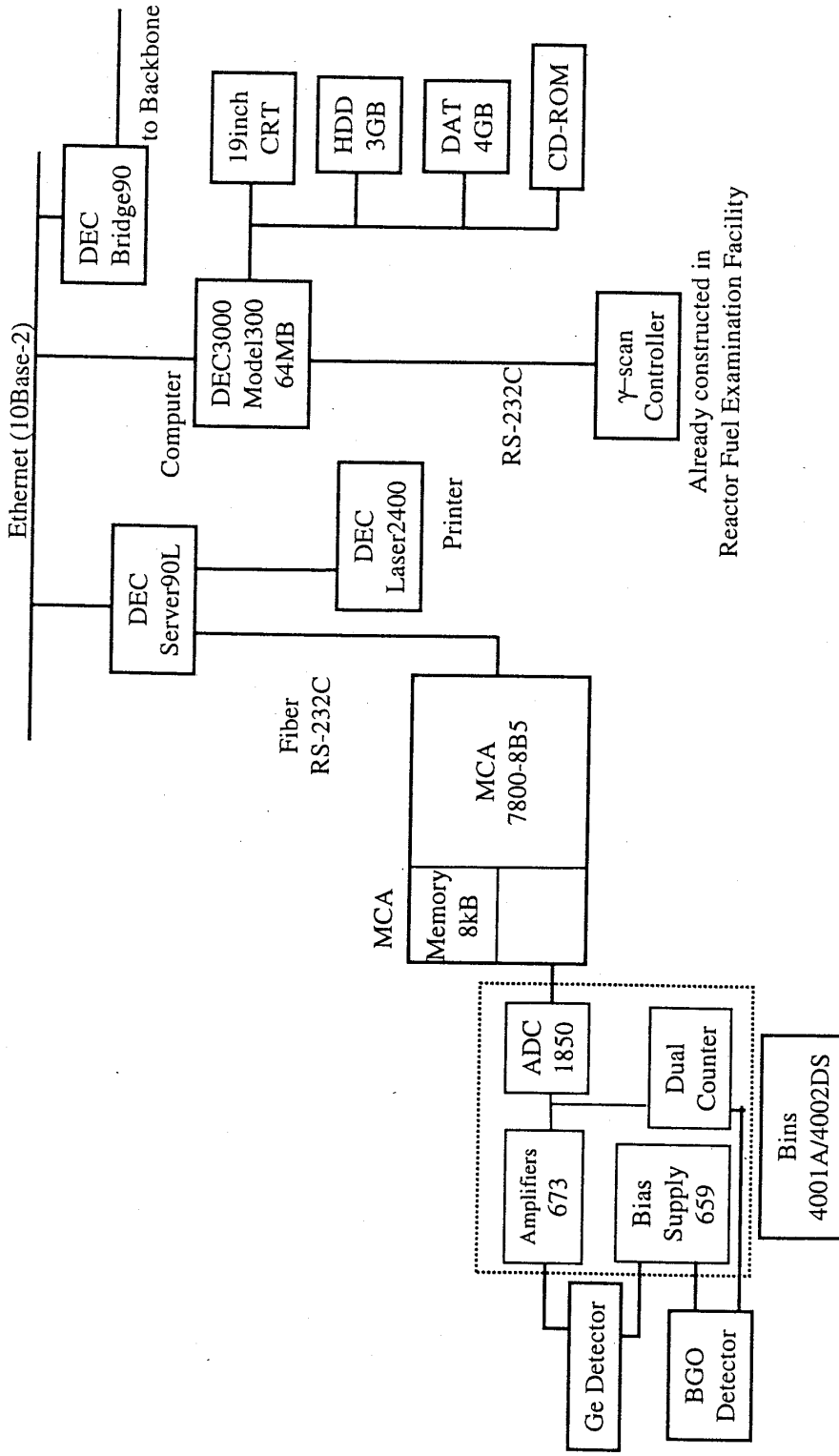


Fig. 2.1.1. Composition of burnup measurement system.

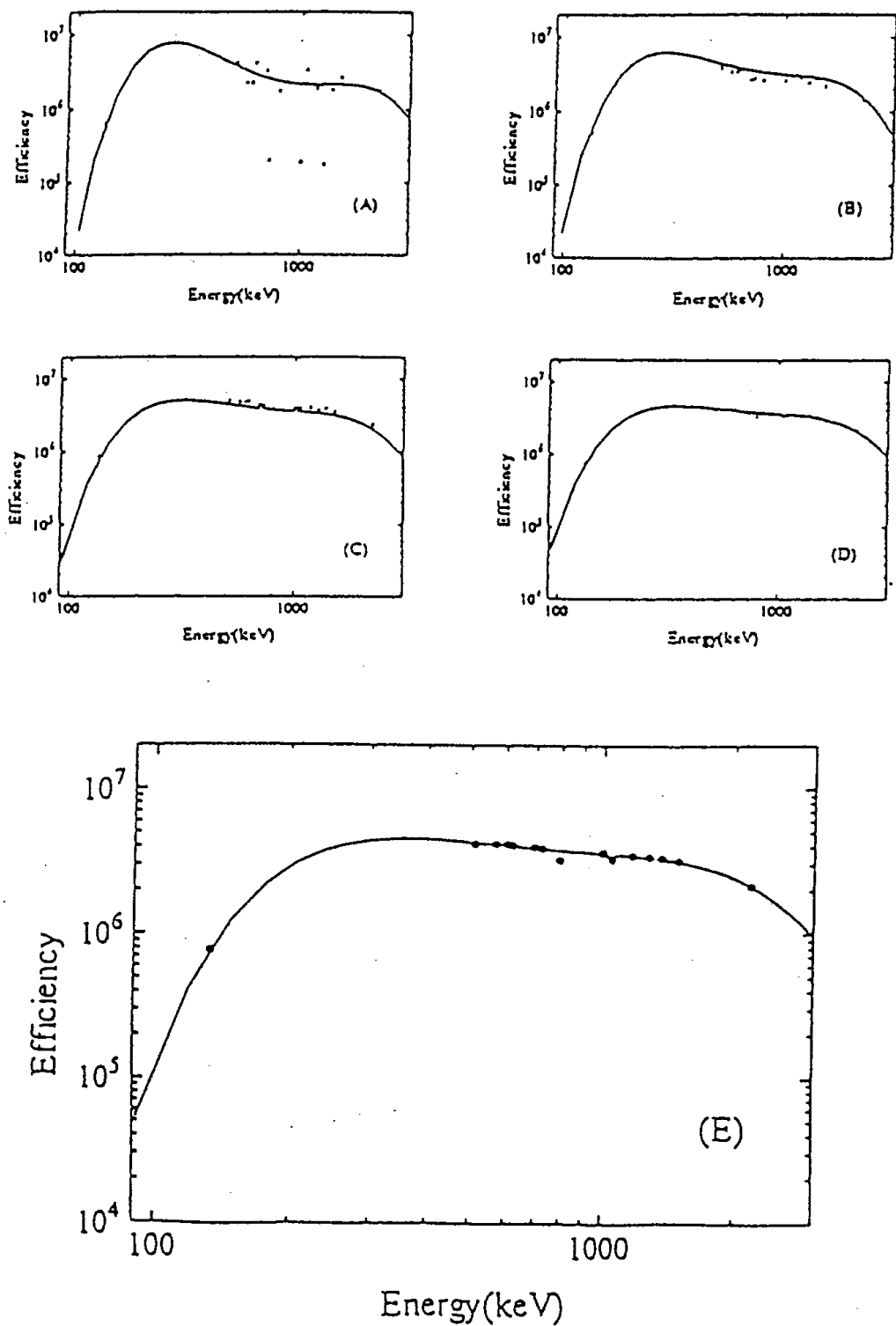


Fig. 2.1.2. Successive approximation of relative efficiency curve  
 (Iteration: 5, A→E).

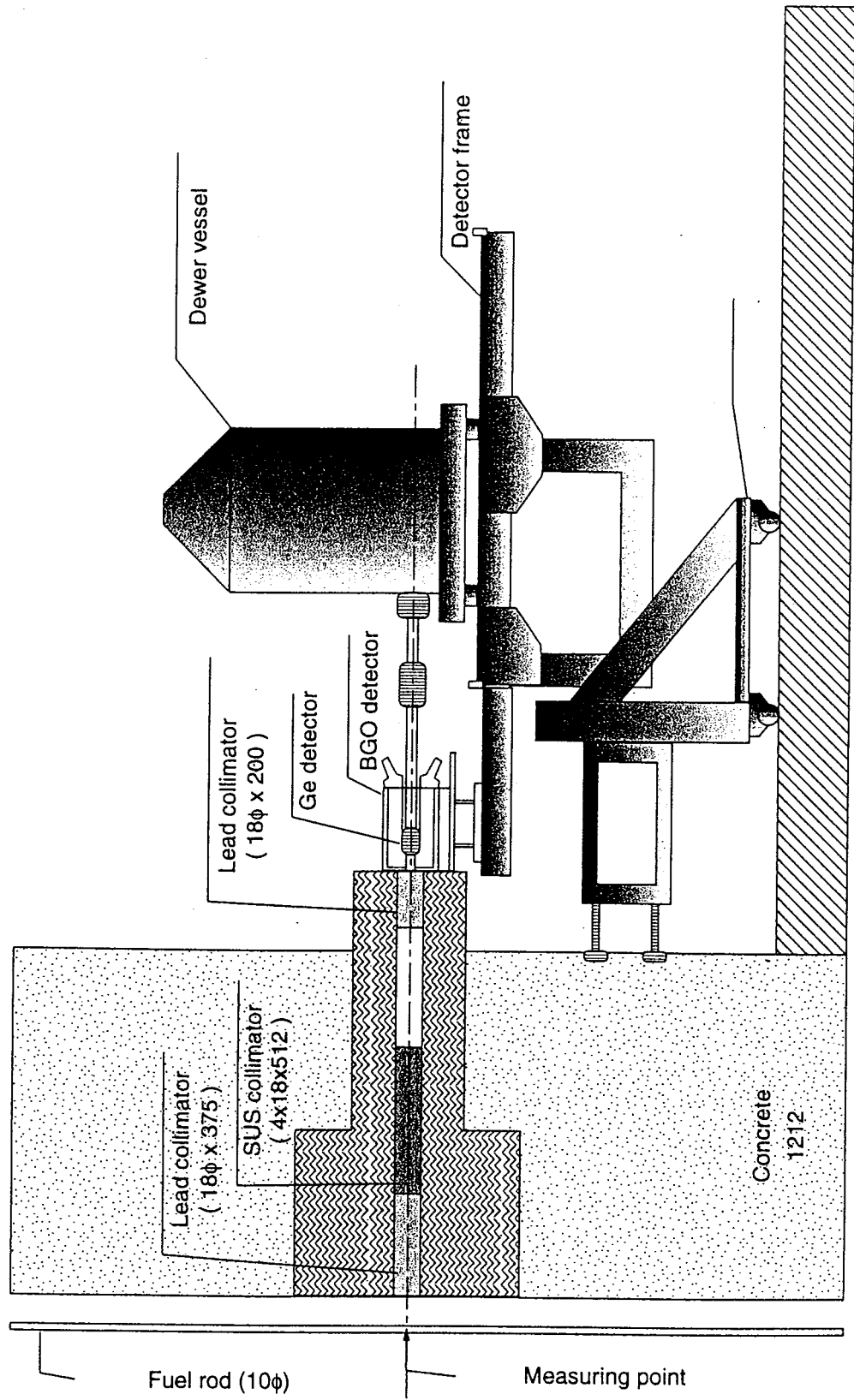


Fig. 2.1.3. The geometry of gamma scanning measurement.

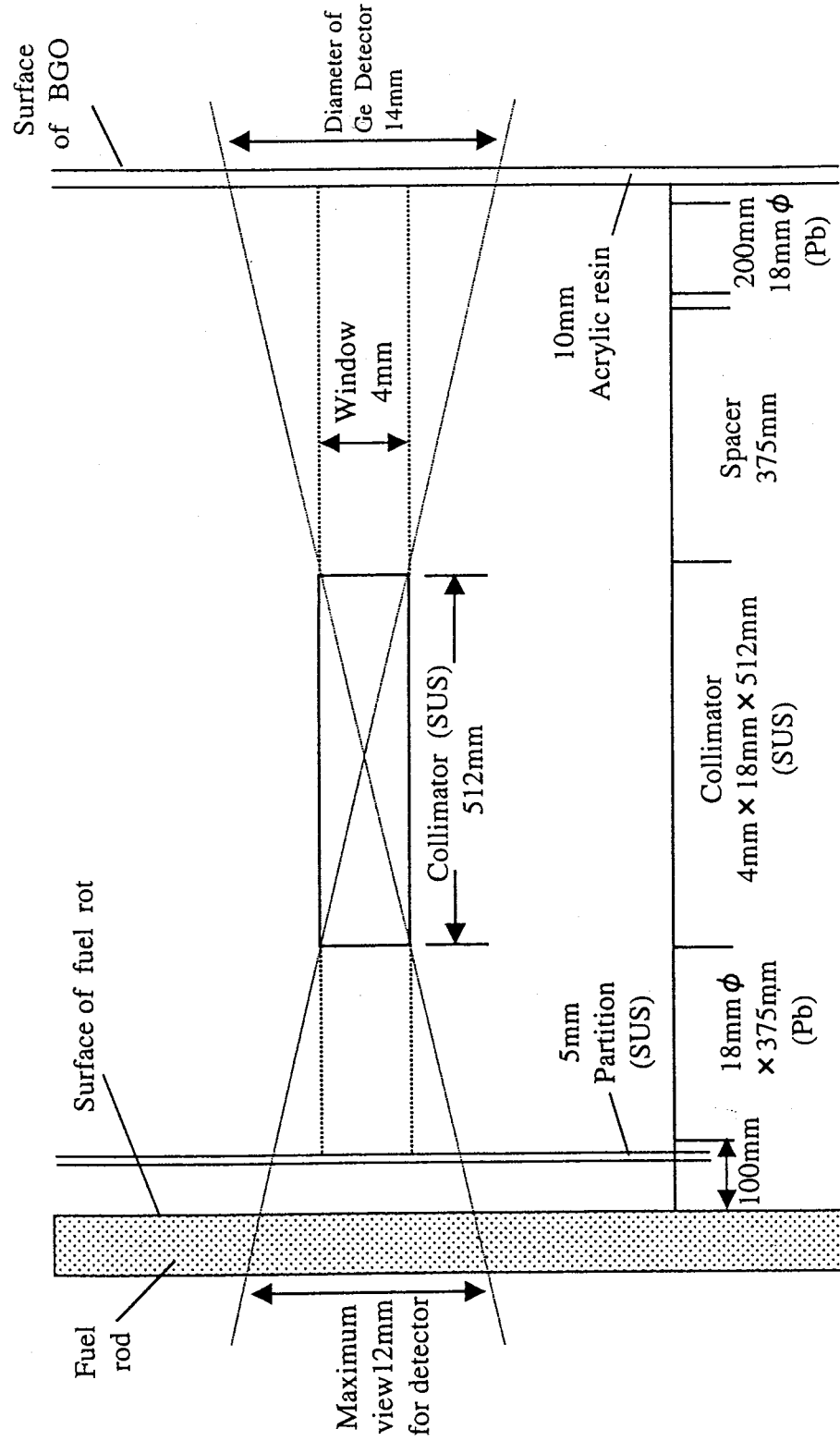


Fig. 2.1.4. A diagram of collimator arrangement.

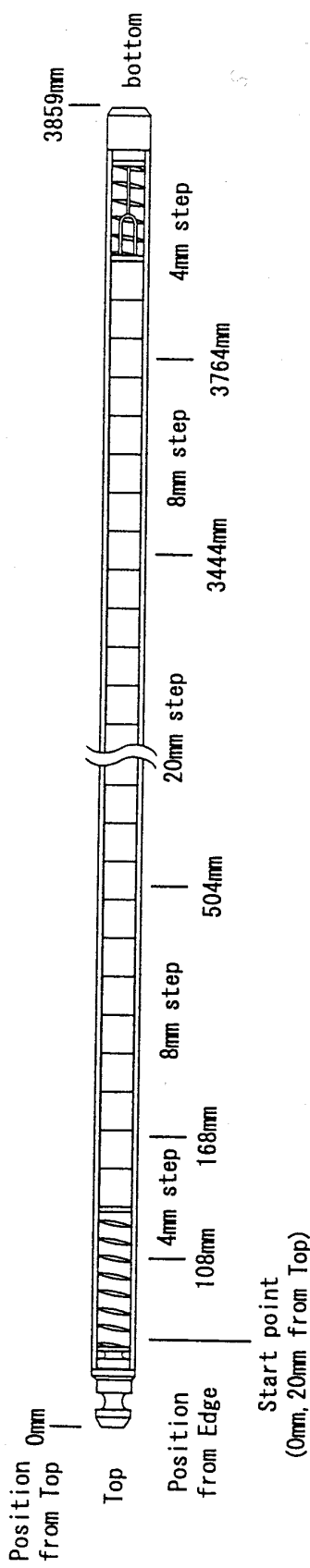


Fig. 2.1.5 An Example of  $\gamma$ -scanning measurement steps in PWR spent fuel rod (NT3G24-G7, burnup 44, 300MWd/t)

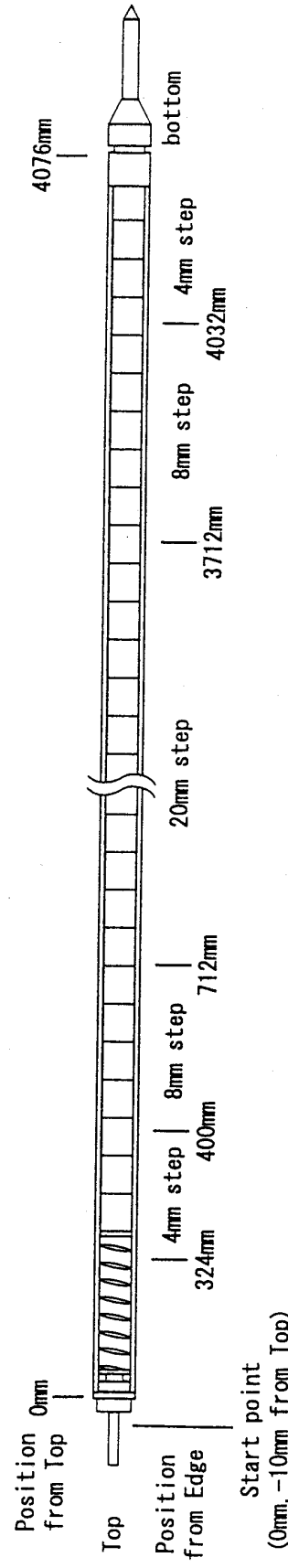


Fig. 2.1.6 An Example of  $\gamma$ -scanning measurement steps in BWR spent fuel rod (2F2DN23-07, burnup 27, 900MWd/t)

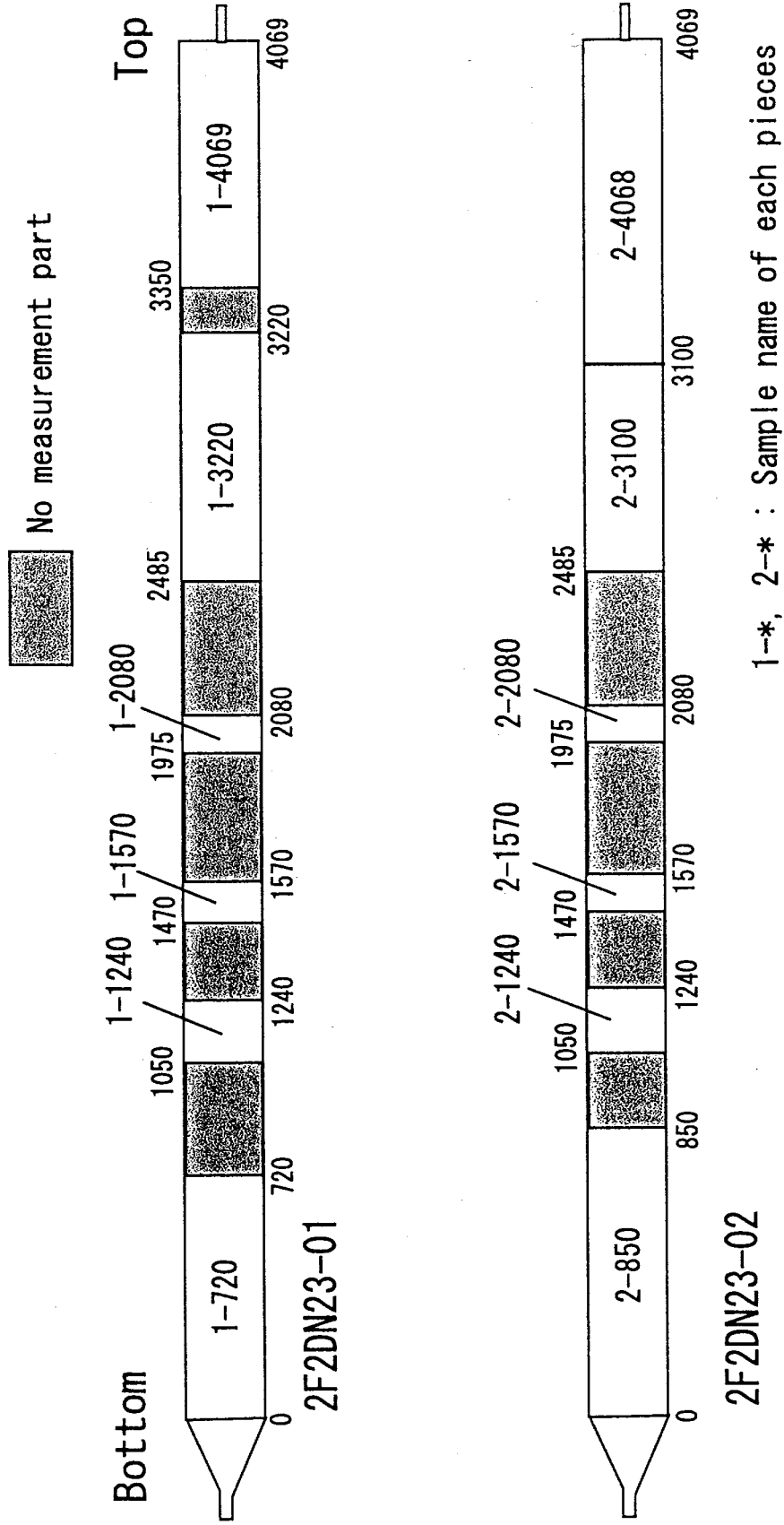


Fig. 2.1.7. Fuel rod pieces used for  $\gamma$ -scanning measurement in BWR (2F2DN23-01, 02).

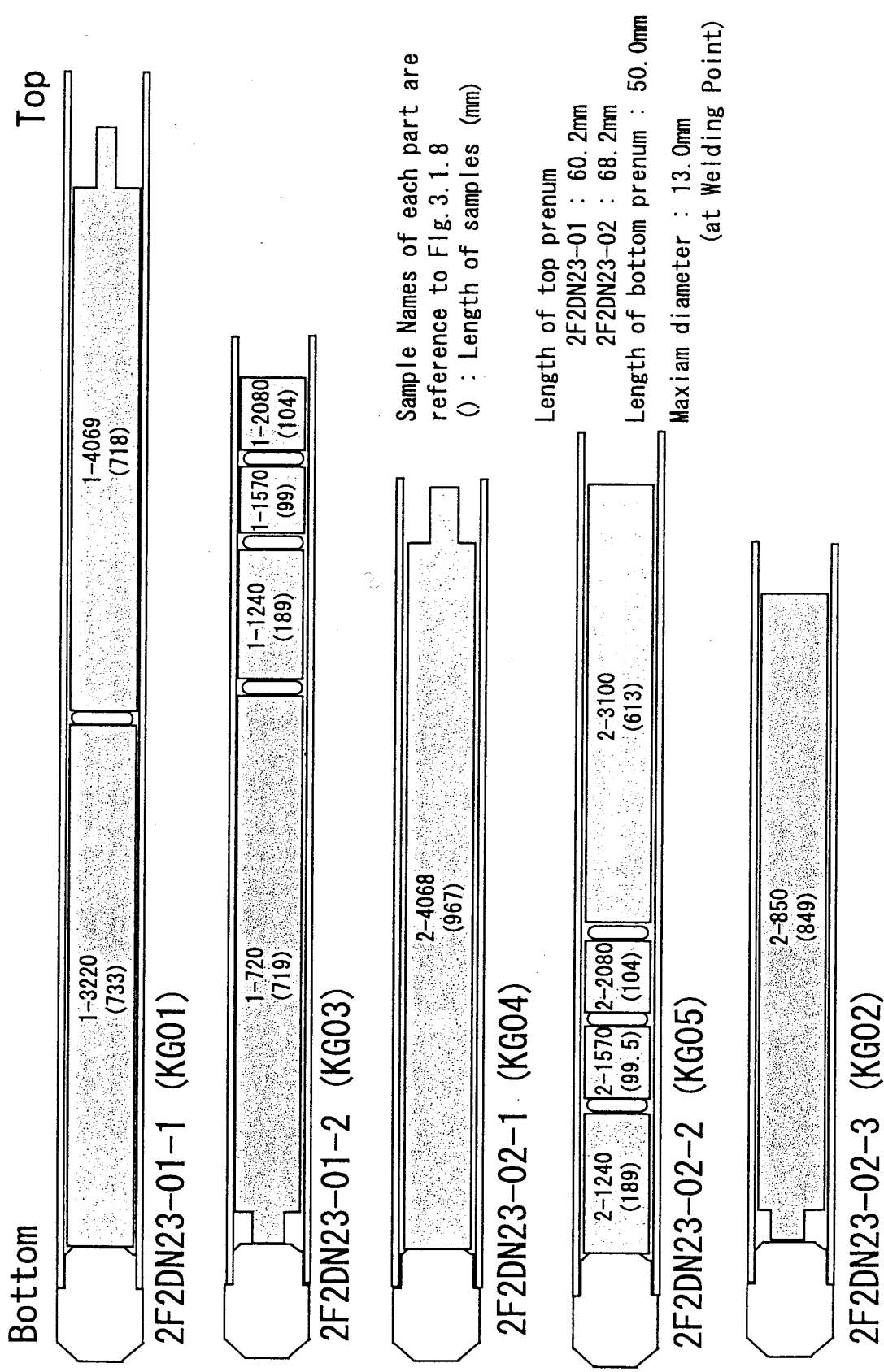


Fig. 2.1.8. Arrangement of BWR rod pieces in Al-case.

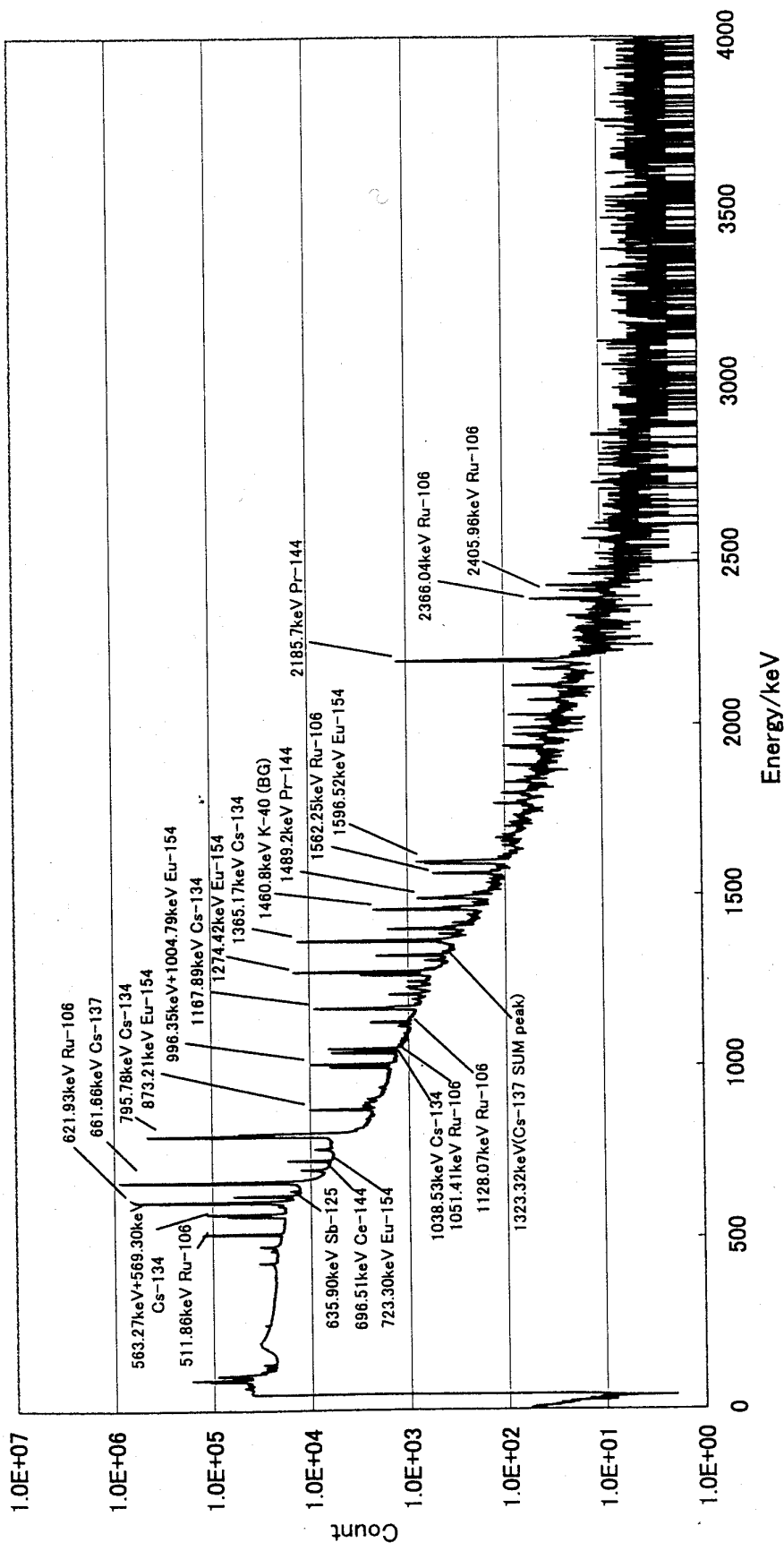


Fig. 2.1.9. An example of  $\gamma$ -spectrum (NT3G24-C7, 1444 mm from top).

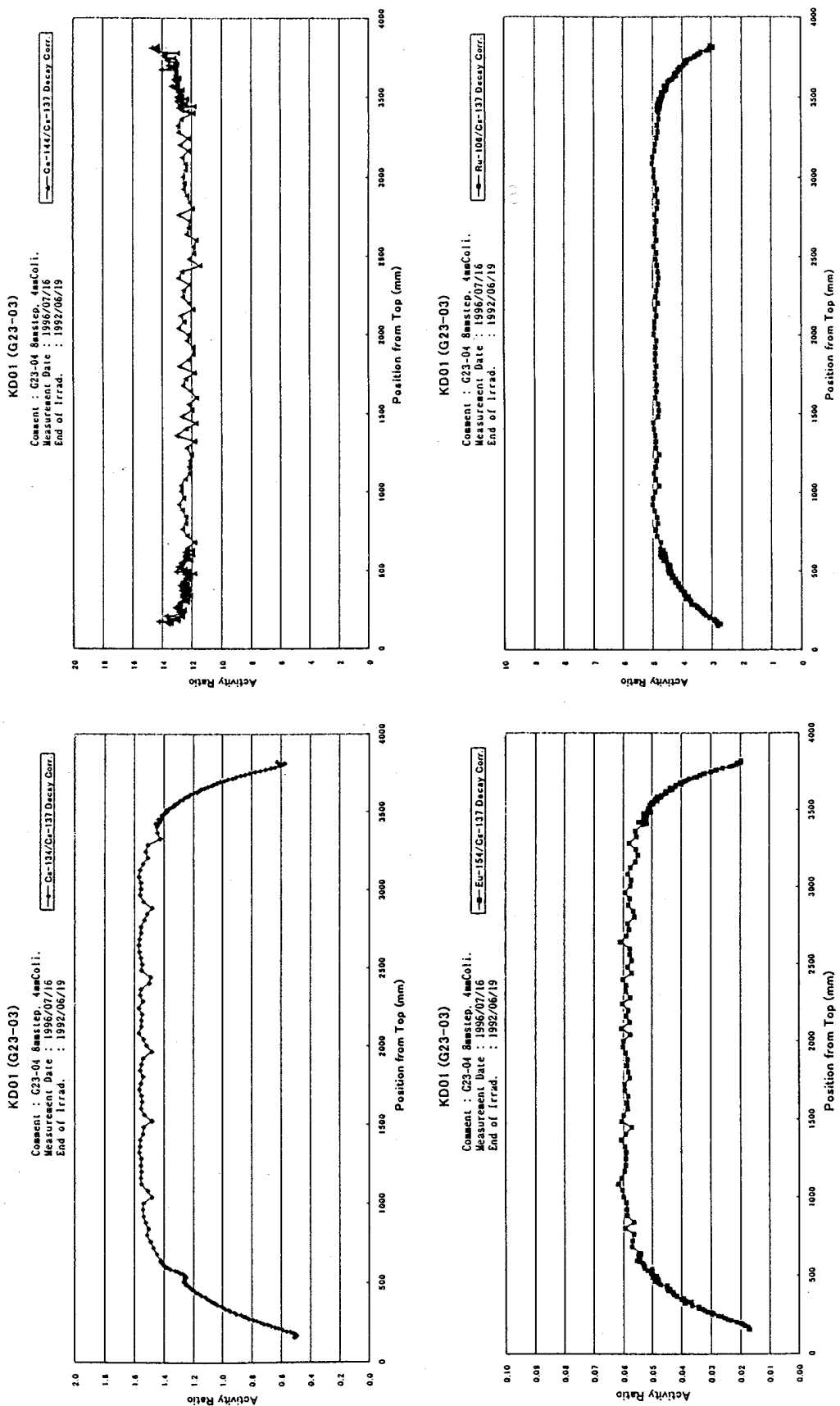


Fig. 2.1.10. Axial profiles of activity ratios measured in NT3G23-C3 (KD01).

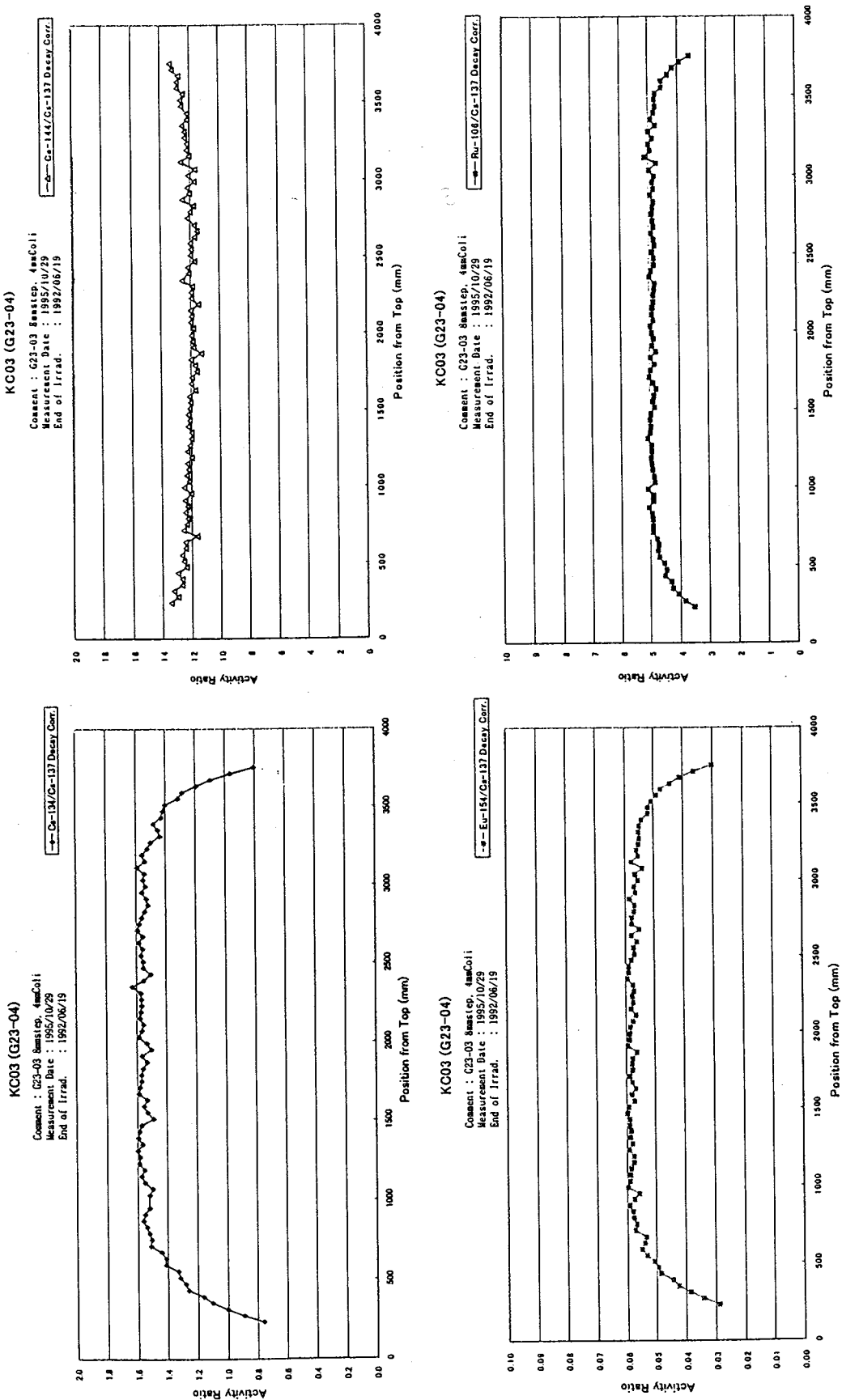


Fig. 2.1.11. Axial profiles of activity ratios measured in NT3G23-A4 (KC03).

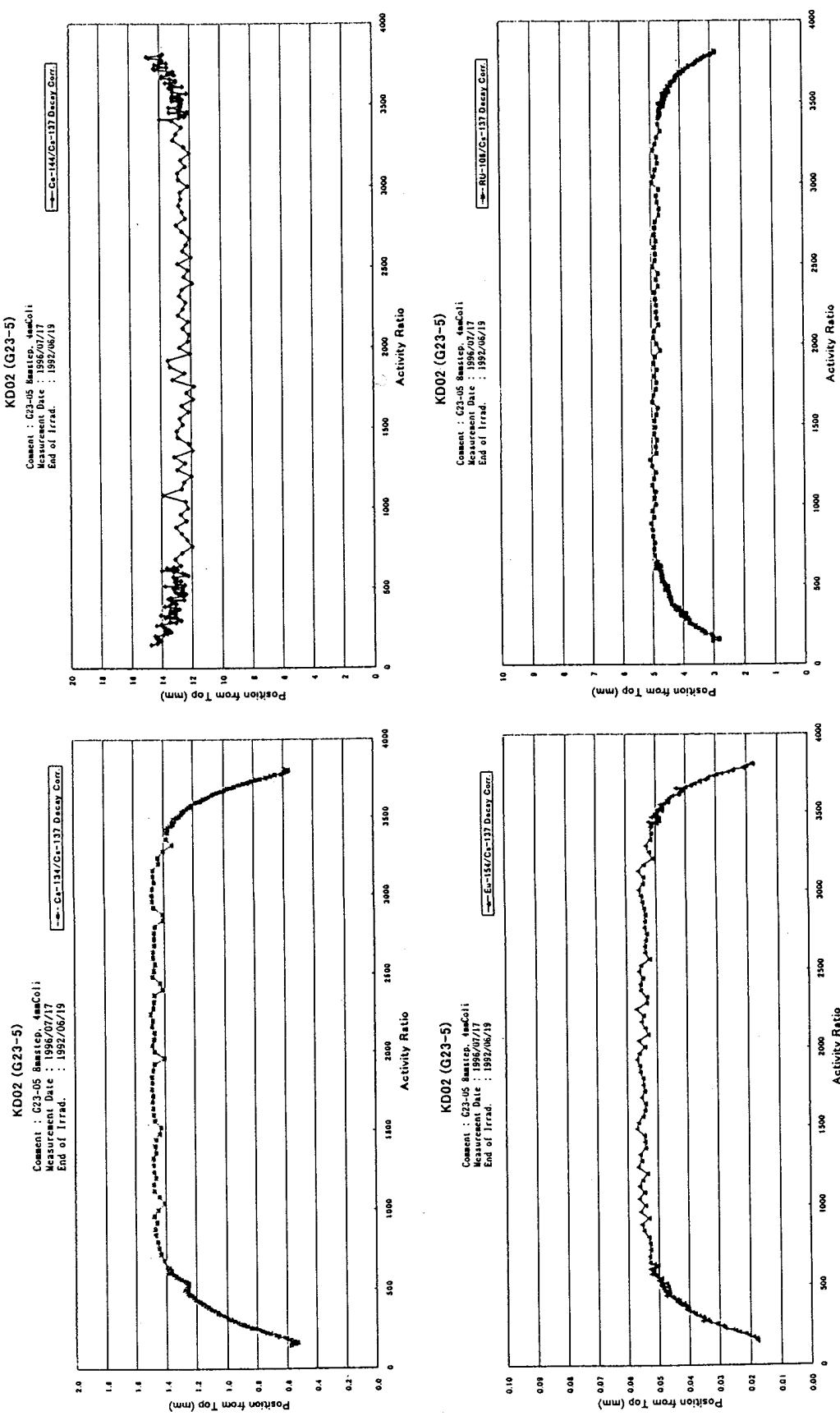


Fig. 2.1.12. Axial profiles of activity ratios measured in NT3G23-C5 (KD02).

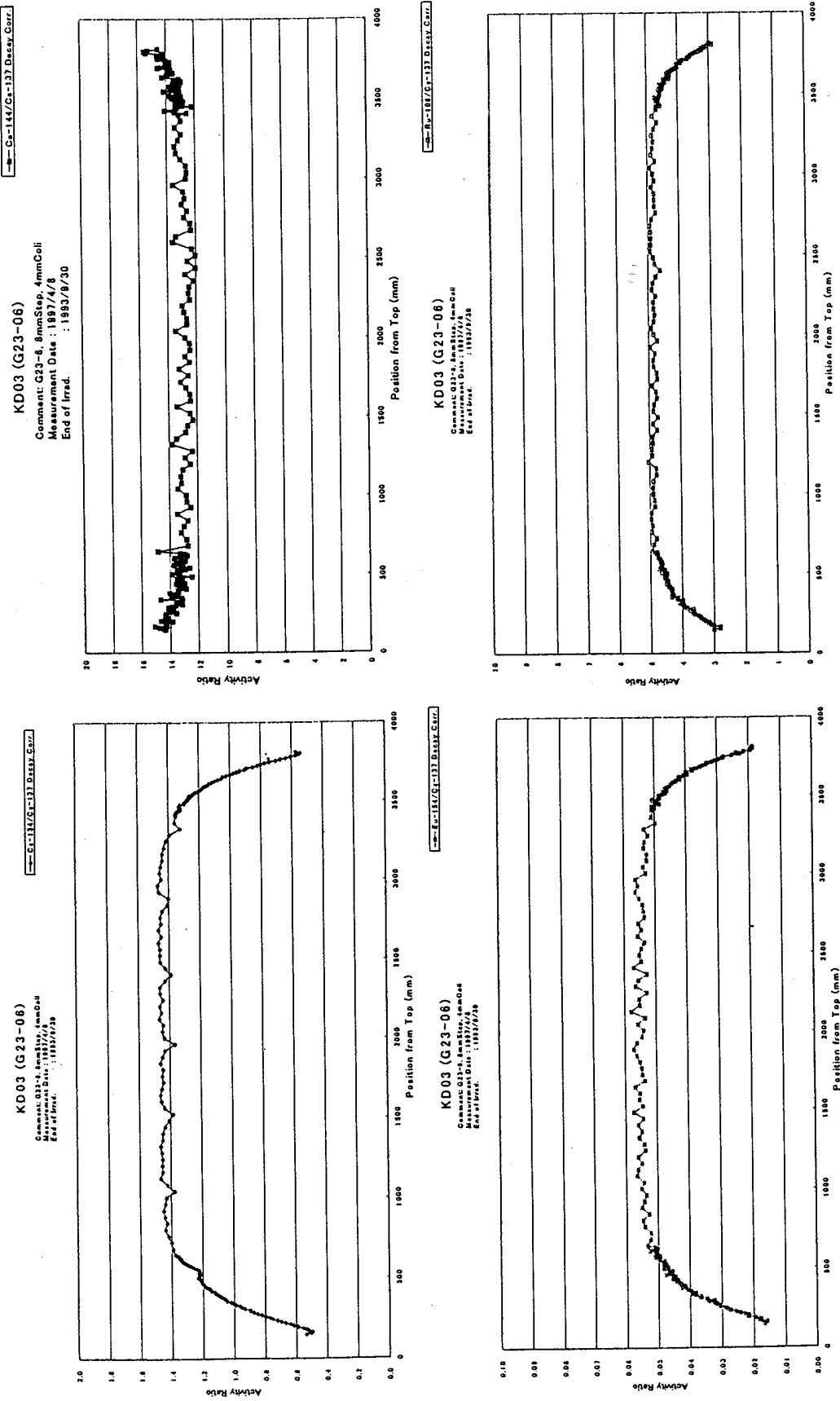


Fig. 2.1.13. Axial profiles of activity ratios measured in NT3G23-A6 (KD03).

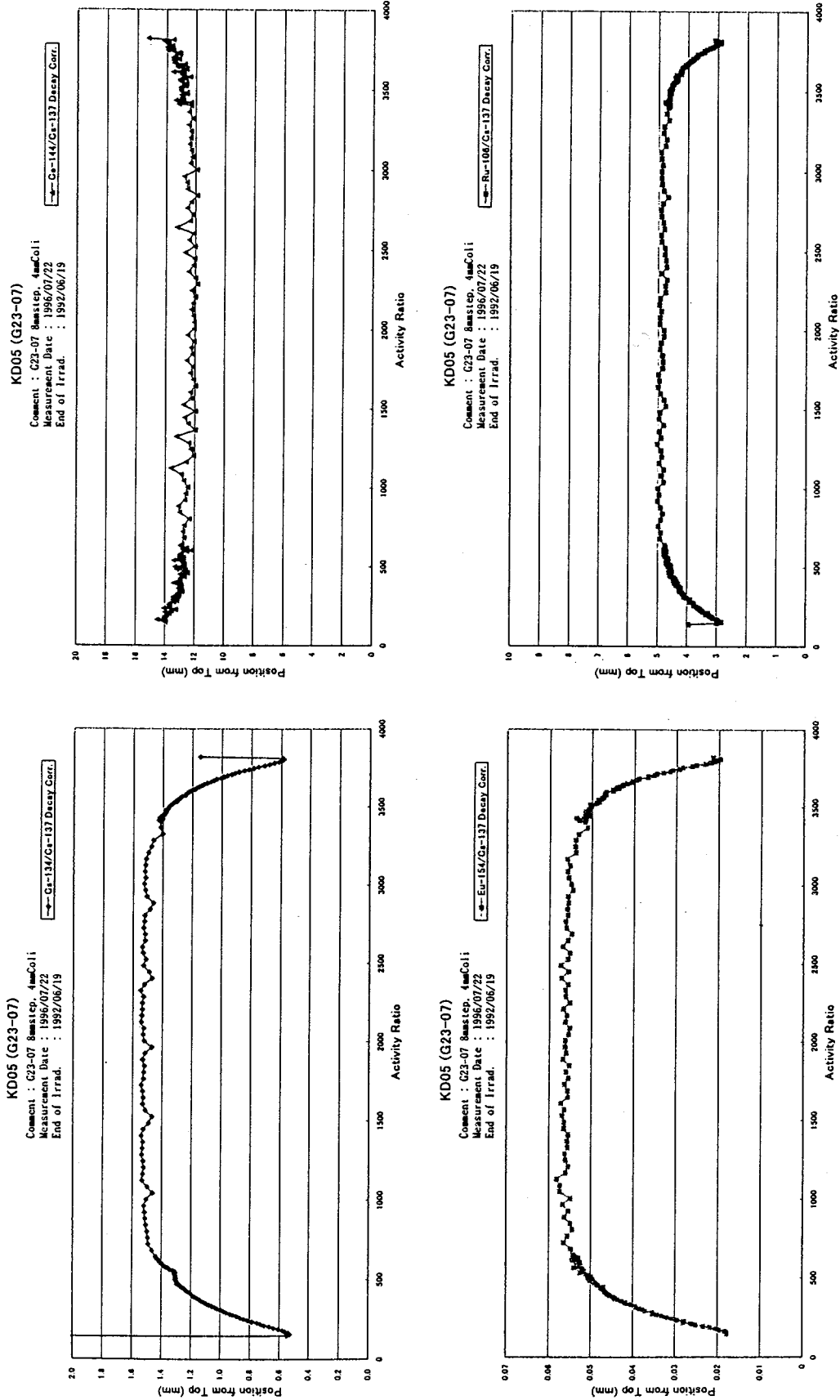


Fig. 2.1.14. Axial profiles of activity ratios measured in NT3G23-C7 (KD05).

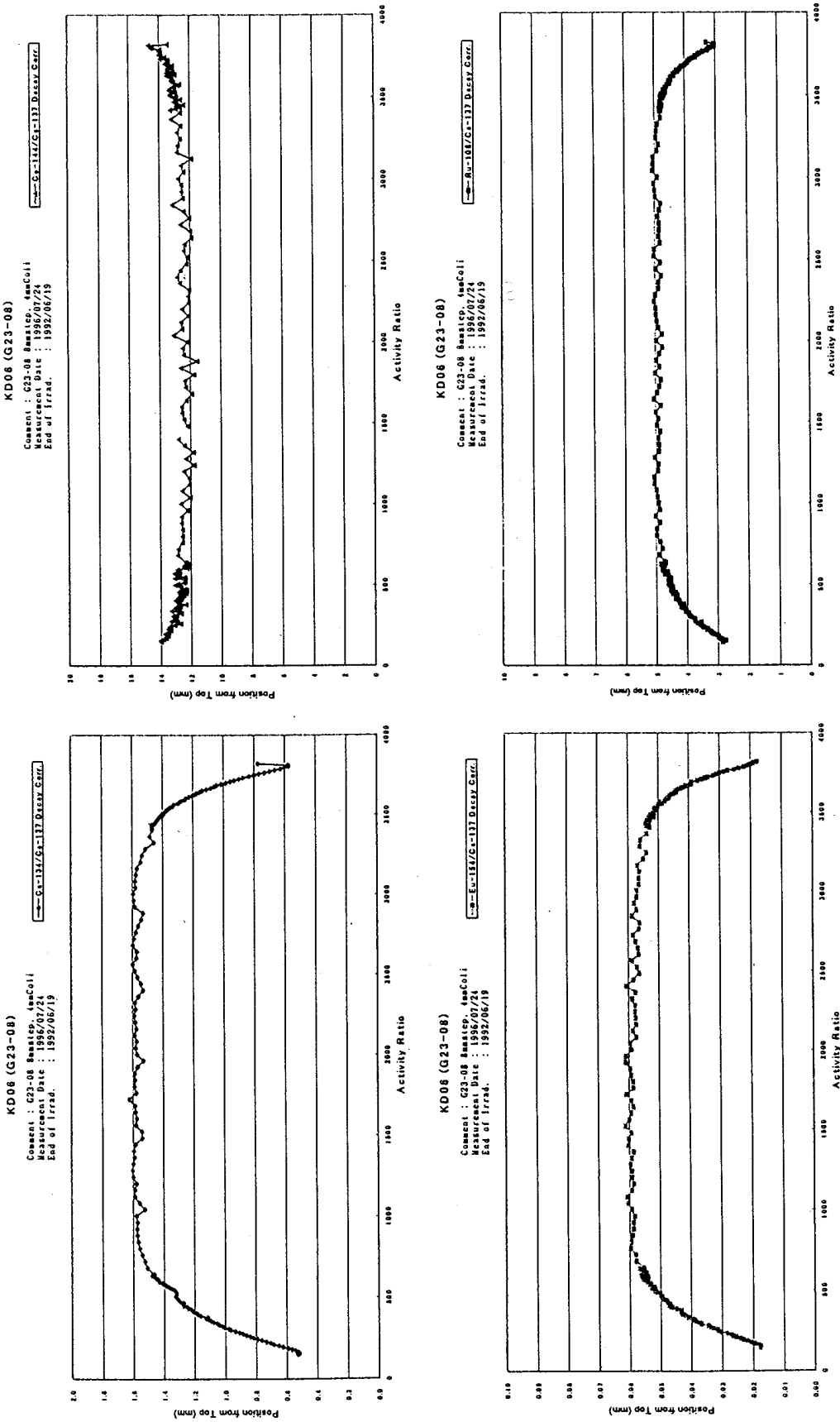


Fig. 2.1.15. Axial profiles of activity ratios measured in NT3G23-A8 (KD06).

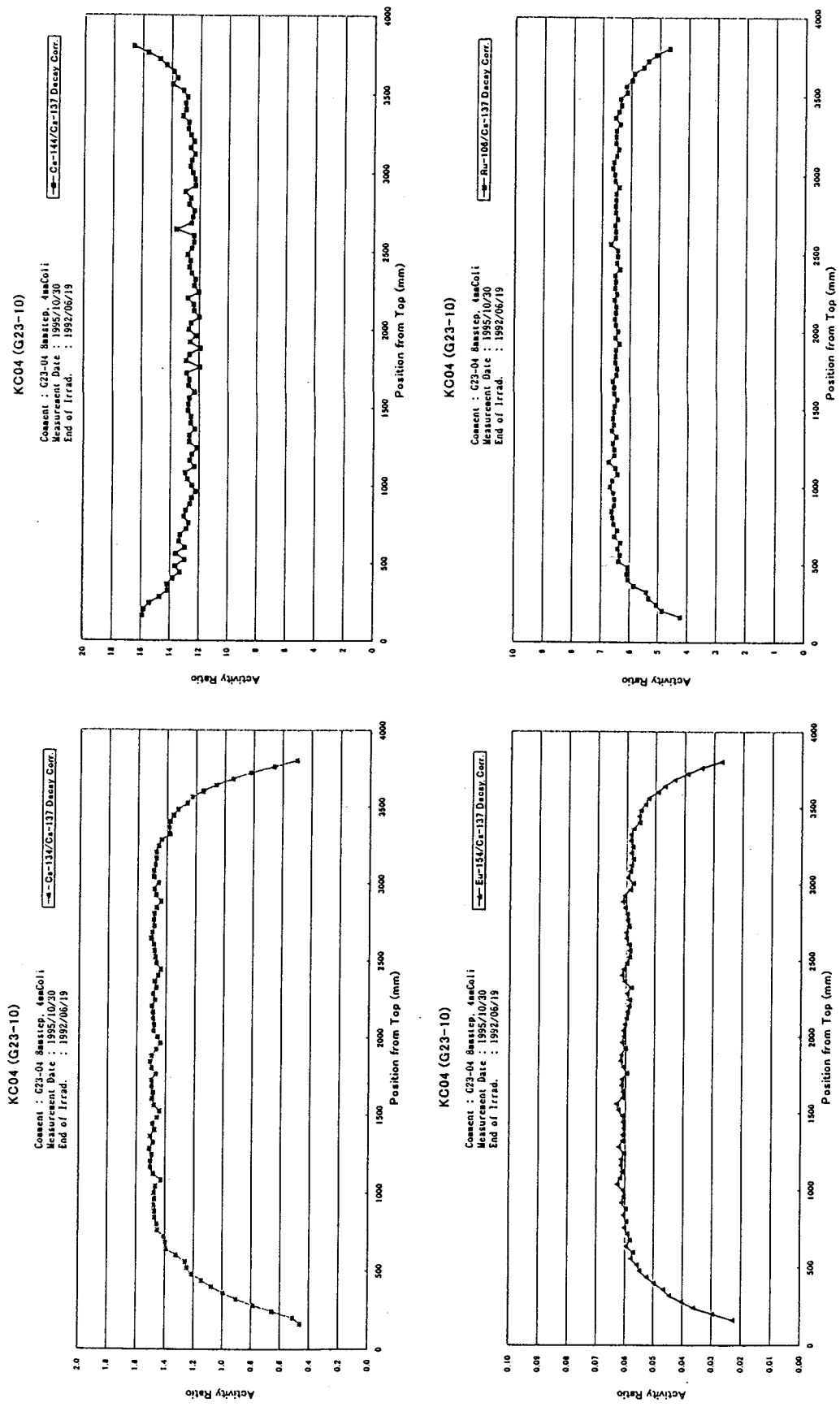


Fig. 2.1.16. Axial profiles of activity ratios measured in NT3G23-B10 (KC04).

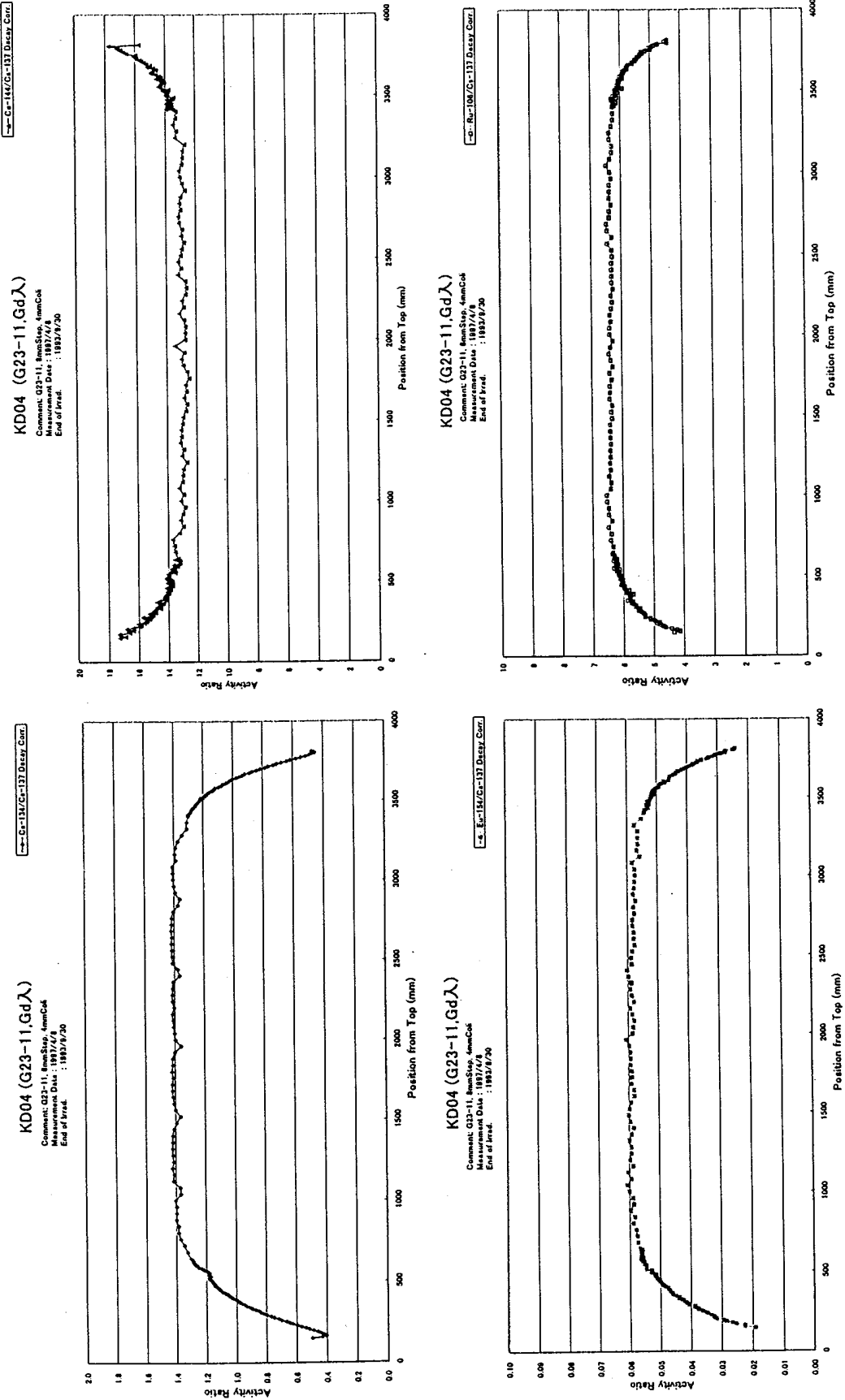


Fig. 2.1.17. Axial profiles of activity ratios measured in NT3G23-D11 (KD04).

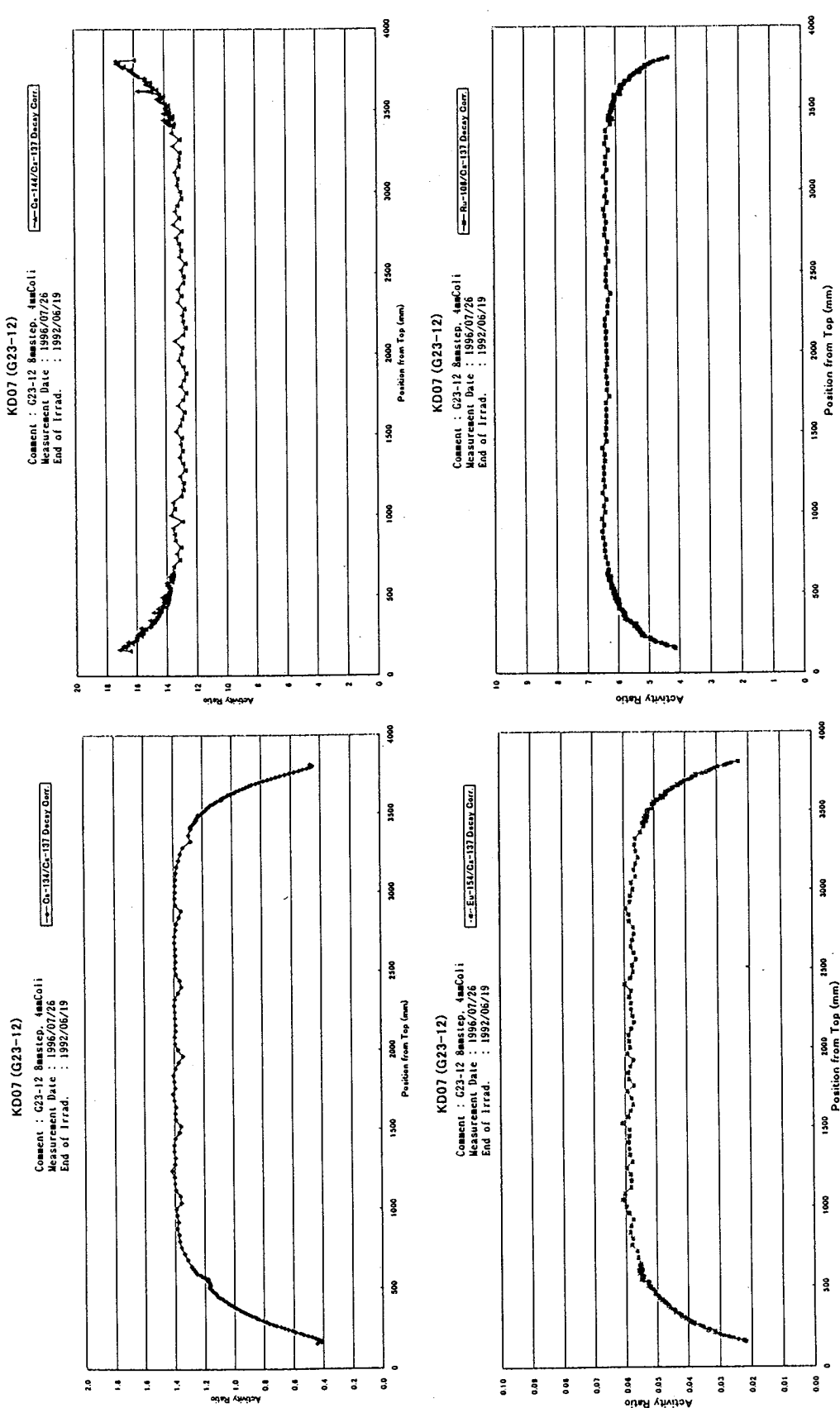


Fig. 2.1.18. Axial profiles of activity ratios measured in NT3G23-B12 (KD07).

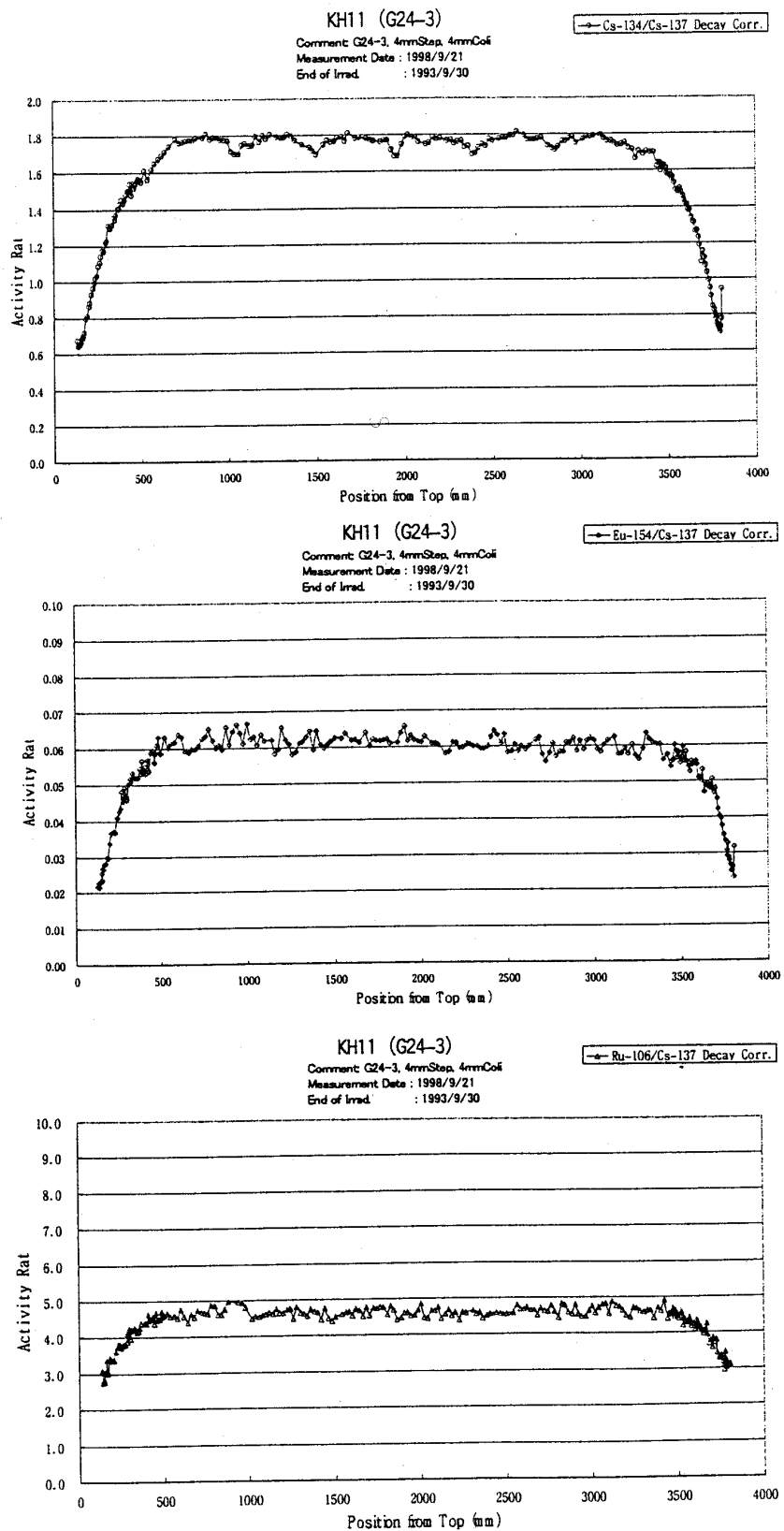


Fig. 2.1.19. Axial profiles of activity ratios measured in NT3G24-C3 (KH11).

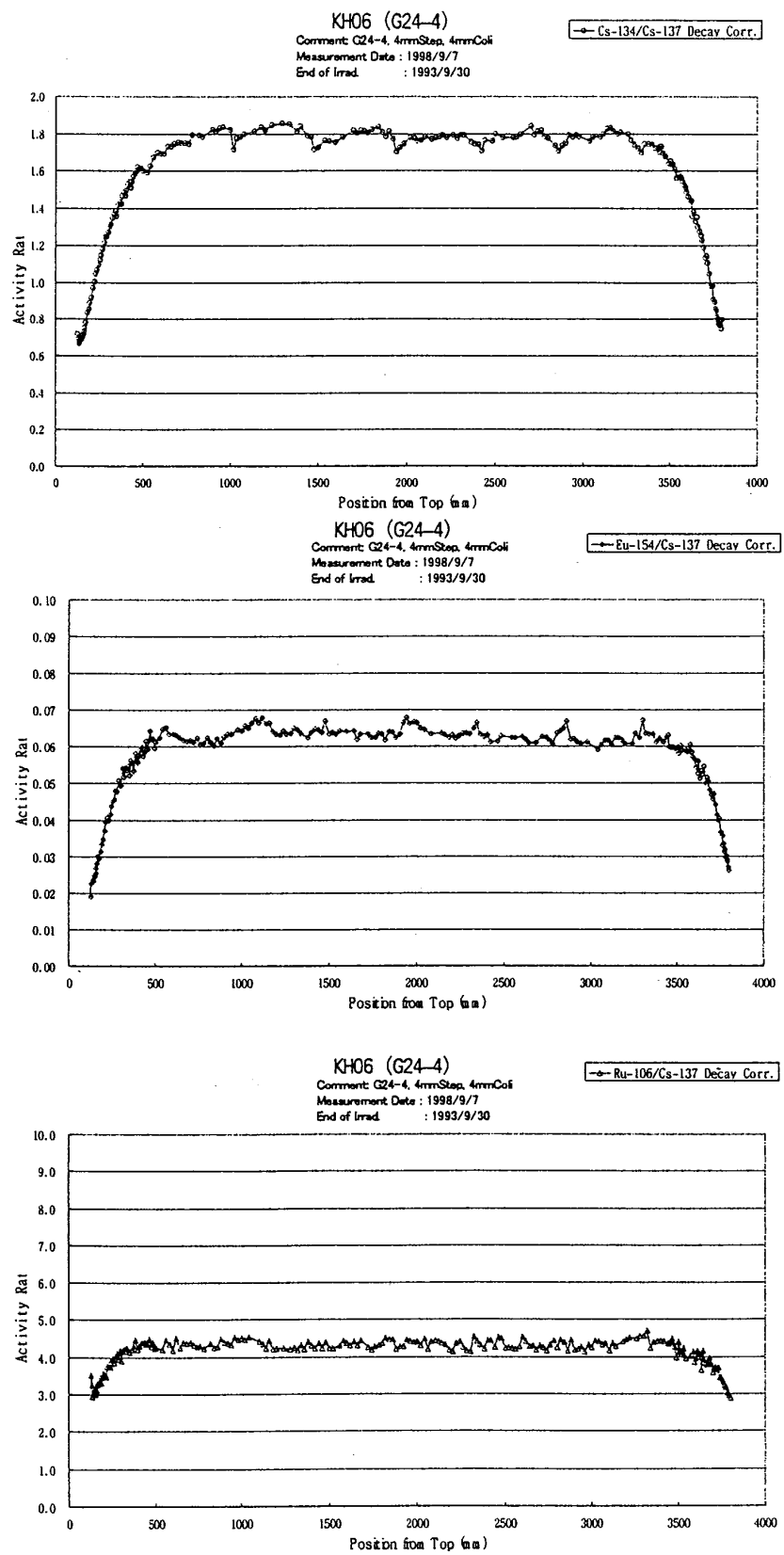


Fig. 2.1.20. Axial profiles of activity ratios measured in NT3G24-A4 (KH06).

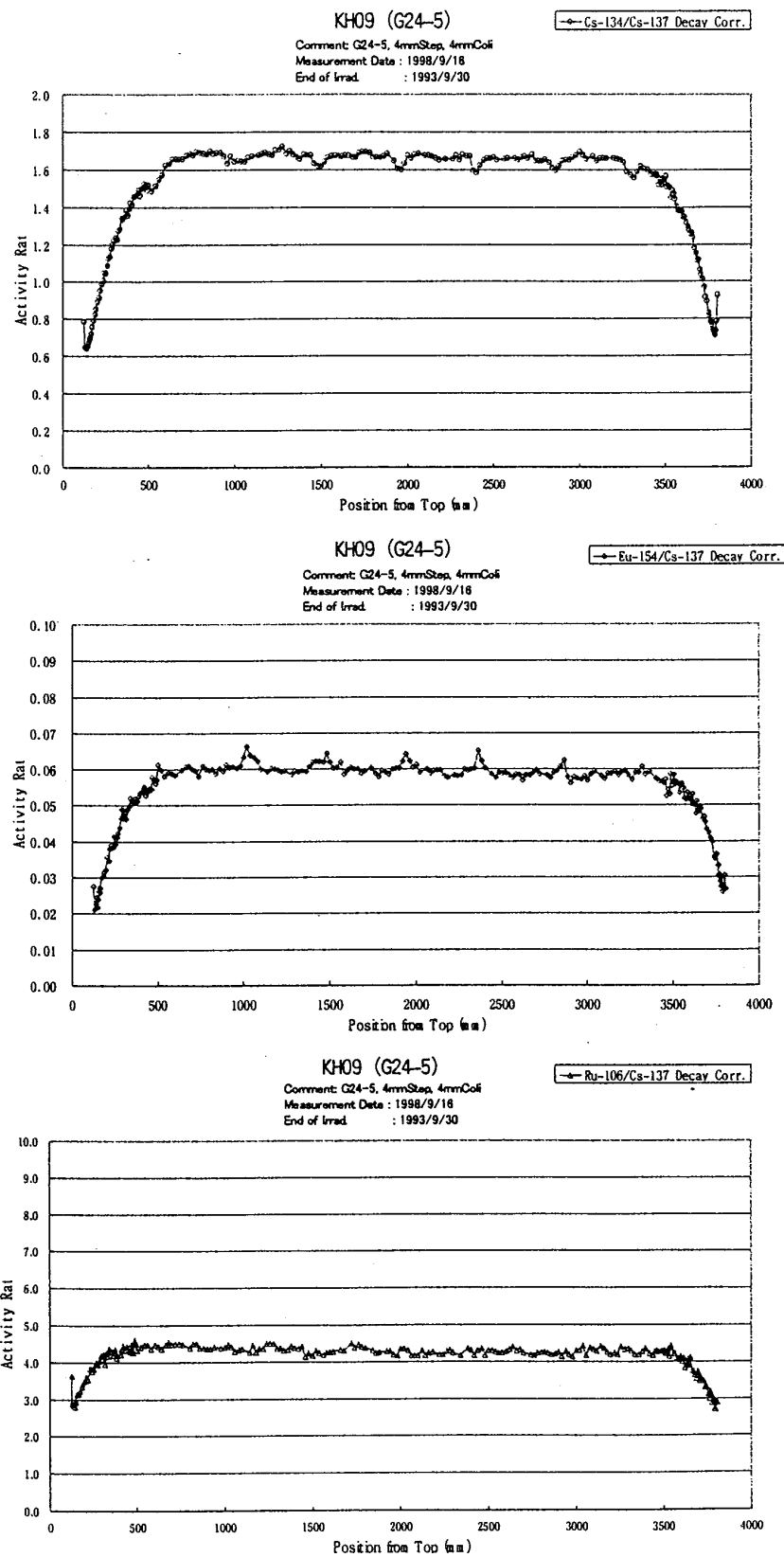


Fig. 2.1.21. Axial profiles of activity ratios measured in NT3G24-C5 (KH09).

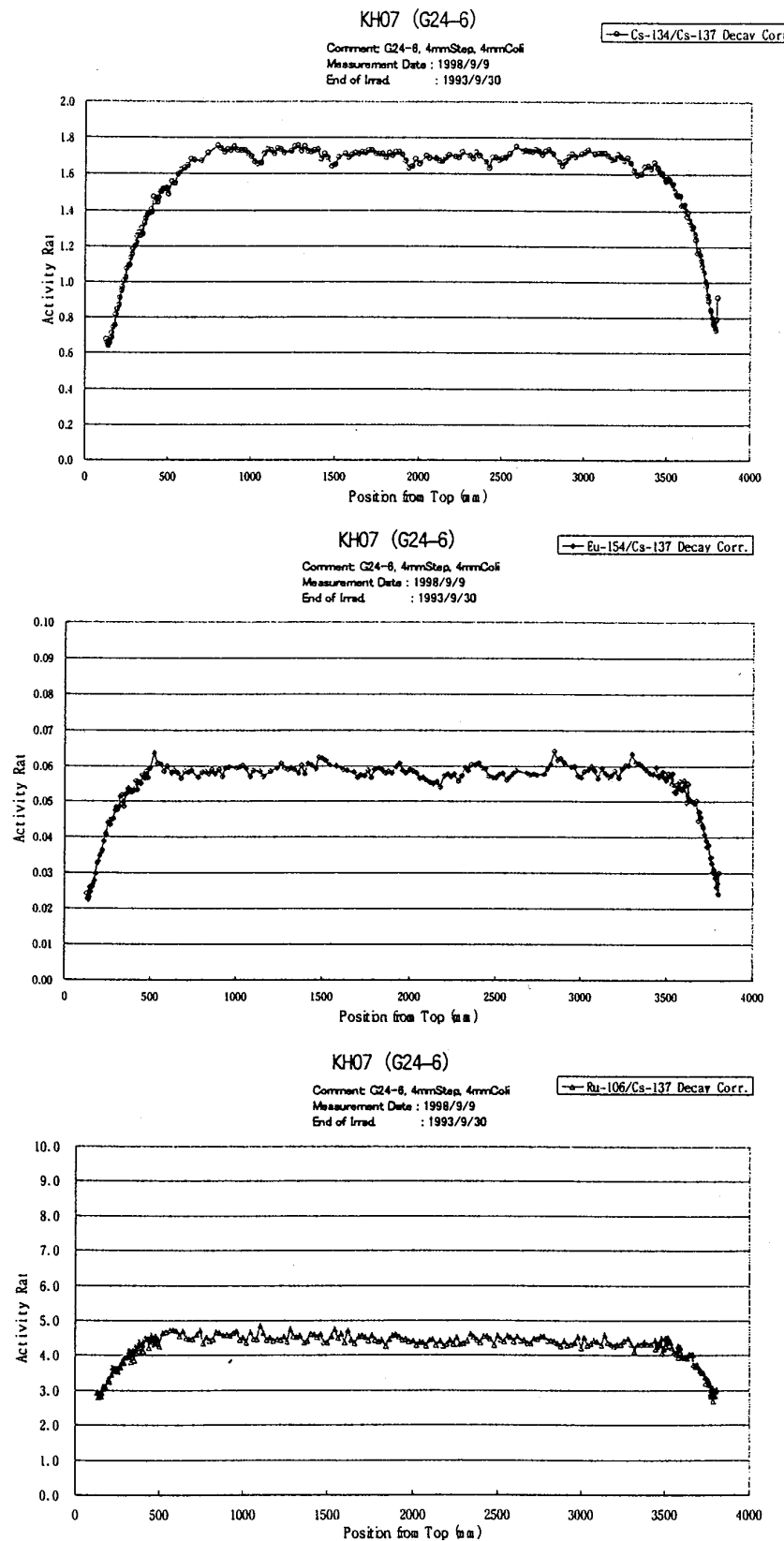


Fig. 2.1.22. Axial profiles of activity ratios measured in NT3G24-A6 (KH07).

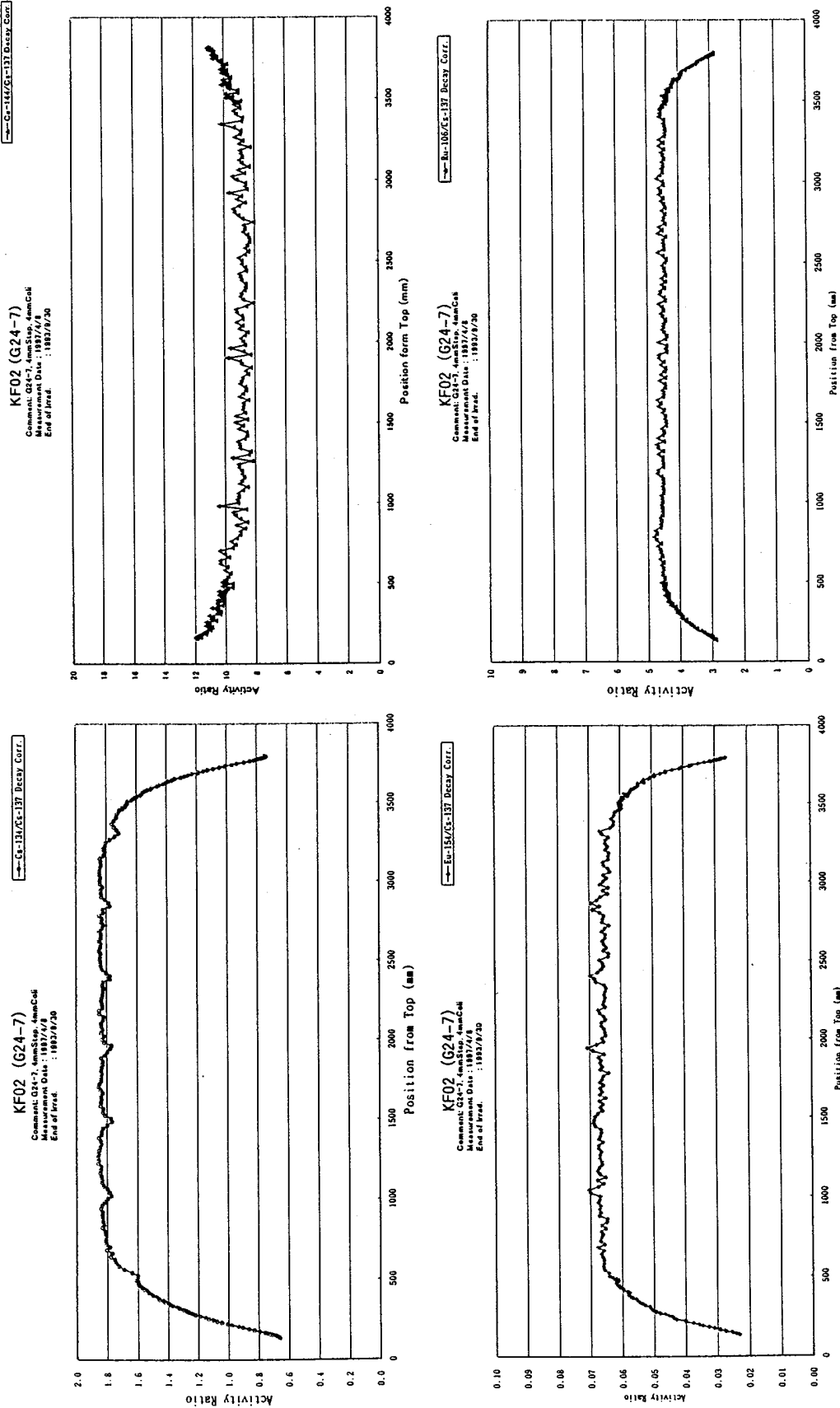


Fig. 2.1.23. Axial profiles of activity ratios measured in NT3G24-C7 (KF02).

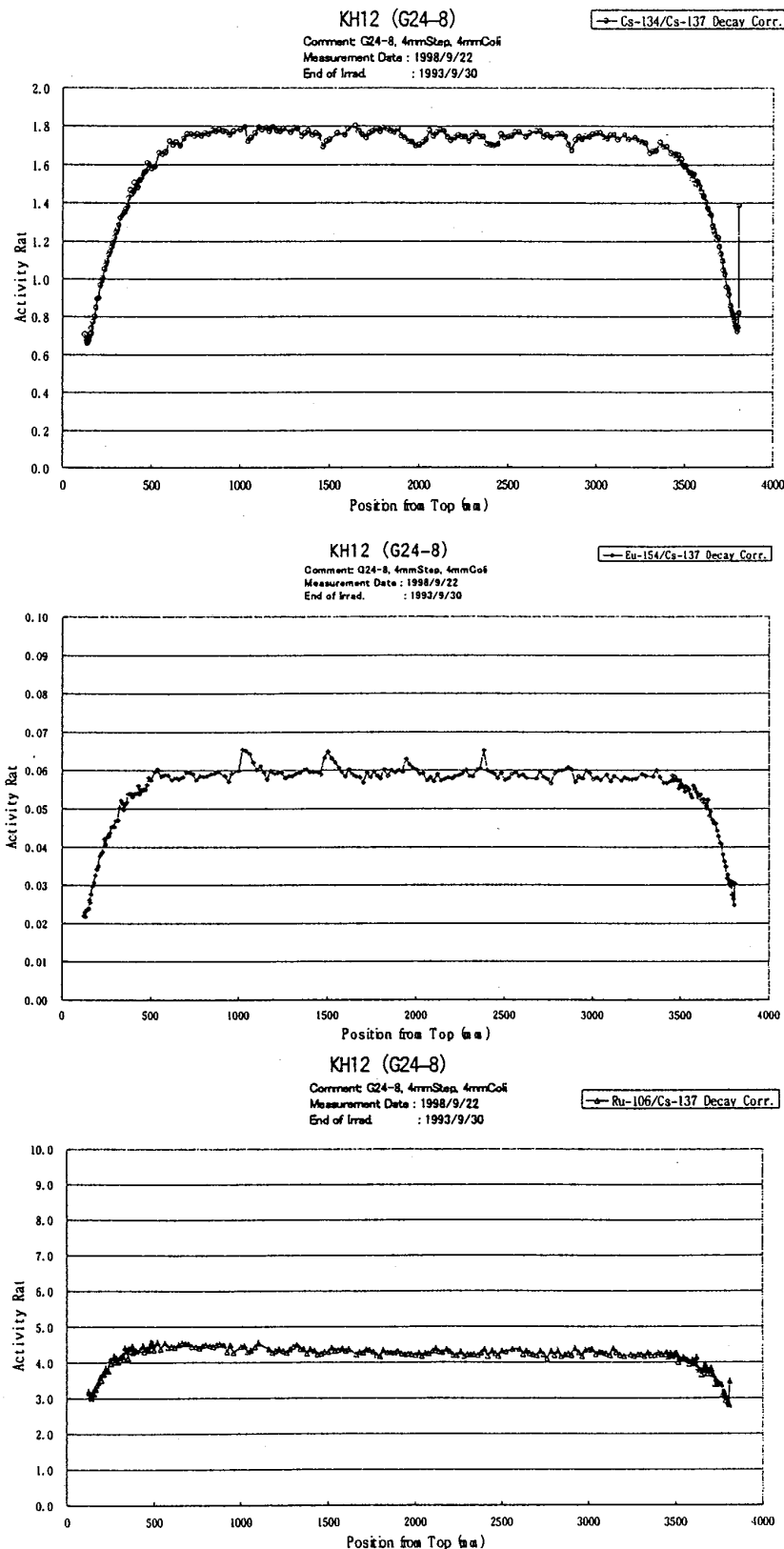


Fig. 2.1.24. Axial profiles of activity ratios measured in NT3G24-A8 (KH12).

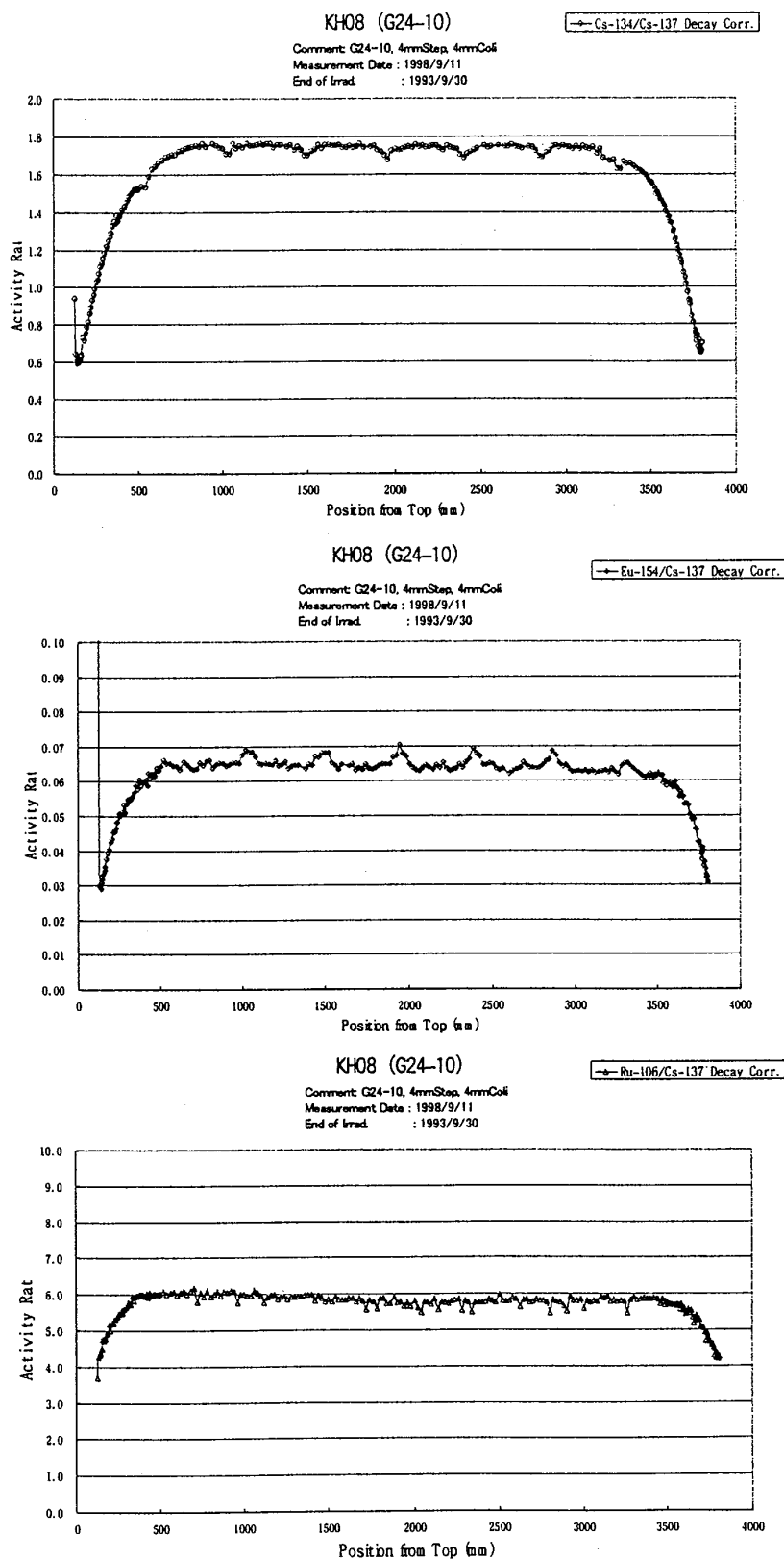


Fig. 2.1.25. Axial profiles of activity ratios measured in NT3G24-B10 (KH08).

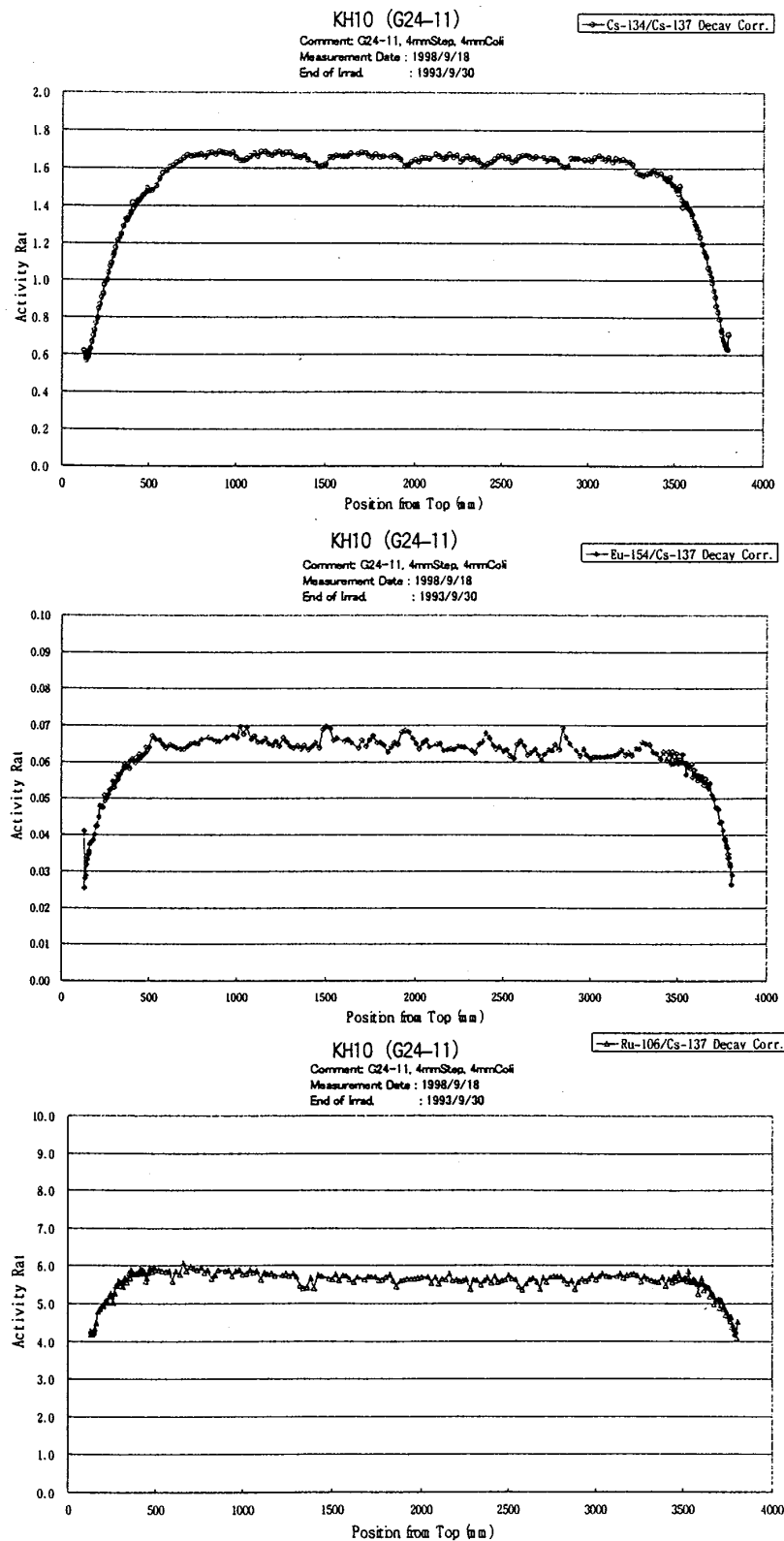


Fig. 2.1.26. Axial profiles of activity ratios measured in NT3G24-D11 (KH10).

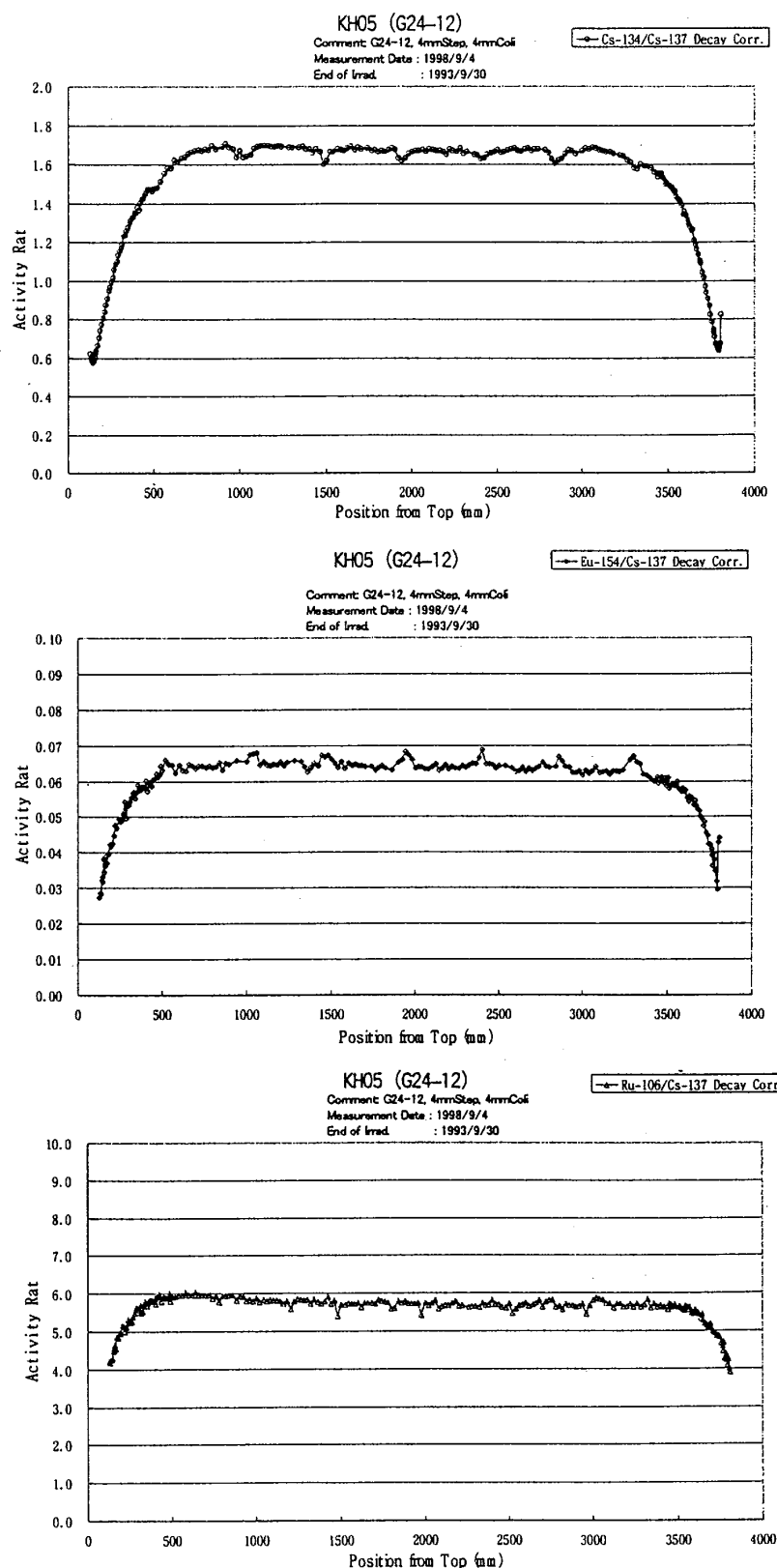


Fig. 2.1.27. Axial profiles of activity ratios measured in NT3G24-B12 (KH05).

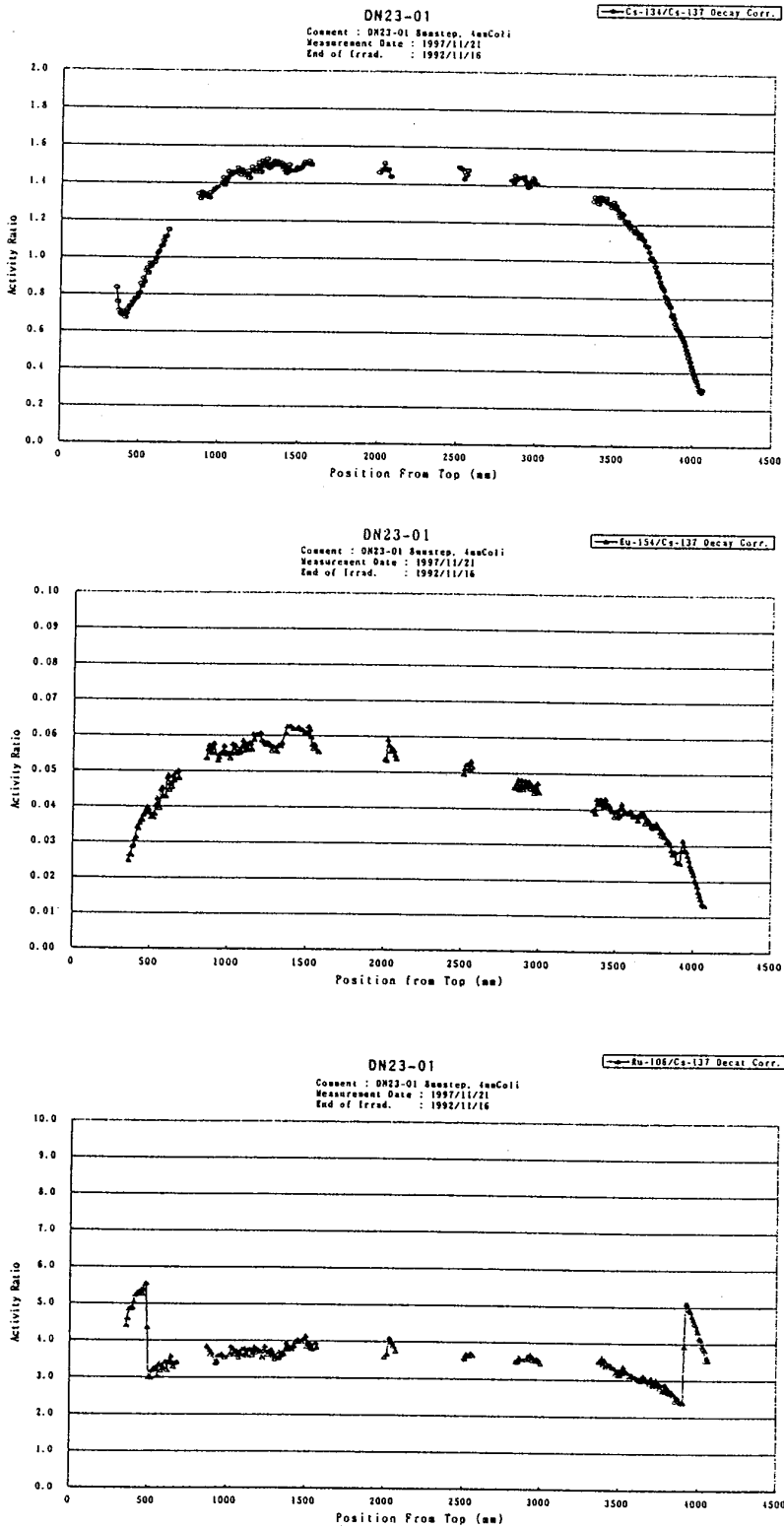


Fig. 2.1.28. Axial profiles of activity ratios measured in 2F2DN23-01.

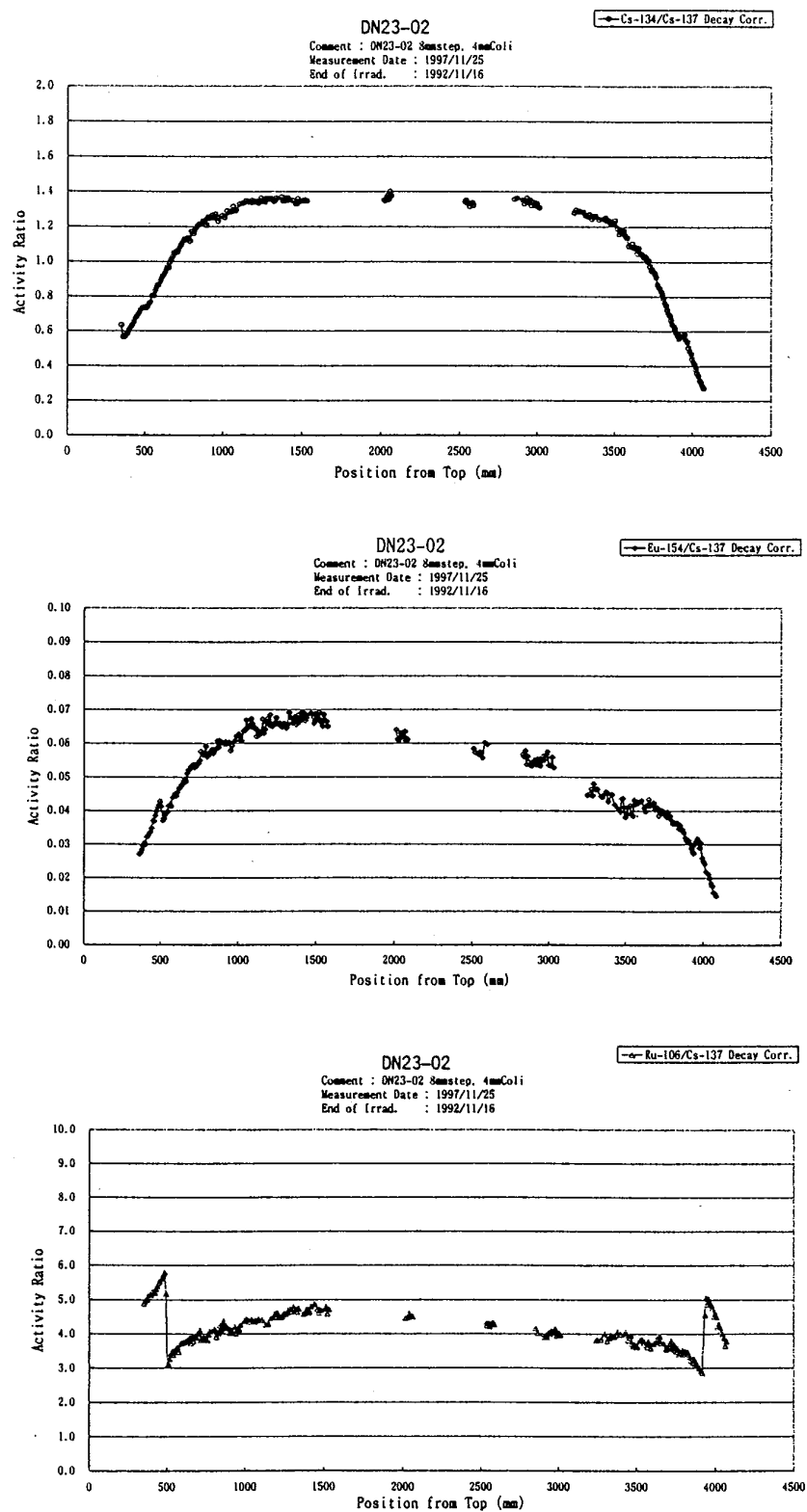


Fig. 2.1.29. Axial profiles of activity ratios measured in 2F2DN23-02.

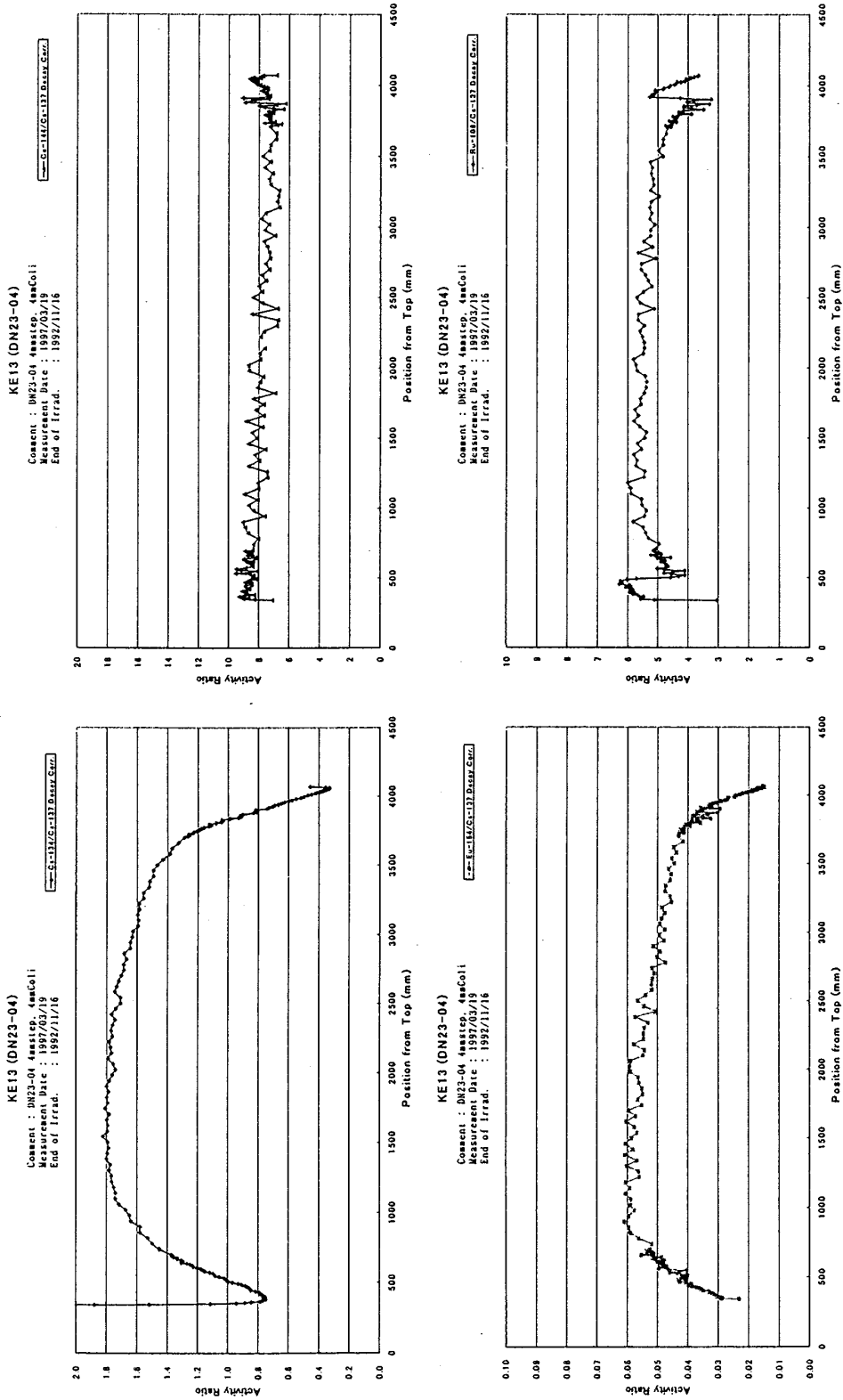


Fig. 2.1.30. Axial profiles of activity ratios measured in 2F2DN23-04 (KE13).

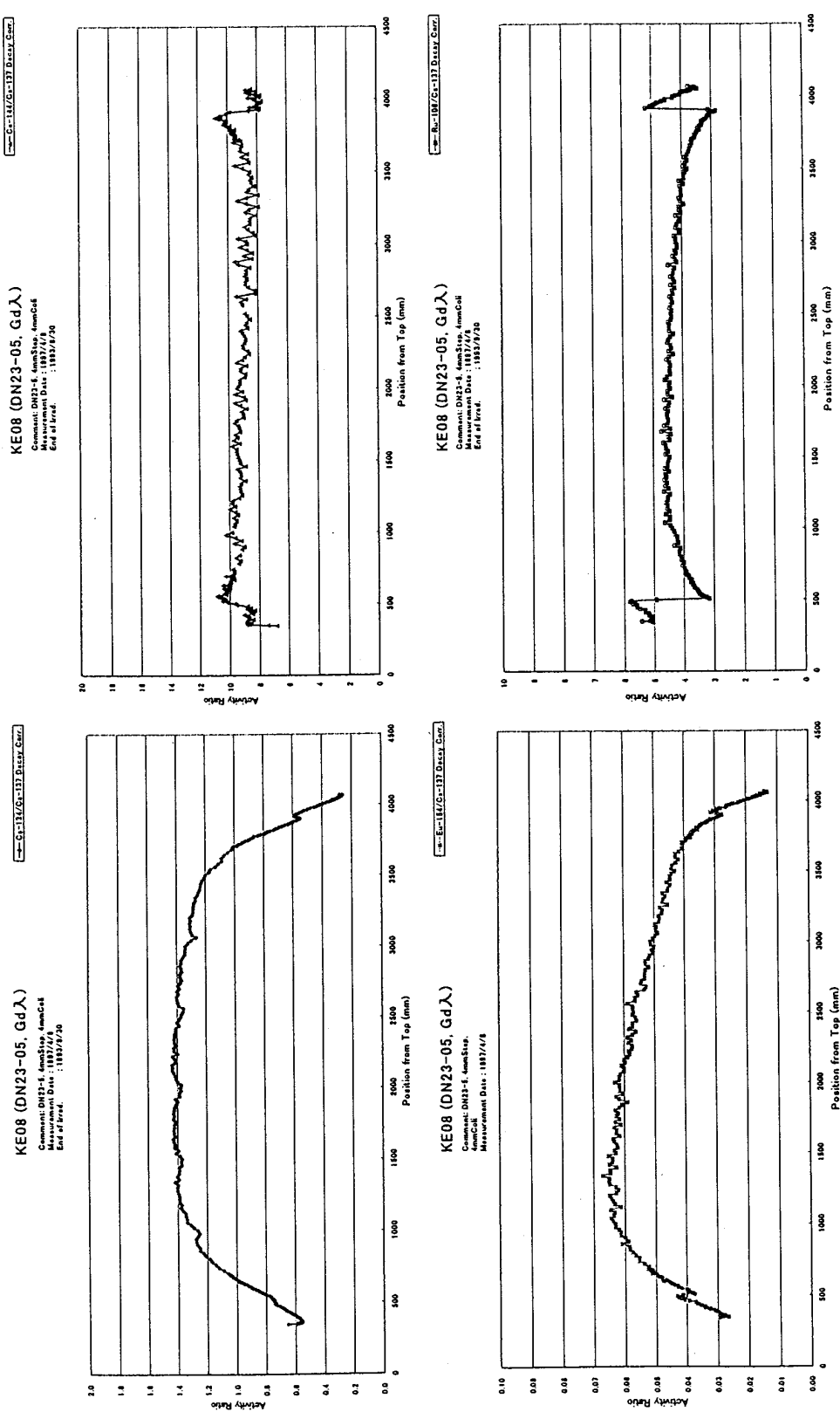


Fig. 2.1.31. Axial profiles of activity ratios measured in 2F2DN23-05 (KE08).

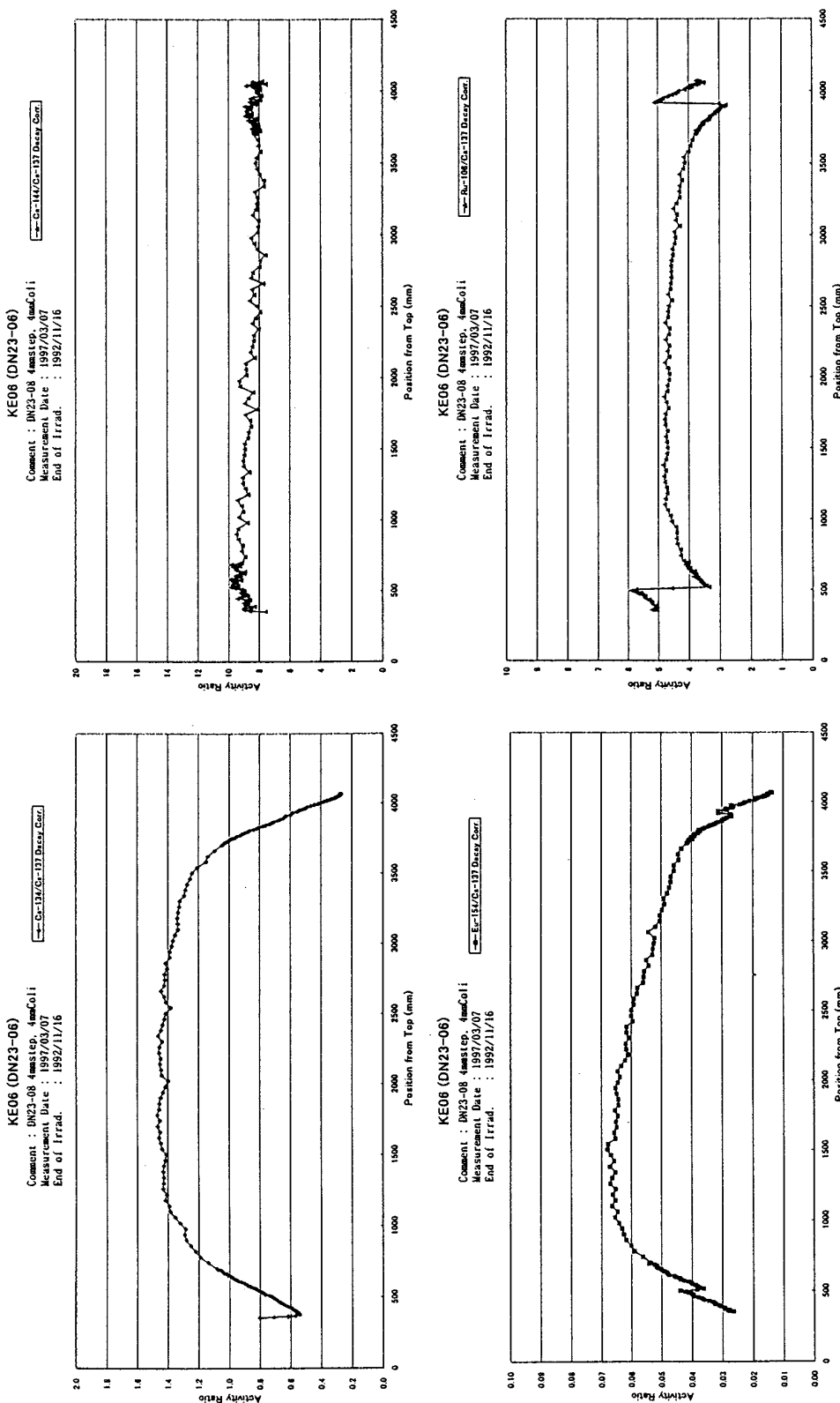


Fig. 2.1.32. Axial profiles of activity ratios measured in 2F2DN23-06 (KE-06).

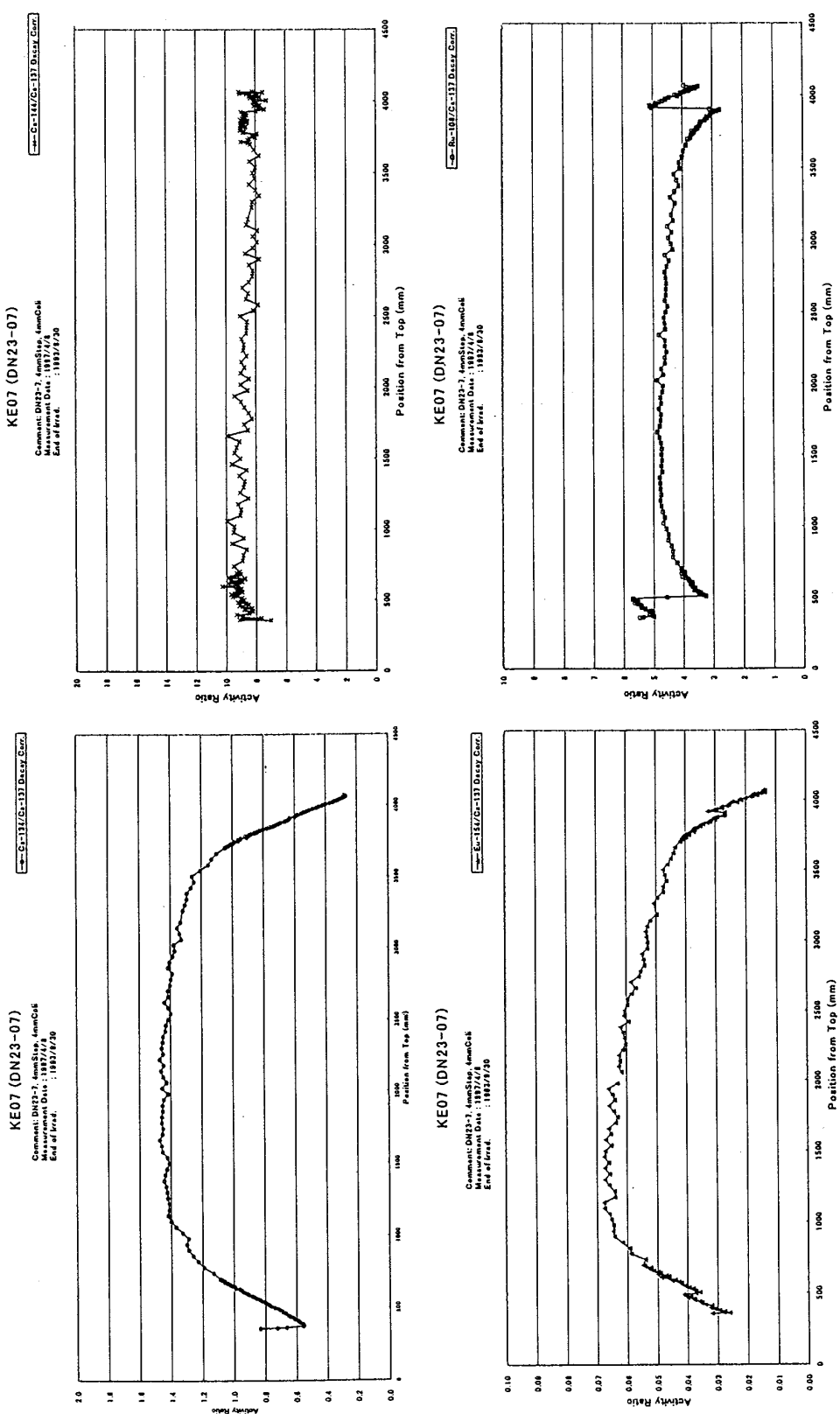


Fig. 2.1.33. Axial profiles of activity ratios measured in 2F2DN23-07 (KE07).

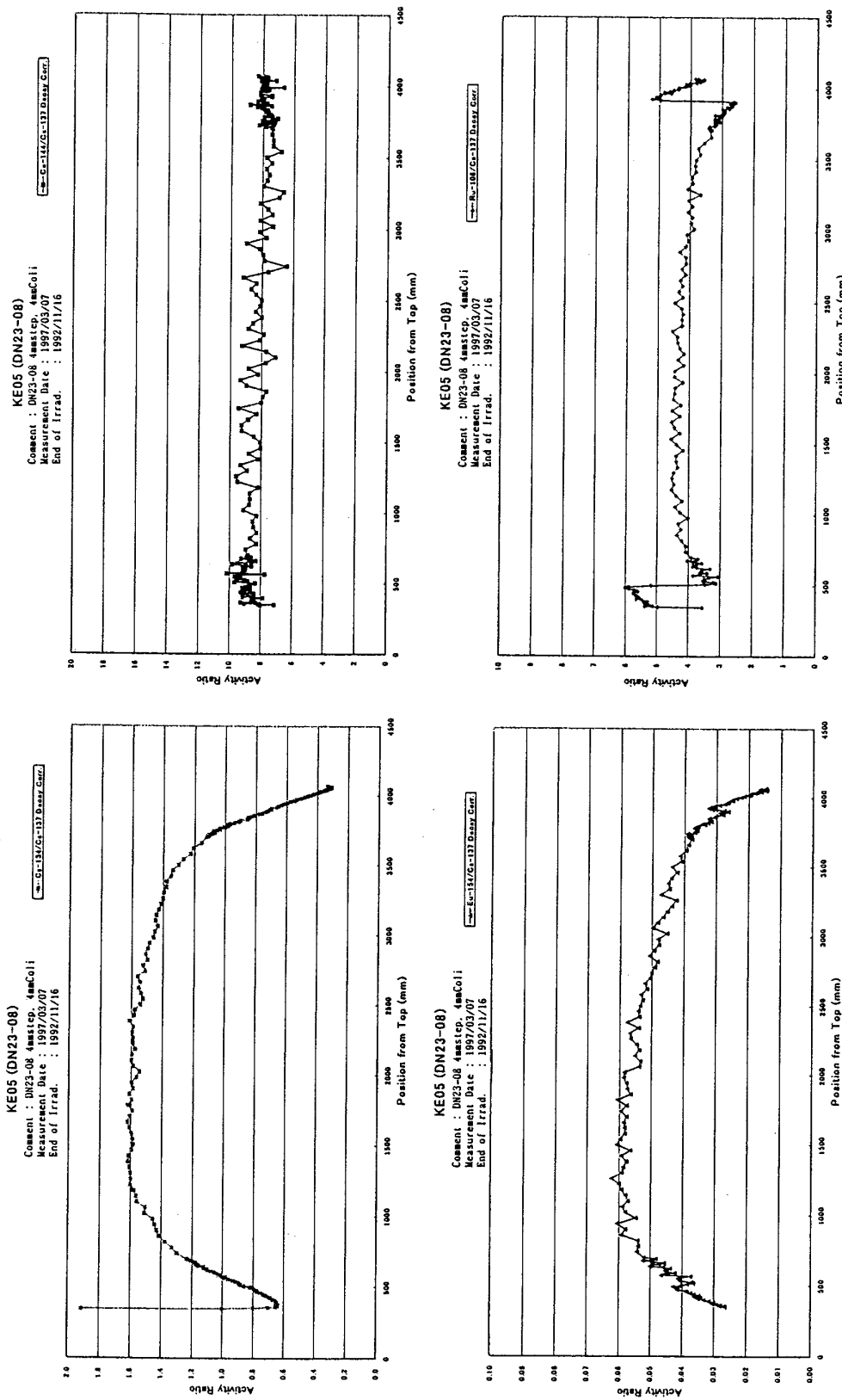


Fig. 2.1.34. Axial profiles of activity ratios measured in 2F2DN23-08 (KE05).

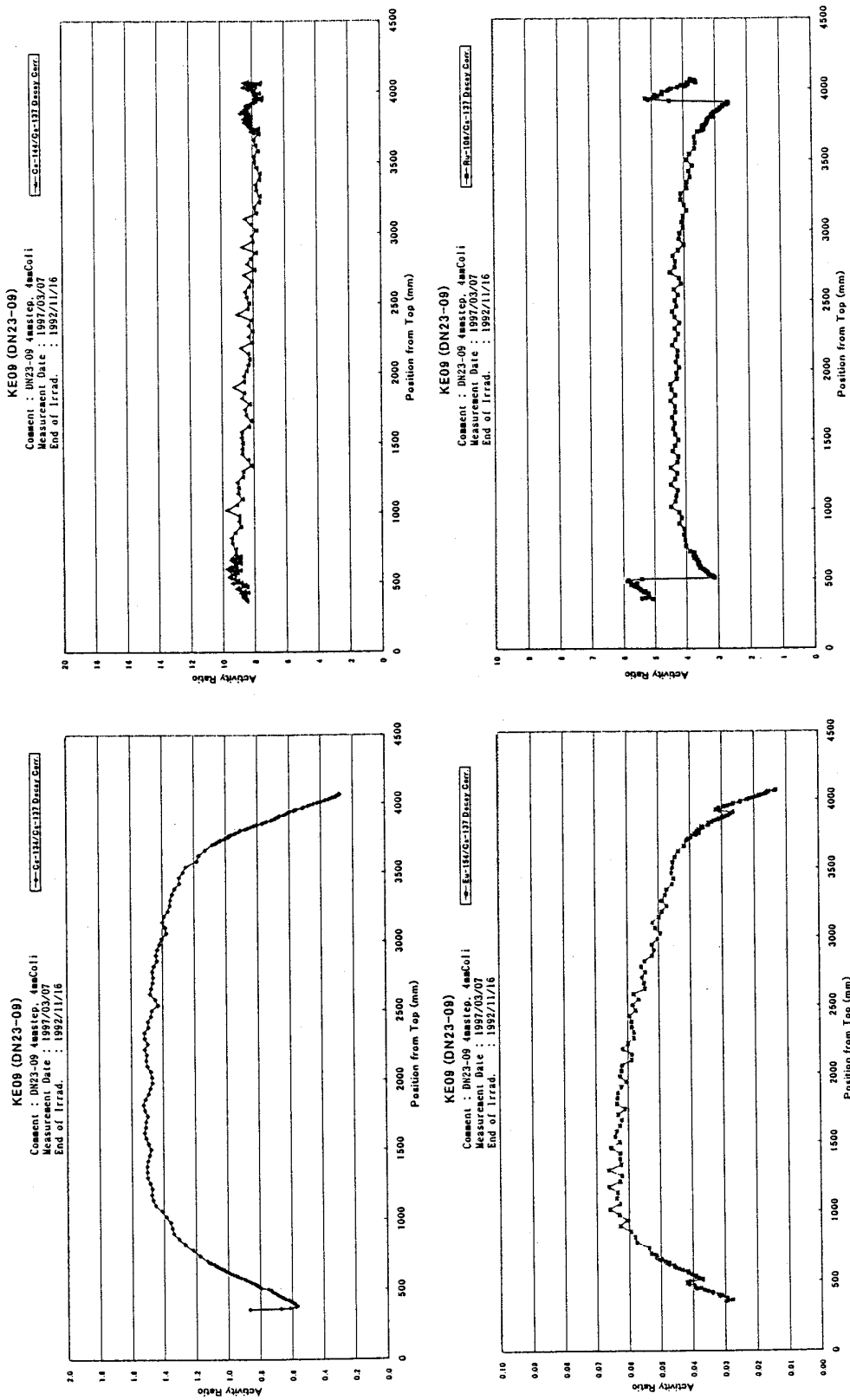


Fig. 2.1.35. Axial profiles of activity ratios measured in 2F2DN23-09 (KE09).

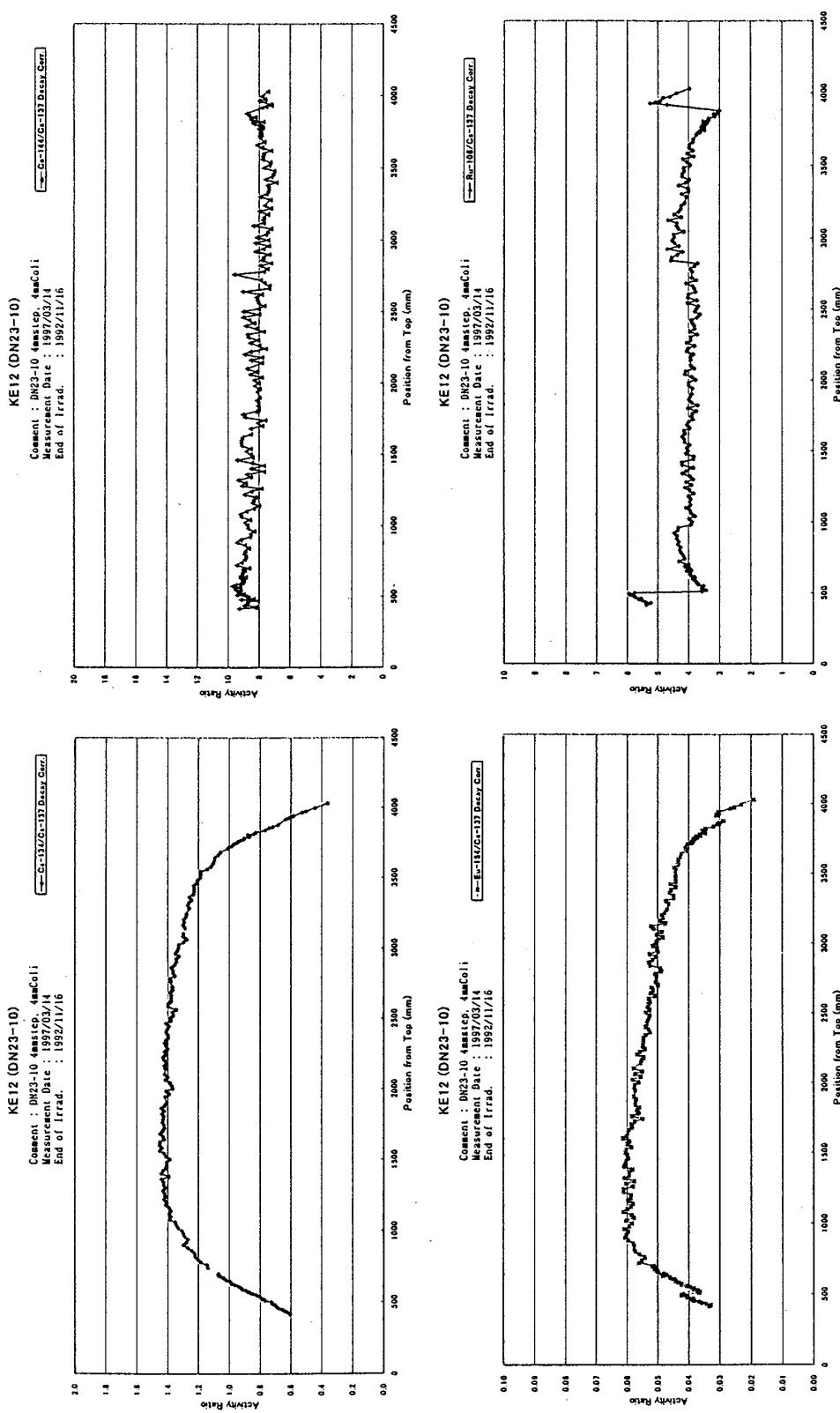


Fig. 2.1.36. Axial profiles of activity ratios measured in 2F2DN23-10 (KE12).

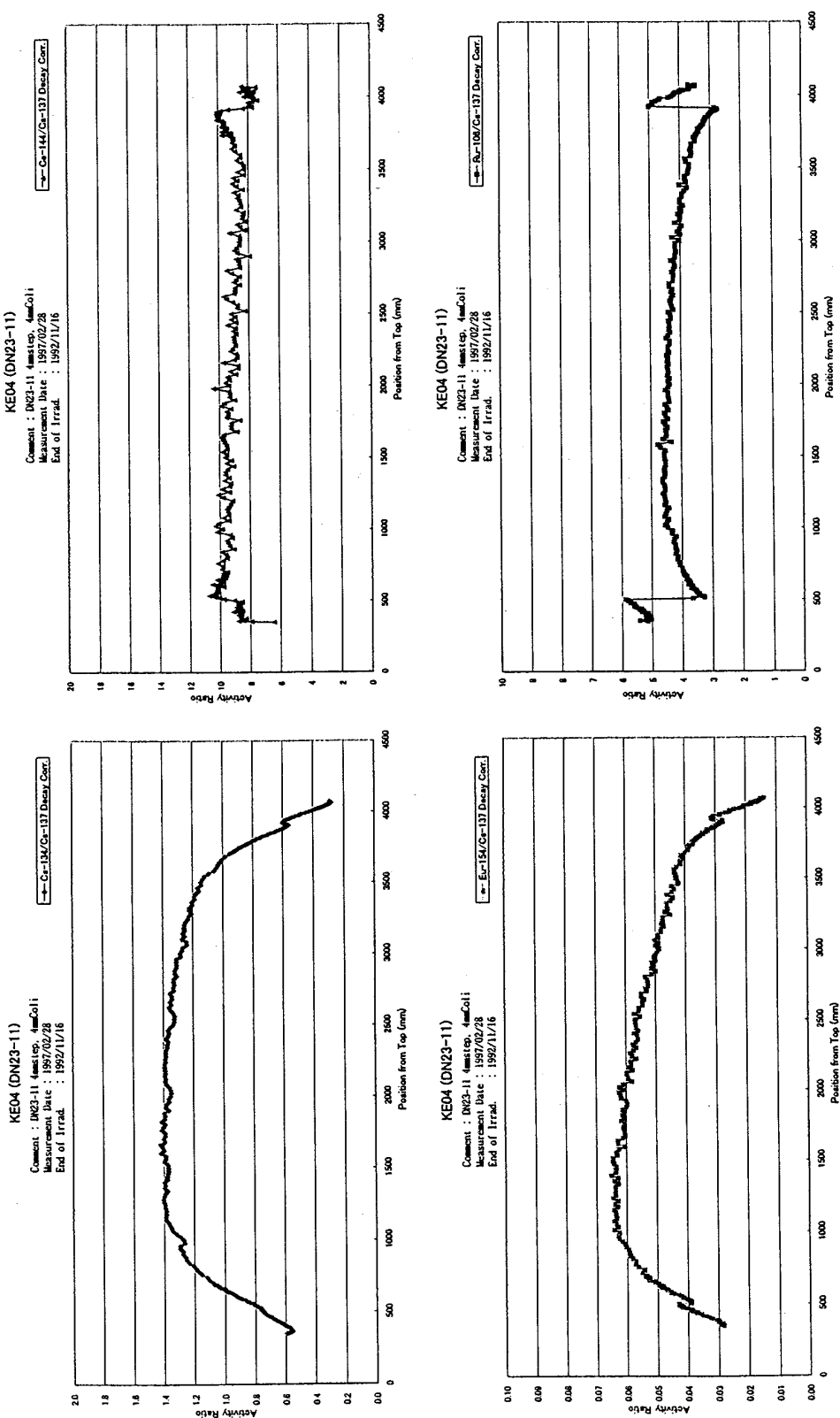


Fig. 2.1.37. Axial profiles of activity ratios measured in 2F2DN23-11 (KE04).

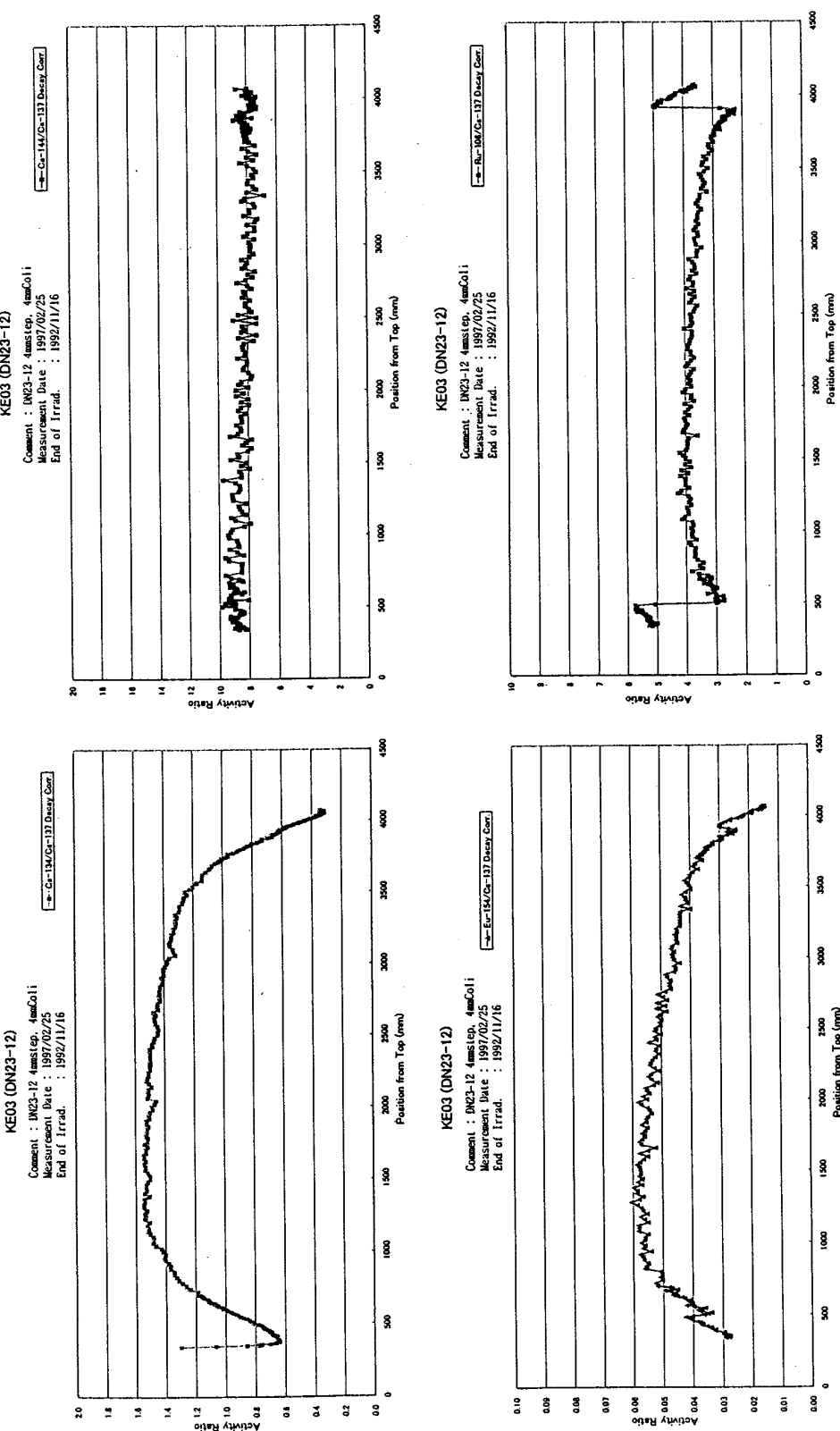


Fig. 2.1.38. Axial profiles of activity ratios measured in 2F2DN23-12 (KE03).

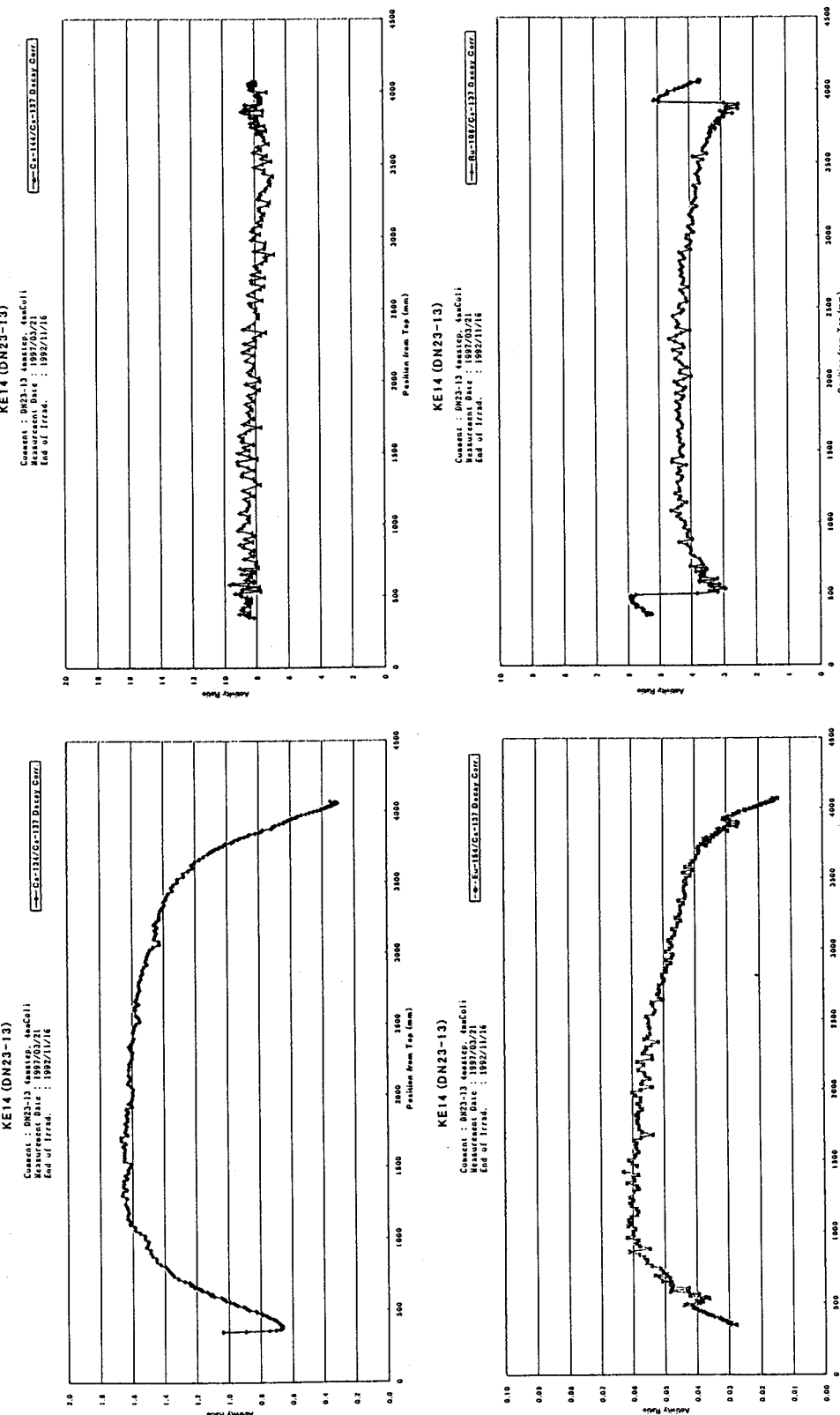


Fig. 2.1.39. Axial profiles of activity ratios measured in 2F2DN23-13 (KE14).

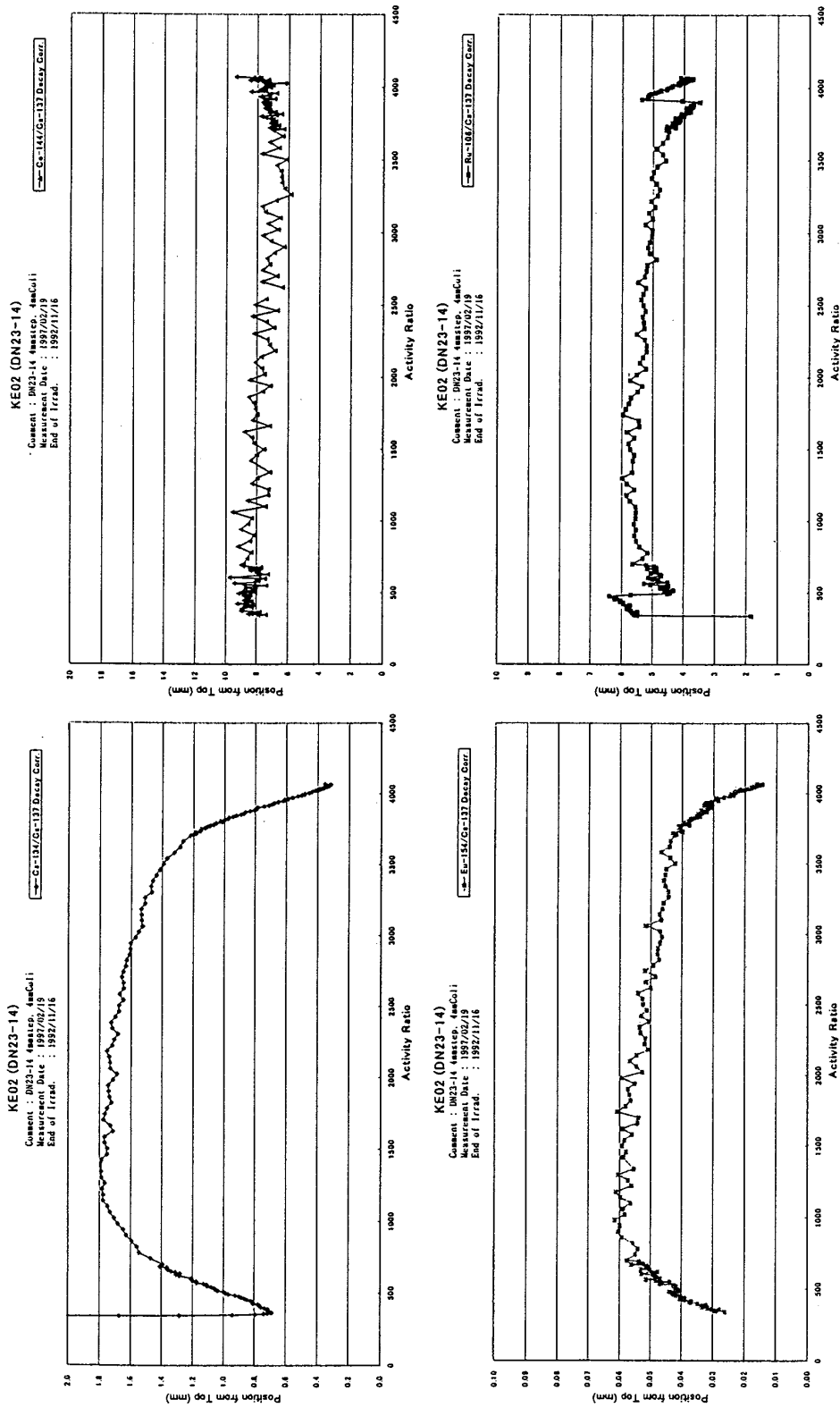


Fig. 2.1.40. Axial profiles of activity ratios measured in 2F2DN23-14 (KE02).

## **2.2. Radiochemical Analyses of Spent Fuel Samples**

Destructive analyses were carried out with a view to obtaining the experimental data on nuclide compositions and burn-up rates of spent LWR fuels.

Nuclides were measured by  $\alpha$ -ray and  $\gamma$ -ray spectrometry and mass spectrometry after dissolving the collected samples and separating the elements by anion exchange separation.

The destructive analyses of spent nuclear fuels began in 1995, and by 1999, a total 34 samples had been analyzed. The analyses are for the elements U, Np, Pu, Am, Cm, and certain FP elements starting with Nd.

Furthermore, starting in 1997, analyses of nuclide compositions were also carried out on elemental Sm as well, in view of its importance in assessing criticality safety, given that this element accounts for about 25% of the proportion of neutron absorption by all FP nuclides.

### **2.2.1. Samples and Analytical Items**

#### **(1) Samples**

Samples were cut out of the spent fuel elements NT3G23 and NT3G24, which had been irradiated for 2 or 3 cycles in the No. 3 reactor of Kansai Electric's Takahama Nuclear Power Plant, and the spent fuel assembly 2F2DN23 irradiated for 5 cycles in the No. 2 reactor of Tokyo Electric's Fukushima No. 2 Nuclear Power Plant, to provide the samples for chemical analyses.

The cutting positions of various samples are shown in Fig. 2.2.1 together with average burn-up and sample No.

#### **(2) Analytical Items**

The nuclides of concern in the destructive analyses are as follows:

- U isotopes (U-234, U-235, U-236, U-238)
- Pu isotopes (Pu-238, Pu-239, Pu-240, Pu-241, Pu-242)
- Am isotopes (Am-241, Am-242m, Am-243)
- Cm isotopes (Cm-242, Cm-243, Cm-244, Cm-245, Cm-246, Cm-247)
- Np isotopes (Np-237)
- Nd isotopes (Nd-142, Nd-143, Nd-144, Nd-145, Nd-146, Nd-148, Nd-150)
- Sm isotopes (Sm-147, Sm-148, Sm-149, Sm-150, Sm-151, Sm-152, Sn-154)
- Gd isotopes (Gd-154, Gd-155, Gd-156, Gd-157, Gd-158, Gd-160): for fuels with Gd
- FP radioactivity (Cs-134, Cs-137, Eu-154, Ce-144, Sb-125, Ru-106)

### **2.2.2. Samples Dissolution Method**

The samples were collected by cutting circular slices 0.5 mm thick from respective positions with a diamond cutter. A resin was injected to prevent the pellets from collapsing during cutting.

The samples were dissolved with the use of the dissolution apparatus shown in Fig. 2.2.2 installed in an  $\alpha\text{-}\gamma$  cell.

The dissolution apparatus is made up of 3 stages of gas washing bottles, a glass hood, a heater, and an exhaust pump, while keeping in mind the prevention of contamination in the cell due to nitric acid mists and FP gases (Ru-106, etc.) that are generated in conjunction with the dissolution operation.

The gas washing bottles were filled with a caustic soda solution as an acid neutralizer.

Each specimen (about 300 mg) that had been cut out of a fuel element was dissolved by heating (about 100°C) in about 15 mL of 7 M nitric acid.

During observation at the time of dissolution, a general increase in black turbidity due to insoluble residue was noted as the burn-up increased. The final dissolution end point was identified by referring to the state of bubble generation in dissolving samples with low burn-up rates.

The dissolution time was about 1 hour. An example of dissolution behavior is summarized in Table 2.2.1.

The dissolved sample solution was allowed to stand overnight or longer, then the supernatant was collected in a vial with the use of a polyethylene pipette.

In other words, the insoluble residue and covering material in solution are not separated.

Table 2.2.2 shows the solution collecting vial surface equivalent doses rates and the dose rates of the fuel sample specimens.

Table 2.2.1. Dissolution behavior of spent fuel sample

Progress time (min)	Temperature (°C)	Dissolution behavior
0	Room temp.	Start (addition of 15 ml of 7 M HNO <sub>3</sub> solution).
5	50	Dissolution was initiated with the finely bubbles.
15	80	NO x gas appeared in the solution. Dissolved sample becomes blackish and then comes to seldom be visible inside vial. Yellow of the uranyl nitrate could be observed around the blackish residue.
20	~ 100	A turbid of the residue made the solution invisible inside vial.
30		The large bubbles were generated in the boiling solution.
60		End.

Table 2.2.2. Surface equivalent dose rate of sample

Sample ID	Sample specimen (mSv/h)	Aliquoting dissolved solution ( $\mu$ Sv/h)	Collecting volume (drop) *
SF95-1	60	20	4
SF95-2	---	20	3
SF95-3	---	20	1
SF95-4	255	20	1
SF95-5	---	20	2
SF96-1	7	100	17
SF96-2	20	300	13
SF96-3	10	100	7
SF96-4	70	500	7
SF96-5	50	400	7
SF97-1	35	---	4
SF97-2	60	---	3
SF97-3	90	---	2
SF97-4	110	---	2
SF97-5	90	---	3
SF97-6	110	---	2
SF98-1	3	100	---
SF98-2	9	100	---
SF98-3	33	150	---
SF98-4	52	400	---
SF98-5	17	300	---
SF98-6	16	600	---
SF98-7	15	300	---
SF98-8	11	200	---
SF99-1	40	400	4
SF99-2	180	700	2
SF99-3	140	380	1
SF99-4	210	450	1
SF99-5	250	1700	2
SF99-6	170	800	2
SF99-7	170	1000	1
SF99-8	110	800	2
SF99-9	40	420	2
SF99-10	30	560	4

\*: 1 drop  $\approx$  15  $\mu$ l

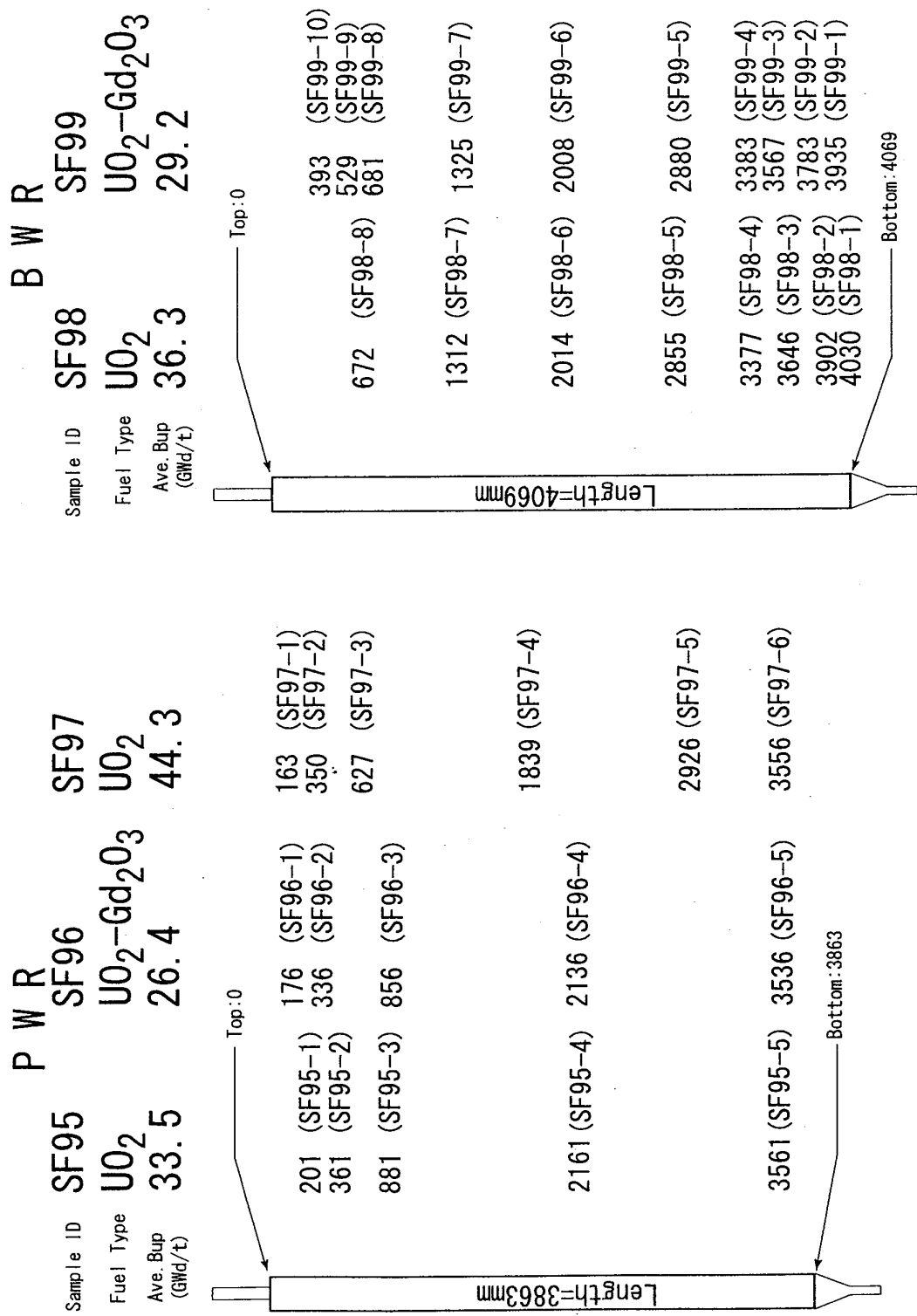


Fig. 2.2.1. Cutting position of samples for the destructive analysis (from top : unit (mm)).

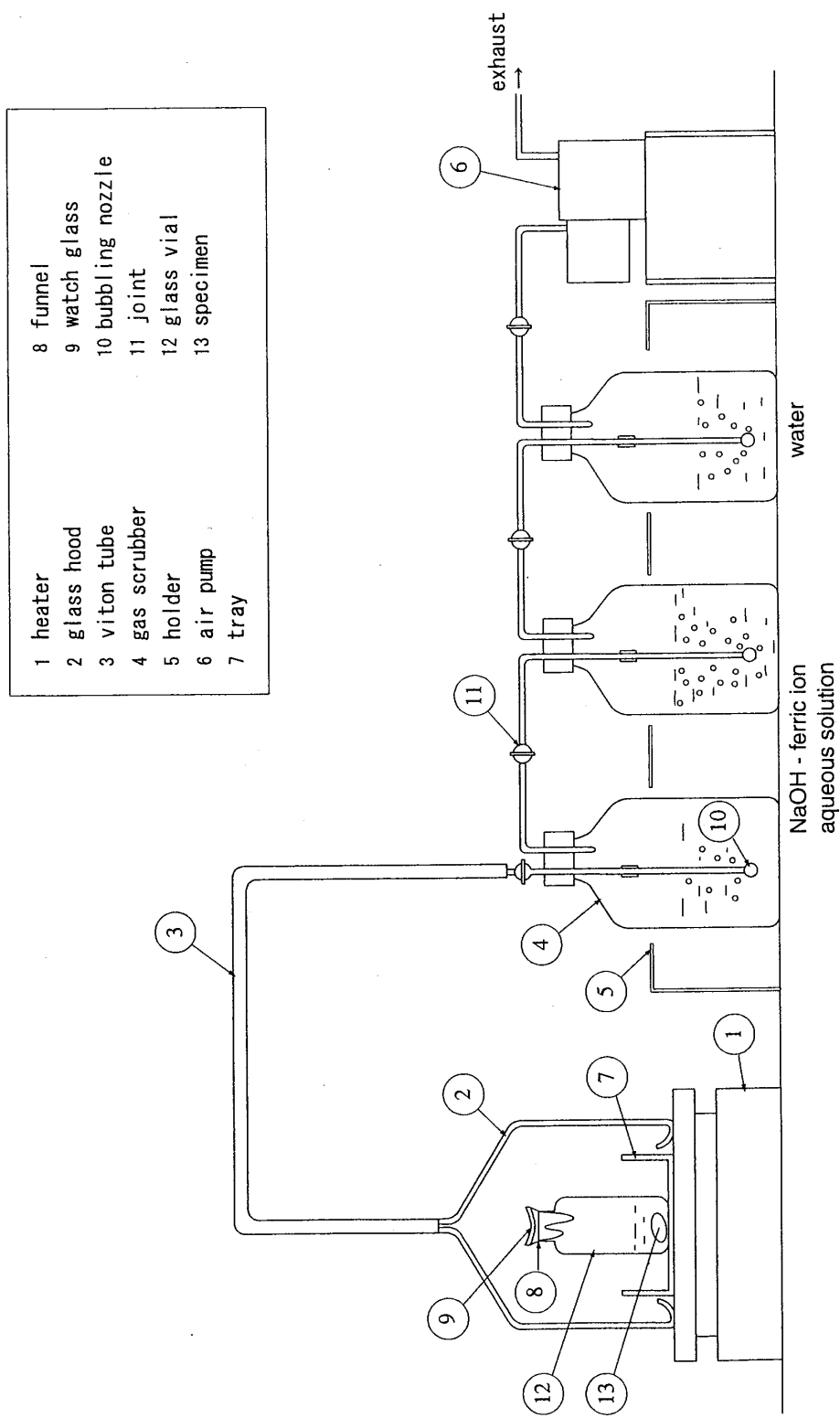


Fig. 2.2.2. Dissolution of apparatus for spent fuel sample.

## 2.2.3. Chemical Separation Method<sup>1</sup>

### (1) Analytical Methods for Nuclide Compositions

For this study, we used the anion exchange separation method for the separation and purification of elements, a surface ionizing mass spectrometer and an  $\alpha$ -ray spectrometer for the measurement of isotopic ratios, and the isotope dilution method for quantification of the elements.

Furthermore, the quantity of Np-237 was determined by  $\alpha$ -ray spectrometry after its isolation and purification, and the quantities of  $\gamma$ -ray-emitting FP nuclides starting with Cs-137 were determined by  $\gamma$ -ray spectrometry using an intrinsic Ge semiconductor detector.

The isotope dilution method is a technique in which a solution (SD = a spiked solution) that contains an added enriched isotope (S = a spike solution) of the object element, and a solution (U = an unspiked solution) without the addition of said isotope are prepared from the same sample, and the quantities of specific nuclides in very small quantities are determined precisely from respective analysis results.

In this case, the relation between a nuclide "i" in the sample to be quantitatively analyzed and a nuclide "j" to be added can be expressed as

$$C_i = \frac{(1 - R_{SD} / R_S)}{R_{SD} - R_U} \cdot \frac{M_S}{M_U} \cdot S_j$$

In this equation,  $C_i$  is the concentration of nuclide "i" in the sample to be quantitatively analyzed;  $S_j$  is the concentration of nuclide "j" in the enriched isotope solution;  $R$  is isotopic ratio i/j; and  $M$  is the weight at the time of preparation of the sample with an added enriched isotope. Since the quantity of nuclide "i" can be thus determined essentially from relative values ( $R_{SD}$ ,  $R_U$ ), this method is a technique that is not influenced by the recovery rate in chemical separation.

On the basis of the above-mentioned method, the dissolved sample was divided into the following portions: (1) one for an added sample; (2) one for an unadded sample; and (3) one for stock, then these samples were prepared. (1) and (2) were used for ion exchange separation, and (3) was used mainly for the measurement of  $\gamma$ -ray spectra.

The compositions of enriched isotopes of analysis target elements used for preparing the spikes are shown below.

Nuclide : atom%	Nuclide : atom%	Nuclide : atom%	Nuclide : atom%
U-233 : 98.2840	Pu-238 : 0.00253	Nd-142 : 1.4602	Sm-144 : 0.0200
U-234 : 0.8425	Pu-239 : 0.01934	Nd-143 : 1.0008	Sm-147 : 0.1453
U-235 : 0.02090	Pu-240 : 0.08403	Nd-144 : 1.5503	Sm-148 : 0.1284
U-236 : 0.00039	Pu-241 : 0.04925	Nd-145 : 0.9135	Sm-149 : 0.1807
U-238 : 0.85180	Pu-242 : 99.8450	Nd-146 : 1.5148	Sm-150 : 0.1246
		Nd-148 : 1.0824	Sm-152 : 0.7669
		Nd-150 : 92.4780	Sm-154 : 98.6341

The amount of an enriched isotope to be added as a spike must be added according to the amount of the object nuclide in the sample. In this study, the amount of a spike to be added to each sample was determined by estimating the burn-up from the measured Cs-137  $\gamma$ -ray radioactivity of a sample collected from the dissolved fuel solution.

## (2) Analytical Procedure

A flow diagram of the analytical procedure is shown in Fig. 2.2.3. After a sliced pellet specimen collected from a spent fuel was dissolved, about 1/1,000 to 1/3,000 of the solution was transferred to a glass vial as a sample to be analyzed. Under a hood, this sample was transferred from the  $\alpha\text{-}\gamma$  cell and subjected to chemical separation. In carrying out the chemical separation, the amount of the sample to be used in analysis was determined by referring to the Cs-137 radioactivity as determined by measurement of the  $\gamma$ -rays of each analysis sample.

The sample in the vial was diluted with nitric acid, then a fixed amount of the solution was collected accurately to provide a sample to be spiked and a sample that was not to be spiked for chemical separation, as well as a sample for measuring the  $\gamma$ -rays of the FP nuclides.

For quantification, an accurate known amount of enriched isotope was added to the sample to be spiked.

Next, a fraction for each target element was obtained by ion exchange separation, which will be discussed later.

In these fractions obtained by chemical separation, the isotopic ratios of spiked samples and non-spiked samples were measured by isotope dilution-mass spectrometry. The quantities of Nd, U, and Pu were obtained at this point and the ratios of the numbers of atoms of these elements were determined.

Furthermore,  $\alpha$ -ray spectra were measured on the non-spiked samples, and from the peak counts of Pu, Am, and Cm isotopes on the same spectrum, the ratios of the numbers of atoms of these elements were calculated. From these elementary ratios by  $\alpha$ -ray measurement and the U/Pu ratio which can be obtained by mass spectrometry, the ratios of Am and Cm per uranium were determined.

With regard to Np, in which no peaks can be obtained on the same spectrum by  $\alpha$ -ray measurement, and  $\gamma$ -ray emitting FP nuclides, absolute values were obtained on the basis of the counting efficiency, the amount of sample collected, etc., and divided by the concentration of uranium in the sample, to find the ratio of the number of atoms per uranium.

In this analytical operation, the following two techniques were used to obtain more accurate values.

One technique is to use a mixed spike in the isotope dilution method. This study used a mixed spike consisting of U-233, Pu-242, and Nd-150 in order to determine the quantities of U-238, Pu-239, and Nd-148.

A mixed spike solution can raise the accuracy of the results by adjusting the concentration (better knowledge of the mixing ratio) in advance, since the amount added and its error do not affect the results.

The other technique to improve accuracy is to measure the  $\alpha$ -ray spectrum of a sample solution before chemical separation.

More accurate  $\alpha$ -nuclide radioactivity ratios can be obtained by determining  $\alpha$ -radioactivity ratios associated with Pu, Am, and Cm from the same spectrum and comparing the measured  $\alpha$ -ray spectrum of a Pu fraction isolated by ion exchange separation.

### (3) Ion Exchange Separation [2]

#### a) Reagents and Instruments

- Ion-Exchange Resin: Mitsubishi Chemicals (Ltd.) Diaion and gelled resin
- Other Reagents: Tamapure-AA100 from Tama Chemical Industries (Ltd.) for nitric acid and hydrochloric acid, and analytical reagent quality for the other reagents.
- Ion-Exchange Column: made of glass; inner diameter, 3 mm and length, 90 mm; top liquid reservoir, 30 mL
- Intrinsic Ge Semiconductor Detector for Low-Energy Measurements: EG&G Ortec LO-AX (Be edge window)
- Multichannel Analyzer: EG&G Ortec Model 7800

#### b) Operation

A schematic diagram for preparation of a dissolved sample and anion exchange separation is shown in Fig. 2.2.4. This scheme is divided into three parts, and each part consists of a sample pretreatment (valence adjustment) and ion exchange separation:

- (a) FP, Np, Pu, U separation: Diaion SA#100 resin (3 mm  $\phi \times 70$  mm <sup>h</sup>; volume 0.5 mL); mainly hydrochloric acid systems
- (b) Np fraction purification: Diaion SA#100 resin (3 mm  $\phi \times 70$  mm <sup>h</sup>; volume 0.5 mL); hydrochloric acid systems
- (c) Cm, Am, Nd, etc., separation: CA06Y resin (3 mm  $\phi \times 50$  mm <sup>h</sup>; volume 0.35 mL); hydrochloric acid and methanol systems

Ion-exchange separation was carried out basically at room temperature, but in the nitric acid and methanol systems for separating Cm, Am, Nd, etc., the temperature was kept at 28°C by circulating water, which was temperature controlled in a thermostated vessel, through the column jacket.

The temperature could be controlled within  $\pm 2^\circ\text{C}$ , but it did fluctuate to some extent due to the air conditioning in the laboratory and the day and night temperatures outside.

The flow-out velocity of the eluate was 0.5–0.8 mL/h, though there were small differences depending on the nature of solution.

Furthermore, in the separation of Cm, Am, Nd, etc., because some fractions are eluted in close proximity, we proceeded while checking the radioactivity distributions of Am-241, Eu-152, and Ce-144 by  $\gamma$ -ray scanning in the axial direction of the ion-exchange column.

Moreover, we tried to reduce the corrosive environment under the working hood and in the exhaust system by using as little hydrochloric acid as possible, and to simplify the separation scheme by focusing on  $\alpha$ -ray spectrum measurements in the separation and on the target elements in mass spectrometry.

## 2.2.4. Isotopic Ratio Measurement and Radioactivity Measurement Methods

### (1) Mass Spectrometry

#### (a) Equipment Used

The mass spectrometer used was a MAT-262 surface ionization-type multiple-detector mass spectrometer equipped with 9 Faraday cups and one secondary-electron multiplier in the ion detector.

The configuration of the multiple detectors is shown in Fig. 2.2.5.

#### (b) Measurement

Each fraction of U, Pu, Nd, Am, or Cm obtained by ion exchange separation was evaporated to dryness under the hood and placed in a glove box for mass spectrometry, then it was dissolved in about 10  $\mu$ L of 1 N nitric acid.

Next, 1/3 of the dissolved solution was applied on a rhenium filament ribbon (1 mm  $\times$  10 mm  $\times$  0.1 mm) with the use of a micropipette, then turned into oxides by passing a current of about 2A through the filament.

The amount applied on the filament was about 1  $\mu$ g, about 10 ng, about 5 ng, about 5 ng, and < 1 ng for U, Pu, Nd, Am, and Cm, respectively, and about 50 ng and about 100 ng for Gd and Sm.

The filament assembly is a double filament system consisting of an ionization filament and an evaporation filament for evaporating the sample. The filament magazine (13 samples) was attached to the ion source section of the mass spectrometer, which was then evacuated ( $< 10^{-8}$  mb), and the respective isotopic ratios were measured under the following conditions.

The isotopic ratios were measured by adjusting the evaporation filament current to 1.6–1.8 A, 1.5–1.7 A, 1.8–2.0 A, 1.8–2.0 A, and 1.9–2.1 A for U, Pu, Nd, Am, and Cm, and 1.7–1.9 and 2.1–2.3 A for Sm and Gd.

Furthermore, the ionization filament current was adjusted (5.4–5.7 A) so as to keep the amount of the Re-187 ion constant (output 100 mV).

The mass discrimination bias was measured by using NBS U-500 for U, NBS-947 for Pu, and various reagents (Shin-etsu Chemicals) for Nd, Gd, and Sm, then corrections were made.

Since no standard materials are available for Am and Cm, the measured values were used as-is.

## (2) $\alpha$ -Ray Spectrum Measurement

### (a) Equipment Used

- Si Surface Barrier-Type Semiconductor Detector (SSB): EG&G Ortec product; effective sensitive area  $100 \text{ mm}^2$
- Multichannel Analyzer: EG&G Ortec product, Model 7800

### (b) Measurement

A portion of the spent fuel specimen dissolved solution and a portion or the whole of each fraction after chemical separation were applied, respectively, to tantalum disks ( $24 \text{ mm } \phi \times 0.1 \text{ mm t}$ ) and  $\alpha$ -ray source samples for  $\alpha$ -ray spectrum measurement were prepared by tetraethylene glycol dispersion and evaporation by high-temperature heating.

The distance between the SSB detector and the  $\alpha$ -ray source sample was adjusted to 20–40 mm and the measurement time was adjusted as appropriate (3,000–500,000 s) so as to make it possible to obtain the necessary counts.

The  $\alpha$  radioactivity ratios  $(\text{Pu-238} + \text{Am-241})/(\text{Pu-239} + \text{Pu-240})$ ,  $\text{Cm-242}/(\text{Pu-239} + \text{Pu-240})$ ,  $\text{Cm-244}/(\text{Pu-239} + \text{Pu-240})$  were obtained from the  $\alpha$ -ray spectra of the dissolved solutions, the  $\alpha$  radioactivity ratio  $\text{Am-241}/\text{Cm-244}/\text{Cm-242}$  was obtained from the  $\alpha$ -ray spectrum of the FP fraction, and the  $\alpha$  radioactivity ratio  $\text{Pu-238}/(\text{Pu-239} + \text{Pu-240})$  was obtained from the  $\alpha$ -ray spectrum of the Pu fraction.

Examples of the measured  $\alpha$ -ray spectra are shown in Figs. 2.2.6–2.2.9. The amount of each nuclide per uranium was calculated by using the value of  $(\text{Pu-239} + \text{Pu-240})/\text{U}$  calculated from the quantities determined by isotope dilution-mass spectrometry of U and Pu as a reference.

The quantity of Np-237 was determined on the basis of the counts of Np-237 in the  $\alpha$ -ray spectrum measurement of the Np fraction, the count efficiency, the amount of dissolved solution used, and the concentration of uranium in the dissolved solution, because the method using a reference value cannot be applied. The recovery rate of Np associated with chemical separation was evaluated as 0.95.<sup>3</sup>

## (3) $\gamma$ -Ray Spectrum Measurement

### (a) Equipment Used

- Intrinsic Ge semiconductor detector: EG&G Ortec product
- Multichannel analyzer: EG&G Ortec product, Model 7800
- Spectral analysis: EG-BOB (JAERI 1277 (1973))

### (b) Measurement

The  $\gamma$ -ray spectra of the dissolved solutions were measured in order to compare them with the  $\gamma$ -ray spectra obtained by nondestructive measurement. The measured samples were from spent fuels several (3–5.5) years after the end of irradiation. The spectra were measured on  $\gamma$ -ray emitting nuclides with relatively long lifetimes, such as Cs-134, Cs-137, Ce-144, and Eu-154.

Furthermore, for reference purposes, spectra were also measured for Ru-106 and Sb-125, which remain as insoluble residues and whose total amounts do not exist in the dissolved solution.

A portion of the dissolved solution was separated and diluted, and about 1 mL of the dilute solution was placed in a polyethylene vial, weighed, and then measured with a measurement time ranging from 160 ks to 320 ks.

The distance between the sample and the detector was set at 160 cm, and the configuration as shown in Fig. 2.2.10 was used.

Furthermore, the count efficiency was determined with the use of standard  $\gamma$ -ray sources of Cs-137 and Eu-152, and the radioactivity of each nuclide was calculated.

A typical example of a  $\gamma$ -ray spectrum is shown in Fig. 2.2.11.

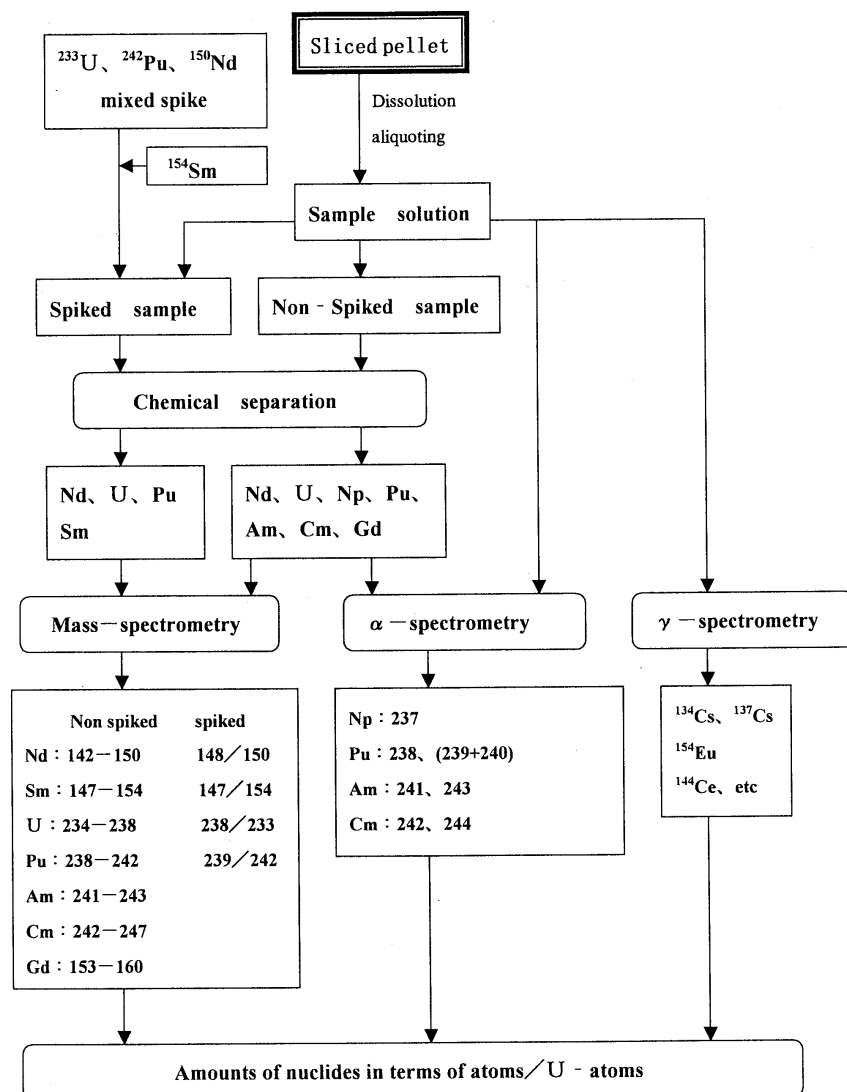


Fig. 2.2.3. Flow diagram for analysis of the spent fuel sample.

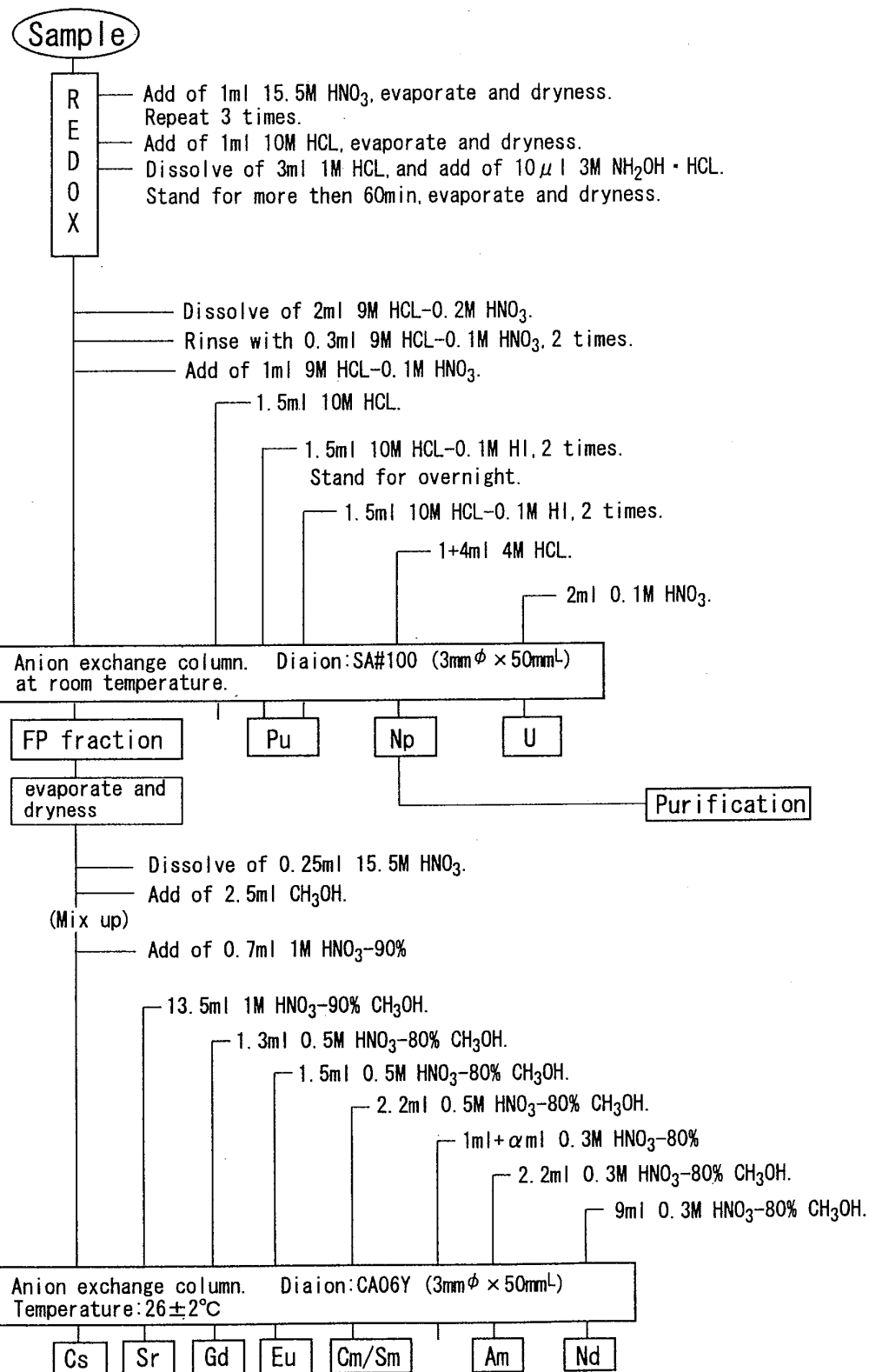


Fig. 2.2.4. Schematic diagram for the separation of dissolved solution (1/2).

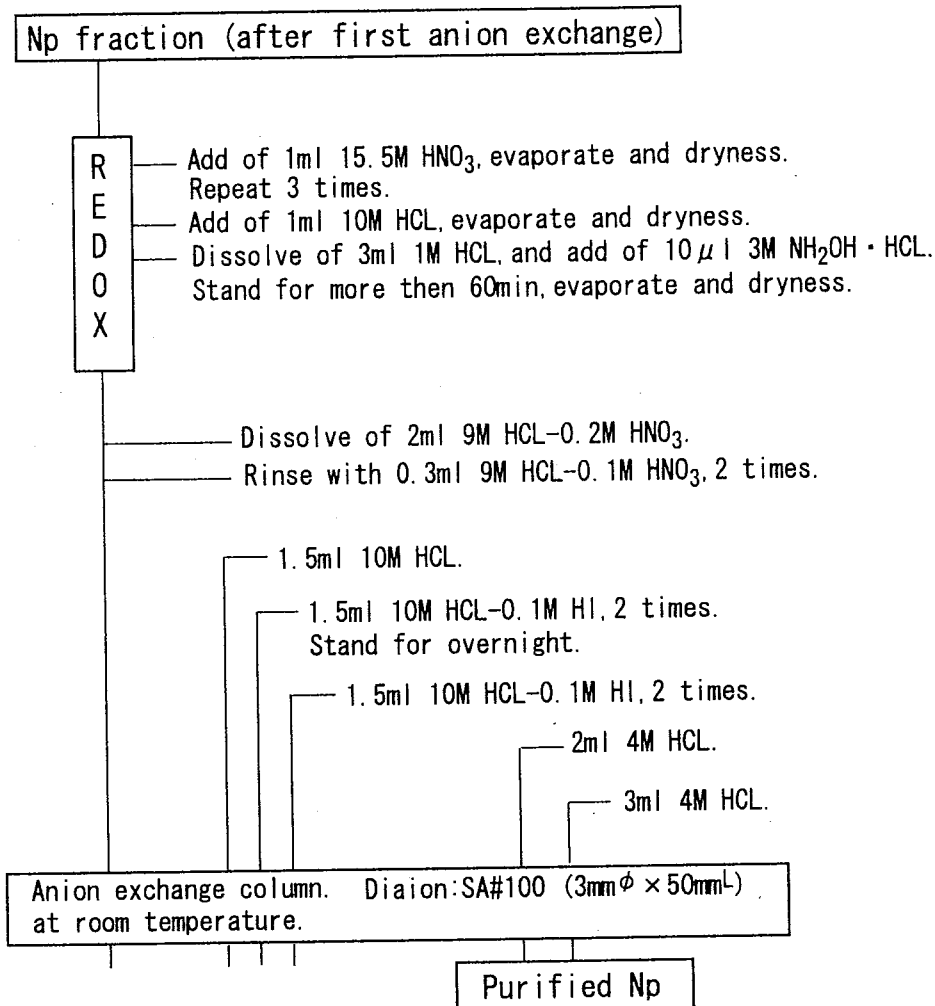
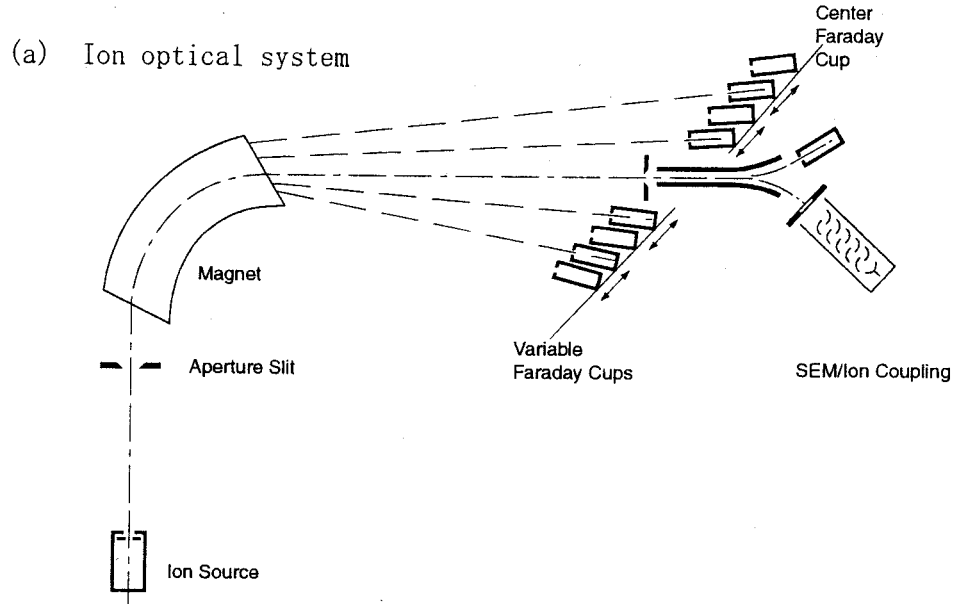


Fig. 2.2.4. Schematic diagram for the separation of dissolved solution (2/2)  
 - Np purification -.



(b) Multiple detector configuration

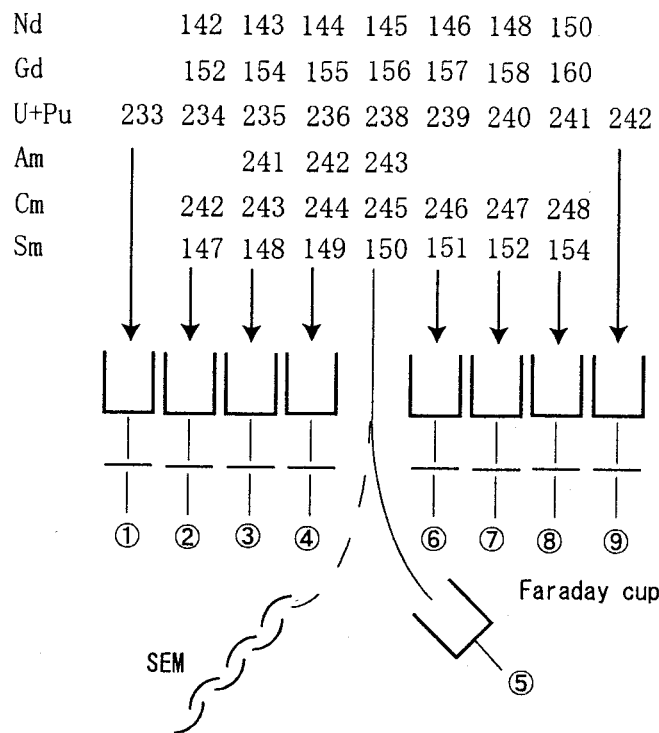


Fig. 2.2.5. Ion optical system and variable multiple detector configuration for mass-spectrometer.

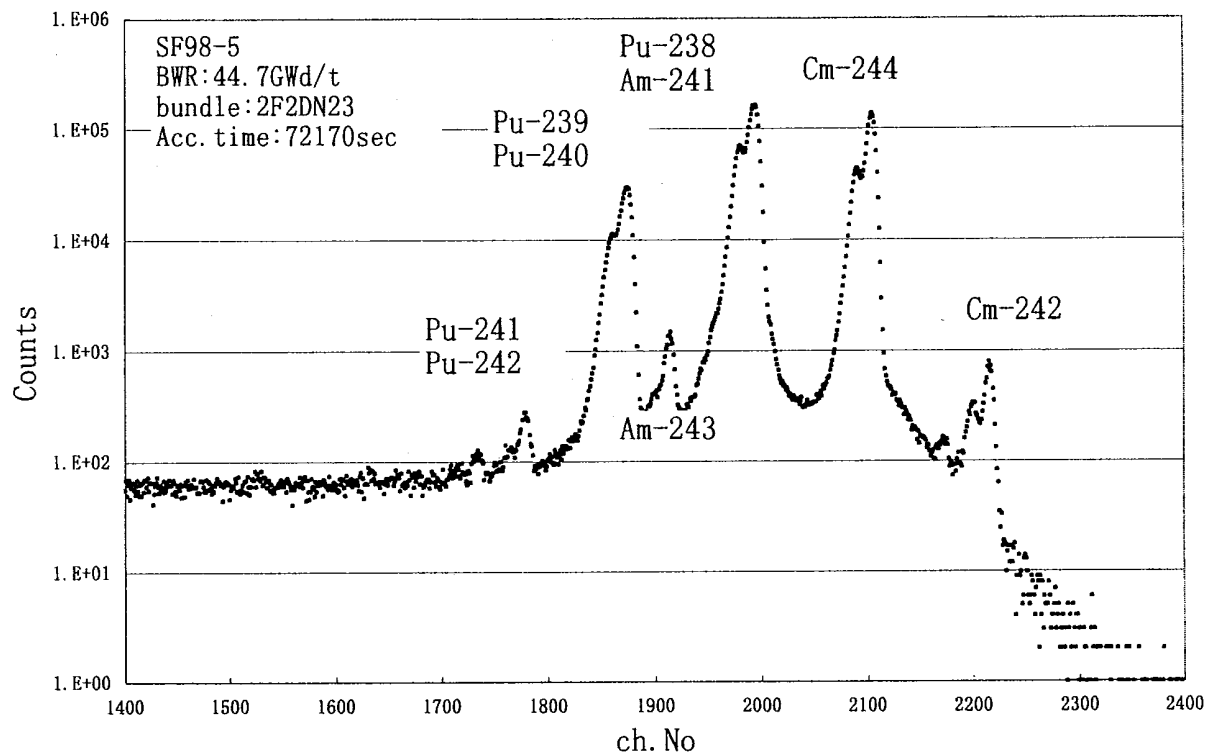


Fig. 2.2.6.  $\alpha$ -ray spectrum of dissolved solution before chemical separation.

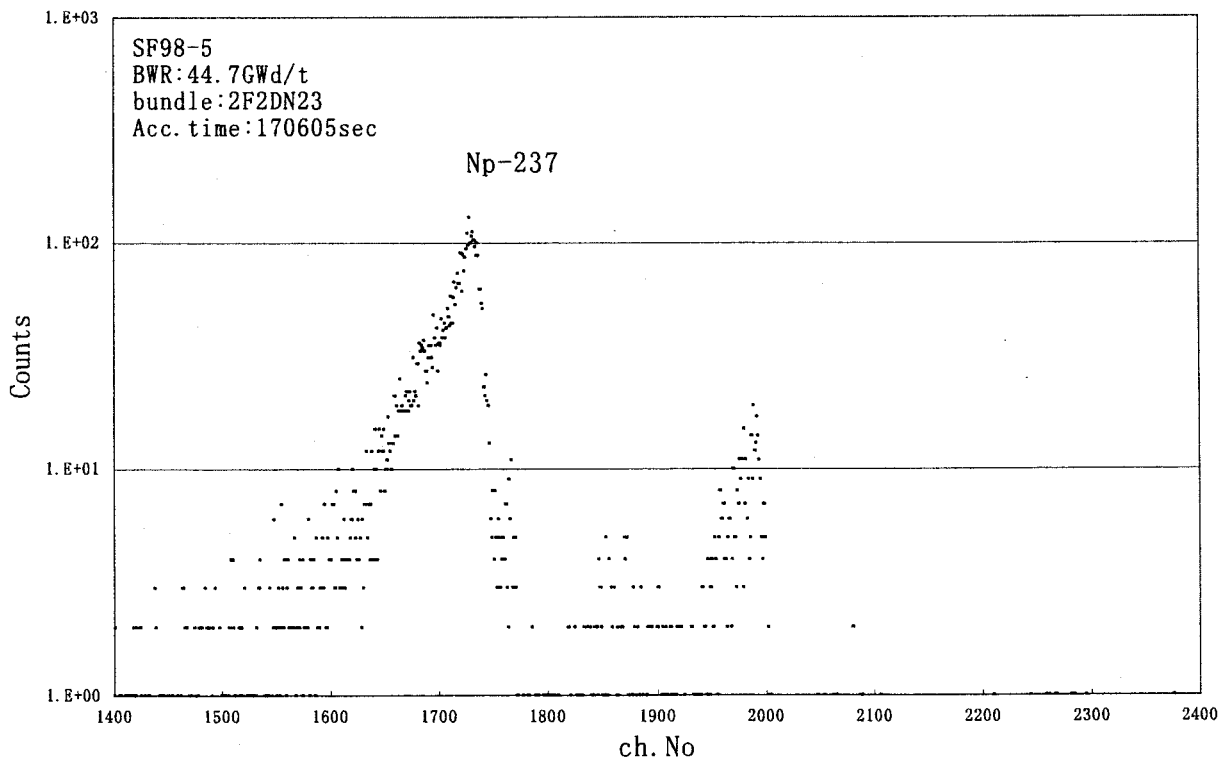


Fig. 2.2.7.  $\alpha$ -ray spectrum of Neptunium fraction.

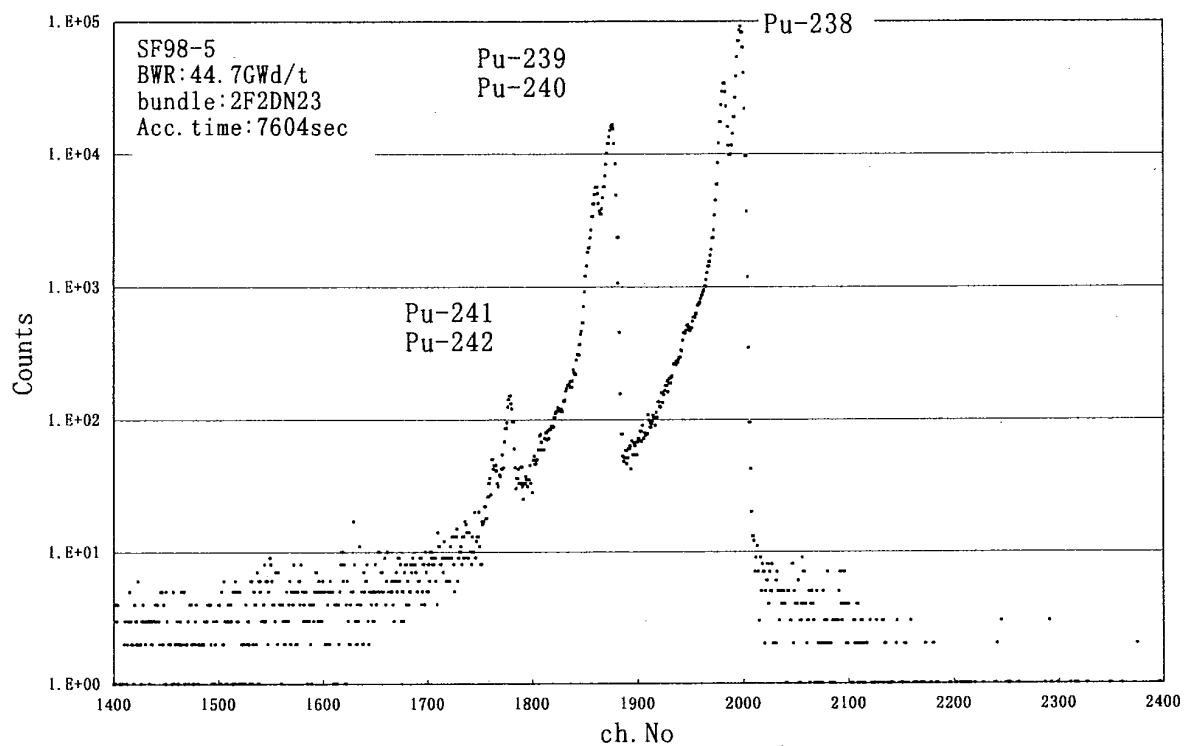


Fig. 2.2.8.  $\alpha$ -ray spectrum of Plutonium fraction.

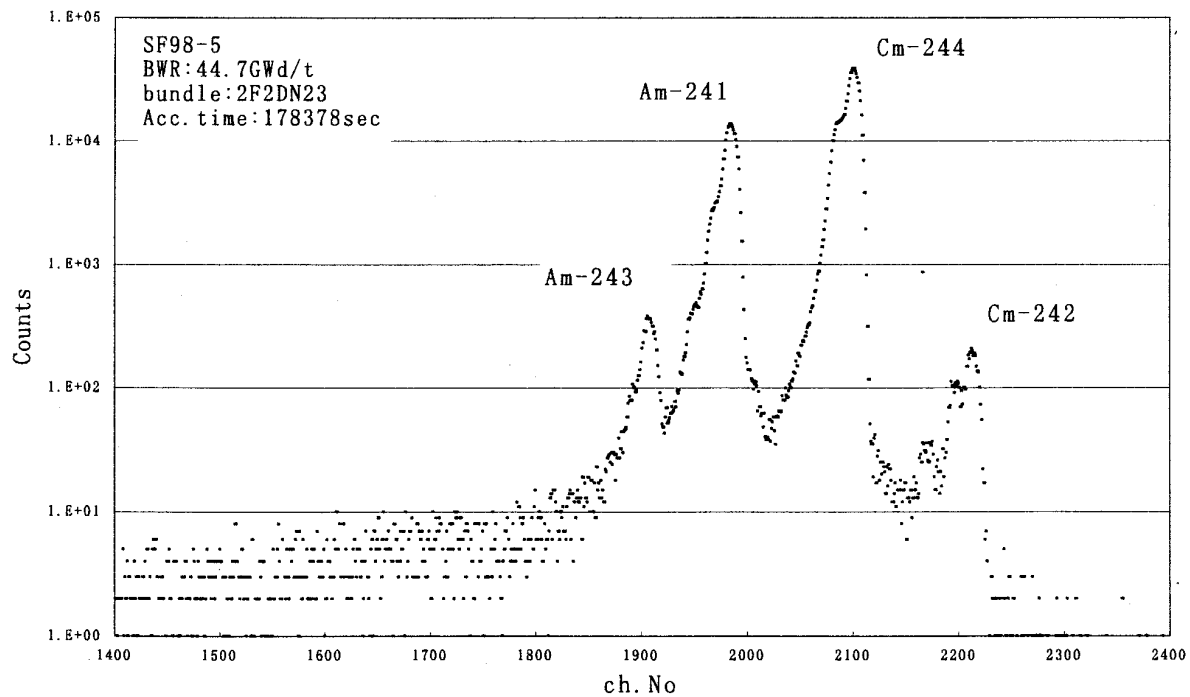


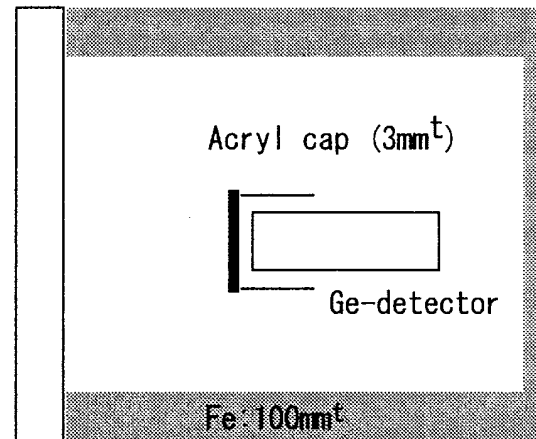
Fig. 2.2.9.  $\alpha$ -ray spectrum of FP fraction.

(a) Sample

Diluted sample in the  
10ml polyethylene vial  
(about 1ml)



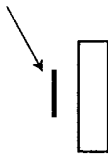
Acryl plate (15mm<sup>t</sup>)



← 160cm →

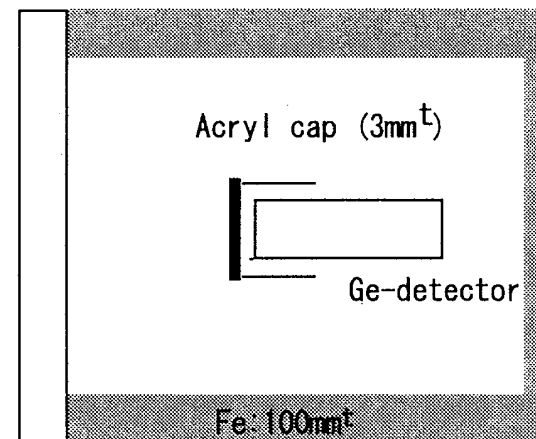
(b) Standard source

standard  $\gamma$ -ray source  
( $^{137}\text{Cs}$ ,  $^{152}\text{Eu}$ )



Acryl plate (6mm<sup>t</sup>)  
(Compensate for self  
absorption of sample)

Acryl plate (15mm<sup>t</sup>)



← 160cm →

Fig. 2.2.10. Allocation of sample/standard source and Ge-detector for  $\gamma$ -ray measurement.

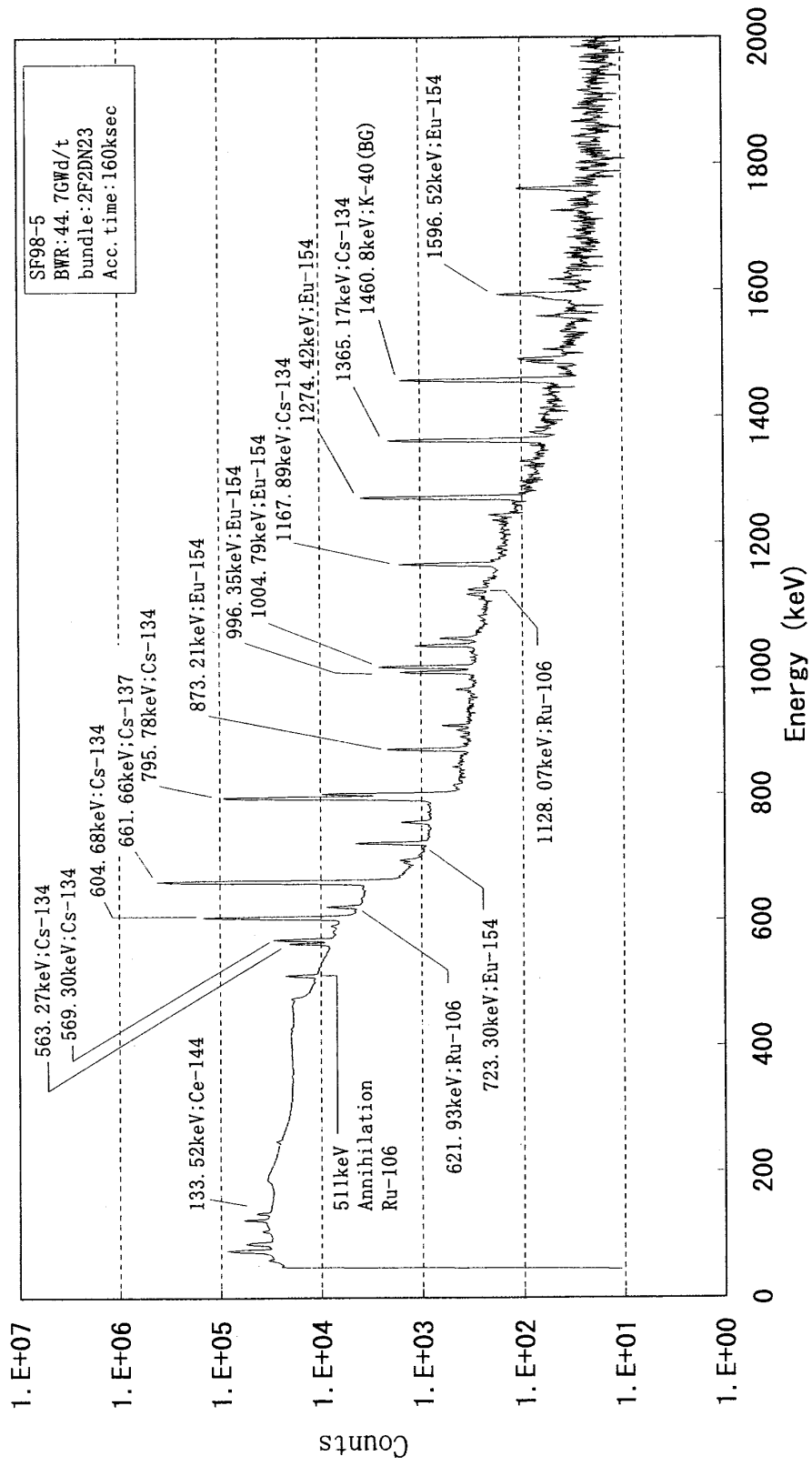


Fig. 2.2.11. An example of  $\gamma$ -ray spectrum profile for dissolved solution.

## 2.2.5. Burn-Up Rate (Degree) Calculation Method

From the analysis results for the compositions of nuclides such as U, Pu, etc., obtained by destructive analysis, the burn-up rate of the sample concerned was calculated by the following equation:<sup>4</sup>

$$\text{burnup rate (\%FMA)} = \frac{F}{U_0} = \frac{\text{Nd-148 / U / Y(eff.)}}{(1 + \text{Pu/U} + (\text{Am} + \text{Cm} + \text{Np})/\text{U} + \text{F/U})} \times 100.$$

Here,  $F/U_0$  is the number of fissions per initial uranium. The number of fissions (F) can be obtained by dividing the amount of Nd-148 which is a stable FP isotope by the effective fission field (Y(eff.)). The initial amount of uranium in the denominator is expressed as the sum of the total amount of actinides such as U, Pu, etc., after irradiation and the number of fissions, as shown in the second term. The value of the fission yield of Nd-148 relative to U-235, Pu-239, U-238, and Pu-241 was taken from LA-UR-94-3106 (ENDF-349), by T. R. England and B. F. Rider, 1994/10, and the proportion of fission of the above-mentioned 4 fissionable nuclides was determined by SWAT burn-up calculation code<sup>5</sup> and used as a weight to determine the value of Y(eff.).

Here, the analytical value of Nd-148 to be used in the burn-up calculation is the value at the end of irradiation, but this value includes Nd-148 originating in the  $(n, \gamma)$  reaction from Nd-147, which forms during burning.

Furthermore, the value of the burn-up degree (GWd/t) was determined by multiplying the value of the burn-up rate (%FIMA = Fissions per Initial Metal Atom in percent) by 9.6. The error of burn-up by this method is 3% or less.<sup>4</sup>

## 2.2.6. Analytical Results and Errors

The analytical results for actinides and FP nuclides are shown in Tables 2.2.3–2.2.12 for the various samples cut from spent fuel rods. The analytical value of the isotopes is shown in the ratio of the number of atoms per atom of initial uranium at the end of irradiation (atoms/IMA), but the value for Pu-239 includes the amount of Np-239 because the correction is difficult. Furthermore, the value of each isotope of Sm is the value at the time of analysis, because it is difficult to assess the contribution from Pm during the cooling period until analysis.

In these tables, the value of the burn-up rate (degree) evaluated by the Nd-148 method and the sampling position from the top of the fuel rod are also shown in numerical values.

The relative standard deviations of these results are within the following ranges, depending on the nuclide and the measurement method.

In isotope dilution—mass spectrometry: Nd, Sm < 0.1%; U-235, U-238 < 0.1%; U-234 < 1%; U-236 < 2%; Pu-239, Pu-240, Pu-241, Pu-242 < 0.3%; and Pu-238 < 0.5%.

In the measurement of isotopic ratios by  $\alpha$ -ray measurement and mass spectrometry: Am-241, Cm-243, Cm-244, Cm-245 < 2%; Am-243, Cm-246 < 5%; and Am-242m, Cm-242, Cm-247 < 10%.

In the measurement of isotopic ratios of Gd elements by mass spectrometry: < 0.1%.

In the quantification of Np-237 by  $\alpha$ -ray measurement: < 10%.

In the  $\gamma$ -ray measurement: Cs-134, Cs-137, Eu-154 < 3%, Ru-106 < 5%, Sb-125, Ce-144 < 10%.

## REFERENCES

1. Author(s) not given: Dissolution Test Group, Chemistry Department, Japan Atomic Energy Research Institute. JAERI-M 91-010, 1991.
2. S. Usuda, N. Kohno, *Sep. Sci. Tech.*, **23**, 1119 (1988).
3. N. Kohno, K. Gunji, et al., "Abstracts of Papers," *Autumn Meeting of the Atomic Energy Society of Japan*, K26, 1991.
4. Standard Test Method for Atom Percent Fission in Uranium and Plutonium Fuel (Neodymium-148 Method), ANSI/ASTM E 321 – 79.
5. K. Suyama, T. Kiyosumi and H. Mochizuki, "Revised SWAT – The Integrated Burn-up Calculation Code System," JAERI-Data/Code 2000-027, May 2000 (in Japanese).

Table 2.2.3. SF95: Destructive analytical results of actinide nuclides for PWR spent fuel ( $\text{UO}_2$ ) sample, normalized in zero cooling

Sample ID	SF95-1	SF95-2	SF95-3	SF95-4	unit atoms/IMA
Sampling position (from top, mm)	201	361	881	2161	3561
Initial	After irradiation				
Burnup (FIMA)	1.490E-02	2.536E-02	3.690E-02	3.822E-02	3.167E-02
Burnup (GWd/t)	14.30	24.35	35.42	36.69	30.40
U-234	3.680E-04	3.031E-04	2.605E-04	2.170E-04	2.175E-04
U-235	4.108E-02	2.707E-02	1.956E-02	1.340E-02	1.243E-02
U-236	0	2.689E-03	4.020E-03	4.957E-03	5.041E-03
U-238	9.585E-01	9.494E-01	9.420E-01	9.333E-01	9.330E-01
U total	1.000E+00	9.795E-01	9.658E-01	9.519E-01	9.507E-01
dU-235		1.401E-02	2.153E-02	2.769E-02	2.866E-02
F5		1.120E-02	1.722E-02	2.221E-02	2.308E-02
F5/Ftotal		0.752	0.679	0.602	0.604
dU-238		9.114E-03	1.655E-02	2.524E-02	2.554E-02
Np-237		1.364E-04	2.639E-04	4.302E-04	4.561E-04
Pu-238		1.716E-05	7.122E-05	1.543E-04	1.588E-04
Pu-239 (*)		4.207E-03	5.628E-03	6.164E-03	5.976E-03
Pu-240		7.734E-04	1.525E-03	2.167E-03	2.187E-03
Pu-241		3.642E-04	9.456E-04	1.466E-03	1.447E-03
Pu-242		3.726E-05	1.810E-04	4.438E-04	4.716E-04
Pu total		5.399E-03	8.351E-03	1.040E-02	1.024E-02
Am-241		1.360E-05	2.314E-05	3.267E-05	2.320E-05
Am-242m		1.809E-07	5.121E-07	7.711E-07	7.147E-07
Am-243		2.625E-06	2.240E-05	7.878E-05	8.293E-05
Am total		1.641E-05	4.606E-05	1.122E-04	1.068E-04
Cm-242		1.484E-06	7.541E-06	1.930E-05	2.288E-05
Cm-243		1.420E-08	1.217E-07	3.635E-07	3.889E-07
Cm-244		2.644E-07	4.916E-06	2.498E-05	2.766E-05
Cm-245		5.362E-09	1.908E-07	1.355E-06	1.542E-06
Cm-246		2.554E-10	1.112E-08	1.017E-07	1.207E-07
Cm total		1.768E-06	1.278E-05	4.610E-05	5.259E-05
Pu + Am + Cm		5.417E-03	8.410E-03	1.055E-02	1.040E-02
F8		3.697E-03	8.144E-03	1.469E-02	1.514E-02
F8/Ftotal		2.482E-01	3.211E-01	3.982E-01	3.960E-01
U + Np + Pu + Am + Cm +		1.000	1.000	1.000	1.000
Fission					

## F5 : U-235 fission

= FIMA-F8

## FIMA : Fission per Initial Metal Atom

### dU-235 : U-235 depletion

$\equiv$  U=235 (initial) = U=235 (after)

### F8 : U-238 fission

$$\equiv dU-238 - (P_{11} + A_m + C_m)$$

### dU-238 : U-238 depletion

$\equiv U-238$  (initial) =  $U-238$  (after)

(\*) : The Pu-239 at zero cooling includes the amount of Np-239

Table 2.2.4. SF95: Destructive analytical results of FP nuclides  
for PWR spent fuel ( $\text{UO}_2$ ) sample, normalized in zero cooling

Sample ID	SF95-1	SF95-2	SF95-3	unit:atoms/IMA	
				SF95-4	SF95-5
Sampling position (from top mm)	201	361	881	2161	3561
Initial					
Burnup (FIMA)	1.490E-02	2.536E-02	3.690E-02	3.822E-02	3.167E-02
Burnup (GWd/t)	14.30	24.35	35.42	36.69	30.40
Nd-143	7.709E-04	1.190E-03	1.548E-03	1.560E-03	1.383E-03
Nd-144	5.416E-04	9.997E-04	1.545E-03	1.693E-03	1.311E-03
Nd-145	5.465E-04	8.840E-04	1.214E-03	1.247E-03	1.070E-03
Nd-146	4.645E-04	8.142E-04	1.213E-03	1.260E-03	1.023E-03
Nd-148	2.560E-04	4.401E-04	6.400E-04	6.638E-04	5.469E-04
Nd-150	1.143E-04	1.996E-04	3.009E-04	3.111E-04	2.496E-04
Nd total	2.694E-03	4.528E-03	6.462E-03	6.735E-03	5.583E-03
Cs-137	9.39E-04	1.62E-03	2.34E-03	2.43E-03	2.00E-03
Cs-134	4.16E-05	1.24E-04	2.50E-04	2.61E-04	1.80E-04
Eu-154	6.33E-06	2.02E-05	3.91E-05	4.11E-05	2.81E-05
Ce-144	3.21E-04	5.23E-04	7.54E-04	7.11E-04	6.40E-04
Sb-125	2.80E-06	5.52E-06	7.11E-06	6.04E-06	6.21E-06
Ru-106	1.00E-04	1.87E-04	3.06E-04	3.15E-04	2.71E-04

Table 2.2.5. SF96: Destructive analytical results of actinide nuclides for PWR spent fuel ( $\text{UO}_2\text{-Gd}_2\text{O}_3$ ) sample, normalized in zero cooling

	unit atoms/IMA				
Sample ID	SF96-1	SF96-2	SF96-3	SF96-4	SF96-5
Sampling position (from top, mm)	176	336	856	2136	3536
Initial	After irradiation				
Burnup (FIMA)	8.115E-03	1.713E-02	2.938E-02	3.011E-02	2.520E-02
Burnup (GWd/t)	7.79	16.44	28.20	28.91	24.19
U-234	2.2000E-04	1.836E-04	1.548E-04	1.272E-04	1.271E-04
U-235	2.6250E-02	1.968E-02	1.426E-02	8.746E-03	8.164E-03
U-236	0	1.432E-03	2.430E-03	3.271E-03	3.329E-03
U-238	9.7246E-01	9.657E-01	9.577E-01	9.473E-01	9.472E-01
U total	9.9900E-01	9.870E-01	9.745E-01	9.594E-01	9.588E-01
dU-235		6.570E-03	1.199E-02	1.750E-02	1.809E-02
F5		6.068E-03	1.035E-02	1.470E-02	1.523E-02
F5/Ftotal		0.748	0.604	0.500	0.506
dU-238		6.780E-03	1.479E-02	2.519E-02	2.527E-02
Np-237		6.148E-05	1.329E-04	2.176E-04	2.261E-04
Pu-238		8.534E-06	4.171E-05	1.205E-04	1.248E-04
Pu-239 (*)		3.764E-03	5.434E-03	5.974E-03	5.792E-03
Pu-240		6.706E-04	1.482E-03	2.283E-03	2.307E-03
Pu-241		2.588E-04	8.573E-04	1.479E-03	1.461E-03
Pu-242		2.399E-05	1.587E-04	5.017E-04	5.319E-04
Pu total		4.726E-03	7.973E-03	1.036E-02	1.022E-02
Am-241		5.908E-06	1.713E-05	2.808E-05	3.055E-05
Am-242m		1.198E-07	4.502E-07	6.305E-07	6.678E-07
Am-243		1.123E-06	1.692E-05	8.687E-05	9.397E-05
Am total		7.151E-06	3.449E-05	1.156E-04	1.252E-04
Cm-242		8.359E-07	5.684E-06	1.601E-05	1.650E-05
Cm-244		9.321E-08	3.015E-06	2.790E-05	3.050E-05
Cm total		9.291E-07	8.698E-06	4.391E-05	4.701E-05
Pu + Am + Cm		4.734E-03	8.016E-03	1.052E-02	1.039E-02
F8		2.046E-03	6.774E-03	1.467E-02	1.488E-02
F8/Ftotal		2.522E-01	3.955E-01	4.995E-01	4.941E-01
U + Np + Pu + Am + Cm + Fission		1.000	1.000	1.000	1.000

F5 : U-235 fission = FIMA-F8 FIMA : Fission per Initial Metal Atom

dU-235 : U-235 depletion = U-235(initial) - U-235 (after)

F8 : U-238 fission = dU-238 - (Pu + Am + Cm)

dU-238 : U-238 depletion = U-238 (initial) - U-238 (after)

(\*) : The Pu-239 at zero cooling includes the amount of Np-239.

Table 2.2.6. SF96: Destructive analytical results of FP nuclides  
for PWR spent fuel ( $\text{UO}_2\text{-Gd}_2\text{O}_3$ ) sample, normalized in zero cooling

Sample ID	SF96-1	SF96-2	SF96-3	SF96-4	SF96-5	
Sampling position (from top, mm)	176	336	856	2136	3536	
Initial	After irradiation					
Burnup (FIMA)	8.115E-03	1.713E-02	2.938E-02	3.011E-02	2.520E-02	
Burnup (GWd/t)	7.79	16.44	28.20	28.91	24.19	
Nd-143	4.198E-04	7.957E-04	1.192E-03	1.196E-03	1.071E-03	
Nd-144	2.540E-04	5.934E-04	1.206E-03	1.242E-03	9.802E-04	
Nd-145	2.956E-04	5.870E-04	9.469E-04	9.656E-04	8.367E-04	
Nd-146	2.505E-04	5.326E-04	9.452E-04	9.700E-04	8.008E-04	
Nd-148	1.411E-04	2.978E-04	5.150E-04	5.277E-04	4.397E-04	
Nd-150	6.556E-05	1.424E-04	2.525E-04	2.584E-04	2.113E-04	
Nd total	1.427E-03	2.949E-03	5.057E-03	5.160E-03	4.340E-03	
Cs-137	4.89E-04	1.04E-03	1.77E-03	1.83E-03	1.49E-03	
Cs-134	1.53E-05	6.68E-05	1.78E-04	1.86E-04	1.27E-04	
Eu-154	3.57E-06	1.32E-05	3.05E-05	3.08E-05	2.20E-05	
Ce-144	1.95E-04	3.72E-04	5.56E-04	5.71E-04	5.20E-04	
Sb-125	2.73E-06	5.39E-06	6.97E-06	8.85E-06	7.03E-06	
Ru-106	6.36E-05	1.36E-04	3.15E-04	2.90E-04	3.02E-04	
Natural Gd						
Gd-154	2.2	2.043	2.004	1.922	1.889	1.938
Gd-155	14.8	0.702	0.903	0.812	0.571	1.474
Gd-156	20.5	34.86	34.43	34	34.05	34.09
Gd-157	15.7	0.092	0.116	0.095	0.059	0.178
Gd-158	24.8	40.5	40.63	41.09	41.26	40.6
Gd-160	21.9	21.55	21.43	21.57	21.74	21.18

Table 2.2.7. SF97: Destructive analytical results of actinide nuclides  
for PWR high burnup spent fuel ( $\text{UO}_2$ ) sample, normalized in zero cooling

Sample ID	SF97-1	SF97-2	SF97-3	SF97-4	SF97-5	SF97-6
Sampling position (from top, mm)	163	350	627	1839	2926	3556
	Initial			After irradiation		unit atoms/IMA
Burnup (FIMA)	1.843E-02	3.201E-02	4.392E-02	4.899E-02	4.922E-02	4.249E-02
Burnup (GWd/t)	17.69	30.73	42.16	47.03	47.25	40.79
U-234	3.800E-05	2.988E-04	2.387E-04	2.043E-04	1.903E-04	1.896E-04
U-235	4.158E-02	2.376E-02	1.590E-02	1.043E-02	8.279E-03	8.029E-03
U-236	0	3.140E-03	4.596E-03	5.354E-03	5.572E-03	5.576E-03
U-238	9.584E-01	9.488E-01	9.372E-01	9.277E-01	9.241E-01	9.242E-01
U total	1.000E+00	9.760E-01	9.579E-01	9.437E-01	9.381E-01	9.380E-01
dU-235		1.782E-02	2.632E-02	3.252E-02	3.529E-02	3.576E-02
F5		1.417E-02	2.034E-02	2.459E-02	2.657E-02	2.684E-02
F5/Ftotal		0.769	0.636	0.560	0.542	0.545
dU-238		9.530E-03	2.119E-02	3.063E-02	3.430E-02	3.418E-02
Np-237		1.527E-04	4.049E-04	5.867E-04	6.629E-04	6.726E-04
Pu-238		2.369E-05	1.249E-04	2.580E-04	3.197E-04	3.186E-04
Pu-239 (*)		3.826E-03	5.900E-03	6.188E-03	6.009E-03	5.948E-03
Pu-240		9.264E-04	1.854E-03	2.449E-03	2.644E-03	2.625E-03
Pu-241		4.182E-04	1.219E-03	1.667E-03	1.747E-03	1.731E-03
Pu-242		6.079E-05	3.098E-04	6.406E-04	8.105E-04	8.199E-04
Pu total		5.255E-03	9.407E-03	1.120E-02	1.153E-02	1.144E-02
Am-241		1.473E-05	3.965E-05	4.845E-05	5.242E-05	5.258E-05
Am-242m		2.231E-07	8.687E-07	1.159E-06	1.212E-06	1.180E-06
Am-243		4.354E-06	5.024E-05	1.380E-04	1.883E-04	1.894E-04
Am total		1.931E-05	9.076E-05	1.876E-04	2.420E-04	2.431E-04
Cm-242		2.098E-06	1.031E-05	1.808E-05	2.009E-05	1.871E-05
Cm-243		2.431E-08	2.714E-07	6.775E-07	8.537E-07	8.487E-07
Cm-244		4.856E-07	1.349E-05	5.553E-05	8.589E-05	8.601E-05
Cm-245		1.055E-08	6.649E-07	3.626E-06	5.866E-06	5.743E-06
Cm-246		3.738E-10	4.082E-08	3.527E-07	7.194E-07	7.299E-07
Cm-247		—	3.893E-10	4.790E-09	1.057E-08	1.035E-08
Cm total		2.619E-06	2.477E-05	7.826E-05	1.134E-04	1.121E-04
Pu + Am + Cm		5.277E-03	9.522E-03	1.130E-02	1.189E-02	1.180E-02
F8		4.253E-03	1.167E-02	1.933E-02	2.241E-02	2.238E-02
F8/Ftotal		0.231	0.364	0.440	0.458	0.455
U + Np + Pu + Am + Cm + Fission		1.000	1.000	1.000	1.000	1.000

F5 : U-235 fission

= FIMA-F8

FIMA : Fission per Initial Metal Atom

dU-235 : U-235 depletion

= U-235 (initial) - U-235 (after)

F8 : U-238 fission

= dU-238 - (Pu+Am+Cm)

dU-238 : U-238 depletion

= U-238 (initial) - U-238 (after)

(\*) : The Pu-239 at zero cooling includes the amount of Np-239.

Table 2.2.8. SF97: Destructive analytical results of FP nuclides  
for PWR high burnup spent fuel ( $\text{UO}_2$ ) sample, normalized in zero cooling  
unit: atoms/IMA

Sample ID	SF97-1	SF97-2	SF97-3	SF97-4	SF97-5	SF97-6
Sample position (from top, mm)	163	350	627	1839	2926	3556
After irradiation						
Burnup (FIMA)	1.843E-02	3.201E-02	4.392E-02	4.899E-02	4.922E-02	4.249E-02
Burnup (GWd/t)	17.69	30.73	42.16	47.03	47.25	40.79
Nd-142	9.866E-06	2.454E-05	4.558E-05	5.745E-05	5.827E-05	4.283E-05
Nd-143	9.074E-04	1.383E-03	1.679E-03	1.745E-03	1.746E-03	1.621E-03
Nd-144	7.706E-04	1.462E-03	2.200E-03	2.591E-03	2.644E-03	2.167E-03
Nd-145	6.642E-04	1.064E-03	1.377E-03	1.497E-03	1.507E-03	1.354E-03
Nd-146	5.710E-04	1.028E-03	1.456E-03	1.644E-03	1.654E-03	1.400E-03
Nd-148	3.129E-04	5.452E-04	7.499E-04	8.371E-04	8.406E-04	7.244E-04
Nd-150	1.360E-04	2.510E-04	3.546E-04	3.993E-04	3.996E-04	3.381E-04
Nd total	3.372E-03	5.756E-03	7.861E-03	8.771E-03	8.849E-03	7.647E-03
Cs-137	1.15E-03	2.00E-03	2.75E-03	3.04E-03	3.06E-03	2.66E-03
Cs-134	5.30E-05	1.83E-04	3.25E-04	3.80E-04	3.81E-04	2.90E-04
Eu-154	8.12E-06	3.05E-05	5.09E-05	5.78E-05	5.73E-05	4.42E-05
Ce-144	3.35E-04	5.06E-04	6.15E-04	6.21E-04	6.20E-04	6.14E-04
Sb-125	4.69E-06	9.75E-06	9.46E-06	1.16E-05	1.43E-05	8.66E-06
Ru-106	1.16E-04	2.61E-04	4.11E-04	4.35E-04	2.61E-04	4.40E-04
Ag-110m	4.45E-08	3.69E-07	1.08E-06	2.11E-06	—	1.01E-06
(Sm : As for 3.96 years cooling time)						
Sm-147	2.477E-04	3.320E-04	3.814E-04	3.997E-04	4.015E-04	3.839E-04
Sm-148	6.582E-05	1.921E-04	3.182E-04	3.761E-04	3.792E-04	2.913E-04
Sm-149	4.689E-06	6.352E-06	6.805E-06	6.300E-06	6.070E-06	6.138E-06
Sm-150	2.100E-04	3.966E-04	5.712E-04	6.466E-04	6.527E-04	5.407E-04
Sm-151	1.473E-05	2.126E-05	2.372E-05	2.351E-05	2.307E-05	2.040E-05
Sm-152	1.022E-04	1.495E-04	1.866E-04	2.033E-04	2.065E-04	1.887E-04
Sm-154	2.202E-05	4.601E-05	7.011E-05	8.118E-05	8.190E-05	6.544E-05
Sm total	6.672E-04	1.144E-03	1.558E-03	1.737E-03	1.751E-03	1.497E-03

Table 2.2.9. SF98: Destructive analytical results of actinide nuclides for BWR spent fuel ( $\text{UO}_2$ ) sample, normalized in zero cooling

Sample ID	SF98-1	SF98-2	SF98-3	SF98-4	SF98-5	SF98-6	SF98-7	SF98-8
Sampling position (from top, mm)	4030	3902	3646	3377	2855	2014	1312	672
unit atoms/IMA								
Initial								
Burnup (FIMA)	4.323E-03	2.761E-02	3.848E-02	4.411E-02	4.582E-02	4.158E-02	4.105E-02	2.831E-02
Burnup (GWd/t)	4.15	26.51	36.94	42.35	43.99	39.92	39.41	27.18
U-234	0	4.961E-05	2.722E-04	2.214E-04	2.009E-04	1.935E-04	1.891E-04	1.987E-04
U-235	3.900E-02	4.179E-03	1.764E-02	8.243E-03	6.040E-03	6.393E-03	9.173E-03	9.472E-03
U-236	0	4.897E-04	3.580E-03	5.034E-03	5.326E-03	5.350E-03	5.181E-03	5.159E-03
U-238	9.610E-01	9.879E-01	9.455E-01	9.401E-01	9.354E-01	9.323E-01	9.330E-01	9.328E-01
U total	1.000E+00	9.926E-01	9.670E-01	9.536E-01	9.469E-01	9.443E-01	9.475E-01	9.476E-01
dU-235		3.021E-03	2.136E-02	3.076E-02	3.296E-02	3.261E-02	2.983E-02	2.953E-02
F5		2.474E-03	1.720E-02	2.490E-02	2.675E-02	2.627E-02	2.358E-02	2.335E-02
F5/Ftotal		0.572	0.623	0.647	0.606	0.573	0.567	0.648
dU-238		4.840E-03	1.546E-02	2.088E-02	2.562E-02	2.867E-02	2.803E-02	2.825E-02
Np-237		2.388E-05	1.484E-04	3.359E-04	4.334E-04	3.876E-04	5.176E-04	4.590E-04
Pu-238		3.134E-06	2.825E-05	1.167E-04	1.677E-04	1.935E-04	1.691E-04	2.082E-04
Pu-239 (*)		2.286E-03	3.357E-03	3.677E-03	3.774E-03	4.245E-03	5.280E-03	5.601E-03
Pu-240		5.426E-04	1.111E-03	2.116E-03	2.436E-03	2.590E-03	2.607E-03	2.645E-03
Pu-241		1.314E-04	4.253E-04	8.833E-04	1.019E-03	1.157E-03	1.275E-03	1.338E-03
Pu-242		1.659E-05	9.134E-05	4.544E-04	6.509E-04	6.821E-04	5.339E-04	5.347E-04
Pu total		2.980E-03	5.012E-03	7.247E-03	8.047E-03	8.868E-03	9.865E-03	1.033E-02
Am-241		1.015E-05	2.270E-05	3.229E-05	3.373E-05	3.685E-05	4.038E-05	4.332E-05
Am-242m		7.848E-08	2.916E-07	4.914E-07	5.207E-07	6.308E-07	8.476E-07	8.822E-07
Am-243		5.716E-07	6.844E-06	6.537E-05	1.114E-04	1.246E-04	1.093E-04	1.065E-04
Am total		1.080E-05	2.984E-05	9.815E-05	1.457E-04	1.621E-04	1.505E-04	1.512E-05
Cm-242		5.219E-07	3.520E-06	1.667E-05	2.224E-05	3.401E-05	5.824E-05	2.843E-05
Cm-243		—	3.632E-08	3.069E-07	4.158E-07	4.842E-07	5.234E-07	5.806E-07
Cm-244		3.017E-08	7.802E-07	1.654E-05	3.544E-05	4.874E-05	4.192E-05	4.372E-05
Cm-245		—	1.598E-08	5.326E-07	1.299E-06	2.255E-06	2.408E-06	2.654E-06
Cm-246		—	—	7.412E-08	2.234E-07	3.722E-07	2.838E-07	2.908E-07
Cm total		5.520E-07	4.352E-06	3.412E-05	5.962E-05	8.586E-05	1.034E-04	7.568E-05
Pu + Am + Cm		2.991E-03	5.047E-03	7.298E-03	8.253E-03	9.116E-03	1.003E-02	1.055E-02
F8		1.849E-03	1.041E-02	1.358E-02	1.737E-02	1.955E-02	1.800E-02	1.770E-02
F8/Ftotal		0.428	0.377	0.353	0.394	0.427	0.433	0.431
U + Np + Pu + Am + Cm + Fission		1.000	1.000	1.000	1.000	1.000	1.000	1.000

F5 : U-235 fission = FIMA-F8 FIMA : Fission per Initial Metal Atom

dU-235 : U-235 depletion = U-235 (initial) - U-235 (after)

F8 : U-238 fission = dU-238 - (Pu + Am + Cm)

dU-238 : U-238 depletion = U-238 (initial) - U-238 (after)

(\*) : The Pu-239 at zero cooling includes the amount of Np-239.

Table 2.2.10. SF98: Destructive analytical results of FP nuclides  
for BWR spent fuel ( $\text{UO}_2$ ) sample, normalized in zero cooling

Sample ID	SF98-1	SF98-2	SF98-3	SF98-4	SF98-5	SF98-6	SF98-7	SF98-8	unit: atoms/IMA
Sampling position (from top mm)	4030	3902	3646	3377	2855	2014	1312	672	
After irradiation									
Burnup (FIMA)	4.323E-03	2.761E-02	3.848E-02	4.411E-02	4.582E-02	4.158E-02	4.105E-02	2.831E-02	
Burnup (GWd/t)	4.15	26.51	36.94	42.35	43.99	39.92	39.41	27.18	
Nd-142	2.256E-06	2.839E-05	3.985E-05	7.147E-05	5.629E-05	4.38E-05	4.433E-05	2.037E-05	
Nd-143	2.011E-04	1.260E-03	1.371E-03	1.413E-03	1.505E-03	1.53E-03	1.529E-03	1.225E-03	
Nd-144	1.907E-04	1.407E-03	2.109E-03	2.468E-03	2.440E-03	2.12E-03	1.996E-03	1.236E-03	
Nd-145	1.509E-04	9.808E-04	1.256E-03	1.383E-03	1.423E-03	1.31E-03	1.288E-03	9.475E-04	
Nd-146	1.267E-04	8.607E-04	1.244E-03	1.454E-03	1.520E-03	1.37E-03	1.358E-03	9.050E-04	
Nd-148	7.335E-05	4.673E-04	6.527E-04	7.499E-04	7.802E-04	7.09E-04	7.007E-04	4.821E-04	
Nd-150	3.471E-05	2.030E-04	2.963E-04	3.480E-04	3.641E-04	3.33E-04	3.301E-04	2.205E-04	
Nd total	7.798E-04	5.207E-03	6.968E-03	7.887E-03	8.089E-03	7.420E-03	7.247E-03	5.037E-03	
Cs-137	2.84E-04	1.44E-03	2.31E-03	2.74E-03	2.76E-03	2.62E-03	2.71E-03	1.65E-03	
Cs-134	6.36E-06	5.71E-05	1.79E-04	2.50E-04	2.76E-04	2.69E-04	2.88E-04	1.24E-04	
Eu-154	1.26E-06	1.06E-05	2.81E-05	3.73E-05	4.02E-05	4.53E-05	4.52E-05	2.64E-05	
Ce-144	4.60E-05	3.03E-04	4.95E-04	5.85E-04	6.79E-04	5.82E-04	6.26E-04	4.74E-04	
Ru-106	3.93E-05	1.12E-04	2.45E-04	2.78E-04	2.98E-04	2.50E-04	2.94E-04	1.69E-04	
(Nd and $\gamma$ FP : As for zero-cooling)									
Sm-147	7.737E-05	3.731E-04	5.006E-04	5.193E-04	4.899E-04	2.984E-04	4.535E-04	3.974E-04	
Sm-148	9.624E-06	9.284E-05	2.462E-04	3.170E-04	3.252E-04	5.392E-06	2.980E-04	1.735E-04	
Sm-149	1.017E-06	3.517E-06	4.080E-06	3.998E-06	5.913E-06	5.612E-04	6.709E-06	6.523E-06	
Sm-150	5.305E-05	2.842E-04	5.251E-04	6.135E-04	6.044E-04	2.005E-05	5.563E-04	3.821E-04	
Sm-151	4.026E-06	1.293E-05	1.449E-05	1.535E-05	1.638E-05	—	2.066E-05	1.963E-05	
Sm-152	3.492E-05	1.412E-04	2.232E-04	2.435E-04	2.242E-04	1.931E-04	1.914E-04	1.530E-04	
Sm-154	7.050E-06	2.896E-05	6.106E-05	7.464E-05	7.593E-05	6.766E-05	6.912E-05	4.534E-05	
Sm total	1.871E-04	9.367E-04	1.575E-03	1.787E-03	1.742E-03	1.146E-03	1.596E-03	1.178E-03	

(Sm SF98-1 ~ -4 : As for 5.5 years cooling time)  
(SF98-5 ~ -8 : As for 5.9 years cooling time)

Table 2.2.11. SF99: Destructive analytical results of actinide nuclides for BWR spent fuel ( $\text{UO}_2\text{-Gd}_2\text{O}_3$ ) sample, normalized in zero cooling

Sample ID	SF99-1 3935 Nat. U	SF99-2 3783	SF99-3 3567	SF99-4 3383	SF99-5 2880	SF99-6 2008	SF99-7 1325	SF99-8 681	SF99-9 529	SF99-10 393 Nat. U
Initial										
Burnup (FIMA)										
Burnup (GWd/t)										
U-234	0	3.964E-05	2.040E-04	1.812E-04	1.693E-04	1.629E-04	1.677E-04	1.670E-04	1.993E-04	2.221E-04
U-235	3.400E-02	2.950E-03	1.416E-02	8.764E-03	7.067E-03	7.473E-03	1.059E-02	1.106E-02	1.595E-02	1.929E-02
U-236	0	6.926E-04	3.495E-03	4.285E-03	4.516E-03	4.559E-03	4.329E-03	4.285E-03	3.485E-03	2.856E-03
U-238	9.660E-01	9.838E-01	9.518E-01	9.448E-01	9.428E-01	9.390E-01	9.405E-01	9.399E-01	9.489E-01	9.534E-01
U total	1.000E+00	9.875E-01	9.697E-01	9.581E-01	9.546E-01	9.512E-01	9.556E-01	9.554E-01	9.686E-01	9.758E-01
dU-235				2.524E-02	2.693E-02	2.653E-02	2.341E-02	2.294E-02	1.805E-02	1.471E-02
F5				2.022E-02	2.167E-02	2.118E-02	1.828E-02	1.785E-02	1.386E-02	1.133E-02
F5/Ftotal		0.440	0.668	0.598	0.587	0.543	0.542	0.533	0.609	0.653
dU-238				1.417E-02	2.117E-02	2.319E-02	2.547E-02	2.614E-02	1.708E-02	1.259E-02
Np-237		5.698E-03	2.185E-04	3.646E-04	3.680E-04	4.634E-04	4.162E-04	4.481E-04	2.768E-04	1.983E-04
Pu-238		1.130E-05	3.959E-05	9.692E-05	1.144E-04	1.233E-04	1.374E-04	1.376E-04	6.473E-05	3.425E-05
Pu-239 (*)		2.997E-03	3.889E-03	3.961E-03	3.847E-03	4.528E-03	5.607E-03	6.009E-03	5.423E-03	4.709E-03
Pu-240		1.055E-03	1.505E-03	2.113E-03	2.273E-03	2.513E-03	2.424E-03	2.465E-03	1.632E-03	1.171E-03
Pu-241		3.553E-04	6.676E-04	9.330E-04	9.971E-04	1.181E-03	1.247E-03	1.296E-03	8.224E-04	5.302E-04
Pu-242		8.100E-05	1.864E-04	4.300E-04	5.478E-04	5.970E-04	4.260E-04	4.144E-04	1.694E-04	8.192E-05
Pu total		4.500E-03	6.288E-03	7.534E-03	7.780E-03	8.942E-03	9.841E-03	1.032E-02	8.112E-03	6.526E-03
Am-241		2.664E-05	2.082E-05	3.899E-05	3.366E-05	4.307E-05	4.499E-05	4.785E-05	3.572E-05	2.848E-05
Am-242m		2.428E-07	4.167E-07	5.351E-07	5.326E-07	6.799E-07	9.148E-07	9.083E-07	6.697E-07	4.008E-07
Am-243		5.666E-06	1.855E-05	6.359E-05	8.847E-05	1.104E-04	8.335E-05	8.275E-05	2.520E-05	9.061E-06
Am total		3.255E-05	3.979E-05	1.031E-04	1.227E-04	1.541E-04	1.293E-04	1.315E-04	6.159E-05	3.794E-05
Cm-242		2.800E-06	1.597E-05	2.231E-05	3.418E-05	6.026E-05	3.778E-05	3.998E-05	1.566E-05	5.440E-06
Cm-243		2.937E-08	9.114E-08	2.701E-07	3.614E-07	4.650E-07	4.321E-07	4.662E-07	1.595E-07	3.211E-08
Cm-244		5.746E-07	3.101E-06	1.604E-05	2.624E-05	3.774E-05	2.933E-05	2.925E-05	5.998E-06	6.665E-07
Cm-245		9.771E-09	8.508E-08	5.530E-07	9.844E-07	1.716E-06	1.685E-06	1.741E-06	2.623E-07	7.947E-08
Cm-246		9.261E-10	-----	6.720E-08	1.446E-07	2.333E-07	1.550E-07	1.509E-07	1.394E-08	1.281E-08
Cm-247		3.80E-10	1.925E-05	3.924E-05	6.192E-05	1.004E-04	6.938E-05	3.744E-09	1.179E-08	-----
Cm total		3.415E-06	6.347E-03	7.505E-03	7.964E-03	9.197E-03	1.004E-02	1.052E-02	8.196E-03	6.571E-03
Pu + Am + Cm		4.536E-03	4.394E-03	7.823E-03	1.357E-02	1.523E-02	1.779E-02	1.543E-02	8.884E-03	6.019E-03
F8		0.560	0.332	0.402	0.413	0.457	0.458	0.467	0.391	0.347
U + Np + Pu + Am + Cm + Fission		1.000	1.000	1.000	1.000	1.000	1.000	1.000	1.000	1.000
F5 : U-235 fission		= FIMA-F8								
dU-235 : U-235 depletion		= U-235(initial) - U-235(after)								
F8 : U-238 fission		= dU-238 - (Pu + Am + Cm)								
dU-238 : U-238 depletion		= U-238 (initial) - U-238 (after)								
(*) : The Pu-239 at zero cooling includes the amount of Np-239.										

Table 2.2.12. SF99: Destructive analytical results of FP nuclides for BWR spent fuel ( $\text{UO}_2\text{-Gd}_2\text{O}_3$ ) sample, normalized in zero cooling

Sample ID	SF99-1	SF99-2	SF99-3	SF99-4	SF99-5	SF99-6	SF99-7	SF99-8	SF99-9	SF99-10
Sampling position (from top, mm)	3935 Nat. U	3783	3567	3383	2830	2008	1325	681	529	393 Nat. U
Initial	After irradiation									
Burnup (FIMA)	7.84E-03									
Burnup (GWd/t)	7.53	2.375E-02	3.379E-02	3.690E-02	3.897E-02	3.371E-02	3.347E-02	2.274E-02	1.734E-02	7.490E-03
Nd-142	4.288E-06	1.395E-05	3.209E-05	3.844E-05	3.959E-05	2.918E-05	2.826E-05	1.312E-05	7.848E-06	5.629E-06
Nd-143	3.244E-04	1.022E-03	1.270E-03	1.300E-03	1.398E-03	1.329E-03	1.347E-03	1.023E-03	8.337E-04	3.156E-04
Nd-144	4.348E-04	1.081E-03	2.184E-03	1.989E-03	1.929E-03	1.541E-03	1.351E-03	9.145E-04	7.285E-04	4.150E-04
Nd-145	2.594E-04	8.074E-04	1.105E-03	1.182E-03	1.233E-03	1.074E-03	1.069E-03	7.670E-04	6.084E-04	2.492E-04
Nd-146	2.300E-04	7.300E-04	1.078E-03	1.193E-03	1.268E-03	1.088E-03	1.084E-03	7.170E-04	5.394E-04	2.228E-04
Nd-148	1.333E-04	3.998E-04	5.743E-04	6.279E-04	6.644E-04	5.751E-04	5.721E-04	3.878E-04	2.955E-04	1.283E-04
Nd-150	6.633E-05	1.813E-04	2.657E-04	2.926E-04	3.141E-04	2.753E-04	2.736E-04	1.803E-04	1.339E-04	6.414E-05
Nd total	1.452E-03	4.235E-03	6.509E-03	6.623E-03	6.846E-03	5.909E-03	5.724E-03	4.003E-03	3.147E-03	1.401E-03
Cs-137	4.97E-04	1.48E-03	2.14E-03	2.34E-03	2.48E-03	2.17E-03	2.20E-03	1.45E-03	1.10E-03	4.82E-04
Cs-134	1.85E-05	8.25E-05	1.62E-04	2.00E-04	2.32E-04	2.02E-04	2.12E-04	1.01E-04	5.71E-05	1.94E-05
Eu-154	4.12E-06	1.58E-05	2.77E-05	3.08E-05	3.81E-05	3.94E-05	4.11E-05	2.17E-05	1.27E-05	4.26E-06
Ce-144	-----	3.56E-04	-----	4.82E-04	6.36E-04	5.24E-04	7.01E-04	4.20E-04	2.74E-04	-----
SB-125	1.84E-06	7.00E-06	8.01E-06	8.74E-06	8.89E-06	9.66E-06	7.31E-06	4.63E-06	2.35E-06	1.71E-06
Ru-106	5.98E-05	7.37E-05	1.81E-04	1.76E-04	1.57E-04	1.55E-04	1.12E-04	9.81E-05	1.13E-04	8.68E-05
(Nd and $\gamma$ FP : As for zero-cooling)										
Measurement data	1999/8/13	1999/8/13	1999/8/13	1999/8/13	1999/8/13	1999/8/13	1999/8/13	1999/8/13	1999/8/13	1999/8/14
Sm-144	1.261E-04	4.226E-04	4.487E-04	4.239E-04	3.946E-04	3.182E-04	2.645E-04	2.645E-04	2.645E-04	2.645E-04
Sm-147	2.653E-05	1.877E-04	2.539E-04	2.161E-04	2.124E-04	1.214E-04	7.211E-05	7.211E-05	7.211E-05	7.211E-05
Sm-148	1.413E-06	3.944E-06	4.351E-06	5.474E-06	5.474E-06	4.728E-06	4.155E-06	4.155E-06	4.155E-06	4.155E-06
Sm-149	9.803E-05	4.248E-04	5.152E-04	4.409E-04	4.409E-04	2.905E-04	2.085E-04	2.085E-04	2.085E-04	2.085E-04
Sm-150	5.375E-06	1.339E-05	1.616E-05	1.616E-05	2.040E-05	1.821E-05	1.577E-05	1.577E-05	1.577E-05	1.577E-05
Sm-152	6.182E-05	1.846E-04	1.992E-04	1.603E-04	1.603E-04	1.211E-04	9.666E-05	9.666E-05	9.666E-05	9.666E-05
Sm-154	1.451E-05	5.184E-05	6.516E-05	5.533E-05	5.533E-05	3.418E-05	2.381E-05	2.381E-05	2.381E-05	2.381E-05
Sm total	3.337E-04	1.289E-03	1.503E-03	1.293E-03	1.293E-03	9.083E-04	6.855E-04	6.855E-04	6.855E-04	6.855E-04
(Nd and $\gamma$ FP : As for zero-cooling)										
Natural Gd	atom%	atom%	atom%	atom%	atom%	atom%	atom%	atom%	atom%	atom%
Gd-154	2.2	1.81	0.12	1.72	0.17	1.75	0.15	1.98	0.18	0.18
Gd-155	14.8	0.02	5.17	0.03	4.41	0.02	0.47	0.02	1.60	1.60
Gd-156	20.5	34.84	0.04	34.62	0.03	34.35	0.02	34.91	0.03	0.03
Gd-157	15.7	0.01	4.16	0.01	1.52	0.01	0.82	0.01	1.18	1.18
Gd-158	24.8	41.45	0.02	41.77	0.02	41.93	0.02	41.19	0.03	0.03
Gd-160	21.9	21.82	0.02	21.82	0.01	21.88	0.01	21.78	0.02	0.02
Gd total	100	100	100	100	100	100	100	100	100	100

## 2.3. Exponential Experiments of Spent Fuel Assemblies

In storage facilities and transportation vessels for light-water-reactor spent fuels in our country, thick water layers and strong neutron-absorbing materials are provided between fuel assemblies, so that there is no danger that criticality will be reached even if a new fuel is introduced. Incidentally, it is far more difficult for spent fuels to attain criticality than new fuels, due to the wear of the nuclear fuel in the reactor and the accumulation of fission products, which absorb neutrons strongly. This fact is the reason for designations such as spent fuels, which means that they cannot any longer be used advantageously in the reactor. Since the assumption that the burn-up of a fuel is not taken into consideration can become an irrational restriction, especially regarding spent fuels with high initial concentrations (enrichments), each country involved is now trying to introduce criticality safety management with burn-up taken into consideration (i.e., to apply burn-up credit).

The basic idea required for criticality safety regulations is to demonstrate, by experimental data, that the calculation codes to be used in design have sufficient reliability. However, the worldwide situation as it exists today is that there are practically no appropriate benchmark data for systems loaded with spent fuel. For this reason, in this project we obtained criticality benchmark data by noncriticality experiments (exponential experiments), using spent fuel assemblies in Japan, and gathered information on the compositions of fuels and data that can be used for validating the calculation codes.

### 2.3.1. Principle of an Exponential Experiment

#### (1) Exponential Decay Constant and Effective Neutron Multiplication Factor<sup>1</sup>

As shown in Fig. 2.3.1, it can be seen that the natural flux decays as an exponential function in the axial direction in a region pointing away to a certain extent from the neutron source in a fuel assembly system provided with a steady point neutron source (external neutron source). If we represent the decay constant (fundamental mode) as  $\gamma$ , then the axial distribution of neutron flux can be expressed by Eq. (1) (the Equation No. is also given in the figure). On the other hand, the radial distribution can be expressed by Eq. (2) as a function of geometric buckling  $B^2$ , and the effective neutron multiplication factor  $k_{eff}$  of a fuel assembly with an infinite length can be given by Eq. (3) ( $k_\infty$  is the infinite multiplication factor and  $M^2$  is the moving area). The state of formation and disappearance being balanced by the flow-in neutrons in the axial direction can be expressed like Eq. (4) from the fact that material buckling is equal to  $B^2 - \gamma^2$ , and from this equation and Eq. (3), the relationship between  $k_{eff}$  and  $\gamma$  can be derived as in Eq. (5). Here,  $K$  is called the buckling coefficient of reactivity, and has a characteristic such as increasing with increasing  $\gamma$  (refer to Fig. 2.3.2).  $\gamma$  is measured in exponential experiments, but the  $\gamma$  itself is a kind of eigenvalue that provides criticality characteristics, and can be used for validating the calculation codes by comparing directly with the results of axial buckling search calculation. Furthermore, if the value of  $K$  is calculated by a reliable code, the  $k_{eff}$  of a fuel assembly with an infinite length can be calculated by Eq. (5).

## (2) DS Method and SS Method

The exponential decay constant  $g$  can usually be obtained by fixing an external neutron source at a certain position, moving in the axial direction, and measuring the neutron flux distribution (DS method), but also the same  $\gamma$ -value can be obtained from the distribution of neutron importance which can be measured conversely by fixing the position of the detector and moving the neutron source (SS method) (refer to Fig. 2.3.3). This fact can also be seen in the measured examples of Fig. 2.3.4. Furthermore, the axial distribution of neutron flux was compared with that of neutron importance by solving Eqs. (1) and (2) of Fig. 2.3.3, and thereby it was confirmed that the two methods give measured results in agreement even when there is a compositional distribution in the axial direction.<sup>3</sup> The SS method is more advantageous for improving the measurement accuracy of the  $\gamma$ -value, since it is less likely to be affected by local property changes (such as a support lattice with strong neutron absorption) in a fuel assembly than the DS method, as seen in Fig. 2.3.4. Moreover, the background distribution due to an inherent neutron source generating from higher-order actinides in a spent fuel needs to be measured with high accuracy in the DS method, but the SS method requires only one-point measurement at the detector location and so can nearly halve the measurement time.

### 2.3.2. Spent Fuel Assemblies

The following four spent fuel assemblies were used in the experiments: C33 from the Kyushu Electric Genkai Power Station No. 1 reactor (PWR 14 × 14; called assembly P14); J2R from the Kansai Electric Ohi Power Station No. 2 reactor (PWR 17 × 17; called assembly P17); DN23 from the Tokyo Electric Fukushima Power Station No. 2 reactor (BWR 8 × 8; called assembly B8); and G24 from the Kansai Electric Takahama No. 3 reactor (PWR 17 × 17 for high burn-up degrees loaded with a gadolinia fuel; called assembly HP17). The specifications and burn-up histories of these fuel assemblies are assembled in Appendix.

The nuclide composition of the fuel in these fuel assemblies was determined as the radial averaged composition in the region where the exponential decay constant had been measured, by combining chemical analysis data, burn-up management data, and calculation results by burn-up codes (refer to Sect. 4).

### 2.3.3. Experimental Method

A fuel assembly was placed vertically in a cage made of stainless steel provided on the base of a pool 15-m deep at the JAERI examination facility, as shown in Fig. 2.3.5. Aluminum spacers 4-mm thick were placed at two locations in the assembly axial direction between the cage and the assembly so as to adjust the gap to 3.5 cm or more. A  $^{235}\text{U}$  fission counter with an outer diameter of 6 mm and an effective length of 25.4 mm and a  $^{252}\text{Cf}$  neutron source with a diameter of 4 mm and a height of 2 cm were installed, respectively, at the lower end of two stainless steel tubes with an outer diameter of 9.5 mm and a thickness of 0.5 mm, and these stainless steel tubes were inserted in Al guide tubes with an inner diameter of 13 mm and a thickness of 1.5 mm attached inside the assembly for the PWR assemblies and around the assembly for the BWR assembly. The quantities mentioned in the above-mentioned Sect. 2.3.1 were measured by moving these stainless steel tubes in the axial direction of the assembly. The average water temperature of the pool was about 25°C.

### **2.3.4. Experimental Results**

#### **(1) Axial Neutron Flux Distribution Due to an Inherent Neutron Source**

The measured axial distributions of neutron counts due to an inherent neutron source without using the  $^{252}\text{Cf}$  neutron source are shown in Fig. 2.3.6. This distribution contains information on the intensity of an inherent neutron source originating mainly in the spontaneous nuclear fission of  $^{244}\text{Cm}$  accumulated in the fuel and on the neutron multiplication characteristics in the assembly, and is useful for validating the burn-up and criticality calculation codes.

#### **(2) Exponential Decay Constant**

The values of exponential decay constant  $\gamma$  in the assembly axial direction measured by exponential experiments are shown in Table 2.3.1. In the PWR assemblies, the radial arrangement of the  $^{252}\text{Cf}$  neutron source and the detector was selected so as to be able to obtain decay constants of fundamental mode in a region where the burn-up distribution at the axial center is flat.<sup>4, 2, 6</sup> In the BWR assembly, the  $\gamma$ -value changed with the axial measurement location, and was smaller in the upper part than in the lower part.<sup>5</sup> Furthermore, from a comparison with the analytical results, higher-order modes are mixed in the measured  $\gamma$ -values, and the measured values are about 10% smaller than the values of the fundamental mode (refer to Sect. 4).

## **REFERENCES**

1. T. Suzaki, *J. Nucl. Sci. Technol.*, Vol. 28, No. 12, p. 1,067, 1991.
2. Japan Atomic Energy Research Institute: Results Report on 1993 Technical Development on LWR Spent Fuel Criticality Safety Management.
3. Japan Atomic Energy Research Institute: Results Report on 1995 Technical Development on LWR Spent Fuel Criticality Safety Management.
4. Japan Atomic Energy Research Institute: Results Report on 1992 Technical Development on LWR Spent Fuel Criticality Safety Management.
5. Japan Atomic Energy Research Institute: Results Report on 1998 Technical Development on LWR Spent Fuel Criticality Safety Management.
6. Japan Atomic Energy Research Institute: Results Report on 1999 Technical Development on LWR Spent Fuel Criticality Safety Management.

Table 2.3.1. Results of exponential experiments and analyses

(1) P14 and P17 assemblies			
Assembly name	P14	P17	
Burnup (GWd/tU) <sup>1</sup>	40.2		39.0
Cooling time (yr)	13.5	14.5	4.3
Measured $\gamma$ (cm <sup>-1</sup> ) <sup>2,3</sup>	0.1247 ± 0.0014	0.1263 ± 0.0019	0.1156 ± 0.0010
Measured $\phi_{th}$ (cm <sup>-2</sup> s <sup>-1</sup> ) <sup>3</sup>	8,430 ± 660		12,970 ± 360
CITATION calculation			
$\gamma$ (cm <sup>-1</sup> )	0.1261	0.1124	
$\phi_{th}$ (cm <sup>-2</sup> s <sup>-1</sup> )	9,460	14,740	
K (cm <sup>2</sup> )	46.55	44.56	
Estimated $k_{eff}$	0.580	0.627	
MCNP calculation			
$k_{eff}$ <sup>4</sup>	0.566	0.632	

<sup>1</sup>Radial-average value in axial plateau region.

<sup>2</sup>The preceding measurements were made mainly by the DS-method, and the succeeding ones by the SS-method.

<sup>3</sup>The error value represents the scattering among the plural measurements.

<sup>4</sup> $\sigma = 0.002$ .

(2) B8 assembly						
Detector pos. (cm)*	Range of fit. (cm)*	Measured $\gamma$ (/cm)	Avg.	Calculated $\gamma$ (/cm)		C/E
				Buckl. search	Fixed source	
369	325–342	0.133 ± 0.001	—	—	0.135	1.02
304	330–346	0.135 ± 0.002	0.135	0.149	0.134	0.99
	265–276	0.135 ± 0.003			0.138	1.02
264	287–302	0.139 ± 0.002	0.140	0.150	0.136	0.97
	225–240	0.140 ± 0.001			0.139	1.00
154	175–195	0.140 ± 0.003	0.140	0.154	0.140	1.00
	114–133	0.139 ± 0.002			0.141	1.01
94	117–133	0.146 ± 0.004	0.145	0.158	0.141	0.97
	55–72	0.143 ± 0.002			0.142	0.99
69	92–107	0.144 ± 0.004	0.142	0.159	0.141	0.98
	30–47	0.140 ± 0.002			0.136	0.97
(E)				(C)		

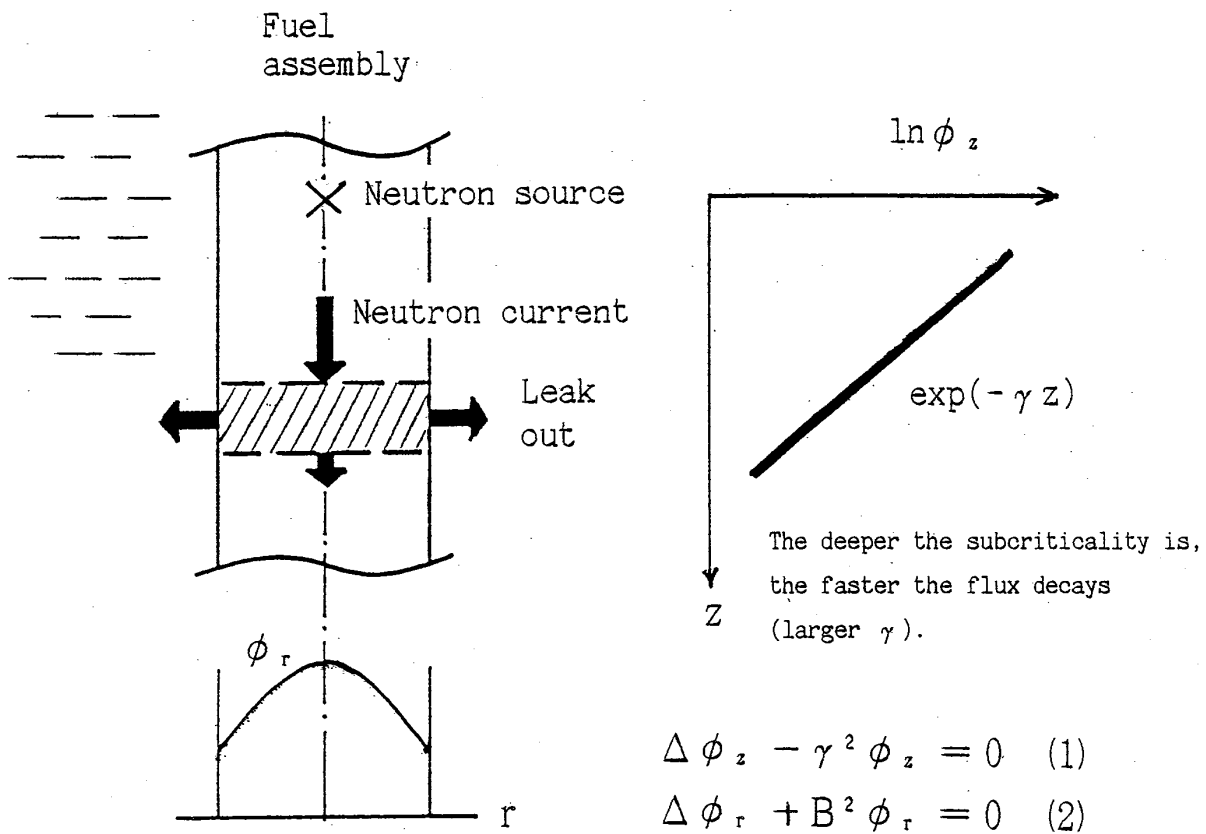
\*Distance from lower end of active fuel.

Table 2.3.1. (continued)

## (3) HP17 assembly

Detector pos. (cm)*	Range of fit. (cm)*	Measured $\gamma$ (/cm)	Calculated $\gamma$ (/cm)	C/E
140	108–124	$0.127 \pm 0.002$	Buckling search ; 0.1176	0.947
185	148–170	$0.123 \pm 0.002$	Fixed source ; 0.1161	0.935
	200–218	$0.126 \pm 0.002$		
230	244–262	$0.121 \pm 0.002$		
	Average	$0.1242 \pm 0.0028(E)$		

\* Distance from lower end of active fuel.



$$k_{\text{eff}} = \frac{k_{\infty}}{1 + M^2 B^2} \quad (3)$$

$$1 = \frac{k_{\infty}}{1 + M^2 (B^2 - \gamma^2)} \quad (4)$$

$$\left. \begin{array}{l} \\ \end{array} \right\} \quad 1 - \frac{1}{k_{\text{eff}}} = -K \gamma^2 \quad (5)$$

$$(K = M^2 / k_{\infty})$$

Fig. 2.3.1. Principle of exponential experiment.

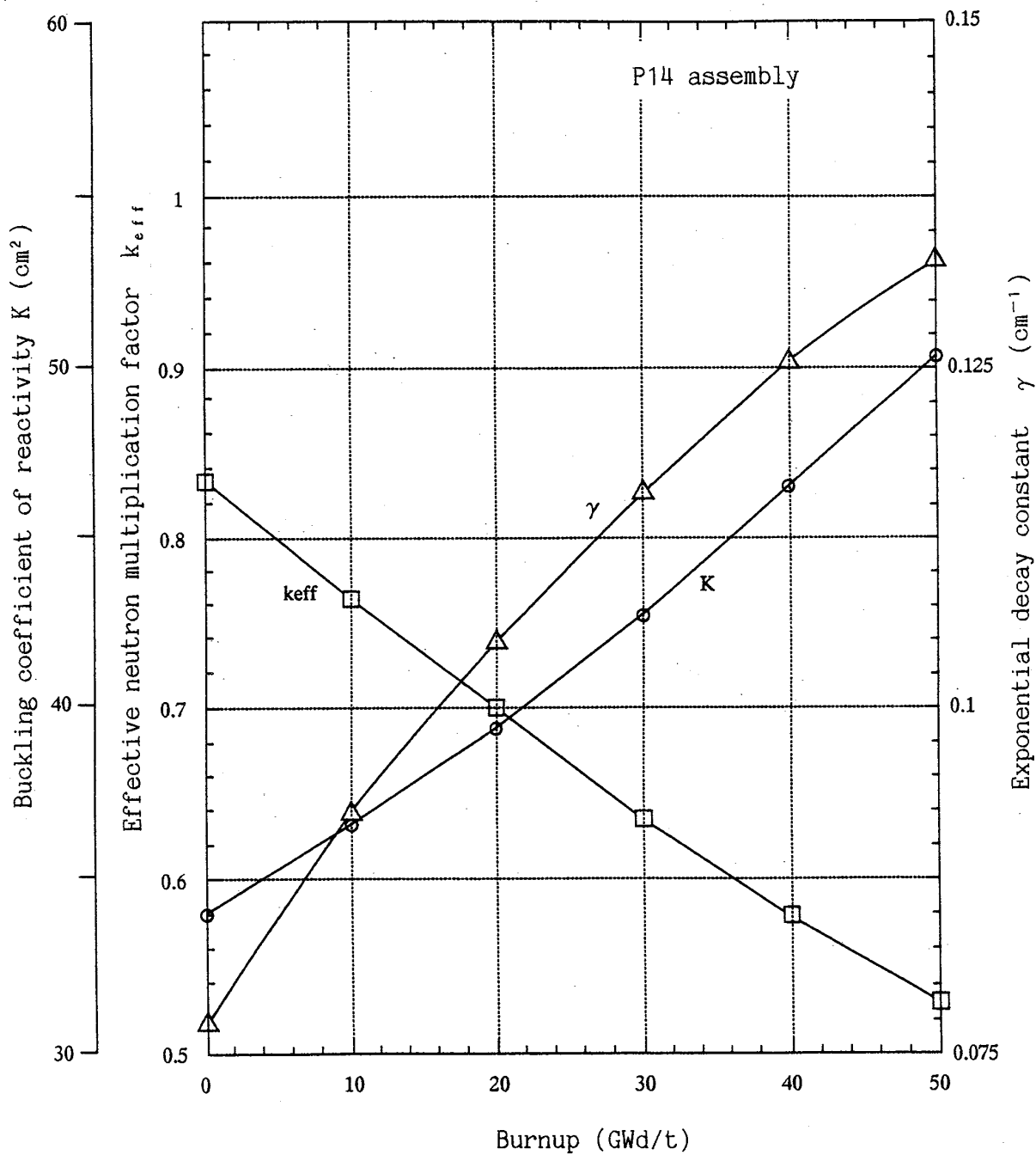


Fig. 2.3.2. Example of calculated variations in  $k_{\text{eff}}$ ,  $\gamma$  and  $K$  with burnup.<sup>2</sup>

Neutron flux  $\phi$  formed by a neutron source at  $r_1$ ;

$$M\phi(r, E; r_1) + S(E) \delta(r - r_1) = 0 . \quad (1)$$

Neutron importance  $\phi^*$  measured by a detector at  $r_2$ ;

$$M^*\phi^*(r, E; r_2) + \Sigma_D(E) \delta(r - r_2) = 0 . \quad (2)$$

Multiplying  $\phi^*$  to Eq. (1) and  $\phi$  to Eq. (2), integrating the products over the whole space and energy, and subtracting each other;

$$\int S(E) \phi^*(r_1, E; r_2) dE = \int \Sigma_D(E) \phi(r_2, E; r_1) dE , \quad (3)$$

which means that if the count rate distribution (R.H.S of Eq. (3)) is proportional to  $\exp(-\gamma |r_1 - r_2|)$ , the importance distribution (L.H.S. of Eq. (3)) forms the same exponential function.

Fig. 2.3.3. Relation between DS- and SS-methods.

$M, M^*$ : Neutron transport and its adjoint operators.

$S, \Sigma_D$ : Neutron source strength and detector reaction cross section.

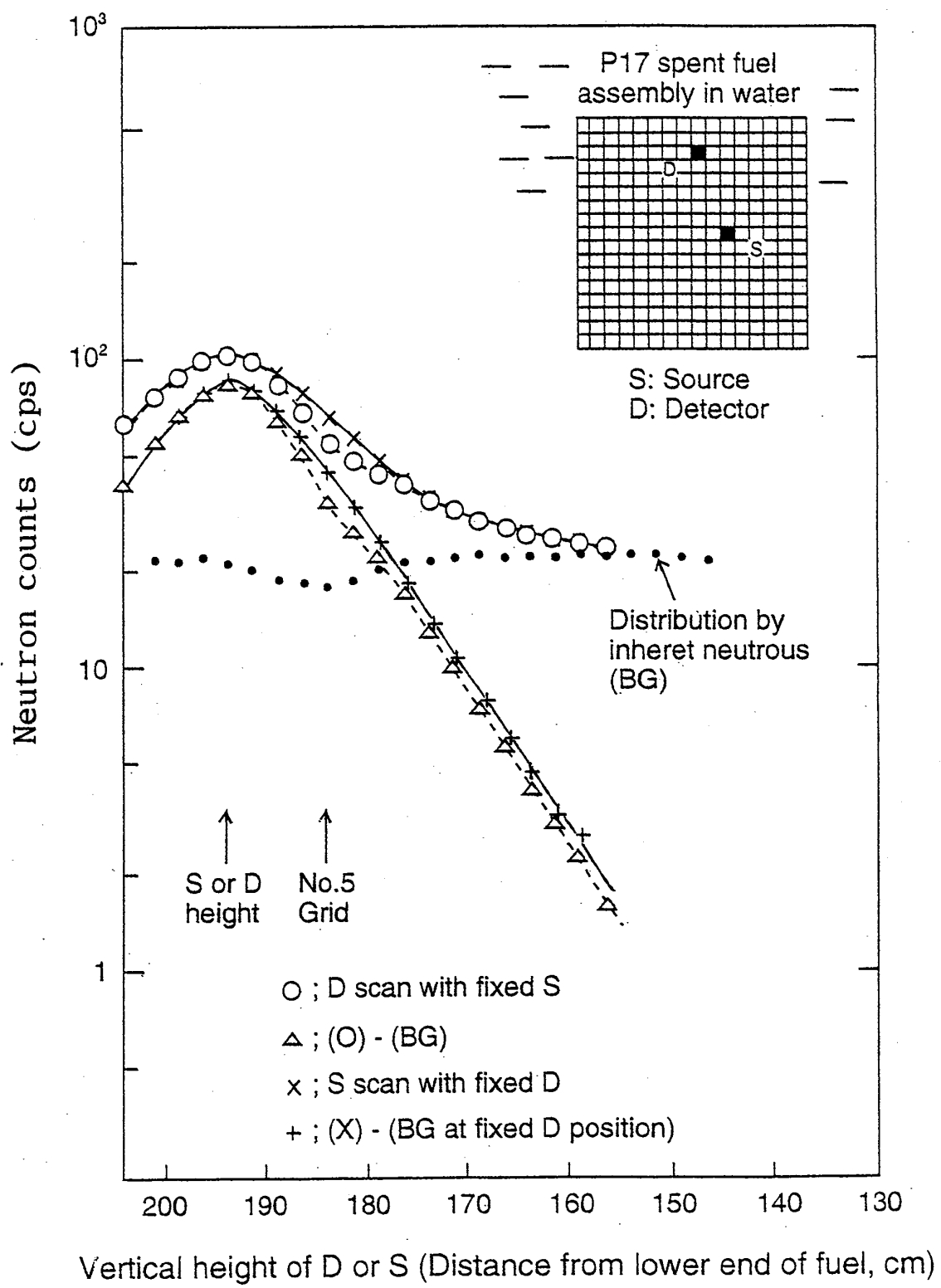


Fig. 2.3.4. Comparison of measured results between DS- and SS-methods.<sup>2</sup>

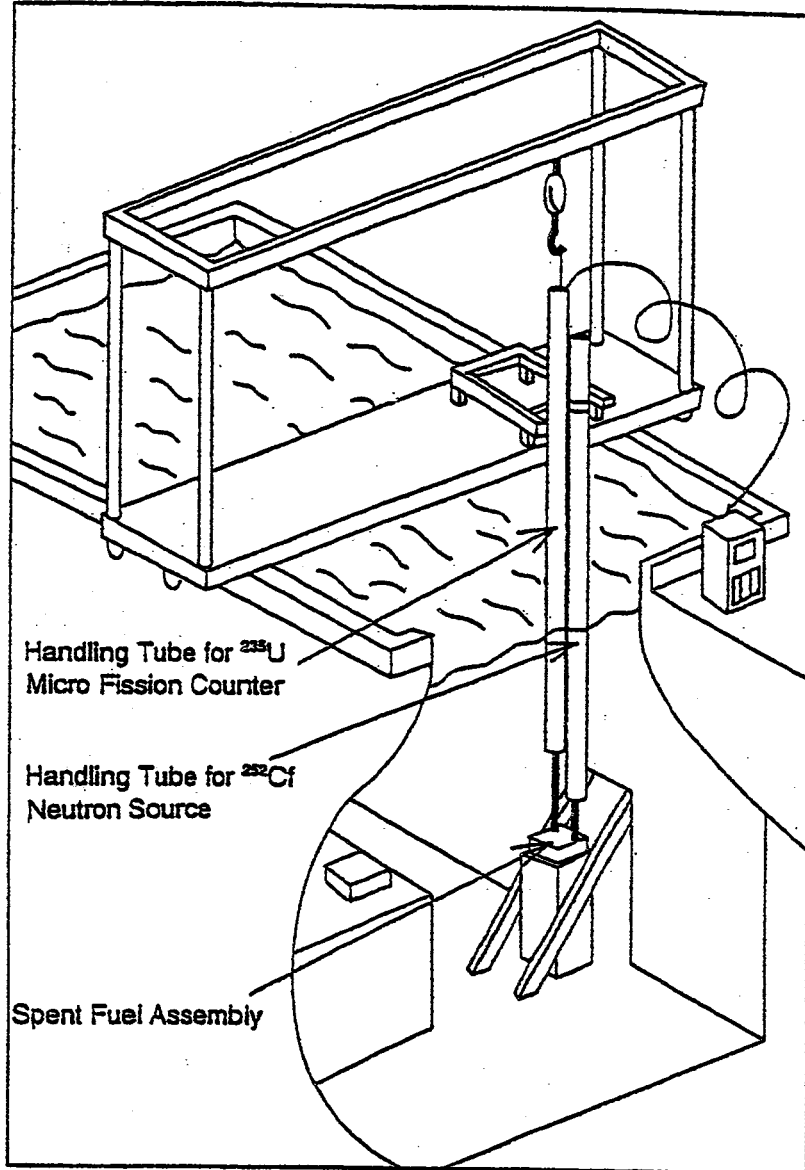
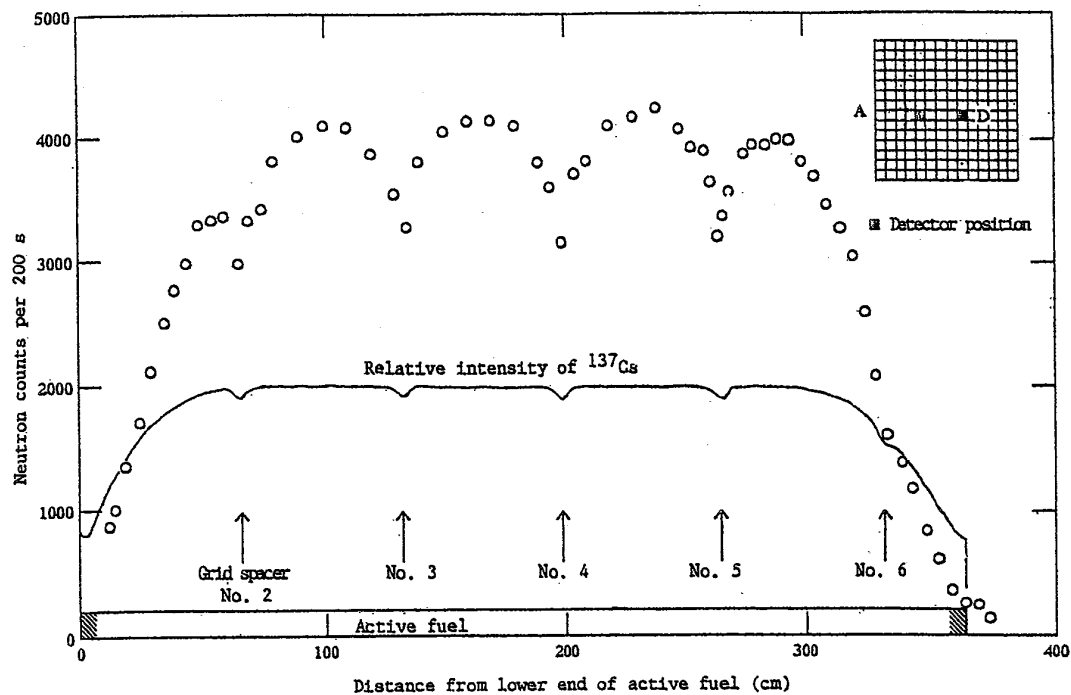
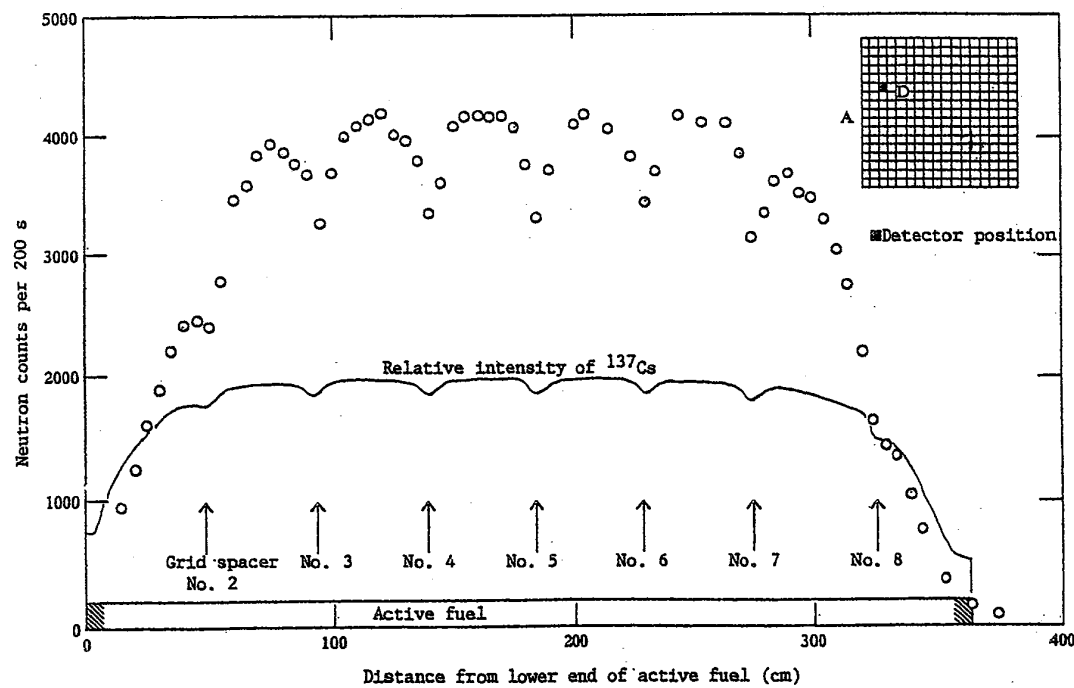


Fig. 2.3.5. Experimental setup at the fuel receiving pool of the Reactor Fuel Examination Facility (REFEF).



(1) P14 assembly



(2) P17 assembly

Fig. 2.3.6. Axial distribution of neutron count rate in spent fuel assembly (without  $^{252}\text{Cf}$  source).

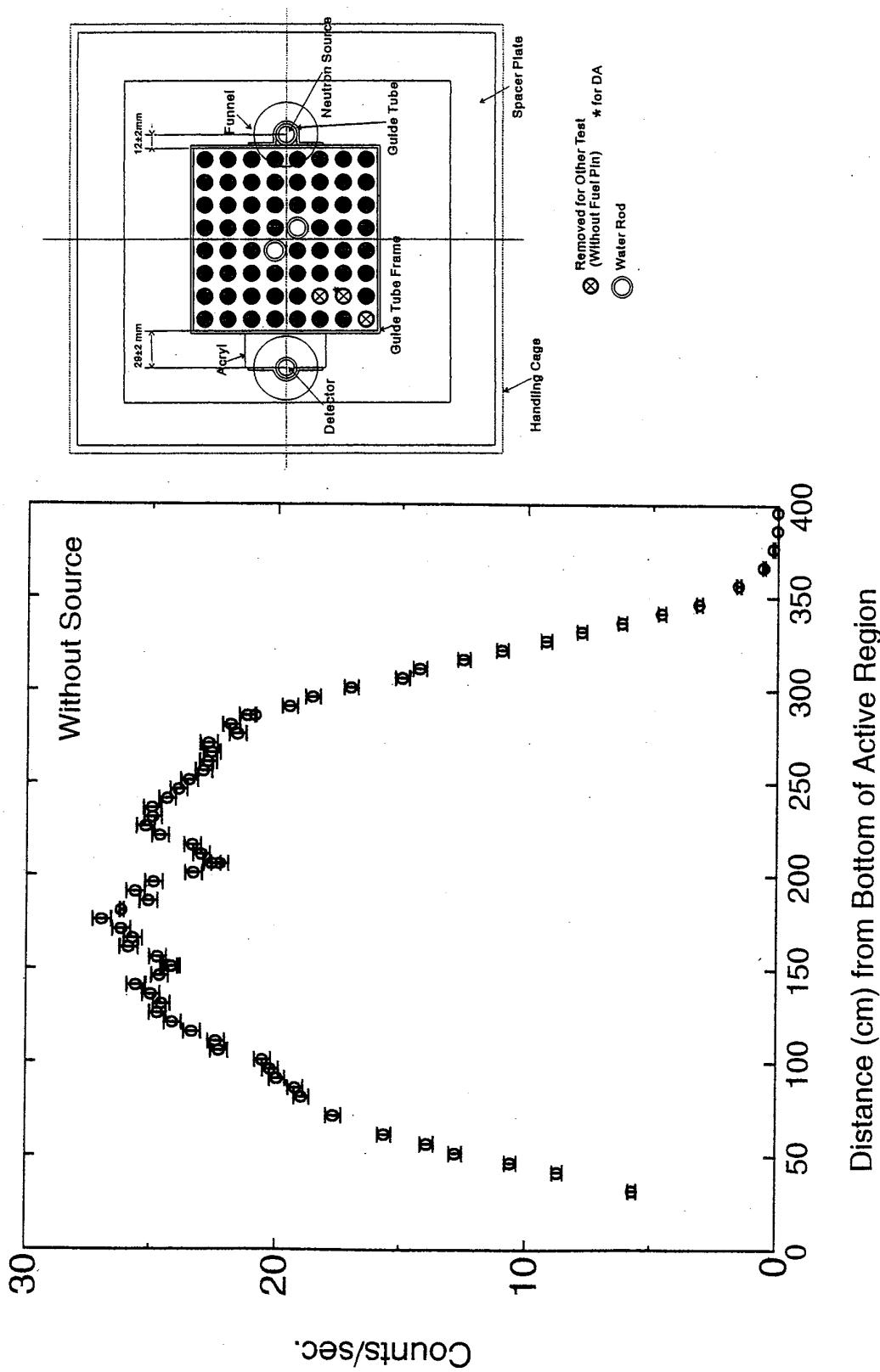
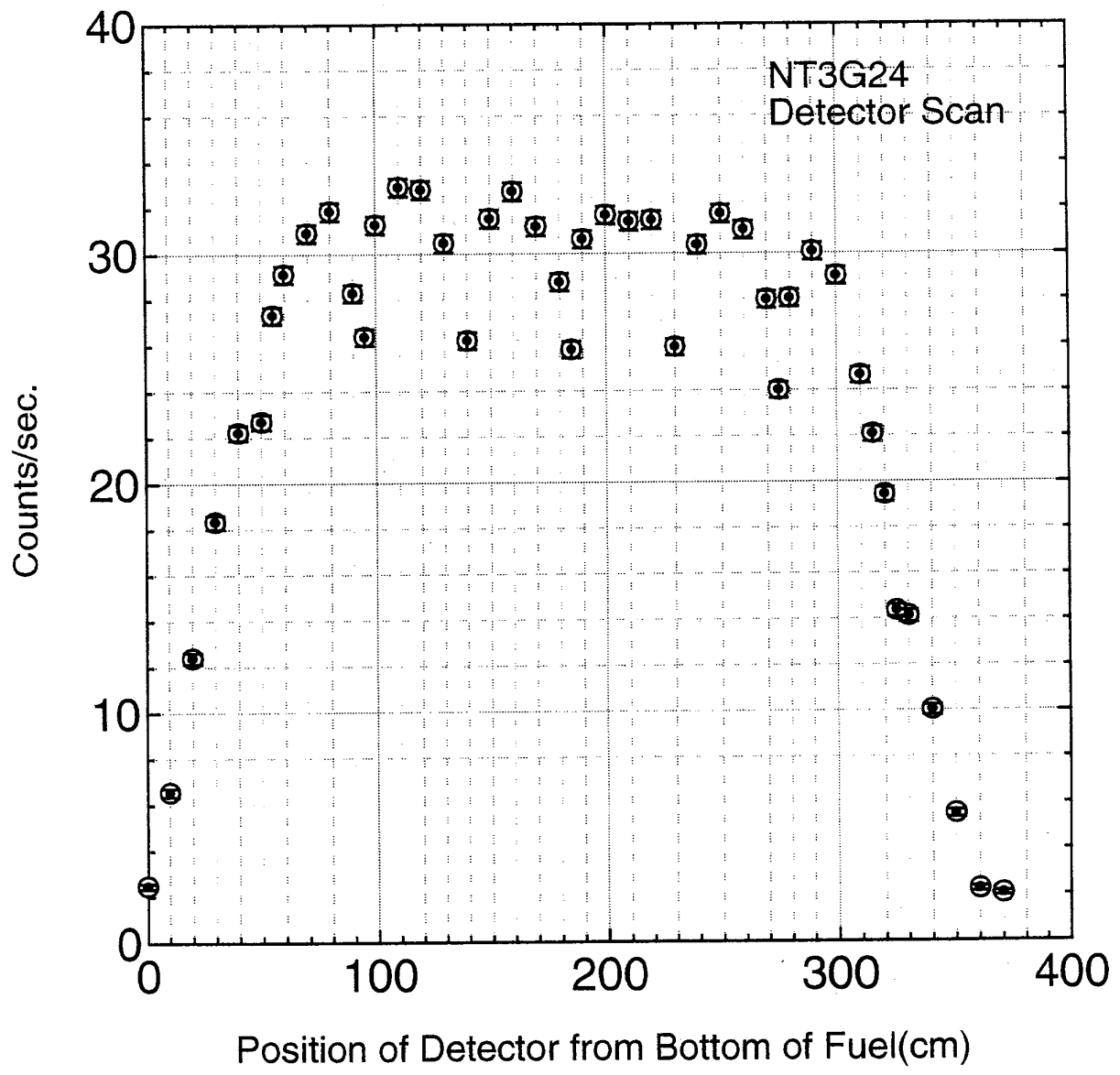


Fig. 2.3.6. (continued) (3) B8 assembly:  
Depression around the middle height is caused by an acrylic spacer of about 15 cm long (see the attached figure).



(4) HP17 assmby

Fig. 2.3.6. (continued)

### 3. VALIDATION OF BURN-UP CODES

#### 3.1. General

The burn-up calculation codes were validated by analyzing the various destructive analysis data of SF95, SF96, SF97, SF98, and SF99. Table 3.1.1 lists an outline of the various destructive analyses. These data are data obtained by the same technique with reliability, and can be considered to be useful for the benchmark of the calculation codes. In the "code accuracy evaluation," work was carried out to better understand the calculation accuracy of SWAT<sup>2</sup> and ORIGEN2.1<sup>3</sup> when using these data.

Samples irradiated with average spectra were selected as the samples to be analyzed. This means that the natural uranium blanket section in use in the BWR fuels and samples obtained from locations close to the top and bottom ends of the fuel were to be excluded from the object of the code accuracy evaluation. As a result, SF96-1 (17 mm from the top end of the fuel), SF97-1 (4 mm from the top end of the fuel), SF98-1 (natural uranium blanket section), SF98-2 (enriched uranium section but near the boundary between the natural uranium blanket section and the enriched uranium), SF99-1 (natural uranium blanket section), and SF99-10 (natural uranium blanket section) were excluded from the analysis objects.

Furthermore, the destructive test results for isotopes other than Sm isotopes are given as values immediately after irradiation, but the data of <sup>239</sup>Pu are not corrected for the increases due to the decay of <sup>239</sup>Np, which existed immediately after irradiation. In other words, it can be said that the experimental value is in consequence the sum of <sup>239</sup>Pu and <sup>239</sup>Np immediately after irradiation. Therefore, the calculated value of <sup>239</sup>Pu + <sup>239</sup>Np was used for the purpose of comparison with the experimental value of <sup>239</sup>Pu. However, the contribution of the decay of <sup>239</sup>Np is 3% at most, and whether or not this effect is incorporated, the tendency with regard to the calculated results for <sup>239</sup>Pu is not changed.

#### 3.2. Equation for Accuracy Evaluation

For evaluation of the accuracy of the codes, the average value of C/E, i.e., the calculated amount of an isotope divided by the experimental value, was calculated for each sample, and the dispersion of population expressed by Eq. (3.2.1) was calculated.

$$S.T.D. = \sqrt{\frac{1}{n-1} \sum_{i=1}^n \left( \left( \frac{C}{E} \right)_i - \left( \frac{C}{E} \right)_{average} \right)^2} \quad (3.2.1)$$

Table 3.1.1. List of destructive analyses samples

Sample group	Reactor type	Reactor name	Assembly type	Assembly average burnup (GWd/t)	Assembly name	ROD POS.	Enrichment
SF95	PWR	Takahama 3	17×17	33.1	NT3G23	A-Q	4.1% UO <sub>2</sub>
SF96	PWR	Takahama 3	17×17	33.1	NT3G23	C-M	2.6% UO <sub>2</sub> – 6% Gd <sub>2</sub> O <sub>3</sub>
SF97	PWR	Takahama 3	17×17	43.2	NT3G24	I-Q	4.1% UO <sub>2</sub>
SF98	BWR	Fukushima-Daini-2	8×8-2	33.4	2F2DN23	B-2	3.9% UO <sub>2</sub>
SF99	BWR	Fukushima-Daini-2	8×8-2	33.4	2F2DN23	C-2	3.4% UO <sub>2</sub> – 3.0 (4.5)% Gd <sub>2</sub> O <sub>3</sub>

### 3.3. SWAT Analyses

#### 3.3.1. Cell Configuration

A "single pin cell model," which is the basic pattern of the SWAT calculation, was used for the SWAT analyses of the uranium fuels. This model consists of three regions, i.e., the "uranium pellet region," the "clad region," and the "coolant region." And the assembly averaged water-to-fuel volume ratio can presumably be conserved by adjusting the area of the coolant region. This assumption is considered to be a good approximation for uranium fuels. The cell geometry data in the analysis of SF95 and SF97 samples are listed in Table 3.3.1, and the cell geometry data in the analysis of SF98 samples are listed in Table 3.3.3. However, in the case of a  $\text{UO}_2\text{-Gd}_2\text{O}_3$  fuel, this cell configuration results in reproducing the condition that it is surrounded entirely by  $\text{UO}_2\text{-Gd}_2\text{O}_3$ . To avoid this condition, we decided to carry out our analysis by considering a multiple-region cell where uranium fuel regions and water regions exist on top of another around the  $\text{UO}_2\text{-Gd}_2\text{O}_3$  fuel. Table 3.3.2 lists the cell geometry data in the analysis of SF96 samples, and Table 3.3.4 lists the cell geometry data in the analysis of SF99 samples.

Table 3.3.1. Cell geometry for SF95 and SF97

Radius (cm)	Region
0.4025	Fuel
0.475	Clad
0.739716	Coolant

Table 3.3.2. Cell geometry for SF96

Radius (cm)	Region
0.4025	Fuel
0.475	Clad
0.739716	Water
1.339091	Water
1.42126	Clad
1.729745	Fuel
1.794111	Clad
2.122887	Water
2.597006	Water
2.682922	Clad
3.128925	Fuel
3.200594	Clad
3.53293	Water
4.0009	Water
4.085952	Clad
4.500199	Fuel
4.575176	Clad
4.945487	Water

Table 3.3.3. Cell geometry for SF98

Radius (cm)	Region
0.529	Fuel
0.615	Clad
0.9221	Water (1) : Void
1.0555	Water (2)

Table 3.3.4. Cell geometry for SF99

Radius (cm)	Region
0.529	Gd <sub>2</sub> O <sub>3</sub> -UO <sub>2</sub>
0.615	Clad
0.91963	Water (Void)
1.046802	Water
1.4477895	Water
1.9915	Water (Void)
2.087967	Clad
2.568723	Fuel (UO <sub>2</sub> )
2.644215	Clad
2.976886	Water (Void)
3.140406	Water
3.444729	Water
3.950457	Water (Void)
4.04885	Clad
4.537708	Fuel (UO <sub>2</sub> )
4.623621	Clad
5.011769	Water (Void)
5.449857	Water

### 3.3.2. Temperature

The analysis is carried out by assuming that the temperature of the fuel pellet is constant at 900 K and that the temperature of the clad is constant at 600 K. These temperatures are considered to be adequate assumptions based on the temperature distribution of a typical LWR fuel. The temperature of the coolant region affects the density of the number of atoms. Therefore, the temperature of the coolant was determined on the basis of the following: First, in the analysis of samples obtained from PWR fuels, temperatures were evaluated by assuming that the increase in coolant temperature in the axial direction is proportional to the integrated power up to the sample position. If the coolant temperature at the reactor core inlet is denoted by  $T_{inlet}$ , the effective fuel length by  $H$ , and the increase in coolant temperature at the reactor core outlet by  $DT$ , the coolant temperature at a sample position "z" measured from the bottom of the effective fuel length is expressed by the following equation:

$$T(z) = T_{inlet} + \frac{\pi\Delta T}{2H} \int_0^z \cos\left(\frac{\pi}{2H} z\right) dz \quad (3.3.1)$$

The temperature of the coolant region as evaluated by Eq. (3.3.1) and using the axial sample positions given in Tables A.2.16–A.2.18 are shown in Tables 3.3.5–3.3.7.

Furthermore, in a BWR the quantity of heat passed to the coolant is not used for temperature rise but for the formation of voids if voids begin to form, and thus the temperature is constant above a certain region. This region was assumed to be the fourth node when the effective fuel length was divided into 24 nodes. The coolant temperature at each sample position is listed in Tables 3.3.8 and 3.3.9.

Table 3.3.5. SF95 : Temperature of coolant (K)

Sample	Temp. (k)
SF95–1	593.04
SF95–2	592.75
SF95–3	589.37
SF95–4	570.40
SF95–5	554.19

Table 3.3.6. SF96 : Temperature of coolant (K)

Sample	Temp. (k)
SF96–1	593.05
SF96–2	592.82
SF96–3	589.62
SF96–4	570.82
SF96–5	554.28

Table 3.3.7. SF97 : Temperature of coolant (K)

Sample	Temp. (k)
SF97–1	593.05
SF97–2	592.78
SF97–3	591.48
SF97–4	575.83
SF97–5	559.14
SF97–6	554.21

Table 3.3.8. SF98 : Temperature of coolant (K)

Sample	Temp. (k)
SF98-1	551.60
SF98-2	553.07
SF98-3	556.00
SF98-4	559.15
SF98-5	559.15
SF98-6	559.15
SF98-7	559.15
SF98-8	559.15

Table 3.3.9. SF99 : Temperature of coolant (K)

Sample	Temp. (k)
SF99-1	552.69
SF99-2	554.95
SF99-3	556.91
SF99-4	559.15
SF99-5	559.15
SF99-6	559.15
SF99-7	559.15
SF99-8	559.15
SF99-9	559.15
SF99-10	559.15

### 3.3.3. Void Rate

The void ratios, which are important in the analysis of BWR fuels, were evaluated for use in the analysis by reading a typical distribution of void ratios given in the application form for the reactor installation permit by a scanner, converting it into numbers with a digitizer, and fitting the numerical data to a quadratic function of axial position. The distribution of void ratios is shown in Fig. A.2.8. The evaluated values of void ratios at the positions of the SF98 and SF99 samples are listed in Tables 3.3.10 and 3.3.11.

Table 3.3.10. SF98 : Void ratio

Sample	Void ratio (%)
SF98-1	0.0
SF98-2	0.0
SF98-3	3.0
SF98-4	11.0
SF98-5	32.0
SF98-6	54.5
SF98-7	68.0
SF98-8	73.0

Table 3.3.11. SF99 : Void ratio

Sample	Void ratio (%)
SF99-1	0.0
SF99-2	1.4
SF99-3	5.8
SF99-4	10.8
SF99-5	27.7
SF99-6	54.7
SF99-7	66.5
SF99-8	71.7
SF99-9	72.9
SF99-10	74.3

### 3.3.4. Power Histories

The power histories of the SF95 samples are listed in Table A.2.21, those of the SF96 samples are listed in Table A.2.22, those of the SF97 samples are listed in Tables A.2.23 and A.2.24, those of the SF98 samples are listed in Table A.2.25, and those of the SF99 samples are listed in Table A.2.26. These data were evaluated so as to give the burn-up degrees of the destructive test samples measured finally by the Nd-148 method, on the basis of the power history data of the fuel assemblies or fuel rods as disclosed to JAERI.

### 3.3.5. Analytical Results by SWAT

The analytical results by SWAT are listed in Tables 3.3.12–3.3.16.

As can be seen from these evaluations, the principal uranium and plutonium are analyzed with an accuracy of 5% in the analysis of PWR-UO<sub>2</sub> fuels by SWAT, and the dispersion is also small, i.e., 2% or less. In the analysis of BWR-UO<sub>2</sub> fuels, the difference in the principal uranium and plutonium is larger

than in PWR-UO<sub>2</sub> fuels and the agreement is within approximately 10%, but the dispersion is about 3%, which is approximately the same as in the PWR-UO<sub>2</sub>.

In the analytical results of the PWR-Gd<sub>2</sub>O<sub>3</sub>-UO<sub>2</sub> fuel (SF96), the differences from the experimental values are within 10% in the C/E averages of principal uranium and plutonium, and larger than in the PWR-UO<sub>2</sub> fuels. This can be said to be a good agreement, considering that the fuel pellet is treated as a separate region in the model used. In the analytical results of the BWR-Gd<sub>2</sub>O<sub>3</sub>-UO<sub>2</sub> fuel (SF99), the <sup>239</sup>Pu is characteristically underestimated, but the overall differences are within 10%, as seen in the PWR-Gd<sub>2</sub>O<sub>3</sub>-UO<sub>2</sub> fuel.

For the plutonium, the calculated value of <sup>238</sup>Pu is underestimated by about 15%, which means that attention is necessary when evaluating the number of emitted neutrons of spent fuels.

As to the minor actinides, the difference from the calculation is larger than for the principal uranium and plutonium. For example, the <sup>241</sup>Am of the SF95 samples shows a difference of 14%, and a large dispersion of 27%. The other minor actinides are underestimated by nearly 20%. For example, the <sup>244</sup>Cm which becomes important in the evaluation of the amount of emitted neutrons, is underestimated by more than 20% overall, so it is clear that care must be taken when evaluating the amount of emitted neutrons, as in the case of <sup>238</sup>Pu.

As to the isotopes of Sm, which become important in burn-up credit with FP taken into account, data are obtained for the SF97, SF98, and SF99 samples. The calculated results for <sup>152</sup>Sm showed differences close to 20%, but the differences for the other isotopes were only about 10%. The difference between the experimental value and calculated value of the <sup>149</sup>Sm, which is important in evaluating reactivity, is close to 10%, and the dispersion is also relatively large, i.e., about 5%, among the Sm isotopes.

### 3.3.6. Analytical Results Without Considering Power Histories

The analytical results shown so far were obtained by considering accurate histories based on disclosed data. However, it is sometimes impossible to evaluate such accurate histories in test results after many irradiations, and also the evaluation of burn-up analysis results must be changed if the calculated results change considerably with the evaluation of the histories. The results are shown in Tables 3.3.17–3.3.21.

From these tables, it can be seen that <sup>241</sup>Am is largely affected by the burn-up history, but the other principal U and Pu do not change all that much overall. For example, the average C/E value for <sup>241</sup>Am was 1.14 when the history was taken into consideration, but if a constant history is assumed, the average C/E value is 1.09, thus a change of 5% occurs. However, the average C/E value does not change for the <sup>235</sup>U of SF95, and, on average, the <sup>241</sup>Pu shows no change either, though there are changes from sample to sample (SF95-1); hence, it can be concluded that analysis can be carried out by assuming a constant power without taking detailed histories into consideration, at least as far as the calculated values of the principal uranium and plutonium go, which become important in the analysis of burn-up credit.

Furthermore, it is known that, in the case of FP, the calculated values of the Sm isotopes change, depending on the history, but results different from those expected were obtained in which there were no large changes in the calculated values of the Sm isotopes obtained in the SF97 samples.

Table 3.3.12. SF95 : Results (C/E by SWAT)

Isotope	SF95-1	SF95-2	SF95-3	SF95-4	SF95-5	nbr	Average	stdv
U-234	1.023	0.928	1.193	1.181	0.866	5	1.04	0.15
U-235	1.010	1.022	1.013	1.015	1.008	5	1.01	0.01
U-236	0.948	0.930	0.948	0.950	0.942	5	0.94	0.01
U-238	1.000	1.000	1.000	1.000	1.000	5	1.00	0.00
Pu-238	0.832	0.778	0.881	0.877	0.837	5	0.84	0.04
Pu-239	1.044	1.006	1.016	1.009	1.011	5	1.02	0.02
Pu-240	1.006	0.980	1.012	1.014	1.008	5	1.00	0.01
Pu-241	1.006	0.944	0.963	0.966	0.964	5	0.97	0.02
Pu-242	0.949	0.895	0.929	0.936	0.938	5	0.93	0.02
Am-241	0.814	1.119	1.139	1.559	1.079	5	1.14	0.27
Am-242m	0.706	0.716	0.731	0.744	0.754	5	0.73	0.02
Am-243	0.862	0.847	0.902	0.918	0.880	5	0.88	0.03
Cm-242	0.752	0.658	0.612	0.532	0.784	5	0.67	0.10
Cm-243	0.588	0.550	0.649	0.629	0.555	5	0.59	0.04
Cm-244	0.766	0.660	0.778	0.761	0.770	5	0.75	0.05
Cm-245	0.896	0.704	0.849	0.787	0.789	5	0.81	0.07
Cm-246	0.374	0.429	0.701	0.685	1.050	5	0.65	0.27
Cs-134	0.900	0.852	0.889	0.887	0.871	5	0.88	0.02
Cs-137	0.983	0.971	0.981	0.978	0.988	5	0.98	0.01
Nd-142	0.757	0.875	0.810	0.834	0.902	5	0.84	0.06
Nd-143	0.968	0.969	0.967	0.974	0.973	5	0.97	0.00
Ce-144	0.970	0.976	0.951	1.044	0.983	5	0.98	0.04
Nd-144	0.989	0.977	0.989	0.955	0.986	5	0.98	0.01
Nd-145	0.996	0.997	1.001	1.006	1.005	5	1.00	0.00
Nd-146	1.000	0.990	0.990	0.989	0.996	5	0.99	0.00
Nd-148	0.999	0.993	0.998	0.997	0.999	5	1.00	0.00
Nd-150	0.967	0.977	0.973	0.975	0.986	5	0.98	0.01
Eu-154	0.865	0.786	0.793	0.764	0.786	5	0.80	0.04

Table 3.3.13. SF96 : Results (C/E by SWAT)

Isotope	SF95–2	SF95–3	SF95–4	SF95–5	nbr	Average	stdv
U-234	1.056	1.044	1.039	1.050	4	1.05	0.01
U-235	1.011	1.010	1.014	0.998	4	1.01	0.01
U-236	0.947	0.950	0.948	0.957	4	0.95	0.00
U-238	1.000	1.001	1.001	1.001	4	1.00	0.00
Np-237	1.311	1.534	1.478	1.403	4	1.43	0.10
Pu-238	0.825	0.843	0.814	0.853	4	0.83	0.02
Pu-239	0.978	0.988	0.982	0.985	4	0.98	0.00
Pu-240	0.992	0.983	0.971	0.997	4	0.99	0.01
Pu-241	0.992	0.980	0.968	0.993	4	0.98	0.01
Pu-242	0.974	0.958	0.943	0.990	4	0.97	0.02
Am-241	1.382	1.197	1.057	1.368	4	1.25	0.15
Am-242m	0.715	0.800	0.701	0.721	4	0.73	0.04
Am-243	0.939	0.959	0.917	0.982	4	0.95	0.03
Cm-242	0.800	0.789	0.769	0.822	4	0.79	0.02
Cm-244	0.779	0.822	0.778	0.848	4	0.81	0.03
Cs-134	0.905	0.965	0.949	0.966	4	0.95	0.03
Cs-137	1.031	1.042	1.033	1.061	4	1.04	0.01
Nd-143	0.961	0.958	0.962	0.951	4	0.96	0.01
Ce-144	1.036	1.143	1.142	1.067	4	1.10	0.05
Nd-144	0.937	0.886	0.900	0.922	4	0.91	0.02
Nd-145	0.996	0.995	0.999	0.992	4	1.00	0.00
Nd-146	0.975	0.970	0.970	0.972	4	0.97	0.00
Nd-148	0.991	0.990	0.991	0.992	4	0.99	0.00
Nd-150	0.979	0.978	0.977	0.984	4	0.98	0.00
Eu-154	1.483	1.265	1.241	1.387	4	1.34	0.11

Table 3.3.14. SF97 : Results (C/E by SWAT)

Isotope	SF97-2	SF97-3	SF97-4	SF97-5	SF97-6	nbr	Average	stdv
U-234	1.024	0.998	0.996	1.002	1.013	5	1.01	0.01
U-235	1.012	1.018	1.018	1.002	1.021	5	1.01	0.01
U-236	0.947	0.947	0.947	0.949	0.946	5	0.95	0.00
U-238	1.000	1.000	1.001	1.001	1.000	5	1.00	0.00
Np-237	0.951	0.985	0.966	0.938	0.943	5	0.96	0.02
Pu-238	0.834	0.839	0.820	0.798	0.838	5	0.83	0.02
Pu-239	1.027	1.038	1.033	1.007	1.044	5	1.03	0.01
Pu-240	1.033	1.044	1.034	1.027	1.039	5	1.04	0.01
Pu-241	0.978	0.992	0.989	0.964	0.998	5	0.98	0.01
Pu-242	0.943	0.950	0.945	0.940	0.946	5	0.94	0.00
Am-241	1.258	1.264	1.139	1.087	1.294	5	1.21	0.09
Am-242m	0.859	0.826	0.748	0.712	0.829	5	0.79	0.06
Am-243	0.875	0.901	0.892	0.877	0.907	5	0.89	0.01
Cm-242	0.985	1.072	1.131	1.190	1.070	5	1.09	0.08
Cm-243	0.632	0.670	0.676	0.655	0.661	5	0.66	0.02
Cm-244	0.739	0.765	0.754	0.732	0.778	5	0.75	0.02
Cm-245	0.780	0.816	0.796	0.754	0.841	5	0.80	0.03
Cm-246	0.640	0.673	0.651	0.629	0.676	5	0.65	0.02
Cm-247	0.569	0.616	0.608	0.592	0.589	5	0.59	0.02
Cs-134	0.830	0.869	0.903	0.896	0.878	5	0.88	0.03
Cs-137	0.982	0.982	0.991	0.989	0.982	5	0.99	0.00
Nd-143	0.994	0.995	1.000	0.990	0.995	5	0.99	0.00
Ce-144	0.896	0.977	1.067	1.075	0.956	5	0.99	0.08
Nd-144	1.002	0.971	0.955	0.952	0.969	5	0.97	0.02
Nd-145	1.014	1.016	1.020	1.019	1.013	5	1.02	0.00
Nd-146	0.989	0.984	0.983	0.982	0.986	5	0.98	0.00
Nd-148	1.007	1.007	1.008	1.008	1.008	5	1.01	0.00
Nd-150	0.999	1.000	1.000	1.001	1.004	5	1.00	0.00
Eu-154	0.789	0.800	0.793	0.779	0.807	5	0.79	0.01
Sm-147	1.042	1.028	1.018	1.023	1.033	5	1.03	0.01
Sm-148	1.044	1.051	1.042	1.032	1.062	5	1.05	0.01
Sm-149	0.859	0.893	0.960	0.960	0.887	5	0.91	0.05
Sm-150	0.983	0.971	0.964	0.955	0.979	5	0.97	0.01
Sm-151	0.986	0.980	0.967	0.933	0.995	5	0.97	0.02
Sm-152	1.222	1.259	1.268	1.265	1.240	5	1.25	0.02
Sm-154	0.984	0.984	0.979	0.971	0.991	5	0.98	0.01

Table 3.3.15. SF98 : Results (C/E by SWAT)

Isotope	SF98-3	SF98-4	SF98-5	SF98-6	SF98-7	SF98-8	nbr	Average	stdv
U-234	0.997	0.994	0.987	1.057	0.990	1.001	6	1.00	0.03
U-235	1.075	1.105	1.066	1.034	1.102	1.069	6	1.08	0.03
U-236	0.948	0.946	0.946	0.933	0.924	0.915	6	0.94	0.01
U-238	0.999	1.000	1.000	1.000	0.999	0.998	6	1.00	0.00
Np-237	1.096	1.044	1.318	0.969	1.151	1.144	6	1.12	0.12
Pu-238	0.909	0.910	0.969	1.052	0.931	0.897	6	0.94	0.06
Pu-239	1.078	1.081	1.089	1.051	1.132	1.148	6	1.10	0.04
Pu-240	0.977	0.962	0.961	0.926	0.934	0.966	6	0.95	0.02
Pu-241	1.082	1.084	1.101	1.089	1.142	1.171	6	1.11	0.04
Pu-242	0.966	0.962	1.008	1.031	0.995	1.018	6	1.00	0.03
Am-241	1.029	1.035	1.102	1.220	1.289	1.353	6	1.17	0.14
Am-242m	0.814	0.825	0.842	0.836	0.978	0.952	6	0.87	0.07
Am-243	0.936	0.940	1.037	0.956	1.007	1.006	6	0.98	0.04
Cm-242	0.718	0.726	0.549	0.299	0.640	0.752	6	0.61	0.17
Cm-243	0.670	0.792	0.872	0.738	0.735	0.690	6	0.75	0.07
Cm-244	0.848	0.856	0.874	0.789	0.818	0.809	6	0.83	0.03
Cm-245	1.000	1.029	0.997	0.823	0.914	0.900	6	0.94	0.08
Cm-246	0.725	0.758	0.739	0.621	0.656	0.972	6	0.75	0.12
Cs-134	1.064	1.016	1.060	0.933	0.891	1.040	6	1.00	0.07
Cs-137	1.022	0.989	1.020	0.974	0.930	1.051	6	1.00	0.04
Nd-143	1.039	1.046	1.028	1.012	1.029	1.024	6	1.03	0.01
Ce-144	1.115	1.059	0.937	0.998	0.912	0.863	6	0.98	0.09
Nd-144	0.957	0.968	0.998	0.973	0.992	1.025	6	0.99	0.02
Nd-145	1.019	1.027	1.022	1.024	1.020	1.015	6	1.02	0.00
Nd-146	0.998	0.995	0.992	0.985	0.984	0.990	6	0.99	0.01
Nd-148	1.013	1.014	1.012	1.009	1.008	1.007	6	1.01	0.00
Nd-150	1.008	1.004	1.009	1.001	1.004	1.004	6	1.00	0.00
Eu-154	0.811	0.775	0.845	0.760	0.839	0.799	6	0.81	0.03
Sm-147	0.891	0.888	0.945	0.944	0.934	0.895	6	0.92	0.03
Sm-148	0.963	0.965	1.035	1.009	1.027	0.976	6	1.00	0.03
Sm-149	0.990	1.100	0.821	0.985	0.880	0.825	6	0.93	0.11
Sm-150	0.874	0.871	0.934	0.922	0.926	0.893	6	0.90	0.03
Sm-151	0.943	0.953	1.005	0.943	1.036	1.003	6	0.98	0.04
Sm-152	1.038	1.055	1.151	1.194	1.160	1.066	6	1.11	0.07
Sm-154	0.888	0.890	0.940	0.945	0.927	0.870	6	0.91	0.03

Table 3.3.16. SF99 : Results (C/E by SWAT)

Isotope	SF99-2	SF99-3	SF99-4	SF99-5	SF99-6	SF99-7	SF99-8	SF99-9	nbr	Average	stdv
U-234	1.064	1.026	1.040	1.032	1.069	1.062	1.052	1.021	8	1.05	0.02
U-235	1.029	0.996	1.048	0.938	0.965	0.978	1.025	1.029	8	1.00	0.04
U-236	0.952	0.968	0.956	0.964	0.940	0.943	0.924	0.935	8	0.95	0.02
U-238	1.000	1.001	1.000	1.002	1.002	1.002	1.001	1.000	8	1.00	0.00
Np-237	0.847	0.841	0.949	0.852	0.879	0.853	0.849	0.829	8	0.86	0.04
Pu-238	0.964	0.904	0.951	1.078	0.837	0.897	0.826	0.826	8	0.91	0.08
Pu-239	0.945	0.947	0.987	0.903	0.857	0.870	0.925	0.989	8	0.93	0.05
Pu-240	0.982	0.972	0.973	0.935	0.904	0.905	0.944	0.994	8	0.95	0.03
Pu-241	0.926	0.956	0.972	0.915	0.898	0.922	0.974	1.071	8	0.95	0.05
Pu-242	0.905	0.968	0.940	0.983	1.006	1.025	1.006	1.075	8	0.99	0.05
Am-241	1.411	0.898	1.060	0.902	1.027	1.052	1.074	1.019	8	1.06	0.16
Am-242m	0.805	0.774	0.801	0.709	0.680	0.780	0.780	0.927	8	0.78	0.07
Am-243	0.805	0.865	0.859	0.879	0.827	0.869	0.799	0.875	8	0.85	0.03
Cm-242	0.341	0.528	0.410	0.268	0.367	0.361	0.412	0.644	8	0.42	0.12
Cm-243	0.649	0.710	0.702	0.692	0.600	0.603	0.541	0.500	8	0.62	0.08
Cm-244	0.638	0.737	0.714	0.722	0.601	0.658	0.573	0.675	8	0.66	0.06
Cm-245	0.610	0.754	0.732	0.700	0.506	0.585	0.512	0.384	8	0.60	0.13
Cm-246	0.000	0.620	0.572	0.611	0.449	0.511	0.420	0.081	7	0.47	0.19
Cm-247	0.000	0.207	0.000	0.476	0.000	0.194	0.000	0.000	4	0.22	0.20
Cs-134	0.820	0.902	0.890	0.886	0.805	0.782	0.781	0.808	8	0.83	0.05
Cs-137	0.976	0.969	0.969	0.966	0.954	0.934	0.960	0.965	8	0.96	0.01
Nd-143	1.007	0.992	1.006	0.971	0.987	0.981	0.996	0.987	8	0.99	0.01
Ce-144	0.984	0.000	1.084	0.858	0.910	0.673	0.789	0.941	7	0.89	0.13
Nd-144	1.002	0.781	0.960	1.044	1.045	1.160	1.083	0.997	8	1.01	0.11
Nd-145	1.024	1.020	1.023	1.020	1.036	1.026	1.023	1.009	8	1.02	0.01
Nd-146	1.000	0.996	0.991	0.991	0.984	0.981	0.985	0.988	8	0.99	0.01
Nd-148	1.010	1.012	1.012	1.011	1.008	1.007	1.006	1.007	8	1.01	0.00
Nd-150	0.998	1.004	1.006	1.001	0.986	0.992	0.992	1.005	8	1.00	0.01
Eu-154	1.185	1.023	1.018	0.922	0.880	0.897	0.927	1.058	8	0.99	0.10
Sm-147		1.023		1.000		1.025	1.007	1.013	5	1.01	0.01
Sm-148		1.021		1.005		0.986	0.929	0.981	5	0.98	0.03
Sm-149	0.914		0.938		0.848	0.892	0.957	5	0.91	0.04	
Sm-150	0.950		0.923		0.937	0.932	0.970	5	0.94	0.02	
Sm-151	0.929		0.859		0.830	0.869	0.950	5	0.89	0.05	
Sm-152	1.161		1.188		1.250	1.178	1.148	5	1.18	0.04	
Sm-154	0.958		0.940		0.945	0.933	0.966	5	0.95	0.01	

Table 3.3.17. SF95 : Results (C/E by SWAT : Constant power)

Isotope	SF95-1	SF95-2	SF95-3	SF95-4	SF95-5	nbr	Average	stdv
U-234	1.023	0.928	1.193	1.181	0.866	5	1.04	0.15
U-235	0.010	1.022	1.013	1.015	1.007	5	1.01	0.01
U-236	0.948	0.930	0.948	0.950	0.942	5	0.94	0.01
U-238	1.000	1.000	1.000	1.000	1.000	5	1.00	0.00
Pu-238	0.829	0.774	0.876	0.872	0.833	5	0.84	0.04
Pu-239	1.044	1.006	1.016	1.010	1.011	5	1.02	0.02
Pu-240	1.005	0.979	1.011	1.013	1.007	5	1.00	0.01
Pu-241	1.008	0.946	0.964	0.968	0.966	5	0.97	0.02
Pu-242	0.951	0.896	0.930	0.936	0.938	5	0.93	0.02
Am-241	0.775	1.065	1.083	1.483	1.027	5	1.09	0.25
Am-242m	0.674	0.684	0.697	0.710	0.720	5	0.70	0.02
Am-243	0.863	0.847	0.901	0.918	0.880	5	0.88	0.03
Cm-242	0.737	0.646	0.602	0.524	0.771	5	0.66	0.10
Cm-243	0.583	0.546	0.645	0.624	0.550	5	0.59	0.04
Cm-244	0.766	0.660	0.778	0.762	0.770	5	0.75	0.05
Cm-245	0.897	0.704	0.849	0.788	0.789	5	0.81	0.07
Cm-246	0.374	0.428	0.701	0.685	1.050	5	0.65	0.27
Cs-134	0.909	0.861	0.898	0.896	0.880	5	0.89	0.02
Cs-137	0.984	0.972	0.982	0.979	0.988	5	0.98	0.01
Nd-142	0.758	0.876	0.811	0.835	0.904	5	0.84	0.06
Nd-143	0.967	0.967	0.965	0.972	0.971	5	0.97	0.00
Ce-144	0.998	1.003	0.978	1.073	1.010	5	1.01	0.04
Nd-144	0.973	0.963	0.977	0.943	0.972	5	0.97	0.01
Nd-145	0.996	0.997	1.001	1.006	1.005	5	1.00	0.00
Nd-146	1.000	0.990	0.990	0.989	0.996	5	0.99	0.00
Nd-148	0.999	0.993	0.998	0.997	0.999	5	1.00	0.00
Nd-150	0.967	0.977	0.973	0.975	0.986	5	0.98	0.01
Eu-154	0.866	0.787	0.794	0.764	0.787	5	0.80	0.04

Table 3.3.18. SF96 : Results (C/E by SWAT : Constant power)

Isotope	SF96–2	SF96–3	SF96–4	SF96–5	nbr	Average	stdv
U-234	1.052	1.042	1.037	1.046	4	1.04	0.01
U-235	1.022	1.030	1.038	1.018	4	1.03	0.01
U-236	0.945	0.951	0.949	0.956	4	0.95	0.00
U-238	1.000	1.001	1.001	1.000	4	1.00	0.00
Np-237	1.332	1.546	1.489	1.416	4	1.45	0.09
Pu-238	0.875	0.880	0.849	0.896	4	0.88	0.02
Pu-239	0.989	0.989	0.982	0.989	4	0.99	0.00
Pu-240	1.016	0.996	0.984	1.015	4	1.00	0.02
Pu-241	1.007	0.987	0.976	1.004	4	0.99	0.01
Pu-242	0.995	0.970	0.955	1.007	4	0.98	0.02
Am-241	1.742	1.499	1.326	1.723	4	1.57	0.20
Am-242m	0.901	1.003	0.881	0.909	4	0.92	0.05
Am-243	0.960	0.973	0.930	1.001	4	0.97	0.03
Cm-242	0.898	0.878	0.858	0.922	4	0.89	0.03
Cm-244	0.792	0.828	0.784	0.860	4	0.82	0.04
Cs-134	0.865	0.922	0.906	0.923	4	0.90	0.03
Cs-137	1.027	1.038	1.029	1.057	4	1.04	0.01
Nd-143	0.967	0.966	0.971	0.959	4	0.97	0.01
Ce-144	0.917	1.013	1.012	0.946	4	0.97	0.05
Nd-144	1.004	0.940	0.953	0.979	4	0.97	0.03
Nd-145	0.995	0.994	0.999	0.992	4	0.99	0.00
Nd-146	0.974	0.968	0.968	0.970	4	0.97	0.00
Nd-148	0.990	0.988	0.989	0.990	4	0.99	0.00
Nd-150	0.983	0.981	0.980	0.988	4	0.98	0.00
Eu-154	1.527	1.300	1.276	1.428	4	1.38	0.12

Table 3.3.19. SF97 : Results (C/E by SWAT : Constant power)

Isotope	SF97-2	SF97-3	SF97-4	SF97-5	SF97-6	nbr	Average	stdv
U-234	1.024	0.998	0.995	1.001	1.013	5	1.01	0.01
U-235	1.012	1.017	1.017	1.001	1.020	5	1.01	0.01
U-236	0.947	0.947	0.947	0.949	0.946	5	0.95	0.00
U-238	1.000	1.000	1.001	1.001	1.000	5	1.00	0.00
Np-237	0.950	0.984	0.965	0.937	0.942	5	0.96	0.02
Pu-238	0.833	0.838	0.819	0.797	0.837	5	0.82	0.02
Pu-239	1.027	1.039	1.033	1.008	1.044	5	1.03	0.01
Pu-240	1.033	1.044	1.033	1.027	1.038	5	1.03	0.01
Pu-241	0.980	0.993	0.990	0.965	0.999	5	0.99	0.01
Pu-242	0.943	0.950	0.945	0.940	0.946	5	0.94	0.00
Am-241	1.217	1.221	1.099	1.049	1.250	5	1.17	0.09
Am-242m	0.834	0.799	0.723	0.689	0.802	5	0.77	0.06
Am-243	0.874	0.900	0.892	0.877	0.907	5	0.89	0.01
Cm-242	0.992	1.079	1.138	1.197	1.076	5	1.10	0.08
Cm-243	0.649	0.687	0.693	0.671	0.678	5	0.68	0.02
Cm-244	0.738	0.765	0.754	0.733	0.778	5	0.75	0.02
Cm-245	0.779	0.816	0.796	0.754	0.841	5	0.80	0.03
Cm-246	0.639	0.672	0.651	0.628	0.675	5	0.65	0.02
Cm-247	0.567	0.615	0.607	0.591	0.587	5	0.59	0.02
Cs-134	0.838	0.877	0.911	0.904	0.886	5	0.88	0.03
Cs-137	0.982	0.982	0.992	0.990	0.982	5	0.99	0.00
Nd-143	0.993	0.994	0.999	0.989	0.994	5	0.99	0.00
Ce-144	0.917	0.998	1.090	1.099	0.977	5	1.02	0.08
Nd-144	0.995	0.965	0.949	0.946	0.963	5	0.96	0.02
Nd-145	1.014	1.016	1.020	1.019	1.013	5	1.02	0.00
Nd-146	0.989	0.984	0.983	0.982	0.986	5	0.98	0.00
Nd-148	1.007	1.007	1.008	1.008	1.008	5	1.01	0.00
Nd-150	0.999	1.000	1.000	1.001	1.004	5	1.00	0.00
Eu-154	0.791	0.800	0.794	0.779	0.807	5	0.79	0.01
Sm-147	1.041	1.027	1.017	1.022	1.032	5	1.03	0.01
Sm-148	1.043	1.051	1.043	1.032	1.062	5	1.05	0.01
Sm-149	0.871	0.908	0.978	0.978	0.902	5	0.93	0.05
Sm-150	0.982	0.970	0.963	0.954	0.978	5	0.97	0.01
Sm-151	0.986	0.980	0.967	0.933	0.996	5	0.97	0.02
Sm-152	1.221	1.259	1.267	1.264	1.239	5	1.25	0.02
Sm-154	0.983	0.984	0.979	0.971	0.991	5	0.98	0.01

Table 3.3.20. SF98 : Results (C/E by SWAT : Constant power)

Isotope	SF98-3	SF98-4	SF98-5	SF98-6	SF98-7	SF98-8	nbr	Average	stdv
U-234	0.997	0.995	0.987	1.057	0.990	1.000	6	1.00	0.03
U-235	1.076	1.106	1.066	1.035	1.103	1.069	6	1.08	0.03
U-236	0.948	0.946	0.946	0.933	0.924	0.915	6	0.94	0.01
U-238	0.999	1.000	1.000	1.000	0.999	0.998	6	1.00	0.00
Np-237	1.097	1.045	1.319	0.970	1.152	1.146	6	1.12	0.12
Pu-238	0.912	0.911	0.971	1.054	0.933	1.899	6	0.95	0.06
Pu-239	1.078	1.081	1.089	1.052	1.133	1.149	6	1.10	0.04
Pu-240	0.978	0.963	0.961	0.926	0.935	0.967	6	0.95	0.02
Pu-241	1.082	1.083	1.100	1.088	1.142	1.172	6	1.11	0.04
Pu-242	0.966	0.962	1.009	1.031	0.996	1.019	6	1.00	0.03
Am-241	1.051	1.058	1.126	1.246	1.316	1.381	6	1.20	0.14
Am-242m	0.830	0.842	0.860	0.852	0.996	0.967	6	0.89	0.07
Am-243	0.938	0.940	1.038	0.957	1.008	1.008	6	0.98	0.04
Cm-242	0.713	0.720	0.545	0.296	0.634	0.745	6	0.61	0.17
Cm-243	0.659	0.779	0.857	0.725	0.723	0.678	6	0.74	0.07
Cm-244	0.849	0.856	0.874	0.789	0.819	0.811	6	0.83	0.03
Cm-245	1.002	1.028	0.997	0.823	0.915	0.903	6	0.94	0.08
Cm-246	0.727	0.759	0.740	0.622	0.657	0.977	6	0.75	0.12
Cs-134	1.059	1.010	1.055	0.929	0.887	1.035	6	1.00	0.07
Cs-137	1.022	0.989	1.020	0.974	0.930	1.051	6	1.00	0.04
Nd-143	1.041	1.047	1.029	1.013	1.030	1.025	6	1.03	0.01
Ce-144	1.101	1.046	0.925	0.985	0.900	0.852	6	0.97	0.09
Nd-144	0.960	0.971	1.001	0.977	0.995	1.029	6	0.99	0.02
Nd-145	1.019	1.027	1.022	1.024	1.020	1.015	6	1.02	0.00
Nd-146	0.998	0.995	0.992	0.985	0.984	0.990	6	0.99	0.01
Nd-148	1.013	1.014	1.012	1.009	1.007	1.007	6	1.01	0.00
Nd-150	1.008	1.004	1.009	1.001	1.004	1.005	6	1.01	0.00
Eu-154	0.811	0.775	0.845	0.760	0.839	0.800	6	0.80	0.03
Sm-147	0.891	0.887	0.945	0.943	0.933	0.895	6	0.92	0.03
Sm-148	0.965	0.966	1.036	1.010	1.028	0.978	6	1.00	0.03
Sm-149	0.975	1.081	0.807	0.972	0.870	0.818	6	0.92	0.11
Sm-150	0.875	0.872	0.934	0.922	0.927	0.894	6	0.90	0.03
Sm-151	0.943	0.952	1.004	0.943	1.036	1.004	6	0.98	0.04
Sm-152	1.039	1.055	1.151	1.194	1.161	1.066	6	1.11	0.07
Sm-154	0.888	0.889	0.940	0.945	0.927	0.870	6	0.91	0.03

Table 3.3.21. SF99 : Results (C/E by SWAT : Constant power)

Isotope	SF99-2	SF99-3	SF99-4	SF99-5	SF99-6	SF99-7	SF99-8	SF99-9	nbr	Average	stdv
U-234	1.065	1.027	1.040	1.032	1.070	1.063	1.052	1.022	8	1.05	0.02
U-235	1.028	0.994	1.045	0.936	0.963	0.977	1.024	1.028	8	1.00	0.04
U-236	0.952	0.967	0.956	0.963	0.940	0.943	0.923	0.935	8	0.95	0.01
U-238	1.000	1.001	1.000	1.002	1.002	1.002	1.001	1.000	8	1.00	0.00
Np-237	0.846	0.841	0.949	0.852	0.879	0.853	0.850	0.829	8	0.86	0.04
Pu-238	0.962	0.904	0.951	1.078	0.837	0.897	0.825	0.861	8	0.91	0.08
Pu-239	0.944	0.946	0.986	0.902	0.857	0.869	0.925	0.988	8	0.93	0.05
Pu-240	0.980	0.971	0.973	0.934	0.903	0.905	0.943	0.993	8	0.95	0.03
Pu-241	0.923	0.954	0.970	0.913	0.896	0.920	0.972	1.068	8	0.95	0.05
Pu-242	0.902	0.966	0.938	0.982	1.005	1.023	1.004	1.073	8	0.99	0.05
Am-241	1.425	0.911	1.077	0.917	1.043	1.066	1.087	1.031	8	1.07	0.16
Am-242m	0.810	0.783	0.811	0.719	0.689	0.789	0.785	0.931	8	0.79	0.07
Am-243	0.801	0.863	0.857	0.878	0.826	0.867	0.798	0.873	8	0.85	0.03
Cm-242	0.335	0.520	0.404	0.264	0.362	0.356	0.406	0.633	8	0.41	0.12
Cm-243	0.633	0.693	0.686	0.678	0.586	0.589	0.528	0.488	8	0.61	0.08
Cm-244	0.635	0.734	0.712	0.720	0.600	0.657	0.572	0.673	8	0.66	0.06
Cm-245	0.607	0.751	0.730	0.698	0.505	0.583	0.511	0.383	8	0.60	0.13
Cm-246	0.000	0.618	0.571	0.610	0.449	0.511	0.419	0.081	7	0.47	0.19
Cm-247	0.000	0.206	0.000	0.475	0.000	0.194	0.000	0.000	4	0.22	0.20
Cs-134	0.817	0.899	0.886	0.882	0.801	0.779	0.778	0.804	8	0.83	0.05
Cs-137	0.976	0.969	0.968	0.965	0.954	0.934	0.960	0.964	8	0.96	0.01
Nd-143	1.007	0.992	1.006	0.971	0.987	0.982	0.996	0.988	8	0.99	0.01
Ce-144	0.972	0.000	1.070	0.847	0.898	0.664	0.779	0.929	7	0.88	0.13
Nd-144	1.007	0.785	0.964	1.048	1.049	1.165	1.088	1.002	8	1.01	0.11
Nd-145	1.024	1.020	1.023	1.020	1.036	1.027	1.023	1.009	8	1.02	0.01
Nd-146	1.000	0.996	0.992	0.991	0.985	0.981	0.985	0.988	8	0.99	0.01
Nd-148	1.010	1.012	1.012	1.011	1.008	1.007	1.006	1.007	8	1.01	0.00
Nd-150	0.997	1.003	1.005	1.001	0.986	0.991	0.992	1.005	8	1.00	0.01
Eu-154	1.185	1.024	1.019	0.922	0.880	0.897	0.927	1.057	8	0.99	0.10
Sm-147		1.022		0.999		1.024	1.007	1.013	5	1.01	0.01
Sm-148		1.023		1.006		0.987	0.931	0.983	5	0.99	0.03
Sm-149		0.900		0.923		0.837	0.884	0.951	5	0.90	0.04
Sm-150		0.650		0.923		0.938	0.932	0.970	5	0.94	0.02
Sm-151		0.928		0.858		0.829	0.868	0.950	5	0.89	0.05
Sm-152		1.161		1.187		1.250	1.177	1.148	5	1.18	0.04
Sm-154		0.957		0.940		0.944	0.933	0.965	5	0.95	0.01

### 3.3.7. Analysis with the Effect of Temperature Change Taken into Consideration

The effect of fuel temperature was analyzed. The history of the fuel temperature was analyzed by using FEMAXI-V.<sup>4</sup> The conditions for the analysis are listed in Table 3.3.22.

Table 3.3.22. Data for FEMAXI-V calculation

Clad	
Material	Zr-4
Inner diam.	0.822 cm
Outer diam.	0.95 cm
Pellet	
Dish	No
Chanfa	No
Pellet diam.	0.805 cm
Pellet length	0.90 cm
<sup>235</sup> U enrichment	4.1%
Density	95% T.D.
Plenum	
Volume of upper plenum	6.813 cm <sup>3</sup>
Initial gas pressure	3.236 MPa
Initial gas contents	He
Pellet total weight	1934.2 g
Volume of lower plenum	1.81 cm <sup>3</sup>
Fast flux	5.0E+11 n/cm <sup>2</sup> s
Coolant temp.	553.75 K
Coolant pressure	15.495 MPa
Coolant flow rate	0.315 Kg/cm <sup>2</sup> s
Initial temperature of fuel element	553.65 K
Temp. difference between plenum and coolant	0.0 K

The distribution of temperatures in the cell as calculated by using FEMAXI-V is shown in Figs. 3.3.1 and 3.3.2.

Furthermore, the change in the fuel pellet temperature associated with burning as calculated by using FEMAXI-V is shown in Figs. 3.3.3 and 3.3.4.

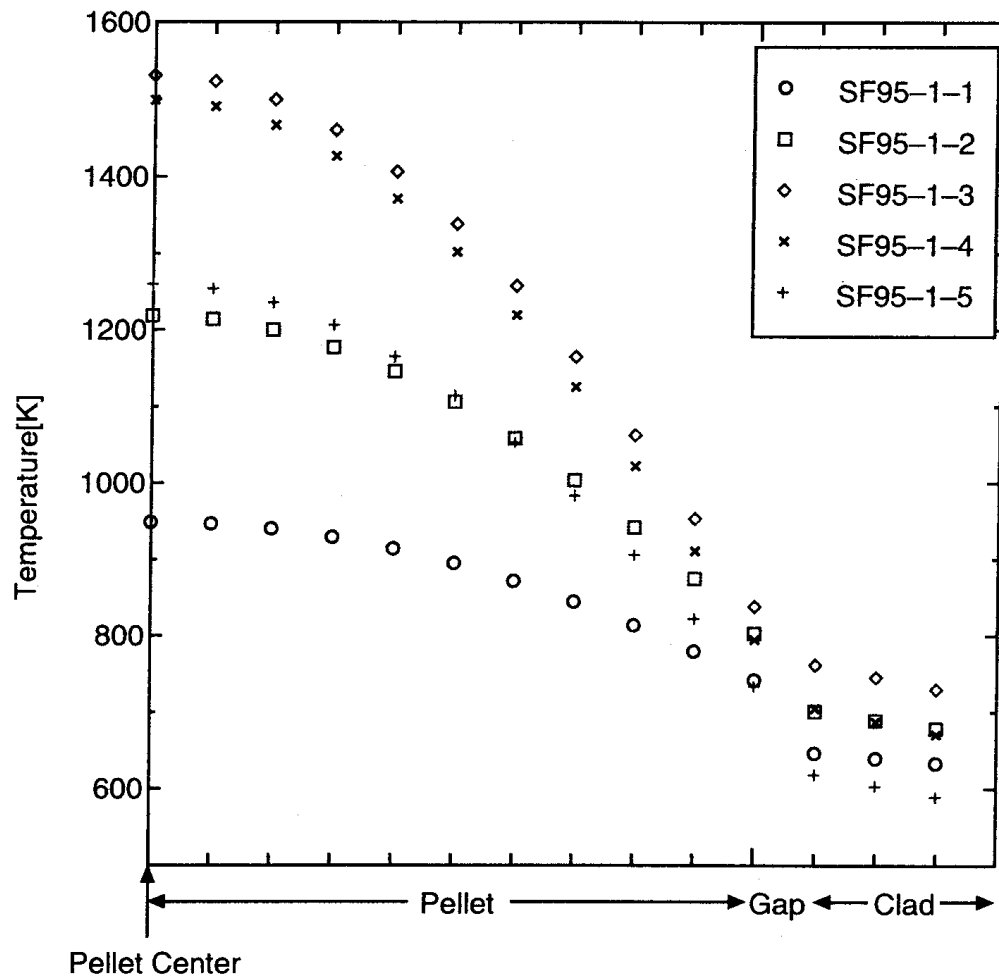


Fig. 3.3.1. Temperature distribution in (SF95).

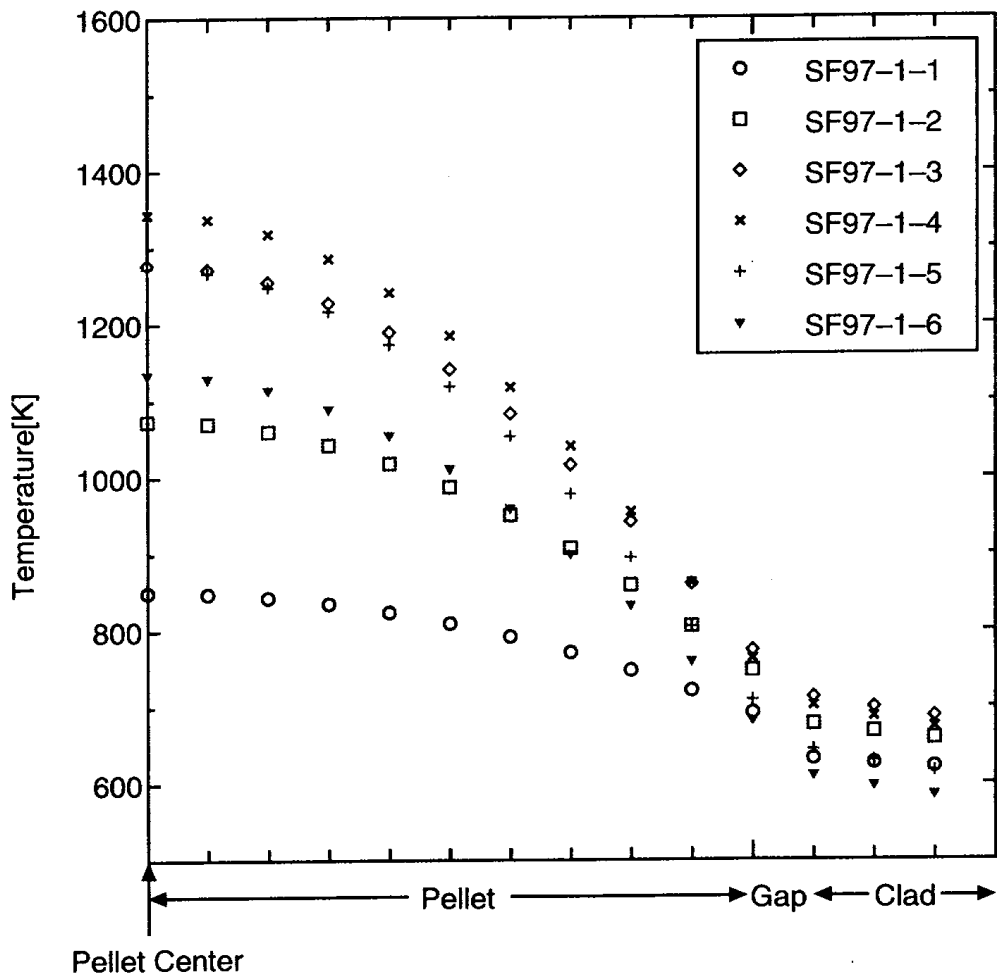


Fig. 3.3.2. Temperature distribution in (SF97).

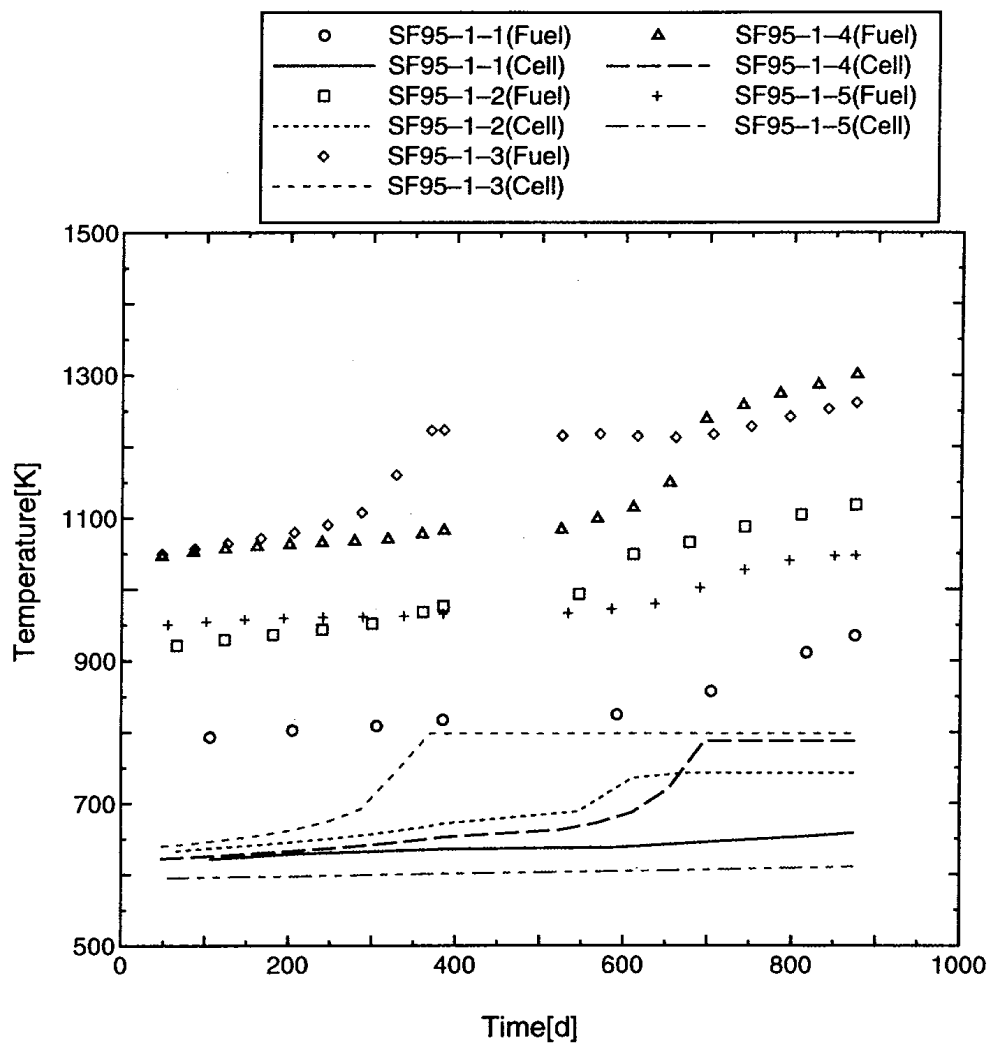


Fig. 3.3.3. Temperature history of SF95 samples.

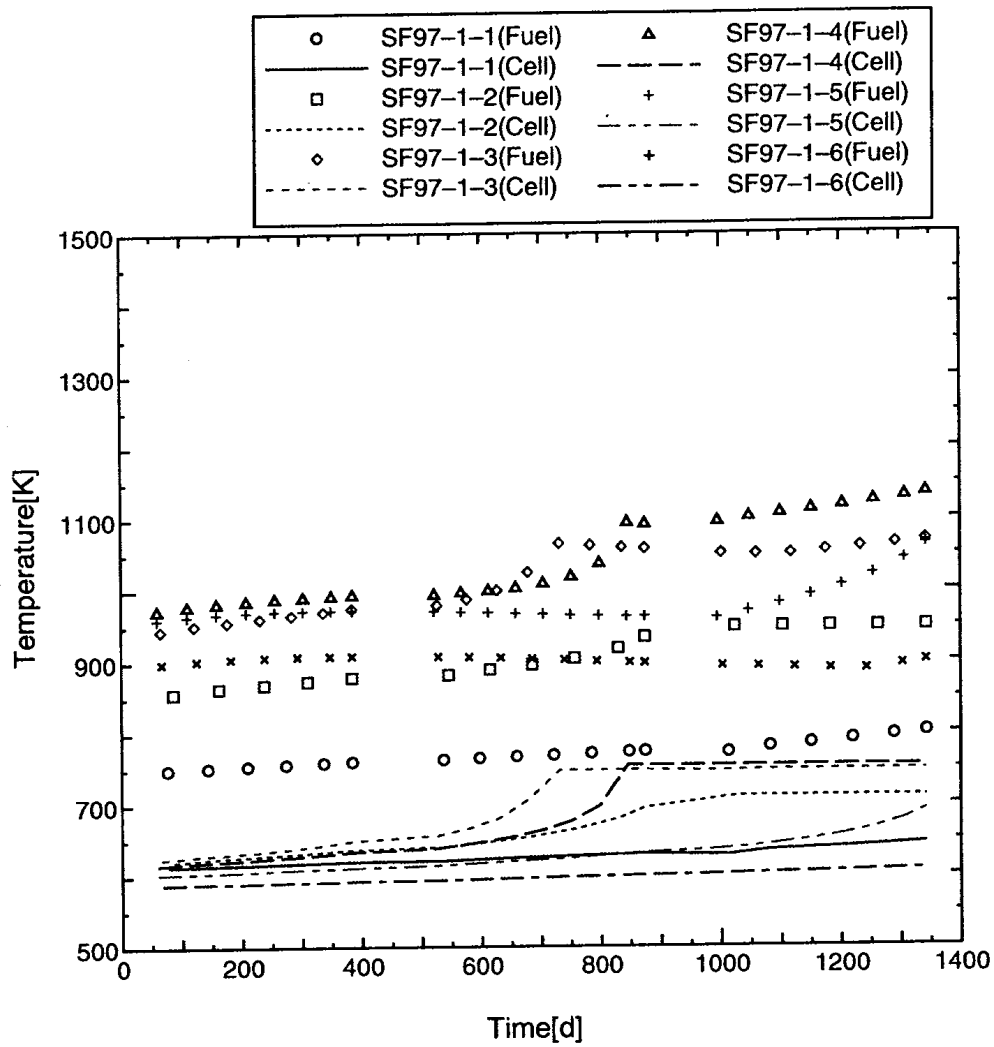


Fig. 3.3.4. Temperature history of SF97 samples.

The SWAT analysis results with the use of these temperature histories are listed in Table 3.3.23 and 3.3.24. Since this analysis was carried out at a preliminary analysis stage, the contribution of U-238 fission to the formation of Nd-148 is not subtracted; thus, the burn-up degrees are 2–3% higher than those in the analysis done so far.

As shown in the analysis, a difference of 2% at most appears only in the calculated values of  $^{241}\text{Pu}$ , even if the history of temperature change in the pellet region is accurately included, the result being no changes at all in many isotopes. Therefore, it can be concluded that the temperature of 900 K employed as the temperature of the pellet region throughout the present analysis is adequate.

Table 3.3.23. SF95 : Results (C/E by SWAT : Considering pellet temp. history)

	SF95-1			SF95-2			SF95-3			SF95-4			SF95-5		
	H*	C**	Diff	H*	C**	Diff	H*	C**	Diff	H*	C**	Diff	H*	C**	Diff
U-234	1.02	1.02	0.00	0.92	0.92	0.00	1.18	1.18	0.00	1.17	1.17	0.00	0.86	0.86	0.00
U-235	1.00	1.00	0.00	1.01	1.01	0.00	1.00	0.99	0.01	1.00	0.99	0.01	0.99	0.99	0.00
U-236	0.96	0.96	0.00	0.94	0.94	0.00	0.95	0.96	0.00	0.96	0.96	0.00	0.95	0.95	0.00
U-238	1.00	1.00	0.00	1.00	1.00	0.00	1.00	1.00	0.00	1.00	1.00	0.00	1.00	1.00	0.00
Pu-238	0.86	0.86	0.00	0.81	0.81	0.00	0.92	0.92	0.00	0.92	0.91	0.00	0.87	0.87	0.00
Pu-239	1.03	1.04	-0.01	1.00	1.00	0.00	1.02	1.00	0.01	1.01	0.99	0.01	1.00	1.00	0.00
Pu-240	1.01	1.03	-0.01	1.00	1.00	0.00	1.04	1.03	0.01	1.04	1.03	0.01	1.03	1.02	0.00
Pu-241	1.02	1.03	-0.02	0.97	0.97	0.00	1.00	0.98	0.02	1.00	0.98	0.01	0.99	0.98	0.00
Pu-242	0.98	0.99	-0.02	0.93	0.93	0.00	0.98	0.97	0.01	0.98	0.98	0.01	0.98	0.98	0.00
Am-241	0.82	0.84	-0.02	1.14	1.14	0.00	1.17	1.15	0.02	1.60	1.57	0.03	1.10	1.10	0.00
Am-242m	0.71	0.73	-0.02	0.73	0.73	0.00	0.76	0.74	0.02	0.77	0.75	0.02	0.77	0.77	0.00
Am-243	0.90	0.92	-0.02	0.90	0.90	0.00	0.97	0.96	0.01	0.98	0.98	0.01	0.93	0.93	0.00
Cm-242	0.77	0.79	-0.01	0.69	0.69	0.00	0.64	0.64	0.01	0.56	0.55	0.01	0.82	0.81	0.00
Cm-243	0.61	0.62	-0.01	0.58	0.58	0.00	0.70	0.69	0.01	0.67	0.67	0.01	0.59	0.59	0.00
Cm-244	0.81	0.83	-0.01	0.71	0.71	0.00	0.85	0.85	0.01	0.83	0.83	0.01	0.83	0.83	0.00
Cm-245	0.97	0.98	-0.02	0.78	0.78	0.00	0.95	0.94	0.01	0.88	0.87	0.01	0.87	0.87	0.00
Cm-246	0.41	0.42	0.00	0.48	0.48	0.00	0.79	0.80	0.00	0.78	0.78	0.00	1.18	1.18	0.00
Cs-134	0.93	0.93	0.00	0.88	0.88	0.00	0.93	0.92	0.01	0.92	0.92	0.00	0.92	0.90	0.02
Cs-137	1.00	1.00	0.00	0.99	0.99	0.00	1.00	1.00	0.00	1.00	1.00	0.00	1.00	1.00	0.00
Nd-142	0.78	0.78	0.00	0.91	0.91	0.00	0.84	0.84	0.00	0.86	0.87	0.00	0.93	0.93	0.00
Nd-143	0.98	0.98	0.00	0.98	0.98	0.00	0.98	0.98	0.00	0.99	0.98	0.00	0.98	0.98	0.00
Ce-144	0.98	0.98	0.00	0.99	0.99	0.00	0.97	0.97	0.00	1.06	1.06	0.00	1.00	1.00	0.00
Nd-144	1.01	1.00	0.00	1.00	1.00	0.00	1.01	1.01	0.00	0.97	0.98	0.00	1.00	1.00	0.00
Nd-145	1.01	1.01	0.00	1.01	1.01	0.00	1.02	1.02	0.00	1.02	1.02	0.00	1.02	1.02	0.00
Nd-146	1.02	1.02	0.00	1.01	1.01	0.00	1.01	1.01	0.00	1.01	1.01	0.00	1.01	1.01	0.00
Nd-148	1.01	1.01	0.00	1.01	1.01	0.00	1.02	1.02	0.00	1.02	1.02	0.00	1.02	1.02	0.00
Nd-150	0.98	0.98	0.00	0.99	0.99	0.00	0.99	0.99	0.00	1.00	0.99	0.00	1.00	1.00	0.00
Eu-154	0.89	0.89	0.00	0.81	0.81	0.00	0.82	0.82	0.00	0.79	0.79	0.00	0.81	0.81	0.00

Table 3.3.24. SF97 : Results (C/E by SWAT : Considering pellet temp. history)

	SF97-2			SF97-3			SF97-4			SF97-5			SF97-6		
	H*	C**	Diff	H*	C**	Diff	H*	C**	Diff	H*	C**	Diff	H*	C**	Diff
U-234	1.02	1.02	0.00	0.98	0.98	0.00	0.98	0.98	0.00	0.99	0.99	0.00	1.00	1.00	0.00
U-235	0.99	0.99	0.00	0.99	0.98	0.00	0.98	0.98	0.01	0.96	0.96	0.00	0.99	0.99	0.00
U-236	0.96	0.96	0.00	0.95	0.95	0.00	0.95	0.95	0.00	0.95	0.95	0.00	0.95	0.95	0.00
U-238	1.00	1.00	0.00	1.00	1.00	0.00	1.00	1.00	0.00	1.00	1.00	0.00	1.00	1.00	0.00
Np-237	0.97	0.97	0.00	1.01	1.01	0.00	0.99	0.99	0.00	0.96	0.96	0.00	0.96	0.96	0.00
Pu-238	0.87	0.87	0.00	0.88	0.88	0.00	0.86	0.86	0.00	0.83	0.83	0.00	0.87	0.87	0.00
Pu-239	1.02	1.02	-0.01	1.03	1.03	0.01	1.02	1.02	0.01	0.99	0.99	0.00	1.03	1.03	0.00
Pu-240	1.05	1.05	0.00	1.06	1.06	0.00	1.05	1.05	0.00	1.04	1.04	0.00	1.05	1.05	0.00
Pu-241	0.99	1.00	-0.01	1.01	1.01	0.01	1.01	1.00	0.01	0.98	0.98	0.00	1.01	1.01	0.00
Pu-242	0.98	0.98	0.00	0.99	0.99	0.00	0.99	0.99	0.00	0.98	0.98	0.00	0.99	0.99	0.00
Am-241	1.27	1.28	-0.01	1.28	1.27	0.01	1.15	1.14	0.01	1.09	1.09	0.00	1.30	1.30	-0.01
Am-242m	0.87	0.88	-0.01	0.84	0.83	0.01	0.76	0.75	0.01	0.72	0.71	0.00	0.83	0.84	-0.01
Am-243	0.92	0.93	0.00	0.96	0.96	0.00	0.95	0.95	0.00	0.93	0.93	0.00	0.96	0.96	0.00
Cm-242	1.02	1.02	-0.01	1.12	1.11	0.00	1.17	1.17	0.00	1.23	1.23	0.00	1.11	1.11	0.00
Cm-243	0.67	0.67	0.00	0.71	0.71	0.00	0.72	0.71	0.00	0.69	0.69	0.00	0.70	0.70	0.00
Cm-244	0.80	0.80	0.00	0.84	0.84	0.00	0.83	0.83	0.00	0.80	0.80	0.00	0.85	0.85	0.00
Cm-245	0.86	0.86	0.00	0.91	0.91	0.00	0.89	0.89	0.00	0.84	0.84	0.00	0.93	0.93	0.00
Cm-246	0.73	0.73	0.00	0.77	0.77	0.00	0.75	0.75	0.00	0.72	0.72	0.00	0.77	0.77	0.00
Cm-247	0.66	0.66	0.00	0.72	0.73	0.00	0.72	0.72	0.00	0.70	0.70	0.00	0.69	0.69	0.00
Cs-134	0.86	0.86	0.00	0.90	0.90	0.00	0.94	0.94	0.00	0.93	0.93	0.00	0.91	0.91	0.00
Cs-137	1.00	1.00	0.00	1.00	1.00	0.00	1.01	1.01	0.00	1.01	1.01	0.00	1.00	1.00	0.00
Nd-143	1.01	1.01	0.00	1.01	1.01	0.00	1.01	1.01	0.00	1.00	1.00	0.00	1.00	1.00	0.00
Ce-144	0.91	0.91	0.00	0.99	0.99	0.00	1.09	1.09	0.00	1.09	1.09	0.00	0.97	0.97	0.00
Nd-144	1.02	1.02	0.00	0.99	1.00	0.00	0.98	0.98	0.00	0.98	0.98	0.00	0.99	0.99	0.00
Nd-145	1.03	1.03	0.00	1.03	1.03	0.00	1.04	1.04	0.00	1.04	1.04	0.00	1.03	1.03	0.00
Nd-146	1.01	1.01	0.00	1.01	1.01	0.00	1.01	1.01	0.00	1.00	1.00	0.00	1.01	1.01	0.00
Nd-148	1.02	1.02	0.00	1.03	1.03	0.00	1.03	1.03	0.00	1.03	1.03	0.00	1.03	1.03	0.00
Nd-150	1.02	1.02	0.00	1.02	1.02	0.00	1.02	1.02	0.00	1.02	1.02	0.00	1.02	1.02	0.00
Eu-154	0.81	0.81	0.00	0.83	0.82	0.00	0.82	0.82	0.00	0.80	0.80	0.00	0.83	0.83	0.00
Sm-147	1.05	1.05	0.00	1.03	1.03	0.00	1.02	1.02	0.00	1.03	1.03	0.00	1.04	1.04	0.00
Sm-148	1.08	1.07	0.00	1.08	1.09	0.00	1.08	1.08	0.00	1.06	1.06	0.00	1.09	1.09	0.00
Sm-149	0.86	0.86	0.00	0.90	0.90	0.00	0.97	0.97	0.00	0.97	0.97	0.00	0.89	0.89	0.00
Sm-150	1.00	1.00	0.00	0.99	0.99	0.00	0.99	0.99	0.00	0.98	0.98	0.00	1.00	1.00	0.00
Sm-151	0.99	0.99	-0.01	0.99	0.99	0.01	0.98	0.97	0.01	0.94	0.94	0.00	1.00	1.00	-0.01
Sm-152	1.24	1.24	0.00	1.28	1.28	0.00	1.29	1.29	0.00	1.28	1.28	0.00	1.26	1.26	0.00
Sm-154	1.00	1.01	0.00	1.01	1.01	0.00	1.01	1.01	0.00	1.00	1.00	0.00	1.02	1.02	0.00

### 3.4. Analysis by ORIGEN2

The data stored in ORIGEN2.1 are given for each reactor core. While considering that the data obtained in the present special project are obtained from spent fuels from light water reactors, we decided to use the libraries listed in the following Table 3.4.1. The libraries from PWR-U to BWR-UE are included in ORIGEN2.1, and those from PWR41J32 to BS170J432 are given in the library ORLIBJ32<sup>1</sup> for ORIGEN2, based on JENDL-3.2. The ORIGEN2 code cannot ensure the accuracy of calculation unless the specifications of the library to be used and those of the fuel to be analyzed are in agreement. Therefore, it is difficult to judge the calculation accuracy of ORIGEN2 by selecting only analysis target fuels that differ from the library's assumed fuel. However, since it is thought that there are cases where users of ORIGEN2 code must sometimes carry out an analysis by disregarding the matching of the fuel with the library, we think that the results shown below could serve as references for such users.

Table 3.4.1. Libraries in ORIGEN2.1

Library	Objectives	SF95	SF96	SF97	SF98	SF99
PWR-U	PWR 33,000 MWd/t (3.2%)	○	○	○		
PWR-US	PWR 33,000 MWd/t (3.2%)	○	○	○		
PUD50	PWR 50,000 MWd/t (3.2%)	○		○		
PWR-UE	PWR 50,000 MWd/t (4.2%)	○	○	○		
BWR-U	BWR 27,500 MWd/t (2.75%)				○	○
BWR-US	BWR 27,500 MWd/t (3.0%)				○	○
BWR-UE	BWR 50,000 MWd/t (3.4%)				○	○
PWR41J32	PWR 60,000 MWd/t (4.1%)	○	○	○		
BS100J32	BWR Step-1 40,000 MWd/t (Void = 0%) (3.0%)				○	○
BS140J32	BWR Step-1 40,000 MWd/t (Void = 40%) (3.0%)				○	○
BS170J32	BWR Step-1 40,000 MWd/t (Void = 70%) (3.0%)				○	○

### 3.4.1. Analytical Results of SF95 Samples

The SF95 samples are taken from the fuel pin located at the corner of the fuel assembly and irradiated with a neutron spectrum that represents the assembly average, without being affected by the water holes that exist in the assembly. Therefore, they are suitable for validating the libraries of ORIGEN2. The analysis results for the SF95 samples are listed in Tables 3.4.2–3.4.6. In these tables, it can be seen that the amount of the uranium or plutonium that forms is underestimated in the analyses using the PWR-U library and the PWR-US library. For example, when the PWR-U was used, the amount of  $^{239}\text{Pu}$  that formed was underestimated by as much as 17%. With PWR-US, the same situation occurs, i.e., the  $^{239}\text{Pu}$  is underestimated by 15%. The reason for this may be the fact that the fuels assumed in the PWR-U and PWR-US libraries have low initial concentrations and soft neutron spectra.

When compared with these, the tendency to underestimate the amounts of U and Pu that form disappears in analyses using the PWR-UE library, and the calculated values agree well with the experimental values. The difference is –3% for  $^{225}\text{U}$  and –1% for  $^{239}\text{Pu}$ .

The analysis using PWR41J32 is also similar to that using the PWR-UE library, namely, there is no tendency to underestimate and there is good agreement with the experimental values. The reason for the similar tendencies shown by PWR-UE and PWR41J32 is thought to be the fact that the conditions of preparation of these libraries (fuel enrichments) are nearly the same.

Am and Cm are also underestimated by PWR-U and PWR-US.  $^{224}\text{Cm}$  is an important isotope from the viewpoint of neutron shielding safety, but it is nevertheless underestimated by more than 30%. This is thought to derive from the underestimation of Pu as the parent nuclide. When compared with these, PWR-UE appears to be improved, which is most likely due to the fact that the  $^{242}\text{Pu}$  is underestimated and the "flow-in" to the path to  $^{244}\text{Cm}$  is increased. As for  $^{244}\text{Cm}$ , its amount is underestimated by 25%, even with the use of PWR41J32. All the libraries give the same underestimating tendency.

As for fission products (FP), whichever library is used, good results are obtained for the isotopes except  $^{142}\text{Nd}$ . The calculated values for  $^{142}\text{Nd}$  can be improved nearly 20% by using PWR41J32. In the other FP, the calculated values of  $^{125}\text{Sb}$  are markedly improved. This is reported to be the result of changing the decay data and fission yield to the newest data.<sup>5</sup> In addition, it can be seen that the calculated values of Cs-134 are also improved on the whole with the use of PWR41J32, such that the underestimating tendency with PWR-U and PWR-US can be corrected by using PWR41J32.

### 3.4.2. Analytical Results for the SF96 Samples

It was thought that a typical ORIGEN2 analysis could not be made of the SF96 samples, since they were obtained from a  $\text{UO}_2\text{-Gd}_2\text{O}_3$  fuel. Tables 3.4.7–3.4.10 list the calculation results. When PWR41J32 was used, the difference between the calculated and experimental values of  $^{235}\text{U}$  was 4% or less for all samples, thus it was not as large as assumed in the past. However, the difference tended to increase with the other libraries, e.g., with the PWR-UE library there was a difference of 7%. Furthermore, as for the amount of Pu that formed, the differences from the experimental values of  $^{239}\text{Pu}$  and  $^{241}\text{Pu}$  are not large when using the PWR41J32 and PWR-UE libraries, but it can be seen that the difference in  $^{240}\text{Pu}$  is large, i.e., about 10%, with both libraries.

As for the FP, it can be seen that the differences between the calculated and experimental values are larger than those in SF95. For example, the calculated value of  $^{137}\text{Cs}$  using PWR41J32 showed a difference of 4%. From the above-mentioned results, the difference between the calculated and experimental values increases from that in the analysis of  $\text{UO}_2$  fuel samples, when the conventional libraries are used to analyze Gd-containing fuel samples by ORIGEN2 code. Moreover, when PWR41J32 is used, the difference between the calculated and experimental values shows a tendency similar to that with the conventional libraries, but the extent of the increase is not as great when compared with the conventional libraries. However, it was seen that  $^{240}\text{Pu}$  tends to be underestimated.

Table 3.4.2. SF95 : Results (C/E by ORIGEN2.1 : PWR41J32)

Isotope	SF95-1	SF95-2	SF95-3	SF95-4	SF95-5	nbr	Average	stdv
U-234	1.020	0.924	1.183	1.160	0.848	5	1.03	0.15
U-235	1.007	1.013	0.997	1.025	1.028	5	1.01	0.01
U-236	0.945	0.929	0.948	0.948	0.940	5	0.94	0.01
U-238	1.000	1.000	1.001	1.000	0.999	5	1.00	0.00
Pu-238	0.811	0.742	0.845	0.889	0.887	5	0.83	0.06
Pu-239	1.024	0.981	0.990	1.027	1.053	5	1.01	0.03
Pu-240	0.991	0.968	1.004	1.026	1.037	5	1.01	0.03
Pu-241	0.988	0.925	0.949	0.998	1.031	5	0.98	0.04
Pu-242	0.934	0.891	0.938	0.959	0.982	5	0.94	0.03
Am-241	0.796	1.095	1.121	1.613	1.156	5	1.16	0.29
Am-242m	0.613	0.590	0.601	0.668	0.719	5	0.64	0.05
Am-243	0.823	0.819	0.895	0.956	0.963	5	0.89	0.07
Cm-242	0.729	0.642	0.606	0.550	0.843	5	0.67	0.11
Cm-243	0.547	0.513	0.612	0.638	0.604	5	0.58	0.05
Cm-244	0.712	0.620	0.756	0.805	0.879	5	0.75	0.10
Cm-245	0.793	0.616	0.764	0.817	0.925	5	0.78	0.11
Cm-246	0.381	0.440	0.734	0.786	1.335	5	0.74	0.38
Cs-137	0.982	0.971	0.982	0.979	0.988	5	0.98	0.01
Cs-134	0.905	0.895	0.950	0.973	0.968	5	0.94	0.04
Eu-154	0.851	0.747	0.747	0.752	0.800	5	0.78	0.05
Ce-144	0.968	0.975	0.951	1.040	0.976	5	0.98	0.03
Nd-142	0.807	0.951	0.889	0.913	0.988	5	0.91	0.07
Nd-143	0.956	0.945	0.931	0.942	0.949	5	0.94	0.01
Nd-144	1.004	1.008	1.033	0.986	1.006	5	1.01	0.02
Nd-145	0.991	0.992	0.994	0.995	0.992	5	0.99	0.00
Nd-146	1.000	0.992	0.995	0.996	1.001	5	1.00	0.00
Nd-148	0.999	0.994	1.000	1.000	1.001	5	1.00	0.00
Nd-150	0.969	0.978	0.976	0.982	0.996	5	0.98	0.01

Table 3.4.3. Results (C/E by ORIGEN2.1 : PWR-UE)

Isotope	SF95-1	SF95-2	SF95-3	SF95-4	SF95-5	nbr	Average	stdv
U-234	1.030	0.938	1.194	1.169	0.860	5	1.04	0.14
U-235	0.998	0.986	0.933	0.953	0.981	5	0.97	0.03
U-236	1.003	0.982	0.994	0.992	0.990	5	0.99	0.01
U-238	1.000	1.001	1.001	1.001	1.000	5	1.00	0.00
Pu-238	0.891	0.842	1.030	1.093	1.045	5	0.98	0.11
Pu-239	0.974	0.929	0.983	1.029	1.020	5	0.99	0.04
Pu-240	0.960	0.911	0.985	1.019	0.995	5	0.97	0.04
Pu-241	1.002	0.919	0.874	0.909	0.976	5	0.94	0.05
Pu-242	0.923	0.861	0.858	0.869	0.921	5	0.89	0.03
Am-241	0.814	1.082	1.053	1.504	1.114	5	1.11	0.25
Am-242m	1.676	1.807	1.900	2.109	2.270	5	1.95	0.24
Am-243	0.905	0.880	0.952	1.017	1.029	5	0.96	0.07
Cm-242	0.688	0.588	0.530	0.478	0.754	5	0.61	0.11
Cm-243	0.732	0.686	0.838	0.875	0.822	5	0.79	0.08
Cm-244	0.772	0.674	0.869	0.932	0.983	5	0.85	0.12
Cm-245	0.611	0.471	0.621	0.671	0.729	5	0.62	0.10
Cm-246	0.360	0.413	0.750	0.815	1.307	5	0.73	0.38
Cs-137	0.955	0.944	0.953	0.950	0.959	5	0.95	0.01
Cs-134	0.911	0.899	0.975	1.002	0.984	5	0.95	0.05
Eu-154	1.149	1.188	1.407	1.441	1.404	5	1.32	0.14
Ce-144	0.964	0.973	0.950	1.040	0.975	5	0.98	0.03
Nd-142	0.996	1.179	1.136	1.173	1.244	5	1.15	0.09
Nd-143	0.967	0.965	0.952	0.964	0.971	5	0.96	0.01
Nd-144	0.986	0.987	1.016	0.971	0.987	5	0.99	0.02
Nd-145	0.994	0.995	0.994	0.995	0.995	5	0.99	0.00
Nd-146	1.004	0.998	1.007	1.008	1.010	5	1.01	0.00
Nd-148	1.005	0.996	0.998	0.997	1.001	5	1.00	0.00
Nd-150	0.967	0.976	0.972	0.979	0.992	5	0.98	0.01

Table 3.4.4. SF95 : Results (C/E by ORIGEN2.1 : PWR-US)

Isotope	SF95-1	SF95-2	SF95-3	SF95-4	SF95-5	nbr	Average	stdv
U-234	1.048	0.961	1.227	1.201	0.883	5	1.06	0.15
U-235	0.981	0.940	0.839	0.849	0.909	5	0.90	0.06
U-236	1.000	0.992	1.011	1.009	1.004	5	1.00	0.01
U-238	1.001	1.003	1.004	1.003	1.003	5	1.00	0.00
Pu-238	0.671	0.669	0.861	0.919	0.855	5	0.80	0.12
Pu-239	0.839	0.803	0.852	0.892	0.884	5	0.85	0.04
Pu-240	0.880	0.866	0.958	0.993	0.959	5	0.93	0.06
Pu-241	0.780	0.748	0.726	0.755	0.804	5	0.76	0.03
Pu-242	0.751	0.754	0.799	0.814	0.837	5	0.79	0.04
Am-241	0.623	0.858	0.840	1.197	0.888	5	0.88	0.21
Am-242m	1.213	1.354	1.431	1.585	1.712	5	1.46	0.20
Am-243	0.623	0.672	0.798	0.860	0.828	5	0.76	0.10
Cm-242	0.512	0.468	0.443	0.401	0.618	5	0.49	0.08
Cm-243	0.478	0.494	0.654	0.688	0.621	5	0.59	0.10
Cm-244	0.457	0.452	0.658	0.716	0.706	5	0.60	0.13
Cm-245	0.299	0.264	0.394	0.431	0.438	5	0.37	0.08
Cm-246	0.189	0.253	0.536	0.593	0.874	5	0.49	0.28
Cs-137	0.956	0.944	0.954	0.950	0.960	5	0.95	0.01
Cs-134	0.808	0.819	0.913	0.940	0.910	5	0.88	0.06
Eu-154	1.010	1.072	1.303	1.340	1.284	5	1.20	0.15
Ce-144	0.975	0.986	0.961	1.051	0.987	5	0.99	0.03
Nd-142	0.983	1.196	1.188	1.230	1.283	5	1.18	0.11
Nd-143	0.970	0.959	0.928	0.937	0.956	5	0.95	0.02
Nd-144	1.004	1.016	1.060	1.014	1.024	5	1.02	0.02
Nd-145	1.004	1.007	1.006	1.006	1.007	5	1.01	0.00
Nd-146	1.003	0.998	1.007	1.008	1.009	5	1.00	0.00
Nd-148	1.003	0.995	0.996	0.995	0.999	5	1.00	0.00
Nd-150	0.950	0.958	0.957	0.963	0.975	5	0.96	0.01

Table 3.4.5. SF95 : Results (C/E by ORIGEN2.1 : PWR-U)

Isotope	SF95-1	SF95-2	SF95-3	SF95-4	SF95-5	nbr	Average	stdv
U-234	1.055	0.977	1.271	1.248	0.906	5	1.09	0.16
U-235	0.987	0.956	0.873	0.888	0.935	5	0.93	0.05
U-236	0.991	0.983	1.006	1.004	0.997	5	1.00	0.01
U-238	1.001	1.003	1.004	1.003	1.002	5	1.00	0.00
Pu-238	0.700	0.663	0.800	0.848	0.814	5	0.77	0.08
Pu-239	0.863	0.806	0.802	0.831	0.858	5	0.83	0.03
Pu-240	0.951	0.963	1.014	1.034	1.052	5	1.00	0.04
Pu-241	0.734	0.704	0.744	0.790	0.781	5	0.75	0.04
Pu-242	0.725	0.716	0.795	0.818	0.811	5	0.77	0.05
Am-241	0.585	0.774	0.755	1.084	0.793	5	0.80	0.18
Am-242m	0.648	0.675	0.690	0.767	0.827	5	0.72	0.07
Am-243	0.583	0.627	0.762	0.827	0.775	5	0.71	0.10
Cm-242	0.602	0.546	0.521	0.475	0.718	5	0.57	0.09
Cm-243	0.540	0.557	0.712	0.751	0.676	5	0.65	0.09
Cm-244	0.424	0.421	0.593	0.643	0.644	5	0.54	0.11
Cm-245	0.292	0.258	0.366	0.398	0.416	5	0.35	0.07
Cm-246	0.198	0.266	0.519	0.568	0.873	5	0.48	0.27
Cs-137	0.956	0.944	0.954	0.950	0.960	5	0.95	0.01
Cs-134	0.827	0.813	0.870	0.892	0.882	5	0.86	0.03
Eu-154	1.301	1.316	1.506	1.539	1.521	5	1.44	0.12
Ce-144	0.971	0.982	0.957	1.047	0.984	5	0.99	0.03
Nd-142	1.044	1.247	1.201	1.240	1.314	5	1.21	0.10
Nd-143	0.960	0.945	0.918	0.926	0.943	5	0.94	0.02
Nd-144	1.013	1.026	1.065	1.019	1.031	5	1.03	0.02
Nd-145	1.001	1.004	1.004	1.005	1.004	5	1.00	0.00
Nd-146	1.005	0.998	1.005	1.006	1.009	5	1.00	0.00
Nd-148	1.005	0.995	0.997	0.996	1.000	5	1.00	0.00
Nd-150	0.956	0.964	0.962	0.968	0.980	5	0.97	0.01

Table 3.4.6. SF95 : Results (C/E by ORIGEN2.1 : PUD50)

Isotope	SF95-1	SF95-2	SF95-3	SF95-4	SF95-5	nbr	Average	stdv
U-234	1.028	0.936	1.201	1.178	0.861	5	1.04	0.15
U-235	0.999	0.991	0.947	0.970	0.991	5	0.98	0.02
U-236	0.996	0.978	0.999	0.998	0.990	5	0.99	0.01
U-238	1.000	1.001	1.002	1.001	1.000	5	1.00	0.00
Pu-238	0.794	0.724	0.843	0.889	0.874	5	0.82	0.07
Pu-239	0.981	0.903	0.901	0.936	0.961	5	0.94	0.04
Pu-240	1.042	0.982	0.978	0.997	1.032	5	1.01	0.03
Pu-241	0.910	0.896	0.914	0.957	0.992	5	0.93	0.04
Pu-242	0.838	0.843	0.918	0.939	0.948	5	0.90	0.05
Am-241	0.728	1.026	1.050	1.509	1.084	5	1.08	0.28
Am-242m	0.741	0.839	0.908	1.010	1.066	5	0.91	0.13
Am-243	0.738	0.771	0.887	0.952	0.931	5	0.86	0.10
Cm-242	0.657	0.617	0.600	0.546	0.824	5	0.65	0.11
Cm-243	0.660	0.678	0.870	0.916	0.829	5	0.79	0.12
Cm-244	0.576	0.533	0.714	0.769	0.796	5	0.68	0.12
Cm-245	0.444	0.360	0.481	0.520	0.563	5	0.47	0.08
Cm-246	0.284	0.338	0.606	0.657	1.064	5	0.59	0.31
Cs-137	0.955	0.944	0.953	0.950	0.959	5	0.95	0.01
Cs-134	0.926	0.890	0.931	0.953	0.955	5	0.93	0.03
Eu-154	1.395	1.392	1.569	1.601	1.597	5	1.51	0.11
Ce-144	0.963	0.972	0.948	1.038	0.974	5	0.98	0.03
Nd-142	1.046	1.220	1.149	1.183	1.271	5	1.17	0.08
Nd-143	0.955	0.946	0.930	0.941	0.949	5	0.94	0.01
Nd-144	1.002	1.007	1.034	0.988	1.006	5	1.01	0.02
Nd-145	0.994	0.995	0.996	0.997	0.995	5	1.00	0.00
Nd-146	1.004	0.997	1.002	1.003	1.007	5	1.00	0.00
Nd-148	1.005	0.996	0.998	0.997	1.001	5	1.00	0.00
Nd-150	0.966	0.976	0.974	0.980	0.993	5	0.98	0.01

Table 3.4.7. SF96 : Results (C/E by ORIGEN2.1 :PWR41J32)

Isotope	SF96-2	SF96-3	SF96-4	SF96-5	nbr	Average	stdv
U-234	1.072	1.048	1.035	1.044	4	1.05	0.02
U-235	0.957	0.958	0.996	0.987	4	0.97	0.02
U-236	0.939	0.931	0.924	0.934	4	0.93	0.01
U-238	1.001	1.001	1.001	1.000	4	1.00	0.00
Np-237	1.270	1.501	1.484	1.453	4	1.43	0.11
Pu-238	0.744	0.831	0.845	0.912	4	0.83	0.07
Pu-239	0.971	1.026	1.062	1.080	4	1.03	0.05
Pu-240	0.843	0.899	0.908	0.925	4	0.89	0.04
Pu-241	0.951	1.011	1.044	1.090	4	1.02	0.06
Pu-242	0.844	0.920	0.913	0.955	4	0.91	0.05
Am-241	1.141	1.166	1.087	1.391	4	1.20	0.13
Am-242m	0.514	0.668	0.641	0.672	4	0.62	0.07
Cm-243	0.799	0.943	0.939	1.020	4	0.93	0.09
Cm-242	0.634	0.736	0.747	0.795	4	0.73	0.07
Cm-244	0.653	0.812	0.825	0.933	4	0.81	0.12
Cs-137	1.030	1.043	1.034	1.061	4	1.04	0.01
Cs-134	1.013	1.075	1.079	1.127	4	1.07	0.05
Eu-154	1.539	1.237	1.256	1.455	4	1.37	0.15
Ce-144	1.040	1.141	1.136	1.060	4	1.09	0.05
Nd-143	0.952	0.928	0.939	0.935	4	0.94	0.01
Nd-144	0.993	0.935	0.936	0.953	4	0.95	0.03
Nd-145	1.000	0.988	0.990	0.983	4	0.99	0.01
Nd-146	0.989	0.984	0.985	0.986	4	0.99	0.00
Nd-148	0.993	0.995	0.996	0.996	4	0.99	0.00
Nd-150	0.965	0.977	0.981	0.988	4	0.98	0.01

Table 3.4.8. SF96 : Results (C/E ORIGEN2.1 : PWR-UE)

Isotope	SF96-2	SF96-3	SF96-4	SF96-5	nbr	Average	stdv
U-234	1.087	1.062	1.048	1.060	4	1.06	0.02
U-235	0.938	0.899	0.931	0.944	4	0.93	0.02
U-236	0.996	0.979	0.971	0.986	4	0.98	0.01
U-238	1.002	1.002	1.001	1.001	4	1.00	0.00
Np-237	1.495	1.868	1.854	1.773	4	1.75	0.17
Pu-238	0.830	0.984	1.004	1.053	4	0.97	0.10
Pu-239	0.913	0.991	1.029	1.024	4	0.99	0.05
Pu-240	0.797	0.864	0.875	0.870	4	0.85	0.04
Pu-241	0.983	0.962	0.991	1.082	4	1.00	0.05
Pu-242	0.840	0.882	0.872	0.931	4	0.88	0.04
Am-241	1.154	1.120	1.038	1.362	4	1.17	0.14
Am-242m	1.520	2.131	2.045	2.116	4	1.95	0.29
Am-243	0.883	1.030	1.025	1.117	4	1.01	0.10
Cm-242	0.602	0.671	0.680	0.738	4	0.67	0.06
Cm-244	0.720	0.938	0.956	1.054	4	0.92	0.14
Cs-137	0.999	1.011	1.001	1.028	4	1.01	0.01
Cs-134	1.020	1.097	1.102	1.145	4	1.09	0.05
Eu-154	1.368	1.714	1.776	1.767	4	1.66	0.19
Ce-144	1.036	1.137	1.132	1.057	4	1.09	0.05
Nd-143	0.968	0.949	0.960	0.955	4	0.96	0.01
Nd-144	0.971	0.917	0.918	0.933	4	0.93	0.03
Nd-145	1.002	0.988	0.989	0.984	4	0.99	0.01
Nd-146	0.994	0.993	0.994	0.993	4	0.99	0.00
Nd-148	0.998	0.992	0.992	0.995	4	0.99	0.00
Nd-150	0.966	0.978	0.981	0.988	4	0.98	0.01

Table 3.4.9. SF96 : Results (C/E ORIGEN2.1 : PWR-US)

Isotope	SF96-2	SF96-3	SF96-4	SF96-5	nbr	Average	stdv
U-234	1.107	1.081	1.067	1.081	4	1.08	0.02
U-235	0.890	0.786	0.809	0.852	4	0.83	0.05
U-236	1.015	1.001	0.993	1.009	4	1.00	0.01
U-238	1.003	1.004	1.003	1.003	4	1.00	0.00
Np-237	1.315	1.710	1.700	1.605	4	1.58	0.18
Pu-238	0.678	0.849	0.869	0.895	4	0.82	0.10
Pu-239	0.793	0.860	0.894	0.888	4	0.86	0.05
Pu-240	0.769	0.851	0.862	0.853	4	0.83	0.04
Pu-241	0.822	0.815	0.840	0.919	4	0.85	0.05
Pu-242	0.768	0.861	0.853	0.893	4	0.84	0.05
Am-241	0.937	0.907	0.840	1.110	4	0.95	0.12
Am-242m	1.176	1.637	1.566	1.638	4	1.50	0.22
Am-243	0.711	0.923	0.923	0.971	4	0.88	0.12
Cm-242	0.497	0.582	0.590	0.633	4	0.58	0.06
Cm-244	0.519	0.779	0.799	0.839	4	0.73	0.15
Cs-137	1.000	1.012	1.002	1.029	4	1.01	0.01
Cs-134	0.942	1.042	1.047	1.079	4	1.03	0.06
Eu-154	1.231	1.601	1.663	1.634	4	1.53	0.20
Ce-144	1.049	1.148	1.143	1.068	4	1.10	0.05
Nd-143	0.963	0.920	0.929	0.935	4	0.94	0.02
Nd-144	1.005	0.966	0.968	0.976	4	0.98	0.02
Nd-145	1.013	0.997	0.997	0.994	4	1.00	0.01
Nd-146	0.994	0.995	0.997	0.995	4	1.00	0.00
Nd-148	0.995	0.989	0.990	0.993	4	0.99	0.00
Nd-150	0.947	0.962	0.966	0.971	4	0.96	0.01

Table 3.4.10. SF96 : Results (C/E by ORIGEN2.1 : PWR-U)

Isotope	SF96-2	SF96-3	SF96-4	SF96-5	nbr	Average	stdv
U-234	1.122	1.119	1.106	1.109	4	1.11	0.01
U-235	0.904	0.821	0.847	0.880	4	0.86	0.04
U-236	1.005	0.997	0.989	1.001	4	1.00	0.01
U-238	1.003	1.004	1.003	1.003	4	1.00	0.00
Np-237	1.300	1.618	1.605	1.543	4	1.52	0.15
Pu-238	0.694	0.817	0.833	0.881	4	0.81	0.08
Pu-239	0.816	0.836	0.865	0.887	4	0.85	0.03
Pu-240	0.869	0.946	0.955	0.959	4	0.93	0.04
Pu-241	0.732	0.790	0.817	0.870	4	0.80	0.06
Pu-242	0.718	0.824	0.819	0.845	4	0.80	0.06
Am-241	0.849	0.807	0.748	0.994	4	0.85	0.10
Am-242m	0.606	0.792	0.757	0.803	4	0.74	0.09
Am-243	0.656	0.851	0.852	0.896	4	0.81	0.11
Cm-242	0.570	0.670	0.680	0.722	4	0.66	0.06
Cm-244	0.476	0.697	0.714	0.760	4	0.66	0.13
Cs-137	1.000	1.011	1.002	1.029	4	1.01	0.01
Cs-134	0.945	0.999	1.001	1.053	4	1.00	0.04
Eu-154	3.233	2.732	2.783	3.167	4	2.98	0.26
Ce-144	1.047	1.145	1.140	1.065	4	1.10	0.05
Nd-143	0.949	0.907	0.916	0.921	4	0.92	0.02
Nd-144	1.016	0.973	0.975	0.987	4	0.99	0.02
Nd-145	1.010	0.995	0.996	0.991	4	1.00	0.01
Nd-146	0.996	0.995	0.996	0.995	4	1.00	0.00
Nd-148	0.996	0.990	0.991	0.994	4	0.99	0.00
Nd-150	0.952	0.967	0.971	0.976	4	0.97	0.01

### 3.4.3. Analytical Results for the SF97 Samples

The SF97 samples differ from the SF95 and SF96 samples. They are fuels that have been irradiated for 3 cycles and are known as high burn-up fuels. Although ORIGEN2 also has libraries for high-burn-up fuels, it has been impossible to assess the suitability of the high-burn-up region of the library concerned, because of the lack of data. The present data are thus to be considered very important in terms of assessing the suitability of ORIGEN2 code for high-burn-up samples.

The analytical results are listed in Tables 3.4.11–3.4.15. In these tables, it can be seen that the analytical results using PWR-U and PWR-US are similar to those for SF95. In other words, the amounts of U and Pu isotopes that form are underestimated; for example the amount of  $^{235}\text{U}$  using these two libraries are underestimated by 20% and 15%, respectively. In the SF95 samples, the underestimating trend with PWR-U and PWR-US disappeared with the use of the PWR-UE library, but the same cannot be said for the SF97 samples. The amount of  $^{235}\text{U}$  is still underestimated, and the Pu isotopes, in contrast, tend to be overestimated. In other words, the PWR-UE library is prepared as a library for high burn-up degrees, but its use reduces the calculation accuracy for higher burn-up degrees.

For the SF97 samples, another library for high-burn-up fuels are included in Table 3.4.7. ORIGEN2 was used to compare the calculated values with the experimental values. When PUD50 is used, the  $^{235}\text{U}$  is underestimated by 5% and the  $^{239}\text{Pu}$  by 4%, but it can be seen that the calculation accuracy is higher on the whole than with the PWR-UE library.

When compared with these results, the effectiveness of the new library PWR41J32 prepared based on JENDL-3.2, i.e., improvements in the calculated values of U and Pu isotopes, can be seen in Table 3.4.11. For example, the difference is 3% for  $^{235}\text{U}$  and 4% for  $^{239}\text{Pu}$ . The difference is similar to those for SF95, and these results taken together with the analytical results for SF95 indicate that the PWR41J32 library enables calculation with similar accuracies for burn-up degrees from low to high.

As for the MA, the analytical results for SF97 are almost the same as for SF95, and the calculation with PWR-U and PWR-US evaluates the amount of the  $^{244}\text{Cm}$  that forms as being larger by underestimating the amount of the  $^{242}\text{Pu}$  that forms.

The amounts of Sm that form are measured in the SF97 samples. For the Sm isotopes also, the use of PWR41J32 led to improvements in the calculated values when compared with PWR-UE; although this library changed the difference for  $^{149}\text{Sm}$  from + 6% to – 14% and gave almost the same difference, i.e., + 25% for  $^{152}\text{Sm}$ , the calculated values of the other Sm isotopes were improved in comparison with the old libraries (PWR-U, PWR-US, and PWR-UE).

In summarizing the above-mentioned results, it can be concluded that the PWR41J32 library can be used to calculate the amounts of the principal U and Pu isotopes ( $^{235}\text{U}$ ,  $^{239}\text{Pu}$ , 240, 241) with differences within about 5% for burn-up degrees ranging from low (14 GWd/t) to high (50 GWd/t). Furthermore, it was found that this library provides calculated values that are improved over those using the old libraries for Sm isotopes as well, which are important isotopes in introducing burn-up credit where the FP are taken into consideration.

Table 3.4.11. SF97 : Results (C/E by ORIGEN2.1 : PWR41J32)

Isotope	SF97–2	SF97–3	SF97–4	SF97–5	SF97–6	nbr	Average	stdv
U-234	1.018	0.989	0.977	0.977	0.988	5	0.99	0.02
U-235	0.999	0.992	1.025	1.048	1.062	5	1.03	0.03
U-236	0.946	0.947	0.945	0.945	0.941	5	0.94	0.00
U-238	1.000	1.001	1.000	1.000	0.999	5	1.00	0.00
Np-237	0.922	0.955	0.960	0.951	0.964	5	0.95	0.02
Pu-238	0.807	0.802	0.820	0.831	0.885	5	0.83	0.03
Pu-239	1.001	1.006	1.043	1.054	1.098	5	1.04	0.04
Pu-240	1.019	1.031	1.039	1.050	1.066	5	1.04	0.02
Pu-241	0.961	0.973	1.010	1.023	1.068	5	1.01	0.04
Pu-242	0.945	0.961	0.960	0.958	0.974	5	0.96	0.01
Am-241	1.233	1.233	1.165	1.162	1.392	5	1.24	0.09
Am-242m	0.702	0.673	0.667	0.686	0.801	5	0.71	0.05
Am-243	0.855	0.895	0.915	0.923	0.972	5	0.91	0.04
Cm-242	0.968	1.059	1.152	1.247	1.135	5	1.11	0.10
Cm-243	0.587	0.624	0.665	0.677	0.702	5	0.65	0.05
Cm-244	0.704	0.745	0.778	0.793	0.867	5	0.78	0.06
Cm-245	0.687	0.727	0.794	0.831	0.964	5	0.80	0.11
Cm-246	0.660	0.693	0.708	0.720	0.813	5	0.72	0.06
Cm-247	0.568	0.619	0.672	0.712	0.751	5	0.66	0.07
Cs-137	0.982	0.981	0.992	0.990	0.982	5	0.99	0.01
Cs-134	0.879	0.934	0.991	0.998	0.981	5	0.96	0.05
Eu-154	0.741	0.746	0.772	0.784	0.817	5	0.77	0.03
Ce-144	0.895	0.976	1.063	1.070	0.949	5	0.99	0.08
Nd-143	0.959	0.946	0.956	0.957	0.964	5	0.96	0.01
Nd-144	1.036	1.012	0.985	0.971	0.987	5	1.00	0.03
Nd-145	1.007	1.006	1.007	1.003	0.997	5	1.00	0.00
Nd-146	0.992	0.990	0.992	0.991	0.993	5	0.99	0.00
Nd-148	1.007	1.009	1.010	1.010	1.010	5	1.01	0.00
Nd-150	1.000	1.002	1.004	1.009	1.013	5	1.01	0.01
Sm-147	1.003	0.970	0.943	0.939	0.957	5	0.96	0.03
Sm-148	1.077	1.089	1.087	1.086	1.131	5	1.09	0.02
Sm-149	0.754	0.809	0.926	0.963	0.850	5	0.86	0.09
Sm-150	1.011	1.010	1.015	1.010	1.031	5	1.02	0.01
Sm-151	0.856	0.877	0.933	0.951	1.005	5	0.92	0.06
Sm-152	1.221	1.240	1.229	1.213	1.197	5	1.22	0.02
Sm-154	0.979	0.983	0.986	0.984	1.007	5	0.99	0.01

Table 3.4.12. SF97 : Results (C/E by ORIGEN2.1 : PWR-UE)

Isotope	SF97-2	SF97-3	SF97-4	SF97-5	SF97-6	nbr	Average	stdv
U-234	1.032	0.989	0.967	0.967	0.991	5	0.99	0.03
U-235	0.953	0.896	0.897	0.915	0.968	5	0.93	0.03
U-236	0.997	0.982	0.970	0.970	0.979	5	0.98	0.01
U-238	1.001	1.001	1.001	1.000	1.000	5	1.00	0.00
Np-237	1.151	1.257	1.286	1.275	1.260	5	1.25	0.05
Pu-238	0.939	1.005	1.060	1.076	1.098	5	1.04	0.06
Pu-239	0.971	1.040	1.122	1.135	1.123	5	1.08	0.07
Pu-240	0.979	1.064	1.135	1.149	1.084	5	1.08	0.07
Pu-241	0.909	0.871	0.876	0.888	0.970	5	0.90	0.04
Pu-242	0.885	0.840	0.806	0.804	0.859	5	0.84	0.03
Am-241	1.184	1.114	1.024	1.019	1.266	5	1.12	0.11
Am-242m	2.208	2.096	2.041	2.096	2.500	5	2.19	0.18
Am-243	0.915	0.946	0.957	0.964	1.030	5	0.96	0.04
Cm-242	0.857	0.886	0.936	1.012	0.958	5	0.93	0.06
Cm-243	0.793	0.848	0.901	0.918	0.953	5	0.88	0.06
Cm-244	0.791	0.888	0.951	0.970	1.025	5	0.92	0.09
Cm-245	0.545	0.618	0.696	0.728	0.811	5	0.68	0.10
Cm-246	0.649	0.756	0.813	0.825	0.875	5	0.78	0.09
Cm-247	0.524	0.650	0.751	0.797	0.774	5	0.70	0.11
Cs-137	0.953	0.952	0.962	0.960	0.953	5	0.96	0.00
Cs-134	0.895	0.976	1.049	1.057	1.021	5	1.00	0.07
Eu-154	1.293	1.511	1.648	1.677	1.626	5	1.55	0.16
Ce-144	0.895	0.975	1.061	1.067	0.948	5	0.99	0.07
Nd-143	0.982	0.964	0.969	0.970	0.984	5	0.97	0.01
Nd-144	1.018	1.002	0.979	0.965	0.975	5	0.99	0.02
Nd-145	1.009	1.003	0.999	0.996	0.995	5	1.00	0.01
Nd-146	1.001	1.006	1.011	1.010	1.007	5	1.01	0.00
Nd-148	1.011	1.008	1.007	1.007	1.009	5	1.01	0.00
Nd-150	0.997	0.999	1.002	1.006	1.010	5	1.00	0.01
Sm-147	0.848	0.755	0.706	0.702	0.753	5	0.75	0.06
Sm-148	1.304	1.224	1.188	1.184	1.281	5	1.24	0.05
Sm-149	0.938	1.005	1.105	1.192	1.061	5	1.06	0.10
Sm-150	1.096	1.124	1.137	1.128	1.142	5	1.13	0.02
Sm-151	1.209	1.274	1.367	1.394	1.456	5	1.34	0.10
Sm-152	1.235	1.274	1.266	1.251	1.226	5	1.25	0.02
Sm-154	1.015	1.027	1.035	1.033	1.051	5	1.03	0.01

Table 3.4.13. SF97 : Results (C/E ORIGEN2.1 : PWR-US)

Isotope	SF97-2	SF97-3	SF97-4	SF97-5	SF97-6	nbr	Average	stdv
U-234	1.060	1.014	0.991	0.990	1.017	5	1.01	0.03
U-235	0.882	0.768	0.742	0.756	0.837	5	0.80	0.06
U-236	1.012	0.998	0.983	0.983	0.995	5	0.99	0.01
U-238	1.004	1.004	1.003	1.003	1.002	5	1.00	0.00
Np-237	1.021	1.149	1.181	1.171	1.149	5	1.13	0.06
Pu-238	0.769	0.858	0.912	0.926	0.936	5	0.88	0.07
Pu-239	0.841	0.895	0.940	0.950	0.973	5	0.92	0.05
Pu-240	0.945	1.034	1.056	1.067	1.063	5	1.03	0.05
Pu-241	0.751	0.747	0.810	0.821	0.813	5	0.79	0.04
Pu-242	0.806	0.807	0.807	0.806	0.819	5	0.81	0.01
Am-241	0.946	0.883	0.822	0.820	1.004	5	0.90	0.08
Am-242m	1.670	1.561	1.525	1.567	1.870	5	1.64	0.14
Am-243	0.739	0.832	0.872	0.880	0.897	5	0.84	0.06
Cm-242	0.709	0.761	0.825	0.893	0.817	5	0.80	0.07
Cm-243	0.603	0.687	0.744	0.758	0.769	5	0.71	0.07
Cm-244	0.571	0.716	0.791	0.808	0.819	5	0.74	0.10
Cm-245	0.328	0.416	0.480	0.503	0.542	5	0.45	0.08
Cm-246	0.436	0.584	0.647	0.660	0.669	5	0.60	0.10
Cm-247	0.306	0.448	0.536	0.571	0.527	5	0.48	0.11
Cs-137	0.954	0.953	0.963	0.961	0.953	5	0.96	0.00
Cs-134	0.830	0.926	0.996	1.003	0.968	5	0.94	0.07
Eu-154	1.187	1.421	1.551	1.579	1.528	5	1.45	0.16
Ce-144	0.906	0.983	1.067	1.072	0.957	5	1.00	0.07
Nd-143	0.966	0.925	0.919	0.920	0.947	5	0.94	0.02
Nd-144	1.054	1.049	1.027	1.013	1.020	5	1.03	0.02
Nd-145	1.022	1.013	1.008	1.004	1.005	5	1.01	0.01
Nd-146	1.001	1.007	1.012	1.012	1.008	5	1.01	0.00
Nd-148	1.010	1.006	1.005	1.006	1.008	5	1.01	0.00
Nd-150	0.980	0.985	0.989	0.994	0.995	5	0.99	0.01
Sm-147	0.889	0.785	0.733	0.729	0.783	5	0.78	0.06
Sm-148	1.249	1.202	1.171	1.168	1.255	5	1.21	0.04
Sm-149	0.810	0.878	1.009	1.050	0.958	5	0.94	0.10
Sm-150	1.076	1.101	1.106	1.102	1.117	5	1.10	0.01
Sm-151	1.009	1.056	1.140	1.163	1.201	5	1.11	0.08
Sm-152	1.262	1.303	1.300	1.284	1.252	5	1.28	0.02
Sm-154	0.968	0.990	1.005	1.003	1.011	5	1.00	0.02

Table 3.4.14. SF97 : Results (C/E by ORIGEN2.1 : PWR-U)

Isotope	SF97-2	SF97-3	SF97-4	SF97-5	SF97-6	nbr	Average	stdv
U-234	1.088	1.066	1.055	1.055	1.066	5	1.07	0.01
U-235	0.907	0.819	0.806	0.822	0.888	5	0.85	0.05
U-236	1.005	0.998	0.988	0.988	0.994	5	0.99	0.01
U-238	1.003	1.004	1.004	1.003	1.002	5	1.00	0.00
Np-237	0.954	1.051	1.077	1.068	1.053	5	1.04	0.05
Pu-238	0.738	0.785	0.824	0.836	0.859	5	0.81	0.05
Pu-239	0.815	1.811	0.840	0.848	0.886	5	0.84	0.03
Pu-240	1.034	1.016	0.996	1.005	1.058	5	1.02	0.02
Pu-241	0.731	0.801	0.853	0.864	0.872	5	0.82	0.06
Pu-242	0.782	0.845	0.864	0.863	0.850	5	0.84	0.03
Am-241	0.848	0.823	0.772	0.769	0.931	5	0.83	0.07
Am-242m	0.811	0.777	0.769	0.790	0.925	5	0.81	0.06
Am-243	0.691	0.826	0.893	0.902	0.883	5	0.84	0.09
Cm-242	0.830	0.934	1.029	1.114	0.997	5	0.98	0.11
Cm-243	0.664	0.767	0.843	0.860	0.855	5	0.80	0.08
Cm-244	0.519	0.646	0.726	0.743	0.736	5	0.67	0.10
Cm-245	0.311	0.381	0.443	0.465	0.495	5	0.42	0.07
Cm-246	0.434	0.544	0.599	0.611	0.626	5	0.56	0.08
Cm-247	0.305	0.409	0.482	0.513	0.484	5	0.44	0.08
Cs-137	0.954	0.953	0.963	0.961	0.953	5	0.96	0.00
Cs-134	0.804	0.866	0.923	0.929	0.908	5	0.89	0.05
Eu-154	1.405	1.597	1.722	1.752	1.727	5	1.64	0.14
Ce-144	0.902	0.980	1.065	1.071	0.954	5	0.99	0.07
Nd-143	0.954	0.918	0.914	0.915	0.939	5	0.93	0.02
Nd-144	1.060	1.050	1.027	1.012	1.022	5	1.03	0.02
Nd-145	1.019	1.014	1.010	1.007	1.005	5	1.01	0.01
Nd-146	1.001	1.003	1.007	1.007	1.005	5	1.00	0.00
Nd-148	1.010	1.008	1.007	1.007	1.009	5	1.01	0.00
Nd-150	0.985	0.990	0.995	0.999	1.001	5	0.99	0.01
Sm-147	0.888	0.801	0.754	0.750	0.797	5	0.80	0.06
Sm-148	1.235	1.180	1.151	1.149	1.233	5	1.19	0.04
Sm-149	0.779	0.855	0.985	1.024	0.932	5	0.92	0.10
Sm-150	1.082	1.093	1.105	1.100	1.116	5	1.10	0.01
Sm-151	0.956	1.006	1.087	1.109	1.151	5	1.06	0.08
Sm-152	1.279	1.329	1.331	1.316	1.279	5	1.31	0.03
Sm-154	0.980	1.001	1.015	1.013	1.023	5	1.01	0.02

Table 3.4.15. SF97 : Results (C/E by ORIGEN2.1 : PUD50)

Isotope	SF97-2	SF97-3	SF97-4	SF97-5	SF97-6	nbr	Average	stdv
U-234	1.034	1.002	0.986	0.986	1.002	5	1.00	0.02
U-235	0.963	0.919	1.928	0.947	0.990	5	0.95	0.03
U-236	0.997	0.996	0.993	0.994	0.991	5	0.99	0.00
U-238	1.001	1.002	1.002	1.001	1.000	5	1.00	0.00
Np-237	0.995	1.046	1.052	1.043	1.052	5	1.04	0.02
Pu-238	0.793	0.808	0.833	0.845	0.890	5	0.83	0.04
Pu-239	0.913	0.920	0.965	0.976	1.004	5	0.96	0.04
Pu-240	1.013	0.985	0.985	0.995	1.023	5	1.00	0.02
Pu-241	0.927	0.930	0.950	0.961	1.020	5	0.96	0.04
Pu-242	0.914	0.942	0.938	0.936	0.955	5	0.94	0.01
Am-241	1.159	1.142	1.067	1.063	1.293	5	1.14	0.09
Am-242m	1.044	1.026	1.002	1.030	1.219	5	1.06	0.09
Am-243	0.828	0.914	0.946	0.954	0.987	5	0.93	0.06
Cm-242	0.952	1.058	1.146	1.240	1.132	5	1.11	0.11
Cm-243	0.812	0.924	1.005	1.024	1.033	5	0.96	0.09
Cm-244	0.639	0.743	0.808	0.825	0.856	5	0.77	0.09
Cm-245	0.419	0.483	0.547	0.573	0.634	5	0.53	0.08
Cm-246	0.527	0.606	0.646	0.658	0.704	5	0.63	0.07
Cm-247	0.391	0.471	0.535	0.568	0.564	5	0.51	0.07
Cs-137	0.953	0.953	0.962	0.960	0.953	5	0.96	0.00
Cs-134	0.869	0.915	0.968	0.975	0.961	5	0.94	0.05
Eu-154	1.475	1.650	1.769	1.800	1.785	5	1.70	0.14
Ce-144	0.893	0.973	1.059	1.065	0.947	5	0.99	0.07
Nd-143	0.960	0.942	0.948	0.949	0.961	5	0.95	0.01
Nd-144	1.036	1.016	0.991	0.977	0.990	5	1.00	0.02
Nd-145	1.010	1.007	1.006	1.003	0.999	5	1.00	0.00
Nd-146	0.999	0.999	1.002	1.001	1.001	5	1.00	0.00
Nd-148	1.011	1.008	1.007	1.008	1.009	5	1.01	0.00
Nd-150	0.998	1.001	1.004	1.008	1.012	5	1.00	0.01
Sm-147	0.851	0.773	0.732	0.728	0.768	5	0.77	0.05
Sm-148	1.297	1.214	1.178	1.175	1.271	5	1.23	0.05
Sm-149	0.865	0.941	1.080	1.122	0.990	5	1.00	0.10
Sm-150	1.086	1.101	1.103	1.098	1.119	5	1.10	0.01
Sm-151	1.062	1.129	1.212	1.237	1.285	5	1.19	0.09
Sm-152	1.237	1.278	1.272	1.257	1.229	5	1.25	0.02
Sm-154	1.021	1.035	1.044	1.042	1.059	5	1.04	0.01

### 3.4.4. Analytical Results for the SF98 Samples

What must be considered in the analysis of BWR fuels is the distribution of void ratios. For this reason, properly speaking, the analysis is supposed to be carried out by considering the void ratio data of the sampling positions. However, the libraries for ORIGEN2 are prepared to obtain reactor core averaged or assembly averaged composition. It is thought to be difficult to evaluate the compositions of specified places such as the test samples after irradiation.

Tables 3.4.16–3.4.19 list the analytical results. The first thing that can be seen is that the C/E value varies largely from sample to sample, even though the averages of C/E show values close to 1. For example, the C/E value for  $^{239}\text{Pu}$  with the use of the BWR-U library is 1.07 on average, but this value in SF98-3 is 1.32 with an overestimate of as much as 32%. In contrast, the C/E value in SF98-8 is 0.86, for an underestimate of 14%. These dispersions in the analytical results can be taken into consideration by Eq. (3.2.1), i.e., the standard deviation when the distribution of C/E values obtained by analysis is assumed to take a normal distribution. The dispersion in C/E for  $^{239}\text{Pu}$  with the use of BWR-U is as large as 0.21, and much larger than the value of 0.03 listed in Table 3.4.14 for the analytical results for the SF97 samples using the PWR-U library. A large dispersion similar to this can be seen in the actinide isotopes as well, and the BWR-U library gives dispersions close to 30%. A dispersion of this kind is caused by the void ratio. Table 3.4.11. For example, for SF98-3, which was located at a position with a low void ratio, the amount of remaining  $^{235}\text{U}$  is large and the amount of Pu that forms is estimated to be smaller, but in SF98-8 irradiated at a location with a high void ratio, the amount of remaining  $^{235}\text{U}$  decreases and the amount of Pu that forms is increased.

The second thing that can be seen is that, on inspecting the C/E averages for the principal actinides and MA, the differences from the experimental values are smaller with BWR-U than with BWR-US and BWR-UE. Although both libraries are prepared on the basis of calculations where the axial distribution of the void ratios is taken into consideration, it can be concluded that, as far as these analytical results go, the old BWR-U library gave better results.

BS1XXJ32 (XX = 0, 40, 70) comprises libraries where the void ratio is assumed to be 0, 40, or 70%, and thus enables void ratio-dependent analysis. In this analysis, the libraries with the closest void ratios were used. From a comparison of the results using these libraries and the results of using BWR-U, it can be seen that the variation from sample to sample is decreased in the results using BS1XXJ32. Furthermore, the average value of C/E itself shows good agreement for the principal isotopes of U and Pu, where the difference is within 5%. From these results, it can be concluded that the effectiveness of the BS1XXJ32 library can be validated.

Table 3.4.16. SF98 : Results (C/E by ORIGEN2.1 : BS1XXJ2)

Isotope	SF98-3	SF98-4	SF98-5	SF98-6	SF98-7	SF98-8	nbr	Average	stdv
Library	BS100J32	BS100J32	BS140J32	BS170J32	BS170J32	BS170J32			
U-234	1.013	1.014	0.990	1.042	0.996	1.019	6	1.01	0.02
U-235	0.981	0.934	0.993	1.032	1.022	1.015	6	1.00	0.04
U-236	0.957	0.955	0.947	0.934	0.929	0.923	6	0.94	0.01
U-238	1.001	1.002	1.001	1.000	1.000	1.000	6	1.00	0.00
Np-237	1.001	0.939	1.290	1.002	1.112	1.045	6	1.06	0.12
Pu-238	0.789	0.766	0.927	1.106	0.872	0.772	6	0.87	0.13
Pu-239	0.975	0.942	1.056	1.120	1.053	1.016	6	1.03	0.06
Pu-240	0.975	0.947	0.972	0.966	0.942	0.956	6	0.96	0.01
Pu-241	0.963	0.941	1.068	1.136	1.069	1.021	6	1.03	0.07
Pu-242	0.887	0.899	0.970	0.995	0.964	0.938	6	0.94	0.04
Am-241	0.874	0.840	1.028	1.240	1.148	1.132	6	1.04	0.16
Am-242m	0.770	0.739	0.795	0.751	0.718	0.608	6	0.73	0.07
Am-243	0.766	0.765	0.954	0.939	0.924	0.840	6	0.86	0.09
Cm-242	0.597	0.590	0.493	1.287	0.575	0.637	6	0.53	0.13
Cm-243	0.552	0.642	0.779	0.708	0.615	0.531	6	0.64	0.09
Cm-244	0.628	0.618	0.772	0.794	0.717	0.619	6	0.69	0.08
Cm-245	0.682	0.664	0.855	0.823	0.696	0.581	6	0.72	0.10
Cm-246	0.451	0.447	0.620	0.707	0.630	0.807	6	0.61	0.14
Cs-137	1.014	0.979	1.013	0.971	0.927	1.049	6	0.99	0.04
Cs-134	1.053	1.023	1.117	1.061	0.966	1.048	6	1.04	0.05
Eu-154	0.782	0.743	0.844	0.760	0.747	0.676	6	0.76	0.05
Ce-144	1.089	1.029	0.913	0.979	0.900	0.861	6	0.96	0.09
Nd-143	1.024	1.036	0.997	0.952	0.948	0.968	6	0.99	0.04
Nd-144	0.965	0.986	1.024	1.020	1.067	1.089	6	1.03	0.05
Nd-145	1.016	1.023	1.008	1.002	1.006	1.013	6	1.01	0.01
Nd-146	0.990	0.985	0.991	0.995	0.992	0.993	6	0.99	0.00
Nd-148	1.006	1.005	1.006	1.007	1.006	1.006	6	1.01	0.00
Nd-150	0.994	0.985	0.999	1.000	0.994	0.992	6	0.99	0.01
Sm-147	0.884	0.881	0.897	0.864	0.879	0.880	6	0.88	0.01
Sm-148	0.969	0.967	1.085	1.095	1.074	0.983	6	1.03	0.06
Sm-149	0.942	1.020	0.781	0.911	0.728	0.641	6	0.84	0.14
Sm-150	0.872	0.865	0.940	0.937	0.932	0.897	6	0.91	0.03
Sm-151	0.963	0.949	1.009	0.888	0.860	0.772	6	0.91	0.09
Sm-152	1.038	1.055	1.125	1.156	1.155	1.088	6	1.10	0.05
Sm-154	0.856	0.852	0.922	0.944	0.908	0.838	6	0.89	0.04

Table 3.4.17. SF98 : Results (C/E by ORIGEN2.1 : BWR-UE)

Isotope	SF98-3	SF98-4	SF98-5	SF98-6	SF98-7	SF98-8	nbr	Average	stdv
U-234	0.916	0.913	0.917	1.015	0.972	1.003	6	0.96	0.05
U-235	1.341	1.450	1.271	1.062	1.051	1.039	6	1.20	0.18
U-236	0.968	0.956	0.961	0.966	0.962	0.969	6	0.96	0.00
U-238	0.994	0.994	0.996	0.999	1.000	1.000	6	1.00	0.00
Np-237	1.896	1.759	2.063	1.365	1.514	1.396	6	1.67	0.28
Pu-238	1.943	1.876	1.779	1.618	1.274	1.103	6	1.60	0.34
Pu-239	1.560	1.583	1.428	1.111	1.043	0.975	6	1.28	0.27
Pu-240	1.015	1.012	0.996	0.889	0.865	0.872	6	0.94	0.07
Pu-241	1.686	1.625	1.459	1.246	1.175	1.270	6	1.41	0.21
Pu-242	1.060	0.947	0.961	1.041	1.016	1.156	6	1.03	0.08
Am-241	1.674	1.613	1.468	1.350	1.257	1.418	6	1.46	0.16
Am-242m	5.455	5.304	4.380	3.232	3.097	2.986	6	4.08	1.13
Am-243	1.772	1.537	1.521	1.330	1.314	1.345	6	1.47	0.18
Cm-242	0.996	0.909	0.624	0.320	0.643	0.823	6	0.72	0.24
Cm-243	1.938	2.031	1.910	1.393	1.214	1.147	6	1.61	0.40
Cm-244	2.546	2.172	1.859	1.419	1.285	1.180	6	1.74	0.54
Cm-245	3.681	3.114	2.184	1.233	1.045	0.918	6	2.03	1.16
Cm-246	2.559	2.179	1.695	1.145	1.022	1.380	6	1.66	0.61
Cs-137	0.989	0.956	0.986	0.934	0.900	1.020	6	0.97	0.04
Cs-134	1.501	1.419	1.389	1.171	1.065	1.160	6	1.28	0.17
Eu-154	2.274	2.225	2.214	1.640	1.603	1.281	6	1.87	0.42
Ce-144	1.069	1.018	0.906	0.973	0.895	0.852	6	0.95	0.08
Nd-143	1.095	1.139	1.087	1.021	1.016	1.009	6	1.06	0.05
Nd-144	0.877	0.889	0.943	0.960	1.004	1.031	6	0.95	0.06
Nd-145	0.972	0.979	0.978	0.992	0.996	1.004	6	0.99	0.01
Nd-146	1.018	1.017	1.016	1.006	1.003	1.000	6	1.01	0.01
Nd-148	1.013	1.010	1.008	1.008	1.006	1.011	6	1.01	0.00
Nd-150	1.044	1.032	1.029	1.012	1.006	1.006	6	1.02	0.02
Sm-147	0.596	0.571	0.612	0.655	0.669	0.725	6	0.64	0.06
Sm-148	1.359	1.255	1.281	1.239	1.221	1.257	6	1.27	0.05
Sm-149	1.757	1.902	1.307	1.375	1.099	0.978	6	1.40	0.36
Sm-150	1.037	1.042	1.105	1.063	1.057	0.987	6	1.05	0.04
Sm-151	2.077	2.114	1.017	1.558	1.505	1.325	6	1.77	0.34
Sm-152	0.925	0.936	1.044	1.132	1.132	1.060	6	1.04	0.09
Sm-154	1.023	1.009	1.046	1.027	0.987	0.917	6	1.00	0.05

Table 3.4.18. SF98 : Results (C/E by ORIGEN2.1 : BWR-US)

Isotope	SF98-3	SF98-4	SF98-5	SF98-6	SF98-7	SF98-8	nbr	Average	stdv
U-234	0.945	0.939	0.944	1.046	1.001	1.033	6	0.98	0.05
U-235	1.181	1.224	1.061	0.914	0.908	0.971	6	1.04	0.14
U-236	0.983	0.970	0.975	0.982	0.977	0.982	6	0.98	0.01
U-238	0.997	0.997	0.999	1.002	1.002	1.002	6	1.00	0.00
Np-237	1.722	1.616	1.899	1.249	1.383	1.232	6	1.52	0.27
Pu-238	1.632	1.601	1.522	1.372	1.078	0.889	6	1.35	0.30
Pu-239	1.350	1.365	1.224	0.961	0.903	0.844	6	1.11	0.23
Pu-240	0.995	0.991	0.964	0.875	0.852	0.842	6	0.92	0.07
Pu-241	1.415	1.380	1.252	1.050	0.989	1.049	6	1.19	0.18
Pu-242	1.004	0.920	0.945	0.999	0.972	1.043	6	0.98	0.04
Am-241	1.341	1.286	1.173	1.077	1.004	1.137	6	1.17	0.13
Am-242m	4.063	3.921	3.241	2.398	2.297	2.238	6	3.03	0.83
Am-243	1.528	1.375	1.380	1.168	1.151	1.073	6	1.28	0.17
Cm-242	0.837	0.775	0.536	0.271	0.544	0.669	6	0.61	0.20
Cm-243	1.535	1.649	1.564	1.118	0.973	0.851	6	1.28	0.34
Cm-244	1.988	1.779	1.543	1.139	1.026	0.831	6	1.38	0.46
Cm-245	2.399	2.126	1.507	0.826	0.697	0.538	6	1.35	0.79
Cm-246	1.897	1.712	1.347	0.878	0.779	0.896	6	1.25	0.47
Cs-137	0.989	0.956	0.985	0.943	0.900	1.019	6	0.97	0.04
Cs-134	1.410	1.345	1.317	1.107	1.006	1.067	6	1.21	0.17
Eu-154	2.124	2.159	2.153	1.542	1.505	1.165	6	1.77	0.43
Ce-144	1.077	1.022	0.909	0.979	0.900	0.861	6	0.96	0.08
Nd-143	1.062	1.090	1.037	0.983	0.980	0.997	6	1.02	0.05
Nd-144	0.915	0.932	0.990	1.004	1.050	1.065	6	0.99	0.06
Nd-145	0.984	0.988	0.987	1.003	1.007	1.017	6	1.00	0.01
Nd-146	1.018	1.017	1.016	1.006	1.003	0.998	6	1.01	0.01
Nd-148	1.011	1.007	1.005	1.005	1.004	1.009	6	1.01	0.00
Nd-150	1.026	1.017	1.013	0.995	0.990	0.987	6	1.00	0.02
Sm-147	0.623	0.593	0.635	0.683	0.697	0.762	6	0.67	0.06
Sm-148	1.322	1.231	1.259	1.211	1.193	1.193	6	1.23	0.05
Sm-149	1.486	1.615	1.113	1.165	0.930	0.825	6	1.19	0.31
Sm-150	1.019	1.024	1.086	1.045	1.039	0.971	6	1.03	0.04
Sm-151	1.719	1.795	1.713	1.286	1.243	1.109	6	1.48	0.30
Sm-152	0.948	0.960	1.071	1.161	1.159	1.084	6	1.06	0.09
Sm-154	0.979	0.973	1.011	0.986	0.947	0.870	6	0.96	0.05

Table 3.4.19. SF98 : Results (C/E ORIGEN2.1 : BWR-U)

Isotope	SF98-3	SF98-4	SF98-5	SF98-6	SF98-7	SF98-8	nbr	Average	stdv
U-234	0.976	0.978	0.986	1.085	1.038	1.055	6	1.02	0.05
U-235	1.139	1.177	1.018	0.880	0.875	0.946	6	1.01	0.13
U-236	0.980	0.969	0.973	0.979	0.975	0.977	6	0.98	0.00
U-238	0.997	0.998	1.000	1.002	1.003	1.002	6	1.00	0.00
Np-237	1.548	1.457	1.714	1.124	1.245	1.099	6	1.36	0.25
Pu-238	1.318	1.291	1.226	1.107	1.870	0.721	6	1.09	0.24
Pu-239	1.317	1.298	1.156	0.924	0.870	0.862	6	1.07	0.21
Pu-240	1.059	0.995	0.952	0.902	0.882	0.948	6	0.96	0.06
Pu-241	1.341	1.352	1.233	1.015	0.954	0.879	6	1.13	0.21
Pu-242	0.940	0.917	0.956	0.971	0.939	0.866	6	0.93	0.04
Am-241	1.175	1.181	1.087	0.971	0.901	0.919	6	1.04	0.13
Am-242m	1.662	1.687	1.409	1.010	0.964	0.861	6	1.27	0.37
Am-243	1.236	1.197	1.225	0.987	0.966	0.769	6	1.06	0.19
Cm-242	0.831	0.819	0.574	0.279	0.557	0.601	6	0.61	0.20
Cm-243	1.304	1.484	1.427	0.982	0.850	0.665	6	1.12	0.33
Cm-244	1.336	1.259	1.110	0.788	0.706	0.515	6	0.95	0.33
Cm-245	1.483	1.367	0.981	0.521	0.438	0.313	6	0.85	0.50
Cm-246	1.254	1.160	0.922	0.588	0.520	0.566	6	0.84	0.32
Cs-137	0.990	0.956	0.985	0.943	0.900	1.020	6	0.97	0.04
Cs-134	1.243	1.175	1.147	0.970	0.883	0.954	6	1.06	0.14
Eu-154	2.320	2.328	2.315	1.716	1.677	1.299	6	1.94	0.44
Ce-144	1.076	1.021	0.907	0.977	0.899	0.864	6	0.96	0.08
Nd-143	1.051	1.077	1.024	0.972	0.969	0.991	6	1.01	0.04
Nd-144	0.928	0.943	1.002	1.017	1.064	1.081	6	1.01	0.06
Nd-145	0.992	0.998	0.997	1.013	1.016	1.025	6	1.01	0.01
Nd-146	1.009	1.006	1.004	0.996	0.993	0.993	6	1.00	0.01
Nd-148	1.008	1.005	1.002	1.002	1.001	1.007	6	1.00	0.00
Nd-150	1.018	1.009	1.007	0.987	0.982	0.978	6	1.00	0.02
Sm-147	0.651	0.626	0.672	0.717	0.732	0.785	6	0.70	0.06
Sm-148	1.293	1.212	1.242	1.190	1.170	1.156	6	1.21	0.05
Sm-149	1.335	1.459	1.006	1.049	0.838	9.732	6	1.07	0.28
Sm-150	0.998	1.000	1.059	1.022	1.015	0.957	6	1.01	0.03
Sm-151	1.515	1.575	1.503	1.163	1.124	0.974	6	1.31	0.25
Sm-152	0.984	1.004	1.122	1.211	1.209	1.111	6	1.11	0.10
Sm-154	0.963	0.960	0.998	0.972	0.934	0.849	6	0.95	0.05

### **3.4.5. Analytical Results for the SF99 Samples**

Tables 3.4.20–3.4.23 show a comparison of the calculated values with the experimental values for the SF99 samples. As can be seen from these tables, the calculation is performed with a difference of 4% for  $^{235}\text{U}$  and a difference of 3% for  $^{239}\text{Pu}$  and  $^{241}\text{Pu}$ , when the BS1XXJ32 library prepared based on JENDL-3.2 is used. And the calculated values of the  $^{240}\text{Pu}$  are underestimated, as in the SF96 samples.

This difference appears notably when the libraries included in ORIGEN2 are used. For example, when the BWR-UE library is used, the  $^{239}\text{Pu}$  is underestimated by 15% and the  $^{241}\text{Pu}$  is overestimated by 38%, but the  $^{240}\text{Pu}$  is underestimated by 13%. This tendency to calculate the amounts of  $^{239}\text{Pu}$  and  $^{241}\text{Pu}$  a little larger and the amount of  $^{240}\text{Pu}$  a little smaller can also be seen when the BWR-US library is used. When compared with the BWR-UE and BWR-US libraries, the BWR-U library gives better agreement with the experimental values. Furthermore, it can be seen that the old library gives more appropriate calculated values than the new PWR-US and PWR-UE libraries that have been included since ORIGEN2.1. This can be seen when PWR fuels such as SF95 are analyzed.

Table 3.4.20. SF99 : Results (C/E by ORIGEN2.1 : BS1XXI32)

Isotope	SF99-2	SF99-3	SF99-4	SF99-5	SF99-6	SF99-7	SF99-8	SF99-9	nbr	Average	stdv
Library	BS100J32	BS100J32	BS140J32	BS140J32	BS170J32	BS170J32	BS170J32	BS170J32			
U-234	1.090	1.048	1.033	1.035	1.059	1.067	1.041	8	1.05	0.02	0.02
U-235	0.954	0.882	1.064	0.900	0.954	0.923	0.979	0.988	8	0.96	0.06
U-236	0.953	0.960	0.931	0.942	0.922	0.929	0.922	0.935	8	0.94	0.01
U-238	1.002	1.002	1.000	1.002	1.001	1.002	1.001	1.001	8	1.00	0.00
Np-237	0.779	0.792	1.030	0.876	0.945	0.869	0.825	0.770	8	0.86	0.09
Pu-238	0.793	0.805	1.065	1.118	0.924	0.908	0.760	0.723	8	0.89	0.14
Pu-239	0.908	0.918	1.173	0.998	1.028	0.958	0.949	0.975	8	0.99	0.08
Pu-240	0.891	0.928	0.980	0.927	0.905	0.884	0.894	0.901	8	0.91	0.03
Pu-241	0.813	0.902	1.127	0.996	1.028	0.981	0.950	0.964	8	0.97	0.09
Pu-242	0.720	0.863	0.887	0.927	0.940	0.951	0.887	0.869	8	0.88	0.07
Am-241	1.052	0.754	1.159	0.917	1.076	1.007	0.923	0.785	8	0.96	0.14
Am-242m	0.586	0.728	0.966	0.767	0.686	0.689	0.562	0.607	8	0.70	0.13
Am-243	0.578	0.713	0.880	0.850	0.833	0.819	0.683	0.663	8	0.75	0.11
Cm-242	0.246	0.426	0.394	0.248	0.353	0.329	0.348	0.489	8	0.35	0.08
Cm-243	0.447	0.569	0.721	0.659	0.559	0.543	0.441	0.361	8	0.54	0.12
Cm-244	0.417	0.561	0.781	0.707	0.649	0.630	0.477	0.484	8	0.59	0.13
Cm-245	0.371	0.554	0.960	0.749	0.604	0.562	0.407	0.257	8	0.56	0.22
Cm-246	0.000	0.398	0.632	0.580	0.543	0.531	0.367	0.059	7	0.44	0.19
Cm-247	0.000	0.128	0.000	0.488	0.000	0.213	0.000	0.000	4	0.21	0.21
Cs-137	0.972	0.963	0.964	0.960	0.952	0.931	0.959	0.963	8	0.96	0.01
Cs-134	0.885	0.973	1.060	1.023	0.988	0.928	0.888	0.901	8	0.96	0.07
Eu-154	1.174	1.027	1.153	0.986	0.929	0.884	0.912	1.057	8	1.02	0.11
Ce-144	0.973	0.000	1.050	0.833	0.888	0.660	0.783	0.938	7	0.87	0.13
Nd-143	1.000	0.986	1.009	0.960	0.949	0.933	0.966	0.970	8	0.97	0.03
Nd-144	1.036	0.801	0.962	1.063	1.087	1.229	1.139	1.044	8	1.05	0.13
Nd-145	1.025	1.015	1.004	1.003	1.013	1.009	1.017	1.009	8	1.01	0.01
Nd-146	1.004	0.996	0.997	0.996	0.998	0.995	0.993	0.994	8	1.00	0.00
Nd-148	1.006	1.006	1.007	1.006	1.006	1.004	1.004	1.004	8	1.01	0.00
Nd-150	0.976	0.986	1.003	0.993	0.983	0.981	0.978	0.984	8	0.99	0.01
Sm-147	0.990	0.990	0.924	0.924	0.937	0.963	0.985	5	0.96	0.03	
Sm-148	1.077	1.109	1.109	1.103	1.103	1.013	1.052	5	1.07	0.04	
Sm-149	0.896	0.962	0.962	0.795	0.791	0.830	5	0.85	0.07		
Sm-150	0.950	0.937	0.937	0.950	0.937	0.968	5	0.95	0.01		
Sm-151	0.965	0.939	1.133	0.769	0.753	0.804	5	0.85	0.10		
Sm-152	1.138	1.133	1.194	1.154	1.128	5	1.15	0.03			
Sm-154	0.914	0.925	0.923	0.896	0.908	5	0.91	0.01			

Table 3.4.21. SF99 : Results (C/E by ORIGEN2.1 : BWR-UE)

Isotope	SF99-2	SF99-3	SF99-4	SF99-5	SF99-6	SF99-7	SF99-8	SF99-9	nbr	Average	stdv
U-234	1.016	0.962	0.973	0.974	1.042	1.050	1.054	1.029	8	1.01	0.04
U-235	1.098	1.194	1.300	1.124	0.991	0.959	1.005	1.008	8	1.09	0.12
U-236	0.988	0.970	0.952	0.960	0.959	0.966	0.969	0.989	8	0.97	0.01
U-238	0.997	0.996	0.996	0.998	1.001	1.002	1.001	1.000	8	1.00	0.00
Np-237	1.446	1.441	1.604	1.366	1.258	1.158	1.083	1.010	8	1.30	0.20
Pu-238	1.909	1.864	1.942	2.045	1.307	1.283	1.068	1.027	8	1.56	0.42
Pu-239	1.284	1.401	1.486	1.286	0.989	0.922	0.910	0.946	8	1.15	0.24
Pu-240	0.926	0.918	0.936	0.898	0.798	0.780	0.825	0.870	8	0.87	0.06
Pu-241	1.569	1.598	1.575	1.371	1.193	1.141	1.222	1.344	8	1.38	0.18
Pu-242	1.120	1.054	0.970	0.977	1.058	1.072	1.130	1.196	8	1.07	0.08
Am-241	2.130	1.436	1.692	1.323	1.244	1.166	1.198	1.091	8	1.41	0.35
Am-242m	4.605	5.105	5.336	4.232	2.981	2.989	2.720	2.879	8	3.86	1.08
Am-243	1.717	1.613	1.501	1.401	1.222	1.203	1.114	1.171	8	1.37	0.22
Cm-242	0.494	0.711	0.532	0.326	0.418	0.390	0.465	0.707	8	0.51	0.14
Cm-243	1.915	1.952	1.855	1.657	1.212	1.101	0.968	0.839	8	1.44	0.46
Cm-244	2.083	2.124	1.918	1.692	1.149	1.115	0.905	0.980	8	1.50	0.51
Cm-245	2.414	2.720	2.442	1.865	0.881	0.821	0.635	0.430	8	1.53	0.93
Cm-246	0.000	1.989	1.683	1.510	0.848	0.830	0.622	0.107	7	1.08	0.66
Cm-247	0.000	1.042	0.000	1.666	0.000	0.355	0.000	0.001	4	0.77	0.74
Cs-137	0.947	0.939	0.937	0.934	0.923	0.905	0.932	0.936	8	0.93	0.01
Cs-134	1.297	1.357	1.312	1.262	1.083	1.017	0.985	1.014	8	1.17	0.16
Eu-154	1.875	2.168	2.298	2.050	1.517	1.435	1.206	1.167	8	1.71	0.44
Ce-144	0.942	0.000	1.037	0.824	0.881	0.655	0.773	0.924	7	0.86	0.12
Nd-143	1.027	1.056	1.085	1.039	1.007	0.990	0.999	0.990	8	1.02	0.03
Nd-144	0.954	0.723	0.884	0.976	1.022	1.156	1.081	0.998	8	0.97	0.13
Nd-145	0.988	0.975	0.977	0.976	1.005	1.000	1.008	0.999	8	0.99	0.01
Nd-146	1.019	1.019	1.015	1.016	1.007	1.003	0.999	0.999	8	1.01	0.01
Nd-148	1.017	1.013	1.011	1.009	1.009	1.007	1.011	1.012	8	1.01	0.00
Nd-150	1.029	1.036	1.035	1.024	0.997	0.996	0.995	1.002	8	1.01	0.02
Sm-147		0.691		0.655		0.738	0.811	0.861	5	0.75	0.08
Sm-148		1.526		1.357		1.308	1.341	1.483	5	1.40	0.10
Sm-149		1.684		1.620		1.209	1.203	1.251	5	1.39	0.24
Sm-150		1.118		1.091		1.065	1.021	1.036	5	1.07	0.04
Sm-151		2.073		1.846		1.354	1.273	1.321	5	1.57	0.36
Sm-152		1.024		1.054		1.170	1.123	1.091	5	1.09	0.06
Sm-154		1.088		1.047		1.006	0.984	1.003	5	1.03	0.04

Table 3.4.22. SF99 : Results (C/E by ORIGEN2.1 : BWR-US)

Isotope	SF99-2	SF99-3	SF99-4	SF99-5	SF99-6	SF99-7	SF99-8	SF99-9	nbr	Average	stdv
U-234	1.043	0.989	1.000	0.999	1.070	1.079	1.081	1.053	8	1.04	0.04
U-235	1.033	1.057	1.124	0.957	0.878	0.851	0.948	0.972	8	0.98	0.09
U-236	1.002	0.988	0.969	0.976	0.976	0.984	0.983	0.997	8	0.98	0.01
U-238	0.999	0.998	0.998	1.000	1.003	1.004	1.003	1.002	8	1.00	0.00
Np-237	1.275	1.311	1.470	1.257	1.145	1.053	0.952	0.868	8	1.17	0.20
Pu-238	1.540	1.571	1.654	1.753	1.102	1.080	0.857	0.800	8	1.29	0.38
Pu-239	1.111	1.212	1.286	1.113	0.856	0.797	0.788	0.818	8	1.00	0.20
Pu-240	0.895	0.902	0.922	0.887	0.784	0.767	0.796	0.826	8	0.85	0.06
Pu-241	1.301	1.348	1.331	1.160	1.006	0.962	1.010	1.091	8	1.15	0.16
Pu-242	1.013	1.004	0.936	0.949	1.008	1.021	1.017	1.035	8	1.00	0.04
Am-241	1.716	1.158	1.358	1.058	1.003	1.941	0.964	0.866	8	1.13	0.28
Am-242m	3.480	3.839	3.987	3.145	2.243	2.249	2.054	2.147	8	2.89	0.81
Am-243	1.372	1.400	1.329	1.257	1.059	1.042	0.882	0.877	8	1.15	0.21
Cm-242	0.403	0.603	0.454	0.279	0.354	0.330	0.378	0.556	8	0.42	0.11
Cm-243	1.425	1.559	1.503	1.354	0.967	0.877	0.715	0.588	8	1.12	0.38
Cm-244	1.470	1.674	1.556	1.397	0.904	0.876	0.632	0.638	8	1.14	0.43
Cm-245	1.424	1.798	1.662	1.291	0.582	0.541	0.371	0.233	8	0.99	0.62
Cm-246	0.000	1.498	1.315	1.207	0.637	0.622	0.401	0.063	7	0.82	0.53
Cm-247	0.000	0.694	0.000	1.193	0.000	0.235	0.000	0.000	4	0.53	0.53
Cs-137	0.947	0.939	0.937	0.934	0.923	0.905	0.932	0.937	8	0.93	0.01
Cs-134	1.192	1.277	1.242	1.199	1.019	0.956	0.904	0.916	8	1.09	0.15
Eu-154	1.683	2.010	2.145	1.922	1.406	1.329	1.083	1.028	8	1.58	0.43
Ce-144	0.954	0.000	1.043	0.828	0.888	0.659	0.782	0.936	7	0.87	0.13
Nd-143	1.019	1.027	1.048	0.998	0.980	0.964	0.992	0.989	8	1.00	0.03
Nd-144	0.985	0.755	0.926	1.024	1.066	1.206	1.115	1.024	8	1.01	0.13
Nd-145	1.001	0.986	0.987	0.986	1.016	1.012	1.021	1.012	8	1.00	0.01
Nd-146	1.018	1.018	1.015	1.016	1.006	1.002	0.998	0.998	8	1.01	0.01
Nd-148	1.014	1.011	1.009	1.006	1.007	1.005	1.009	1.010	8	1.01	0.00
Nd-150	1.009	1.018	1.018	1.008	0.980	0.978	0.975	0.982	8	1.00	0.02
Sm-147		0.719		0.678		0.770	0.849	0.898	5	0.78	0.09
Sm-148			1.480	1.328		1.268	1.264	1.373	5	1.34	0.09
Sm-149			1.419	1.371		1.018	1.014	1.060	5	1.18	0.20
Sm-150			1.100	1.073		1.048	1.005	1.022	5	1.05	0.04
Sm-151			1.716	1.522		1.121	1.069	1.127	5	1.31	0.29
Sm-152			1.048	1.079		1.197	1.146	1.112	5	1.12	0.06
Sm-154			1.042	1.009		0.964	0.933	0.949	5	0.98	0.05

Table 3.4.23. SF99 : Results (C/E by ORIGEN2.1 : BWR-U)

Isotope	SF99-2	SF99-3	SF99-4	SF99-5	SF99-6	SF99-7	SF99-8	SF99-9	nbr	Average	stdv
U-234	1.061	1.016	1.031	1.034	1.100	1.108	1.099	1.065	8	1.06	0.04
U-235	1.006	1.012	1.074	0.913	0.841	0.815	0.926	0.956	8	0.94	0.09
U-236	0.999	0.986	0.967	0.975	0.975	0.982	0.979	0.992	8	0.98	0.01
U-238	0.999	0.999	0.999	1.001	1.004	1.005	1.003	1.002	8	1.00	0.00
Np-237	1.146	1.184	1.330	1.138	1.034	0.950	0.856	0.781	8	1.05	0.18
Pu-238	1.268	1.289	1.353	1.430	0.905	0.887	0.707	0.658	8	1.06	0.31
Pu-239	1.154	1.218	1.267	1.082	0.860	0.802	0.820	0.862	8	1.01	0.19
Pu-240	1.016	1.022	1.009	0.941	0.890	0.870	0.899	0.903	8	0.94	0.06
Pu-241	1.068	1.201	1.244	1.113	0.895	0.855	0.824	0.847	8	1.01	0.17
Pu-242	0.822	0.903	0.874	0.911	0.906	0.915	0.821	0.788	8	0.87	0.05
Am-241	1.369	1.987	1.188	0.946	0.855	0.801	0.767	0.664	8	0.95	0.23
Am-242m	1.337	1.546	1.635	1.315	0.903	0.905	0.790	0.811	8	1.16	0.34
Am-243	0.969	1.100	1.085	1.053	0.832	0.816	0.622	0.583	8	0.88	0.20
Cm-242	0.356	0.581	0.451	0.284	0.341	0.318	0.332	0.462	8	0.39	0.10
Cm-243	1.105	1.312	1.292	1.185	1.814	0.737	0.554	0.435	8	0.93	0.34
Cm-244	0.917	1.127	1.068	0.972	0.608	0.588	0.394	0.379	8	0.76	0.30
Cm-245	0.843	1.126	1.053	0.824	0.364	0.338	0.220	0.133	8	0.61	0.39
Cm-246	0.000	1.018	0.899	0.827	0.433	0.422	0.262	0.040	7	0.56	0.36
Cm-247	0.000	0.422	0.000	0.728	0.000	0.143	0.000	0.000	4	0.32	0.32
Cs-137	0.948	0.939	0.938	0.934	0.924	0.905	0.933	0.937	8	0.93	0.01
Cs-134	1.077	1.136	1.098	1.055	0.907	0.852	0.818	0.838	8	0.97	0.13
Eu-154	3.283	3.023	3.034	2.668	2.118	2.013	1.875	2.081	8	2.51	0.55
Ce-144	0.956	0.000	1.042	0.827	0.888	0.659	0.785	0.941	7	0.87	0.13
Nd-143	1.013	1.015	1.035	0.985	0.969	0.953	0.986	0.986	8	0.99	0.03
Nd-144	1.001	0.767	0.940	1.039	1.084	1.225	1.133	1.039	8	1.03	0.14
Nd-145	1.008	0.994	0.995	0.994	1.024	1.020	1.028	1.018	8	1.01	0.01
Nd-146	1.015	1.011	1.007	1.007	1.000	0.996	0.995	0.997	8	1.00	0.01
Nd-148	1.012	1.008	1.006	1.003	1.004	1.002	1.006	1.009	8	1.01	0.00
Nd-150	0.997	1.008	1.009	1.000	0.971	0.969	0.965	0.971	8	0.99	0.02
Sm-147		0.745		0.709		0.797	0.868	0.912	5	0.81	0.08
Sm-148		1.448		1.307		1.241	1.226	1.326	5	1.31	0.09
Sm-149		1.265		1.233		0.907	0.893	0.926	5	1.04	0.19
Sm-150		1.079		1.049		1.028	0.992	1.103	5	1.03	0.03
Sm-151		1.504		1.376		0.982	0.935	0.980	5	1.16	0.26
Sm-152		1.081		1.124		1.235	1.169	1.130	5	1.15	0.06
Sm-154		1.022		0.995		0.945	0.909	0.921	5	0.96	0.05

### 3.5. Comparison of the Calculated Results for the Isotopes Important for Burn-Up Credit

In this section, the calculated results for the isotopes important for introducing burn-up credit will be compared with one another. The isotopes selected for comparison are the uranium and plutonium isotopes,  $^{234}\text{U}$ ,  $^{235}\text{U}$ ,  $^{238}\text{U}$ ,  $^{239}\text{Pu}$ ,  $^{240}\text{Pu}$ ,  $^{241}\text{Pu}$ , and  $^{242}\text{Pu}$ , which are supposed to be considered in introducing burn-up credit. Furthermore, the calculated values, which are compared, are the results calculated by ORIGEN2 using PWR-UE, PUD50, and ORLIBJ32, as well as the results calculated by SWAT for the PWR. For the BWR, the results calculated by ORIGEN2 using BWR-U, BWR-US, and ORLIBJ32, as well as the results calculated by SWAT were compared. Tables 3.5.24–3.5.26 show the corresponding C/E values.

With regard to PWR fuels, it is clearly shown that the values calculated by SWAT and ORLIBJ32 are better. The library included in ORIGEN2 that is suitable for analysis of the PWR fuel samples obtained is either PWR-UE or PUD50, but when compared with the results of these, it can be seen that the calculated values for  $^{235}\text{U}$  and  $^{239}\text{Pu}$  [using SWAT and ORLIBJ32] are better. In particular, when the SF97 samples are analyzed using the PWR-UE library, the  $^{235}\text{U}$  is underestimated and the  $^{239}\text{Pu}$  tends to be overestimated. In a comparison of SWAT with ORLIBJ32, it can be seen that the dispersion in the C/E values in the SWAT results is smaller, i.e., 2% at most. This is because the axial distribution of coolant temperatures is taken into consideration in the SWAT calculation.

With regard to the BWR fuels, the dispersion in the difference between the calculated and experimental values increases, because the conventional libraries included in ORIGEN2 cannot be used for an analysis in which the difference in void ratios is taken into consideration. Of these, it can be seen that the analytical results using the BWR-US library show large differences. In particular, the result for  $^{238}\text{Pu}$  shows a difference of 35% and moreover a dispersion of as large as 30%. On the other hand, among the libraries included in the same ORIGEN2, the old BWR-U library gives better results. In a comparison of SWAT with ORLIBJ32, both show similar results, but the dispersion is larger when ORLIBJ32 is used. This is because the distribution of void ratios at the sample position can be considered in SWAT, but cannot be considered in ORIGEN2.

Table 3.5.24. Comparison between several results (SF95)

	SWAT	ORLIBJ32	PWR-UE	PUD50
U-234	1.04 (0.15)	1.03 (0.15)	1.04 (0.14)	1.04 (0.15)
U-235	1.01 (0.01)	1.01 (0.01)	0.97 (0.03)	0.98 (0.02)
Pu-238	0.84 (0.04)	0.83 (0.06)	0.98 (0.11)	0.82 (0.07)
Pu-239	1.02 (0.02)	1.01 (0.03)	0.99 (0.04)	0.94 (0.04)
Pu-240	1.00 (0.01)	1.01 (0.03)	0.97 (0.04)	1.01 (0.03)
Pu-241	0.97 (0.02)	0.98 (0.04)	0.94 (0.05)	0.93 (0.04)
Pu-242	0.93 (0.02)	0.94 (0.03)	0.89 (0.03)	0.90 (0.05)

Table 3.5.25. Comparison between several results (SF97)

	SWAT	ORLIBJ32	PWR-UE	PUD50
U-234	1.01 (0.01)	0.99 (0.02)	0.99 (0.03)	1.00 (0.02)
U-235	1.01 (0.01)	1.03 (0.03)	0.93 (0.03)	0.95 (0.03)
Pu-238	0.83 (0.02)	0.83 (0.03)	1.04 (0.06)	0.83 (0.04)
Pu-239	1.03 (0.01)	1.04 (0.04)	1.06 (0.07)	0.96 (0.04)
Pu-240	1.04 (0.01)	1.04 (0.02)	1.08 (0.07)	1.00 (0.02)
Pu-241	0.98 (0.01)	1.01 (0.04)	0.90 (0.04)	0.96 (0.04)
Pu-242	0.94 (0.00)	0.96 (0.01)	0.84 (0.03)	0.94 (0.01)

Table 3.5.26. Comparison between several results (SF98)

	SWAT	ORLIBJ32	PWR-UE	PUD50
U-234	1.00 (0.03)	1.01 (0.02)	0.98 (0.05)	1.02 (0.05)
U-235	1.08 (0.03)	1.00 (0.04)	1.04 (0.14)	1.01 (0.13)
Pu-238	0.94 (0.06)	0.87 (0.13)	1.35 (0.30)	1.09 (0.24)
Pu-239	1.10 (0.04)	1.03 (0.06)	1.11 (0.23)	1.07 (0.21)
Pu-240	0.95 (0.02)	0.96 (0.01)	0.92 (0.07)	0.96 (0.06)
Pu-241	1.11 (0.04)	1.03 (0.07)	1.19 (0.18)	1.13 (0.21)
Pu-242	1.00 (0.03)	0.94 (0.04)	0.98 (0.04)	0.93 (0.04)

### **3.6. Conclusions**

In the code accuracy evaluation, we analyzed samples from SF95 to SF99 by SWAT and ORIGEN2 codes, and obtained the following results.

#### **Regarding the Analysis by SWAT**

1. In the analysis by SWAT, the difference between the calculated and experimental values for the principal U and Pu is 5% at most for PWR-UO<sub>2</sub> fuels.
2. The analysis of the BWR samples by SWAT showed that the difference tends to be larger than in PWR fuels, but satisfactory calculated values can be obtained if the assumed void ratios and simple modeling are taken into consideration, i.e., the difference between the calculated and experimental values for the principal U and Pu was 10% at most.
3. Even SWAT analysis underestimates the amounts of <sup>238</sup>Pu and <sup>244</sup>Cm, which are the principal sources of the amount of neutrons emitted, by nearly 20%.
4. As for Sm isotopes, the difference between the calculated and experimental values was close to 30% for <sup>152</sup>Sm, but was only about 10% overall.

#### **Regarding the PWR Fuels (Analysis by ORIGEN2)**

1. Regarding the libraries included in the ORIGEN2 code, the calculation accuracy is not improved any more with PWR-US than it is with PWR-U in the analysis of PWR 17 × 17 fuels.
2. The PWR-UE library, despite the fact that it is a library for high burn-up fuels, gives calculated values that differ considerably from the experimental values for burn-up degrees of 40 GWd/t or more.
3. PWR41J32, which is included in the library for ORIGEN2, i.e., "ORLIBJ32", based on JENDL-3.2, produced good agreement between the calculated and experimental values in the range of all burn-up degrees, and gave calculated values that differed by about 5% from the experimental values for the principal U and Pu.
4. When UO<sub>2</sub>-Gd<sub>2</sub>O<sub>3</sub> fuel elements are analyzed by ORIGEN2 code, the differences become larger than for UO<sub>2</sub> fuels, but even in this case, the difference between the calculated and experimental values is about 10%.
5. The calculated values for Sm isotopes are several percent worse than those calculated by SWAT.

### **Regarding the BWR Fuels (Analysis by ORIGEN2)**

1. If the libraries included in ORIGEN2 are used for analysis of the BWR fuels, the difference between the calculated and experimental values varies even more. This is because the effect of the void ratio at the sampling location cannot be incorporated in the libraries included in ORIGEN2.
2. As seen for the PWR, the BWR-U library, which has been conventionally used, gives smaller differences from the experimental values than the new BWR-US and BWR-UE libraries.
3. If the library included in ORLIBJ32 is used, the dispersion in the differences between the calculated and experimental values decreases, but this is because the analysis is carried out by considering the differences in the void ratios.

## REFERENCES

1. K. Suyama, J. Katakura, U. Ohkawa, and M. Ishikawa: Library for ORIGEN2 based on JENDL-3.2: ORLIBJ32. JAERI-Data/Code 90-003, February 1999.
2. K. Suyama, T. Iwasaki, and N. Hirakawa: Integrated Burn-up Calculation Code System = SWAT. JAERI-Data/Code 97-047, November 1997.
3. K. J. Notz, "ORIGEN2, Version 2.1 Release Notes," CCC-371, pp. 200–208, August 1991.
4. M. Suzuki and H. Uezuka, "Light-Water-Reactor Fuel Analysis Code FEMAXI-V (Ver. 1) — Detailed Structure and User Manual," JAERI-Data/Code 99-046, November 1999.
5. Kenya Suyama, Tomohiko Iwasaki, and Naohiro Hirakawa, "Improvement of Burnup Code System SWAT for Use in Burnup Credit Problem," in *Proceedings of International Conference on the Physics of Reactors (PHYSOR96)*, Vol. 4, pp. L-53-L62, Mito, Ibaraki, Japan, September 1996. Japan Atomic Energy Research Institute.
6. K. Tasaka, J. Katakura, H. Ihara, T. Yoshida, S. Iijima, T. Nakashima, Y. Nakagawa, and H. Tanano, "Nuclear Data Library of Fission Products by JNDC — Second Edition," JAERI 1320, September 1990.
7. Y. Nakahara, R. Nagaishi, N. Kawano, Y. Knagawa, M. Ohnuki, and K. Gunji, "Evaluation of the Effective Fission Yield of Nd-148," *Autumn Meeting of the Atomic Energy Society of Japan, 1996 Autumn Meeting*. F23, Tohoku University, Sendai, September 23–25, 1996.
8. Tsuneo Nakagawa, Satoshi Shiba, Toshiro Ohsaki, and Masayuki Igashira, "Maxwellian-Averaged Cross Sections Calculated from JENDL-3.2," JAERI-Research 2000-002, February 2000.



## 4. VALIDATION OF CRITICALITY CALCULATION CODES

### 4.1. General

Criticality calculation codes were validated by analyzing subcritical experiments on spent fuels. Table 4.1.1 shows an outline of various subcritical experiments.

Table 4.1.1. List of subcritical experiment of spent fuel

Sample group	Reactor type	Assembly type	Assembly average burnup (GWd/t)	Assembly name	Enrichment (%)
P14	PWR	14 × 14	36.1	C33	3.4
P17	PWR	17 × 17	34.3	J2R	3.4
B8	BWR	8 × 8-2	33.4	2F2DN23	3.9
HP17	PWR	17 × 17	43.2	NT3G24	4.1

The details of the subcritical experiments are described in Sect. 2, but these particular experiments are to measure the axial spatial profile of the neutron flux created by a spent fuel with the use of a nuclear fission counter tube, by inserting the neutron source into the spent fuel assembly, as shown in Fig. 4.1.1. In this figure, the neutron source is inserted into the spent fuel, but in the B8 assembly the axial spatial profile of the neutron flux created by the neutron source is measured by placing the source outside the spent fuel, as shown in Fig. 4.1.2.

It is shown that, if the measured neutron flux is fitted with an exponential function, the decay constant  $\gamma$  of the axial neutron flux obtained is related to the neutron multiplication factor  $k_{\text{eff}}$  and the buckling coefficient of reactivity  $K$  by Eq. (4.1.1) [Ref. 1]. Since the criticality buckling  $B_g^2$  obtained in axial criticality buckling search calculation and the neutron flux decay constant  $\gamma$  are related as  $\sqrt{|B_g^2|} = \gamma$ ,  $K$  can thus be calculated by Eq. (4.1.1) from the value of  $\gamma$  thus obtained and  $k_{\text{eff}}$  obtained by solving an eigenvalue problem.

$$1 - \frac{1}{k_{\text{eff}}} = -K\gamma^2 \quad (4.1.1)$$

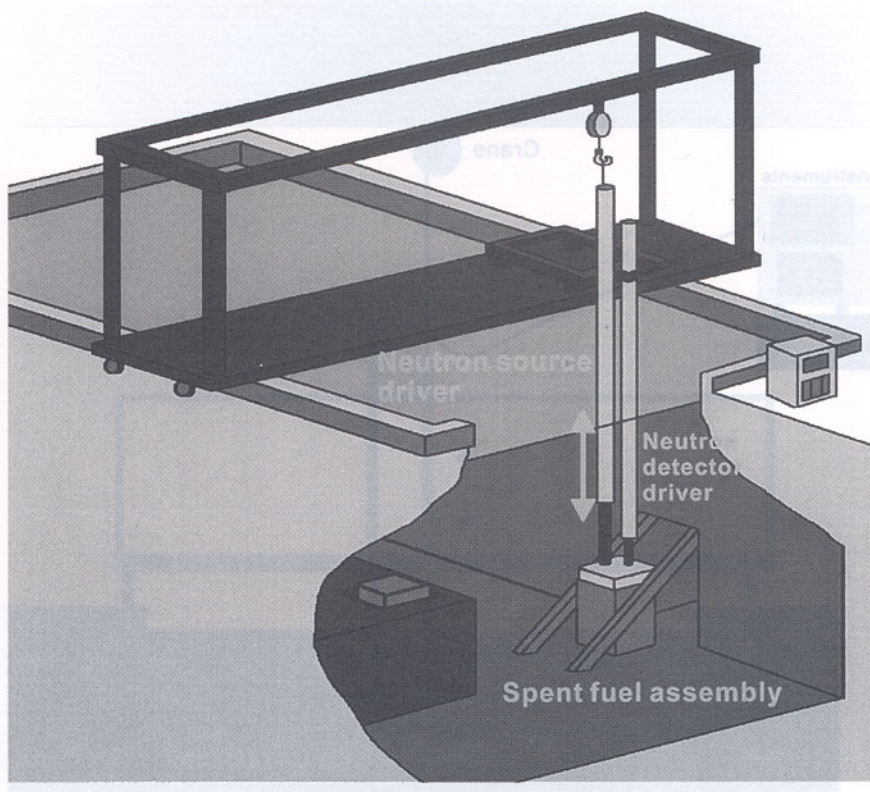


Fig. 4.1.1. Schematic figure of subcritical experiment of spent fuel (for C33, P17 and HP17).

The analysis was carried out by the following procedure.

1. Evaluate burnup (including the profile) in the region where the neutron flux decay constant has been measured.
2. Determine the isotopic composition of a fuel assembly on the basis of the obtained burnup.
3. Calculate the profile of neutron flux that simulates the fuel assembly by a fixed neutron source mode on the basis of the obtained isotopic composition, and determine the exponential decay constant  $\gamma$  by fitting. Furthermore, calculate the neutron multiplication factor and calculate the buckling  $B_g^2$  which results in criticality by carrying out a criticality buckling search in an eigenvalue problem mode in an X-Y two-dimensional system, and calculate  $\gamma$  by the relationship  $\sqrt{|B_g^2|} = \gamma$ .
4. From the above-mentioned results, determine the neutron flux decay constant  $\gamma$  and the buckling conversion coefficient of reactivity  $K$ , then evaluate the neutron multiplication factor by Eq. (4.1.1).

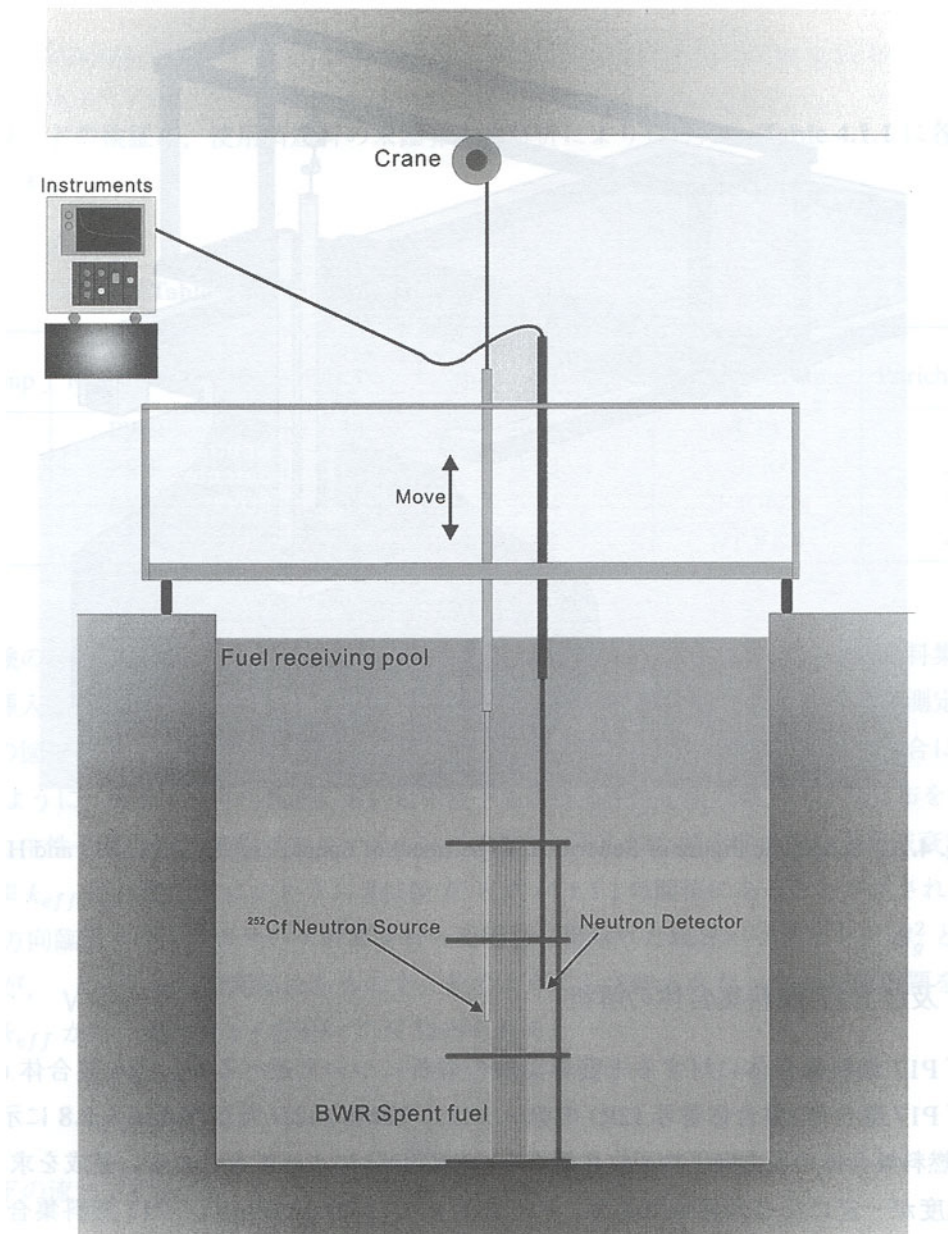


Fig. 4.1.2. Schematic figure of subcritical experiment of spent fuel (for H8).

## 4.2. Analysis of the P14 and P17 Fuel Assemblies

The analysis of subcritical experiments on the P14 and P17 fuel assemblies will be described in this section.<sup>2</sup> Data for the P14 assembly (assembly No. C33) and P17 assembly (assembly No. J2R) are shown in Tables A.2.7 and A.2.8.

First, the radial average isotopic composition of the fuel assembly is determined by ORIGEN2. The region in which the composition is determined is a region where axial burnup is constant, which was 40.2 GWd/t in the P14 assembly and 39.0 GWd/t in the P17 assembly. The radial averaged composition in

the region of interest of the fuel assembly was calculated by using the ratios of the calculated values to the destructive test data obtained from each assembly (the so-called C/E values) as correction factors, then dividing the calculated values by the correction factors.

With the use of the composition obtained, effective sectional areas were prepared by a collision probability method for 107 energy groups by SRAC,<sup>5</sup> and effective sectional areas of 4 groups were prepared by contraction. Then  $\gamma$  (buckling search in the two-dimensional axial direction),  $k_{\text{eff}}$  (X-Y two-dimensional system), and  $\phi^{\text{th}}$  (three-dimensional fixed neutron source problem) were calculated by carrying out diffusion calculations by CITATION for X-Y two-dimensional systems. Then  $K$  was evaluated from  $\gamma$  and  $k_{\text{eff}}$  by Eq. (4.1.1).

The  $k_{\text{eff}}$  was evaluated with the use of  $\gamma$  obtained by experiments and  $K$  was calculated by the above-mentioned method. Furthermore,  $k_{\text{eff}}$  was evaluated by MCNP4A [Ref. 4] with the use of the radial averaged composition. The results are shown in Table 4.2.2. As can be seen from this table,  $k_{\text{eff}}$  estimated with the use of the measured  $\gamma$  and  $k_{\text{eff}}$  determined by calculation are in agreement with a difference of only 3%. This fact indicates that the criticality calculation code used at present is accurate enough in terms of evaluating burnup credit.

Table 4.2.2. Results of subcritical experiment of spent fuel assemblies (P14 and P17)

Assemblies	P14	P17
Burnup (GWd/t)	40.2	39.0
Cooling time (year)	13.5                  14.5	4.3                  5.4
Measured $\gamma$ (1/cm)	$0.1247 \pm 0.0014$	$0.1263 \pm 0.0019$
Measured $\phi^{\text{th}}$ (1/(cm <sup>2</sup> s))	$8400 \pm 660$	$12970 \pm 360$
CITATION Results		
$\gamma$ (1/s)	0.1261	0.1124
$\phi^{\text{th}}$ (1/(cm <sup>2</sup> s))	9460	14740
$K$ (cm <sup>2</sup> )	46.55	44.56
Estimated $k_{\text{eff}}$	0.580	0.627
MCNP Results		
$k_{\text{eff}}$	0.566	0.632

### 4.3. Analysis of a B8 Fuel Assembly

The analysis of subcritical experiments on a B8 fuel assembly<sup>3</sup> will be described in this section. The data for the B8 assembly (assembly No. 2F2DN23) are listed in Table A.2.6. The method of analysis is the same as for the P14 and P17 fuel assemblies, but because the B8 assembly is a BWR fuel and the effect of void distribution must be considered, the assembly was divided into 24 nodes in the axial direction, and the composition was evaluated in each region, in order to analyze the experiments. The initial <sup>235</sup>U enrichment of each region is shown in Fig. A.2.7. Furthermore, the burnups and void ratios were obtained from the axial burnup distribution shown in Fig. A.2.8. The burnup and void ratio numerical values are shown in Table 4.3.3. The burnup calculations were performed by SWAT, and a corrected fuel composition was obtained by dividing the composition obtained by SWAT by the average value of the ratio of the calculated value to the measured value of the destructive test (SF98) shown in Table 3.3.15. Then,

effective sectional areas were calculated by 107-group collision probability calculation by SRAC95 [Ref. 6], and the results were contracted to 4 groups. The library used was JENDL-3.2 [Ref. 8]. Two kinds of calculations were carried out by CITATION with the use of the above-mentioned set of 4-group sectional areas, namely, a two-dimensional axial buckling search calculation and a three-dimensional fixed neutron source problem.

A fixed neutron source was placed at the location of a detector in the experiments, and the profile of the thermal neutron flux in the axial direction was calculated. Then the value of  $\gamma$  was determined by fitting the calculated profile of thermal neutron flux with an exponential function.

The calculated results and experimental results are compared in Table 4.3.4. The values of the decay constant  $\gamma$  obtained by fixed source calculation with no correction for the fuel composition based on the destructive test results are also compared with the experimental values. The values of  $\gamma$  by the fixed source calculation agree with the experimental values with a difference of only 3%, and the decay constants obtained by calculation are nearly the same, even if the composition is not corrected. On the other hand, the values of  $\gamma$  by the buckling search calculation are about 10% larger.

Table 4.3.3. Burnup and void distribution for 2F2DN23

Node	Normalized burnup (-)*	Burnup (MWd/t)	Void ratio (%)
1	0.13	4.37E+03	0.0
2	0.57	1.89E+04	1.0
3	0.84	2.80E+04	4.0
4	1.00	3.33E+04	10.0
5	1.11	3.69E+04	18.0
6	1.13	3.78E+04	27.0
7	1.15	3.84E+04	34.5
8	1.16	3.87E+04	41.0
9	1.20	4.00E+04	45.5
10	1.20	4.00E+04	50.5
11	1.20	4.00E+04	54.0
12	1.21	4.06E+04	58.0
13	1.21	4.05E+04	60.5
14	1.15	3.86E+04	63.0
15	1.15	3.86E+04	65.0
16	1.17	3.89E+04	66.5
17	1.16	3.87E+04	68.0
18	1.14	3.80E+04	69.5
19	1.15	3.86E+04	70.5
20	1.11	3.71E+04	71.5
21	1.00	3.33E+04	72.5
22	0.89	2.98E+04	73.3
23	0.75	2.51E+04	73.7
24	0.22	7.28E+03	74.1
Average		33400	

\* Averaged burnup is 1.0.

Table 4.3.4. Results of subcritical experiment of spent fuel assemblies (B8)

Detector position (cm)	Range of fitting (cm)	Measured $\gamma$ (1/cm)	Average	Calculated $\gamma$ (1/cm)		Fixed source	
				Buckling search	Fixed source	C/E	C/E
369	325 – 342	$0.133 \pm 0.001$	—	—	0.135	1.02	1.01
304	330 – 346	$0.135 \pm 0.002$	0.135	0.149	0.134	0.99	0.99
	265 – 276	$0.135 \pm 0.003$			0.138	1.02	1.01
264	287 – 302	$0.139 \pm 0.002$	0.140	0.150	0.136	0.97	0.97
	225 – 240	$0.140 \pm 0.001$			0.139	1.00	0.99
154	175 – 195	$0.140 \pm 0.003$	0.140	0.154	0.140	1.00	0.99
	114 – 133	$0.139 \pm 0.002$			0.141	1.01	1.01
94	117 – 133	$0.146 \pm 0.004$	0.145	0.158	0.141	0.97	0.96
	55 – 72	$0.143 \pm 0.002$			0.142	0.99	0.99
69	92 – 107	$0.144 \pm 0.004$	0.142	0.159	0.141	0.98	0.97
	30 – 47	$0.140 \pm 0.002$			0.136	0.97	0.96

\* No corrected composition.

### 4.3.1 Evaluation of the Neutron Multiplication Factor Based on the Fixed Neutron Source Calculation

The buckling coefficient of reactivity will be evaluated below based on the results of the fixed neutron source calculation. Here, the buckling coefficient of reactivity  $K$  can also be calculated by deriving the following equation from Eq. (4.1.1) by using  $k_{\text{eff}}^{\text{cal}}$  obtained by solving an eigenvalue problem and the decay constant  $\gamma_{\text{cal}}$  obtained by the fixed source calculation

$$K = \frac{1}{\gamma_{\text{cal}}^2} \left( \frac{1}{k_{\text{eff}}^{\text{cal}}} - 1 \right) \quad (4.3.2)$$

Using this  $K$  and the exponential decay constant  $\gamma_{\text{exp}}$  obtained by experiment (shown in Table 4.3.4), the neutron multiplication factor is evaluated by the following Eq. (4.3.3). The obtained neutron multiplication factors are shown in Table 4.3.5. As shown in this table, the neutron multiplication factor obtained by CITATION and those obtained by Eq. (4.3.3) are in good agreement.

$$k_{\text{eff}}^{\text{eval}} = \frac{1}{1 + K \gamma_{\text{exp}}^2} \quad (4.3.3)$$

Table 4.3.5. Evaluated  $k_{eff}$  of spent fuel assemblies (B8) (Fixed source)

Detector position (cm)	Range of fitting (cm)	Calculated $\gamma_{cal}$ (1/s)	$K$ (cm <sup>2</sup> )	Evaluated $k_{eff}$	Difference (%)
369	325 – 342	0.135	64.31	0.4678	0.74
	330 – 346	0.134	61.54	0.4713	1.09
304	265 – 276	0.138	65.27	0.4567	-0.37
	287 – 302	0.136	60.66	0.4604	0.00
264	225 – 240	0.139	63.36	0.4460	-1.44
	175 – 195	0.140	58.95	0.4675	0.71
154	114 – 133	0.141	59.79	0.4604	0.00
	117 – 133	0.141	58.12	0.4569	-0.35
94	55 – 72	0.142	58.95	0.4432	-1.73
	92 – 107	0.141	63.36	0.4460	-1.44
69	30 – 47	0.136	58.95	0.4500	-1.04

$k_{eff}^{cal}$  by CITATION is 0.46041.

#### 4.3.2 Evaluation of the Neutron Multiplication Factor Based on Buckling Search Calculation

The buckling coefficient of reactivity will be evaluated below based on the results of the buckling search calculation. In the buckling search calculation, a radial averaged composition is assumed in each region where the neutron detector is placed. Negative buckling was produced in each calculation, but the neutron flux decay constant  $\gamma_{cal}$  of the fundamental mode was calculated by finding the square root of the absolute value of buckling. Using this value and the obtained neutron multiplication factor  $k_{eff}^{cal}$ ,  $K$  was evaluated by Eq. (4.3.2) and the neutron multiplication factor was calculated by Eq. (4.3.3). The results are listed in Table 4.3.6.

Table 4.3.6. Evaluated  $k_{eff}$  of spent fuel assemblies (B8) (Buckling search)

Detector position (cm)	$k_{eff}^{cal}$	$\gamma_{cal}$ (1/cm)	$K$ (cm <sup>2</sup> )	Evaluated $k_{eff}$	Difference (%)
369	0.3755	0.159	65.88	0.4618	8.63
304	0.4566	0.149	53.86	0.5047	4.80
264	0.4501	0.150	54.61	0.4848	3.47
154	0.4157	0.154	58.93	0.4658	5.01
94	0.3928	0.158	62.23	0.4349	4.21
69	0.3849	0.159	63.48	0.4386	5.37

The neutron multiplication factors evaluated by Eq. (4.3.3) show differences of from 3 to 8% from the neutron multiplication factors obtained by criticality calculation by CITATION. These are larger than those obtained in the P14 and P17 fuel assemblies, and there are large differences between the neutron flux

decay constants obtained by experiment and those obtained by buckling search, which suggests that there is likely to be a problem in the neutron flux decay constants obtained by experiment.

### 4.3.3 Neutron Flux Decay Constant

To examine whether or not the  $\gamma$  obtained by experiment is affected by higher-order modes,  $\gamma$  was determined in regions away from the source in the fixed source calculation. The location of the detector was at 264 cm. The results are listed in Table 4.3.7. As can be seen from the results,  $\gamma$  increases as the distance between the source and the neutron detector increases. Furthermore, since  $\gamma$  obtained by buckling search calculation is 0.150 (L/cm),  $\gamma$  by fixed source calculation comes to agree with the calculated value by buckling search as the distance increases. From this fact, it can be imagined that the measured values are affected by higher-order modes. Therefore, it can be understood that the distance between the neutron source and the detector must be increased past what it is now in order to avoid the effect of higher-order modes, but this is difficult to do because of problems such as providing safeguards against exposure to radiation, as the strength of the neutron source needs to be increased to a higher value than it is now in order to acquire significant neutron counts in a system with this type of deep subcriticality. An examination was done to see if there are any measurement points that are unaffected by higher-order modes.

Table 4.3.7. Difference of  $\gamma$ : Effect of distance between source and detector

Region (cm) from detector position (264 cm)	$\gamma$ (1/cm)
-27 ~ -43	0.134
-43 ~ -58	0.146
-58 ~ -73	0.150

For this purpose, the detector was placed at locations rotated 90 degrees from the neutron source, instead of placing them face-to-face, and  $\gamma$  was thus examined. Figure 4.3.3 shows their locations. The value of  $\gamma$  was evaluated by the fixed neutron source calculation at the "evaluation position" indicated in this figure.

The results are shown in Table 4.3.8. The values obtained are closer to those of the buckling search even when the distance between the neutron source and the detector is not very large; it can thus be seen why the selection of the measurement location is very important.

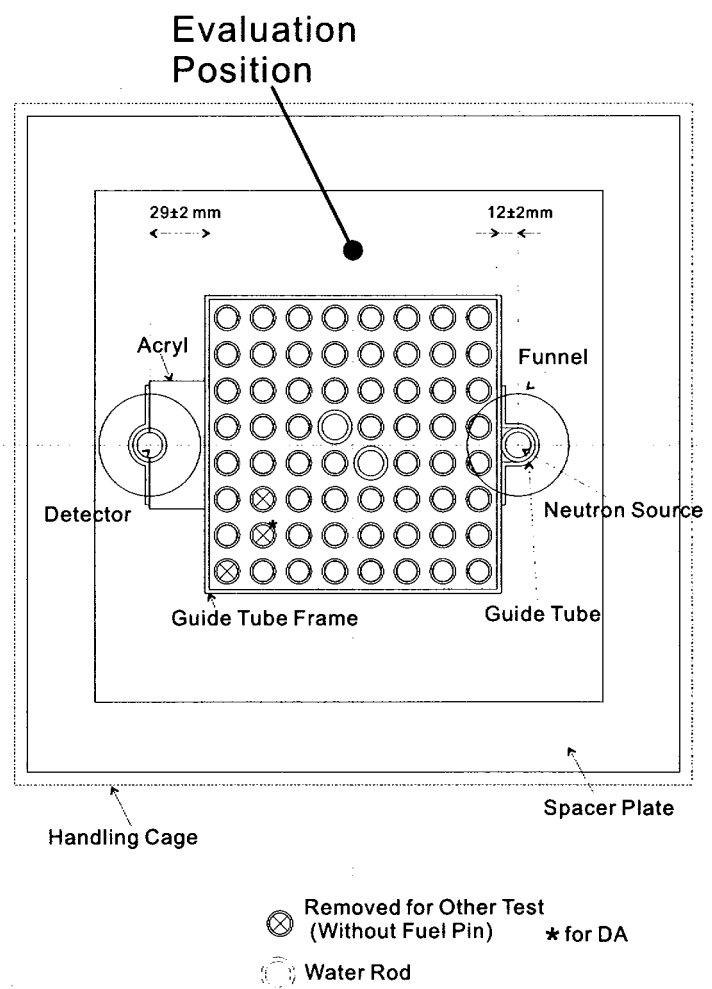


Fig. 4.3.3. B8 subcritical experiment: Position for  $\gamma$  evaluation (90 deg. rotation).

Table 4.3.8. Difference of  $\gamma$ : 90 deg. revolution

Region (cm) from detector position (264 cm)	$\gamma$ (1/cm)
-27 ~ -43	0.145
24 ~ 40	0.147

#### 4.4. Analysis of an HP17 Fuel Assembly

The analysis of subcritical experiments on an HP17 fuel assembly will be described in this section. The data for the HP17 assembly (assembly No. G24) are listed in Table A.2.5. The method of analysis is the same as for the P14 and P17 fuel assemblies.

In the past, the relationship between the burnup (BU) (GWd/t) and the reactivity ratio ( $^{134}\text{Cs}/^{137}\text{Cs}$ ) $^2/(^{106}\text{Ru}/^{137}\text{Cs})$ , which is denoted by X, is obtained as  $\text{BU} = 58.1 \times X^{0.652}$  by combining the gamma scanning measurements and destructive test data for fuel rods obtained from PWR and BWR fuel assemblies, including HP17. So, from the activity profile measured by the  $\gamma$ -scanning of a C7 fuel rod obtained from the HP fuel assembly, the burnup distribution of the C7 fuel rod was determined with the use of an equation for the measured activity profile, and the average burnup was calculated. As a result, the axial averaged burnup of this fuel rod was 44.437 GWd/t. By assuming that the profile of the burnup distribution of the fuel assembly is proportional to the burnup distribution of this fuel rod, the data could be normalized to 43.2 GWd/t, which is the average burnup of the fuel assembly, then the axial burnup distribution of the fuel assembly was determined. The burnup distributions thus obtained are shown in Fig. 4.4.4. As a result of this normalization, the burnup at the burnup flat part (referring to a region 100–300 cm from the top of the assembly) of the HP fuel assembly was determined to be 46.72 GWd/t.

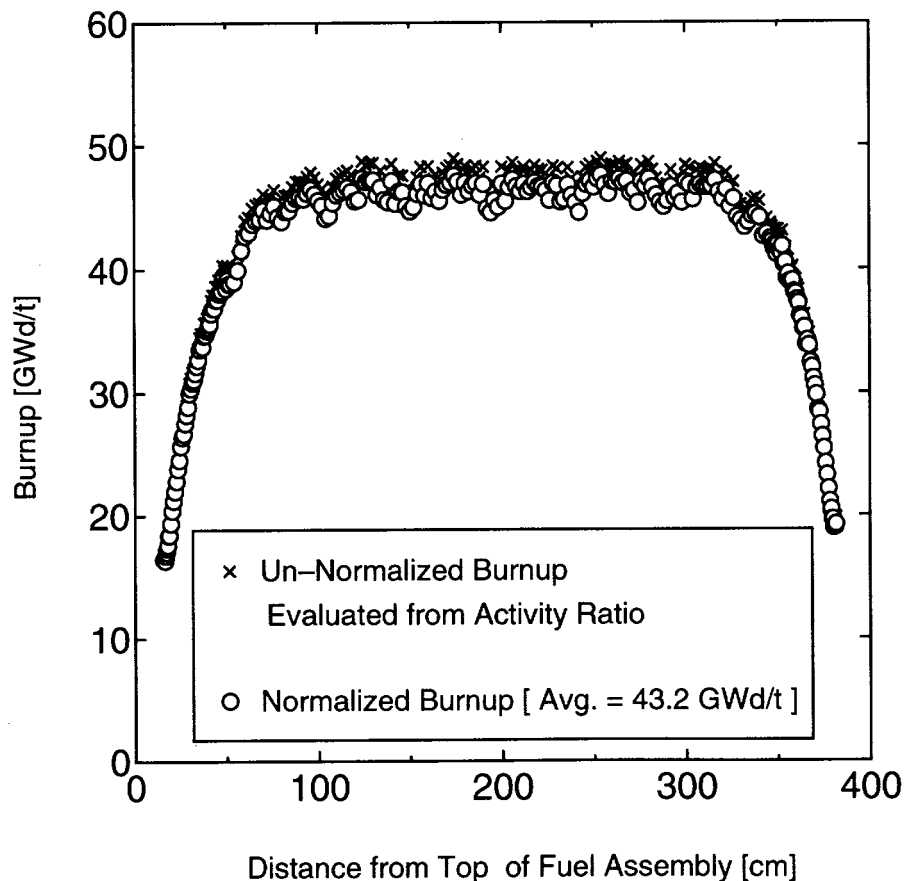


Fig. 4.4.4. Burnup distribution of HP17.

The fuel composition after burnup was calculated by ORIGEN2 by using the evaluated burnup at the burnup flat part and the library ORLIBJ32 [Ref. 9] for ORIGEN2 prepared from JENDL-3.2. And the calculated values were divided by the average values of C/E shown in Table 3.4.11, to provide a corrected nuclide composition of the burned fuel. For isotopes for which no experimental values are available, the calculated values are used as-is.

With this composition, cell calculation for 107 groups was performed with the use of SRAC95, and the group constants of 4 groups were prepared. A system for the cell calculation was determined based on a PWR  $17 \times 17$  fuel assembly system. Then, diffusion calculation was performed by CITATION with the use of the obtained 4-group constants. In this calculation, the neutron flux decay constant  $\gamma$  was calculated by the relationship  $\sqrt{|B_g^2|} = \gamma$  by buckling search calculation in an axially infinite system in an X-Y two-dimensional system, and the neutron flux decay constant  $\gamma$  was determined by determining the profile of neutron flux at the location of the neutron detector by fixed source calculation and fitting the calculated result, in a manner similar to the analysis of the subcritical experiments so far. Figure 4.4.5 shows the locations of the neutron sources and the neutron detectors.

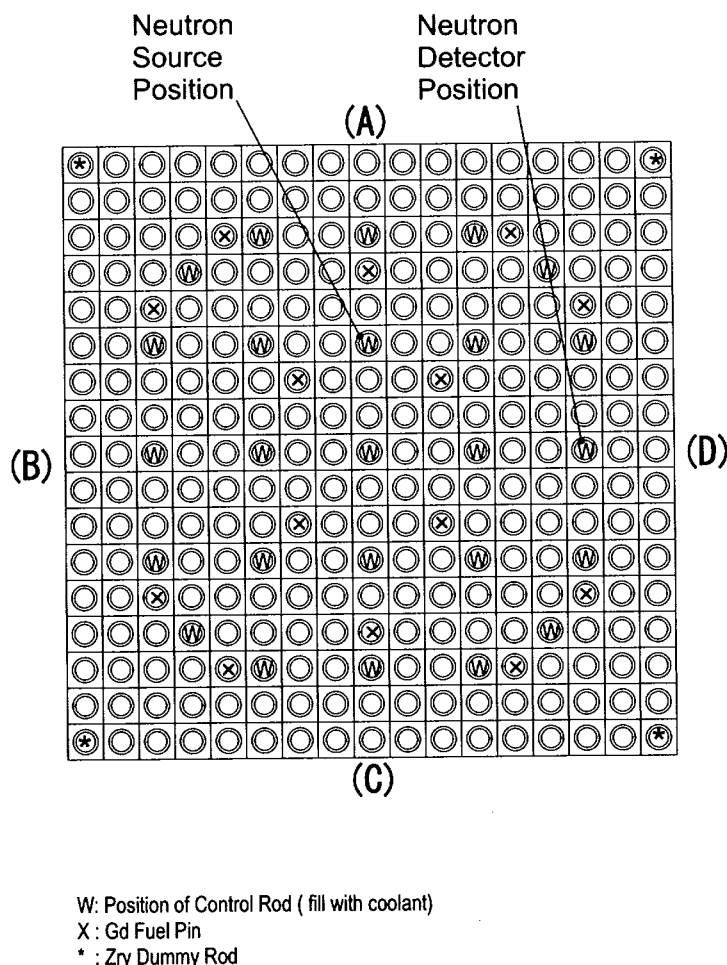


Fig. 4.4.5. HP17 subcritical experiment : Position of source and detector.

The calculated results are summarized in Table 4.4.9. Also shown in this table are the values of  $k_{\text{eff}}$  evaluated by using  $\gamma$  calculated by the respective calculation methods, in a manner similar to the analysis of the subcritical experiment for the B8 assembly. As can be seen from Table 4.4.9, the values of  $\gamma$  obtained by experiment and calculation show a difference of about 6% in buckling search calculation and fixed source calculation, and this difference is larger than in the P14 and P17 fuel assemblies for the same PWR fuel. In the B8 fuel assembly, the fixed source calculation showed differences of about 3%, though the buckling search calculation gave differences of 10%; taking these results together, the analytical results of the HP17 fuel assembly differ more with respect to the experimental results than do the other analytical results.

Table 4.4.9. Evaluated  $\gamma$  (Exp. : 0.1256 (1/cm))

	$\gamma$ (1/cm)	Error of $\gamma$ (%)	Evaluated $k_{\text{eff}}$	Error (%) of $k_{\text{eff}}$
Buckling search	1.176E-1	-6.3	0.5913	-3.2
Fixed source	1.161E-1	-7.6	0.5838	-3.8

With the possibility of a problem in system modeling in mind from the above-mentioned result, Monte Carlo code MCNP4B2, which can deal with the system strictly, was used to try to solve the fixed neutron source problem. The number of histories in this case was 1,000,000. In forming a model, the structure in the fuel rod cell and the guide tube were included accurately. The fuel composition was the same as in the analysis using SRAC95 and CITATION. As a result,  $\gamma = 1.193\text{E}-1$  (L/cm) was obtained with a difference of 5.3% from the experimental value. This means that the difference from the experimental value dropped by about 1% when compared with the analysis using SRAC95 and CITATION, but still the difference is large when compared with the P17, P18, and B8 fuel assemblies.

One conceivable reason for the larger difference between the calculated and measured results for the HP17 fuel assembly than in the earlier analysis of subcritical experiments for the P14 and P17 assemblies, is nonuniformity in the assembly. In other words, it can be imagined that nonuniformity (i.e., scatter in the radial burnup distribution) in the fuel assembly is greater because gadolinia-containing fuel rods are used, but the radial burnup distribution is assumed to be constant in the analysis, which is thought to be the reason.

## 4.5. Conclusions

Subcritical experiments for P14, P17, B8, and HP17 fuel assemblies were analyzed in order to validate the criticality calculation codes.

In the P14 and P17 fuel assemblies, the difference between the measured neutron flux decay constants and the neutron flux decay constants obtained by buckling search calculation was less than 3%, and the calculated values agreed well with the experimental values.

In the B8 fuel assembly, the difference between the measured neutron flux decay constants and the neutron flux decay constants obtained by buckling search calculation were larger, i.e., about 10%, but the difference dropped to about 3% when the neutron flux decay constant was evaluated by analyzing the

experiments by fixed source calculation, and a good agreement was obtained from the standpoint of analyzing the experiments. The cause of the difference between the neutron flux decay constants obtained by buckling search and the measured values were thought to be the effect of higher-order modes on the experimental results. Calculations were made to verify this assumption, and it was shown that measured results unaffected by higher-order modes can be obtained even if the distance from the neutron source is small, by placing the neutron detector at locations rotated 90 degrees from the present location. When carrying out similar experiments in the future, meticulous care should be taken to locate the neutron source and the neutron detector so as to avoid the effect of higher-order modes, in order to assure that experimental values are obtained by measurement of the fundamental mode.

In the HP17 fuel assembly, the difference became larger than in the analysis of the other assemblies. That is, the neutron flux decay constants obtained by buckling search calculation and fixed source calculation showed differences of about 6% from the measured values. The reason is thought to be that a constant radial burnup distribution is assumed in the analyses, in spite of the greater nonuniformity (i.e., scatter in the radial burnup distribution) in the HP17 fuel assembly due to the use of gadolinia-containing fuel rods in the fuel assembly.

## REFERENCES

1. Suzaki Takenori, "Subcriticality Determination of Low-Enriched UO<sub>2</sub> Lattices in Water by Exponential Experiment," *J. Nucl. Sci. Technol.*, **Vol. 28**, pp. 1067–1077, December 1991.
2. Suzaki Takenori et al., "Exponential Experiments of PWR Spent Fuel Assemblies of Acquiring Subcriticality Benchmarks Usable in Burnup Credit Evaluations," in *Proceedings of the Fifth International Conference on Nuclear Criticality Safety (ICNC'95)*, **Vol. 1**, pp. 1B.11–1B.18, Albuquerque, New Mexico, USA, September 17–21, 1995.
3. Suzaki Takenori et al., "Measurement of Criticality Properties of A BWR Spent Fuel Assembly," in *Proceedings of the Sixth International Conference on Nuclear Criticality Safety (ICNC'99)*, **Vol. IV**, pp. 1386–1393, Versailles, France, September 20–24, 1999.
4. J. F. Briesmeister, editor, "MCNP — A General Monte Carlo N-Particle Transport Code Version 4A," LA-12625-M, March 1997.
5. K. Tsuchihashi, Y. Ishiguro, K. Kaneko, and M. Ido, "Revised Version of the SRAC Code System," in *JAERI 1302*, September 1986.
6. K. Okumura, K. Kaneko, and K. Tsuchihashi, "SRAC95: General-Purpose Nuclear Calculation Code System, in *JAERI-Data/Code 96-015*, March 1996.
7. T. B. Flower, D. R. Vondy, and G. W. Cunningham, *Nuclear Reactor Core Analysis Code: CITATION*, ORNL/TM-2496, Rev. 2, July 1971.
8. Tsuneo Nakagawa, Keiichi Shibata, Satoshi Chiba, Tokio Fukahori, Yutaka Nakajima, Yasuyuki Kikuchi, Toshihiko Kawano, Yukinori Kanda, Takaai Ohsawa, Hiroyuki Matsunobu, Masayoshi Kawai, Atsushi Zukeran, Takashi Watanabe, Sin-iti Igarasi, Kazuaki Kosako, and Tetsuo Asami, "Japanese Evaluated Nuclear Data Library Version 3 Revision-2: JENDL-3.2," *J. Nucl. Sci. Technol.*, **Vol. 32**, pp. 1259–1271, December 1995.

9. K. Suyama, J. Katakura, U. Ohkawa, and M. Ishikawa, "Library for ORIGEN2 based on JENDL-3.2: ORLIBJ32," in JAERI-Data/Code 99-003, February 1999.

## 5. EXAMINATION OF THE BURNUP ESTIMATION METHOD

### 5.1. Evaluation of Axial Burnup Profiles Based on the Measured Data

#### 5.1.1. General

The most appropriate nuclide for the purpose of evaluating the burnup from  $\gamma$ -ray emitting FP nuclides is  $^{137}\text{Cs}$ . If the quantity of  $^{137}\text{Cs}$  (atoms/IMA) determined by measuring the  $\gamma$ -ray spectra of destructive analysis samples using a standard source is plotted against burnup, the relationship as shown in Fig. 5.1.1 can be obtained, and burnup can be determined in a straightforward manner, regardless of the type of reactor, the type of fuel, the initial enrichment, or the irradiation cycles. However, for measurement objects such as spent fuel rods or assemblies, it is practically difficult to prepare relevant standards, so most of the measurements are made in relative terms. This report will described the relationships between two activity ratios, i.e.,  $^{134}\text{Cs}/^{137}\text{Cs}$  and  $(^{134}\text{Cs}/^{137}\text{Cs})^2/(^{106}\text{Ru}/^{137}\text{Cs})$  [Ref. 1], and burn-up, as examined by using the measured data for burnup and FP activity ratios (Bq/Bq) obtained by the nondestructive  $\gamma$ -scanning measurement of PWR/BWR spent fuel rods and the destructive analysis of fuel samples cut from these fuel rods. The relationship between  $^{134}\text{Cs}/^{137}\text{Cs}$  and burnup was found to be approximately linear and practically unaffected by the type of fuel ( $\text{UO}_2$  fuel and  $\text{UO}_2\text{-Gd}_2\text{O}_3$  fuel), but to depend on the initial enrichment and the irradiation cycle. On the other hand, the relationship between  $(^{134}\text{Cs}/^{137}\text{Cs})^2/(^{106}\text{Ru}/^{137}\text{Cs})$  and burnup was found to be practically unaffected by the initial enrichment and the irradiation cycle and to have excellent properties as the FP activity ratio for the evaluation of burnup. However, both activity ratios depend on the neutron spectrum in the relationship with burnup, and are affected strongly by spectral changes due to differences in the void ratio (fuel rod position), especially in BWR fuels. Accordingly, the relationship between the burnup and the activity ratio with consideration of the void ratio (fuel rod location) was determined for BWR, and a burnup evaluation method from only measured activity ratios including  $^{154}\text{Eu}/^{137}\text{Cs}$  was also examined. Furthermore, the axial burnup profiles of both PWR and BWR spent fuel rods were evaluated by using the burnup evaluation equations (empirical equations) for PWR and BWR which were constructed on the basis of experimental data.

#### 5.1.2. Data Measurement

Nondestructive  $\gamma$ -scanning of PWR/BWR spent fuel rods and destructive analysis of spent fuel samples collected by cutting said fuel rods were carried out as shown in Sects. 3.1 and 3.2. Figure 5.1.2 shows examples of the axial profiles of the activity ratios, i.e.,  $^{134}\text{Cs}/^{137}\text{Cs}$  (single ratio),  $^{106}\text{Ru}/^{137}\text{Cs}$ , and  $(^{134}\text{Cs}/^{137}\text{Cs})^2/(^{106}\text{Ru}/^{137}\text{Cs})$  (multiple ratio: MPR) obtained by  $\gamma$ -scanning measurement of PWR/BWR spent fuel rods. The  $\gamma$ -scanning measurement was carried out on 9–13 fuel rods from each of 3 assemblies selected, and destructive analysis samples were cut and collected from 5 of those fuel rods. Samples were collected from locations over the entire length of the rod, as indicated by the symbol "O" (sampling position) in the PWR profile in the left-hand figure, and the number of samples per fuel rod was 5–10. Table 5.1.1 shows the data for FP activity ratios and burnup on samples subjected to destructive analysis.

### 5.1.3. Correlation Between Burnup and FP Activity Ratios in PWR Fuels

The correlation between  $^{134}\text{Cs}/^{137}\text{Cs}$  or  $(^{134}\text{Cs}/^{137}\text{Cs})^2/(^{106}\text{Ru}/^{137}\text{Cs})$  and burnup was examined on three PWR fuel rods (SF95, SF96, and SF97). These relationships are shown in Figs. 5.1.3 and 5.1.4.  $^{134}\text{Cs}/^{137}\text{Cs}$  shows an approximately linear relationship with burnup, but this relationship has different slopes in the three fuel rods. Fuel rods with the symbols ● and ▲ belong to the same assembly but differ in initial enrichment and fuel type. On the other hand, fuel rods with symbols ● and □ belong to different assemblies and differ in irradiation cycle, but are identical in initial enrichment and fuel type. From these results, the relationship of burnup with  $^{134}\text{Cs}/^{137}\text{Cs}$  was found to be affected by differences in initial enrichment and irradiation cycles. On the other hand, the relationship of burnup with  $(^{134}\text{Cs}/^{137}\text{Cs})^2/(^{106}\text{Ru}/^{137}\text{Cs})$  is not affected by the differences in initial enrichment and irradiation cycles. It was found experimentally that even in fuel rods with such different properties, the relationship between burnup and the activity ratio  $(^{134}\text{Cs}/^{137}\text{Cs})^2/(^{106}\text{Ru}/^{137}\text{Cs})$  can be expressed by the following approximation equation:

$$\text{Burnup (GWd/t)} = 58.1 \times \text{MPR(PWR)}^{0.652} \quad (1)$$

Here, MPR(PWR) represents the activity ratio  $(^{134}\text{Cs}/^{137}\text{Cs})^2/(^{106}\text{Ru}/^{137}\text{Cs})$  at the end of irradiation for PWR spent fuels.

### 5.1.4. Correlation Between Burnup and FP Activity Ratios in BWR Fuels

#### (1) Relationship of Burnup with Activity Ratios in BWR Fuels

The relationships of burnup with  $^{134}\text{Cs}/^{137}\text{Cs}$  and  $(^{134}\text{Cs}/^{137}\text{Cs})^2/(^{106}\text{Ru}/^{137}\text{Cs})$  for BWR fuels are shown in Figs. 5.1.5 and 5.1.6. As is clear from the figures, neither of these activity ratios show any unique values for burnup. Dependence on initial enrichment appears in  $^{134}\text{Cs}/^{137}\text{Cs}$  in BWR as well, just as seen in PWR. The relationship of burnup with  $(^{134}\text{Cs}/^{137}\text{Cs})^2/(^{106}\text{Ru}/^{137}\text{Cs})$  in BWR fuels seems to separate into two different curves for the upper and lower parts of the rod, with the curve of Eq. (1) (solid line) for PWR fuels in between. A relationship like this is thought to originate in the void rate, which changes with the axial position of the fuel rod (changes in the neutron spectrum). However, the average values (● and ■) of  $(^{134}\text{Cs}/^{137}\text{Cs})^2/(^{106}\text{Ru}/^{137}\text{Cs})$  and burnup for two BWR fuel rods were found to show values on the PWR evaluation curve. From this fact, the average neutron spectrum of the entire reactor may be said to be approximately the same in a PWR and a BWR.

#### (2) Burnup Evaluation Equation with Consideration of the Void Rate (Fuel Rod Location)

As shown in (1), it is difficult to determine an unequivocal relationship for the activity ratio and burnup from only these two parameters in BWR fuels. For this reason, a void factor (Vf) or a position factor Pf was introduced into the relationship between the activity ratio  $(^{134}\text{Cs}/^{137}\text{Cs})^2/(^{106}\text{Ru}/^{137}\text{Cs})$  and burnup in the present examination, and an attempt was made to construct a burnup evaluation equation for BWR fuels normalized by the PWR evaluation equation.

Figures 5.1.7 and 5.1.8 show the relationship between void factor (Vf) and void rate, and the relationship between position factor (Pf) and axial position (position), respectively. In these figures, both Vf and Pf are defined as the ratio of the value of MPR, i.e.,  $(^{134}\text{Cs}/^{137}\text{Cs})^2/(^{106}\text{Ru}/^{137}\text{Cs})$  in the PWR, to the

value of MPR in the BWR, i.e.,  $\text{MPR(PWR)}/\text{MPR(BWR)}$ , for the same burnup, and  $V_f$  was assumed to be a function of the void rate and  $P_f$  was assumed to be a function of axial position, then these functions were determined as 4th degree polynomials by least-square fitting.

### (1) Burnup Evaluation Equation Based on $V_f$

A burnup evaluation equation based on  $V_f$  can be determined as follows by replacing  $\text{MPR(PWR)}$  in the PWR evaluation equation by  $[V_f \times \text{MPR(BWR)}]$ :

$$\text{Burnup (GWde/t)} = 58.1 \times [V_f \times \text{MPR(BWR)}]^{0.652} \quad (2)$$

Here,  $V_f = \text{MPR(PWR)}/\text{MPR(BWR)}$ , which can be expressed as

$$= 7.192E-1 + 1.049E-1 \times (\text{Void \%}) - 5.640E-3 \times (\text{Void \%})^2 + \\ 1.050E-4 \times (\text{Void \%})^3 - 6.476E-7 \times (\text{Void \%})^4$$

Void \% is the void rate (%).

Furthermore, Equation (2) can be expressed as follows by using  $P_f$ :

$$\text{Burnup (GWde/t)} = 58.1 \times [P_f \times \text{MPR(BWR)}]^{0.652} \quad (3)$$

Here,  $P_f = \text{MPR(PWR)}/\text{MPR(BWR)}$ , which can be expressed as

$$= 4.437E-1 + 2.493E-3 \times (\text{Pos.}) - 2.473E-7 \times (\text{Pos.})^2 + \\ 8.941E-10 \times (\text{Pos.})^3 - 1.091E-13 \times (\text{Pos.})^4$$

Pos. is the axial position (mm) from the lower end of the fuel rod.

A comparison of the estimated burnup value ( $C$ ) as evaluated by Eqs. (2) and (3) and the burnup ( $E$ ) as evaluated by destructive analysis is listed in Table 5.1.2. The values of  $C/E$  show that the deviation is within about 10%, except in some data. In particular, the value of  $C/E$  of SF98-2 showed a very low value, i.e., 0.58. The reason is unclear, but a subtle deviation in sampling position can be considered responsible, from the fact that the burnup by destructive analysis was not consistent with the other burnup data and was a little higher, and that there was no obvious analytical mistake.

### (3) Examination of a Burnup Evaluation Method Using Only Measured FP Activity Ratios

Figure 5.1.10 shows the relationship (called the dolphin profile) between burnup (BU) and MPR multiplied by the ratio of  $^{154}\text{Eu}/^{137}\text{Cs}$  for both axes. This relationship is still represented by two curves under the influence of neutron spectral changes in much the same way as in Fig. 5.1.6, but all five fuel rods with different average burnups show the same profile as shown in Fig. 5.1.11. This property could be explained as follows from Eqs. (3) and (5) by first approximation as shown below in Fig. 5.1.11 [sic; “Fig. 5.1.10” -- Tr. Ed.]. The parameter  $BU \times (^{154}\text{Eu}/^{137}\text{Cs})$  of Equation (3) is proportional to the square of the epithermal neutron fluence, and the parameter  $\text{MPR} \times (^{154}\text{Eu}/^{137}\text{Cs})^2$  of Eq. (4) is proportional to the product of spectral index ( $\phi E/\phi T$ ) normalized with the burnup ( $E\phi T$ ) and (epithermal neutron fluence),<sup>4</sup>

and both parameters have characteristics values at a specific position of the fuel rod, which is thought to be the reason. When using this relationship in the evaluation of burnup, which of the two curves to use must be decided from the relationship with the measurement position shown in Fig. 5.1.12. The following empirical equations were derived from the two curves obtained from experimental values by fitting data with a 4th degree polynomial:  $Y = 4.234E-2 + 2.817E3 \times X - 8.693E5 \times X^2 - 1.930E8 \times X^3 + 9.274E10 \times X^4$  for areas including the lower part of the fuel rod, and  $Y = 134.76 \times X^{0.655}$  for areas including the upper part of the fuel rod.

### **5.1.5. Axial Burnup Distributions of Spent Fuel Rods**

The axial burnup distribution of a spent fuel rod in PWR fuels becomes the same as the profile of  $^{134}\text{Cs}/^{137}\text{Cs}$  shown on the left-hand side of Fig. 5.1.2, because the relationship between the ratio of  $^{134}\text{Cs}/^{137}\text{Cs}$  and burnup is linear in PWR fuels, and this profile is nearly flat over the entire fuel rod. On the other hand, the profile is very different in BWR fuels. The burn profile estimated by the above-mentioned Eqs. (2) and (3) on a BWR spent fuel rod (KE12) shown in Fig. 5.1.2 is shown in Fig. 5.1.9. In this fuel rod, the profile of  $^{134}\text{Cs}/^{137}\text{Cs}$  rises from the lower end of the rod to the top, but the burnup profile shows an opposite trend, though its slope is smaller. This is presumably because the rate of formation of  $^{134}\text{Cs}$  increases due to neutron spectrum hardening by the increase in the void ratio.

## **REFERENCE**

1. A. S. Chesterman and P. A. Clark, *Spent Fuel and Residue Measurement Instrumentation at the Shellfield Nuclear Fuel Processing Facility*, BNFL Instruments Ltd., Pelham House, Calderbridge, Seascale, Cumbria, CA20 1PG, UK, Oct. (1995).

Table 5.1.1. Measured data on burnup and activity ratios

Reactor and fuel type	Name of DA sample	Axial position** (mm, from bottom)	Burnup (DA) (GWd/t)	Activity ratio in zero-cooling (NDA)			Void rate %*
				$\frac{^{134}\text{Cs}}{^{137}\text{Cs}}$	$\frac{^{100}\text{Ru}}{^{137}\text{Cs}}$	$\frac{(^{134}\text{Cs}/^{137}\text{Cs})^2}{(^{106}\text{Ru}/^{137}\text{Cs})}$	
PWR (G23) 4.1% $^{235}\text{UO}_2$ (2 cycle irrad.)	SF95-1	3695	14.7	0.59	2.96	0.12	0.021
	SF95-2	3535	25.2	1.11	4.25	0.29	0.043
	SF95-3	3015	36.7	1.56	5.07	0.48	0.059
	SF95-4	1735	38.1	1.58	4.91	0.51	0.058
	SF95-5	335	31.4	1.32	4.54	0.38	0.049
PWR (G23) 2.6% $^{235}\text{UO}_2$ - 6.0% $\text{Gd}_2\text{O}_3$ (3 cycle irrad.)	SF96-1	3685	8.0	0.45	4.42	0.05	0.027
	SF96-2	3525	16.8	0.95	5.75	0.16	0.046
	SF96-3	3005	28.9	1.47	6.55	0.33	0.062
	SF96-4	1727	29.6	1.49	6.50	0.34	0.060
	SF96-5	327	24.7	1.26	6.15	0.26	0.054
PWR (G24) 4.1% $^{235}\text{UO}_2$ (3 cycle irrad.)	SF97-1	3699	18.0	0.67	3.03	0.15	0.025
	SF97-2	3515	31.3	1.35	4.15	0.44	0.054
	SF97-3	3235	43.0	1.74	4.53	0.67	0.065
	SF97-4	2019	48.0	1.83	4.47	0.75	0.066
	SF97-5	937	48.2	1.83	4.49	0.75	0.067
BWR (DN23) 3.9% $^{235}\text{UO}_2$ (3 cycle irrad.)	SF98-1	39	4.2	0.34	3.89	0.03	0.017
	SF98-2	167	26.8	0.64	2.40	0.17	0.025
	SF98-3	423	37.4	1.16	3.11	0.43	0.039
	SF98-4	692	43.0	1.34	3.53	0.51	0.046
	SF98-5	1214	44.8	1.42	3.60	0.56	0.048
BWR (DN23) 3.4% $^{235}\text{UO}_2$ - 4.5% $\text{Gd}_2\text{O}_3$ (3 cycle irrad.)	SF98-6	2050	40.7	1.50	3.87	0.58	0.059
	SF98-7	2757	40.2	1.57	3.72	0.66	0.057
	SF98-8	3397	27.2	1.17	3.51	0.39	0.050
	SF99-1	134	7.7	0.57	3.60	0.09	0.027
	SF99-2	286	22.9	0.87	3.46	0.22	0.037
BWR (DN23) 3.4% $^{235}\text{UO}_2$ - 4.5% $\text{Gd}_2\text{O}_3$ (3 cycle irrad.)	SF99-3	502	32.9	1.11	3.68	0.33	0.043
	SF99-4	686	36.0	1.26	4.05	0.39	0.043
	SF99-5	1189	38.1	1.36	4.00	0.46	0.053
	SF99-6	2061	33.0	1.35	4.45	0.41	0.064
	SF99-7	2744	32.8	1.43	4.65	0.44	0.066
	SF99-8	3388	22.3	1.02	3.80	0.27	0.052
	SF99-9	3540	17.0	0.75	3.28	0.17	0.039
	SF99-10	3676	7.4	0.59	5.15	0.07	0.030

\*Application for a reactor installation permit (July 1995);

\*\*Fuel length (PWR: 3863 mm, BWR: 4069 mm).

Table 5.1.2. Estimated burnup by Vf and Pf fitting curve

Fuel type	Sample I.D.	MPR (PWR)/MPR (BWR)		Burnup (GWd/t)		Burnup (C/E)	
		Measured	from Vf	Measured	from Vf	from Pf	from Vf
BWR (DN23) 3.9% $^{235}\text{UO}_2$ (3 cycle irrad.)	SF98-1	0.63	0.72	0.54	4.2	4.66	3.85
	SF98-2	1.81	0.72	0.80	26.8	14.65	15.68
	SF98-3	1.18	1.05	1.12	37.4	34.63	36.06
	SF98-4	1.23	1.32	1.26	43.0	45.04	43.58
	SF98-5	1.20	1.13	1.19	44.8	42.97	44.34
	SF98-6	0.99	0.97	0.94	40.7	40.10	39.08
	SF98-7	0.86	0.98	0.95	40.2	43.71	42.96
	SF98-8	0.82	0.84	0.89	27.7	28.13	29.14
BWR (DN23) 3.4% $^{235}\text{UO}_2$ - 4.5% $\text{Gd}_2\text{O}_3$ (3 cycle irrad.)	SF99-1	0.50	0.69	0.74	7.7	9.56	9.98
	SF99-2	1.09	0.86	0.97	22.9	19.60	21.31
	SF99-3	1.25	1.16	1.18	32.9	31.22	31.60
	SF99-4	1.22	1.32	1.25	36.0	37.77	36.58
	SF99-5	1.13	1.15	1.20	38.1	38.57	39.57
	SF99-6	1.02	0.98	0.93	33.0	31.95	31.06
	SF99-7	0.94	0.98	0.95	32.8	33.59	32.94
	SF99-8	0.85	0.85	0.89	22.3	22.24	23.06
	SF99-9	0.90	0.79	0.80	17.0	15.73	15.83
	SF99-10	0.64	0.73	0.67	7.4	8.06	7.67

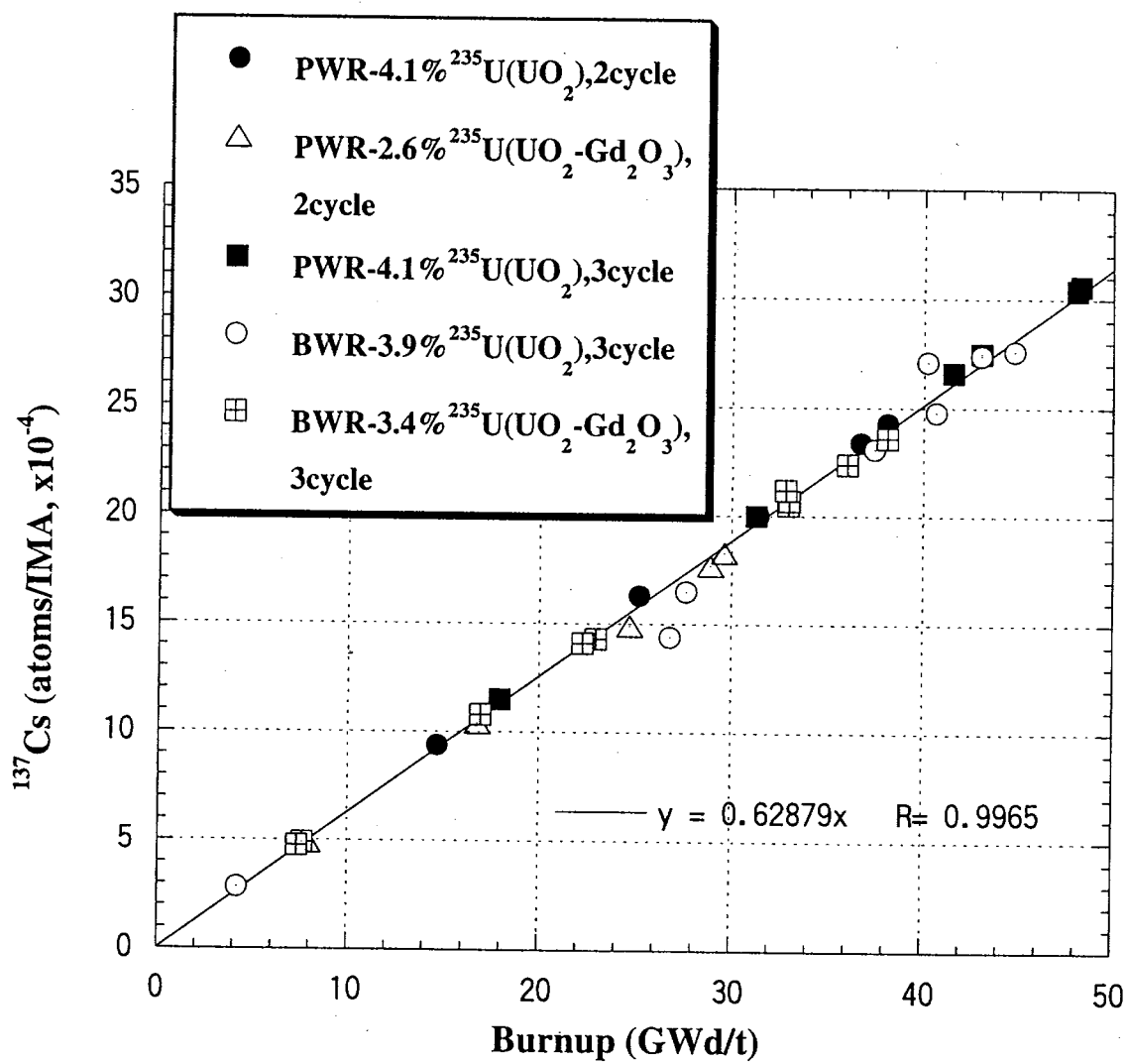


Fig. 5.1.1. Relation of  $^{137}\text{Cs}$  with burnup.

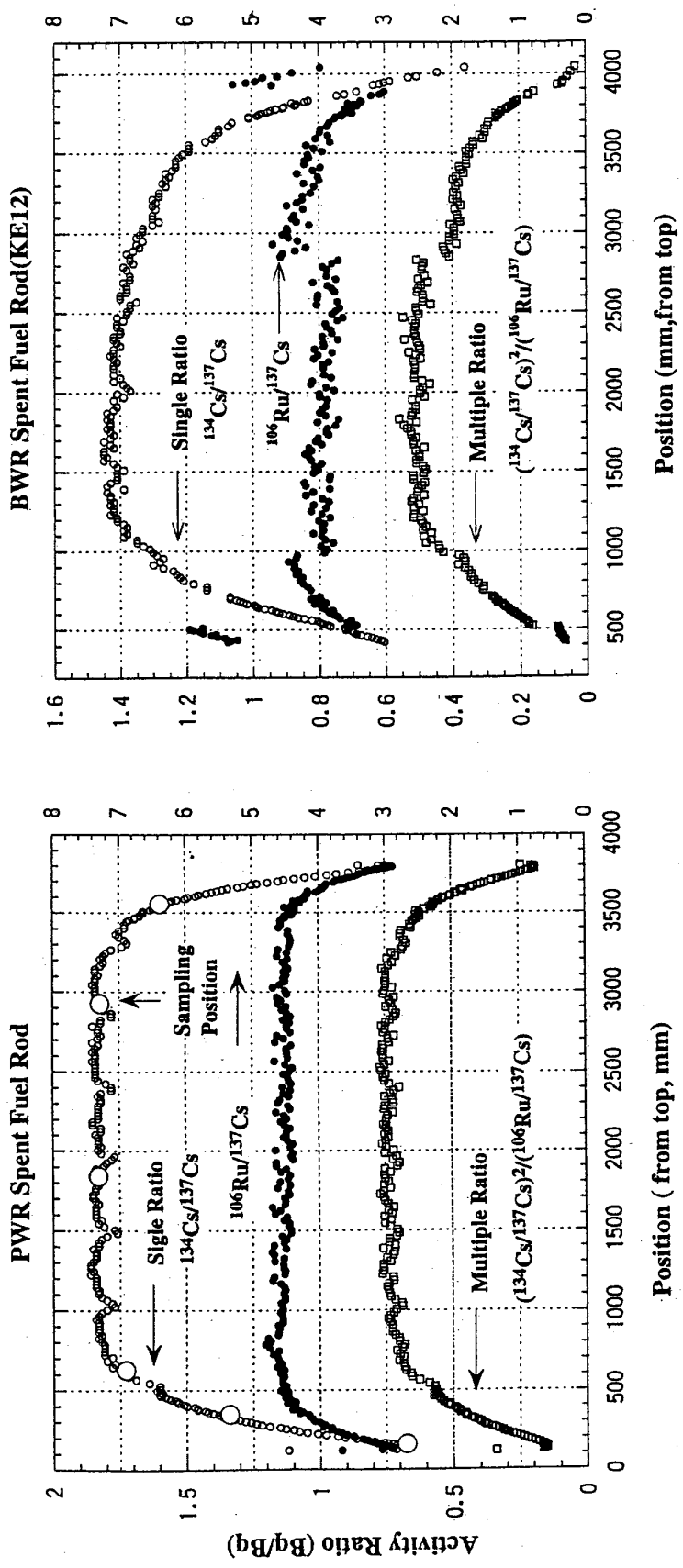


Fig. 5.1.2 Examples of axial profiles on FP activity ratios in both PWR and BWR spent fuel rods.

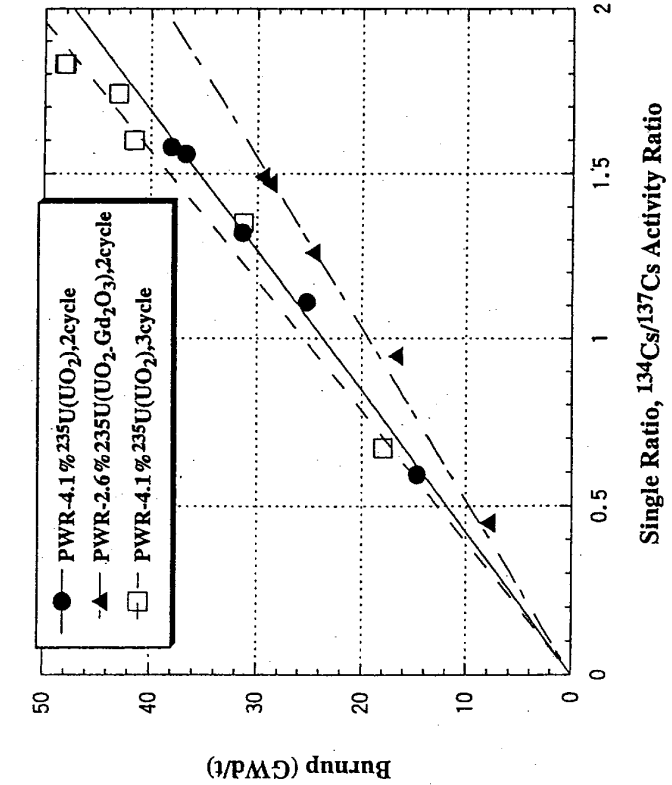


Fig. 5.1.3. Relation of burnup with single ratio in PWR.

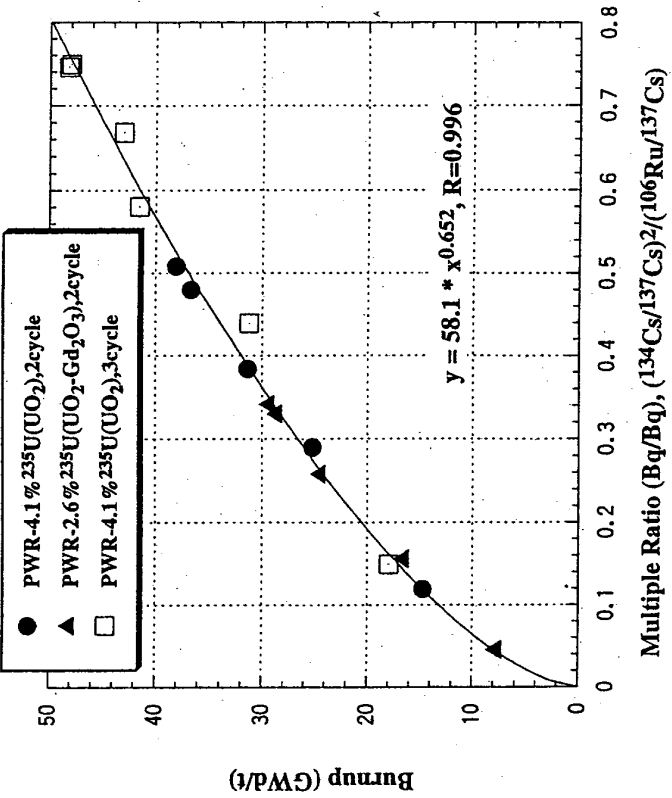


Fig. 5.1.4. Relation of burnup with multiple ratio in PWR.

Fig. 5.1.6. Relation of burnup with multiple ratio.

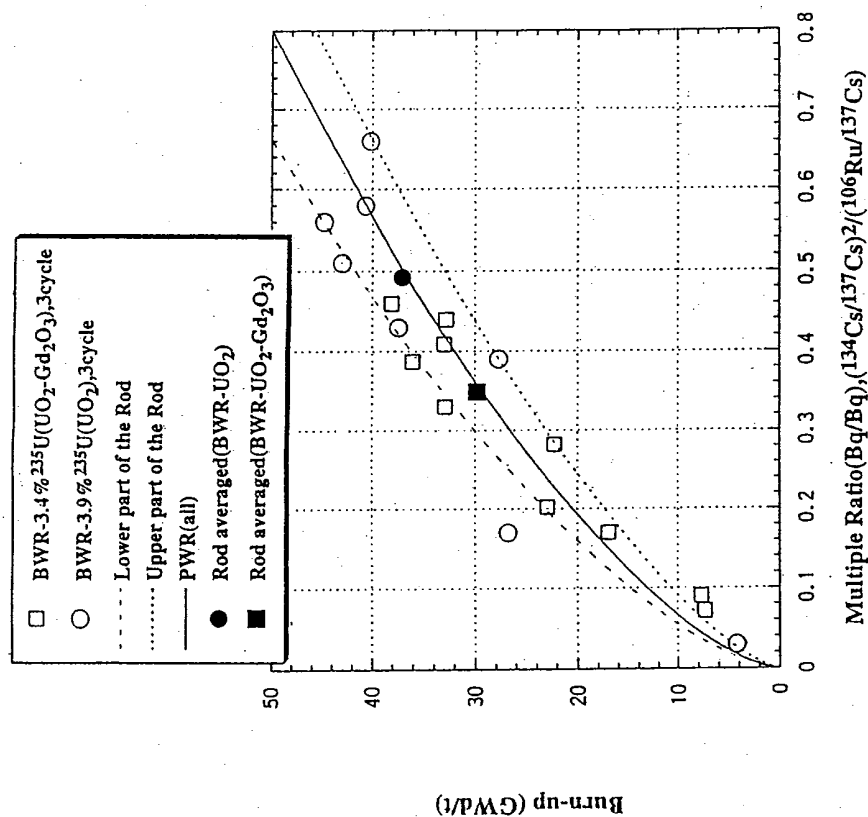
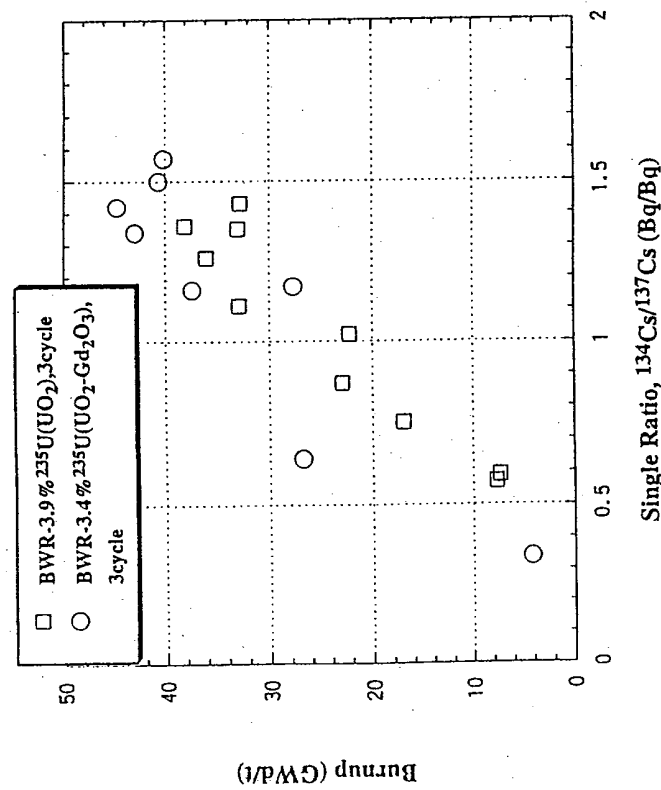


Fig. 5.1.5. Relation of burnup with single ratio.



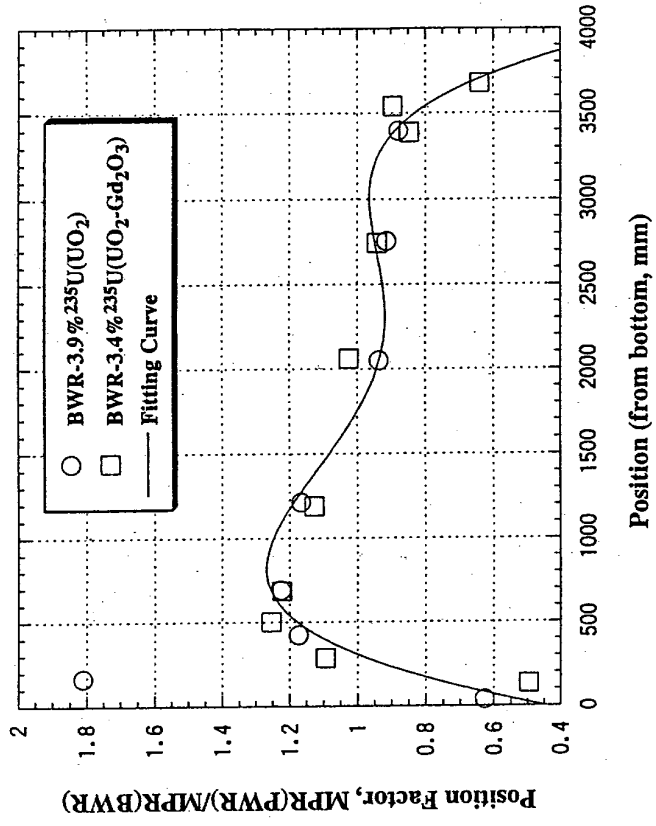


Fig. 5.1.8. Relation of position factor with rod position.

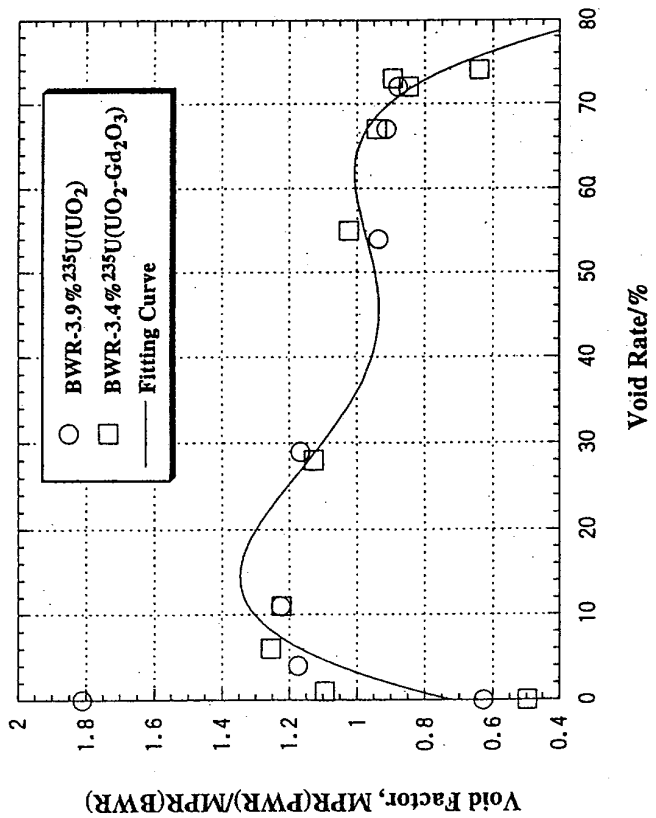


Fig. 5.1.7. Relation of void factor with void rate.

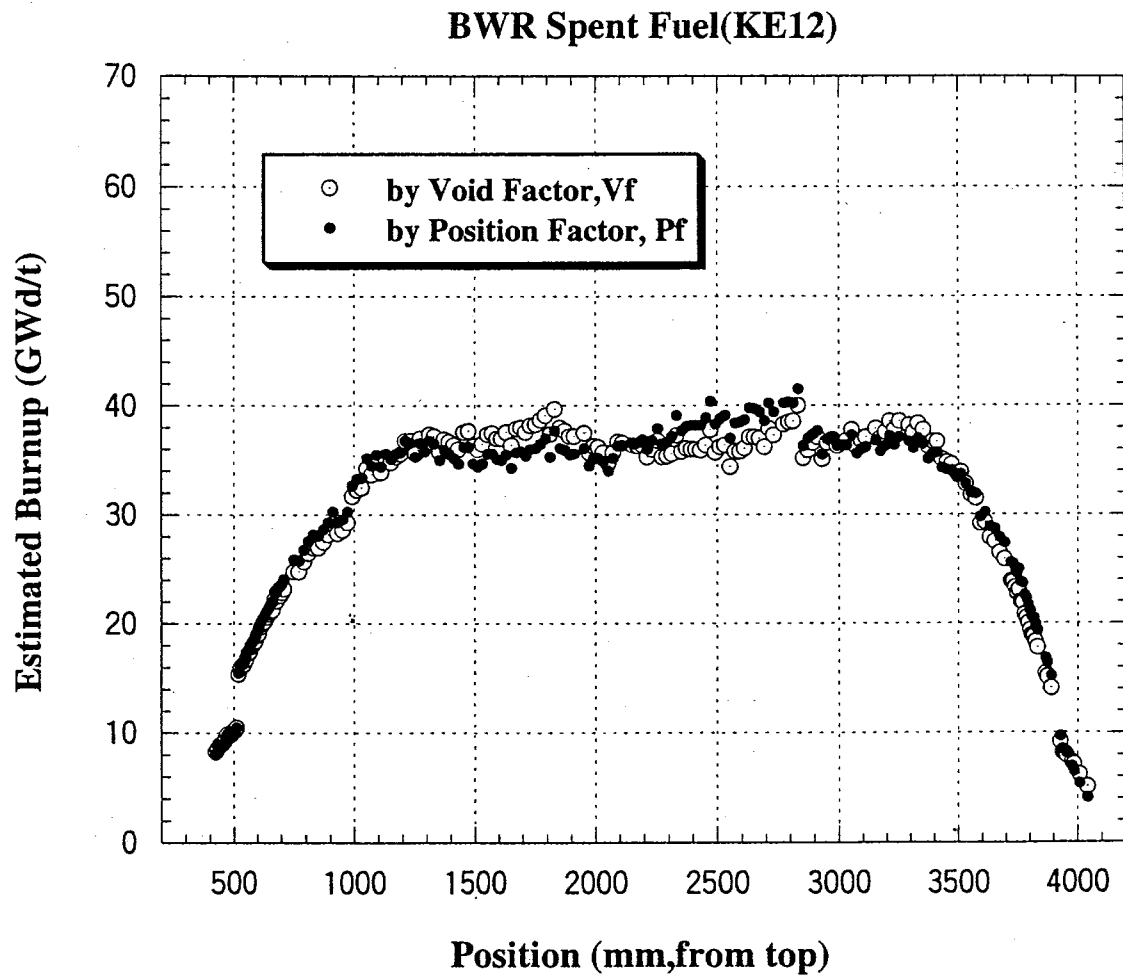


Fig. 5.1.9. Axial burnup profile estimated by Vf and Pf.

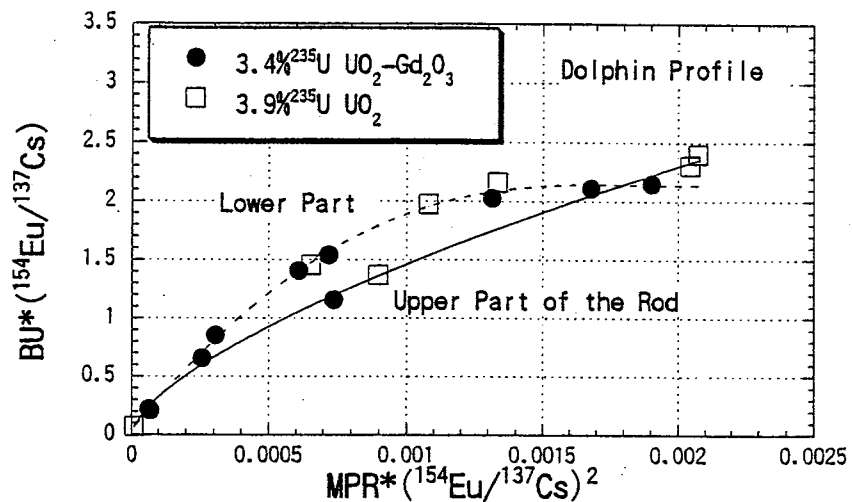


Fig.5.1.10 Relation between Activity Ratios and Burn-up based on Measured Data

$$BU \propto E \cdot \phi_t \cdot T \quad (1)$$

$$\frac{N(154\text{Eu})}{N(137\text{Cs})} \propto \frac{(\phi_e \cdot T)^2}{E \cdot \phi_t \cdot T} \propto BU \cdot \frac{1}{E^2} \cdot \left(\frac{\phi_e}{\phi_t}\right)^2 \quad (2)$$

$$BU \cdot \frac{N(154\text{Eu})}{N(137\text{Cs})} \propto (\phi_e \cdot T)^2 \equiv \text{Const.(Pos.)} \quad (3)$$

$$FPR \cdot \left[ \frac{N(154\text{Eu})}{N(137\text{Cs})} \right]^2 \propto \frac{(\phi_e / \phi_t)}{E \cdot \phi_t \cdot T} \cdot (\phi_e \cdot T)^4 \equiv \text{Const.(Pos.)} \quad (4)$$

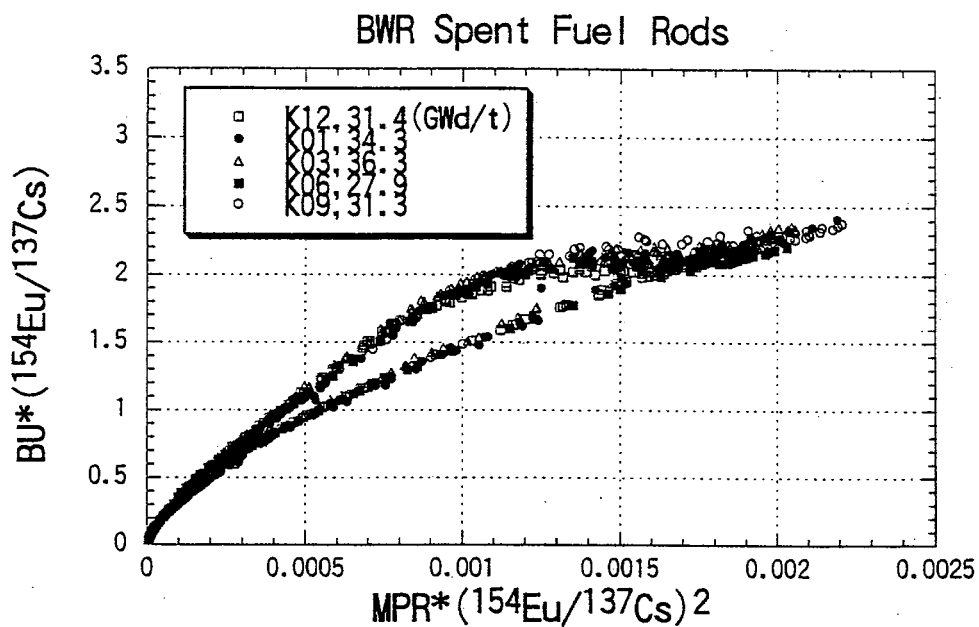


Fig. 5.1.11. Relation between activity ratios and burnup with different spent fuel rods.

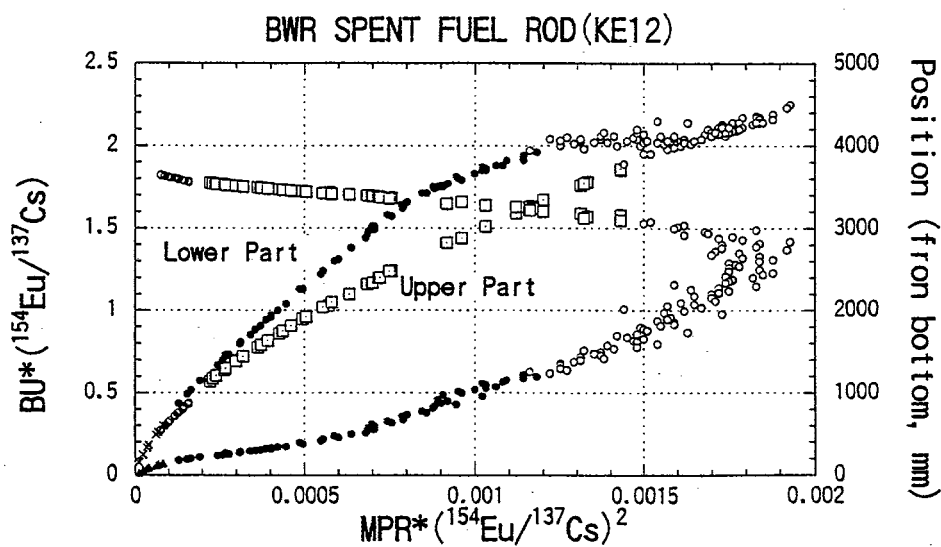


Fig. 5.1.12. Relation between Dolphin profile and measurement positions.

## 5.2. Sensitivity Analysis of Irradiation Parameters Affecting the Correlation Between Burnup and FP Activity Ratios

Burnup calculations were carried out on PWR and BWR fuels, and the sensitivity of three types of FP activity ratios to parameters such as initial enrichment, power history, moderator boron content (PWR), and moderator void ratio (BWR) was examined. Burnup calculations were carried out up to 50 GWd/t and 40 GWd/t, respectively, on PWR and BWR fuels.

The relationship between the following three FP activity ratios and burnup was examined as an index of burnup.

- (1)  $^{134}\text{Cs}/^{137}\text{Cs}$
- (2)  $^{154}\text{Eu}/^{137}\text{Cs}$
- (3)  $(^{134}\text{Cs}/^{137}\text{Cs})^2/(^{106}\text{Ru}/^{137}\text{Cs})$

### 5.2.1. Sensitivity Analysis on PWR Fuels

#### (1) Calculation Conditions

##### 1) Fuel Rod Specifications

The fuel rod selected for the calculations was 1100 MW class PWR ( $17 \times 17$  fuel assembly). Specifically, the fuel rod specifications given in JAERI- Data/Code 99-0003 were selected, which are listed in Table 5.2.1.

The atomic number densities used in the calculations are listed in Table 5.2.2.

##### 2) Burnup Step

The relative power was set at 42.74 MW/tU so as to be able to achieve a burnup of 50 GWd/t in 3 cycles, with one cycle of operation as 13 months. Furthermore, the partway cooling period between cycles to simulate periodic inspection was assumed to be 2 months. Burnup for one step was set at about 2 GWd/t. Burnup calculation steps in various cases are shown in Table 5.2.3.

##### 3) The Dancoff Factor

The value 0.305 evaluated separately was used for the Dancoff factor so as to be able to simulate assembly-averaged calculations by unit cell calculations.

#### (2) Parameters to be Examined

The parameters to be examined in PWR fuels are three, i.e., initial enrichment, power history, and boron content. The ranges of these parameters are shown below. When changing one parameter, the values of the other parameters were those of a standard case. The range of each parameter is listed in Tables 5.2.4, 5.2.5, and 5.2.6.

### (3) Calculation Results

The effect of each parameter on FP activity ratios and burnup is described below.

#### 1) Initial Enrichment

The change in each burnup index with a change in initial enrichment is shown in Tables 5.2.7–5.2.9 and Figs. 5.2.1–5.2.3. In the figures, the activity ratios for various burnups were fitted with a quadratic equation that did not include a constant term.

At the same burnup, each activity ratio decreases as the initial enrichment increases, without depending on relative power and the partway-cooling period.

To examine the difference in activity ratio due to the difference in enrichment, relative values of the activity ratio at each burnup point were calculated. Here, the relative values were taken relative to the values at the initial enrichment of 4 wt %. The results are shown in Tables 5.2.10–5.2.12 and Figs. 5.2.4–5.2.6. It can be seen that the Cs activity ratio is nearly constant for the change in burnup, but in the Ru and Eu activity ratios the difference decreases with the progress of burnup. The Ru activity ratio shows the smallest enrichment dependency, and the difference is less than 5%.

#### 2) Power History

The change in each burnup index with a change in power history is shown in Tables 5.2.13–5.2.15 and Figs. 5.2.7–5.2.9.

To examine the difference in the activity ratio due to the difference in power history, relative values of the activity ratio at each burnup point were calculated. Here, the relative values were taken relative to the values in case B with a constant power. The results are shown in Tables 5.2.16–5.2.18 and Figs. 5.2.10–5.2.12. The Eu activity ratio shows the smallest power history dependency, and the difference is less than 2%. The Ru activity ratio shows a monotonous increase in case A, and a monotonous decrease in case C.

#### 3) Boron Content

The change in each burnup index with a change in boron content is shown in Tables 5.2.19–5.2.22 and Figs. 5.2.13–5.2.15.

At the same burnup, the activity ratio increases as the boron content increases, but the difference is much smaller than that in enrichment dependency.

To examine the difference in the activity ratio due to the difference in boron content, relative values of the activity ratio at each burnup point were calculated. Here, the relative values were taken relative to the values at a constant boron content of 500 ppm. The results are shown in Tables 5.2.23–5.2.25 and Figs. 5.2.16–5.2.18. In all the activity ratios, the change with a change in burnup is not as large as that in the examination of initial enrichment dependency, and the differences are less than about 1% in all cases.

## 5.2.2. Sensitivity Analysis on BWR Fuels

### (1) Calculation Conditions

#### 1) Fuel Rod Specification

The fuel rod selected for the calculations was STEP II fuel. Specifically, the fuel rod specifications given in JAERI-Data/Code 99-0003 were selected, which are shown in Table 5.2.26.

The atomic number densities used in the calculations are shown in Table 5.2.27.

#### 2) Burnup Step

The relative power was set at 25.64 MW/tU so as to be able to achieve a burnup of 40 GWd/t in a 4-cycle operation, with one cycle of operation consisting of 390-day running and 90-day cooling. Burnup in one step was set at about 2 GWd/t. Burnup calculation steps for various cases are shown in Table 5.2.28.

#### 3) The Dancoff Factor

The values in Table 5.2.29 evaluated separately (values given in JAERI- Data/Code 99-003) were used for the Dancoff factor so as to be able to simulate assembly-averaged calculations by unit cell calculations.

### (2) Parameters to be Examined

The parameters to be examined in BWR fuels are three, i.e., initial enrichment, power history, and moderator void ratio. The ranges of these parameters are shown below. When changing one parameter, the values of the other parameters were those of a standard case. The range of each parameter is shown in Tables 5.2.30–5.2.32.

### (3) Calculation Results

The effect of each parameter on the relationship between FP activity ratios and burnup is described below.

#### 1) Initial Enrichment

The changes in each burnup index with a change in initial enrichment are shown in Tables 5.2.33–5.2.35 and Figs. 5.2.19–5.2.21.

To examine the difference in activity ratio due to the difference in enrichment, relative values of the activity ratio at each burnup point were calculated. Here, the relative values were taken relative to the values at an initial enrichment of 4 wt %. The results are shown in Tables 5.2.36–5.2.38 and Figs. 5.2.22–5.2.24. The relative Cs activity ratio is nearly constant for the change in burnup, but in the Ru and Eu activity ratios the difference decreases with the progress of burnup. The Ru activity ratio shows the smallest enrichment dependency, and the difference is less than about 8%.

## 2) Power History

The change in each burnup index with a change in power history is shown in Tables 5.2.39–5.2.41 and Figs. 5.2.25–5.2.27.

To examine the difference in the activity ratio due to the difference in power history, the relative values of the activity ratio at each burnup point were calculated. Here, the relative values were taken relative to the values in case B with a constant power. The results are shown in Tables 5.2.42–5.2.44 and Figs. 5.2.28–5.2.30. The Eu activity ratio shows the smallest power history dependency, and the difference is less than 2%. The relative Cs activity ratio decreases monotonously in case A, and increases monotonously in case C, but the difference between cases tends to increase as the burnup increases.

The relative Ru activity ratio increases monotonously in case A, and decreases monotonously in case C, but the difference between cases tends to decrease as the burnup increases.

## 3) Moderator Void Ratio

The change in each burnup index with a change in the void ratio is shown in Tables 5.2.45–5.2.47 and Figs. 5.2.31–5.2.33.

At the same burnup, the activity ratio increases as the void ratio increases.

To examine the difference in the activity ratio due to the difference in void ratio, relative values of the activity ratio at each burnup point were calculated. Here, the relative values were taken relative to the values at a void ratio of 40%. The results are shown in Tables 5.2.48–5.2.50 and Figs. 5.2.34–5.2.36. In all the activity ratios, the change with a change in burnup is larger than that in the examination of initial enrichment dependency, and the difference is about 20% in all cases.

## **5.2.3. Summary**

### (1) PWR Fuels

The results of examination of initial enrichment dependency, burnup history dependency, and boron content dependency of the relationships between the Cs, Eu, and Ru activity ratios and burnup will be summarized below.

#### 1) Initial Enrichment Dependency

The relationships between the Cs and Eu activity ratios and burnup differ largely at initial enrichments of 3 to 5%, and the difference is about 10%, but the Ru activity ratio shows a small initial enrichment dependency, and the difference at different enrichments is about 5% in an early stage of burnup and decreases with the progress of burnup.

#### 2) Burnup History Dependency

The relationship between the Eu activity ratio and burnup shows the smallest burnup history dependency. The Ru activity ratio shows a large dependency in an early stage of burnup with the difference in different cases being about 10%, but this difference decreases with the progress of burnup, and reduces to less than 5% at burnups of more than 30 GWd/tU.

### 3) Boron Content Dependency

The relationships between the Cs, Eu, and Ru activity ratios and burnup all show small boron content dependencies, and the difference at different contents is about 1%.

## (2) BWR Fuels

The results of examination of initial enrichment dependency, burnup history dependency, and moderator void ratio dependency of the relationship between the Cs, Eu, and Ru activity ratios and burnup will be summarized below.

### 1) Initial Enrichment Dependency

The relationships between the Cs and Eu activity ratios and burnup show differences of more than about 10% at different initial enrichments, but the Ru activity ratio shows a relatively small dependency on initial enrichment, and the difference at different enrichments is less than about 10%, even in an early stage of burnup, and becomes even smaller with the progress of burnup, reducing to less than 5% at burnups of more than 30 GWd/t.

### 2) Burnup History Dependency

The relationship between the Eu activity ratio and burnup shows the smallest burnup history dependency, and the difference in different cases is less than 2%. The Ru activity ratio shows a large dependency with the difference in different cases being about 10% in an early stage of burnup, but this difference decreases with the progress of burnup, and reduces to less than 5% at burnups of more than 20 GWd/t.

### 3) Moderator Void Ratio Dependency

The relationships between the Cs, Eu, and Ru activity ratios and burnup all show large void ratio dependencies, and the difference at different void ratios is about 20%.

From the above-mentioned results, the relationship between the Ru activity ratio and burnup shows relatively small dependencies on the various parameters in PWR fuels; thus, the Ru activity ratio is suitable as an index of burnup.

In BWR fuels also, the relationship between the Ru activity ratio and burnup shows relatively small dependencies on the various parameters, but shows a large dependency on the moderator void ratio; thus, if the Ru activity ratio is to be used as an index of burnup, a parameter on void ratio must be considered separately.

Table 5.2.1. PWR fuel rod specification

Cell pitch [cm]	1.265
Pellet radius [cm]	0.412
Clad radius [cm]	0.476
Clad thickness [cm]	0.064
Cell pitch [cm]	0.7138
Fuel temperature [K]	968.8
Clad temperature [K]	604.0
Moderator temperature [K]	574.2

Table 5.2.4. Initial enrichment

Case	Initial enrichment (wt %)	Remark
A	3	
B	4	Standard case
C	5	

Table 5.2.5. Power history

Case	Power history			Remark
A	1 <sup>st</sup> cycle	64.11 MW/tU	(Standard case × 1.5)	
	2 <sup>nd</sup> cycle	42.74 MW/tU	(Standard case × 1.0)	
	3 <sup>rd</sup> cycle	21.37 MW/tU	(Standard case × 0.5)	
B	Every cycle	42.74 MW/tU	Constant	Standard case
C	1 <sup>st</sup> cycle	21.37 MW/tU	(Standard case × 0.5)	
	2 <sup>nd</sup> cycle	42.74 MW/tU	(Standard case × 1.0)	
	3 <sup>rd</sup> cycle	64.11 MW/tU	(Standard case × 1.5)	

Table 5.2.6. Boron content

Case	Boron content	Remark
A	0 ppm constant	
B	500 ppm constant	Standard case
C	1000 ppm constant	
D	Linear change from 1000 ppm to 0 ppm	

Table 5.2.2. Number densities (PWR fuel cell)

	Fuel			Clad	Moderator
	3 wt %	4 wt %	5 wt %		
U-235	6.841E-04	9.121E-04	1.140E-03	—	—
U-238	2.184E-02	2.161E-02	2.139E-02	—	—
Zr-nat	—	—	—	3.786E-02	—
Fe-nat	—	—	—	2.382E-04	1.306E-04
Cr-nat	—	—	—	6.770E-05	1.609E-04
H-1	—	—	—	8.730E-05	5.572E-02
O-16	4.505E-02	4.505E-02	4.505E-02	—	2.786E-02
C-12	—	—	—	7.912E-05	3.366E-06
B-10	—	—	—	—	4.592E-06
Ni-nat	—	—	—	—	3.688E-04
Al-27	—	—	—	—	8.985E-06
Si-nat	—	—	—	—	1.079E-05
Cu-nat	—	—	—	—	4.767E-06
Mn-55	—	—	—	—	3.676E-06

Table 5.2.3(a). Power history (Pattern A)

Step	Step days	Operated days	Integrated days	Power ratio [MW/tU]	Integrated burnup [MWd/tU]
1	31.000	31.000	31.000	64.11	1987.41
2	31.000	62.000	62.000	64.11	3974.82
3	31.000	93.000	93.000	64.11	5962.23
4	31.000	124.000	124.000	64.11	7949.64
5	31.985	155.985	155.985	64.11	10000.20
6	31.000	186.985	186.985	64.11	11987.61
7	31.000	217.985	217.985	64.11	13975.02
8	31.000	248.985	248.985	64.11	15962.43
9	31.000	279.985	279.985	64.11	17949.84
10	31.980	311.965	311.965	64.11	20000.08
11	31.000	342.965	342.965	64.11	21987.49
12	31.000	373.965	373.965	64.11	23974.90
13	16.035	390.000	390.000	64.11	25002.90
14	60.000	—	450.000	0	25002.90
15	47.000	47.000	497.000	42.74	27011.68
16	47.000	94.000	544.000	42.74	29020.46
17	22.920	116.920	566.920	42.74	30000.06
18	47.000	163.920	613.920	42.74	32008.84
19	47.000	210.920	660.920	42.74	34017.62
20	47.000	257.920	707.920	42.74	36026.40
21	47.000	304.920	754.920	42.74	38035.18
22	45.970	350.890	800.890	42.74	39999.94
23	39.110	390.000	840.000	42.74	41671.50
24	60.000	—	900.000	0	41671.50
25	94.000	94.000	994.000	21.37	43680.28
26	94.000	188.000	1088.000	21.37	45689.06
27	94.000	282.000	1182.000	21.37	47697.84
28	94.000	376.000	1276.000	21.37	49706.62
29	13.730	389.730	1289.730	21.37	50000.03

Table 5.2.3(b). Power history (Pattern B)

Step	Step days	Operated days	Integrated days	Power ratio [MW/tU]	Integrated burnup [MWd/tU]
1	50.000	50.000	50.000	42.74	2137.00
2	50.000	100.000	100.000	42.74	4274.00
3	50.000	150.000	150.000	42.74	6411.00
4	50.000	200.000	200.000	42.74	8548.00
5	33.973	233.973	233.973	42.74	10000.01
6	50.000	283.973	283.973	42.74	12137.01
7	50.000	333.973	333.973	42.74	14274.01
8	50.000	383.973	383.973	42.74	16411.01
9	6.027	390.000	390.000	42.74	16668.60
10	60.000	—	450.000	0	16668.60
11	50.000	50.000	500.000	42.74	18805.60
12	27.946	77.946	527.946	42.74	20000.01
13	50.000	127.946	577.946	42.74	22137.01
14	50.000	177.946	627.946	42.74	24274.01
15	50.000	227.946	677.946	42.74	26411.01
16	50.000	277.946	727.946	42.74	28548.01
17	33.973	311.919	761.919	42.74	30000.02
18	50.000	361.919	811.919	42.74	32137.02
19	28.081	390.000	840.000	42.74	33337.20
20	60.000	—	900.000	0	33337.20
21	50.000	50.000	950.000	42.74	35474.20
22	50.000	100.000	1000.000	42.74	37611.20
23	50.000	150.000	1050.000	42.74	39748.20
24	5.892	155.892	1055.892	42.74	40000.02
25	50.000	205.892	1105.892	42.74	42137.02
26	50.000	255.892	1155.892	42.74	44274.02
27	50.000	305.892	1205.892	42.74	46411.02
28	50.000	355.892	1255.892	42.74	48548.02
29	33.973	389.865	1289.865	42.74	50000.03

Table 5.2.3(c). Power history (Pattern C)

Step	Step days	Operated days	Integrated days	Power ratio [MW/tU]	Integrated burnup [MWd/tU]
1	94.000	94.000	94.000	21.37	2008.78
2	94.000	188.000	188.000	21.37	4017.56
3	94.000	282.000	282.000	21.37	6026.34
4	94.000	376.000	376.000	21.37	8035.12
5	14.000	390.000	390.000	21.37	8334.30
6	60.000	—	450.000	0	8334.30
7	38.978	38.978	488.978	42.74	10000.22
8	47.000	85.978	535.978	42.74	12009.00
9	47.000	132.978	582.978	42.74	14017.78
10	47.000	179.978	629.978	42.74	16026.56
11	47.000	226.978	676.978	42.74	18035.34
12	45.968	272.946	722.946	42.74	20000.01
13	47.000	319.946	769.946	42.74	22008.79
14	47.000	366.946	816.946	42.74	24017.57
15	23.054	390.000	840.000	42.74	25002.90
16	60.000	—	900.000	0	25002.90
17	31.000	31.000	931.000	64.11	26990.31
18	31.000	62.000	962.000	64.11	28977.72
19	15.950	77.950	977.950	64.11	30000.27
20	31.000	108.950	1008.950	64.11	31987.68
21	31.000	139.950	1039.950	64.11	33975.09
22	31.000	170.950	1070.950	64.11	35962.50
23	31.000	201.950	1101.950	64.11	37949.91
24	31.980	233.930	1133.930	64.11	40000.15
25	31.000	264.930	1164.930	64.11	41987.56
26	31.000	295.930	1195.930	64.11	43974.97
27	31.000	326.930	1226.930	64.11	45962.38
28	31.000	357.930	1257.930	64.11	47949.79
29	32.000	389.930	1289.930	64.11	50001.31

Table 5.2.7. Activity and activity ratio  
(Enrichment 3.0 wt %, Power constant, Boron content 500 ppm)

Burnup [GWd/tU]	Activity [Ci / g]					Activity ratio	
	Cs-134	Cs-137	Eu-154	Ru-106	Cs-134 / Cs-137	Eu-154 / Cs-137	$(Cs-134/Cs-137)^2 / (Ru-106/Cs-137)$
10.0	1.520E-02	2.894E-02	4.988E-04	1.393E-01	0.5252	0.0172	0.0573
20.0	5.641E-02	5.747E-02	1.965E-03	3.068E-01	0.9816	0.0342	0.1805
30.0	1.214E-01	8.590E-02	4.142E-03	5.110E-01	1.4128	0.0482	0.3355
40.0	1.939E-01	1.137E-01	6.513E-03	6.509E-01	1.7063	0.0573	0.5083
50.0	2.829E-01	1.414E-01	8.847E-03	8.268E-01	2.0011	0.0626	0.6848

Table 5.2.8. Activity and activity ratio  
(Enrichment 4.0 wt %, Power constant, Boron content 500 ppm)

Burnup [GWd/tU]	Activity [Ci / g]					Activity ratio	
	Cs-134	Cs-137	Eu-154	Ru-106	Cs-134 / Cs-137	Eu-154 / Cs-137	$(Cs-134/Cs-137)^2 / (Ru-106/Cs-137)$
10.0	1.361E-02	2.891E-02	4.369E-04	1.180E-01	0.4707	0.0151	0.0543
20.0	5.072E-02	5.736E-02	1.767E-03	2.559E-01	0.8842	0.0308	0.1753
30.0	1.100E-01	8.568E-02	3.861E-03	4.279E-01	1.2841	0.0451	0.3302
40.0	1.776E-01	1.133E-01	6.272E-03	5.530E-01	1.5675	0.0553	0.5035
50.0	2.628E-01	1.410E-01	8.759E-03	7.167E-01	1.8640	0.0621	0.6835

Table 5.2.9. Activity and activity ratio  
(Enrichment 5.0 wt %, Power constant, Boron content 500 ppm)

Burnup [GWd/tU]	Activity [Ci / g]					Activity ratio	
	Cs-134	Cs-137	Eu-154	Ru-106	Cs-134 / Cs-137	Eu-154 / Cs-137	$(Cs-134/Cs-137)^2 / (Ru-106/Cs-137)$
10.0	1.249E-02	2.889E-02	3.941E-04	1.047E-01	0.4322	0.0136	0.0515
20.0	4.654E-02	5.729E-02	1.615E-03	2.223E-01	0.8124	0.0282	0.1701
30.0	1.012E-01	8.555E-02	3.620E-03	3.702E-01	1.1834	0.0423	0.3236
40.0	1.641E-01	1.131E-01	6.037E-03	4.796E-01	1.4512	0.0534	0.4966
50.0	2.445E-01	1.407E-01	8.644E-03	6.257E-01	1.7378	0.0614	0.6789

Table 5.2.10. Cs-134/Cs-137 Activity ratio enrichment dependency  
(Power constant, Boron content 500 ppm)

Burnup [GWd/tU]	Eu-134/Cs-137 Activity ratio			Relative activity Ratio (4 wt % value = 1.0)	
	Initial enrichment (wt %)			Initial enrichment (wt %)	
	3	4	5	3	5
10.0	0.525	0.471	0.432	1.116	0.918
20.0	0.982	0.884	0.812	1.110	0.919
30.0	1.413	1.284	1.183	1.100	0.922
40.0	1.706	1.568	1.451	1.089	0.926
50.0	2.001	1.864	1.738	1.074	0.932

Table 5.2.11. Eu-154/Cs-137 Activity ratio enrichment dependency  
(Power constant, Boron content 500 ppm)

Burnup [GWd/tU]	Eu-154/Cs-137 Activity ratio			Relative activity Ratio (4 wt % value = 1.0)	
	Initial enrichment (wt %)			Initial enrichment (wt %)	
	3	4	5	3	5
10.0	0.017	0.015	0.014	1.140	0.903
20.0	0.034	0.031	0.028	1.110	0.915
30.0	0.048	0.045	0.042	1.070	0.939
40.0	0.057	0.055	0.053	1.035	0.964
50.0	0.063	0.062	0.061	1.007	0.989

Table 5.2.12.  $(\text{Cs-134/Cs-137})^2 / (\text{Ru-106/Cs-137})$  Activity ratio enrichment dependency  
(Power constant, Boron content 500 ppm)

Burnup [GWd/tU]	$(\text{Cs-134/Cs-137})^2 / (\text{Ru-106/Cs-137})$ Activity ratio			Relative activity Ratio (4 wt % value = 1.0)	
	Initial enrichment (wt %)			Initial enrichment (wt %)	
	3	4	5	3	5
10.0	0.057	0.054	0.052	1.056	0.949
20.0	0.180	0.175	0.170	1.030	0.971
30.0	0.336	0.330	0.324	1.016	0.980
40.0	0.508	0.503	0.497	1.010	0.986
50.0	0.685	0.683	0.679	1.002	0.993

Table 5.2.13. Activity and activity ratio  
(Enrichment 4.0 wt %, Power CASE : A, Boron content 500 ppm)

Burnup [GWd/tU]	Activity [Ci / g]					Activity ratio	
	Cs-134	Cs-137	Eu-154	Ru-106	Cs-134 / Cs-137	Eu-154 / Cs-137	$(Cs-134/Cs-137)^2 / (Ru-106/Cs-137)$
10.0	1.344E-02	2.898E-02	4.328E-04	1.246E-01	0.4638	0.0149	0.0500
20.0	5.414E-02	5.782E-02	1.785E-03	3.067E-01	0.9363	0.0309	0.1653
30.0	1.102E-01	8.602E-02	3.847E-03	4.453E-01	1.2811	0.0447	0.3170
40.0	1.838E-01	1.140E-01	6.316E-03	6.031E-01	1.6119	0.0554	0.4912
50.0	2.263E-01	1.397E-01	8.589E-03	5.366E-01	1.6202	0.0615	0.6832

Table 5.2.14. Activity and activity ratio  
(Enrichment 4.0 wt %, Power CASE : B, Boron content 500 ppm)

Burnup [GWd/tU]	Activity [Ci / g]					Activity ratio	
	Cs-134	Cs-137	Eu-154	Ru-106	Cs-134 / Cs-137	Eu-154 / Cs-137	$(Cs-134/Cs-137)^2 / (Ru-106/Cs-137)$
10.0	1.361E-02	2.891E-02	4.369E-04	1.180E-01	0.4707	0.0151	0.0543
20.0	5.072E-02	5.736E-02	1.767E-03	2.559E-01	0.8842	0.0308	0.1753
30.0	1.100E-01	8.568E-02	3.861E-03	4.279E-01	1.2840	0.0451	0.3301
40.0	1.776E-01	1.133E-01	6.272E-03	5.530E-01	1.5676	0.0553	0.5035
50.0	2.628E-01	1.410E-01	8.759E-03	7.167E-01	1.8640	0.0621	0.6835

Table 5.2.15. Activity and activity ratio  
(Enrichment 4.0 wt %, Power CASE : C, Boron content 500 ppm)

Burnup [GWd/tU]	Activity [Ci / g]					Activity ratio	
	Cs-134	Cs-137	Eu-154	Ru-106	Cs-134 / Cs-137	Eu-154 / Cs-137	$(Cs-134/Cs-137)^2 / (Ru-106/Cs-137)$
10.0	1.295E-02	2.867E-02	4.320E-04	9.840E-02	0.4516	0.0151	0.0594
20.0	5.223E-02	5.731E-02	1.784E-03	2.633E-01	0.9114	0.0311	0.1808
30.0	1.101E-01	8.555E-02	3.845E-03	4.269E-01	1.2874	0.0449	0.3321
40.0	1.929E-01	1.140E-01	6.325E-03	6.557E-01	1.6914	0.0555	0.4976
50.0	2.884E-01	1.423E-01	8.811E-03	8.747E-01	2.0266	0.0619	0.6682

Table 5.2.16. Activity ratio (Enrichment 4.0 wt %, Boron content 500 ppm)

Burnup [GWd/tU]	Cs-134/Cs-137 Activity ratio			Relative activity Ratio (CASE : B value = 1.0)	
	Power pattern			Power pattern	
	A	B	C	A	C
10.0	0.4638	0.4707	0.4516	0.985	0.959
20.0	0.9363	0.8842	0.9114	1.059	1.031
30.0	1.2811	1.2840	1.2874	0.998	1.003
40.0	1.6119	1.5676	1.6914	1.028	1.079
50.0	1.6202	1.8640	2.0266	0.869	1.087

Table 5.2.17. Activity ratio (Enrichment 4.0 wt %, Boron content 500 ppm)

Burnup [GWd/tU]	Eu-154/Cs-137 Activity ratio			Relative activity Ratio (CASE : B value = 1.0)	
	Power pattern			Power pattern	
	A	B	C	A	C
10.0	0.0149	0.0151	0.0151	0.988	0.997
20.0	0.0309	0.0308	0.0311	1.002	1.010
30.0	0.0447	0.0451	0.0449	0.992	0.997
40.0	0.0554	0.0553	0.0555	1.001	1.002
50.0	0.0615	0.0621	0.0619	0.990	0.997

Table 5.2.18. Activity ratio (Enrichment 4.0 wt %, Boron content 500 ppm)

Burnup [GWd/tU]	$(\text{Cs-134}/\text{Cs-137})^2 / (\text{Ru-106}/\text{Cs-137})$ Activity ratio			Relative activity Ratio (CASE : B value = 1.0)	
	Power pattern			Power pattern	
	A	B	C	A	C
10.0	0.0500	0.0543	0.0594	0.921	1.094
20.0	0.1653	0.1753	0.1808	0.943	1.031
30.0	0.3170	0.3301	0.3321	0.960	1.006
40.0	0.4912	0.5035	0.4976	0.975	0.988
50.0	0.6832	0.6835	0.6682	1.000	0.978

Table 5.2.19. Activity and activity ratio  
(Enrichment 4.0 wt %, Power constant, Boron content 500 ppm)

Burnup [GWd/tU]	Activity [Ci / g]					Activity ratio	
	Cs-134	Cs-137	Eu-154	Ru-106	Cs-134 / Cs-137	Eu-154 / Cs-137	(Cs-134/Cs-137) <sup>2</sup> / (Ru-106/Cs-137)
10.0	1.361E-02	2.891E-02	4.369E-04	1.180E-01	0.4707	0.0151	0.0543
20.0	5.072E-02	5.736E-02	1.767E-03	2.559E-01	0.8842	0.0308	0.1753
30.0	1.100E-01	8.568E-02	3.861E-03	4.279E-01	1.2841	0.0451	0.3302
40.0	1.776E-01	1.133E-01	6.272E-03	5.530E-01	1.5675	0.0553	0.5035
50.0	2.628E-01	1.410E-01	8.759E-03	7.167E-01	1.8640	0.0621	0.6835

Table 5.2.20. Activity and activity ratio  
(Enrichment 4.0 wt %, Power constant, Boron content 0 ppm)

Burnup [GWd/tU]	Activity [Ci / g]					Activity ratio	
	Cs-134	Cs-137	Eu-154	Ru-106	Cs-134 / Cs-137	Eu-154 / Cs-137	(Cs-134/Cs-137) <sup>2</sup> / (Ru-106/Cs-137)
10.0	1.351E-02	2.891E-02	4.331E-04	1.174E-01	0.4672	0.0150	0.0537
20.0	5.038E-02	5.736E-02	1.750E-03	2.547E-01	0.8783	0.0305	0.1737
30.0	1.094E-01	8.568E-02	3.821E-03	4.264E-01	1.2766	0.0446	0.3275
40.0	1.768E-01	1.133E-01	6.202E-03	5.516E-01	1.5597	0.0547	0.4998
50.0	2.617E-01	1.410E-01	8.652E-03	7.155E-01	1.8560	0.0614	0.6788

Table 5.2.21. Activity and activity ratio  
(Enrichment 4.0 wt %, Power constant, Boron content 1000 ppm)

Burnup [GWd/tU]	Activity [Ci / g]					Activity ratio	
	Cs-134	Cs-137	Eu-154	Ru-106	Cs-134 / Cs-137	Eu-154 / Cs-137	(Cs-134/Cs-137) <sup>2</sup> / (Ru-106/Cs-137)
10.0	1.371E-02	2.891E-02	4.408E-04	1.185E-01	0.4742	0.0152	0.0548
20.0	5.105E-02	5.736E-02	1.784E-03	2.570E-01	0.8899	0.0311	0.1768
30.0	1.106E-01	8.568E-02	3.901E-03	4.294E-01	1.2913	0.0455	0.3327
40.0	1.785E-01	1.133E-01	6.341E-03	5.544E-01	1.5751	0.0560	0.5071
50.0	2.639E-01	1.410E-01	8.864E-03	7.178E-01	1.8716	0.0629	0.6880

Table 5.2.22. Activity and activity ratio  
(Enrichment 4.0 wt %, Power constant, Boron content 1000–0 ppm linear change)

Burnup [GWd/tU]	Activity [Ci / g]					Activity ratio	
	Cs-134	Cs-137	Eu-154	Ru-106	Cs-134 / Cs-137	Eu-154 / Cs-137	(Cs-134/Cs-137) <sup>2</sup> / (Ru-106/Cs-137)
10.0	1.363E-02	2.891E-02	4.377E-04	1.183E-01	0.4713	0.0151	0.0543
20.0	5.073E-02	5.736E-02	1.770E-03	2.560E-01	0.8844	0.0309	0.1753
30.0	1.100E-01	8.568E-02	3.858E-03	4.281E-01	1.2835	0.0450	0.3297
40.0	1.778E-01	1.133E-01	6.286E-03	5.531E-01	1.5687	0.0555	0.5042
50.0	2.624E-01	1.410E-01	8.727E-03	7.167E-01	1.8614	0.0619	0.6816

Table 5.2.23. Cs-134/Cs-137 Activity ratio boron content dependency  
(Enrichment 4 wt %, Power constant)

Burnup [GWd/tU]	Cs-134/Cs-137 Activity ratio				Relative activity ratio (500 ppm value = 1.0)		
	Boron content [ppm]				Boron content [ppm]		
	0	500	1000	Linear	0	1000	Linear
10.0	0.467	0.471	0.474	0.471	0.993	1.007	1.001
20.0	0.878	0.884	0.890	0.884	0.993	1.007	1.000
30.0	1.277	1.284	1.291	1.284	0.994	1.006	1.000
40.0	1.560	1.568	1.575	1.569	0.995	1.005	1.001
50.0	1.856	1.864	1.872	1.861	0.996	1.004	0.999

Table 5.2.24. Eu-154/Cs-137 Activity ratio boron content dependency  
(Enrichment 4 wt %, Power constant)

Burnup [GWd/tU]	Cs-154/Cs-137 Activity ratio				Relative activity ratio (500 ppm value = 1.0)		
	Boron content [ppm]				Boron content [ppm]		
	0	500	1000	Linear	0	1000	Linear
10.0	0.015	0.015	0.015	0.015	0.991	1.009	1.002
20.0	0.031	0.031	0.031	0.031	0.990	1.010	1.001
30.0	0.045	0.045	0.046	0.045	0.990	1.010	0.999
40.0	0.055	0.055	0.056	0.055	0.989	1.011	1.002
50.0	0.061	0.062	0.063	0.062	0.988	1.012	0.996

Table 5.2.25.  $(\text{Cs-134/Cs-137})^2 / (\text{Ru-106/Cs-137})$  Activity ratio boron content dependency  
(Enrichment 4 wt %, Power constant)

Burnup [GWd/tU]	$(\text{Cs-134/Cs-137})^2 / (\text{Ru-106/Cs-137})$ Activity ratio				Relative activity ratio (500 ppm value = 1.0)		
	Boron content [ppm]				Boron content [ppm]		
	0	500	1000	Linear	0	1000	Linear
10.0	0.054	0.054	0.055	0.054	0.990	1.010	1.000
20.0	0.174	0.175	0.177	0.175	0.991	1.009	1.000
30.0	0.327	0.330	0.333	0.330	0.992	1.008	0.999
40.0	0.500	0.503	0.507	0.504	0.993	1.007	1.001
50.0	0.679	0.683	0.688	0.682	0.993	1.007	0.997

Table 5.2.26. BWR fuel rod specification

Cell pitch [cm]	1.63
Pellet radius [cm]	0.529
Clad radius [cm]	0.615
Clad thickness [cm]	0.086
Cell pitch [cm]	0.9296
Fuel temperature [K]	900
Clad temperature [K]	559
Moderator temperature [K]	559

Table 5.2.27. Number densities (BWR fuel cell)

	Fuel			Clad	Moderator		
	3%	4%	5%		Void 0%	Void 40%	Void 70%
U-235	6.758E-04	9.009E-04	1.126E-03	–	–	–	–
U-238	2.157E-02	2.135E-02	2.112E-02	–	–	–	–
Zr-nat	–	–	–	4.337E-02	–	–	–
Fe-nat							
Cr-nat	–	–	–	–	–	–	–
H-1	–	–	–	–	8.198E-02	6.270E-02	4.824E-02
O-16	4.647E-02	4.647E-02	4.647E-02	–	4.099E-02	3.135E-02	2.412E-02
C-12				–			
B-10	–	–	–	–	–	–	–
Ni-nat	–	–	–	–	–	–	–
Al-27	–	–	–	–	–	–	–
Si-nat	–	–	–	–	–	–	–
Cu-nat	–	–	–	–	–	–	–
Mn-55	–	–	–	–	–	–	–

Table 5.2.28(a). Power history (Pattern A)

Step	Step days	Operated days	Integrated days	Power ratio [MW/tU]	Integrated burnup [MWd/tU]
1	52.000	52.000	52.000	38.46	1999.92
2	52.000	104.000	104.000	38.46	3999.84
3	52.000	156.000	156.000	38.46	5999.76
4	52.000	208.000	208.000	38.46	7999.68
5	52.010	260.010	260.010	38.46	10000.00
6	52.000	312.010	312.010	38.46	11999.92
7	52.000	364.010	364.010	38.46	13999.84
8	25.990	390.000	390.000	38.46	14999.40
9	90.000	—	480.000	0	14999.40
10	62.441	62.441	542.441	32.04	17000.00
11	62.422	124.863	604.863	32.04	19000.00
12	31.211	156.074	636.074	32.04	20000.00
13	62.422	218.496	698.496	32.04	22000.00
14	62.422	280.918	760.918	32.04	24000.00
15	62.422	343.340	823.340	32.04	26000.00
16	46.660	327.578	870.000	32.04	27495.00
17	90.000	—	960.000	0	27495.00
18	26.262	26.262	986.262	19.23	28000.02
19	104.00	130.265	1090.265	19.23	30000.00
20	104.00	234.265	1194.265	19.23	31999.92
21	104.00	338.265	1298.265	19.23	33999.84
22	51.735	390.000	1350.000	19.23	34994.70
23	90.000	—	1440.000	0	34994.70
24	156.00	156.000	1596.000	12.82	36994.62
25	156.00	312.000	1752.000	12.82	38994.54
26	78.429	390.429	1830.429	12.82	40000.00

Table 5.2.28(b). Power history (Pattern B)

Step	Step days	Operated days	Integrated days	Power ratio [MW/tU]	Integrated burnup [MWd/tU]
1	78.000	78.000	78.000	25.64	1999.92
2	78.000	156.000	156.000	25.64	3999.84
3	78.000	234.000	234.000	25.64	5999.76
4	78.000	312.000	312.000	25.64	7999.68
5	78.016	390.016	390.016	25.64	10000.00
6	90.000	—	480.016	0	10000.00
7	78.000	78.000	558.016	25.64	11999.92
8	78.000	156.000	636.016	25.64	13999.84
9	78.000	234.000	714.016	25.64	15999.76
10	78.000	312.000	792.016	25.64	17999.68
11	78.016	390.016	870.031	25.64	20000.00
12	90.000	—	960.031	0	20000.00
13	78.000	78.000	1038.031	25.64	21999.92
14	78.000	156.000	1116.03	25.64	23999.84
15	78.000	234.000	1194.03	25.64	25999.76
16	78.000	312.000	1272.031	25.64	27999.68
17	78.016	390.016	1350.047	25.64	30000.00
18	90.000	—	1440.047	0	30000.00
19	78.000	78.000	1518.047	25.64	31999.92
20	78.000	156.000	1596.047	25.64	33999.84
21	78.000	234.000	1674.047	25.64	25999.76
22	78.000	312.000	1752.047	25.64	37999.68
23	78.016	312.016	1830.062	25.64	40000.00

Table 5.2.28(c). Power history (Pattern C)

Step	Step days	Operated eays	Integrated days	Power ratio [MW/tU]	Integrated burnup [MWd/tU]
1	156.00	156.000	156.000	12.82	1999.92
2	156.00	312.000	312.000	12.82	3999.84
3	78.000	390.000	390.000	12.82	4999.80
4	90.000	—	480.000	0	4999.80
5	104.00	104.000	584.000	19.23	6999.72
6	104.00	208.000	688.000	19.23	8999.64
7	52.021	260.021	740.021	19.23	10000.00
8	104.00	364.021	844.021	19.23	11999.92
9	25.979	390.000	870.000	19.23	12499.50
10	90.000	—	960.000	0	12499.50
11	62.000	62.000	1022.000	32.04	14485.98
12	62.000	124.000	1084.000	32.04	16472.46
13	63.000	187.000	1147.000	32.04	18490.98
14	47.098	234.098	1194.098	32.04	20000.00
15	63.000	297.098	1257.098	32.04	22018.52
16	63.000	360.098	1320.098	32.04	24037.04
17	29.902	390.000	1350.000	32.04	24995.10
18	90.000	—	1440.000	0	24995.10
19	52.000	52.000	1492.000	38.46	26995.02
20	52.000	104.000	1544.000	38.46	28994.94
21	26.133	130.133	1570.133	38.46	30000.00
22	52.000	182.133	1622.133	38.46	31999.92
23	52.000	234.133	1674.133	38.46	33999.84
24	52.000	286.133	1726.133	38.46	35999.76
25	52.000	338.133	1778.133	38.46	37999.68
26	52.010	390.143	1830.143	38.46	39999.98

Table 5.2.29. Dancoff factor

Void ratio (%)	Dancoff factor
0	0.276
40	0.399
70	0.551

Table 5.2.30. Initial enrichment

Case	Initial enrichment (wt %)	Remark
A	3	
B	4	Standard case
C	5	

Table 5.2.31. Initial enrichment

Case	Power history			Remark
A	1 <sup>st</sup> Cycle	38.46 MW/tU	(Standard case × 1.5)	
	2 <sup>nd</sup> Cycle	32.04 MW/tU	(Standard case × 1.25)	
	3 <sup>rd</sup> Cycle	19.23 MW/tU	(Standard case × 0.75)	
	4 <sup>th</sup> Cycle	12.82 MW/tU	(Standard case × 0.5)	
B	Every cycle	25.64 MW/tU	Constant	Standard case
C	1 <sup>st</sup> Cycle	38.46 MW/tU	(Standard case × 0.5)	
	2 <sup>nd</sup> Cycle	32.04 MW/tU	(Standard case × 0.75)	
	3 <sup>rd</sup> Cycle	19.23 MW/tU	(Standard case × 1.25)	
	4 <sup>th</sup> Cycle	12.82 MW/tU	(Standard case × 1.5)	

Table 5.2.32. Void ratio

Case	Void ratio	Remark
A	0%	
B	40%	Standard case
C	70%	

Table 5.2.33. Activity and activity ratio  
(Enrichment 3.0 wt %, Power constant, Void ratio 40%)

Burnup [GWd/tU]	Activity [Ci/g]				Activity ratio		
	Cs-134	Cs-137	Eu-154	Ru-106	Cs-134 / Cs-137	Eu-154 / Cs-137	$(Cs-134/Cs-137)^2 / (Ru-106/Cs-137)$
10.0	1.273E-02	2.879E-02	4.112E-04	1.110E-01	0.4420	0.0143	0.0507
20.0	4.675E-02	5.690E-02	1.551E-03	2.376E-01	0.8217	0.0273	0.1617
30.0	9.580E-02	8.432E-02	3.140E-03	3.561E-01	1.1361	0.0372	0.3056
40.0	1.551E-01	1.111E-01	4.822E-03	4.629E-01	1.3966	0.0434	0.4679

Table 5.2.34. Activity and activity ratio  
(Enrichment 4.0 wt %, Power constant, Void ratio 40%)

Burnup [GWd/tU]	Activity [Ci/g]				Activity ratio		
	Cs-134	Cs-137	Eu-154	Ru-106	Cs-134 / Cs-137	Eu-154 / Cs-137	$(Cs-134/Cs-137)^2 / (Ru-106/Cs-137)$
10.0	1.125E-02	2.876E-02	3.582E-04	9.360E-02	0.3912	0.0125	0.0470
20.0	4.117E-02	5.680E-02	1.386E-03	1.943E-01	0.7248	0.0244	0.1536
30.0	8.424E-02	8.411E-02	2.906E-03	2.889E-01	1.0016	0.0345	0.2921
40.0	1.373E-01	1.107E-01	4.619E-03	3.783E-01	1.2399	0.0417	0.4498

Table 5.2.35. Activity and activity ratio  
(Enrichment 5.0 wt %, Power constant, Void ratio 40%)

Burnup [GWd/tU]	Activity [Ci/g]				Activity ratio		
	Cs-134	Cs-137	Eu-154	Ru-106	Cs-134 / Cs-137	Eu-154 / Cs-137	$(Cs-134/Cs-137)^2 / (Ru-106/Cs-137)$
10.0	1.027E-02	2.874E-02	3.224E-04	8.321E-02	0.3571	0.0112	0.0441
20.0	3.736E-02	5.674E-02	1.267E-03	1.672E-01	0.6585	0.0223	0.1471
30.0	7.607E-02	8.398E-02	2.719E-03	2.451E-01	0.9058	0.0324	0.2811
40.0	1.235E-01	1.105E-01	4.445E-03	3.190E-01	1.1178	0.0402	0.4328

Table 5.2.36. Cs-134/Cs-137 Activity ratio enrichment dependency  
(Power constant, Void ratio 40%)

Burnup [GWd/tU]	Cs-134/Cs-137 Activity ratio			Relative activity ratio (4 wt % value = 1.0)	
	Initial enrichment (wt %)			Initial enrichment (wt %)	
	3	4	5	3	5
10.0	0.4420	0.3912	0.3571	1.130	0.913
20.0	0.8217	0.7248	0.6585	1.134	0.909
30.0	1.1361	1.0016	0.9058	1.134	0.904
40.0	1.3966	1.2399	1.1178	1.126	0.902

Table 5.2.37. Eu-154/Cs-137 Activity ratio enrichment dependency  
(Power constant, Void ratio 40%)

Burnup [GWd/tU]	Eu-154/Cs-137 Activity ratio			Relative activity ratio (4 wt% value = 1.0)	
	Initial enrichment (wt %)			Initial enrichment (wt %)	
	3	4	5	3	5
10.0	0.0143	0.0125	0.0112	1.147	0.901
20.0	0.0273	0.0244	0.0223	1.117	0.915
30.0	0.0372	0.0345	0.0324	1.078	0.937
40.0	0.0434	0.0417	0.0402	1.041	0.964

Table 5.2.38.  $(\text{Cs-134/Cs-137})^2 / (\text{Ru-106/Cs-137})$  Activity ratio enrichment dependency  
(Power constant, Void ratio 40%)

Burnup [GWd/tU]	$(\text{Cs-134/Cs-137})^2 / (\text{Ru-106/Cs-137})$ Activity ratio			Relative activity ratio (4 wt % value = 1.0)	
	Initial enrichment (wt %)			Initial enrichment (wt %)	
	3	4	5	3	5
10.0	0.0507	0.0470	0.0441	1.077	0.937
20.0	0.1617	0.1536	0.1471	1.052	0.958
30.0	0.3056	0.2921	0.2811	1.046	0.963
40.0	0.4679	0.4498	0.4328	1.040	0.962

Table 5.2.39. Activity and activity ratio (Enrichment 4.0 wt %, Power CASE : A, Void 40%)

Burnup [GWd/tU]	Activity [Ci/g]				Activity ratio		
	Cs-134	Cs-137	Eu-154	Ru-106	Cs-134 / Cs-137	Eu-154 / Cs-137	$(Cs-134 / Cs-137)^2 / (Ru-106/Cs-137)$
10.0	1.145E-02	2.888E-02	3.582E-04	1.026E-01	0.3964	0.0124	0.0442
20.0	4.187E-02	5.710E-02	1.385E-03	2.082E-01	0.7332	0.0243	0.1474
30.0	8.152E-02	8.436E-02	2.875E-03	2.745E-01	1.9663	0.0341	0.2869
40.0	1.129E-01	1.092E-01	4.490E-03	2.604E-01	1.0332	0.0411	0.4478

Table 5.2.40. Activity and activity ratio (Enrichment 4.0 wt %, Power CASE : B, Void 40%)

Burnup [GWd/tU]	Activity [Ci/g]				Activity ratio		
	Cs-134	Cs-137	Eu-154	Ru-106	Cs-134 / Cs-137	Eu-154 / Cs-137	$(Cs-134 / Cs-137)^2 / (Ru-106/Cs-137)$
10.0	1.125E-02	2.876E-02	3.582E-04	9.360E-02	0.3912	0.0125	0.0470
20.0	4.117E-02	5.680E-02	1.386E-03	1.943E-01	0.7248	0.0244	0.1536
30.0	8.424E-02	8.411E-02	2.906E-03	2.889E-01	1.0016	0.0345	0.2921
40.0	1.373E-01	1.107E-01	4.619E-03	3.783E-01	1.2399	0.0417	0.4498

Table 5.2.41. Activity and activity ratio (Enrichment 4.0 wt %, Power CASE : C, Void 40%)

Burnup [GWd/tU]	Activity [Ci/g]				Activity ratio		
	Cs-134	Cs-137	Eu-154	Ru-106	Cs-134 / Cs-137	Eu-154 / Cs-137	$(Cs-134 / Cs-137)^2 / (Ru-106/Cs-137)$
10.0	1.092E-02	2.851E-02	3.552E-04	7.962E-02	0.3831	0.0125	0.0526
20.0	4.207E-02	5.661E-02	1.388E-03	1.941E-01	0.7430	0.0245	0.1610
30.0	8.846E-02	8.431E-02	2.909E-03	3.122E-01	1.0491	0.0345	0.2972
40.0	1.563E-01	1.122E-01	4.664E-03	4.822E-01	1.3938	0.0416	0.4519

Table 5.2.42. Cs-134/Cs-137 Activity ratio power history dependency  
(Enrichment 4.0 wt %, Void ratio 40%)

Burnup [GWd/tU]	Cs-134/Cs-137 Activity ratio			Relative activity ratio (CASE B value = 1.0)	
	Power pattern			Power pattern	
	A	B	C	A	C
10.0	0.396	0.391	0.383	1.013	0.979
20.0	0.733	0.725	0.743	1.012	1.025
30.0	0.966	1.002	1.049	0.965	1.047
40.0	1.033	1.240	1.394	0.833	1.124

Table 5.2.43. Eu-154/Cs-137 Activity ratio power history dependency  
(Enrichment 4.0 wt %, Void ratio 40%)

Burnup [GWd/tU]	Eu-154/Cs-137 Activity ratio			Relative activity ratio (CASE B value = 1.0)	
	Power pattern			Power pattern	
	A	B	C	A	C
10.0	0.012	0.012	0.012	0.996	1.001
20.0	0.024	0.024	0.025	0.994	1.004
30.0	0.034	0.035	0.034	0.987	0.999
40.0	0.041	0.042	0.042	0.985	0.997

Table 5.2.44.  $(\text{Cs-134/Cs-137})^2 / (\text{Ru-106/Cs-137})$  Activity ratio power history dependency  
(Enrichment 4.0 wt %, Void ratio 40%)

Burnup [GWd/tU]	$(\text{Cs-134/Cs-137})^2 / (\text{Ru-106/Cs-137})$ Activity ratio			Relative activity ratio (CASE B value = 1.0)	
	Power pattern			Power pattern	
	A	B	C	A	C
10.0	0.044	0.047	0.053	0.941	1.117
20.0	0.147	0.154	0.161	0.960	1.048
30.0	0.287	0.292	0.297	0.982	1.018
40.0	0.448	0.450	0.452	0.996	1.005

Table 5.2.45. Activity and activity ratio (Enrichment 4.0 wt %, Power constant, Void ratio 0%)

Burnup [GWd/tU]	Activity [Ci/g]				Activity ratio		
	Cs-134	Cs-137	Eu-154	Ru-106	Cs-134 / Cs-137	Eu-154 / Cs-137	$(Cs-134/Cs-137)^2 / (Ru-106/Cs-137)$
10.0	9.750E-03	2.876E-02	3.069E-04	8.638E-02	0.3390	0.0107	0.0383
20.0	3.614E-02	5.679E-02	1.158E-03	1.788E-01	0.6364	0.0204	0.1287
30.0	7.546E-02	8.409E-02	2.407E-03	2.694E-01	0.8974	0.0286	0.2514
40.0	1.263E-01	1.107E-01	3.826E-03	3.617E-01	1.1412	0.0346	0.3985

Table 5.2.46. Activity and activity ratio (Enrichment 4.0 wt %, Power constant, Void ratio 40%)

Burnup [GWd/tU]	Activity [Ci/g]				Activity ratio		
	Cs-134	Cs-137	Eu-154	Ru-106	Cs-134 / Cs-137	Eu-154 / Cs-137	$(Cs-134/Cs-137)^2 / (Ru-106/Cs-137)$
10.0	1.125E-02	2.876E-02	3.582E-04	9.360E-02	0.3912	0.0125	0.0470
20.0	4.117E-02	5.680E-02	1.386E-03	1.943E-01	0.7248	0.0244	0.1536
30.0	8.424E-02	8.411E-02	2.906E-03	2.889E-01	1.0016	0.0345	0.2921
40.0	1.373E-01	1.107E-01	4.619E-03	3.783E-01	1.2399	0.0417	0.4498

Table 5.2.47. Activity and activity ratio (Enrichment 4.0 wt %, Power constant, Void ratio 70%)

Burnup [Gwd/tU]	Activity [Ci/g]				Activity ratio		
	Cs-134	Cs-137	Eu-154	Ru-106	Cs-134 / Cs-137	Eu-154 / Cs-137	$(Cs-134/Cs-137)^2 / (Ru-106/Cs-137)$
10.0	1.297E-02	2.876E-02	4.237E-04	1.017E-01	0.4509	0.0147	0.0575
20.0	4.693E-02	5.681E-02	1.688E-03	2.108E-01	0.8261	0.0297	0.1839
30.0	9.443E-02	8.412E-02	3.591E-03	3.092E-01	1.1226	0.0427	0.3428
40.0	1.506E-01	1.107E-01	5.763E-03	3.964E-01	1.3604	0.0521	0.5168

Table 5.2.48. Cs-134/Cs-137 Activity ratio void ratio dependency  
(Power constant, Enrichment 4 wt %)

Burnup [GWd/tU]	Cs-134/Cs-137 Activity ratio			Relative activity ratio (Void 40% value = 1.0)	
	Void ratio (%)			Void ratio (%)	
	0	40	70	0	70
10.0	0.339	0.391	0.451	0.867	1.153
20.0	0.636	0.725	0.826	0.878	1.140
30.0	0.897	1.002	1.123	0.896	1.121
40.0	1.141	1.240	1.360	0.920	1.097

Table 5.2.49. Eu-154/Cs-137 Activity ratio void ratio dependency  
(Power constant, Enrichment 4 wt %)

Burnup [GWd/tU]	Eu-154/Cs-137 Activity ratio			Relative activity ratio (Void 40% value = 1.0)	
	Void ratio (%)			Void ratio (%)	
	0	40	70	0	70
10.0	0.011	0.012	0.015	0.857	1.183
20.0	0.020	0.024	0.030	0.836	1.218
30.0	0.029	0.035	0.043	0.829	1.236
40.0	0.035	0.042	0.052	0.828	1.248

Table 5.2.50.  $(\text{Cs-134/Cs-137})^2 / (\text{Ru-106/Cs-137})$  Activity ratio void ratio dependency  
(Power constant, Enrichment 4 wt %)

Burnup [GWd/tU]	$(\text{Cs-134/Cs-137})^2 / (\text{Ru-106/Cs-137})$ Activity ratio			Relative activity ratio (Void 40% value = 1.0)	
	Void ratio (%)			Void ratio (%)	
	0	40	70	0	70
10.0	0.038	0.047	0.058	0.814	1.223
20.0	0.129	0.154	0.184	0.838	1.197
30.0	0.251	0.292	0.343	0.861	1.174
40.0	0.399	0.450	0.517	0.886	1.149

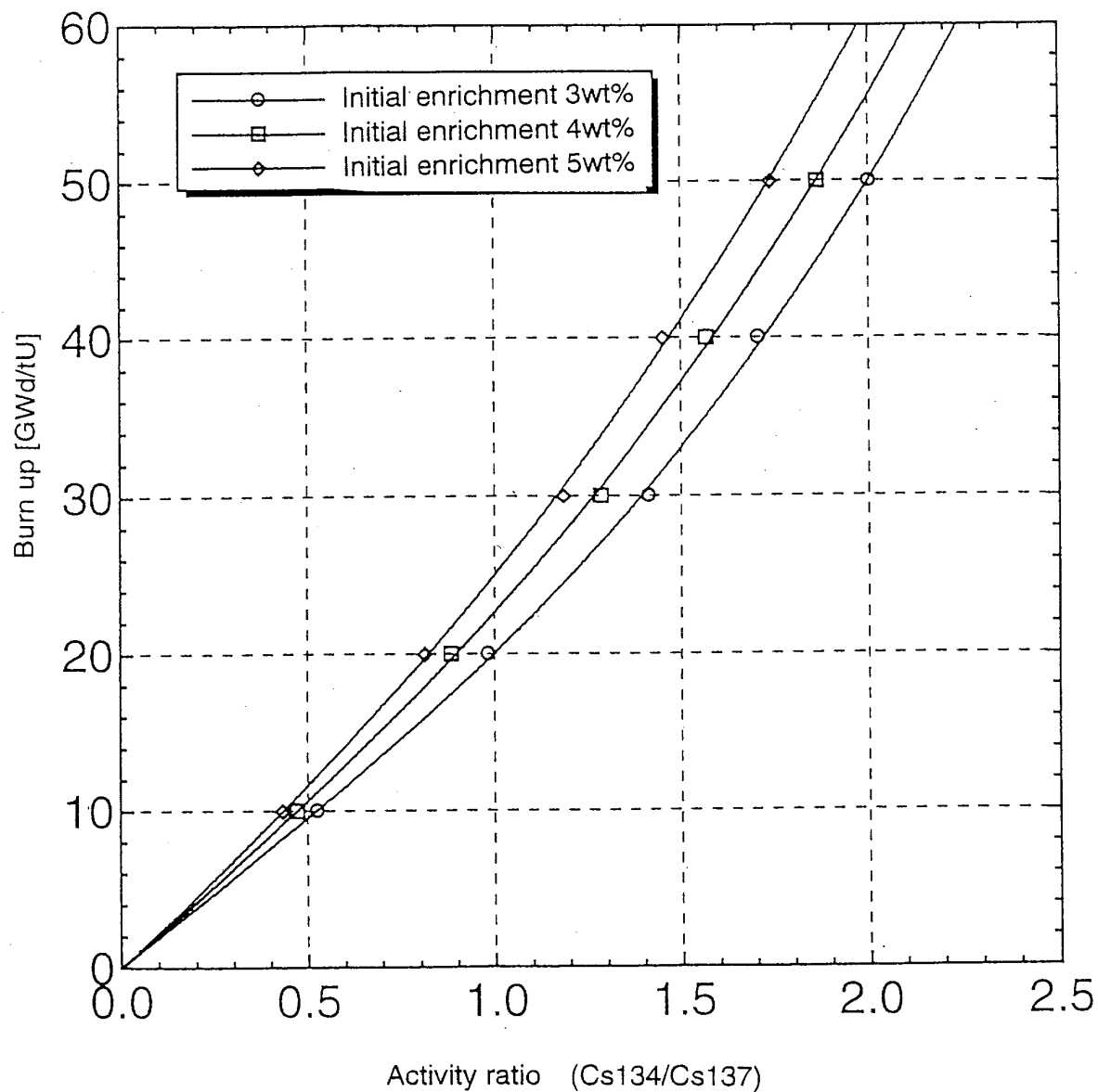


Fig. 5.2.1. Cs Activity ratio (Cs-134/Cs-137) vs. burnup  
(Initial enrichment dependency, PWR).

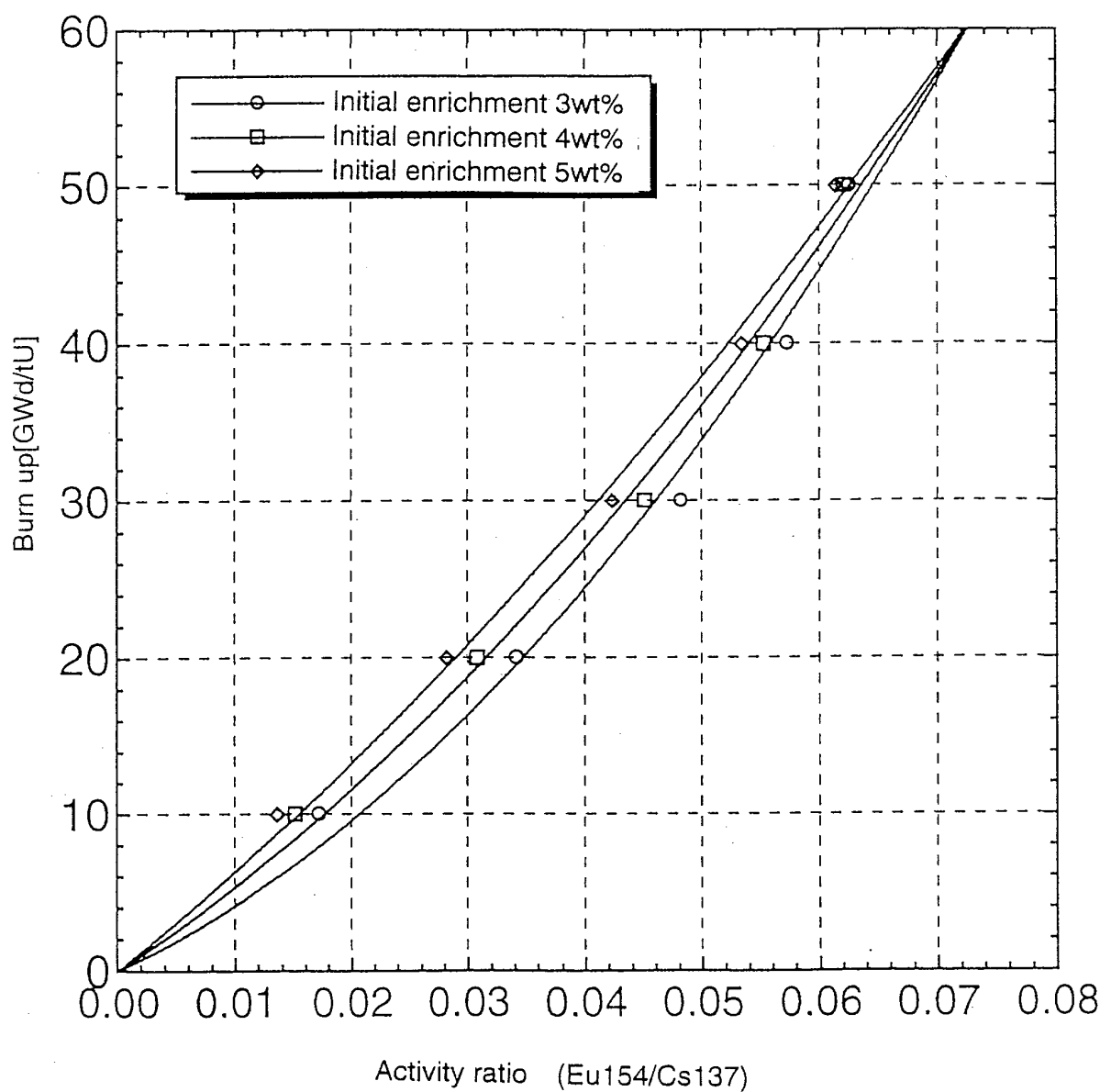


Fig. 5.2.2. Eu Activity ratio (Eu-154/Cs-137) vs. burnup  
(Initial enrichment dependency, PWR).

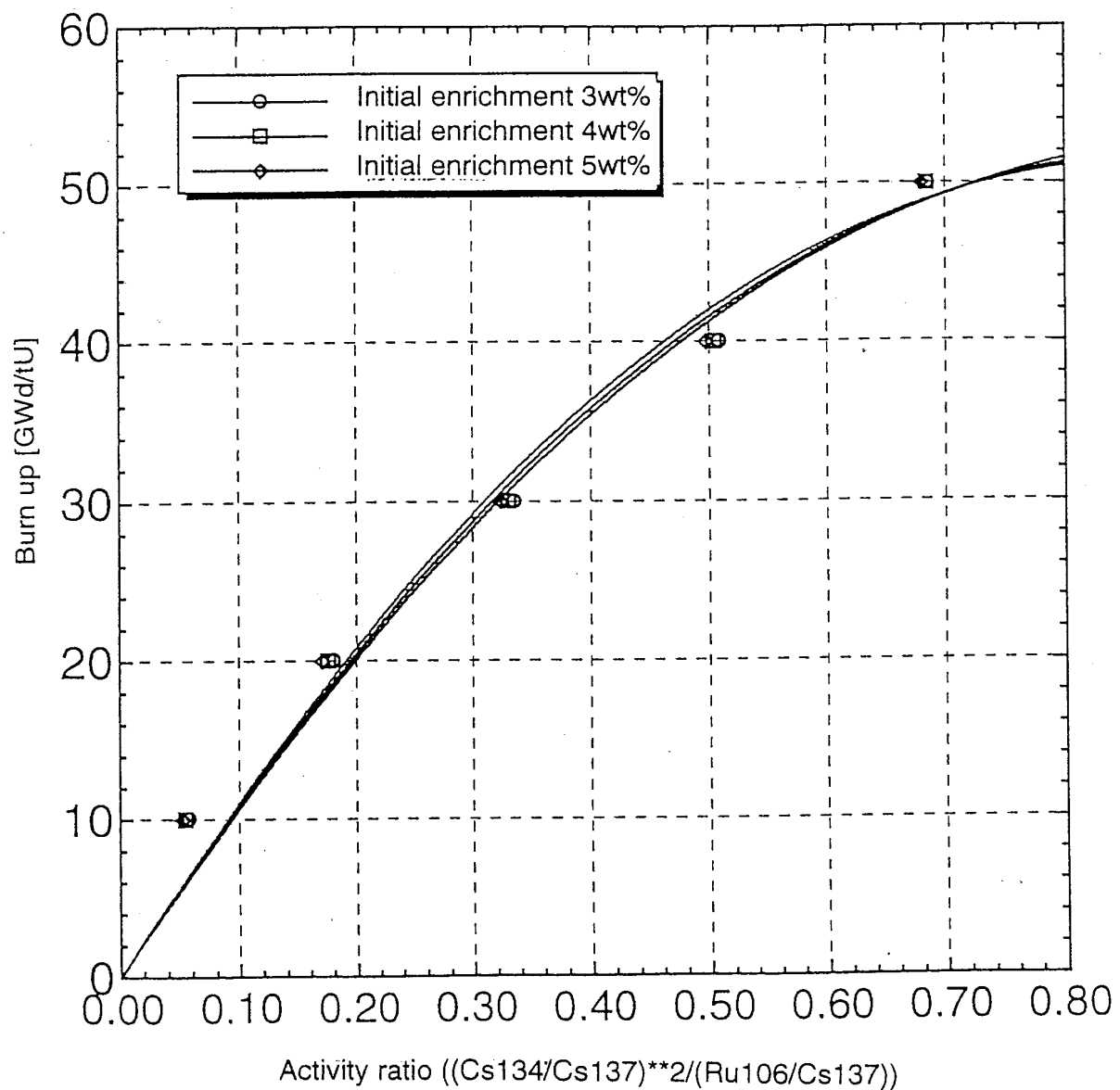


Fig. 5.2.3. Ru Activity ratio  $(\text{Cs-134}/\text{Cs-137})^2 / (\text{Ru-106}/\text{Cs-137})$  vs. burnup  
(Initial enrichment dependency, PWR).

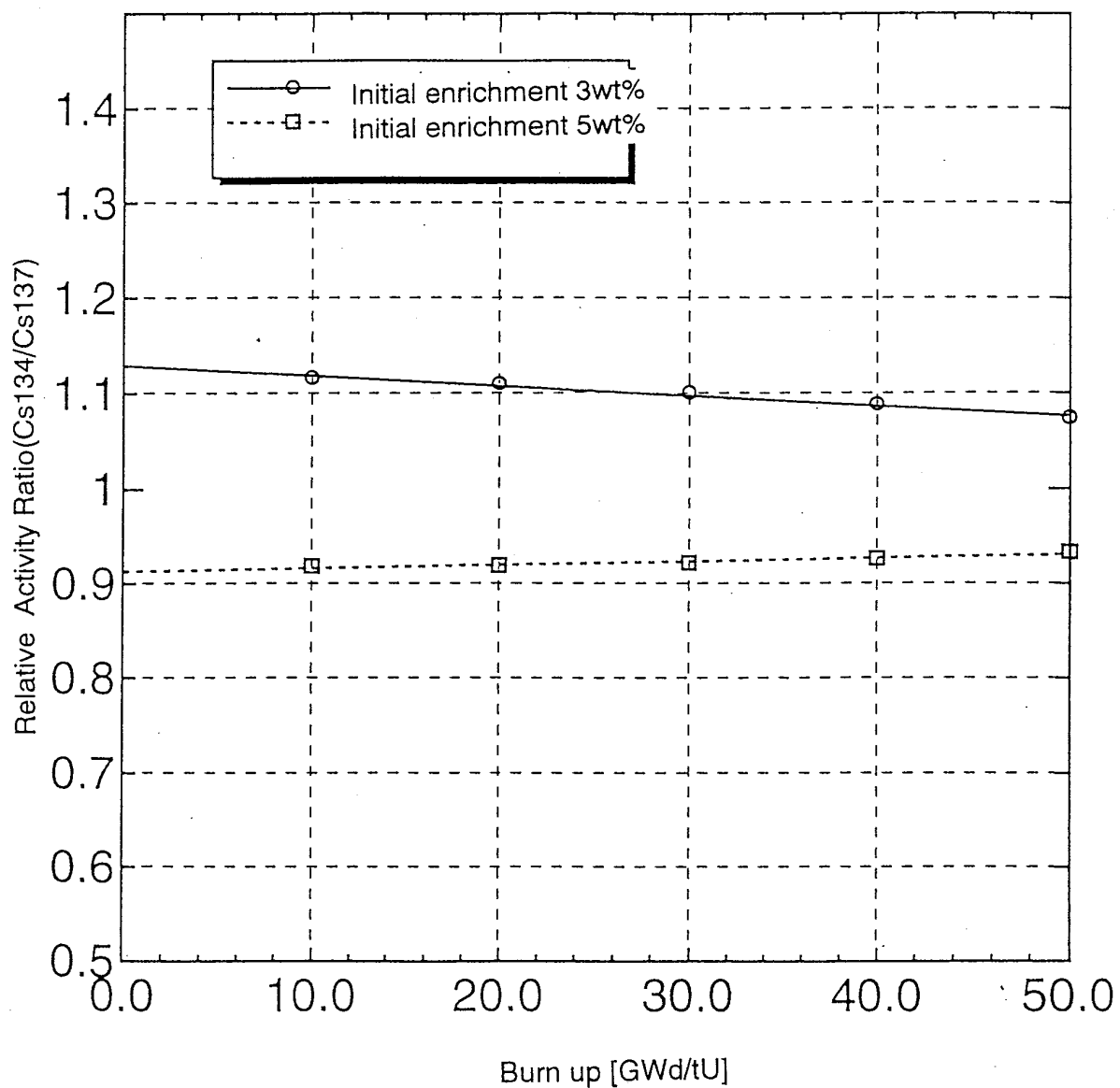


Fig. 5.2.4. Relative activity ratio (Cs-134/Cs-137)  
(Initial enrichment dependency, PWR).

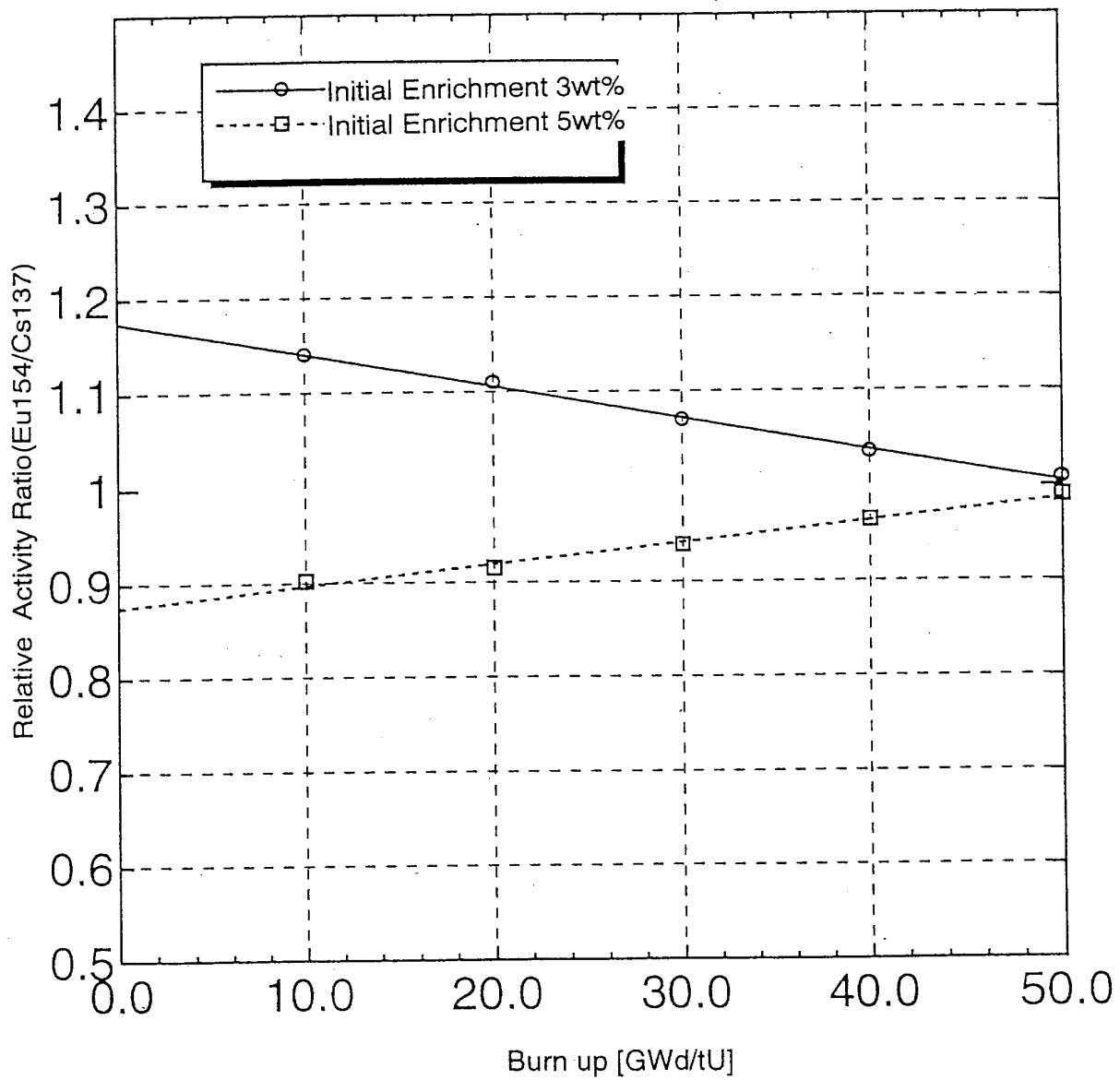


Fig. 5.2.5. Relative activity ratio (Eu-154/Cs-137)  
(Initial enrichment dependency, PWR).

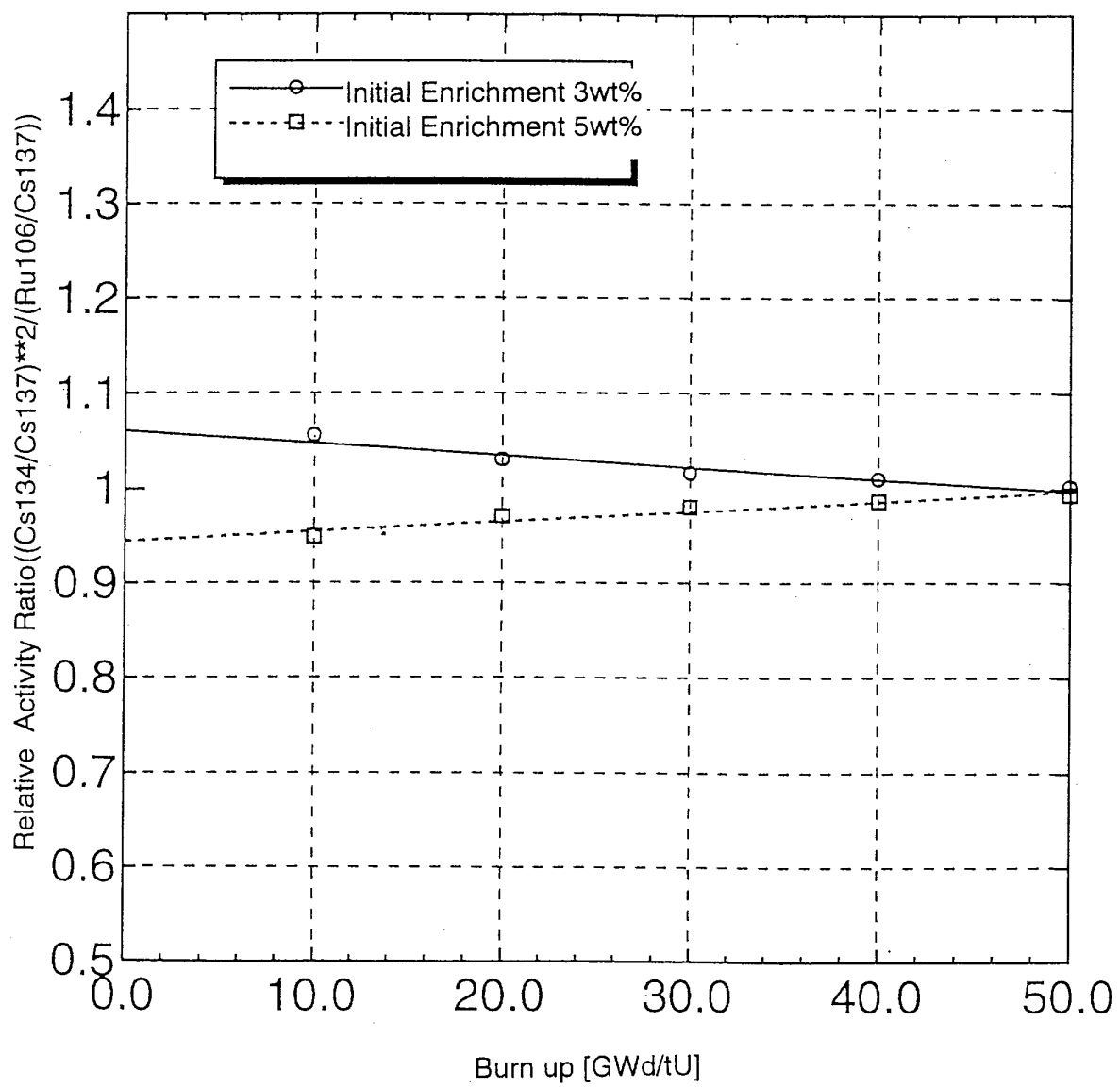


Fig. 5.2.6. Relative activity ratio  $((\text{Cs-134}/\text{Cs-137})^2 / (\text{Ru-106}/\text{Cs-137}))$   
(Initial enrichment dependency, PWR).

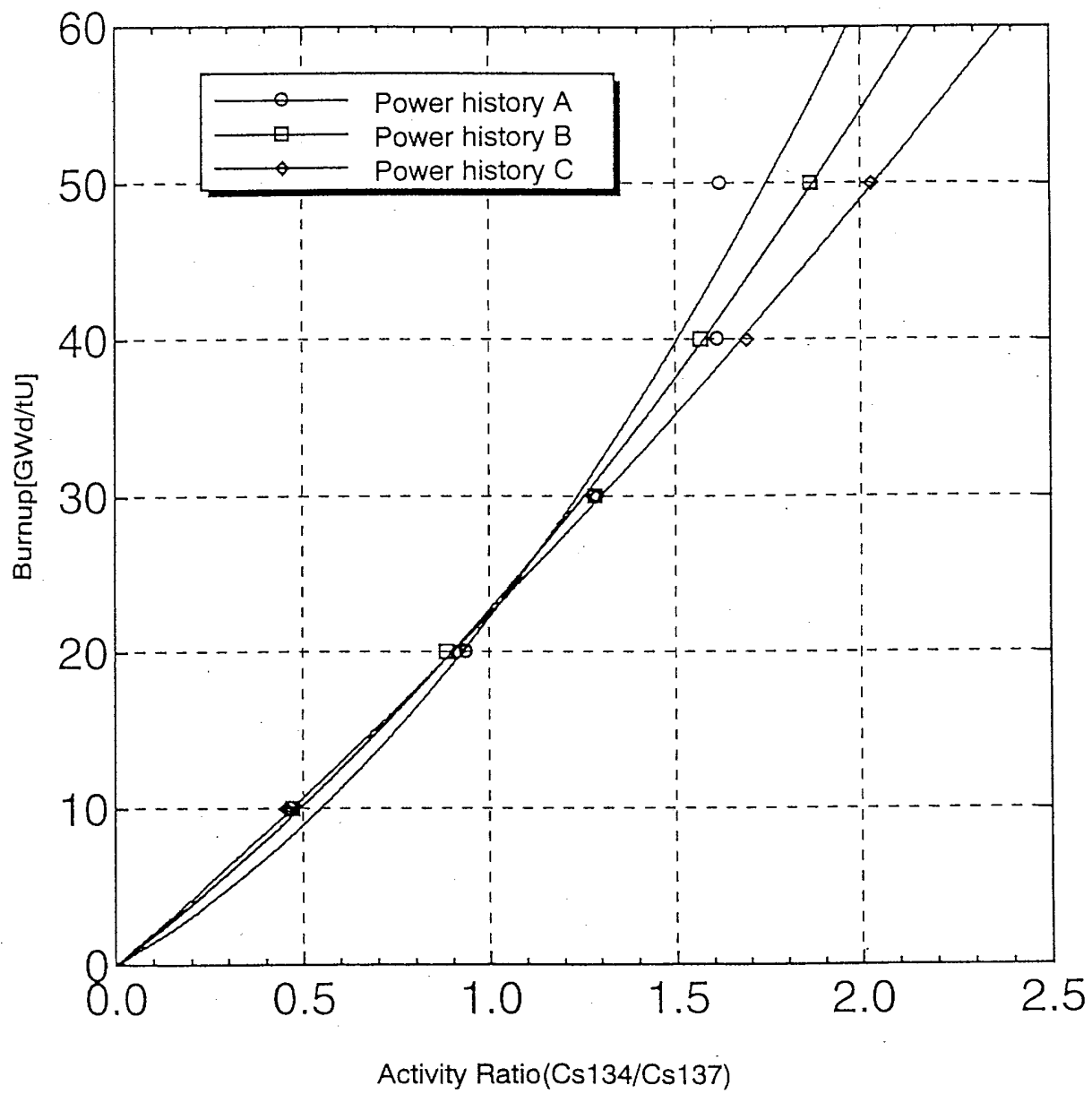


Fig. 5.2.7. Cs Activity ratio (Cs-134/Cs-137) vs. burnup  
(Power history dependency, PWR).

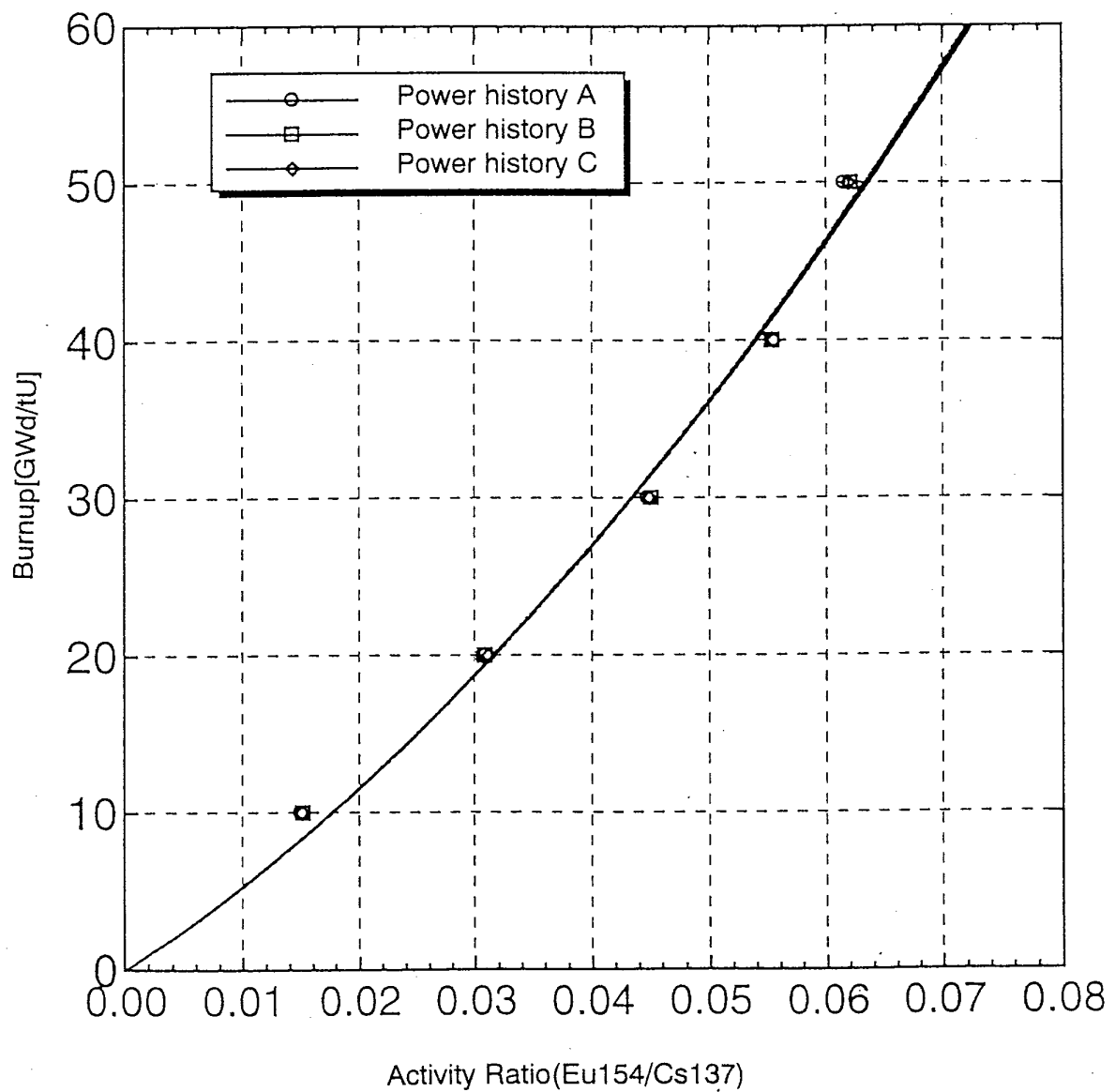


Fig. 5.2.8. Eu Activity ratio (Eu-154/Cs-137) vs. burnup  
(Power history dependency, PWR).

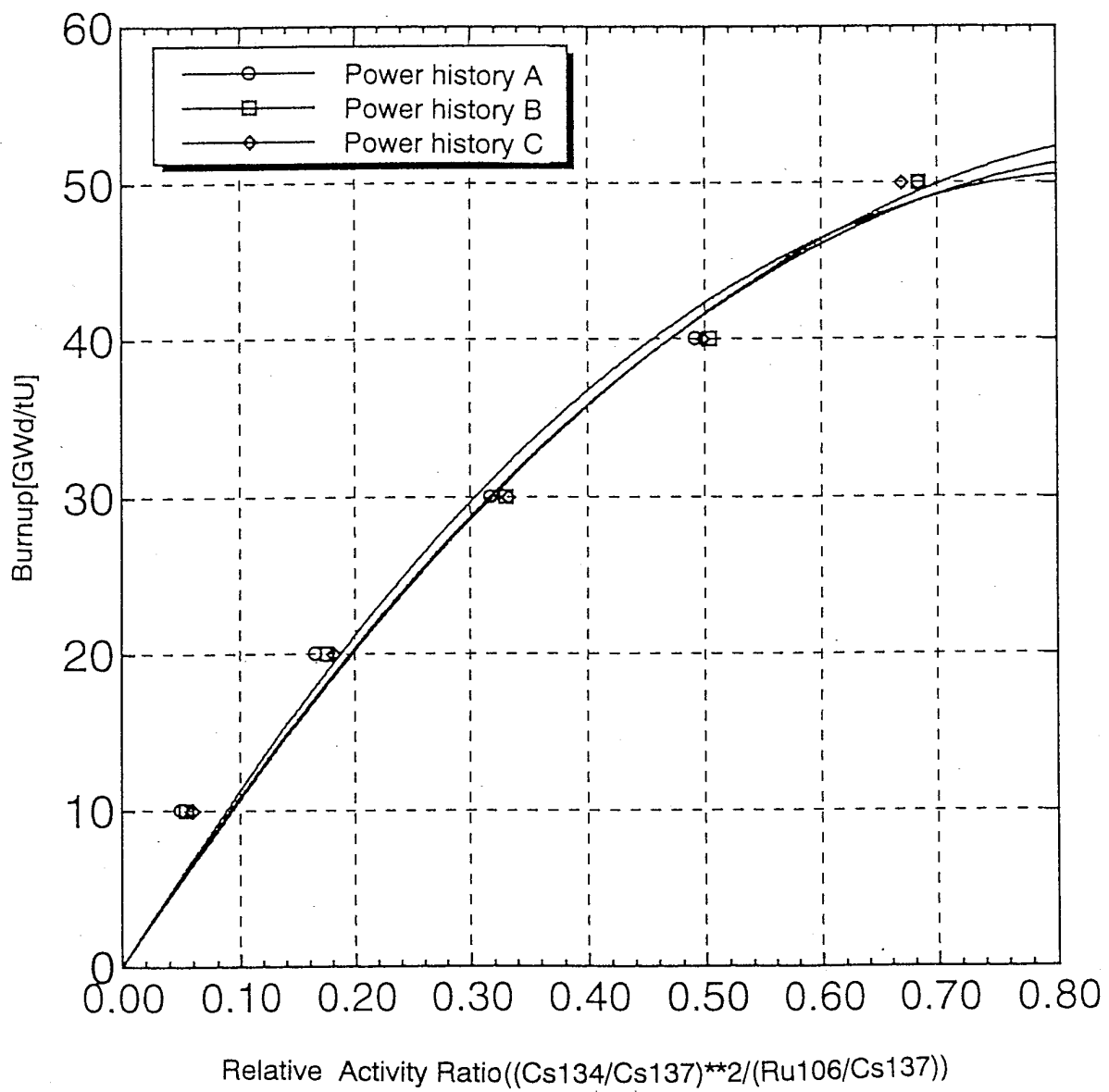


Fig. 5.2.9. Ru Activity ratio  $((\text{Cs-134}/\text{Cs-137})^2 / (\text{Ru-106}/\text{Cs-137}))$  vs. burnup  
(Power history dependency, PWR).

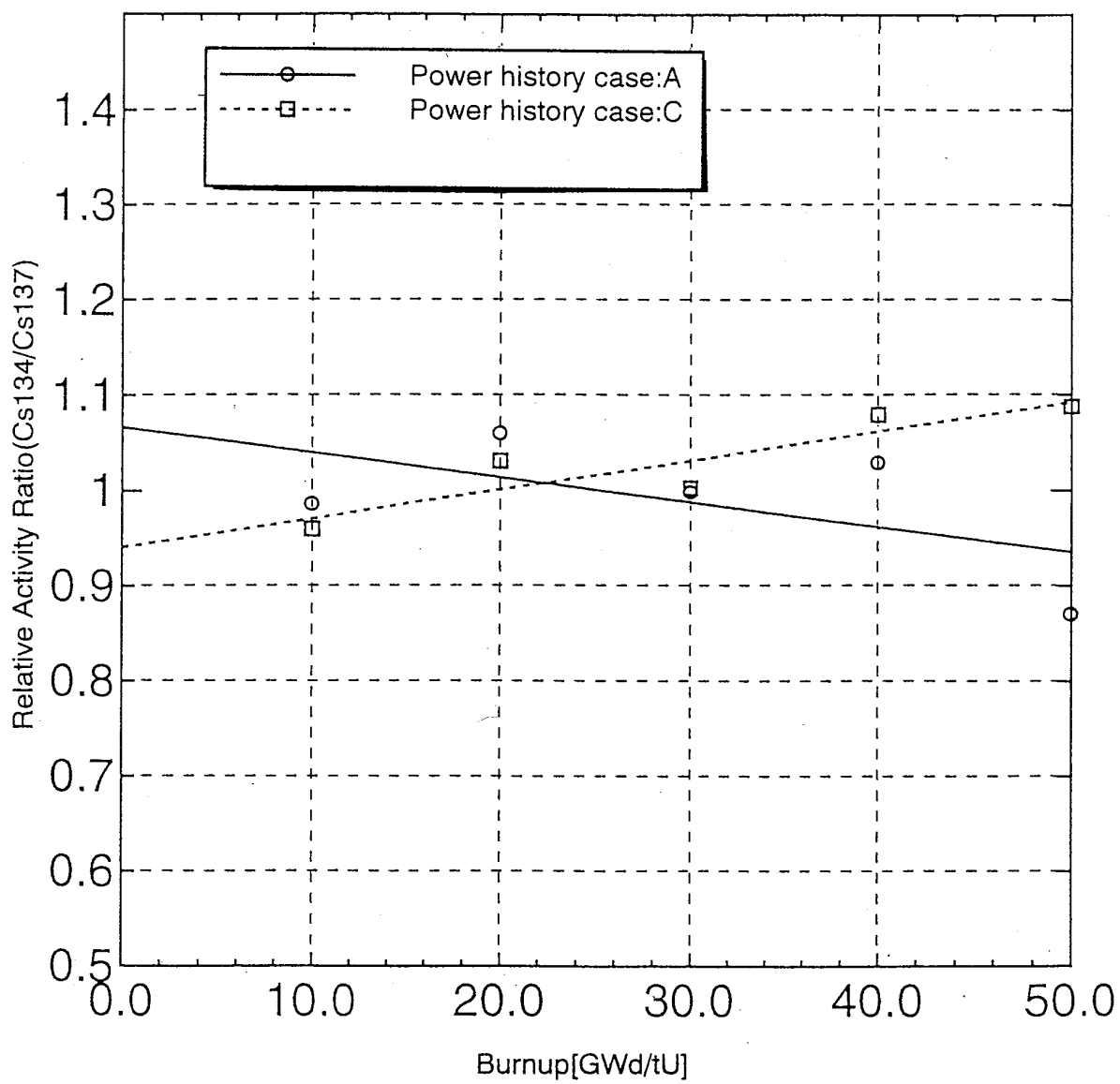


Fig. 5.2.10. Relative activity ratio (Cs-134/Cs-137)  
(Power history dependency, PWR).

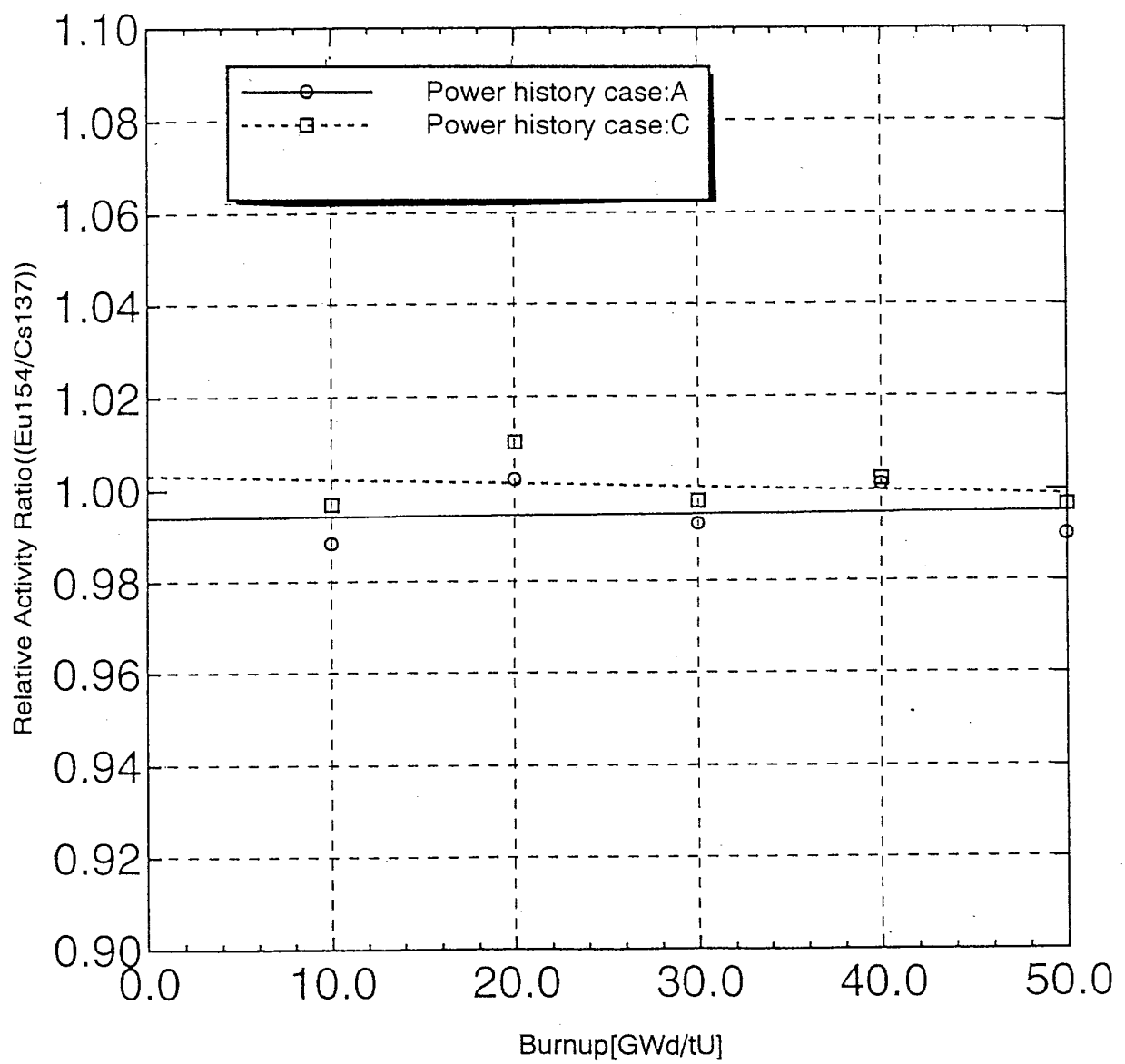


Fig. 5.2.11. Relative activity ratio (Eu-154/Cs-137)  
(Power history dependency, PWR).

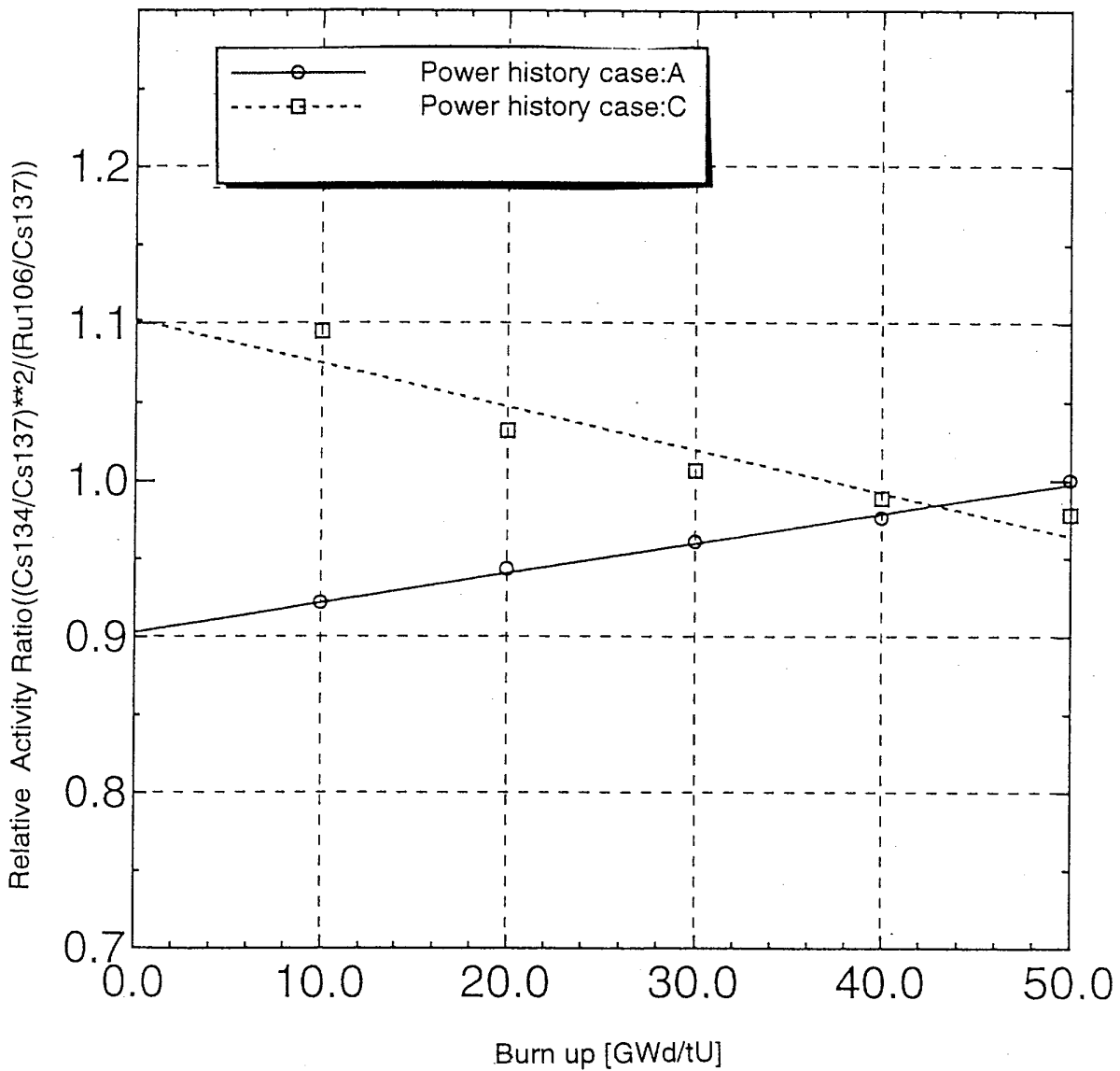


Fig. 5.2.12. Relative activity ratio  $((\text{Cs-134}/\text{Cs-137})^2 / (\text{Ru-106}/\text{Cs-137}))$  vs. burnup  
(Power history dependency, PWR).

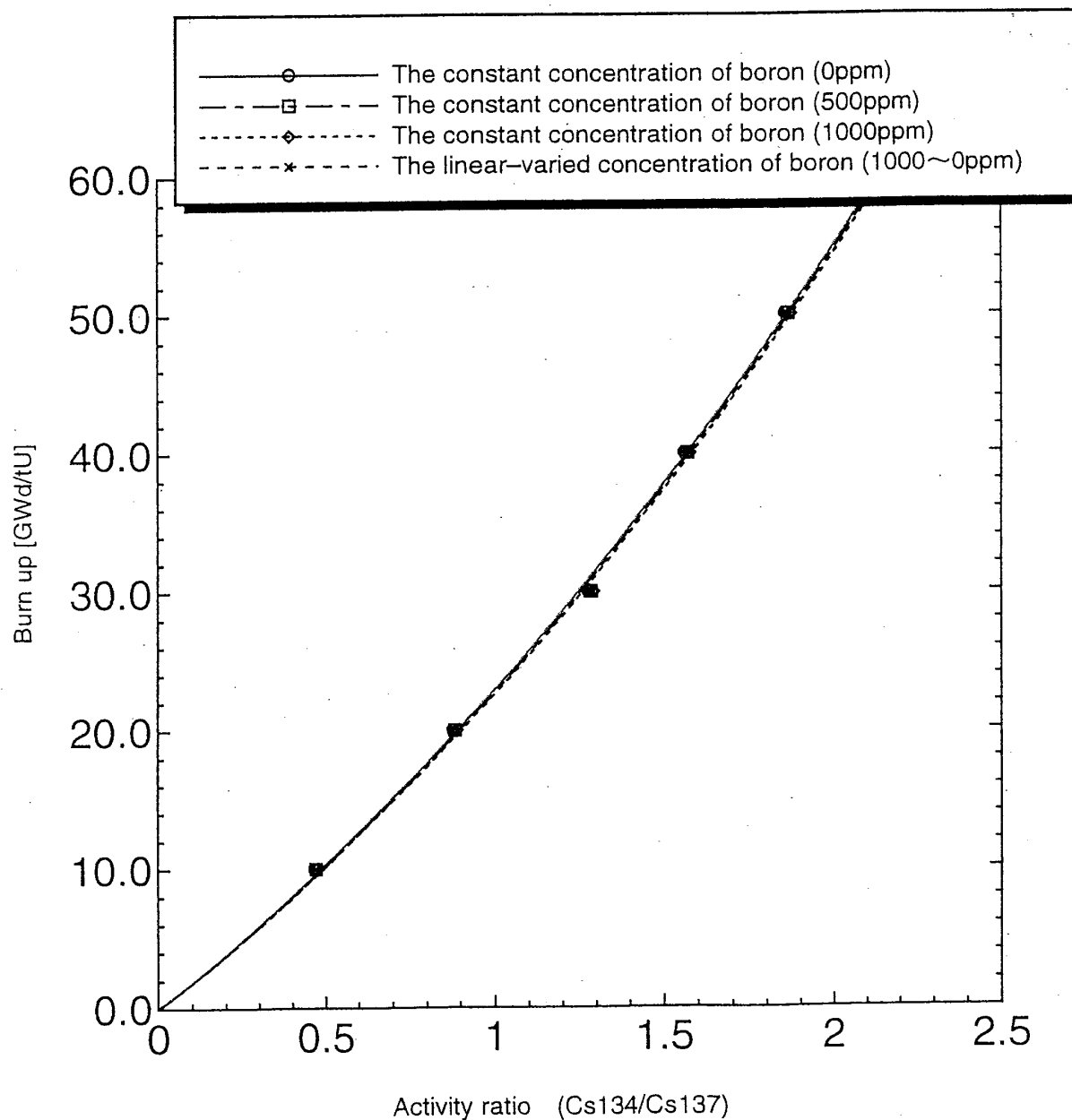


Fig. 5.2.13. Cs Activity ratio (Cs-134/Cs-137) vs. burnup  
(Boron content dependency, PWR).

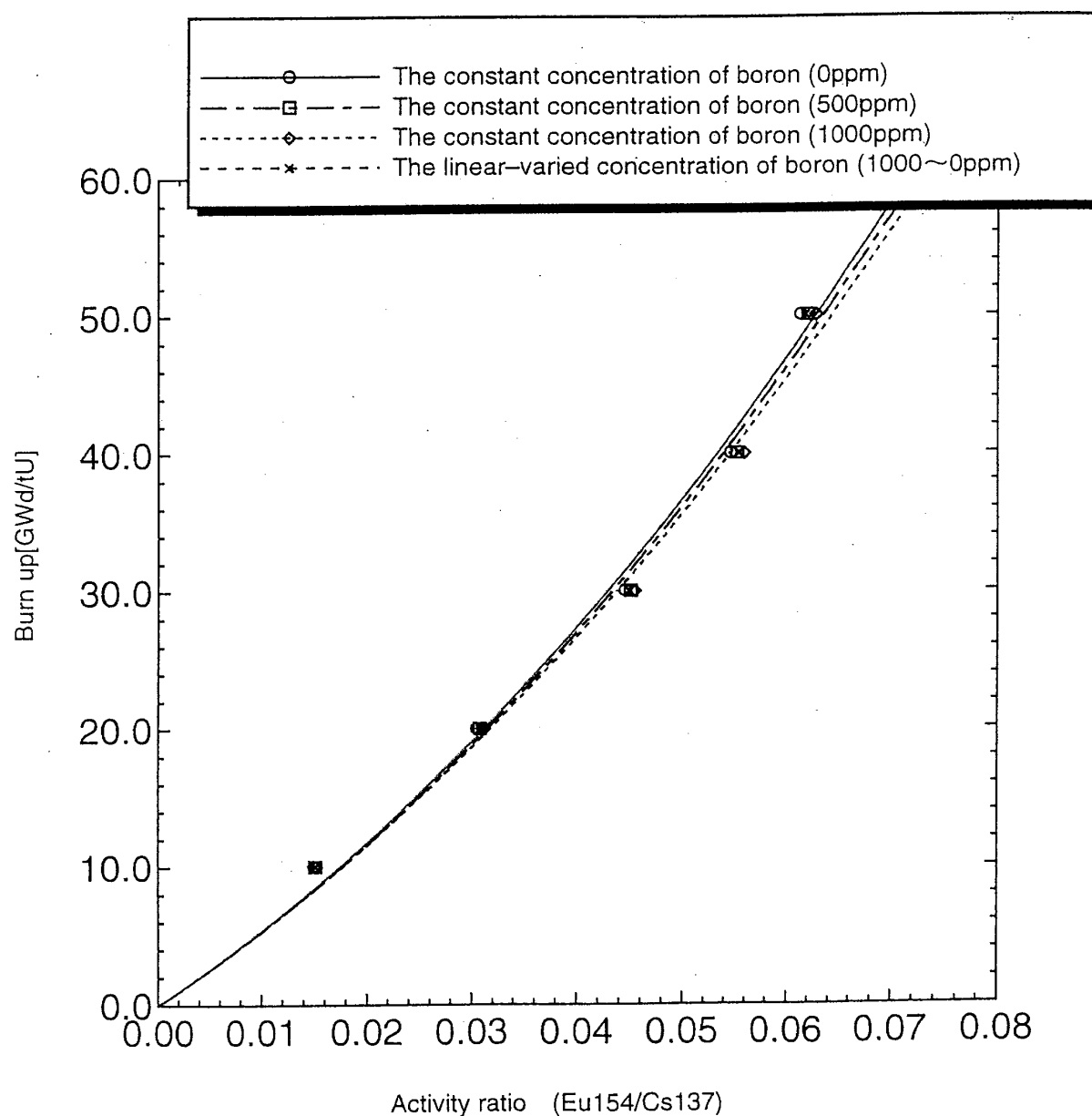


Fig. 5.2.14. Eu Activity ratio (Eu-154/Cs-137) vs. burnup  
(Boron content dependency, PWR).

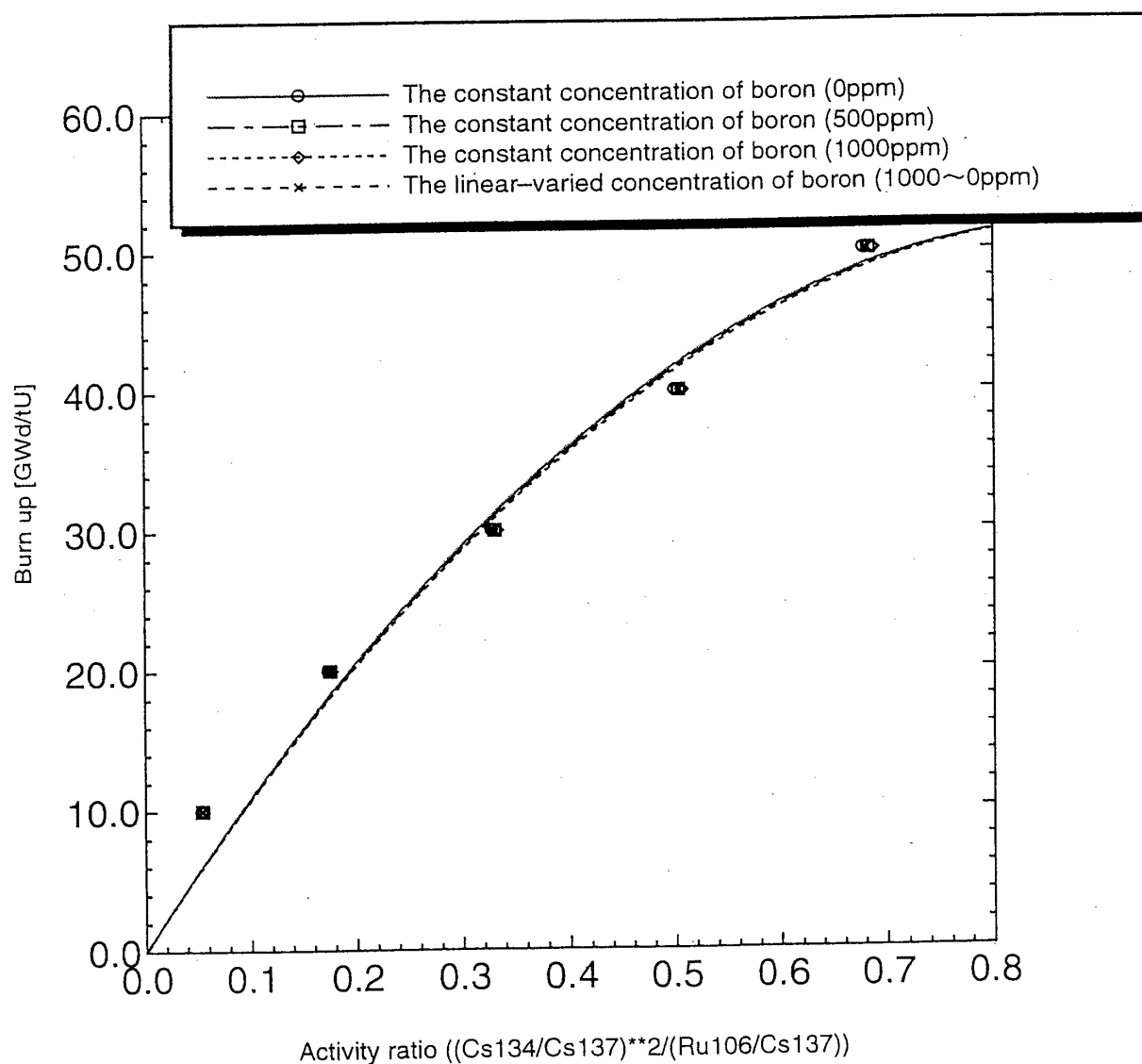


Fig. 5.2.15. Ru Activity ratio  $((\text{Cs-134}/\text{Cs-137})^2 / (\text{Ru-106}/\text{Cs-137}))$   
(Boron content dependency, PWR).

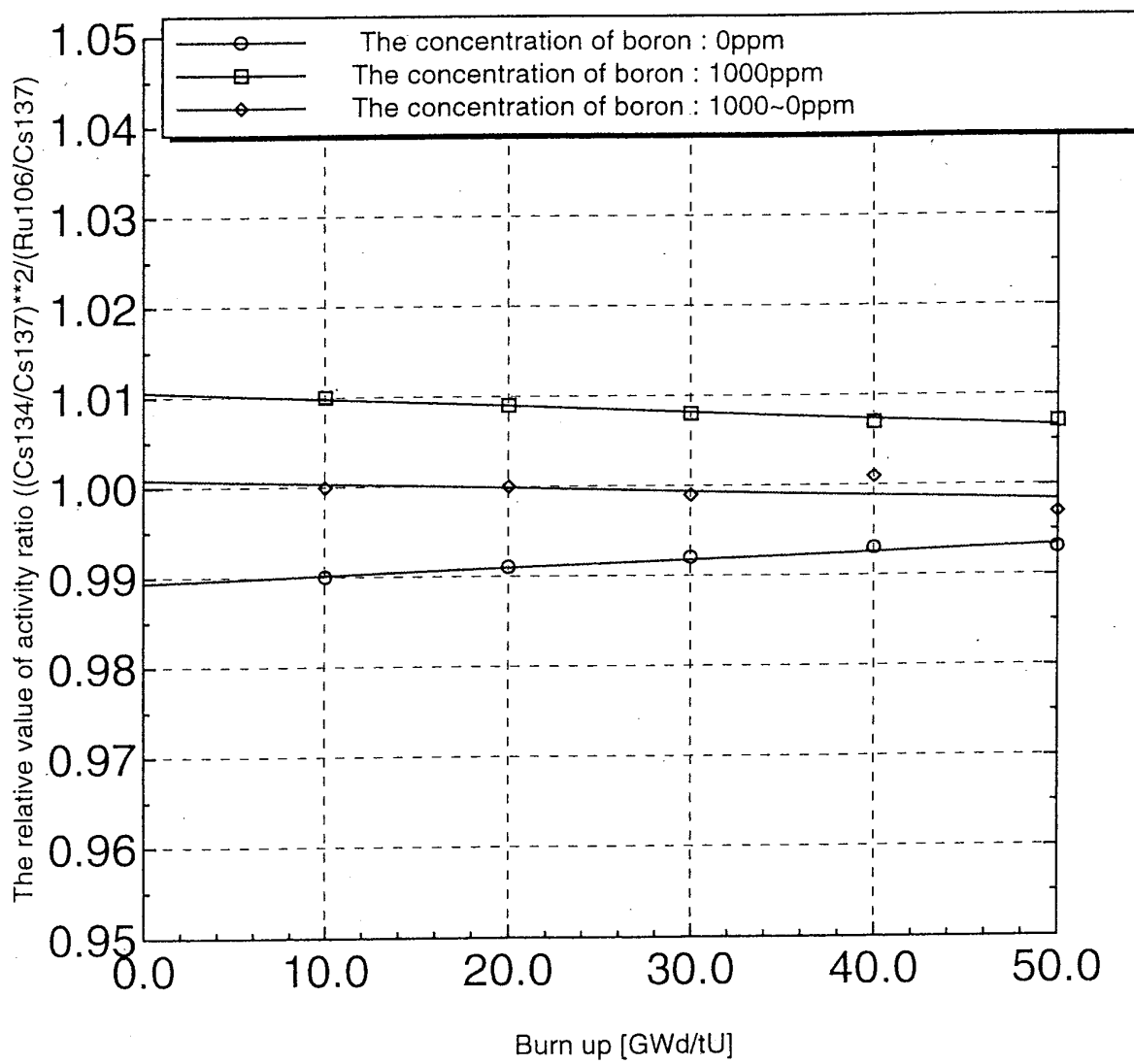


Fig. 5.2.16. Relative activity ( $\text{Cs-134}/\text{Cs-137}$ )  
(Boron content dependency, PWR).

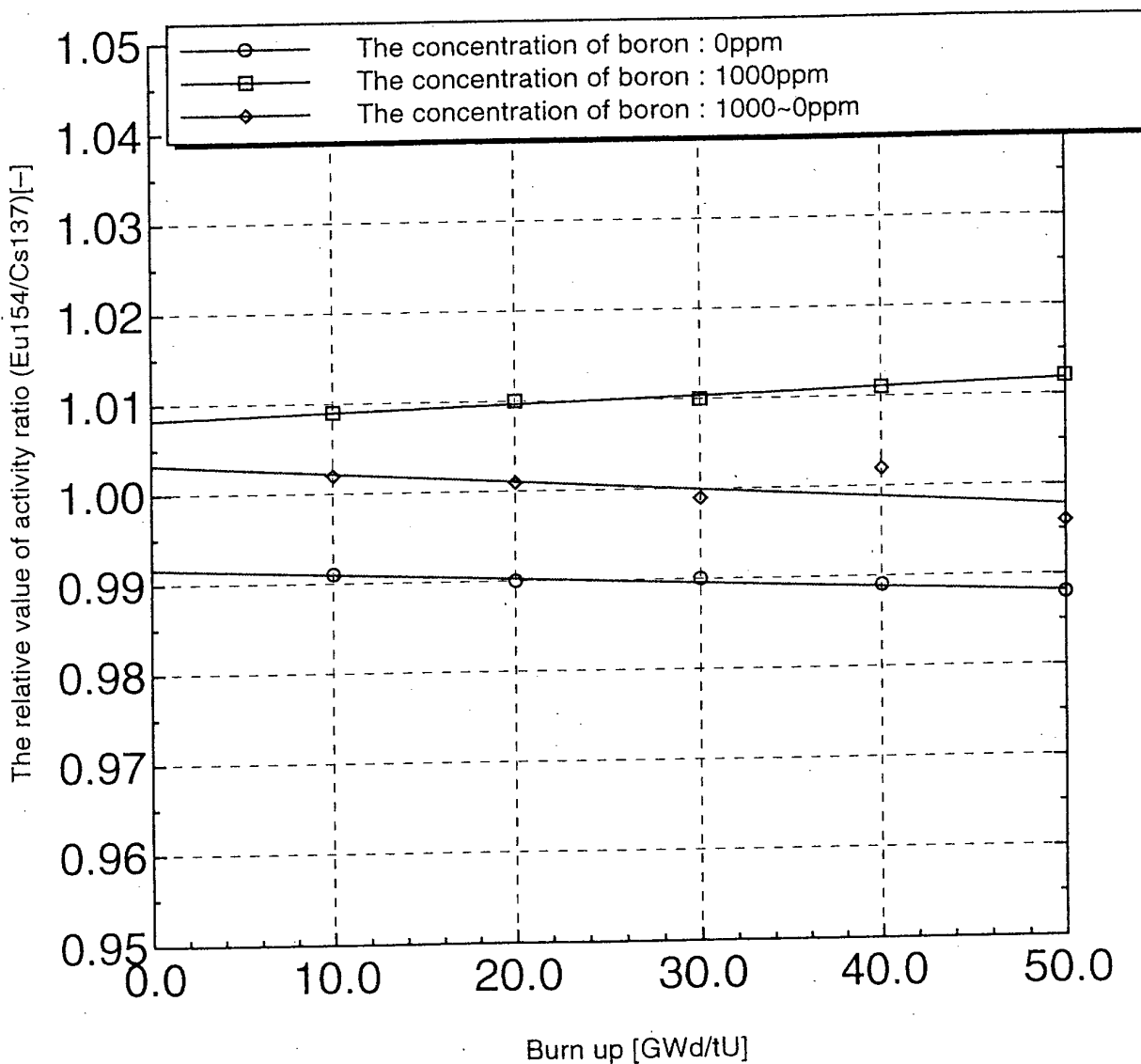


Fig. 5.2.17. Relative activity ratio ( $\text{Eu}-154/\text{Cs}-137$ )  
(Boron content dependency, PWR).

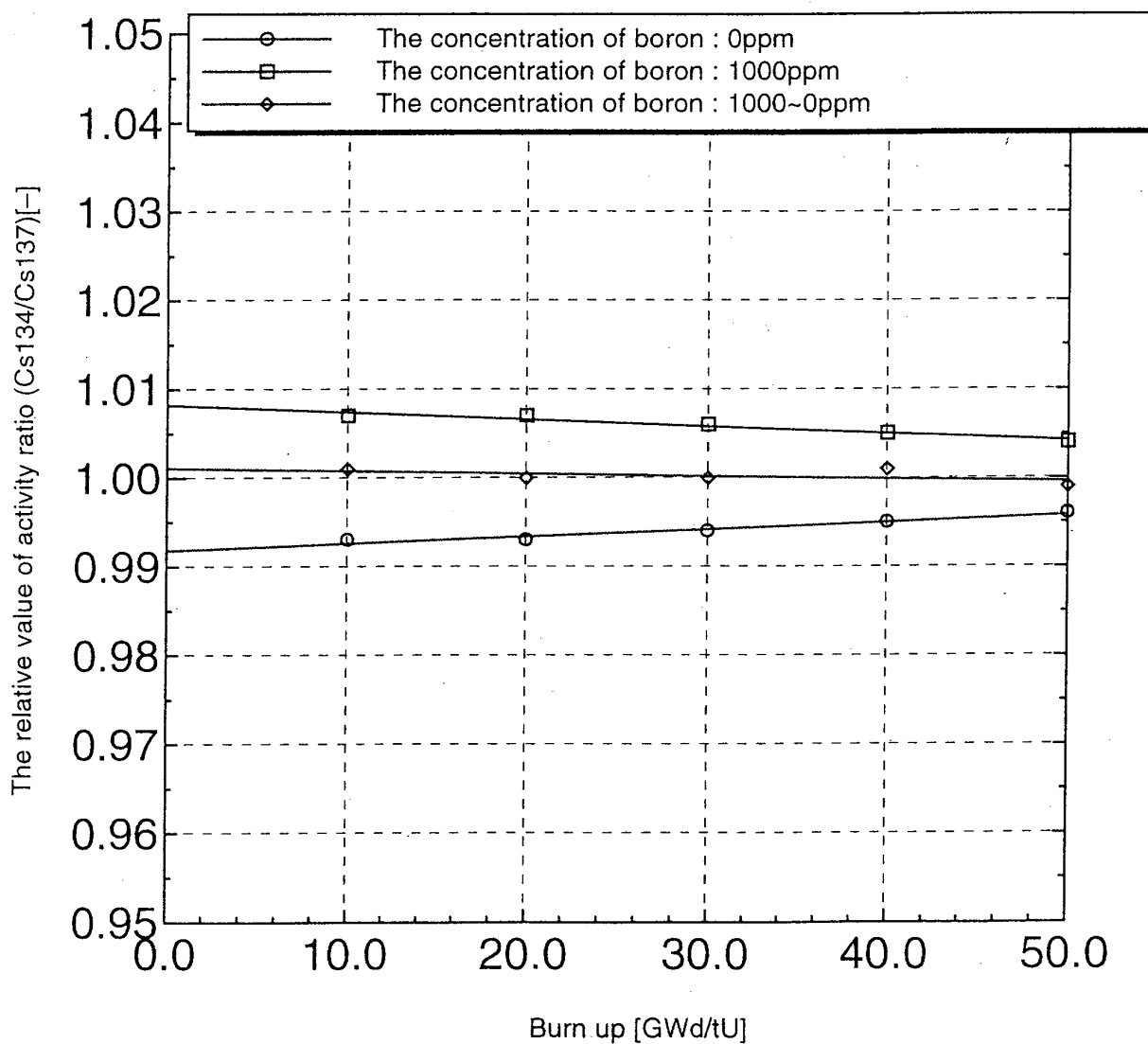


Fig. 5.2.18. Relative activity ratio  $((\text{Cs}-134/\text{Cs}-137)^2 / (\text{Ru}-106/\text{Cs}-137))$  vs. burnup  
(Boron content dependency, PWR).

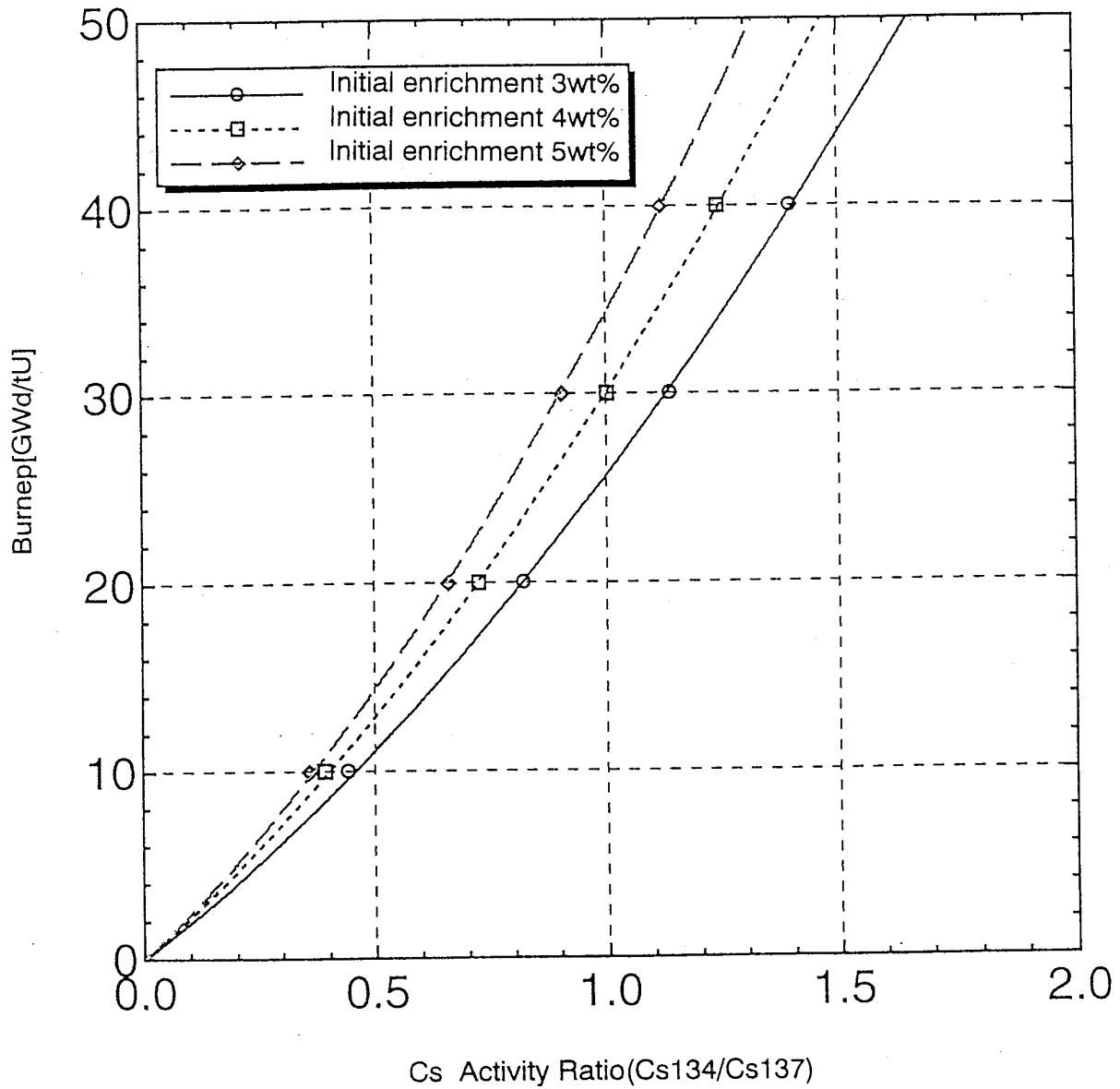


Fig. 5.2.19. Cs Activity ratio (Cs-134/Cs-137) vs. burnup  
(Initial enrichment dependency, BWR).

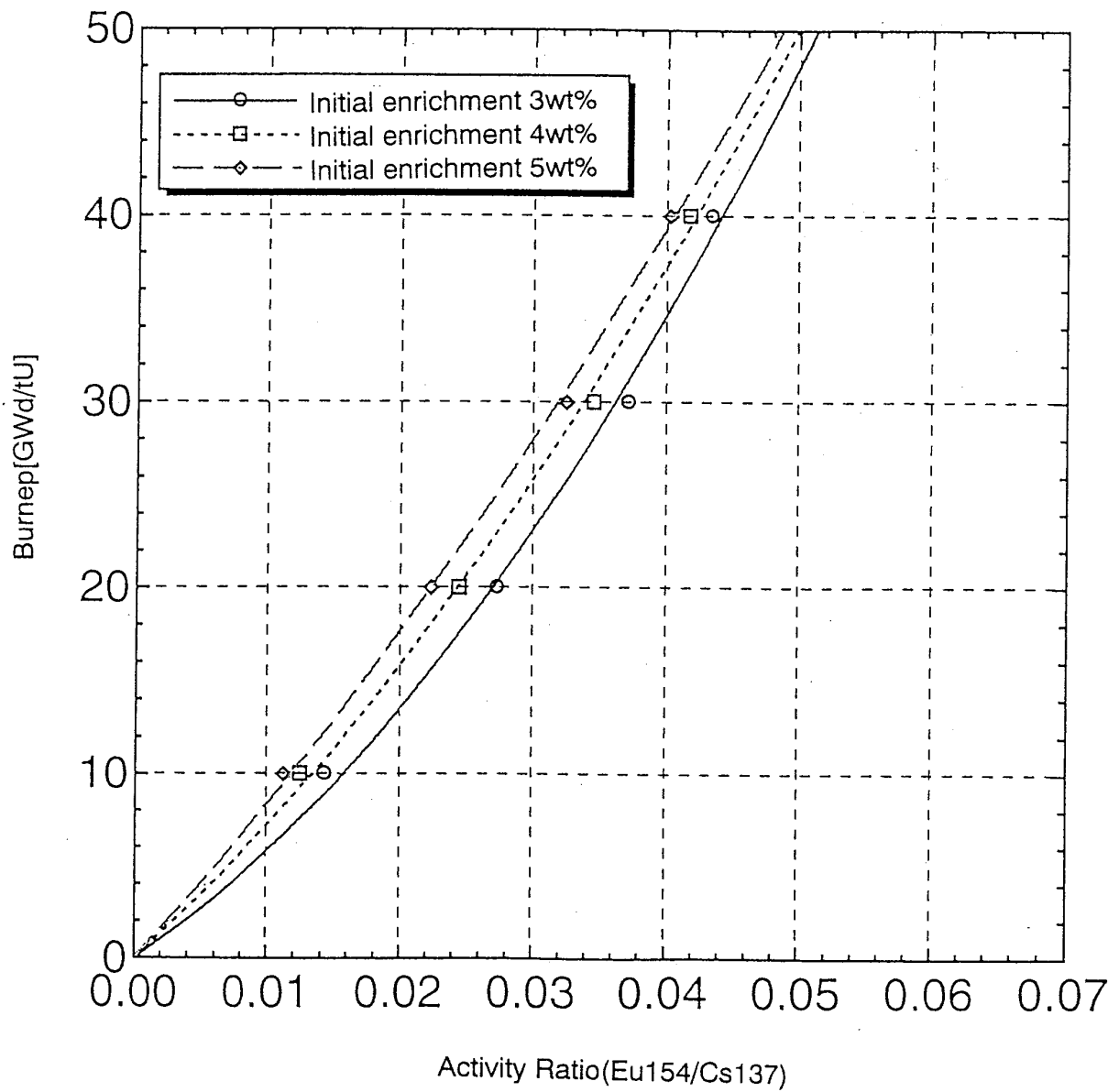


Fig. 5.2.20. Eu Activity ratio (Eu-154/Cs-137) vs. burnup  
(Initial enrichment dependency, BWR).

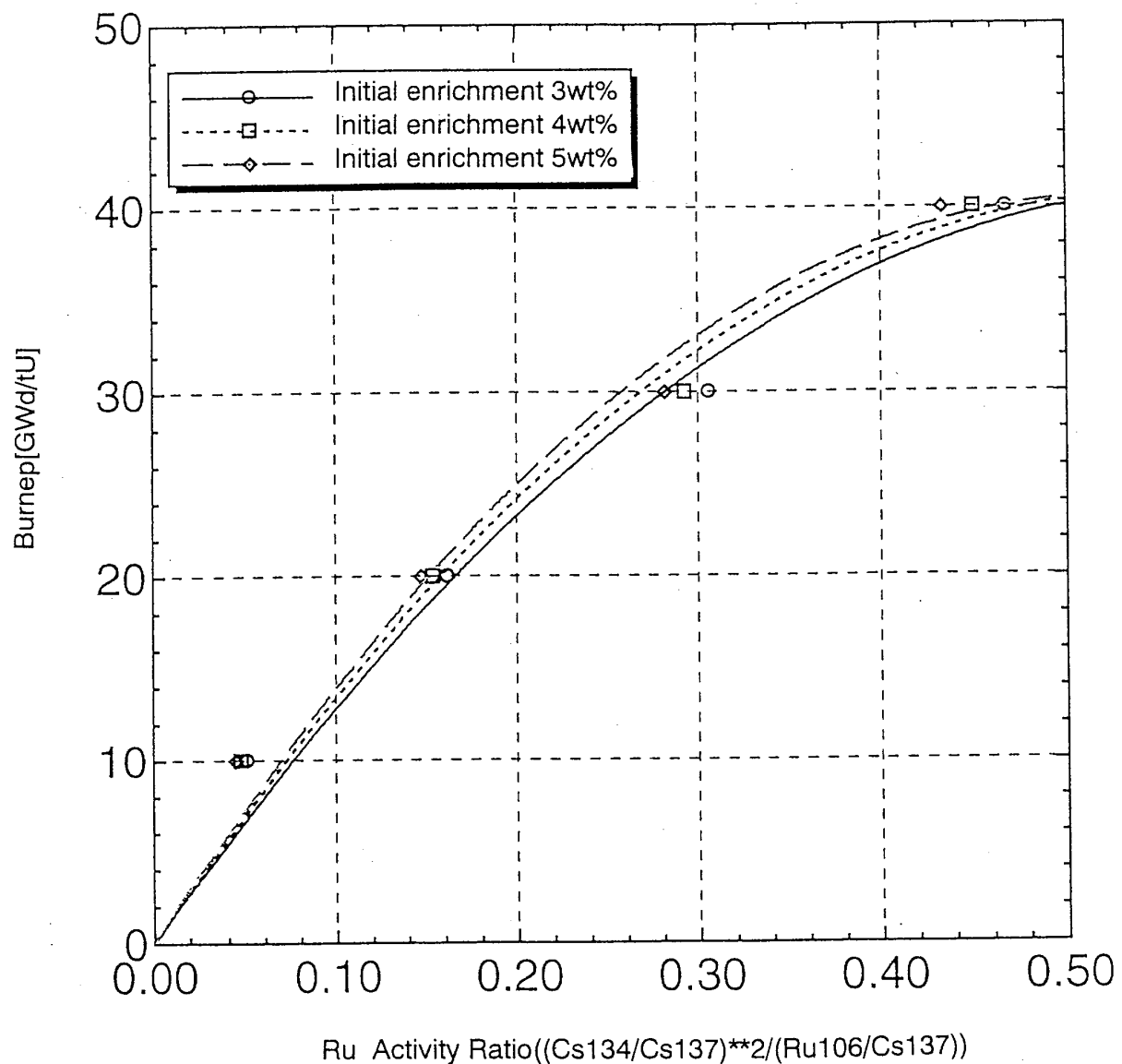


Fig. 5.2.21. Ru Activity ratio  $((\text{Cs-134}/\text{Cs-137})^2 / (\text{Ru-106}/\text{Cs-137}))$  vs. burnup  
(Initial enrichment dependency, BWR).

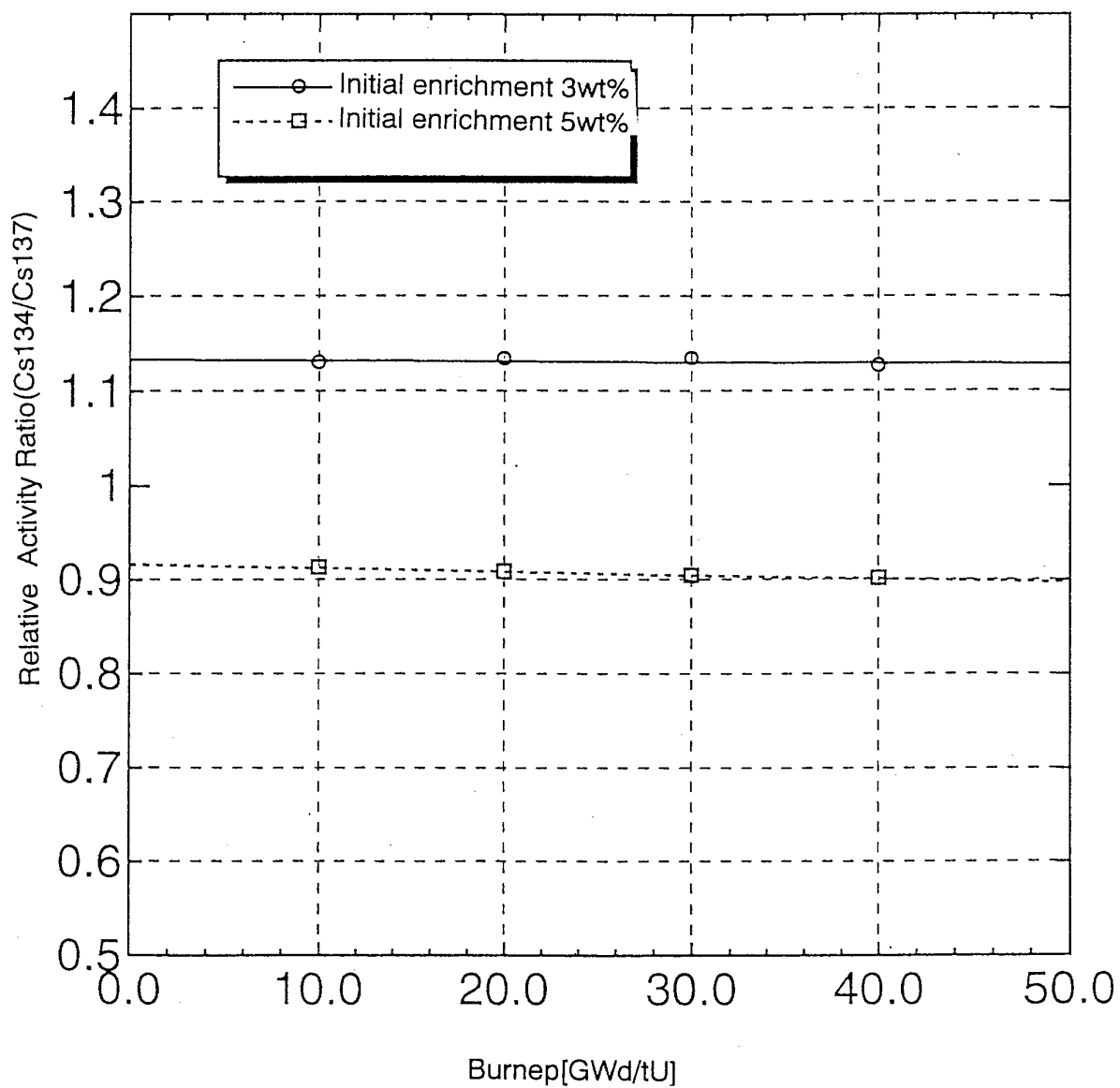


Fig. 5.2.22. Relative activity ratio (Cs-134/Cs-137)  
(Initial enrichment dependency, BWR).

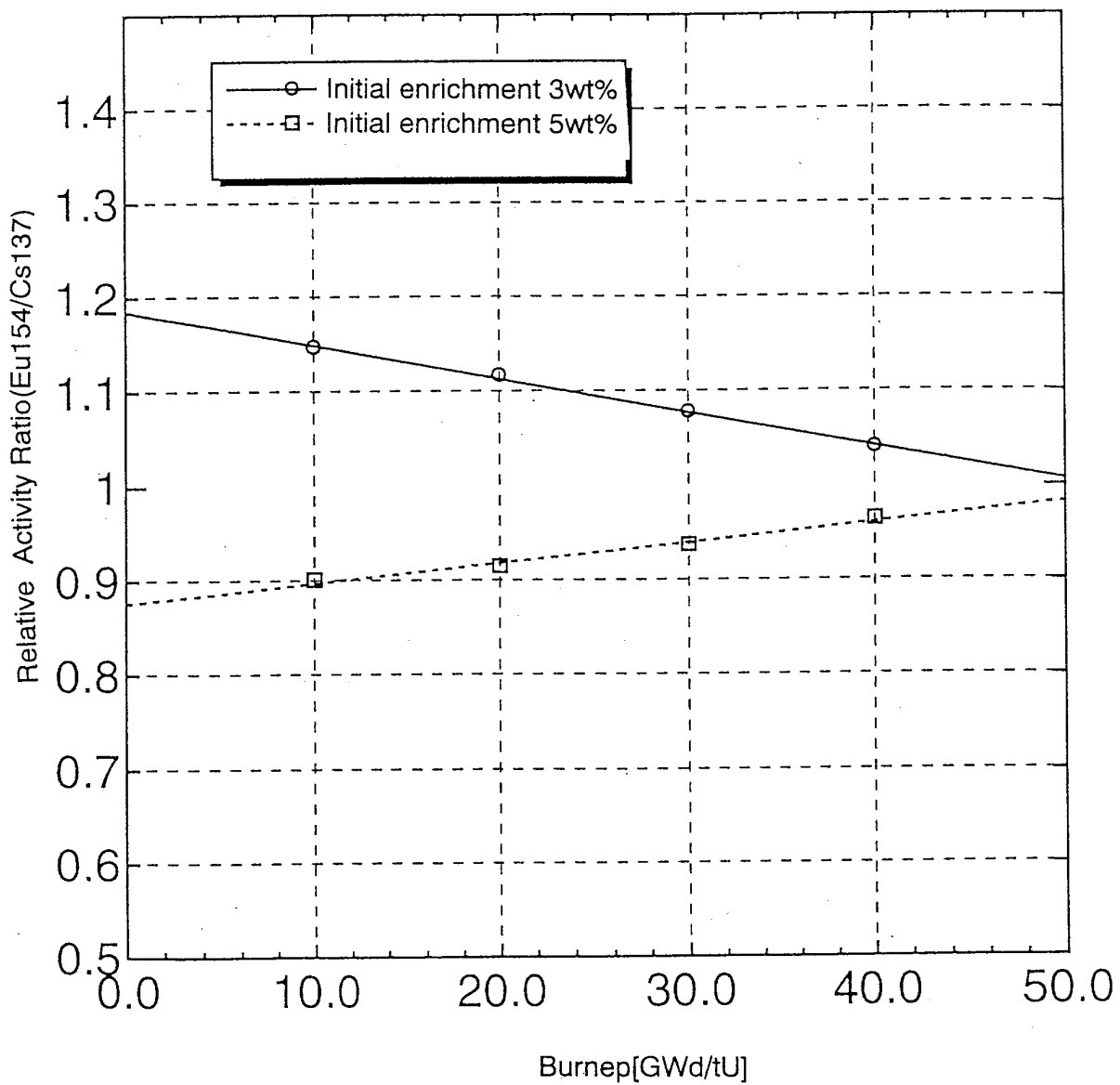


Fig. 5.2.23. Relative activity ratio (Eu-154/Cs-137)  
(Initial enrichment dependency, BWR).

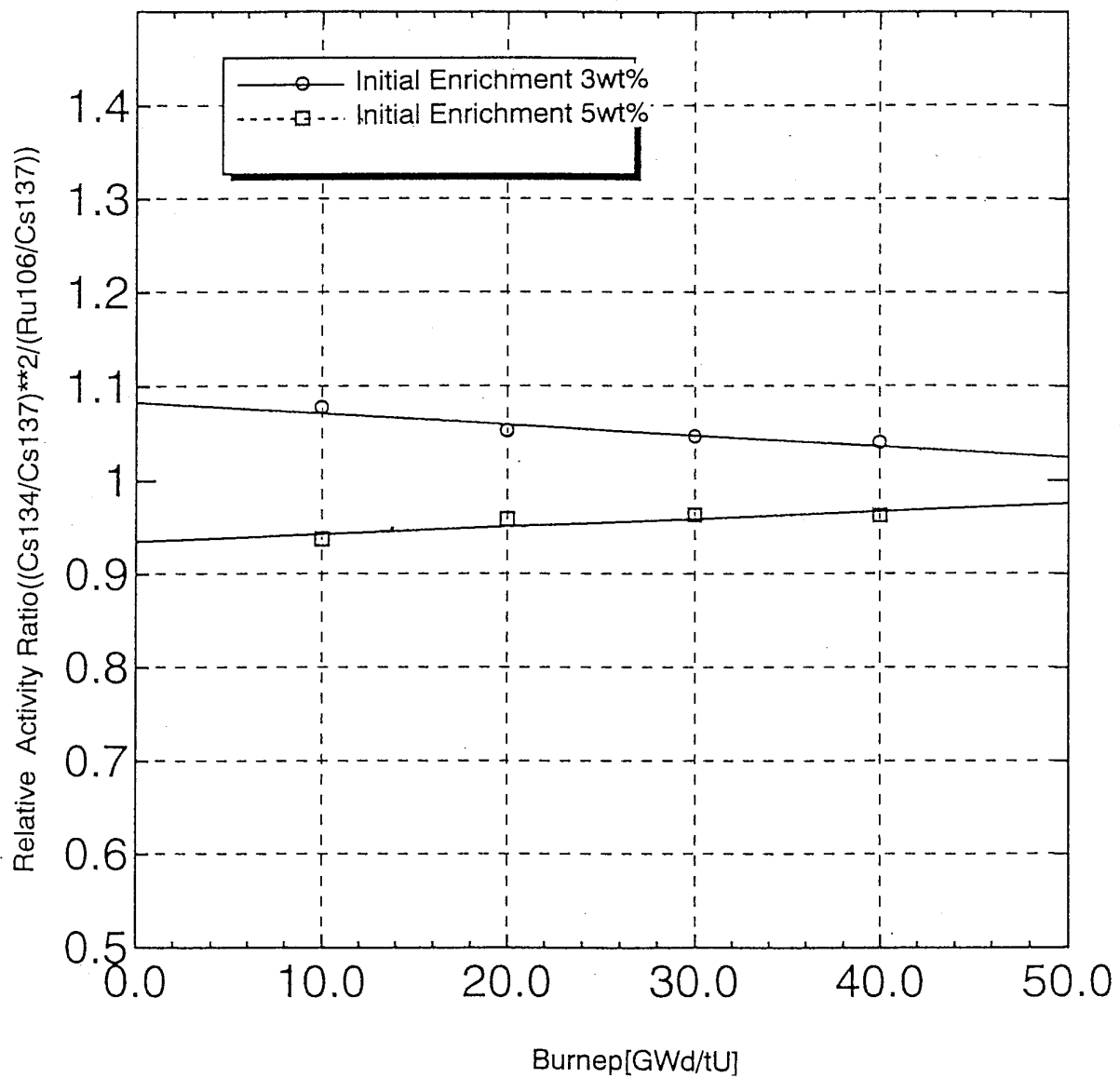


Fig. 5.2.24. Relative activity ratio  $((\text{Cs-134}/\text{Cs-137})^2 / (\text{Ru-106}/\text{Cs-137}))$   
(Initial enrichment dependency, BWR).

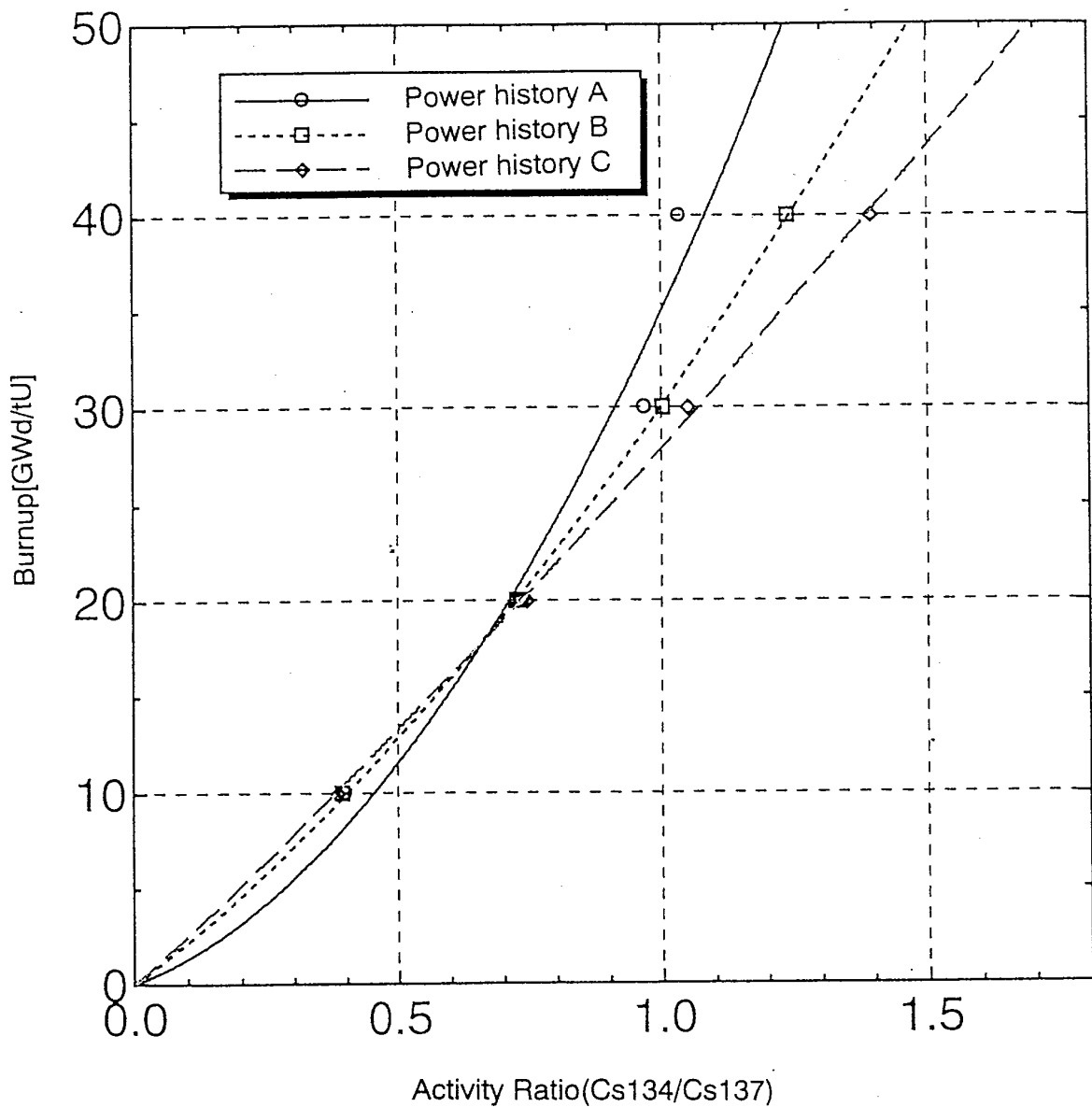


Fig. 5.2.25. Cs Activity ratio (Cs-134/Cs-137) vs. burnup  
(Power history dependency, BWR).

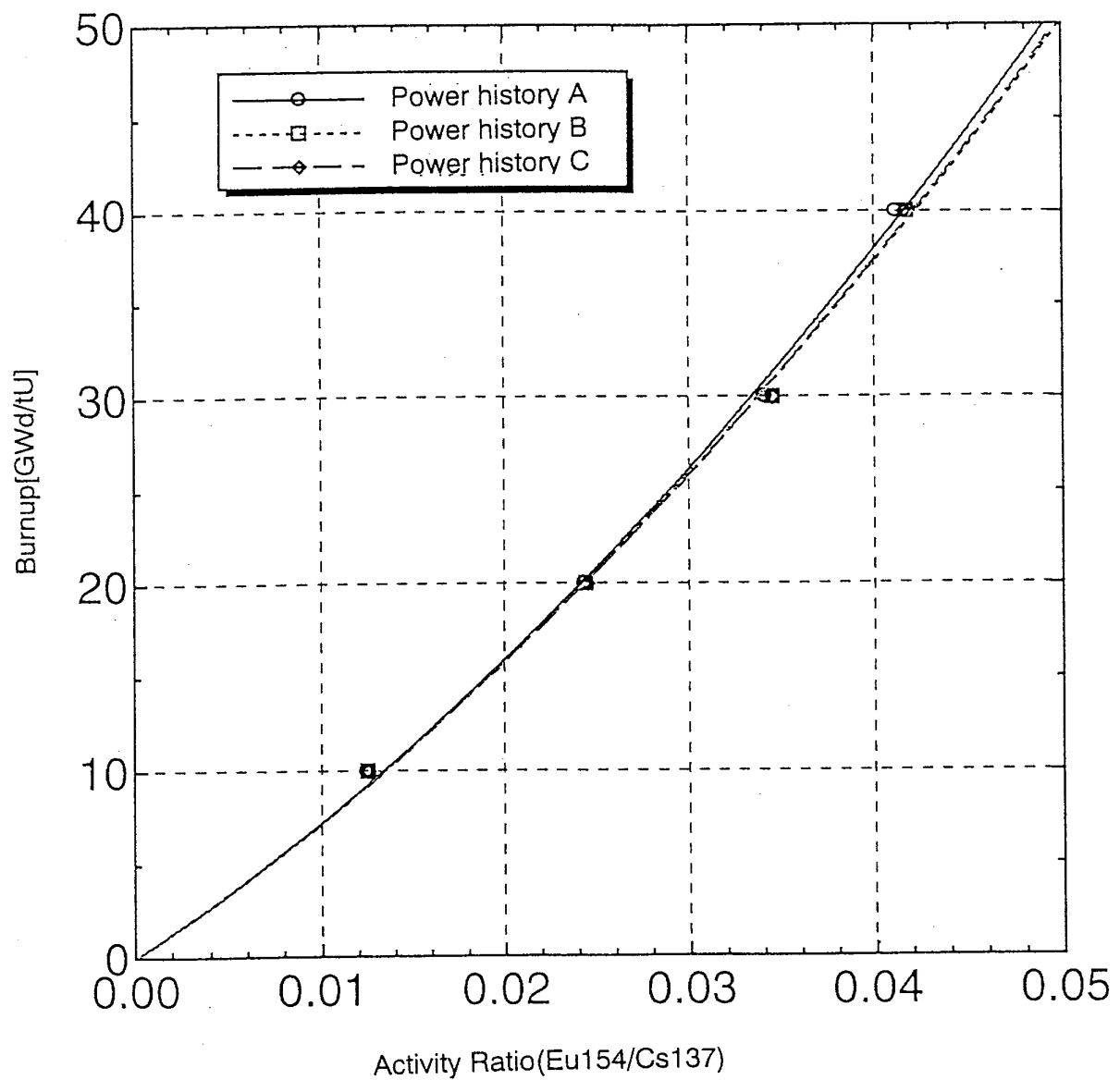


Fig. 5.2.26. Eu Activity ratio (Eu-154/Cs-137) vs. burnup  
(Power history dependency, BWR).

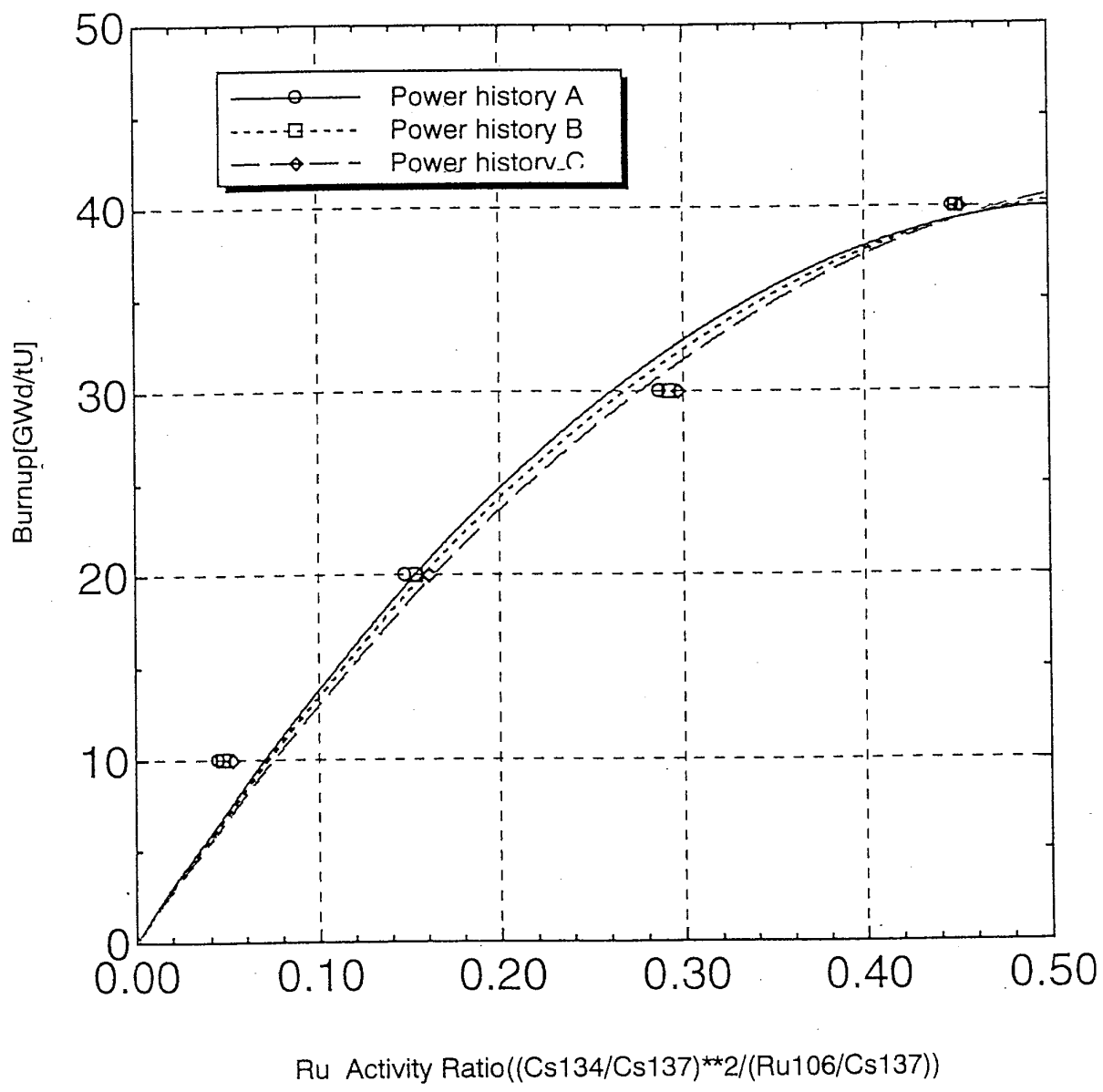


Fig. 5.2.27. Ru Activity ratio  $((\text{Cs-134}/\text{Cs-137})^2 / (\text{Ru-106}/\text{Cs-137}))$  vs. burnup  
(Power history dependency, PWR).

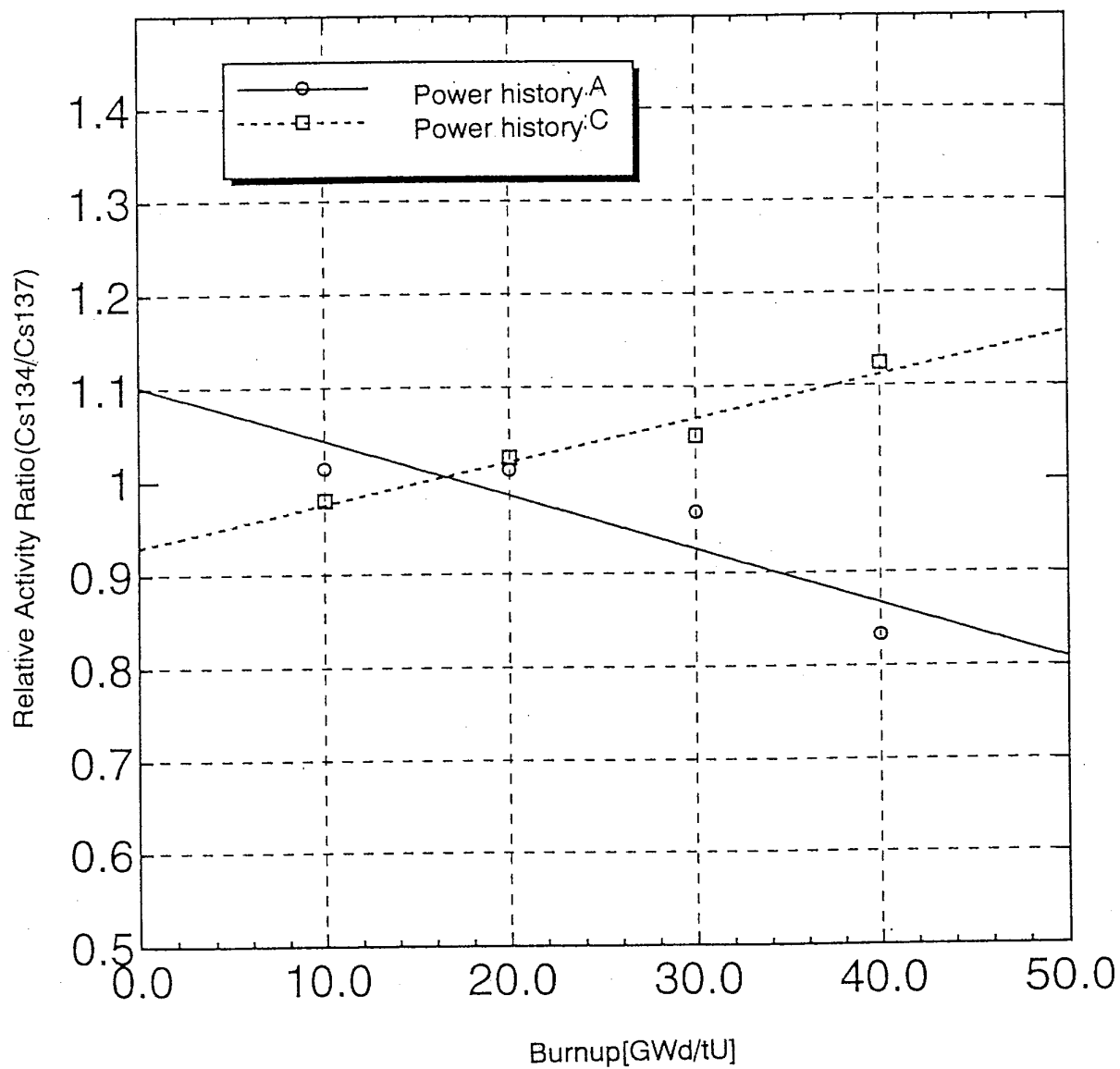


Fig. 5.2.28. Relative activity ratio ( $\text{Cs}-134/\text{Cs}-137$ )  
(Power history dependency, BWR).

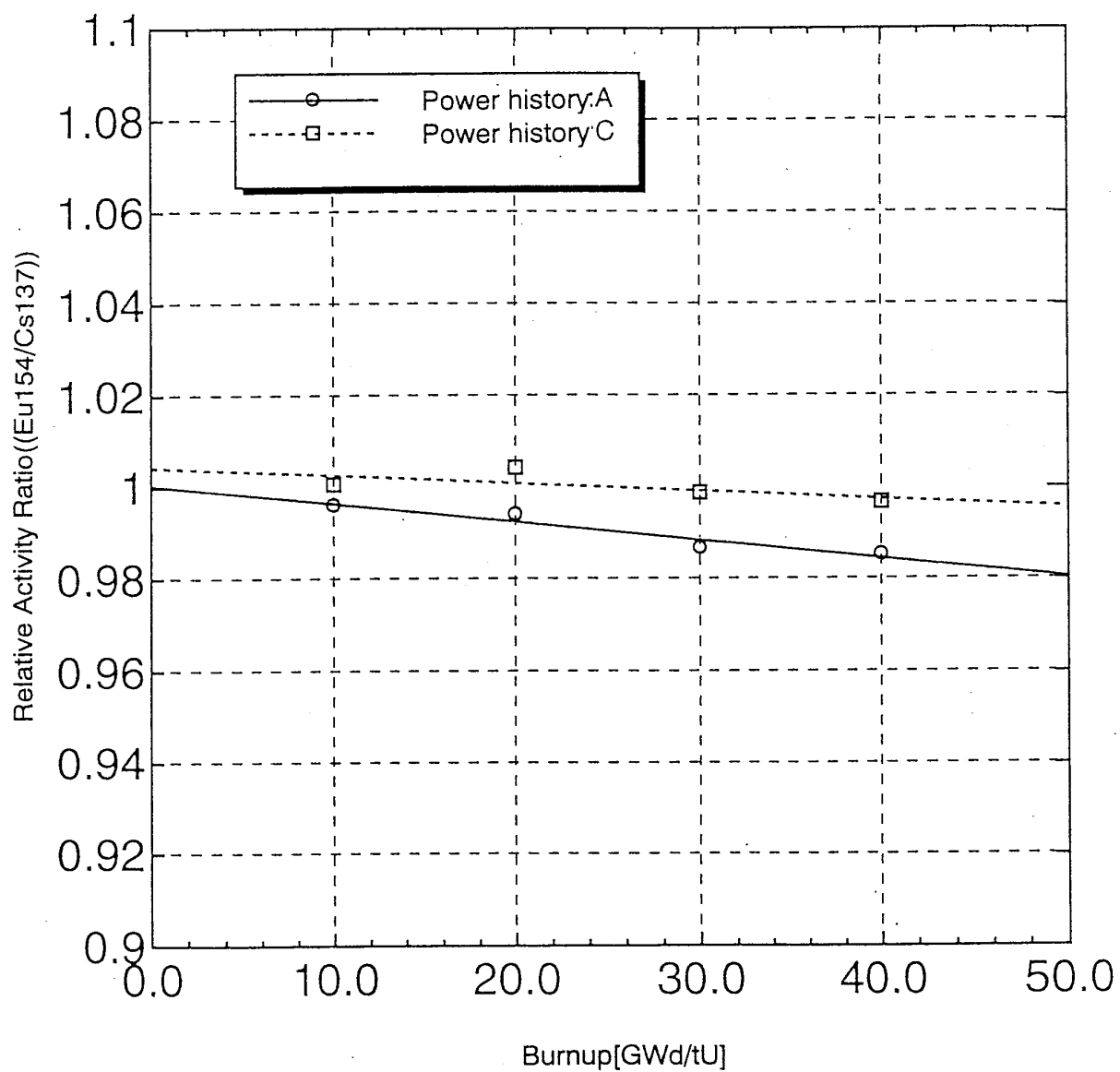


Fig. 5.2.29. Relative activity ratio (Eu-154/Cs-137)  
(Power history dependency, BWR).

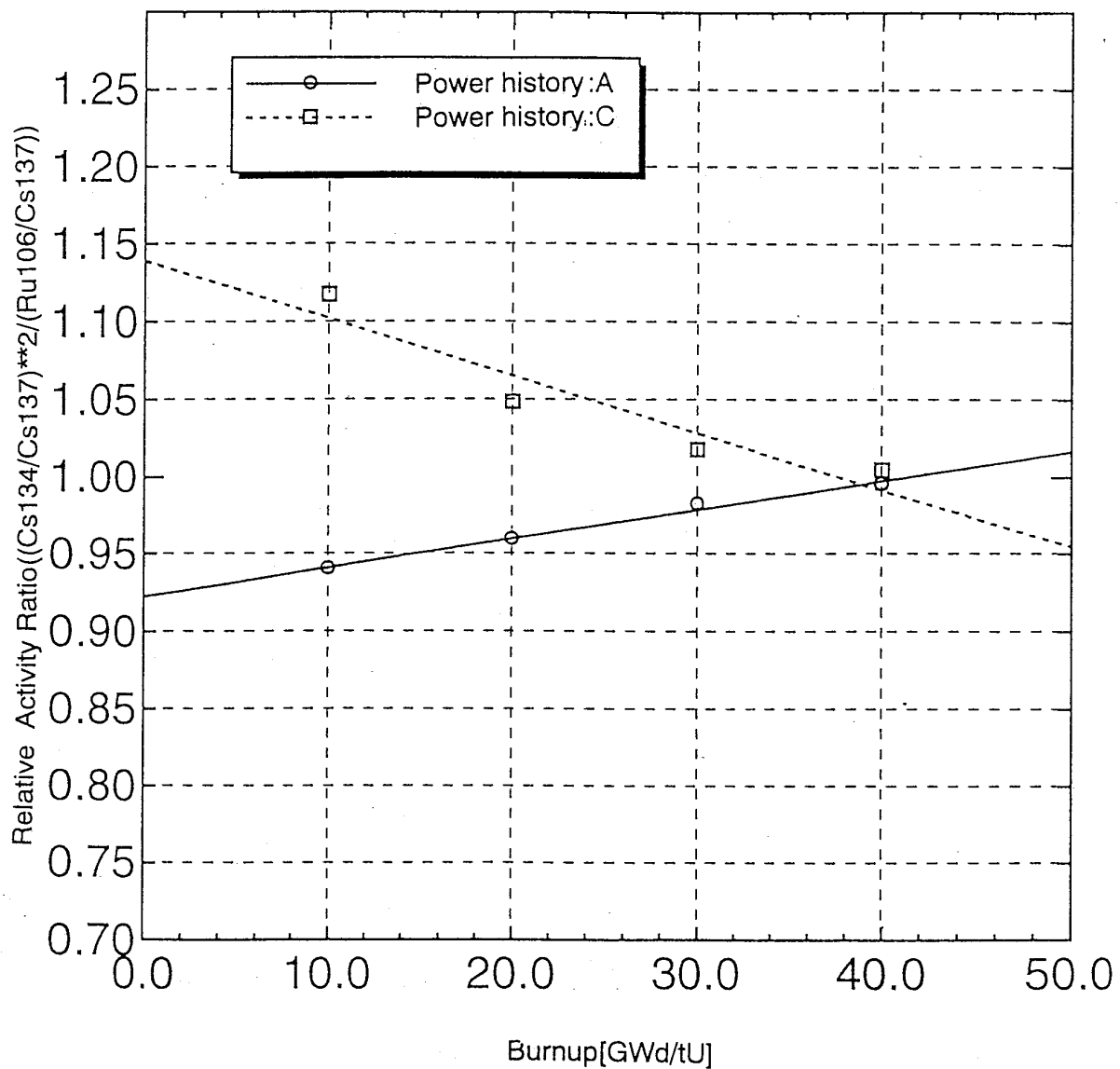


Fig. 5.2.30. Relative activity ratio  $((\text{Cs-134}/\text{Cs-137})^2 / (\text{Ru-106}/\text{Cs-137}))$  vs. burnup  
(Power history dependency, BWR).

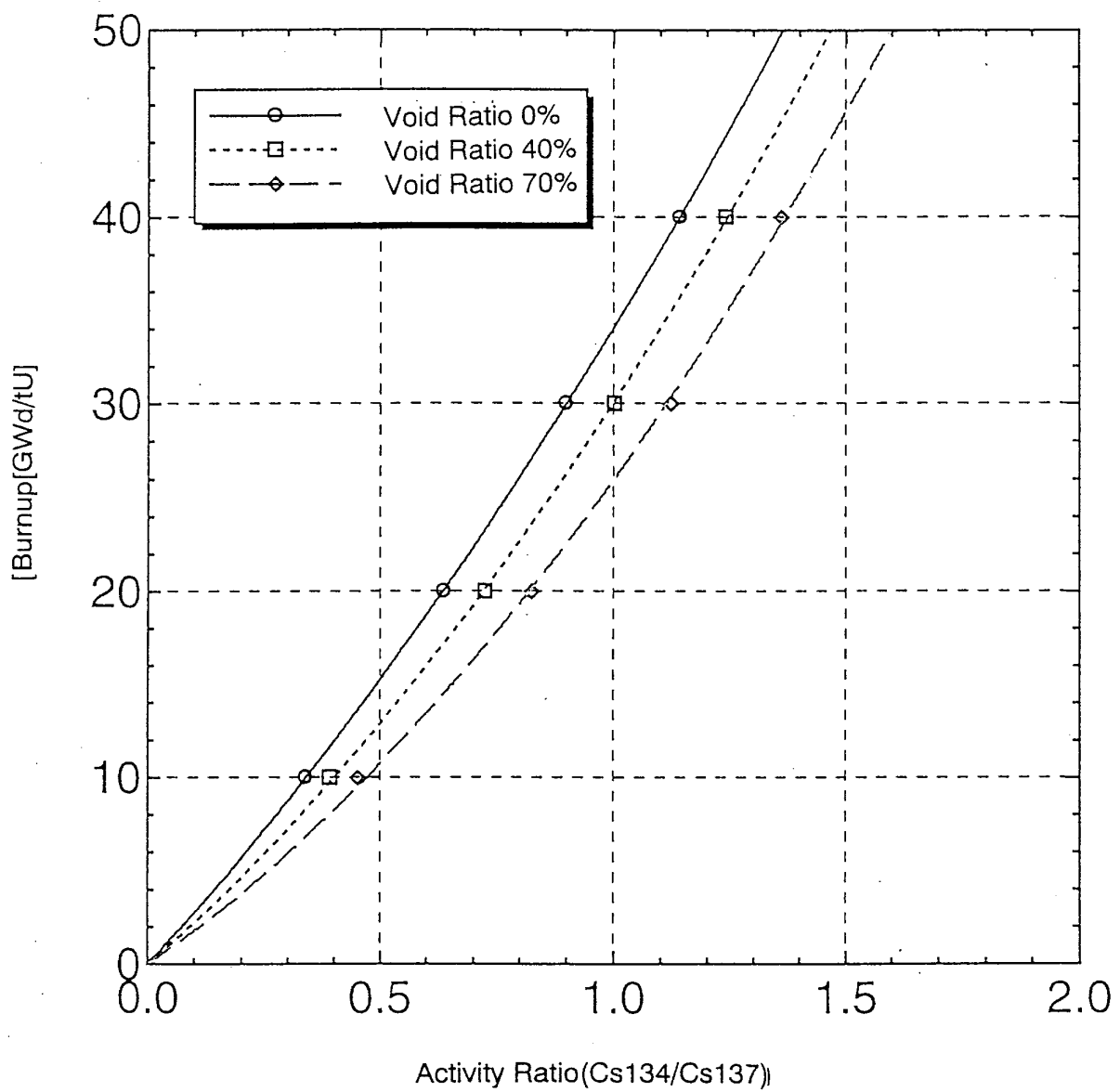


Fig. 5.2.31. Cs Activity ratio (Cs-134/Cs-137) vs. burnup  
(Void ratio dependency, BWR).

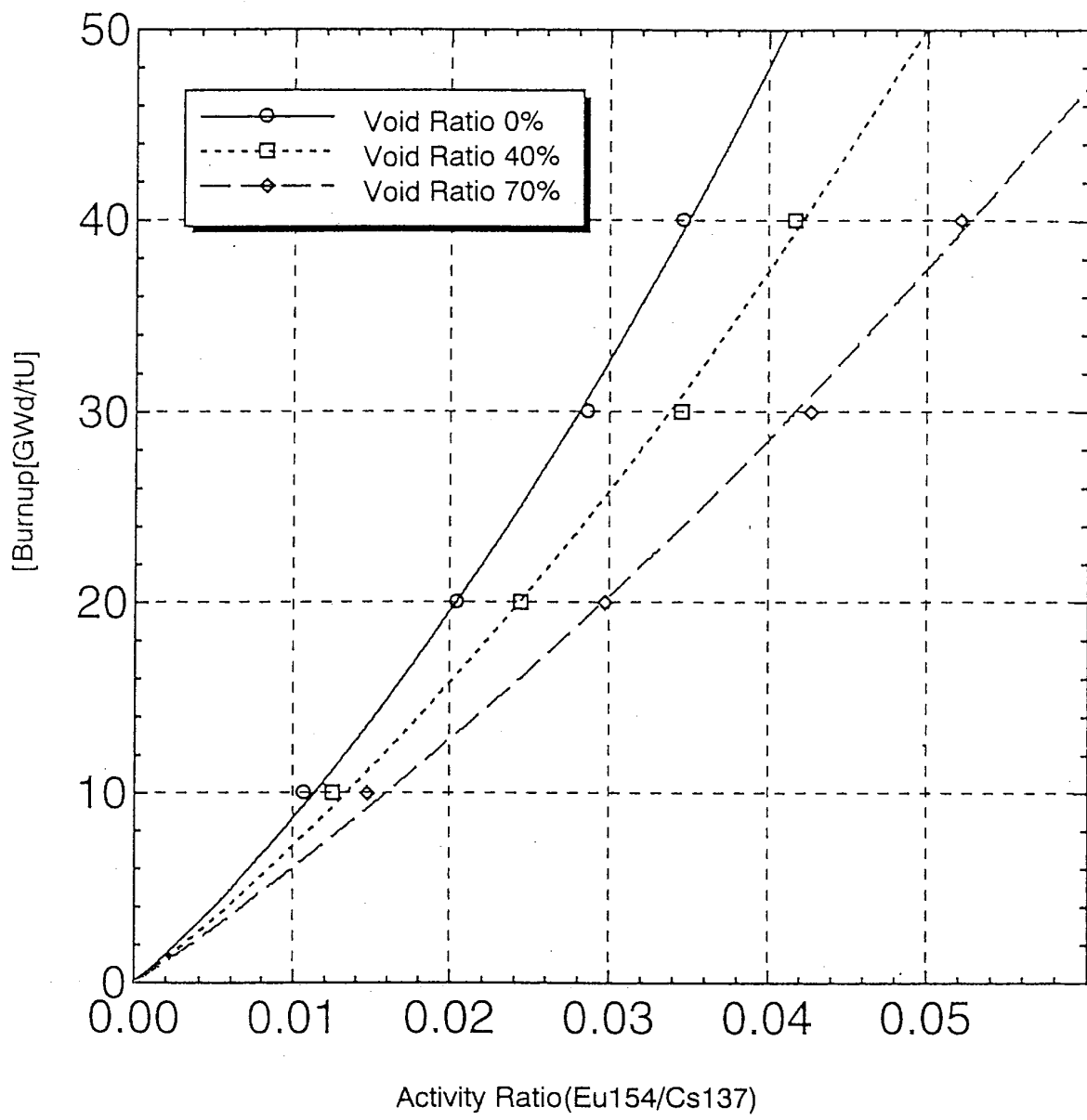


Fig. 5.2.32. Eu Activity ratio (Eu-154/Cs-137) vs. burnup  
(Void ratio dependency, BWR).

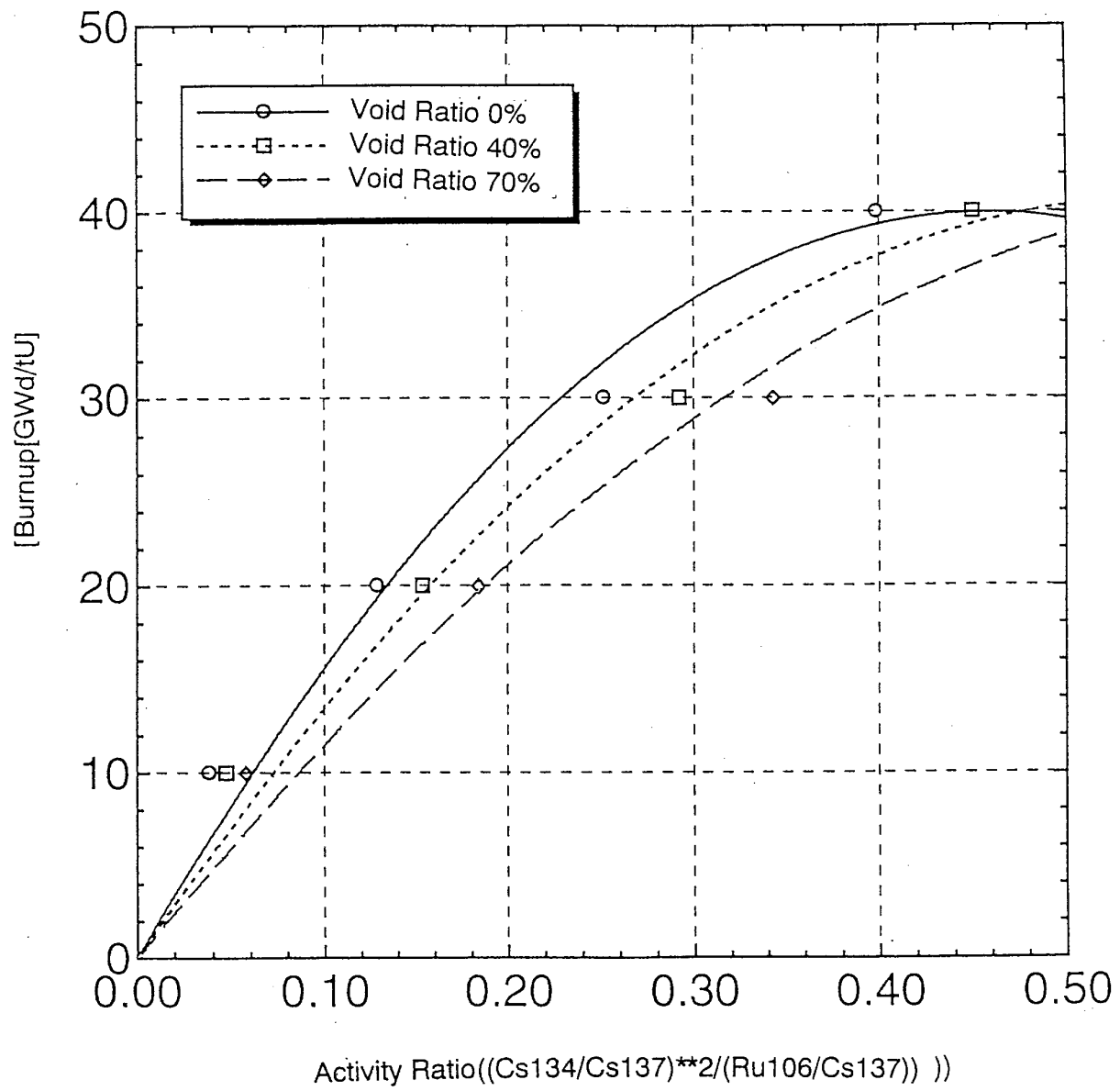


Fig. 5.2.33. Ru Activity ratio  $((\text{Cs}^{134}/\text{Cs}^{137})^2 / (\text{Ru}^{106}/\text{Cs}^{137}))$  vs. burnup  
(Void ratio dependency, BWR).

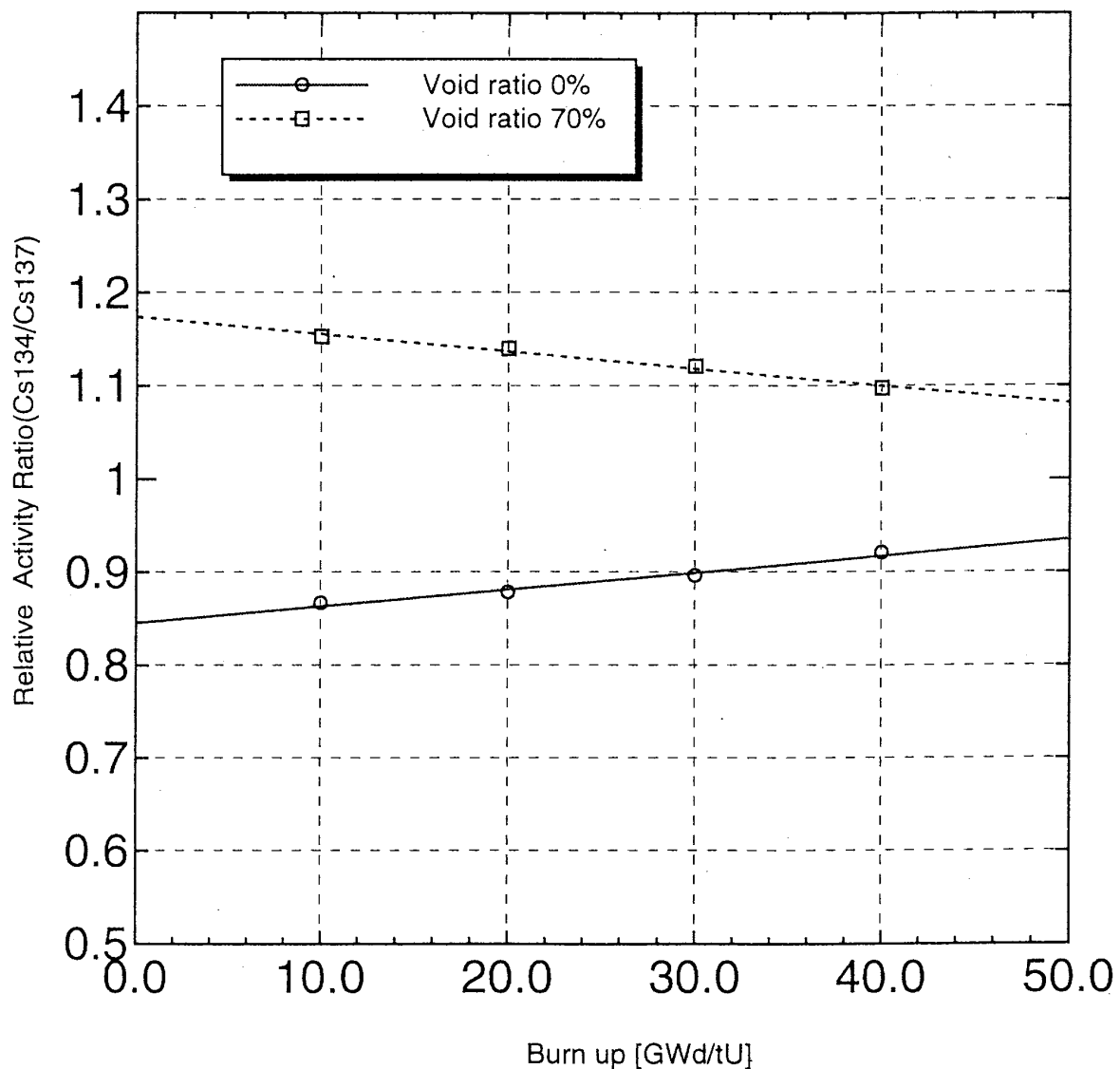


Fig.5.2.34. Relative activity ratio (Cs-134/Cs-137)  
(Void ratio dependency, BWR).

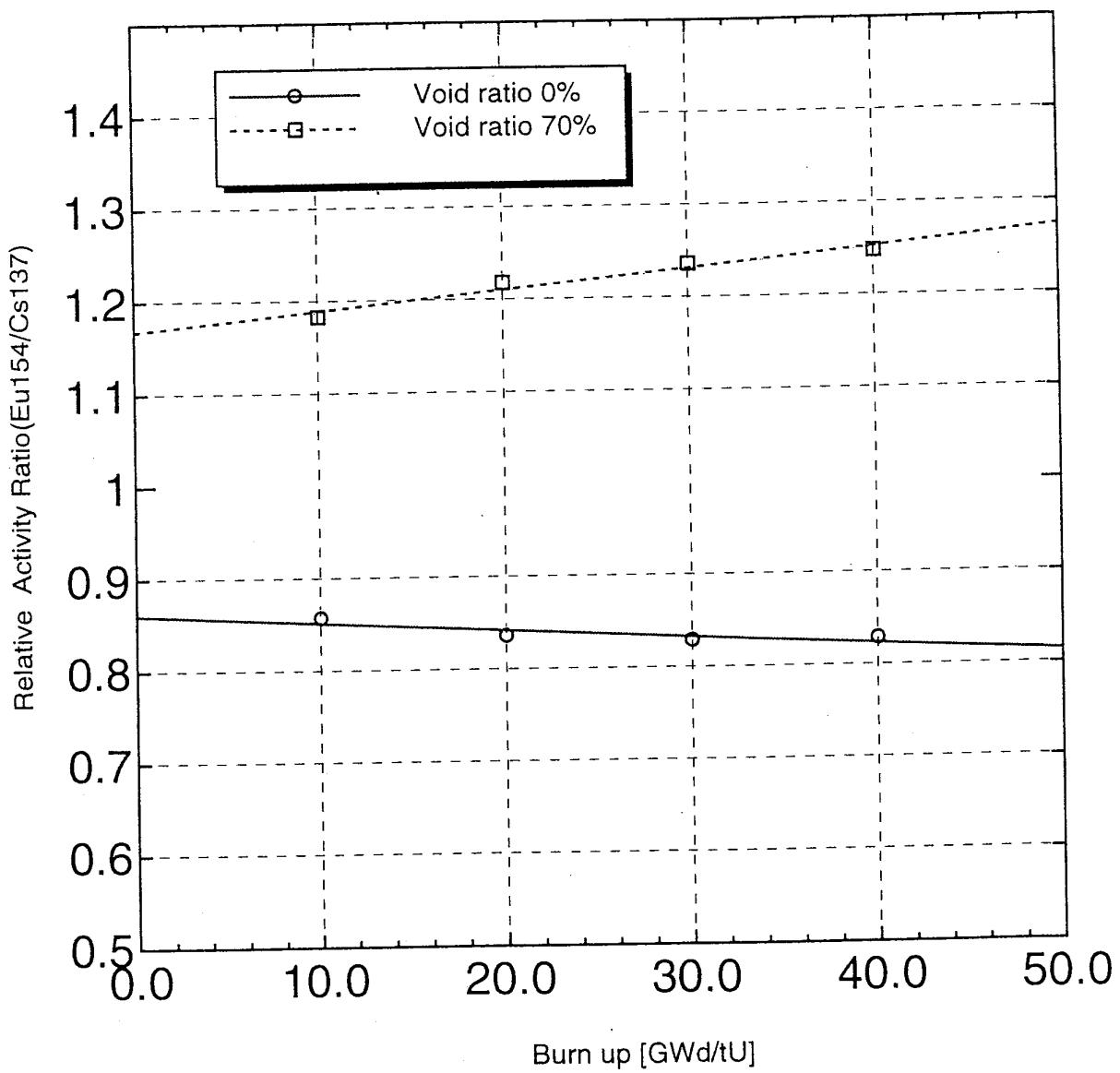


Fig. 5.2.35. Relative activity ratio (Eu-154/Cs-137)  
(Void ratio dependency, BWR).

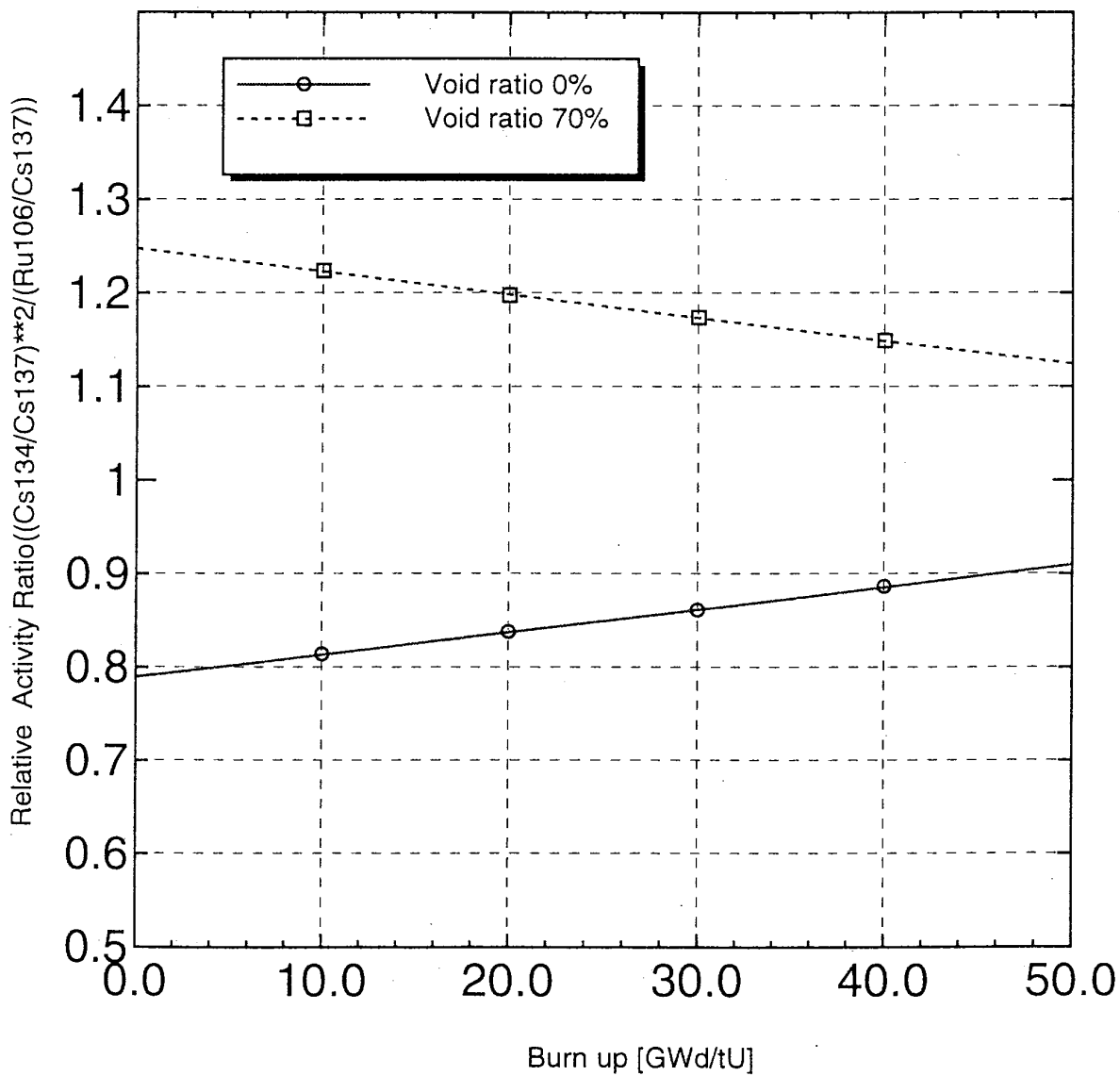


Fig. 5.2.36. Relative activity ratio  $((\text{Cs-134}/\text{Cs-137})^2 / (\text{Ru-106}/\text{Cs-137}))$  vs. burnup  
(Void ratio dependency, BWR).



## **6. EXAMINATION OF THE SAFETY MARGIN**

In Sect. 6, we will examine the safety margin for a change in burnup for models of spent fuel transport and mid-storage casks, similar to those to be actually used, by comparing the results of criticality analysis using actually measured nuclide compositions obtained by the destructive analysis of spent fuels actually irradiated in PWRs and BWRs at this present special committee with the results of criticality analysis using calculated nuclide compositions obtained by ORIGEN2.1 burnup calculation code which is usually used, and by SWAT calculation code which enables detailed burnup analysis in which changes in environmental conditions during irradiation are included. For the evaluation of the source term for safety analysis of shielding and heating, changes in the strength of a source with cooling time as a parameter will be determined by ORIGEN2 calculation and evaluated by comparison, based on the neutron strength that can be obtained from actually measured nuclide compositions immediately after cooling, and from the calculated values of burnup by ORIGEN2.1 or SWAT.

### **6.1. Examination of the Criticality Safety Margin for a Spent Fuel Transport Cask Model**

#### **6.1.1. General**

We carry out criticality safety analysis with burnup taken into consideration for the transport cask to be used for transporting the spent fuels (PWR type) of light-water-reactor power stations to reprocessing plants. We use two types of the compositions of nuclides in a spent fuel, i.e., those calculated from initial composition specifications by ORIGEN2.1 or SWAT burnup calculation code, and those obtained by actually cutting out a piece of the spent fuel and carrying out destructive analysis.

We carry out criticality analysis with burnup and cooling time as parameters by MCNP-4A or KENO-V, assuming that fuel assemblies with the same burnup are arranged in a transport cask, and compare and evaluate the calculated values of the neutron multiplication factor  $k_{\text{eff}}$ .

Furthermore, assuming that fuel assemblies with different average burnups are arranged in the horizontal direction in a transport cask, we carry out criticality analyses with consideration of their horizontal burnup distribution and with consideration of the axial burnup distribution of a spent fuel, and compare these results with the results of analysis with no burnup distribution taken into consideration. We also carry out analyses with consideration of both the axial burnup distribution and the horizontal burnup distribution in the cask.

## **6.1.2. Objective, Conditions, and Modeling for Analysis**

### **(1) Object of Analysis**

The particulars of a fuel element and a fuel assembly as the object of analysis are shown in Table 6.1.1.

### **(2) Analytical Conditions**

For the compositions of nuclides in a spent fuel, we consider 12 nuclides of fission products (FPs) which have been recommended for criticality safety analysis in the Criticality Safety Handbook in Japan, in addition to actinides (ACs) such as principal uranium and plutonium with a fresh fuel and burnup as parameters. Furthermore, we analyze neutron multiplication factors for the case of using actually measured isotopic number densities and for the case of using these densities calculated by ORIGEN2 code or SWAT unified code in criticality calculation, and compare and evaluate these results in order to examine the extent to which the accuracy of the data of nuclide compositions by burnup calculation affects the criticality safety margin. We use the measured values by destructive analysis of 5 spent fuels (we also consider calculated values by ORIGEN2 for comparison) for the compositions of nuclides of principal ACs, and use values calculated by the SWAT code system for the compositions of 12 FP nuclides, because of no measured values. Moreover, we calculate by ORIGEN2 the compositions of nuclides immediately after removing the fuel from the reactor and after cooling periods of 5 years, 10 years, 30 years, and 50 years, carry out criticality calculation based on these compositions, and compare the results. Table 6.1.2 shows the operating history, output, and burnup of each sample, and Tables 6.1.3(1)–6.1.3(5) show the atomic number densities of nuclide compositions determined as sample cases for each sample No. as mentioned above.

The material of the baskets in which fuel assemblies are placed is boron- containing stainless steel (B-containing SS), which is a neutron absorbing material for maintaining noncriticality, but we also carry out analysis for the case of using stainless steel (SS) in place of the above-mentioned material, and examine the effect of the change in the neutron spectrum associated with the change in the burnup of the spent fuel placed in the basket.

We place 14 fuel assemblies in a transport cask. We arrange the fuel assemblies equally in the transport cask. We then carry out analysis by considering only the fuel assembly average burnup and not considering the axial and horizontal distributions of the burnups.

In criticality analysis, taking the distribution of the burnups into consideration, we use the measured values of nuclide compositions of SF95-1-4, which gives the highest burnup. We also carry out criticality analysis with consideration of both the axial burnup distribution in the effective fuel section and the horizontal burnup distribution in the transport cask at the same time, and compare the results with the analytical results obtained without considering the burnup distributions.

### **(3) Modeling**

With regard to the geometric configuration, to be on the safe side, we assume a damaged state as a model, which can be applied commonly to the respective states of isolated systems and arranged systems of undamaged and damaged transported matter. We also disregard the neutron shield, the fins, and the upper

and lower buffers, and replace them by voids. For the boundary condition, we assume an infinite arrangement and mirror-surface complete reflection. Taken together, these assumptions give tough results from the viewpoint of criticality analysis. We consider only the area corresponding to the effective fuel length as the area to be considered as a fuel assembly region, and construct a model in which the upper and lower nozzle sections are replaced by water. We also replace the grid, in which control-rod guide thimbles to hold the burnable poison rods in a fuel assembly are placed, by water. Furthermore, we assume that all cylinders in the transport cask are filled with water.

Figures 6.1.1 and 6.1.2 show a calculation model common to MCNP-4A/KENO-V.a. As shown in Fig. 6.1.3, we represent each fuel assembly by a heterogeneous model, without further homogenization.

We represent the axial burnup distribution of the effective fuel section by a model, with reference to the mesh-forming method being employed by the burnup credit evaluation working group of OECD/NEA, based on the charts disclosed in ANS, etc., obtained by processing a large number of data on burned fuels from the U.S. Yankee reactor. The axial burnup profile models of a PWR fuel thus prepared are shown in Fig. 6.1.4.

When considering the horizontal burnup distribution in the transport cask, we assume from the actual transport results of Haranen Yuso (Ltd.) that there are variations of  $\pm 30\%$  for the average burnup of fuel assemblies to be placed in one transport cask. We arrange 7 fuel assemblies with the maximum burnup (average burnup  $\times 130\%$ ) in a cluster at the center and 7 fuel assemblies with the minimum burnup (average burnup  $\times 70\%$ ) in a cluster at the periphery, as shown in Fig. 6.1.5, with consideration of the shielding aspect. When considering both axial distribution and horizontal distribution in the cask of burnups at the same time, we calculate the burnup in each fuel assembly region by combining the above-mentioned methods. Table 6.1.4 shows the burnup in each region of the effective fuel section when the burnup distributions are taken into consideration.

### 6.1.3. Calculation Codes Used and Their Calculation Conditions

For criticality calculation, we selected the continuous energy Monte Carlo code MNNP-4A (Ref. 1) which enables detailed calculation, and the conventionally used multi-group energy Monte Carlo code KENO-V.a (Ref. 2) from among generally used criticality analysis codes.

The MCNP-4A Monte Carlo calculation conditions are as follows:

- Number of batches: 500
- Number of neutrons generated: 10,000
- Cross-section library used: FSXLIB-J3R2 [Ref. 3] (JENDL-3.2 [Ref. 4]; endl7167 used only for  $^{234}\text{U}$ )

The KENO-V.a Monte Carlo calculation conditions are as follows:

- Number of generations (cycles): 300 or 500
- Number of neutrons generated: 10,000
- Cross-section library used: 44 groupendf5 (SCALE-4.3 built-in library)

In the KENO-V.a calculation, we calculate the Bondarenko resonance self shielding factor in order to determine the 44-group constant data library. Because of this, we carried out processing by BONAMI and NITAWL, using the CSAS25 control module in the SCALE-4.3 code system.<sup>2</sup>

#### 6.1.4. Results and Discussion

(1) The neutron multiplication factor  $k_{\text{eff}}$  obtained by calculating the compositions of AC and FP nuclides in the spent fuel by ORIGEN2 burnup code for general use, and carrying out a criticality calculation using multi-group Monte Carlo code KENO-V.a for general use, and the  $k_{\text{eff}}$  determined by using measured AC compositions and calculating FP compositions by SWAT code for detailed burnup calculation, and carrying out criticality calculation using high-precision continuous energy Monte Carlo code MCNP-4A are plotted against burnup in Fig. 6.1.6. The vertical axis of this figure shows the value of  $k_{\text{eff}}$  obtained by Monte Carlo calculation plus  $3 \times$  standard deviation  $\sigma$  (likewise for the rest). From this figure, it can be seen that the calculated value of  $k_{\text{eff}}$  is about 5% lower in SF95-1-2 (25238 MWd/MTU) and about 7% lower in SF95-1-4 (38064 MWd/MTU) when the all-nuclide compositions in the fuel region are calculated by ORIGEN2 for general use, and the difference increases as the burnup increases.

For reference, Figs. 6.1.6-1 and 6.1.6-2 show a comparison of the calculated values of  $k_{\text{eff}} + 3\sigma$  in criticality analysis by KENO-V.a and MCNP-4A Monte Carlo codes using the measured values of nuclide compositions of only actinides in spent fuels. As can be seen from these figures, there is some difference depending on whether or not boron (B) is contained in the SUS304 basket material, but the difference in the calculated value of  $k_{\text{eff}} + 3\sigma$  due to the difference in the calculation code is very small (1.5% at most).

(2) As can be seen similarly from Fig. 6.1.6, the calculated value of  $k_{\text{eff}}$  by a combination of ORIGEN2 burnup calculation code and KENO-V.a criticality calculation code is about 17% lower at 25,238 MWd/MTU corresponding to sample SF95-1-2, and about 26% lower at 38,064 MWd/MTU corresponding to sample SF95-1-4, when compared with the calculated value of  $k_{\text{eff}} + 3\sigma$ , i.e., about 0.86 in a fresh fuel composition with zero burnup, and this difference is larger at higher burnup. The value of  $k_{\text{eff}}$  becomes higher when calculated by a combination of SWAT burnup calculation code for detailed calculation, measured values of AC compositions, and MCNP-4A criticality calculation code, as mentioned in (1).

(3) Figure 6.1.7 shows a comparison of the results of criticality calculation by KENO-V.a using the calculated values of all nuclide compositions in the fuel region by ORIGEN2 (lower curve of Fig. 6.1.6) with the results of calculation disregarding FPs from the same calculation conditions. If FPs are disregarded, the calculated value of  $k_{\text{eff}}$  becomes about 3% higher in SF95-1-2 (25,238 MWd/MTU), and about 5% higher in SF95-1-4 (38,064 MWd/MTU). Furthermore, when only the measured values of AC nuclide compositions are taken into consideration, this difference increases further, i.e., about 6% and about 8%, respectively.

(4) Figure 6.1.8 shows the calculated value of  $k_{\text{eff}}$  versus cooling time when the ORIGEN2 calculated values of AC and FP nuclide compositions in the fuel region are used. As can be seen from this figure, the  $k_{\text{eff}}$  of the system decreases monotonously with cooling time on account of the accumulation of FPs with thermal neutron absorbing property, such as  $^{155}\text{Gd}$ .

(5) The above-mentioned results were obtained without considering the axial and horizontal burnup distributions. Figure 6.1.9 shows the calculated values of  $k_{\text{eff}}$  with the burnup distributions taken into consideration. In this calculation, both actinides (Ac) and fission products (FP) are taken into consideration. As this figure shows, the  $k_{\text{eff}}$  becomes 1–5% larger with consideration of the horizontal burnup distribution than without, and 0.2–3.6% larger with consideration of the axial burnup distribution than without, for the change in burnup from 15,000 (MWd/MTU) to 38,000 (MWd/MTU) with consideration of Ac and FP.

(6) With only Ac taken into consideration, the  $k_{\text{eff}}$  becomes 0.5–4% larger with consideration of the horizontal burnup distribution than without, and about 0.4–1.6% larger with consideration of the axial burnup distribution than without, as shown in Fig. 6.1.10. On the basis of these considerations and the results mentioned in (5), the difference in the calculated  $k_{\text{eff}}$  tends to be larger with consideration of the horizontal burnup distribution than with consideration of the axial burnup distribution, when compared with the  $k_{\text{eff}}$  with no burnup distribution consideration. With only Ac taken into consideration, the  $k_{\text{eff}}$  becomes 0.1–4.2% larger when both horizontal and axial distributions are taken into consideration than without such consideration.

Table 6.1.1. Main feature of fuel assembly for criticality analysis

Type of fuel assembly	PWR fuel assembly
Fuel material	$\text{UO}_2$
Covering tube material	Zircaloy-4
Fuel rod diameter, mm	10.72
Fuel rod pellet diameter, mm	9.29
Covering tube thickness, mm	0.62
Effective fuel length, mm	3642
Fuel rod arrangement	$15 \times 15$
Fuel rods per assembly (number)	214
Fuel rod pitch, mm	14.30
Width of assembly, mm	214.5
Uranium weight per assembly, kg	470 or less
$\text{UO}_2$ enrichment, %	4.1 (initial)

Table 6.1.2. Spent fuel irradiation conditions

Sample No.		SF95-1-1	SF95-1-2	SF95-1-3	SF95-1-4	SF95-1-5
Operating history		385-day operating (cycle 5) 88-day cooling 402 day operating (cycle 6)				
Output	Cycle 5	18.65	32.07	46.63	48.37	39.85
(MW/MTU)	Cycle 6	18.65	32.07	46.63	48.37	39.85
Burnup (MWd/MTU)		14678	25238	36700	38064	31063

Table 6.1.3 (1). Atomic number density of actinide and fission products (1)  
 Sample No: SF95-1-1 Burnup: 14678 (MWd/MTU)

	Nuclide	Immediately after cooling		Cooling 5 years	Cooling 10 years	Cooling 30 years	Cooling 50 years
		Exp&SWAT	ORIGEN-2				
Ac	U-234	7.060E-06	7.427E-06	7.439E-06	7.450E-06	7.491E-06	7.526E-06
	U-235	6.295E-04	6.166E-04	6.166E-04	6.166E-04	6.166E-04	6.166E-04
	U-236	6.263E-05	6.290E-05	6.293E-05	6.293E-05	6.297E-05	6.300E-05
	U-238	2.207E-02	2.210E-02	2.210E-02	2.210E-02	2.210E-02	2.210E-02
	Pu-238	3.992E-07	2.796E-07	2.926E-07	2.812E-07	2.403E-07	2.054E-07
	Pu-239	9.782E-05	8.442E-05	8.514E-05	8.514E-05	8.509E-05	8.504E-05
	Pu-240	1.798E-05	1.750E-05	1.750E-05	1.749E-05	1.745E-05	1.741E-05
	Pu-241	8.467E-06	6.391E-06	5.024E-06	3.949E-06	1.508E-06	5.758E-07
	Pu-242	8.662E-07	6.605E-07	6.607E-07	6.607E-07	6.607E-07	6.607E-07
	Am-241	3.163E-07	1.813E-07	1.541E-06	2.600E-06	4.913E-06	5.673E-06
	Am-242m	4.205E-09	3.094E-09	3.024E-09	2.955E-09	2.699E-09	2.464E-09
	Am-243	6.104E-08	3.808E-08	3.815E-08	3.812E-08	3.805E-08	3.796E-08
	Cm-242	3.450E-08	2.138E-08	1.655E-11	7.169E-12	6.527E-12	5.958E-12
	Cm-243	3.301E-10	1.907E-10	1.688E-10	1.495E-10	9.190E-11	5.651E-11
	Cm-244	6.148E-09	2.851E-09	2.357E-09	1.946E-09	9.051E-10	4.209E-10
	Cm-245	1.246E-10	4.246E-11	4.246E-11	4.244E-11	4.237E-11	4.230E-11
	Cm-246	5.756E-12	9.777E-13	9.771E-13	9.764E-13	9.735E-13	9.705E-13
FP	Mo-95	1.759E-05	1.770E-05	2.150E-05	2.150E-05	2.150E-05	2.150E-05
	Tc-99	2.076E-05	2.050E-05	2.062E-05	2.062E-05	2.062E-05	2.062E-05
	Rh-103	1.076E-05	1.079E-05	1.185E-05	1.185E-05	1.185E-05	1.185E-05
	Cs-133	2.237E-05	2.263E-05	2.290E-05	2.290E-05	2.290E-05	2.290E-05
	Nd-143	1.750E-05	1.789E-05	1.841E-05	1.841E-05	1.841E-05	1.841E-05
	Nd-145	1.280E-05	1.293E-05	1.294E-05	1.294E-05	1.294E-05	1.294E-05
	Sm-147	1.576E-06	1.534E-06	4.820E-06	5.697E-06	6.013E-06	6.017E-06
	Sm-149	9.403E-08	1.107E-07	1.311E-07	1.311E-07	1.311E-07	1.311E-07
	Sm-150	4.008E-06	4.184E-06	4.184E-06	4.184E-06	4.184E-06	4.184E-06
	Sm-152	2.104E-06	2.077E-06	2.077E-06	2.077E-06	2.078E-06	2.078E-06
	Eu-153	1.090E-06	1.098E-06	1.105E-06	1.105E-06	1.105E-06	1.105E-06
	Gd-155	1.157E-09	2.123E-09	5.838E-08	8.638E-08	1.123E-07	1.139E-07

Unit:atoms/b•cm

Table 6.1.3 (2). Atomic number density of actinide and fission products (2)  
 Sample No: SF95-1-2      Burnup: 25238 (MWd/MTU)

	Nuclide	Immediately after cooling		Cooling 5 years	Cooling 10 years	Cooling 30 years	Cooling 50 years
		Exp&SWAT	ORIGEN-2				
Ac	U-234	6.737E-06	6.540E-06	6.585E-06	6.632E-06	6.796E-06	6.937E-06
	U-235	4.536E-04	4.262E-04	4.262E-04	4.262E-04	4.265E-04	4.265E-04
	U-236	9.431E-05	9.386E-05	9.388E-05	9.391E-05	9.398E-05	9.405E-05
	U-238	2.190E-02	2.195E-02	2.195E-02	2.195E-02	2.195E-02	2.195E-02
	Pu-238	1.651E-06	1.110E-06	1.176E-06	1.131E-06	9.660E-07	8.254E-07
	Pu-239	1.309E-04	1.047E-04	1.061E-04	1.061E-04	1.060E-04	1.060E-04
	Pu-240	3.546E-05	3.489E-05	3.489E-05	3.487E-05	3.482E-05	3.475E-05
	Pu-241	2.198E-05	1.583E-05	1.244E-05	9.779E-06	3.734E-06	1.426E-06
	Pu-242	4.214E-06	3.177E-06	3.177E-06	3.177E-06	3.177E-06	3.177E-06
	Am-241	5.380E-07	4.053E-07	3.773E-06	6.394E-06	1.212E-05	1.401E-05
	Am-242m	1.189E-08	9.592E-09	9.377E-09	9.164E-09	8.367E-09	7.635E-09
	Am-243	5.209E-07	3.498E-07	3.503E-07	3.500E-07	3.494E-07	3.487E-07
	Cm-242	1.753E-07	9.884E-08	6.532E-11	2.223E-11	2.023E-11	1.847E-11
	Cm-243	2.823E-09	1.705E-09	1.510E-09	1.337E-09	8.219E-10	5.053E-10
	Cm-244	1.143E-07	5.288E-08	4.370E-08	3.608E-08	1.678E-08	7.806E-09
	Cm-245	4.428E-09	1.396E-09	1.396E-09	1.395E-09	1.393E-09	1.391E-09
	Cm-246	2.675E-10	6.367E-11	6.362E-11	6.358E-11	6.338E-11	6.320E-11
FP	Mo-95	2.888E-05	2.922E-05	3.546E-05	3.546E-05	3.546E-05	3.546E-05
	Tc-99	3.436E-05	3.404E-05	3.424E-05	3.424E-05	3.424E-05	3.424E-05
	Rh-103	1.778E-05	1.759E-05	1.958E-05	1.958E-05	1.958E-05	1.958E-05
	Cs-133	3.668E-05	3.717E-05	3.762E-05	3.763E-05	3.762E-05	3.762E-05
	Nd-143	2.700E-05	2.780E-05	2.865E-05	2.865E-05	2.865E-05	2.865E-05
	Nd-145	2.076E-05	2.105E-05	2.106E-05	2.106E-05	2.106E-05	2.106E-05
	Sm-147	2.246E-06	2.120E-06	6.567E-06	7.753E-06	8.182E-06	8.186E-06
	Sm-149	9.846E-08	1.211E-07	1.629E-07	1.629E-07	1.629E-07	1.629E-07
	Sm-150	7.250E-06	8.070E-06	8.070E-06	8.070E-06	8.070E-06	8.070E-06
	Sm-152	3.529E-06	3.598E-06	3.598E-06	3.598E-06	3.599E-06	3.600E-06
	Eu-153	2.345E-06	2.451E-06	2.472E-06	2.472E-06	2.472E-06	2.472E-06
	Gd-155	1.461E-09	2.426E-09	1.195E-07	1.777E-07	2.317E-07	2.350E-07

Unit:atoms/b•cm

Table 6.1.3 (3). Atomic number density of actinide and fission products (3)  
 Sample No: SF95-1-3 Burnup: 36700 (MWd/MTU)

	Nuclide	Immediately after cooling		Cooling 5 years	Cooling 10 years	Cooling 30 years	Cooling 50 years
		Exp&SWAT	ORIGEN-2				
Ac	U-234	4.426E-06	5.557E-06	5.680E-06	5.803E-06	6.240E-06	6.614E-06
	U-235	3.121E-04	2.636E-04	2.636E-04	2.636E-04	2.636E-04	2.636E-04
	U-236	1.151E-04	1.169E-04	1.169E-04	1.169E-04	1.170E-04	1.171E-04
	U-238	2.170E-02	2.177E-02	2.177E-02	2.177E-02	2.177E-02	2.177E-02
	Pu-238	3.577E-06	2.961E-06	3.119E-06	2.998E-06	2.561E-06	2.188E-06
	Pu-239	1.433E-04	1.130E-04	1.154E-04	1.154E-04	1.153E-04	1.153E-04
	Pu-240	5.037E-05	5.190E-05	5.194E-05	5.197E-05	5.199E-05	5.194E-05
	Pu-241	3.410E-05	2.607E-05	2.050E-05	1.611E-05	6.153E-06	2.350E-06
	Pu-242	1.032E-05	8.643E-06	8.643E-06	8.643E-06	8.643E-06	8.643E-06
	Am-241	7.595E-07	5.519E-07	6.102E-06	1.042E-05	1.987E-05	2.297E-05
	Am-242m	1.800E-08	1.514E-08	1.480E-08	1.447E-08	1.321E-08	1.206E-08
	Am-243	1.832E-06	1.507E-06	1.509E-06	1.509E-06	1.506E-06	1.503E-06
	Cm-242	4.488E-07	2.413E-07	1.399E-10	3.510E-11	3.195E-11	2.916E-11
FP	Cm-243	8.467E-09	6.619E-09	5.861E-09	5.189E-09	3.191E-09	1.962E-09
	Cm-244	5.807E-07	3.828E-07	3.162E-07	2.611E-07	1.215E-07	5.651E-08
	Cm-245	3.151E-08	1.484E-08	1.483E-08	1.483E-08	1.480E-08	1.478E-08
	Cm-246	2.358E-09	1.158E-09	1.157E-09	1.156E-09	1.153E-09	1.149E-09
	Mo-95	4.041E-05	4.101E-05	4.971E-05	4.971E-05	4.971E-05	4.971E-05
	Tc-99	4.839E-05	4.787E-05	4.817E-05	4.816E-05	4.816E-05	4.816E-05
	Rh-103	2.450E-05	2.372E-05	2.690E-05	2.690E-05	2.690E-05	2.690E-05
	Cs-133	5.102E-05	5.170E-05	5.236E-05	5.236E-05	5.236E-05	5.236E-05
	Nd-143	3.497E-05	3.609E-05	3.726E-05	3.726E-05	3.726E-05	3.726E-05
	Nd-145	2.865E-05	2.902E-05	2.903E-05	2.903E-05	2.903E-05	2.903E-05
	Sm-147	2.665E-06	2.389E-06	7.320E-06	8.634E-06	9.112E-06	9.116E-06
	Sm-149	9.782E-08	1.258E-07	1.990E-07	1.990E-07	1.990E-07	1.990E-07
	Sm-150	1.108E-05	1.355E-05	1.355E-05	1.355E-05	1.355E-05	1.355E-05
	Sm-152	4.883E-06	5.134E-06	5.134E-06	5.138E-06	5.138E-06	5.138E-06
	Eu-153	3.913E-06	4.374E-06	4.421E-06	4.421E-06	4.421E-06	4.421E-06
	Gd-155	1.739E-09	3.084E-09	2.397E-07	3.574E-07	4.667E-07	4.731E-07

Unit:atoms/b•cm

Table 6.1.3 (4). Atomic number density of actinide and fission products (4)  
 Sample No: SF95-1-4      Burnup: 38064 (MWd/MTU)

	Nuclide	Immediately after cooling		Cooling 5 years	Cooling 10 years	Cooling 30 years	Cooling 50 years
		Exp&SWAT	ORIGEN-2				
Ac	U-234	4.421E-06	5.446E-06	5.583E-06	5.715E-06	6.193E-06	6.602E-06
	U-235	2.896E-04	2.485E-04	2.485E-04	2.485E-04	2.485E-04	2.485E-04
	U-236	1.172E-04	1.187E-04	1.187E-04	1.188E-04	1.189E-04	1.190E-04
	U-238	2.169E-02	2.175E-02	2.175E-02	2.175E-02	2.175E-02	2.175E-02
	Pu-238	3.691E-06	3.237E-06	3.407E-06	3.274E-06	2.798E-06	2.389E-06
	Pu-239	1.390E-04	1.134E-04	1.160E-04	1.160E-04	1.159E-04	1.159E-04
	Pu-240	5.086E-05	5.333E-05	5.339E-05	5.342E-05	5.349E-05	5.344E-05
	Pu-241	3.364E-05	2.726E-05	2.143E-05	1.684E-05	6.430E-06	2.456E-06
	Pu-242	1.098E-05	9.439E-06	9.439E-06	9.439E-06	9.439E-06	9.439E-06
	Am-241	5.395E-07	5.616E-07	6.364E-06	1.088E-05	2.075E-05	2.400E-05
	Am-242m	1.664E-08	1.557E-08	1.522E-08	1.488E-08	1.358E-08	1.240E-08
	Am-243	1.928E-06	1.717E-06	1.720E-06	1.719E-06	1.716E-06	1.713E-06
	Cm-242	5.320E-07	2.603E-07	1.491E-10	3.611E-11	3.284E-11	2.998E-11
	Cm-243	9.049E-09	7.449E-09	6.598E-09	5.842E-09	3.591E-09	2.208E-09
	Cm-244	6.431E-07	4.583E-07	3.785E-07	3.126E-07	1.454E-07	6.764E-07
	Cm-245	3.583E-08	1.836E-08	1.835E-08	1.835E-08	1.832E-08	1.828E-08
	Cm-246	2.812E-09	1.511E-09	1.510E-09	1.509E-09	1.504E-09	1.500E-09
FP	Mo-95	4.183E-05	4.226E-05	5.122E-05	5.122E-05	5.122E-05	5.122E-05
	Tc-99	5.002E-05	4.937E-05	4.967E-05	4.967E-05	4.967E-05	4.966E-05
	Rh-103	2.508E-05	2.430E-05	2.762E-05	2.762E-05	2.762E-05	2.762E-05
	Cs-133	5.271E-05	5.324E-05	5.390E-05	5.390E-05	5.390E-05	5.390E-05
	Nd-143	3.543E-05	3.684E-05	3.805E-05	3.805E-05	3.805E-05	3.805E-05
	Nd-145	2.958E-05	2.984E-05	2.986E-05	2.986E-05	2.986E-05	2.986E-05
	Sm-147	2.737E-06	2.399E-06	7.343E-06	8.660E-06	9.139E-06	9.142E-06
	Sm-149	9.059E-08	1.255E-07	2.027E-07	2.027E-07	2.027E-07	2.027E-07
	Sm-150	1.147E-05	1.404E-05	1.404E-05	1.404E-05	1.404E-05	1.404E-05
	Sm-152	5.080E-06	5.276E-06	5.280E-06	5.280E-06	5.280E-06	5.280E-06
	Eu-153	4.069E-06	4.598E-06	4.649E-06	4.649E-06	4.649E-06	4.649E-06
	Gd-155	1.595E-09	3.161E-09	2.569E-07	3.831E-07	5.003E-07	5.074E-07

Unit:atoms/b•cm

Table 6.1.3 (5). Atomic number density of actinide and fission products (5)  
 Sample No: SF95-1-5 Burnup: 31363 (MWd/MTU)

	Nuclide	Immediately after cooling		Cooling 5 years	Cooling 10 years	Cooling 30 years	Cooling 50 years
		Exp&SWAT	ORIGEN-2				
Ac	U-234	6.688E-06	6.008E-06	6.091E-06	6.172E-06	6.465E-06	6.715E-06
	U-235	3.634E-04	3.316E-04	3.316E-04	3.316E-04	3.319E-04	3.319E-04
	U-236	1.070E-04	1.078E-04	1.079E-04	1.079E-04	1.080E-04	1.081E-04
	U-238	2.182E-02	2.186E-02	2.186E-02	2.186E-02	2.186E-02	2.186E-02
	Pu-238	2.371E-06	1.979E-06	2.092E-06	2.011E-06	1.718E-06	1.468E-06
	Pu-239	1.304E-04	1.104E-04	1.124E-04	1.123E-04	1.123E-04	1.122E-04
	Pu-240	4.197E-05	4.494E-05	4.496E-05	4.496E-05	4.491E-05	4.485E-05
	Pu-241	2.646E-05	2.120E-05	1.666E-05	1.310E-05	5.001E-06	1.910E-06
	Pu-242	6.801E-06	5.782E-06	5.782E-06	5.782E-06	5.782E-06	5.782E-06
	Am-241	6.516E-07	4.989E-07	5.010E-06	8.519E-06	1.620E-05	1.872E-05
	Am-242m	1.300E-08	1.299E-08	1.270E-08	1.241E-08	1.133E-08	1.034E-08
	Am-243	1.001E-06	8.319E-07	8.330E-07	8.325E-07	8.310E-07	8.294E-07
	Cm-242	2.298E-07	1.698E-07	1.039E-10	3.012E-11	2.740E-11	2.502E-11
	Cm-243	5.218E-09	3.835E-09	3.396E-09	3.007E-09	1.849E-09	1.137E-09
	Cm-244	2.412E-07	1.708E-07	1.411E-07	1.165E-07	5.419E-08	2.520E-08
	Cm-245	1.092E-08	5.664E-09	5.661E-09	5.659E-09	5.650E-09	5.641E-09
	Cm-246	4.389E-10	3.507E-10	3.503E-10	3.500E-10	3.491E-10	3.480E-10
FP	Mo-95	3.551E-05	3.574E-05	4.336E-05	4.336E-05	4.336E-05	4.336E-05
	Tc-99	4.227E-05	4.169E-05	4.194E-05	4.194E-05	4.194E-05	4.193E-05
	Rh-103	2.142E-05	2.112E-05	2.373E-05	2.373E-05	2.373E-05	2.373E-05
	Cs-133	4.489E-05	4.533E-05	4.591E-05	4.591E-05	4.591E-05	4.591E-05
	Nd-143	3.141E-05	3.268E-05	3.371E-05	3.371E-05	3.371E-05	3.371E-05
	Nd-145	2.531E-05	2.552E-05	2.553E-05	2.553E-05	2.553E-05	2.553E-05
	Sm-147	2.575E-06	2.310E-06	7.109E-06	8.389E-06	8.853E-06	8.856E-06
	Sm-149	8.763E-08	1.181E-07	1.762E-07	1.762E-07	1.762E-07	1.762E-07
	Sm-150	9.225E-06	1.102E-05	1.102E-05	1.102E-05	1.102E-05	1.102E-05
	Sm-152	4.366E-06	4.442E-06	4.442E-06	4.442E-06	4.446E-06	4.446E-06
	Eu-153	3.135E-06	3.444E-06	3.476E-06	3.476E-06	3.476E-06	3.476E-06
	Gd-155	1.382E-09	2.741E-09	1.766E-07	2.630E-07	3.432E-07	3.482E-07

Unit:atoms/b•cm

Table 6.1.4. Averaged burnup for each fuel region in the assumed PWR  
(UO<sub>2</sub>) fuel rods by considering axial and horizontal burnup distribution

		SF95-1-1	SF95-1-2	SF95-1-3	SF95-1-4	SF95-1-5	SF97-1-5
		14678 MWd/MTU	25238 MWd/MTU	36700 MWd/MTU	38064 MWd/MTU	31363 MWd/MTU	48220 MWd/MTU
Axial burnup distribution considered	Region-1	7382	13443	19653	20384	16795	25822
	Region-2	8808	15716	22497	23334	19226	29559
	Region-3	10948	19125	26764	27759	22872	35165
	Region-4	14839	25219	34422	35701	29416	45226
	Region-5	16245	27405	39664	41139	33896	52115
	Region-6	6903	16665	26731	27725	22844	35122
	Region-7	4866	11216	19398	20119	16578	25488
	Region-8	3793	8444	15640	16221	13366	20549
	Region-9	3078	6596	13134	13623	11224	17257
Horizontal	Center	—	19081	32809	47710	49483	40772
	Periphe.	—	10275	17667	25690	26645	21954
Axial × Horizontal	Center × Horizontal	Region-1	9596	17476	25549	26499	21834
		Region-2	11451	20430	29247	30334	24994
		Region-3	14232	24862	34793	36086	29733
		Region-4	19291	32785	44748	46411	38241
		Region-5	21118	35626	51564	53480	44065
		Region-6	8974	21664	34751	36042	29697
		Region-7	6326	14580	25218	26155	21551
		Region-8	4931	10977	20332	21088	17375
		Region-9	4001	8575	17075	17709	14592
(MWd/MTU)							

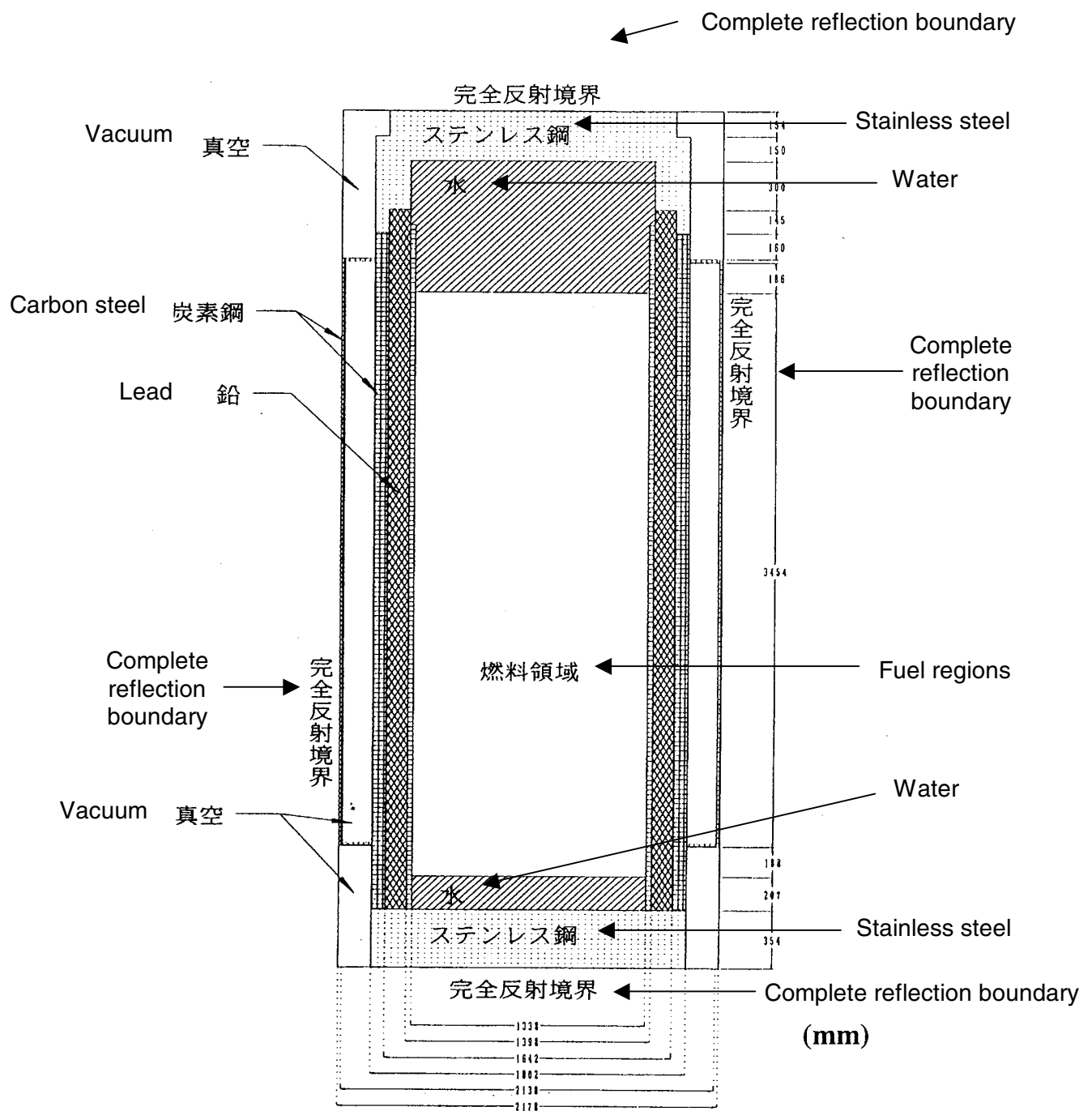


Fig. 6.1.1. Criticality calculation model for MCNP-4A/KENO-V.a  
(Longitudinal cross section of transport cask).

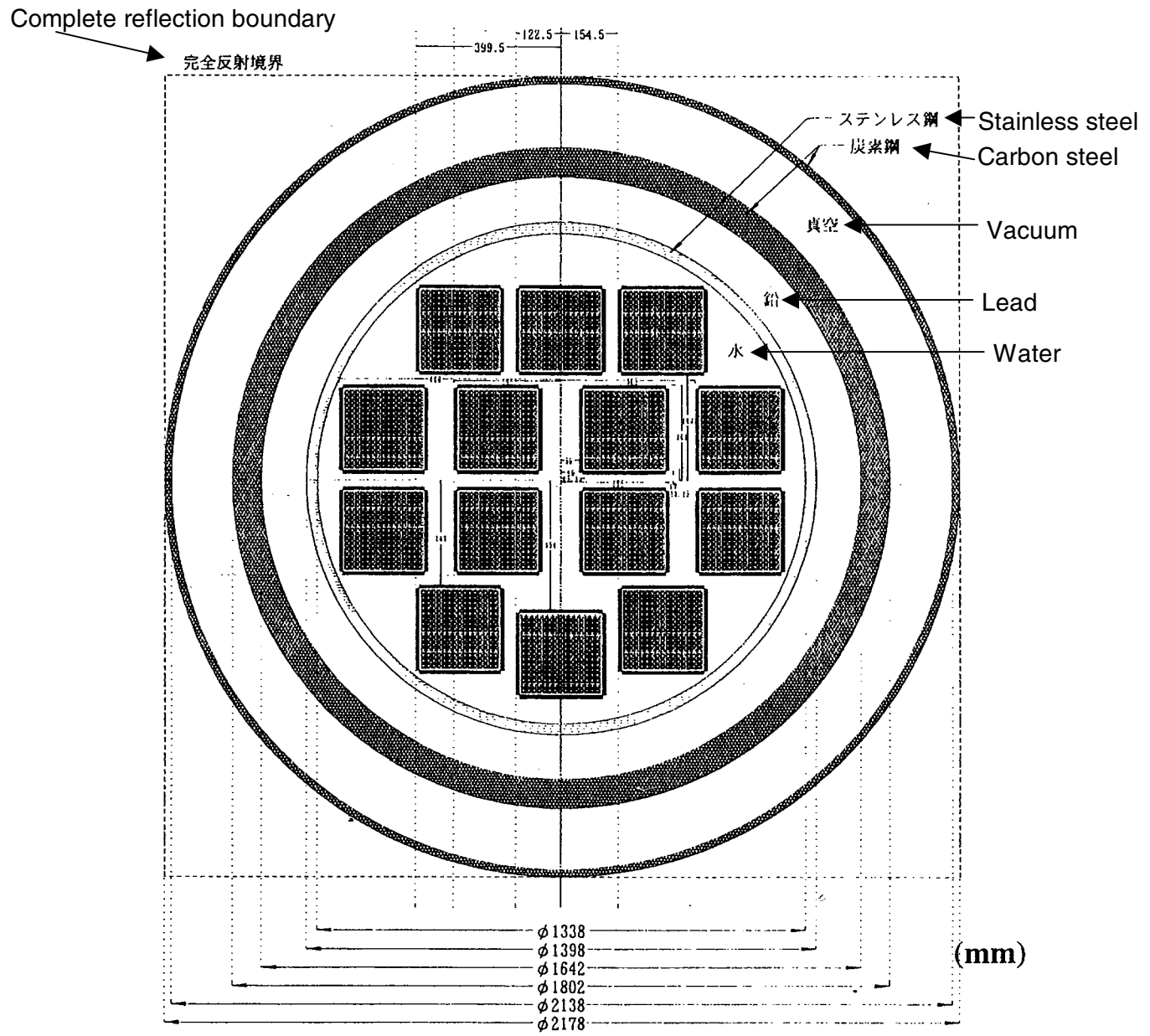


Fig. 6.1.2. Criticality calculation model for MCNP-4A/KENO-V.a  
(Horizontal cross section of transport cask).

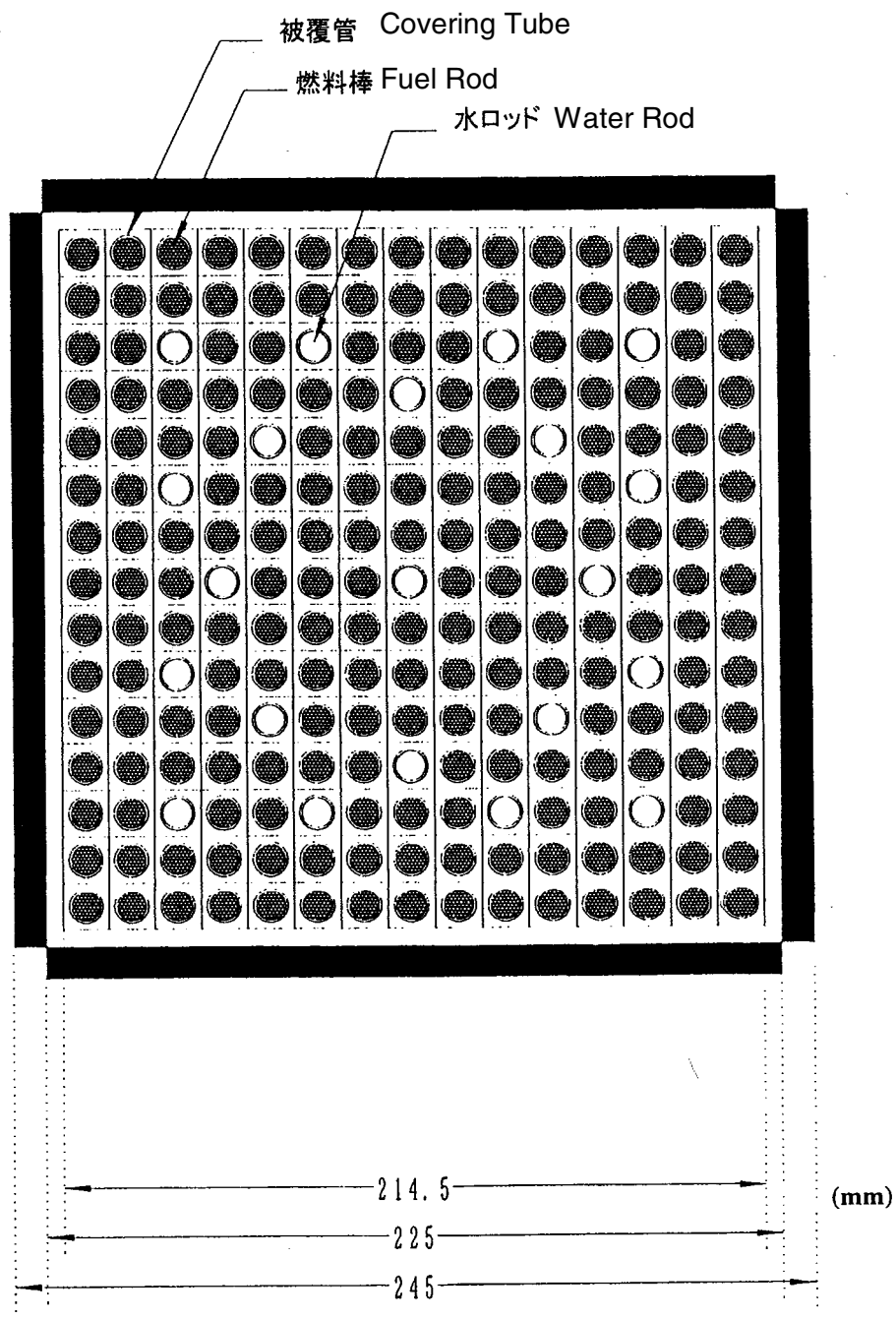


Fig. 6.1.3. Criticality calculation model for MCNP-4A/KENO-V.a  
(Horizontal cross section of fuel assembly).

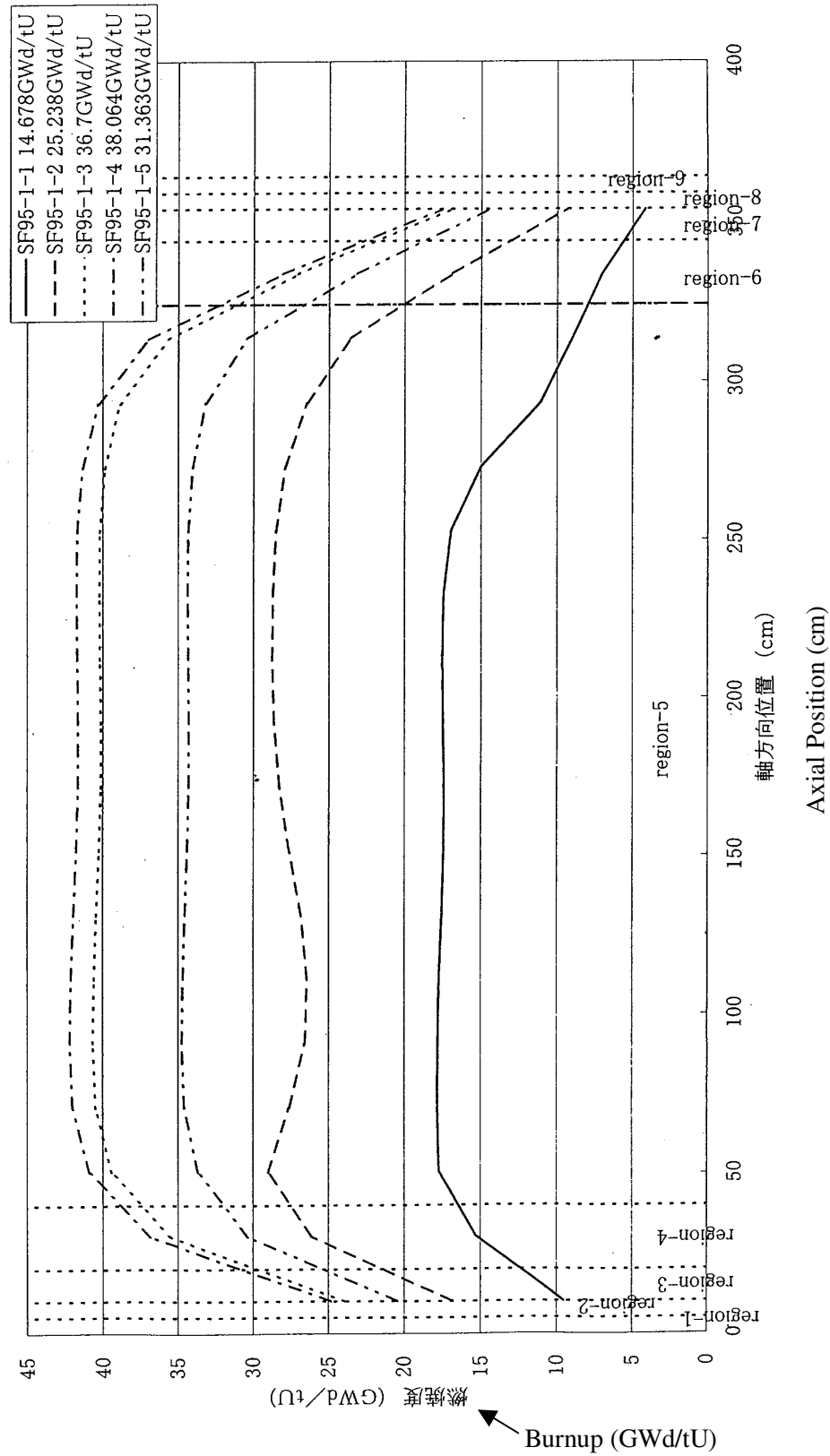


Fig. 6.1.4. Axial burnup distribution profile in PWR fuel pin.

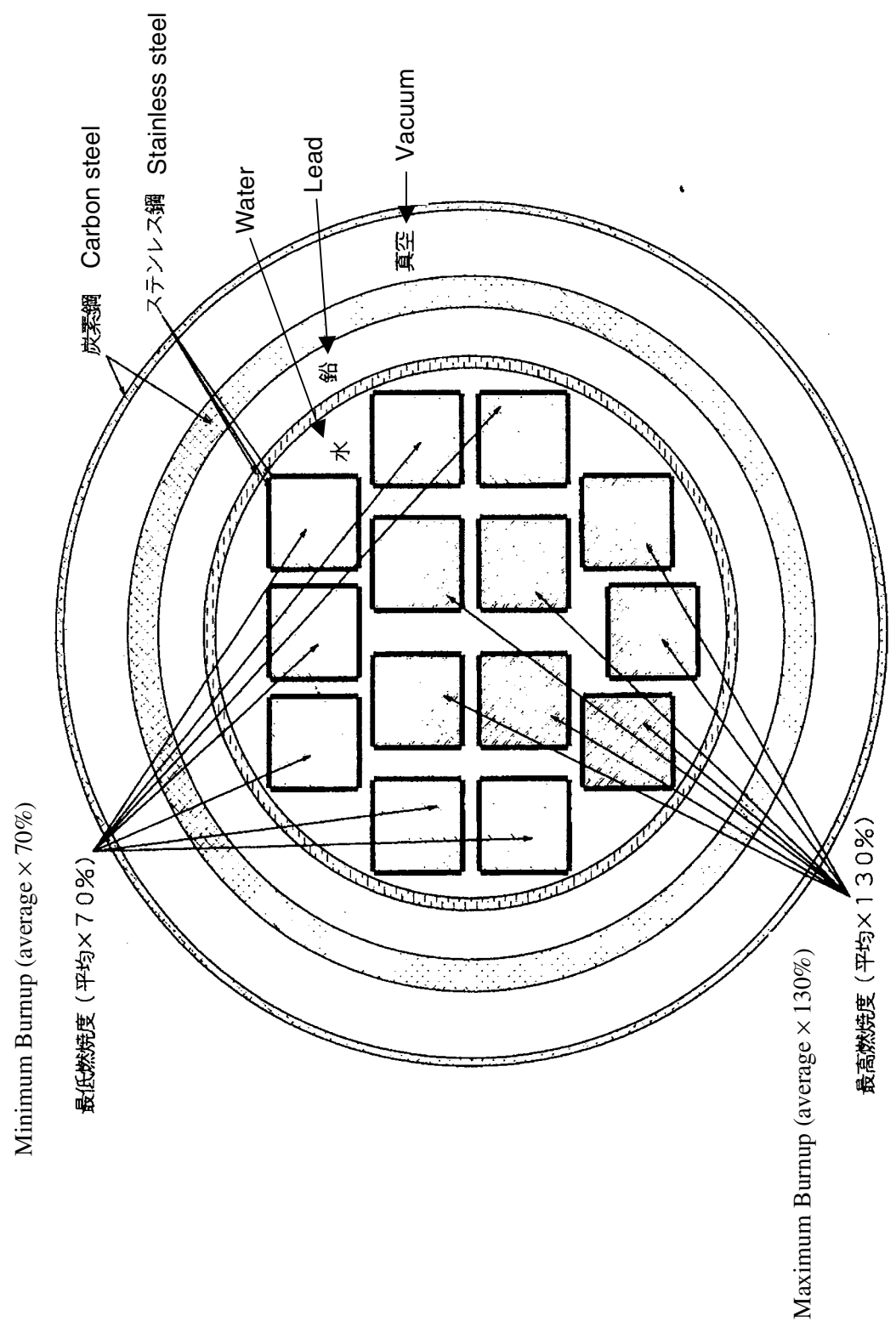


Fig. 6.1.5. Horizontal burnup distribution of spent fuel assemblies.

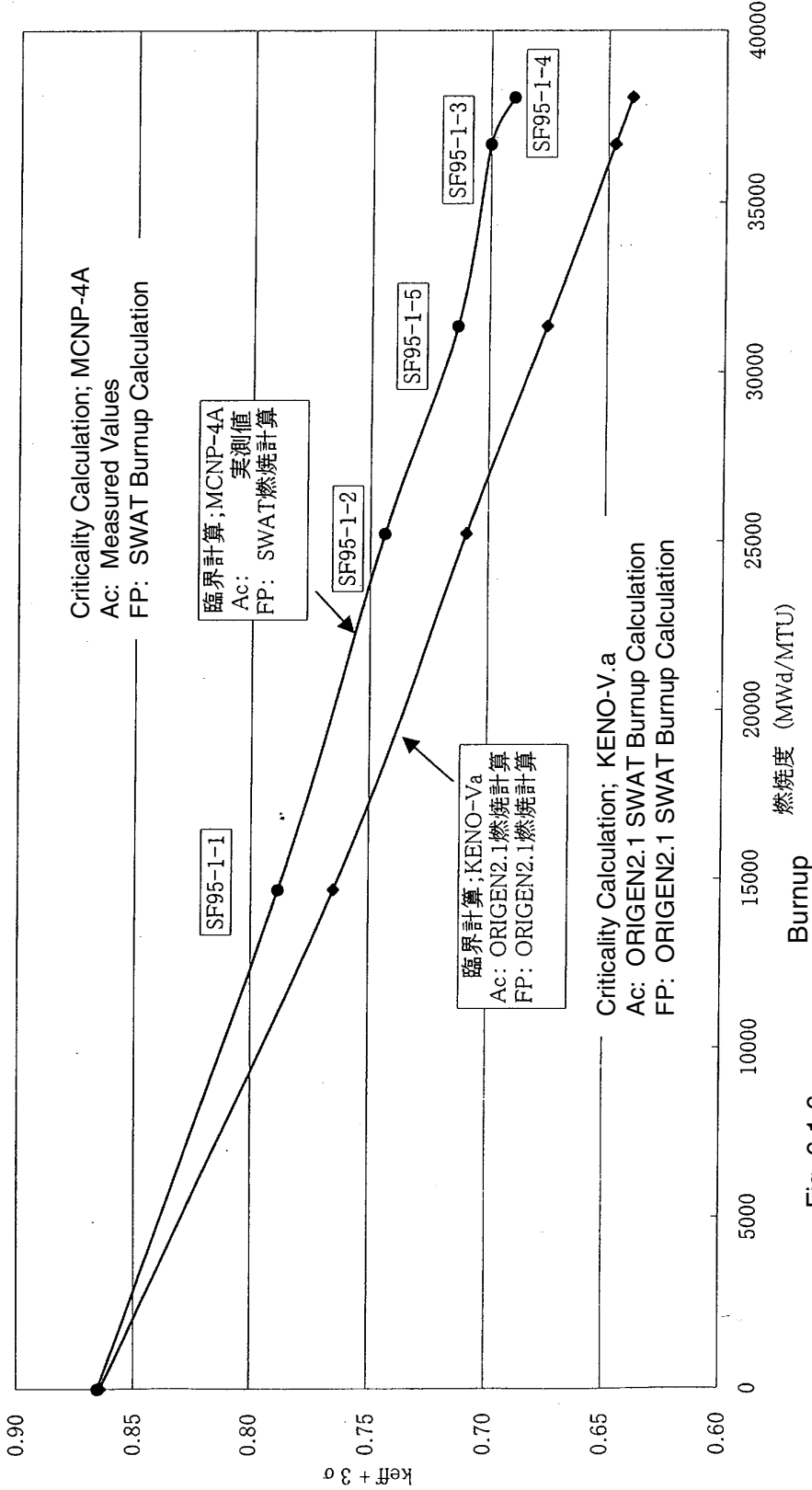


Fig. 6.1.6.

-Table 6.1.6 ( $k_{\text{eff}} + 3 \sigma$ ) changing curve with burnup of spent fuel in transport cask  
(considering Ac and FP to compare its measured and calculated values in effect of criticality)

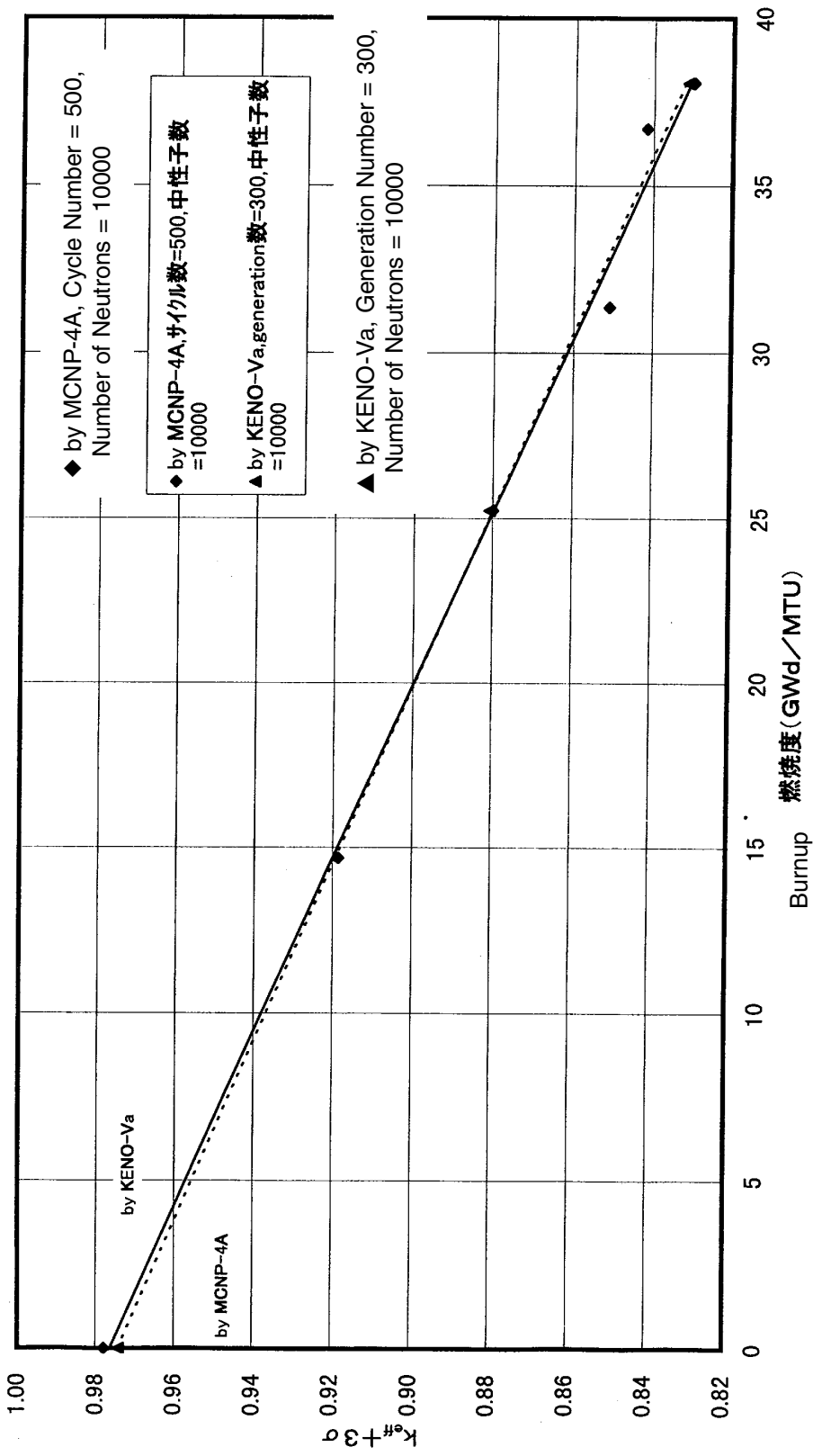


Fig. 6.1.6-1 ( $K_{\text{eff}} + 3\sigma$ ) changing curve with burnup of spent fuel in transport task considering only actinoid-burkett material is SUS304 stainless steel (reference 1)  
actinide, basket material

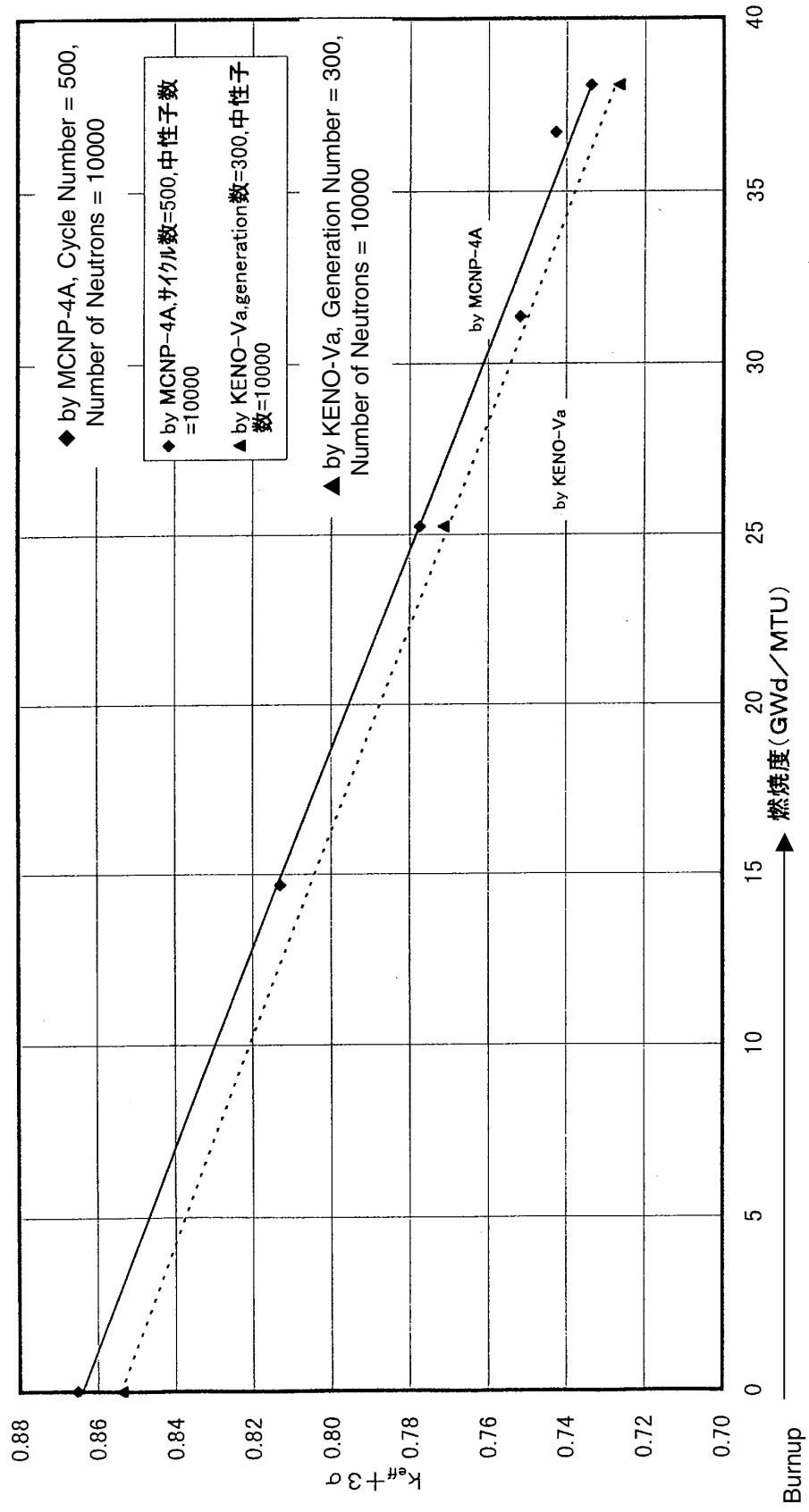


Fig. 6.1.6-2 ( $K_{\text{eff}} + 3\sigma$ ) changing curve with burnup of spent fuel in transport cask  
considering only actinoid-busket material is borated SUS304 stainless steel (reference 2)  
actinide, basket material

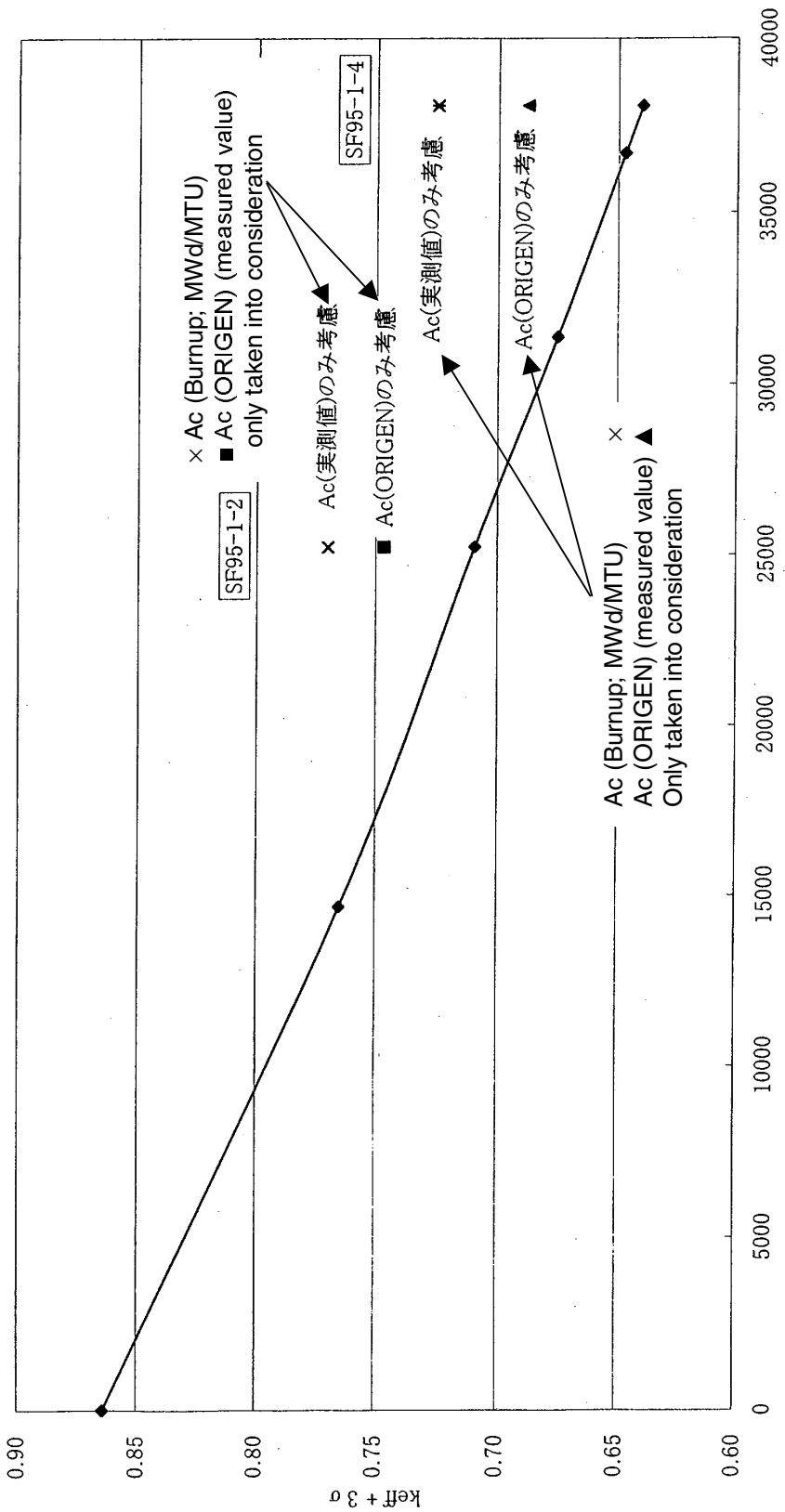


Fig. 6.1.7.

-Table 6.1.7 ( $k_{eff} + 3\sigma$ ) changing curve with burnup of spent fuel in transport cask  
(to compare  $k_{eff}$  considering Ac and FP obtained by ORIGEN2 with  $k_{eff}$  considering Ac only )

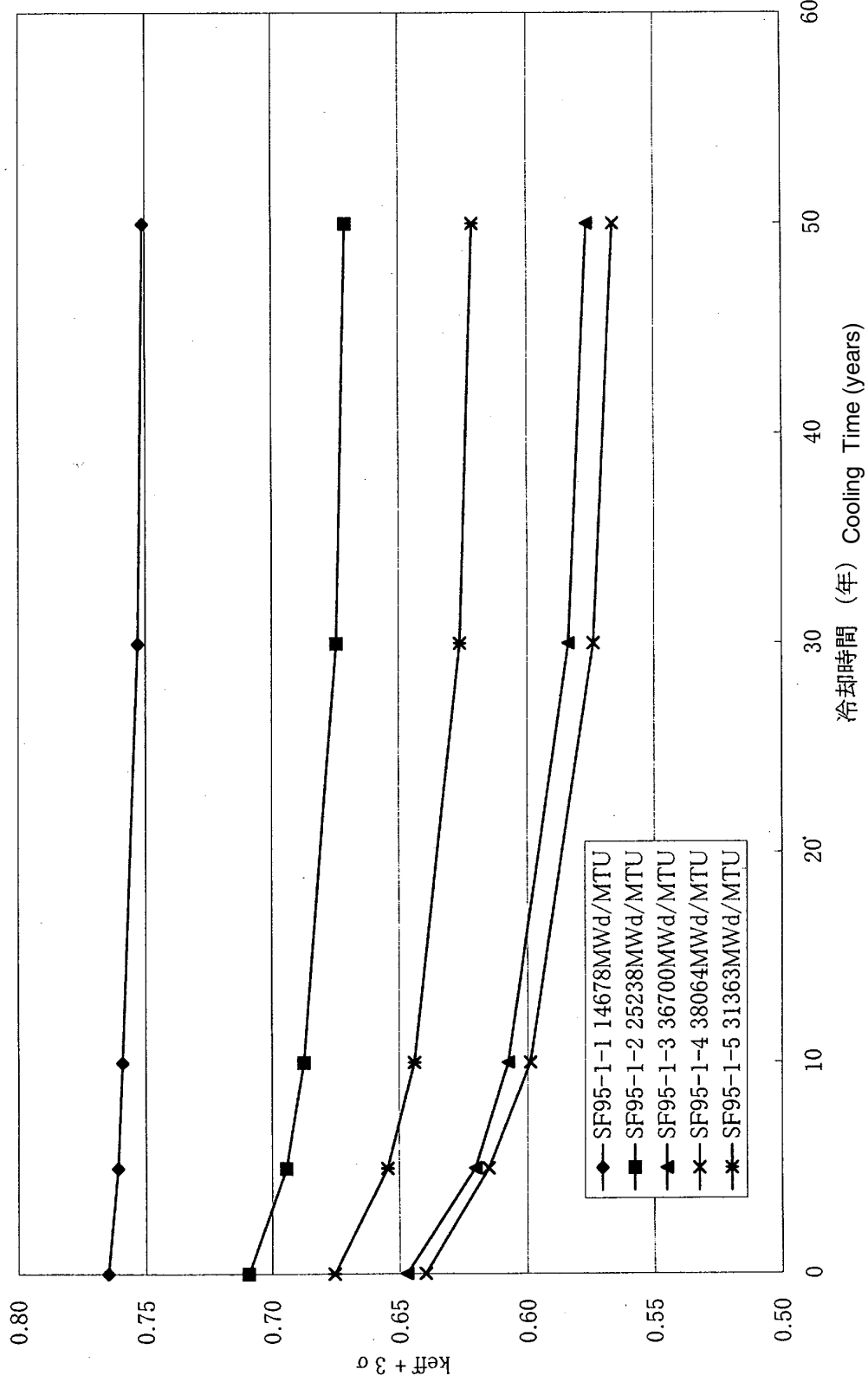


Fig. 6.1.8  $(k_{\text{eff},+3\sigma})$  changing curve with burnup of spent fuel in transport cask considering Ac and FP calculated by ORIGEN2.1

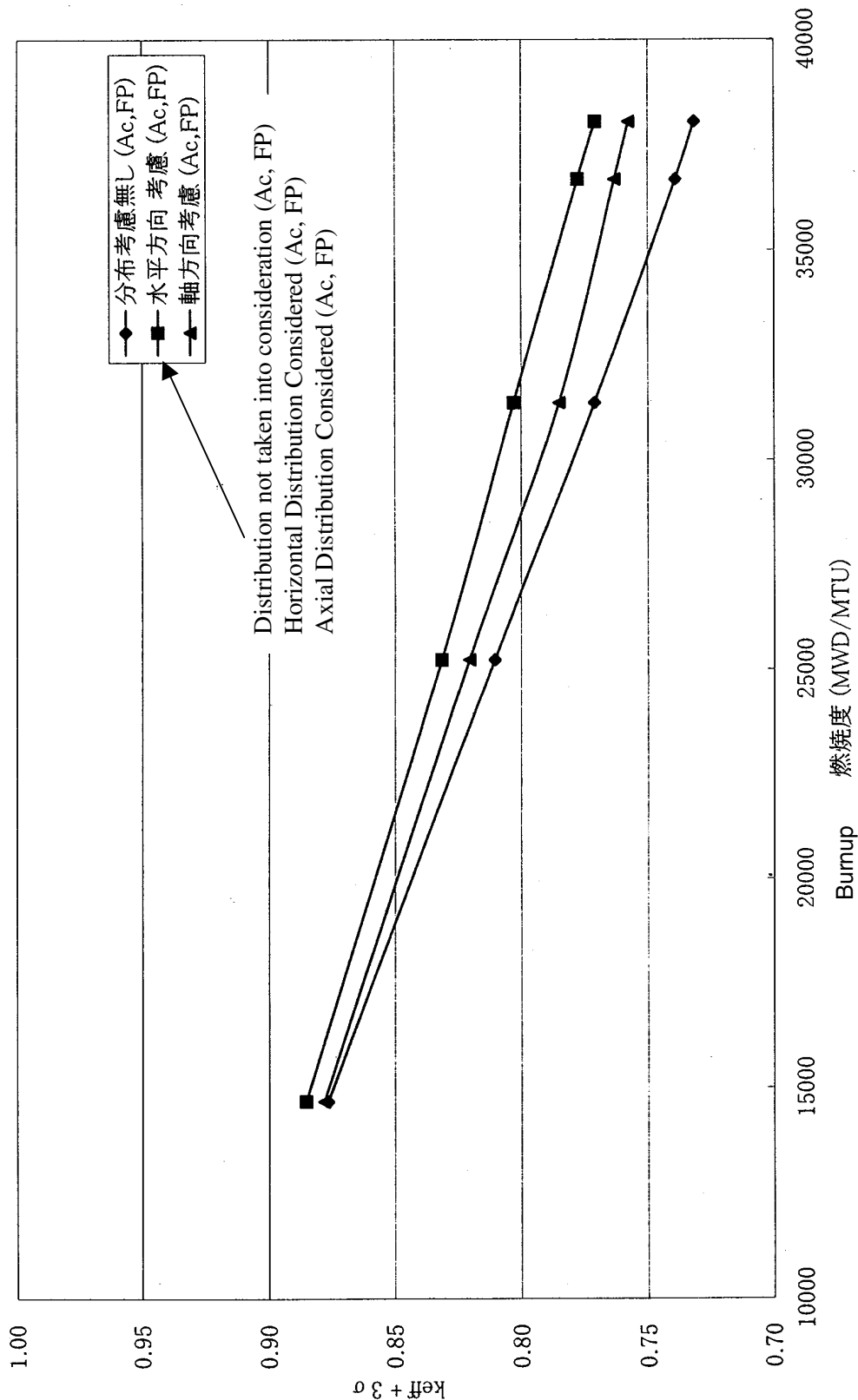


Fig. 6.1.9 Criticality analysis results obtained by KENO-Va considering burnup distribution with Ac and FP of spent fuel inside transport cask

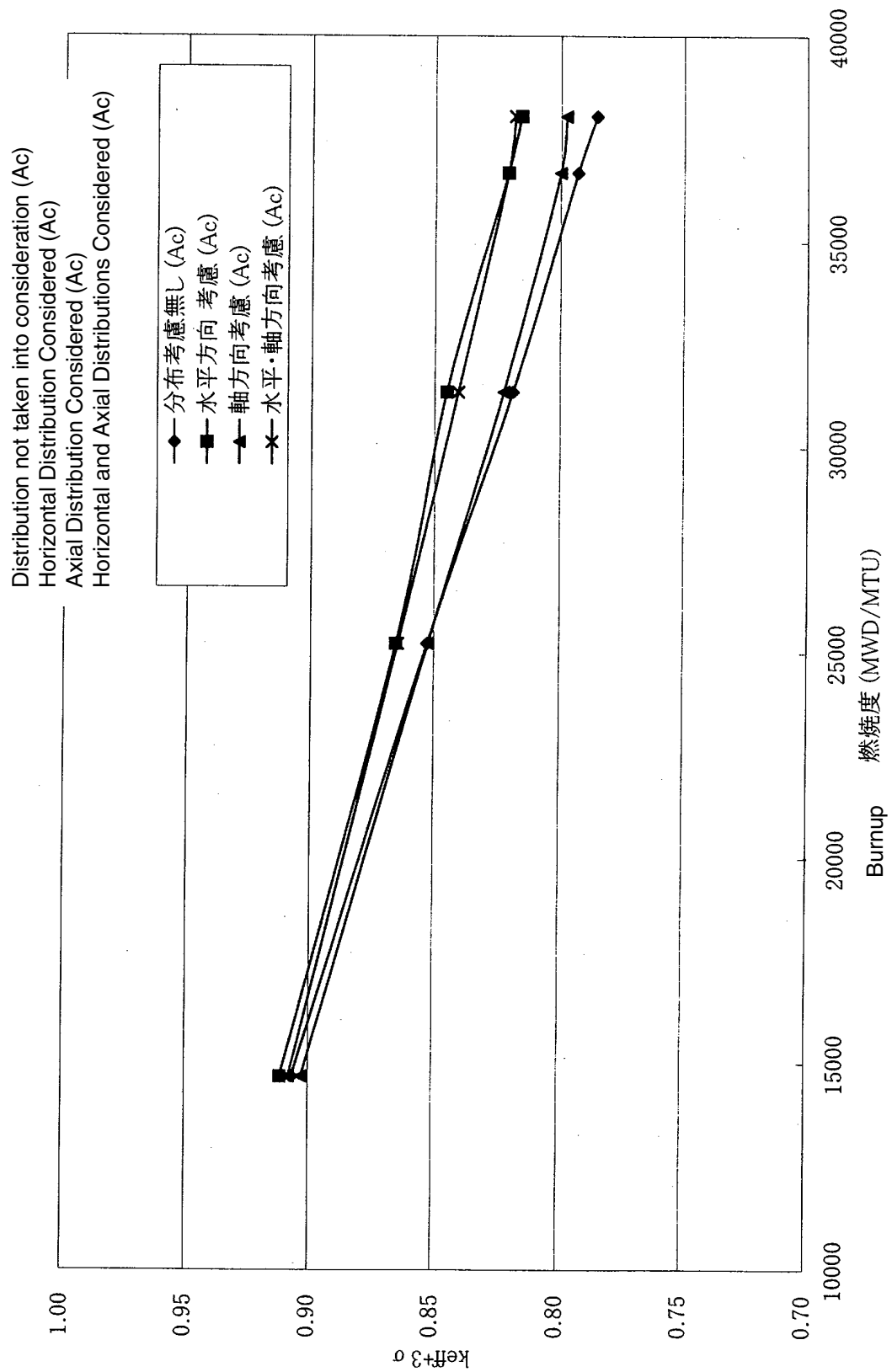


Fig. 6.1.10 Criticality analysis results obtained by KENO-Va considering burnup distribution with only Ac of spent fuel inside transport cask

## **6.2. Examination of Safety Margin for a Concrete Storage Model**

### **6.2.1. General**

Criticality safety analysis with burnup taken into consideration will be carried out in this section for a concrete dry storage cask for spent fuel mid-storage, using the currently disclosed conceptual design data. MCNP or KENO-V criticality analysis with burnup and cooling time as parameters will be carried out, using both the nuclide compositions in spent fuels obtained from the initial compositions of fuel specifications by ORIGEN2.1 or SWAT burnup calculation code, and the compositions obtained by actually cutting pieces from spent fuels and carrying out destructive analysis. And the neutron multiplication factor  $k_{eff}$  will be compared and evaluated.

Since the cask uses the dry storage mode, we construct a model, with dried air as the atmosphere inside and outside the canister and the cask at normal time. Furthermore, we carry out a criticality safety analysis using the moisture density of the atmosphere inside and outside the cask as a parameter, with rainfall and snowfall taken into consideration, under the assumption of outdoor installation. In this case, the inside of the canister is assumed to be dried air, since it is welded shut. Moreover, we carry out an analysis by changing the moisture density of the atmosphere in the canister, because a spent fuel is loaded in the canister under water, even though it is stored in dry mode. We also carry out a criticality analysis with burnup as a parameter while fixing the moisture density, which gives the toughest results from the standpoint of criticality safety. All the above-mentioned analyses are carried out by assuming that the axial burnup distribution of the spent fuel is uniform.

Furthermore, we carry out a criticality analysis in which the burnup distributions in the axial direction of the spent fuel and in the horizontal direction in the storage cask, respectively, are taken into consideration, and compare the results with the analytical results obtained without considering the burnup distribution as mentioned above, to evaluate changes in the effective neutron multiplication factor. We also carry out an analysis with consideration of the burnup distributions in both the axial direction and the horizontal direction in the cask at the same time.

### **6.2.2. Objective, Conditions, and Modeling for Analysis**

#### **(1) Object of Analysis**

The particulars of a fuel element and a fuel assembly as the object of analysis are shown in Table 6.2.1. The operating history, output, and burnup data of each sample of the spent fuel are shown in Table 6.2.2.

#### **(2) Analytical Conditions**

For the compositions in the effective fuel region, we use combinations of respective experimental values and calculated values by SWAT and ORIGEN2.1 for U, Pu, Am, Cm, Np, and isotopes of FPs. We include a total of 15 nuclides of FPs including nuclides measured by experiment in addition to 12 nuclides recommended for criticality analysis in the Criticality Safety Handbook. Table 6.2.3 shows combinations of criticality analysis cases. "Experiment" in this table means to give the nuclide isotope

compositions by experimental values, "Fresh Fuel" means to give fresh fuel specification values, "SWAT" means to give calculated values by the unified burnup calculation code SWAT, and "ORIGEN2.1" means to give calculated values by ORIGEN2.1. Furthermore, we calculate isotopic compositions immediately after removing the fuel from the reactor and after cooling periods of 5 years, 10 years, 30 years, and 50 years for cases 3 [sic; should be "6" -- Tr. Ed.] and 7. Here, the atomic number density in each cooling period is calculated by ORIGEN2.1.

Tables 6.2.4(1)–6.2.4(6) show the measured values of atomic number density in the fuel immediately after irradiation and the calculated values with cooling times of 0, 5, 10, 30, and 50 years for each burnup according to each analysis sample. Here, "SWAT" on each cooling time indicates the values calculated by ORIGEN2.1 based on the SWAT calculated values immediately after fuel removal from the reactor, and "ORIGEN2" indicates the values calculated entirely by ORIGEN2.1. The library used in ORIGEN2.1 was PWR-UE. Table 6.2.5 shows the nuclide % composition and atomic number density in the fuel region when a fresh fuel is assumed.

### (3) Modeling

A model of the entirety simplified for concrete storage cask analysis is shown in Fig. 6.2.1. Figures 6.2.2 and 6.2.3 show a calculation model common to MCNP-4B and KENO-Va. The calculation model for the fuel region is a heterogeneous model, which represents fuel rods faithfully one by one by a model. A canister accommodating 21 fuel assemblies is incorporated in the cask. Figure 6.2.4 shows the arrangement of the fuel assemblies in the canister. Each fuel assembly is supposed to be located at the center of a guide tube. Figure 6.2.5 shows the calculation model for the canister inside. Two materials, boron-containing stainless steel and ordinary stainless steel, are considered as the material of the guide tube shown in the same figure. In calculation with burnup distributions taken into consideration, a model that gives the toughest results from the standpoint of criticality analysis is determined with the canister thickness and liner thickness shown in Fig. 6.2.2, and the moisture density in the gap between the canister and the liner as parameters. Furthermore, the total in the radial direction of the canister, gap, and liner thicknesses is supposed to be kept at 20 cm. Figure 6.2.4 shows the burnup distribution in the horizontal fuel assembly arrangement, and Fig. 6.2.6 shows the calculation model for the axial burnup distribution profile in a fuel rod.

### 6.2.3. Calculation Codes Used and the Associated Calculation

#### Conditions

The MCNP-4B [1] Monte Carlo calculation conditions used in calculation are as follows:

- Number of batches: 500
- Number of neutrons generated: 10,000
- Cross-section library used: FSXLIB-J3R2 [3] (JENDL-3.2 [4]; endl7167 used only for  $^{234}\text{U}$ )

The KENO-V.a [2] Monte Carlo calculation conditions used in comparison calculation are as follows:

- Number of generations (cycles): 300
- Number of neutrons generated: 10,000

- Cross-section library used: SCALE-4.3 built-in library 44 groupendf5 and 238 groupendf5 for comparison with MCNP-4B calculation

In executing KENO-V.a calculation, we calculate the Bondarenko resonance self-shielding factor in order to determine the 44-group constant data library. Because of this, we carried out processing by BONAMI and NITAWL, using the CSAS25 control module in the SCALE-4.3 code system [2].

#### 6.2.4. Results and Discussion

(1) Figure 6.2.7 shows curves of the change in the neutron multiplication factor  $k_{\text{eff}}$  with burnup, which were obtained by Monte Carlo calculation for various cases with combinations of experimental and calculated data of the nuclide compositions immediately after fuel removal from the reactor. Here, the vertical axis of the figure shows the  $k_{\text{eff}}$  obtained by Monte Carlo calculation plus  $3 \times$  the standard deviation  $s$  (likewise for the rest). As shown in the figure, all cases excluding case 7 (ORIGEN2.1 calculated values) show complicated behavior at higher burnup, because of the presence of a discontinuous element due to the difference in the sampling position of an experimental sample with a high burnup (SF97-1-3), but generally the calculated  $k_{\text{eff}}$  value decreases monotonously with burnup. The rate of decrease is about  $2.5\% \Delta k/k$  per 10 GWd/MTU in most cases, and the absolute value of the calculated  $k_{\text{eff}}$  for a fresh fuel is small, i.e., about 0.37, thus the advantage in introducing burnup credit is small.

(2) As we see in Fig. 6.2.7, the calculated  $k_{\text{eff}}$  value is about 0.3% smaller if FPs are taken into consideration, from a comparison of case 1 with consideration of measured FPs (Nd and Sm) (AC is the experimental value with no Cm; FP is the experimental value) with case 2b without consideration of FPs (AC is the experimental value with no Cm; no FPs). The large difference in the extent of the effect of consideration of FPs from the analytical results on the wet transport cask for spent fuels in Sect. 6.1 arises because the neutron spectrum of the system is basically hard in a dry storage system and thus the neutron absorption of FPs is practically ineffective.

(3) Again, as we see in Fig. 6.2.7, the presence of Cm makes the calculated  $k_{\text{eff}}$  value slightly larger (up to 0.1%), from a comparison of case 2a with consideration of Cm (AC is the experimental value; no FPs) with case 2b with no consideration of Cm (AC excluding Cm: experimental value; no FPs). This is also thought to be due to the hard neutron spectrum.

(4) Again, as we see in Fig. 6.2.7, the calculated  $k_{\text{eff}}$  value is smaller in case 3 using SWAT calculated values of FP nuclide compositions (AC = measured; FP = SWAT calculated) and case 4 using ORIGEN2.1 calculated values of the same (AC = measured; FP = ORIGEN calculated) than case 1 using the measured values of both AC and FP compositions, because of the increased types of neutron absorbing nuclides of FPs, but the difference is less than 0.1%.

(5) Again, as we see in Fig. 6.2.7, the difference in the calculated  $k_{\text{eff}}$  value in case 6 and case 7 using, respectively, the SWAT calculated values and ORIGEN2.1 calculated values of AC and FP nuclide compositions immediately after fuel removal from the reactor, and in case 1 using the measured values of nuclide compositions immediately after fuel removal from the reactor, differs with burnup, and exhibits a complicated tendency. In sample SF97-1-1 with a low burnup, the  $k_{\text{eff}}$  decreases in the order case 6 > case 7 > case 1. The difference is about 2% each in comparison with case 1. In samples with high

burnups of more than 30,000 MWd/MTU, the difference is small, and the  $k_{\text{eff}}$  becomes conversely largest in the case with the measured values and decreases in the order case 1 > case 6 > case 7 in samples SF97-1-4 and SF97-1-5. In a comparison of the calculated  $k_{\text{eff}}$  values in case 6 and case 7 using, respectively, the nuclide compositions by SWAT and ORIGEN2.1 calculation,  $k_{\text{eff}}$  is always larger in case 6 than in case 7, regardless of the difference in burnup, and the difference is about 4% at maximum.

(6) Figure 6.2.8 shows cooling time versus  $k_{\text{eff}}$  change curves in case 6 using the SWAT calculated values of nuclide compositions immediately after fuel removal from the reactor, and Fig. 6.2.9 shows cooling time versus  $k_{\text{eff}}$  change curves in case 7 using ORIGEN2.1 calculated values of nuclide compositions immediately after fuel removal from the reactor. The formation and decay of nuclides during cooling periods are based on ORIGEN2.1 code in both cases. The calculated value decreases monotonously with the cooling time in all samples. This is because Am-241 increases with time, and Sm-147 and Gd-155 also increase with time.

(7) Figure 6.2.10 shows the criticality analysis results when the moisture density of the atmosphere in the gap between the canister and liner and around the cask is taken as a parameter. As shown in the figure, the  $k_{\text{eff}}$  decreases monotonously as the moisture density of the atmosphere in the gap between the canister and liner and around the cask increases, regardless of whether or not boron is present in the guide tube material stainless steel. The trend of these analytical results is presumably because the neutrons that leaked from the inside of the canister through the canister are decelerated and made thermal in the water region in the gap and in the trunk concrete. These neutrons are absorbed in the stainless steel in the process of being reflected and thus returning into the canister. For reference, Fig. 6.2.11 shows the criticality analysis results when water is present inside the canister. In this case, the  $k_{\text{eff}}$  increases monotonously as the moisture density in the canister increases.

(8) Figure 6.2.12 shows the  $k_{\text{eff}}$  values calculated with the moisture density in the gap between the canister and liner, with the thickness of the stainless steel of the canister and liner as parameters. From these results, we set the stainless steel thickness of the canister and liner at 1 cm and the moisture density in the gap between the canister and liner at 1 g/cm<sup>3</sup>, to have a system in which the  $k_{\text{eff}}$  becomes maximum when water is taken into consideration. In such a system, the  $k_{\text{eff}}$  is calculated by multi-group energy Monte Carlo code KENO-V.a for the case with no burnup profile consideration for the isotropic compositions of the effective fuel part, and the case with consideration of horizontal and axial burnup distributions; the results are shown in Figs. 6.2.13 and 6.2.14.

### ① A Case with Consideration of Horizontal Burnup Distribution

If the isotopic compositions of all nuclides in the fuel region are taken into consideration, the calculated  $k_{\text{eff}}$  agrees with the  $k_{\text{eff}}$  calculated with no burnup profile consideration within the range of from -0.7% to +2.8%. If the isotopic compositions of only U, Pu, Am, and Np in the fuel region are considered, the calculated  $k_{\text{eff}}$  agrees with the  $k_{\text{eff}}$  calculated with no burnup profile consideration within the range of from -0.93% to +2.6%.

### ② A Case with Consideration of Axial Burnup Distribution

If the isotopic compositions of all nuclides in the fuel region are taken into consideration, the calculated  $k_{\text{eff}}$  agrees with the  $k_{\text{eff}}$  calculated with no burnup profile consideration within the range of

from  $-2.8\%$  to  $-0.83\%$ . If the isotopic compositions of only U, Pu, Am, and Np in the fuel region are considered, the calculated  $k_{\text{eff}}$  agrees with the  $k_{\text{eff}}$  calculated with no burnup profile consideration within the range of from  $-2.7\%$  to  $+0.78\%$ .

### ③ A Case with Consideration of Horizontal and Axial Burnup Distributions

If the isotopic compositions of only U, Pu, Am, and Np in the fuel region are considered, the calculated  $k_{\text{eff}}$  agrees with the  $k_{\text{eff}}$  calculated with no burnup profile consideration within the range of from  $-1.7\%$  to  $+1.8\%$ .

The  $k_{\text{eff}}$  was calculated with the use of continuous energy Monte Carlo code MCNP-4B for validation on the case with no burnup profile consideration for the isotopic compositions of the effective fuel part, or the case with consideration of burnup profiles, but no marked difference was seen in the  $k_{\text{eff}}$  with and without consideration of these burnup profiles in either of the KENO-Va/MCNP-4B evaluations. In a comparison of the absolute values of the calculated  $k_{\text{eff}}$  by KENO-Va/MCNP-4B, KENO-V.a gives about 3% higher values. This is presumably because, in KENO-V.a calculation, the energy spectrum used as a weight when getting energy multi-group cross-section data apportioned to 44 groups differs from that for a dry storage system.

Table 6.2.1. Main feature of fuel assembly for critical analysis

Type of fuel assembly	PWR fuel assembly
Fuel material	UO <sub>2</sub>
Covering tube material	Zircaloy-4
Fuel rod diameter, mm	9.5
Fuel rod pellet diameter, mm	8.19
Covering tube thickness, mm	0.655
Effective fuel length, mm	3642
Fuel rod arrangement	17 × 17
Fuel rods per assembly (number)	264
Fuel rod pitch, mm	12.60
Width of assembly, mm	214.2
Uranium weight per assembly, kg	470 or less
UO <sub>2</sub> enrichment (%)	4.2 (initial)

Table 6.2.2. Spent fuel irradiation conditions

Operating history						
386-day running (Cycle 1) – 86-day cooling – 403-day running (Cycle 2) – 60-day cooling – 407-day running (Cycle 3)						
Output and burnup by sample						
Sample No.		SF97-1-1	SF97-1-2	SF97-1-3	SF97-1-4	SF97-1-5
	Cycle 1	15.01	26.15	35.97	40.15	40.32
(MW/MTU)	Cycle 2	15.01	26.15	35.97	40.15	40.32
	Cycle 3	15.01	26.15	35.97	40.15	40.32
Burnup (MWd/MTU)		17950	31270	43020	48020	48220
						41550

Table 6.2.3. Combination of criticality analysis cases

	U	Pu	Am	Cm	Np	FP
Nuclides under consideration	U-234 U-235 U-236 U-238	Pu-238 Pu-239 Pu-240 Pu-241 Pu-242	Am-241 Am-243	Cm-242 Cm-243 Cm-244 Cm-245 Cm-246 Cm-247	Np-237	Mo-95 Tc-99 Ru-101 Rh-103 Ag-109 Cs-133 Nd-143 Nd-145 Sm-147 Sm-149 Sm-150 Sm-151 Sm-152 Eu-153 Gd-155
Case 1	Experiment	Experiment	Experiment	—	Experiment	Experiment (only isotopes with measured data)
Case 2a	Experiment	Experiment	Experiment	Experiment	Experiment	—
Case 2b	Experiment	Experiment	Experiment	—	Experiment	—
Case 3	Experiment	Experiment	Experiment	Experiment	Experiment	SWAT
Case 4	Experiment	Experiment	Experiment	Experiment	Experiment	ORIGEN2.1
Case 5	Fresh fuel					
Case 6	SWAT	SWAT	SWAT	SWAT	SWAT	SWAT
Case 7	ORIGEN2.1	ORIGEN2.1	ORIGEN2.1	ORIGEN2.1	ORIGEN2.1	ORIGEN2.1

Table 6.2.4 (1). Atomic number density of actinide and fission products (1)  
Sample No.; SF97-1-1, Burnup; 17950 (MWd/MTU)

	Experiment	Immediately after cooling		5-year cooling		10-year cooling		30-year cooling		50-year cooling	
		ORIGEN2	SWAT	ORIGEN2	SWAT	ORIGEN2	SWAT	ORIGEN2	SWAT	ORIGEN2	SWAT
U-234	6.947E-06	6.926E-06	6.850E-06	6.954E-06	6.876E-06	6.981E-06	6.904E-06	7.075E-06	6.998E-06	7.258E-06	7.181E-06
U-235	5.524E-04	5.582E-04	5.699E-04	5.582E-04	5.698E-04	5.582E-04	5.698E-04	5.582E-04	5.698E-04	5.587E-04	5.703E-04
U-236	7.301E-05	7.479E-05	7.075E-05	7.479E-05	7.075E-05	7.479E-05	7.081E-05	7.485E-05	7.086E-05	7.501E-05	7.098E-05
U-238	2.206E-02	2.203E-02	2.201E-02	2.203E-02	2.201E-02	2.203E-02	2.201E-02	2.203E-02	2.201E-02	2.203E-02	2.201E-02
Pu-238	5.508E-07	6.583E-07	6.458E-07	6.904E-07	6.838E-07	6.638E-07	6.572E-07	5.681E-07	5.615E-07	3.847E-07	3.793E-07
Pu-239	8.896E-05	1.059E-04	1.156E-04	1.066E-04	1.163E-04	1.066E-04	1.163E-04	1.065E-04	1.163E-04	1.064E-04	1.161E-04
Pu-240	2.154E-05	2.279E-05	2.452E-05	2.278E-05	2.451E-05	2.276E-05	2.451E-05	2.272E-05	2.446E-05	2.260E-05	2.434E-05
Pu-241	9.723E-06	1.253E-05	1.280E-05	9.847E-06	1.006E-05	7.745E-06	7.911E-06	2.956E-06	3.020E-06	2.664E-07	2.721E-07
Pu-242	1.413E-06	1.572E-06	1.625E-06	1.572E-06	1.625E-06	1.572E-06	1.625E-06	1.572E-06	1.625E-06	1.572E-06	1.625E-06
Am-241	3.425E-07	5.543E-07	5.884E-07	3.219E-06	3.310E-06	5.291E-06	5.427E-06	9.825E-06	1.006E-05	1.161E-05	1.188E-05
Am-243	1.012E-07	1.405E-07	1.373E-08	1.406E-07	1.374E-07	1.405E-07	1.374E-07	1.402E-07	1.371E-07	1.396E-07	1.365E-07
Cm-242	4.878E-08	5.421E-08	6.025E-08	6.450E-11	4.367E-11	4.024E-11	1.733E-11	3.665E-11	1.577E-11	2.918E-11	1.256E-11
Cm-243	5.652E-10	7.114E-10	5.705E-10	6.301E-10	5.054E-10	5.576E-10	4.475E-10	3.429E-10	2.752E-10	1.016E-10	8.154E-11
Cm-244	1.129E-08	1.582E-08	1.616E-08	1.307E-08	1.335E-08	1.079E-08	1.103E-08	5.020E-09	5.129E-09	7.407E-10	7.568E-10
Cm-245	2.453E-10	3.177E-10	4.944E-10	3.176E-10	4.943E-10	3.175E-10	4.941E-10	3.169E-10	4.933E-10	3.157E-10	4.913E-10
Cm-246	8.691E-12	1.140E-11	1.239E-11	1.139E-11	1.239E-11	1.138E-11	1.238E-11	1.135E-11	1.234E-11	1.127E-11	1.225E-11
Cm-247	0.000E+00	4.600E-14	5.671E-14	4.600E-14	5.676E-14	4.600E-14	5.676E-14	4.600E-14	5.676E-14	4.600E-14	5.676E-14
Np-237	3.550E-06	4.635E-06	4.151E-06	4.726E-06	4.230E-06	4.761E-06	4.266E-06	5.015E-06	4.527E-06	5.914E-06	5.448E-06
Mo-95	—	2.296E-05	2.321E-05	2.598E-05	2.603E-05	2.598E-05	2.603E-05	2.598E-05	2.603E-05	2.598E-05	2.603E-05
Tc-99	—	2.498E-05	2.619E-05	2.508E-05	2.625E-05	2.508E-05	2.625E-05	2.508E-05	2.625E-05	2.507E-05	2.624E-05
Ru-101	—	2.284E-05	2.279E-05	2.284E-05	2.277E-05	2.284E-05	2.277E-05	2.284E-05	2.277E-05	2.284E-05	2.277E-05
Rh-103	—	1.345E-05	1.370E-05	1.436E-05	1.457E-05	1.436E-05	1.457E-05	1.436E-05	1.457E-05	1.436E-05	1.457E-05
Ag-109	—	1.353E-06	1.569E-06	1.355E-06	1.569E-06	1.355E-06	1.569E-06	1.355E-06	1.569E-06	1.355E-06	1.569E-06
Cs-133	—	2.762E-05	2.776E-05	2.783E-05	2.794E-05	2.783E-05	2.794E-05	2.783E-05	2.794E-05	2.783E-05	2.794E-05
Nd-143	2.110E-05	2.118E-05	2.121E-05	2.159E-05	2.159E-05	2.159E-05	2.159E-05	2.159E-05	2.159E-05	2.159E-05	2.159E-05
Nd-145	1.544E-05	1.557E-05	1.559E-05	1.557E-05	1.558E-05	1.557E-05	1.558E-05	1.557E-05	1.558E-05	1.557E-05	1.558E-05
Sm-147	5.759E-06	2.385E-06	2.620E-06	5.549E-06	6.185E-06	6.395E-06	7.136E-06	6.699E-06	7.479E-06	6.699E-06	7.479E-06
Sm-149	1.090E-07	9.465E-08	9.602E-08	1.121E-07	1.107E-07	1.121E-07	1.107E-07	1.121E-07	1.107E-07	1.121E-07	1.107E-07
Sm-150	4.883E-06	5.328E-06	5.004E-06	5.328E-06	5.001E-06	5.328E-06	5.001E-06	5.328E-06	5.001E-06	5.328E-06	5.001E-06
Sm-151	3.418E-07	5.004E-07	4.318E-07	4.849E-07	4.185E-07	4.666E-07	4.027E-07	4.000E-07	3.452E-07	2.722E-07	2.349E-07
Sm-152	2.376E-06	2.620E-06	2.602E-06	2.620E-06	2.601E-06	2.621E-06	2.601E-06	2.622E-06	2.602E-06	2.623E-06	2.602E-06
Eu-153	—	1.617E-06	1.506E-06	1.625E-06	1.512E-06	1.625E-06	1.512E-06	1.625E-06	1.512E-06	1.625E-06	1.512E-06
Gd-155	—	2.933E-09	2.065E-09	7.689E-08	4.598E-08	1.136E-07	6.782E-08	1.478E-07	8.807E-08	1.500E-07	8.940E-08

Unit : atoms/b•cm

Table 6.2.4 (2). Atomic number density of actinide and fission products (2)  
 Sample No.; SF97-1-2, Burnup; 31270 (MWd/MTU)

Experiment	Immediately after cooling		5-year cooling		10-year cooling		30-year cooling		50-year cooling	
	ORIGEN2	SWAT	ORIGEN2	SWAT	ORIGEN2	SWAT	ORIGEN2	SWAT	ORIGEN2	SWAT
U-234	5.550E-06	5.919E-06	5.620E-06	6.013E-06	5.731E-06	6.102E-06	5.836E-06	6.428E-06	6.223E-06	7.042E-06
U-235	3.697E-04	3.823E-04	3.703E-04	3.823E-04	3.703E-04	3.823E-04	3.703E-04	3.824E-04	3.704E-04	3.825E-04
U-236	1.069E-04	1.023E-04	1.021E-04	1.024E-04	1.022E-04	1.024E-04	1.022E-04	1.025E-04	1.023E-04	1.027E-04
U-238	2.179E-02	2.186E-02	2.177E-02	2.186E-02	2.178E-02	2.186E-02	2.178E-02	2.186E-02	2.178E-02	2.186E-02
Pu-238	2.904E-06	2.204E-06	2.582E-06	2.306E-06	2.738E-06	2.217E-06	2.633E-06	1.896E-06	2.249E-06	1.282E-06
Pu-239	1.372E-04	1.287E-04	1.427E-04	1.300E-04	1.441E-04	1.300E-04	1.441E-04	1.299E-04	1.440E-04	1.297E-04
Pu-240	4.311E-05	3.908E-05	4.587E-05	3.909E-05	4.589E-05	3.910E-05	4.590E-05	3.908E-05	4.590E-05	3.892E-05
Pu-241	2.834E-05	2.379E-05	2.874E-05	1.870E-05	2.259E-05	1.470E-05	1.776E-05	5.615E-06	6.782E-06	5.057E-07
Pu-242	7.203E-06	5.394E-06	7.114E-06	5.395E-06	7.114E-06	5.395E-06	7.114E-06	5.395E-06	7.114E-06	5.396E-06
Am-241	9.219E-07	9.393E-07	1.211E-06	5.997E-06	7.324E-06	9.935E-06	1.208E-05	1.854E-05	2.247E-05	2.195E-05
Am-243	1.168E-06	8.298E-07	1.101E-06	8.304E-07	1.103E-06	8.298E-07	1.102E-06	8.281E-07	1.100E-06	8.243E-07
Cm-242	2.397E-07	1.737E-07	2.460E-07	1.641E-10	1.492E-10	8.735E-11	4.242E-11	7.949E-11	3.860E-11	6.329E-11
Cm-243	6.310E-09	3.880E-09	4.280E-09	3.435E-09	3.790E-09	3.042E-09	3.356E-09	1.870E-09	2.063E-09	5.543E-11
Cm-244	3.137E-07	1.743E-07	2.584E-07	1.439E-07	2.135E-07	1.189E-07	1.763E-07	5.530E-08	8.198E-08	8.160E-09
Cm-245	1.546E-08	5.525E-09	1.396E-08	5.523E-09	1.396E-08	5.520E-09	1.395E-08	5.511E-09	1.393E-08	5.489E-09
Cm-246	9.491E-10	3.653E-10	7.107E-10	3.650E-10	7.103E-10	3.647E-10	7.098E-10	3.637E-10	7.075E-10	3.610E-10
Cm-247	9.015E-12	2.573E-12	6.255E-12	2.573E-12	6.257E-12	2.573E-12	6.257E-12	2.573E-12	6.257E-12	2.573E-12
Np-237	9.414E-06	9.653E-06	9.286E-06	9.880E-06	9.476E-06	9.946E-06	9.554E-06	1.042E-05	1.014E-05	1.213E-05
Mo-95	—	3.486E-05	3.837E-05	3.984E-05	4.301E-05	3.984E-05	4.301E-05	3.984E-05	4.301E-05	3.984E-05
Tc-99	—	3.844E-05	4.389E-05	3.861E-05	4.401E-05	3.861E-05	4.401E-05	3.860E-05	4.401E-05	3.860E-05
Ru-101	—	3.635E-05	3.954E-05	3.635E-05	3.950E-05	3.635E-05	3.950E-05	3.635E-05	3.950E-05	3.635E-05
Rh-103	—	1.980E-05	2.262E-05	2.154E-05	2.430E-05	2.154E-05	2.430E-05	2.154E-05	2.430E-05	2.154E-05
Ag-109	—	2.645E-06	3.582E-06	2.649E-06	3.584E-06	2.649E-06	3.584E-06	2.649E-06	3.584E-06	2.649E-06
Cs-133	—	4.185E-05	4.533E-05	4.223E-05	4.566E-05	4.223E-05	4.566E-05	4.223E-05	4.566E-05	4.223E-05
Nd-143	3.216E-05	3.008E-05	3.243E-05	3.077E-05	3.306E-05	3.077E-05	3.306E-05	3.077E-05	3.306E-05	3.077E-05
Nd-145	2.472E-05	2.350E-05	2.541E-05	2.351E-05	2.540E-05	2.351E-05	2.540E-05	2.351E-05	2.540E-05	2.351E-05
Sm-147	7.719E-06	2.807E-06	3.599E-06	6.782E-06	8.652E-06	7.839E-06	1.000E-05	8.226E-06	1.049E-05	8.226E-06
Sm-149	1.477E-07	9.935E-08	1.001E-07	1.358E-07	1.292E-07	1.358E-07	1.292E-07	1.358E-07	1.292E-07	1.358E-07
Sm-150	9.221E-06	9.570E-06	9.254E-06	9.570E-06	9.249E-06	9.570E-06	9.249E-06	9.570E-06	9.249E-06	9.570E-06
Sm-151	4.952E-07	5.963E-07	5.104E-07	5.803E-07	4.970E-07	5.587E-07	4.782E-07	4.789E-07	4.099E-07	3.258E-07
Sm-152	3.476E-06	4.052E-06	4.297E-06	4.053E-06	4.294E-06	4.053E-06	4.295E-06	4.054E-06	4.295E-06	4.054E-06
Eu-153	—	3.243E-06	3.287E-06	3.266E-06	3.305E-06	3.266E-06	3.305E-06	3.266E-06	3.305E-06	3.266E-06
Gd-155	—	3.485E-09	2.813E-09	1.651E-07	1.086E-07	2.455E-07	1.611E-07	3.200E-07	2.100E-07	3.249E-07

Unit : atoms/b•cm

Table 6.2.4 (3). Atomic number density of actinide and fission products (3)  
Sample No.; SF97-1-3, Burnup; 43020 (MWd/MTU)

	Experiment	Immediately after cooling		5-year cooling		10-year cooling		30-year cooling		50-year cooling	
		ORIGEN2	SWAT	ORIGEN2	SWAT	ORIGEN2	SWAT	ORIGEN2	SWAT	ORIGEN2	SWAT
U-234	4.750E-06	4.623E-06	4.661E-06	4.883E-06	4.887E-06	5.136E-06	5.106E-06	6.052E-06	5.903E-06	7.800E-06	7.413E-06
U-235	2.425E-04	2.088E-04	2.424E-04	2.088E-04	2.425E-04	2.088E-04	2.425E-04	2.089E-04	2.426E-04	2.092E-04	2.428E-04
U-236	1.245E-04	1.230E-04	1.187E-04	1.231E-04	1.188E-04	1.231E-04	1.188E-04	1.233E-04	1.189E-04	1.263E-04	1.193E-04
U-238	2.157E-02	2.159E-02	2.155E-02	2.159E-02	2.156E-02	2.159E-02	2.156E-02	2.159E-02	2.156E-02	2.159E-02	2.156E-02
Pu-238	5.999E-06	6.334E-06	5.365E-06	6.522E-06	5.654E-06	6.268E-06	5.433E-06	5.357E-06	4.640E-06	3.616E-06	3.129E-06
Pu-239	1.439E-04	1.491E-04	1.505E-04	1.514E-04	1.526E-04	1.513E-04	1.526E-04	1.512E-04	1.525E-04	1.510E-04	1.523E-04
Pu-240	5.694E-05	6.235E-05	6.092E-05	6.257E-05	6.107E-05	6.268E-05	6.118E-05	6.301E-05	6.146E-05	6.301E-05	6.146E-05
Pu-241	3.876E-05	3.391E-05	3.979E-05	2.665E-05	3.129E-05	2.096E-05	2.460E-05	7.999E-06	9.393E-06	7.208E-07	8.464E-07
Pu-242	1.489E-05	1.299E-05	1.479E-05	1.300E-05	1.479E-05	1.300E-05	1.479E-05	1.300E-05	1.479E-05	1.300E-05	1.479E-05
Am-241	1.126E-06	1.217E-06	1.480E-06	8.431E-06	9.946E-06	1.404E-05	1.654E-05	2.631E-05	3.093E-05	3.118E-05	3.664E-05
Am-243	3.209E-06	3.230E-06	3.106E-06	3.232E-06	3.110E-06	3.231E-06	3.108E-06	3.225E-06	3.102E-06	3.210E-06	3.088E-06
Cm-242	4.204E-07	3.867E-07	4.681E-07	2.969E-10	2.569E-10	1.277E-10	5.429E-11	1.163E-10	4.938E-11	9.255E-11	3.931E-11
Cm-243	1.575E-08	1.451E-08	1.132E-08	1.285E-08	1.003E-08	1.138E-08	8.879E-09	6.998E-09	5.460E-09	2.074E-09	1.618E-09
Cm-244	1.291E-06	1.264E-06	1.100E-06	1.043E-06	9.095E-07	8.619E-07	7.507E-07	4.008E-07	3.492E-07	5.914E-08	5.152E-08
Cm-245	8.431E-08	5.842E-08	7.966E-08	5.842E-08	7.966E-08	5.836E-08	7.961E-08	5.831E-08	7.949E-08	5.803E-08	7.916E-08
Cm-246	8.201E-09	7.197E-09	6.466E-09	7.192E-09	6.461E-09	7.186E-09	6.456E-09	7.164E-09	6.439E-09	7.114E-09	6.389E-09
Cm-247	1.114E-10	8.630E-11	8.372E-11	8.630E-11	8.375E-11	8.630E-11	8.375E-11	8.630E-11	8.375E-11	8.630E-11	8.375E-11
Np-237	1.364E-05	1.762E-05	1.392E-05	1.805E-05	1.422E-05	1.814E-05	1.433E-05	1.882E-05	1.514E-05	2.123E-05	1.797E-05
Mo-95	—	5.000E-05	5.047E-05	5.659E-05	5.659E-05	5.659E-05	5.659E-05	5.659E-05	5.659E-05	5.659E-05	5.659E-05
Tc-99	—	5.462E-05	5.817E-05	5.486E-05	5.831E-05	5.485E-05	5.831E-05	5.485E-05	5.831E-05	5.484E-05	5.831E-05
Ru-101	—	5.426E-05	5.402E-05	5.426E-05	5.398E-05	5.426E-05	5.398E-05	5.426E-05	5.398E-05	5.426E-05	5.398E-05
Rh-103	—	2.588E-05	2.909E-05	2.852E-05	3.159E-05	2.852E-05	3.159E-05	2.852E-05	3.159E-05	2.852E-05	3.159E-05
Ag-109	—	4.580E-05	5.561E-06	4.589E-06	5.565E-06	4.589E-06	5.565E-06	4.589E-06	5.565E-06	4.589E-06	5.565E-06
Cs-133	—	5.803E-05	5.922E-05	5.858E-05	5.969E-05	5.858E-05	5.969E-05	5.858E-05	5.969E-05	5.858E-05	5.969E-05
Nd-143	3.904E-05	3.792E-05	3.946E-05	3.881E-05	4.028E-05	3.881E-05	4.028E-05	3.881E-05	4.028E-05	3.881E-05	4.028E-05
Nd-145	3.202E-05	3.258E-05	3.301E-05	3.259E-05	3.300E-05	3.259E-05	3.300E-05	3.259E-05	3.300E-05	3.259E-05	3.300E-05
Sm-147	8.868E-06	3.076E-06	3.978E-06	7.142E-06	9.797E-06	8.226E-06	1.135E-05	8.619E-06	1.192E-05	8.624E-06	1.192E-05
Sm-149	1.582E-07	1.039E-07	9.990E-08	1.635E-07	1.439E-07	1.635E-07	1.439E-07	1.635E-07	1.439E-07	1.635E-07	1.439E-07
Sm-150	1.328E-05	1.542E-05	1.321E-05	1.542E-05	1.320E-05	1.542E-05	1.320E-05	1.542E-05	1.320E-05	1.542E-05	1.320E-05
Sm-151	5.510E-07	7.225E-07	5.646E-07	7.048E-07	5.522E-07	6.782E-07	5.313E-07	5.814E-07	4.554E-07	3.956E-07	3.099E-07
Sm-152	4.339E-06	5.626E-06	5.527E-06	5.626E-06	5.525E-06	5.626E-06	5.525E-06	5.626E-06	5.525E-06	5.626E-06	5.525E-06
Eu-153	—	5.792E-06	4.942E-06	5.842E-06	4.974E-06	5.842E-06	4.974E-06	5.842E-06	4.974E-06	5.842E-06	4.974E-06
Gd-155	—	5.172E-09	3.271E-09	3.667E-07	1.780E-07	5.464E-07	2.649E-07	7.131E-07	3.456E-07	7.241E-07	3.508E-07

Unit : atoms/b•cm

Table 6.2.4 (4). Atomic number density of actinide and fission products (4)  
Sample No.; SF97-1-4, Burnup; 48020 (MWd/MTU)

	Experiment	Immediately after cooling		5-year cooling		10-year cooling		30-year cooling		50-year cooling	
		ORIGEN2	SWAT	ORIGEN2	SWAT	ORIGEN2	SWAT	ORIGEN2	SWAT	ORIGEN2	SWAT
U-234	4.425E-06	4.198E-06	4.320E-06	4.536E-06	4.592E-06	4.864E-06	4.856E-06	6.052E-06	5.814E-06	8.326E-06	7.645E-06
U-235	1.925E-04	1.646E-04	1.918E-04	1.647E-04	1.918E-04	1.647E-04	1.919E-04	1.648E-04	1.920E-04	1.650E-04	1.922E-04
U-236	1.296E-04	1.261E-04	1.233E-04	1.261E-04	1.234E-04	1.262E-04	1.234E-04	1.264E-04	1.235E-04	1.267E-04	1.239E-04
U-238	2.149E-02	2.148E-02	2.147E-02	2.148E-02	2.148E-02	2.148E-02	2.148E-02	2.148E-02	2.148E-02	2.148E-02	2.148E-02
Pu-238	7.433E-06	8.270E-06	6.497E-06	8.469E-06	6.826E-06	8.143E-06	6.615E-06	6.954E-06	5.604E-06	4.692E-06	3.779E-06
Pu-239	1.397E-04	1.552E-04	1.447E-04	1.578E-04	1.470E-04	1.578E-04	1.470E-04	1.577E-04	1.469E-04	1.576E-04	1.468E-04
Pu-240	6.147E-05	7.147E-05	6.497E-05	7.181E-05	6.522E-05	7.203E-05	6.544E-05	7.263E-05	6.594E-05	7.286E-05	6.600E-05
Pu-241	4.062E-05	3.623E-05	4.153E-05	2.848E-05	3.266E-05	2.239E-05	2.567E-05	8.547E-06	9.803E-06	7.706E-07	8.835E-07
Pu-242	1.884E-05	1.576E-05	1.861E-05	1.576E-05	1.862E-05	1.576E-05	1.862E-05	1.576E-05	1.862E-05	1.576E-05	1.862E-05
Am-241	1.219E-06	1.201E-06	1.439E-06	8.906E-06	1.028E-05	1.490E-05	1.715E-05	2.802E-05	3.219E-05	3.323E-05	3.815E-05
Am-243	4.378E-06	4.441E-06	4.197E-06	4.444E-06	4.201E-06	4.442E-06	4.199E-06	4.434E-06	4.191E-06	4.413E-06	4.171E-06
Cm-242	4.671E-07	4.528E-07	5.477E-07	3.264E-10	2.881E-10	1.288E-10	5.140E-11	1.173E-10	4.673E-11	9.338E-11	3.720E-11
Cm-243	1.985E-08	1.932E-08	1.437E-08	1.710E-08	1.273E-08	1.515E-08	1.127E-08	9.310E-09	6.932E-09	2.760E-09	2.054E-09
Cm-244	1.997E-06	2.087E-06	1.679E-06	1.724E-06	1.387E-06	1.423E-06	1.145E-06	6.622E-07	5.327E-07	9.769E-08	7.861E-08
Cm-245	1.364E-07	1.060E-07	1.259E-07	1.060E-07	1.259E-07	1.059E-07	1.259E-07	1.058E-07	1.257E-07	1.053E-07	1.251E-07
Cm-246	1.673E-08	1.574E-08	1.279E-08	1.573E-08	1.279E-08	1.572E-08	1.278E-08	1.568E-08	1.274E-08	1.556E-08	1.265E-08
Cm-247	2.458E-10	2.197E-10	1.829E-10	2.197E-10	1.829E-10	2.197E-10	1.829E-10	2.197E-10	1.829E-10	2.197E-10	1.829E-10
Np-237	1.541E-05	2.033E-05	1.541E-05	2.083E-05	1.576E-05	2.093E-05	1.587E-05	2.165E-05	1.670E-05	2.422E-05	1.966E-05
Mo-95	—	5.465E-05	5.548E-05	6.185E-05	6.218E-05	6.185E-05	6.218E-05	6.185E-05	6.218E-05	6.185E-05	6.218E-05
Tc-99	—	5.963E-05	6.393E-05	5.986E-05	6.412E-05	5.986E-05	6.412E-05	5.986E-05	6.412E-05	5.986E-05	6.412E-05
Ru-101	—	6.035E-05	6.014E-05	6.035E-05	6.008E-05	6.035E-05	6.008E-05	6.035E-05	6.008E-05	6.035E-05	6.008E-05
Rh-103	—	2.720E-05	3.130E-05	3.024E-05	3.415E-05	3.024E-05	3.415E-05	3.024E-05	3.415E-05	3.024E-05	3.415E-05
Ag-109	—	5.251E-06	6.371E-06	5.262E-06	6.378E-06	5.262E-06	6.378E-06	5.262E-06	6.378E-06	5.262E-06	6.378E-06
Cs-133	—	6.273E-05	6.479E-05	6.329E-05	6.533E-05	6.329E-05	6.533E-05	6.329E-05	6.533E-05	6.329E-05	6.533E-05
Nd-143	4.057E-05	3.951E-05	4.120E-05	4.049E-05	4.211E-05	4.049E-05	4.211E-05	4.049E-05	4.211E-05	4.049E-05	4.211E-05
Nd-145	3.481E-05	3.527E-05	3.604E-05	3.528E-05	3.603E-05	3.528E-05	3.603E-05	3.528E-05	3.603E-05	3.528E-05	3.603E-05
Sm-147	9.293E-06	2.985E-06	4.091E-06	6.981E-06	1.016E-05	8.049E-06	1.178E-05	8.436E-06	1.236E-05	8.442E-06	1.237E-05
Sm-149	1.465E-07	1.039E-07	9.209E-08	1.730E-07	1.431E-07	1.730E-07	1.431E-07	1.730E-07	1.431E-07	1.730E-07	1.431E-07
Sm-150	1.503E-05	1.733E-05	1.486E-05	1.733E-05	1.485E-05	1.733E-05	1.485E-05	1.733E-05	1.485E-05	1.733E-05	1.485E-05
Sm-151	5.464E-07	7.662E-07	5.518E-07	7.485E-07	5.412E-07	7.203E-07	5.207E-07	6.174E-07	4.464E-07	4.200E-07	3.037E-07
Sm-152	4.727E-06	6.063E-06	6.060E-06	6.063E-06	6.058E-06	6.063E-06	6.058E-06	6.063E-06	6.058E-06	6.063E-06	6.058E-06
Eu-153	—	6.666E-06	5.615E-06	6.727E-06	5.654E-06	6.727E-06	5.654E-06	6.727E-06	5.654E-06	6.727E-06	5.654E-06
Gd-155	—	5.698E-09	3.081E-09	4.541E-07	2.072E-07	6.771E-07	3.086E-07	8.840E-07	4.028E-07	8.973E-07	4.089E-07

Unit : atoms/b•cm

Table 6.2.4 (5). Atomic number density of actinide and fission products (5)  
Sample No.; SF97-1-5, Burnup; 48220 (MWd/MTU)

	Experiment	Immediately after cooling		5-year cooling		10-year cooling		30-year cooling		50-year cooling	
		ORIGEN2	SWAT	ORIGEN2	SWAT	ORIGEN2	SWAT	ORIGEN2	SWAT	ORIGEN2	SWAT
U-234	4.408E-06	4.181E-06	4.332E-06	4.523E-06	4.598E-06	4.854E-06	4.854E-06	6.058E-06	5.786E-06	8.348E-06	7.562E-06
U-235	1.867E-04	1.630E-04	1.830E-04	1.631E-04	1.831E-04	1.631E-04	1.831E-04	1.632E-04	1.832E-04	1.634E-04	1.833E-04
U-236	1.296E-04	1.262E-04	1.237E-04	1.262E-04	1.238E-04	1.262E-04	1.238E-04	1.264E-04	1.239E-04	1.268E-04	1.242E-04
U-238	2.149E-02	2.148E-02	2.148E-02	2.148E-02	2.149E-02	2.148E-02	2.149E-02	2.148E-02	2.149E-02	2.148E-02	2.149E-02
Pu-238	7.408E-06	8.353E-06	6.300E-06	8.547E-06	6.627E-06	8.221E-06	6.367E-06	7.020E-06	5.440E-06	4.737E-06	3.667E-06
Pu-239	1.383E-04	1.554E-04	1.393E-04	1.580E-04	1.416E-04	1.580E-04	1.416E-04	1.579E-04	1.415E-04	1.577E-04	1.413E-04
Pu-240	6.103E-05	7.181E-05	6.408E-05	7.214E-05	6.434E-05	7.241E-05	6.456E-05	7.302E-05	6.500E-05	7.319E-05	6.511E-05
Pu-241	4.025E-05	3.636E-05	4.006E-05	2.858E-05	3.149E-05	2.247E-05	2.475E-05	8.580E-06	9.449E-06	7.728E-07	8.519E-07
Pu-242	1.906E-05	1.587E-05	1.873E-05	1.587E-05	1.874E-05	1.587E-05	1.874E-05	1.587E-05	1.874E-05	1.587E-05	1.874E-05
Am-241	1.223E-06	1.200E-06	1.375E-06	8.934E-06	9.897E-06	1.495E-05	1.625E-05	2.811E-05	3.102E-05	3.334E-05	3.678E-05
Am-243	4.404E-06	4.493E-06	4.151E-06	4.496E-06	4.155E-06	4.494E-06	4.153E-06	4.485E-06	4.146E-06	4.464E-06	4.126E-06
Cm-242	4.350E-07	4.554E-07	5.364E-07	3.275E-10	2.794E-10	1.288E-10	4.756E-11	1.173E-10	4.323E-11	9.338E-11	3.442E-11
Cm-243	1.973E-08	1.951E-08	1.381E-08	1.728E-08	1.224E-08	1.530E-08	1.083E-08	9.410E-09	6.661E-09	2.788E-09	1.974E-09
Cm-244	2.000E-06	2.125E-06	1.634E-06	1.756E-06	1.350E-06	1.450E-06	1.115E-06	6.743E-07	5.185E-07	9.946E-08	7.651E-08
Cm-245	1.335E-07	1.084E-07	1.168E-07	1.083E-07	1.168E-07	1.083E-07	1.168E-07	1.081E-07	1.166E-07	1.077E-07	1.161E-07
Cm-246	1.697E-08	1.621E-08	1.253E-08	1.620E-08	1.252E-08	1.619E-08	1.251E-08	1.614E-08	1.247E-08	1.602E-08	1.239E-08
Cm-247	2.406E-10	2.274E-10	1.741E-10	2.274E-10	1.741E-10	2.274E-10	1.741E-10	2.274E-10	1.741E-10	2.274E-10	1.741E-10
Np-237	1.564E-05	2.043E-05	1.517E-05	2.094E-05	1.551E-05	2.104E-05	1.562E-05	2.176E-05	1.642E-05	2.435E-05	1.927E-05
Mo-95	—	5.483E-05	5.585E-05	6.207E-05	6.218E-05	6.207E-05	6.218E-05	6.207E-05	6.218E-05	6.207E-05	6.218E-05
Tc-99	—	5.980E-05	6.427E-05	6.008E-05	6.412E-05	6.008E-05	6.412E-05	6.008E-05	6.412E-05	6.008E-05	6.412E-05
Ru-101	—	6.058E-05	6.043E-05	6.058E-05	6.008E-05	6.058E-05	6.008E-05	6.058E-05	6.008E-05	6.058E-05	6.008E-05
Rh-103	—	2.725E-05	3.125E-05	3.031E-05	3.415E-05	3.031E-05	3.415E-05	3.031E-05	3.415E-05	3.031E-05	3.415E-05
Ag-109	—	5.278E-06	6.355E-06	5.289E-06	6.378E-06	5.289E-06	6.378E-06	5.289E-06	6.378E-06	5.289E-06	6.378E-06
Cs-133	—	6.290E-05	6.516E-05	6.345E-05	6.533E-05	6.345E-05	6.533E-05	6.345E-05	6.533E-05	6.345E-05	6.533E-05
Nd-143	4.060E-05	3.957E-05	4.080E-05	4.055E-05	4.211E-05	4.055E-05	4.211E-05	4.055E-05	4.211E-05	4.055E-05	4.211E-05
Nd-145	3.504E-05	3.537E-05	3.624E-05	3.538E-05	3.603E-05	3.538E-05	3.603E-05	3.538E-05	3.603E-05	3.538E-05	3.603E-05
Sm-147	9.335E-06	2.981E-06	4.144E-06	6.976E-06	1.016E-05	8.043E-06	1.178E-05	8.431E-06	1.236E-05	8.431E-06	1.237E-05
Sm-149	1.411E-07	1.039E-07	8.619E-08	1.734E-07	1.431E-07	1.734E-07	1.431E-07	1.734E-07	1.431E-07	1.734E-07	1.431E-07
Sm-150	1.518E-05	1.741E-05	1.485E-05	1.741E-05	1.485E-05	1.741E-05	1.485E-05	1.741E-05	1.485E-05	1.741E-05	1.485E-05
Sm-151	5.371E-07	7.678E-07	5.226E-07	7.507E-07	5.412E-07	7.225E-07	5.207E-07	6.190E-07	4.464E-07	4.212E-07	3.037E-07
Sm-152	4.801E-06	6.080E-06	6.140E-06	6.080E-06	6.058E-06	6.080E-06	6.058E-06	6.080E-06	6.058E-06	6.080E-06	6.058E-06
Eu-153	—	6.699E-06	5.631E-06	6.760E-06	5.654E-06	6.760E-06	5.654E-06	6.760E-06	5.654E-06	6.760E-06	5.654E-06
Gd-155	—	5.720E-09	2.822E-09	4.577E-07	2.072E-07	6.826E-07	3.086E-07	8.912E-07	4.028E-07	9.045E-07	4.089E-07

Unit : atoms/b•cm

Table 6.2.4 (6). Atomic number density of actinide and fission products (6)  
Sample No.; SF97-1-6, Burnup; 41550 (MWd/MTU)

Experiment	Immediately after cooling		5-year cooling		10-year cooling		30-year cooling		50-year cooling		
	ORIGEN2	SWAT	ORIGEN2	SWAT	ORIGEN2	SWAT	ORIGEN2	SWAT	ORIGEN2	SWAT	
U-234	4.861E-06	4.753E-06	4.853E-06	4.992E-06	5.043E-06	5.224E-06	5.228E-06	6.063E-06	5.897E-06	7.673E-06	7.169E-06
U-235	2.390E-04	2.235E-04	2.398E-04	2.235E-04	2.399E-04	2.235E-04	2.399E-04	2.237E-04	2.400E-04	2.238E-04	2.402E-04
U-236	1.236E-04	1.218E-04	1.176E-04	1.218E-04	1.177E-04	1.218E-04	1.177E-04	1.219E-04	1.178E-04	1.223E-04	1.181E-04
U-238	2.163E-02	2.162E-02	2.162E-02	2.162E-02	2.162E-02	2.162E-02	2.162E-02	2.162E-02	2.162E-02	2.162E-02	2.162E-02
Pu-238	5.055E-06	5.803E-06	4.505E-06	5.986E-06	4.761E-06	5.759E-06	4.577E-06	4.918E-06	3.909E-06	3.320E-06	2.636E-06
Pu-239	1.314E-04	1.465E-04	1.372E-04	1.486E-04	1.391E-04	1.486E-04	1.391E-04	1.485E-04	1.391E-04	1.483E-04	1.389E-04
Pu-240	5.359E-05	5.941E-05	5.702E-05	5.958E-04	5.715E-05	5.969E-05	5.726E-05	5.997E-05	5.742E-05	5.991E-05	5.731E-05
Pu-241	3.429E-05	3.372E-05	3.533E-05	2.650E-05	2.777E-05	2.083E-05	2.183E-05	7.955E-06	8.337E-06	7.169E-07	7.512E-07
Pu-242	1.366E-05	1.217E-05	1.353E-05	1.218E-05	1.353E-05	1.218E-05	1.353E-05	1.218E-05	1.353E-05	1.218E-05	1.353E-05
Am-241	9.861E-07	1.213E-06	1.322E-06	8.386E-06	8.835E-06	1.396E-05	1.468E-05	2.617E-05	2.747E-05	3.101E-05	3.253E-05
Am-243	2.662E-06	2.905E-06	2.600E-06	2.908E-06	2.602E-06	2.906E-06	2.601E-06	2.900E-06	2.596E-06	2.887E-06	2.583E-06
Cm-242	3.692E-07	3.670E-07	4.103E-07	2.870E-10	2.225E-10	1.262E-10	4.496E-11	1.150E-10	4.089E-11	9.150E-11	3.255E-11
Cm-243	1.275E-08	1.316E-08	9.032E-09	1.165E-08	7.999E-09	1.031E-08	7.081E-09	6.340E-09	4.355E-09	1.880E-09	1.291E-09
Cm-244	9.568E-07	1.071E-06	8.296E-07	8.846E-07	6.854E-07	7.308E-07	5.659E-07	3.398E-07	2.633E-07	5.014E-08	3.884E-08
Cm-245	5.334E-08	4.803E-08	5.190E-08	4.801E-08	5.189E-08	4.799E-08	5.187E-08	4.791E-08	5.178E-08	4.772E-08	5.157E-08
Cm-246	5.578E-09	5.582E-09	4.410E-09	5.576E-09	4.409E-09	5.576E-09	4.406E-09	5.560E-09	4.393E-09	5.517E-09	4.361E-09
Cm-247	7.029E-11	6.384E-11	5.030E-11	6.384E-11	5.030E-11	6.384E-11	5.030E-11	6.384E-11	5.030E-11	6.384E-11	5.030E-11
Np-237	1.300E-05	1.680E-05	1.267E-05	1.719E-05	1.294E-05	1.729E-05	1.304E-05	1.796E-05	1.375E-05	2.036E-05	1.628E-05
Mo-95	—	4.859E-05	4.943E-05	5.498E-05	5.538E-05	5.498E-05	5.538E-05	5.498E-05	5.538E-05	5.498E-05	5.538E-05
Tc-99	—	5.310E-05	5.667E-05	5.332E-05	5.681E-05	5.332E-05	5.681E-05	5.332E-05	5.681E-05	5.331E-05	5.681E-05
Ru-101	—	5.247E-05	5.230E-05	5.247E-05	5.225E-05	5.247E-05	5.225E-05	5.247E-05	5.225E-05	5.247E-05	5.225E-05
Rh-103	—	2.544E-05	2.813E-05	2.798E-05	3.049E-05	2.798E-05	3.049E-05	2.798E-05	3.049E-05	2.798E-05	3.049E-05
Ag-109	—	4.386E-06	5.188E-06	4.395E-06	5.191E-06	4.395E-06	5.191E-06	4.395E-06	5.191E-06	4.395E-06	5.191E-06
Cs-133	—	5.659E-05	5.794E-05	5.709E-05	5.836E-05	5.709E-05	5.836E-05	5.709E-05	5.836E-05	5.709E-05	5.836E-05
Nd-143	3.769E-05	3.736E-05	3.801E-05	3.823E-05	3.882E-05	3.823E-05	3.882E-05	3.823E-05	3.882E-05	3.823E-05	3.882E-05
Nd-145	3.148E-05	3.175E-05	3.232E-05	3.176E-05	3.231E-05	3.176E-05	3.231E-05	3.176E-05	3.231E-05	3.176E-05	3.231E-05
Sm-147	8.928E-06	3.095E-06	4.071E-06	7.181E-06	9.908E-06	8.270E-06	1.147E-05	8.663E-06	1.204E-05	8.663E-06	1.204E-05
Sm-149	1.428E-07	1.052E-07	8.622E-08	1.613E-07	1.283E-07	1.613E-07	1.283E-07	1.613E-07	1.283E-07	1.613E-07	1.283E-07
Sm-150	1.258E-05	1.489E-05	1.259E-05	1.489E-05	1.259E-05	1.489E-05	1.259E-05	1.489E-05	1.259E-05	1.489E-05	1.259E-05
Sm-151	4.743E-07	7.153E-07	4.919E-07	6.976E-07	4.819E-07	6.716E-07	4.637E-07	5.753E-07	3.975E-07	3.916E-07	2.705E-07
Sm-152	4.394E-06	5.491E-06	5.509E-06	5.492E-06	5.507E-06	5.492E-06	5.507E-06	5.492E-06	5.507E-06	5.493E-06	5.507E-06
Eu-153	—	5.529E-06	4.701E-06	5.571E-06	4.730E-06	5.571E-06	4.730E-06	5.571E-06	4.730E-06	5.571E-06	4.730E-06
Gd-155	—	5.113E-09	2.649E-09	3.425E-07	1.664E-07	5.102E-07	2.478E-07	6.661E-07	3.234E-07	6.760E-07	3.283E-07

Unit : atoms/b•cm

Table 6.2.5. Weight percent and atomic number density for each isotope in an unirradiated UO<sub>2</sub> fuel  
 (UO<sub>2</sub> density : 10.4g/cm<sup>3</sup>)

	Nuclide	Weight (%)	Atomic number density (atoms/b • cm)
Fuel region	U-234	0.0368	8.536E-06
	U-235	4.1082	9.529E-04
	U-236	0.00248	5.752E-07
	U-238	95.8526	2.223E-02
	O	—	4.639E-02

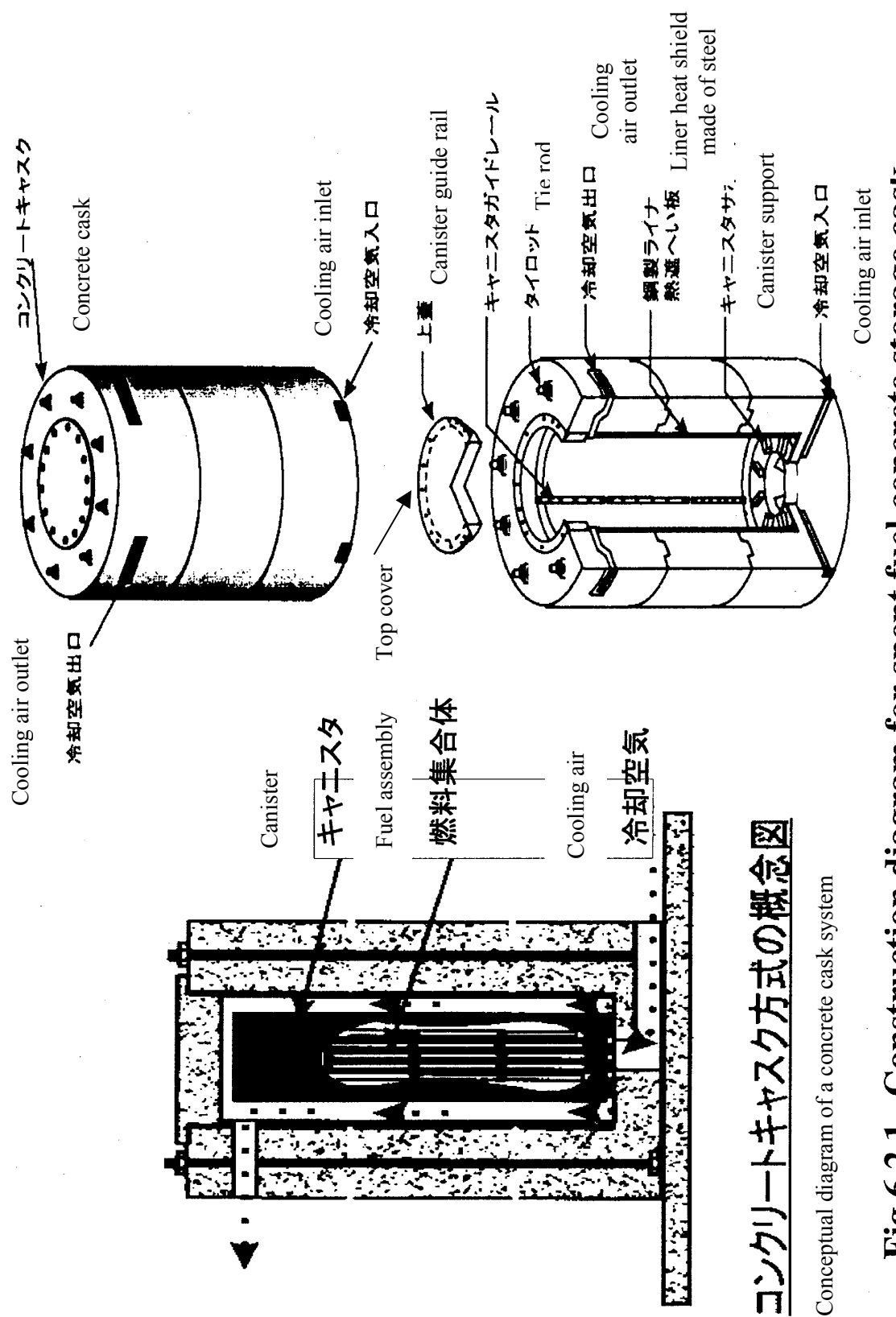


**Fig.6.2.1** Construction diagram for spent fuel concrete storage cask

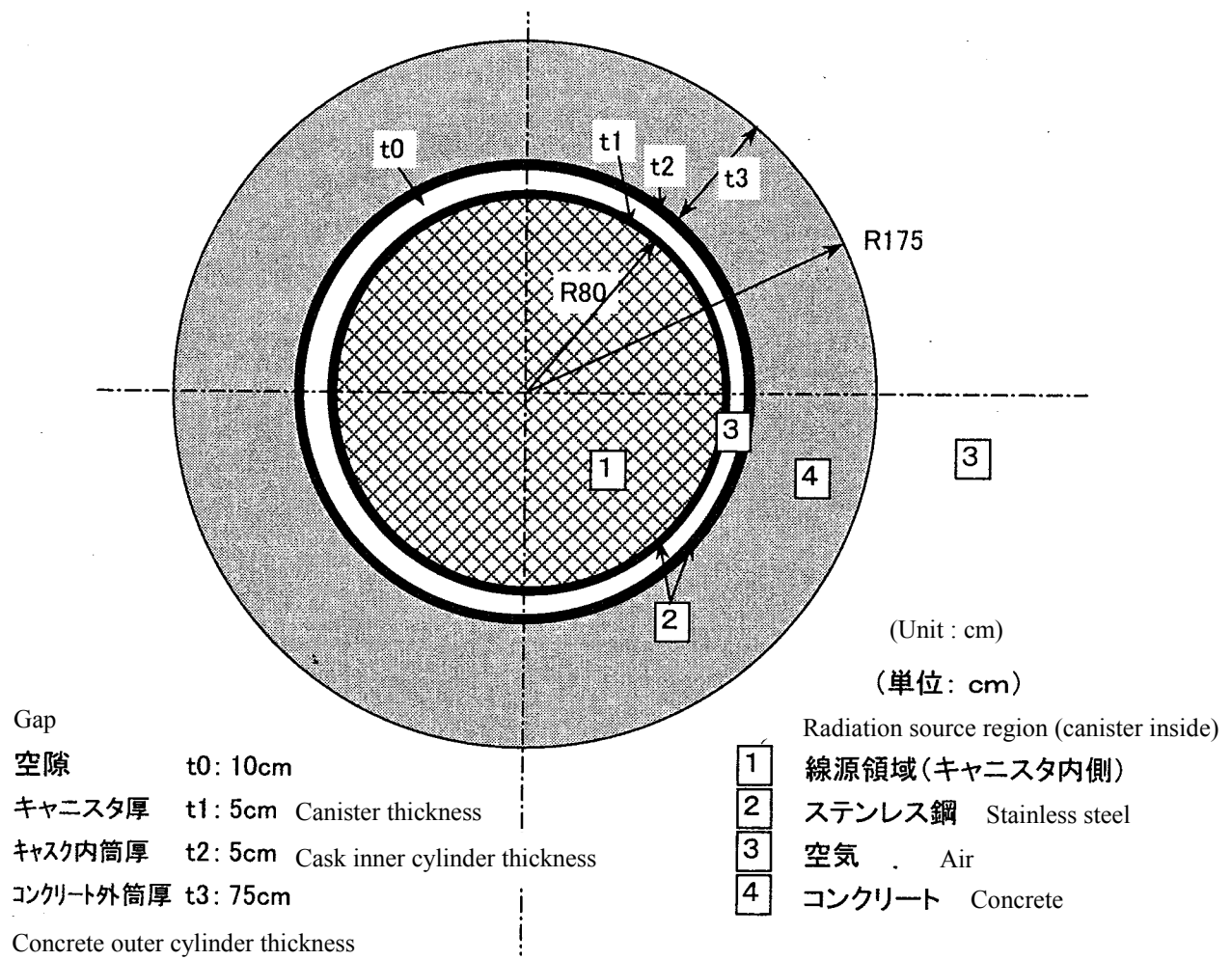


Fig.6.2.2 Calculation model for horizontal cross section

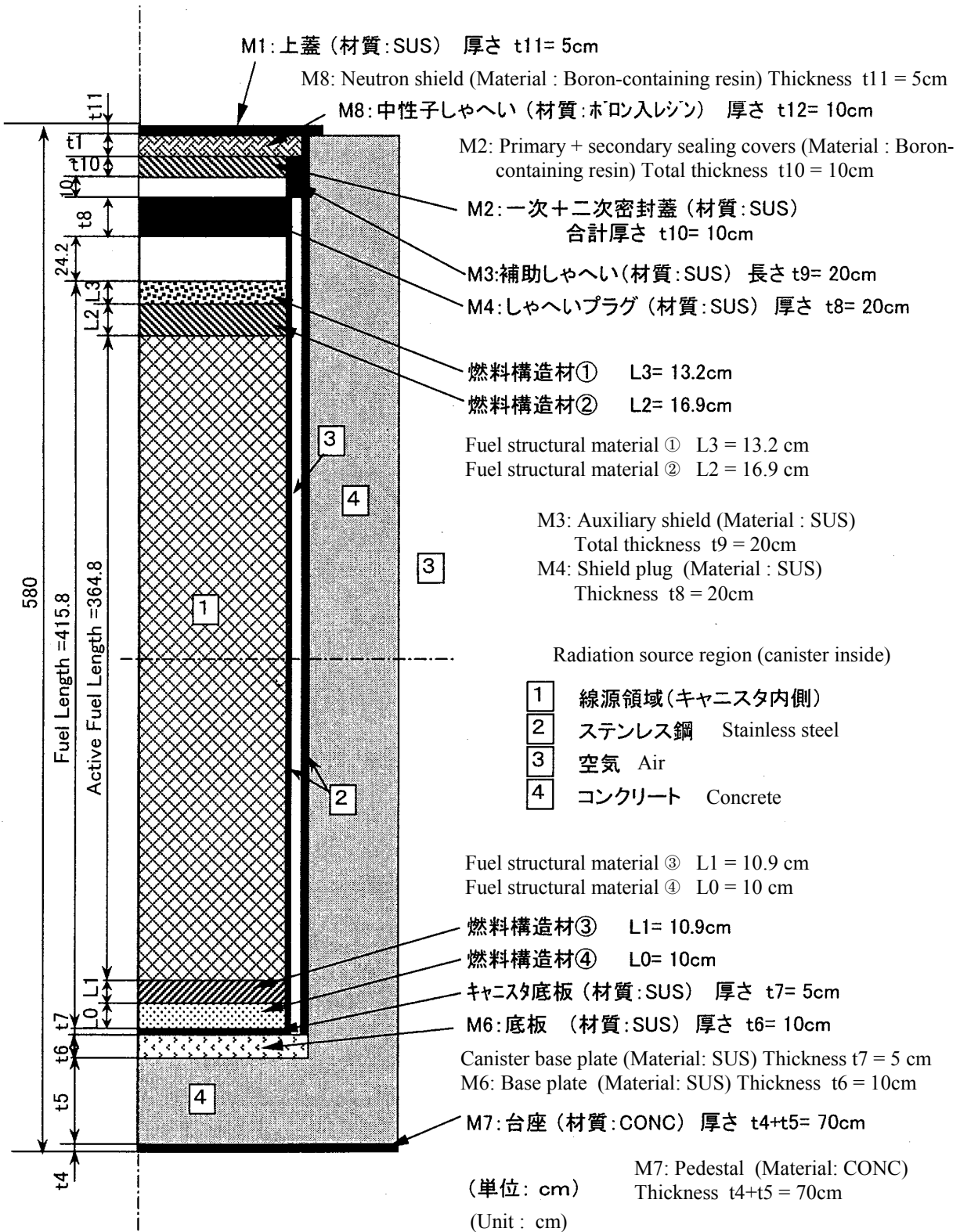
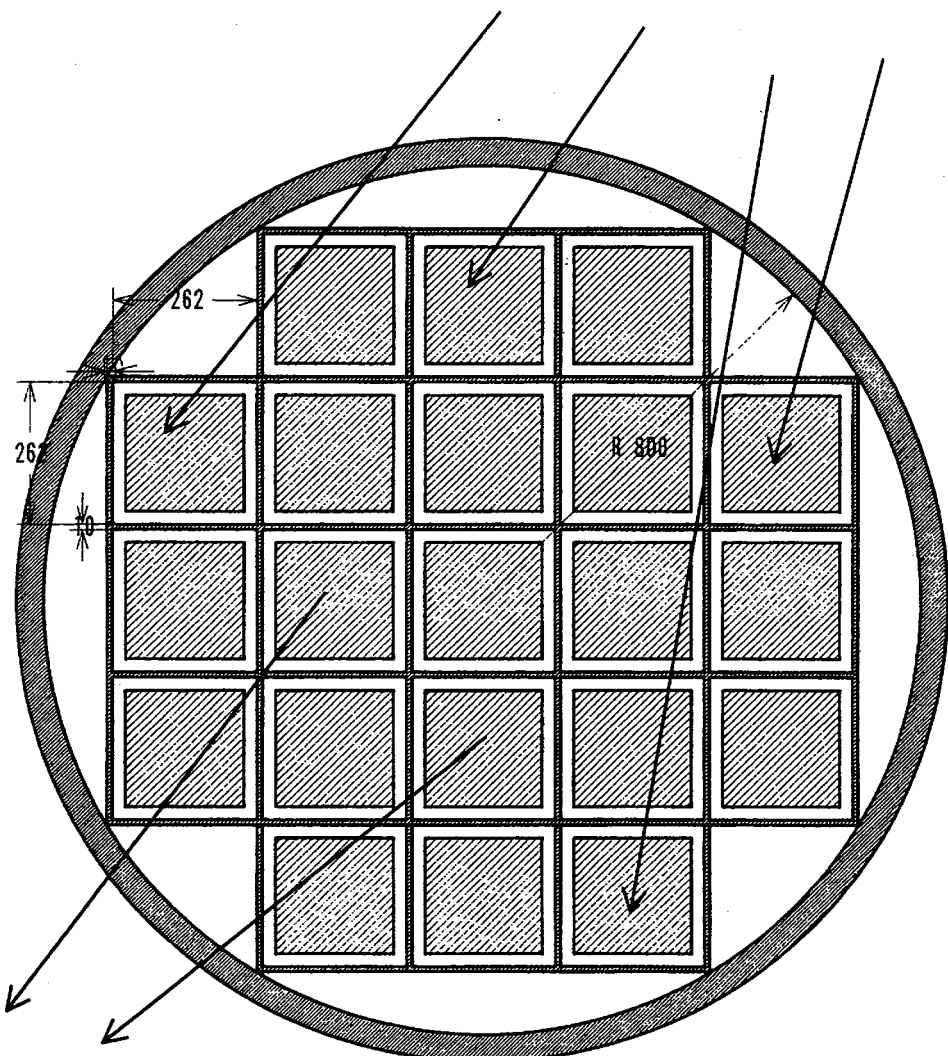


Fig. 6.2.3 Calculation model for longitudinal cross section

12 peripheral fuel assemblies (average burnup  $\times$  70%)

外周燃料集合体12体(平均燃焼度 $\times$ 70%)



中心燃料集合体9体(平均燃焼度 $\times$ 130%)

9 central fuel assemblies (average burnup  $\times$  130%)

单位: mm Unit : mm

Fig. 6.2.4 Calculation model for fuel assembly configuration inside canister

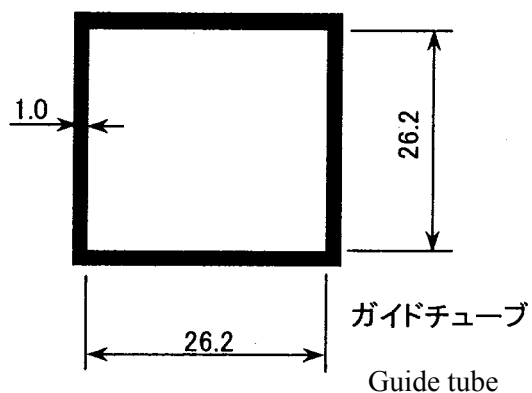
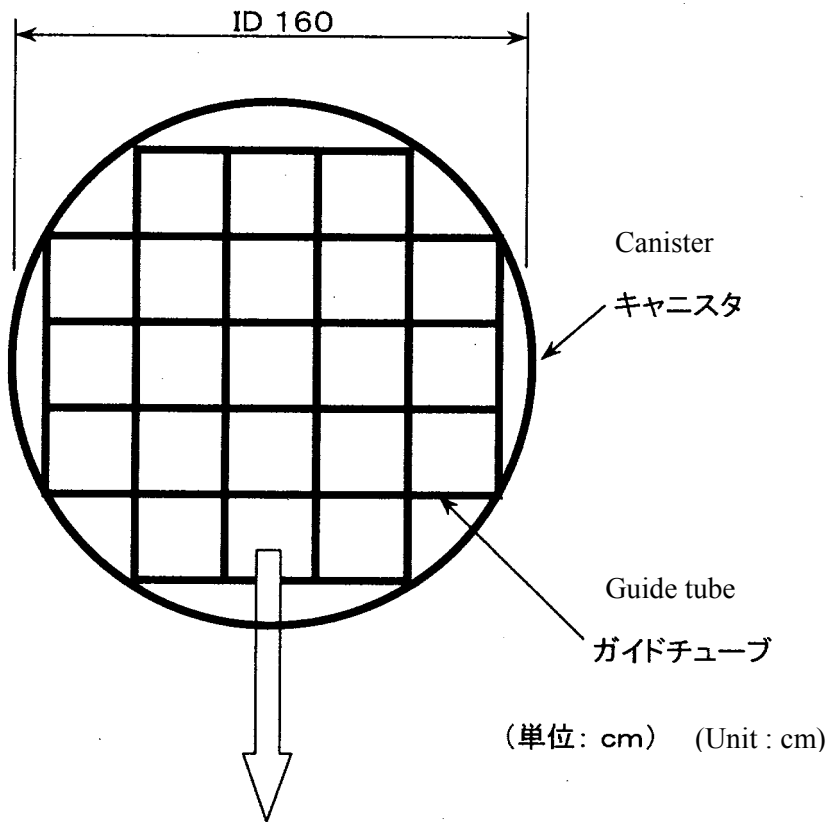


Fig. 6.2.5 Calculation model for canister

horizontal cross section

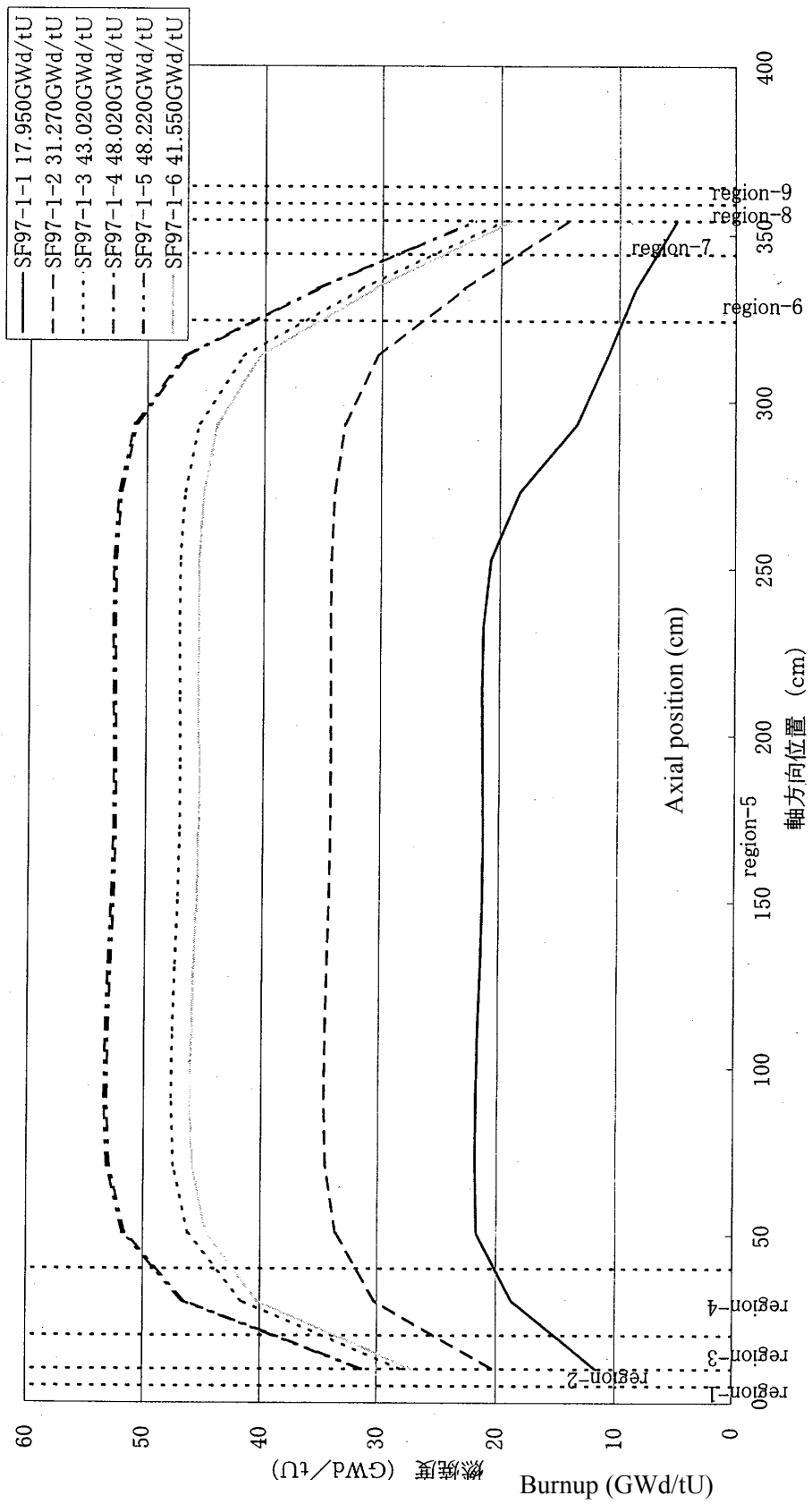


Fig. 6.2.6 Calculation model for axial burnup distribution profile in PWR fuel pin

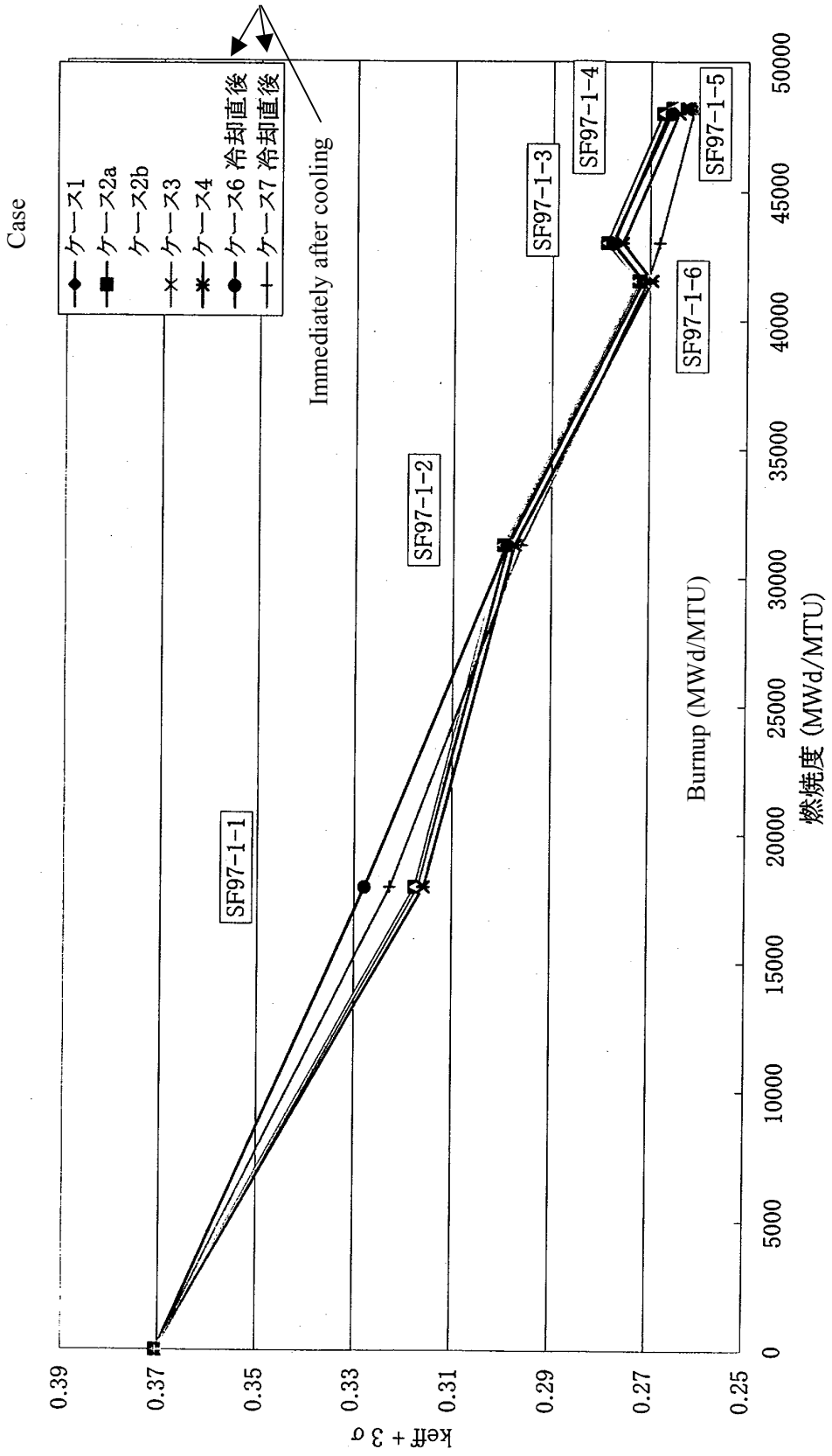


Fig. 6.2.7 ( $k_{\text{eff}} + 3\sigma$ ) changing curve with burnup for spent fuel storage cask model

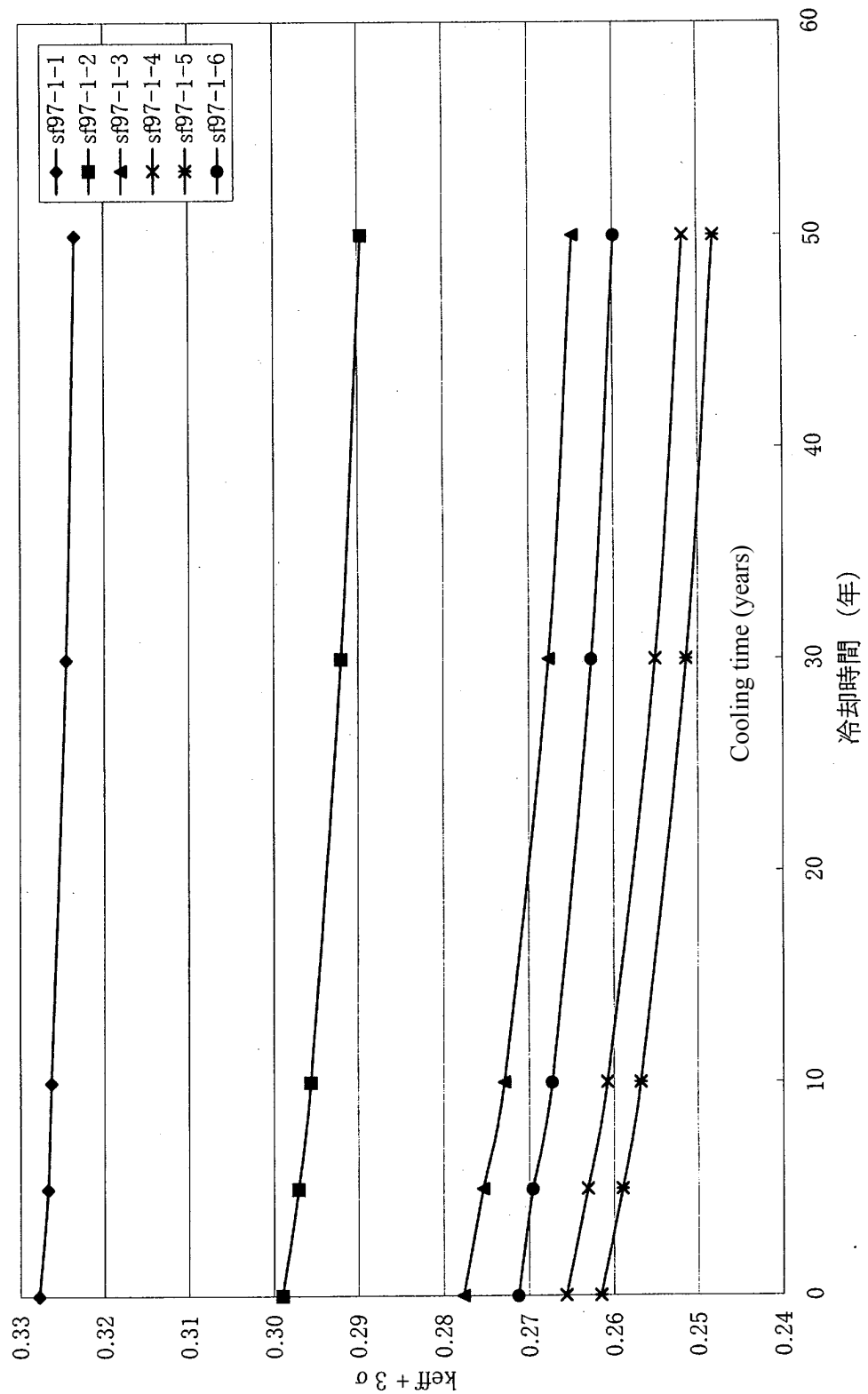


Fig. 6.2.8 ( $k_{\text{eff}}+3\sigma$ ) changing curve with cooling time for case 6 (SWAT) spent fuel storage cask model

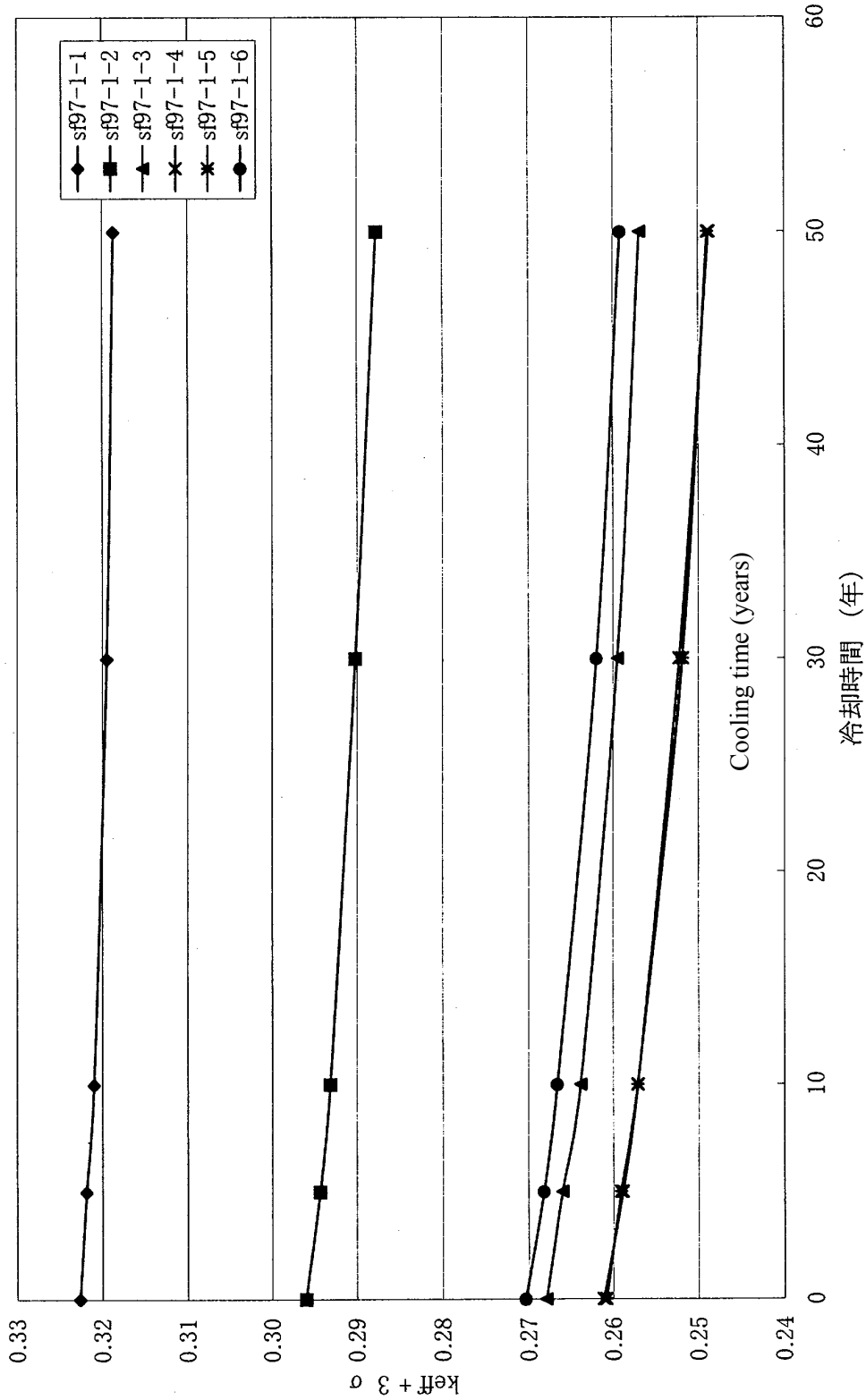


Fig. 6.2.9 ( $k_{\text{eff}}+3\sigma$ ) changing curve with cooling time for case 7 (ORIGEN2.1) spent fuel storage cask model

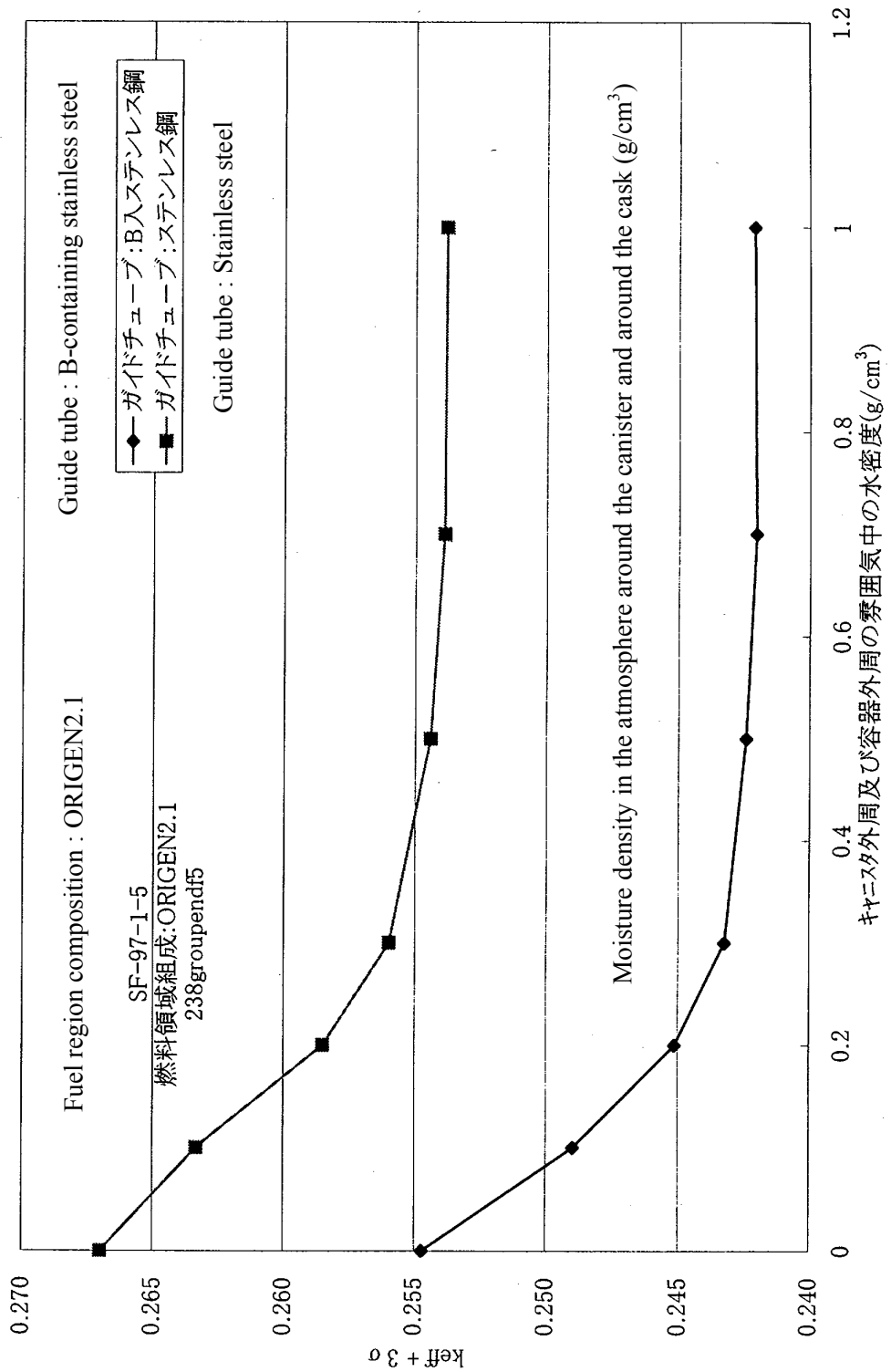


Fig. 6.2.10 ( $k_{\text{eff}}+3\sigma$ ) changing curve with moisture density around canister calculated by KENO-Va

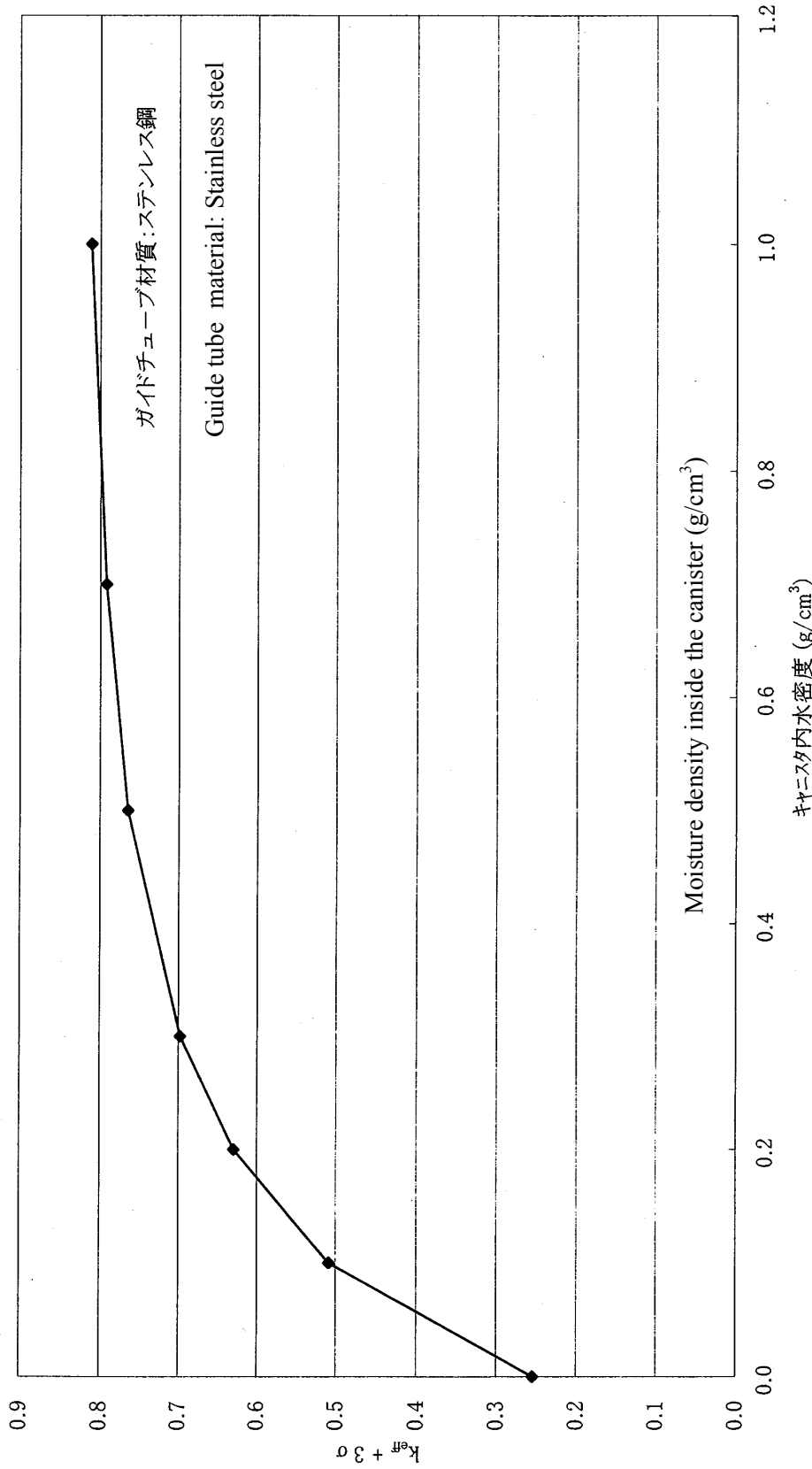


Fig. 6.2.11 ( $(K_{\text{eff}} + 3\sigma)$ ) changing curve with moisture density inside canister calculated by KENO-Va

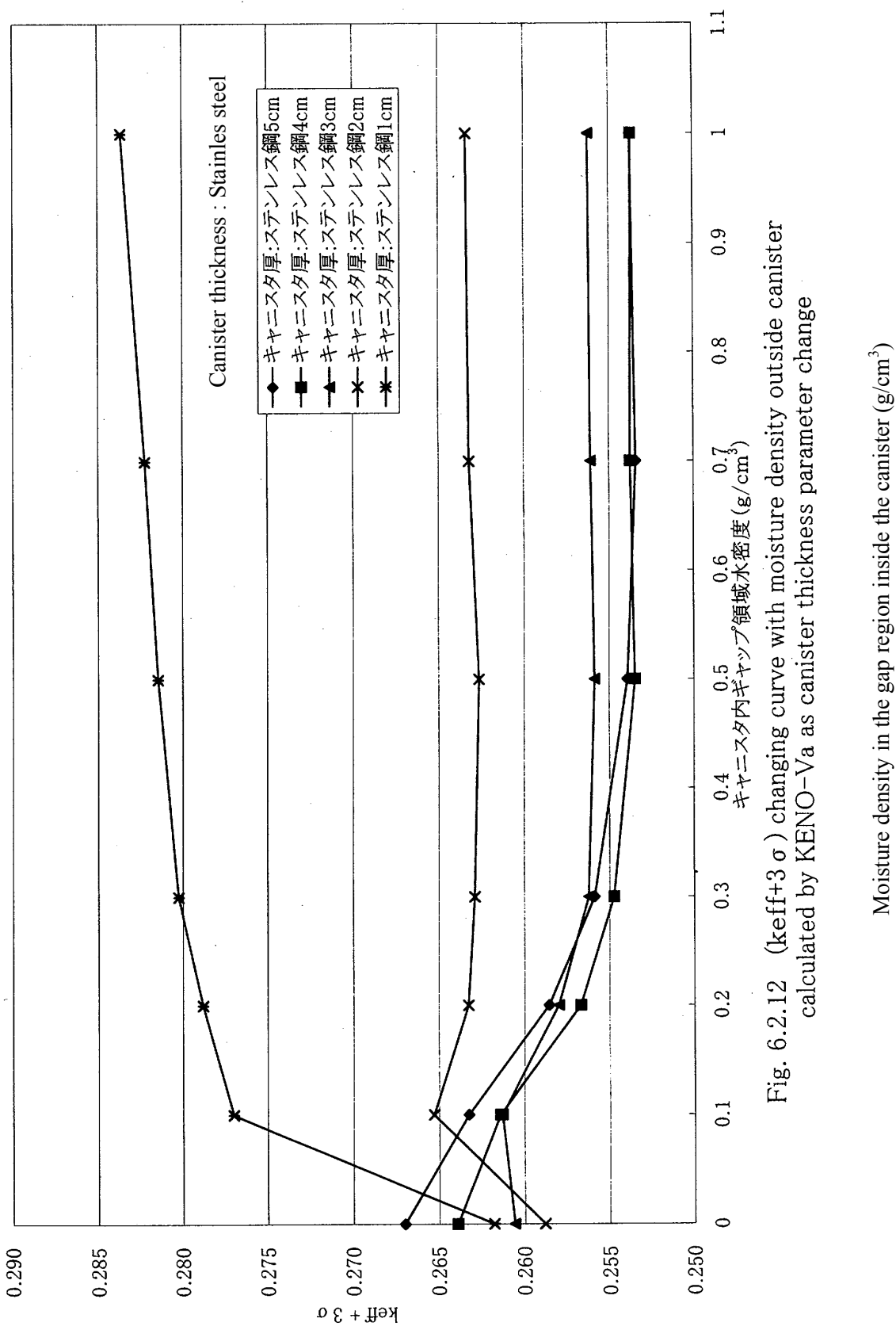


Fig. 6.2.12 ( $k_{eff}+3\sigma$ ) changing curve with moisture density outside canister calculated by KENO-Va as canister thickness parameter change

Moisture density in the gap region inside the canister ( $\text{g}/\text{cm}^3$ )

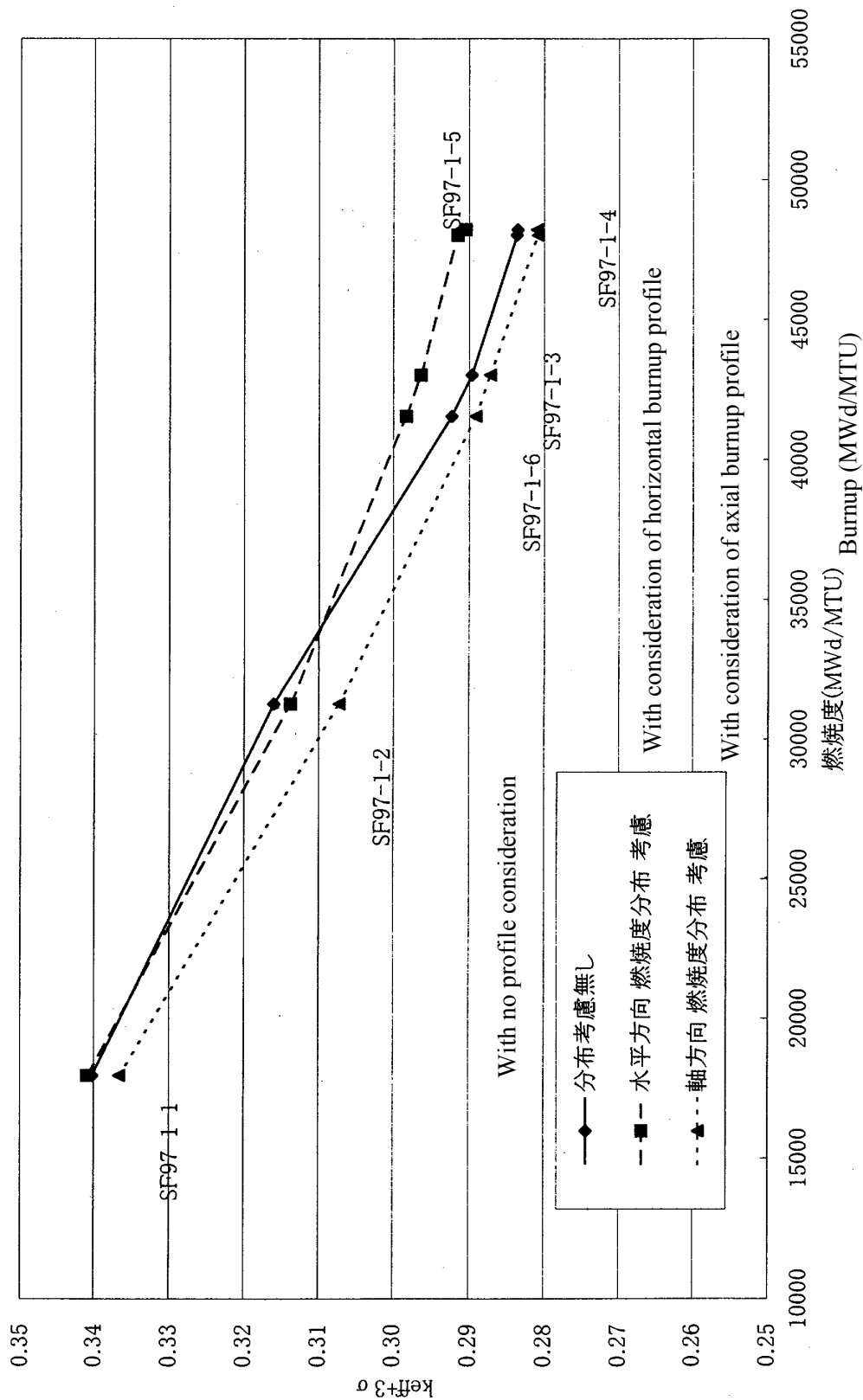


Fig. 6.2.13 ( $k_{\text{eff}} + 3\sigma$ ) changing curve with burnup profile consideration with all isotopic nuclides calculated by ORIGEN2.1 and KENO-Va for spent fuel storage concrete cask

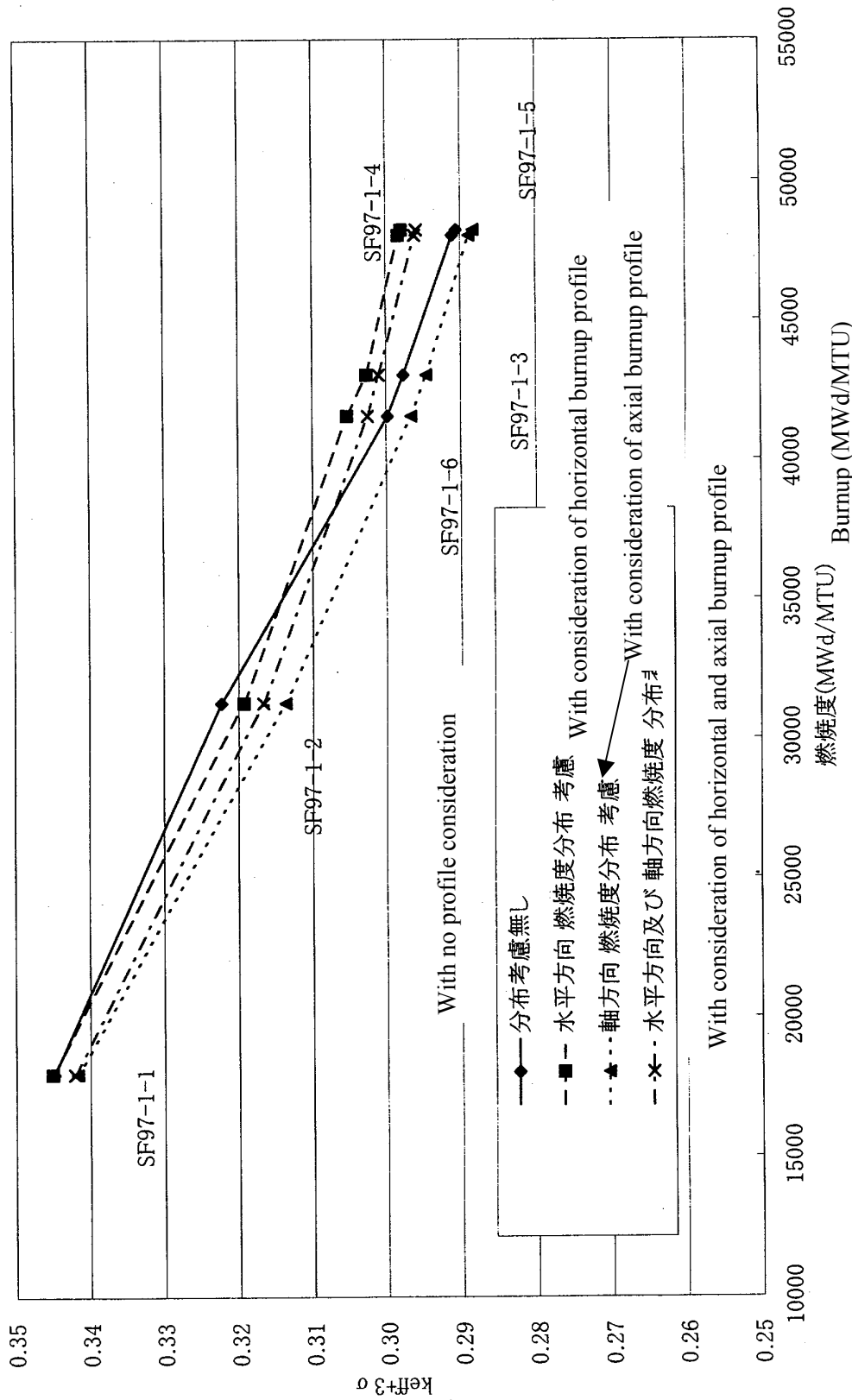


Fig. 6.2.14 ( $k_{\text{eff}} + 3\sigma$ ) changing curve with burnup profile consideration with U,Pu,Am,Np isotopic nuclides calculated by ORIGEN2.1 and KENO-Va for spent fuel storage concrete cask

## **6.3. Examination of the Source Terms for the Safety Analysis of Shielding and Heating**

### **6.3.1. General**

For the safety analysis of spent fuel transport and storage casks, it is important to evaluate not only criticality safety but also radiation shielding in order to control the exposure of operators and the public to radiation and also to evaluate heating and structural safety. In this section, we will examine the neutron source terms important as basic data for the above-mentioned safety analyses, with respect to their cooling time dependence. Since we carry out shielding calculation with respect to neutron sources by using a specified spectrum, the ratio of source strengths is reflected in the source equivalent fraction in shielding analysis.

### **6.3.2. Analysis Objective**

Of the experimental samples used in the concrete storage cask criticality analysis, SF97-1-5 with the highest burnup (48,220 MWd/MTU) and SF97-1-1 with the lowest burnup (17,950 MWd/MTU) are selected for analysis, and ORIGEN2.1 (PWR-UE library) calculation code is used for nuclide formation and decay with cooling time.

Table 6.3.1 shows the object nuclides for criticality safety analysis. Here, neutron source strengths are calculated with compositions of only these object nuclides for criticality safety analysis, and the change in neutron source strength with cooling time is compared and evaluated for the following 4 cases with different nuclide compositions and different calculation codes.

Case 1: Calculation of burnup and attenuation by ORIGEN2.1 for a fresh fuel composition (same as in Table 6.3.1).

Case 2: Calculation of attenuation by ORIGEN2.1 starting from measured values for nuclide compositions of only the measured nuclides shown in Table 6.3.1.

Case 3: Calculation of attenuation by ORIGEN2.1 starting from the calculated burnup values in case 1 for nuclide compositions of only the measured nuclides shown in Table 6.3.1.

Case 4: Calculation of attenuation by ORIGEN2.1 starting from SWAT calculated burnup values for nuclide compositions of only the measured nuclides shown in Table 6.3.1.

However, since FPs made no contribution in the calculation of neutron source strength, the results are the same even if "only the measured nuclides" is replaced by "all nuclides" in case 3 and case 4.

### 6.3.3. Results

Primary neutron source strength based on the calculation of burnup and attenuation by ORIGEN2.1 for a fresh fuel composition of case 1 is shown in Table 6.3.2 and Fig. 6.3.1. As can be seen, the total primary neutron source strength of the minimum burnup sample SF97-1-1 decreases considerably in cooling times of 0–2 years, and then gradually after that. Of the total strength, the neutron source strength due to  $(\alpha, n)$  reaction increases after 5-year cooling, but the contribution of this increase is small. On the other hand, the neutron source strength of SF97-1-5 decreases largely in the beginning in a similar manner, but tends to decrease gradually after 2- to 3-year cooling. Of this strength, the contribution of neutron source strength due to  $(\alpha, n)$  reaction is small, and this strength tends to decrease gradually after 5-year cooling. If the ORIGEN2.1 calculated values are examined in detail, the nuclide that becomes dominant in  $(\alpha, n)$  reaction is Cm-242 for a period of up to 2 years immediately after cooling, and the total neutron source strength due to  $(\alpha, n)$  reaction decreases rapidly as Cm-242 decreases rapidly. The next dominant nuclide is Pu-238, which decreases gradually, and soon Am-241, which increases gradually immediately after cooling, becomes the finally dominant nuclide. In the case of SF97-1-1 with the minimum burnup, Am-241 becomes more dominate than Pu-238 after about 5-year cooling, and thus the primary neutron source strength due to  $(\alpha, n)$  reaction increases with the increasing Am-241 after 5-year cooling. When compared with this, the primary neutron source strength due to  $(\alpha, n)$  reaction shows a gradual monotonous decrease after 5-year cooling in SF97-1-5 with the maximum burnup, since the amount of Pu-238 formed there is about 30 times as great as that of the Am-241 formed (about 6 times in SF97-1-1).

Tables 6.3.3–6.3.4 and Figs. 6.3.2–6.3.3 show the dependence of primary neutron source strength on cooling time in various cases with varied types of nuclides and calculation methods. As can be seen, the calculated values of case 3 with consideration of only the measured nuclides agree approximately with the calculated values of case 1 obtained by burnup and attenuation calculation by ORIGEN2.1 from the composition of a fresh fuel; thus, it can be seen that primary neutron source strength can be calculated by considering only the nuclides for criticality analysis shown in Table 6.3.2. The calculated values of case 4, started from the calculated burnup value by using SWAT, deviate about +10% from the evaluated values of case 1 in SF97-1-1, and about -10% in SF97-1-5, but their attenuation trend is practically the same. The calculated values of case 2 by ORIGEN2.1, started from the measured values of the measured nuclides only, are about 10–25% smaller than the calculated values of case 1 in SF97-1-1, and about 5% smaller in SF97-1-5. The analytical results of case 2 of SF97-1-5 are about +5% larger than those of case 4, but both show the same attenuation trend. If the calculated values are examined in detail, the lowest neutron source strength of case 2 of Fig. 6.3.2 for the low-burnup sample arises from the fact that the values of atomic number density immediately after cooling of Cm-244 and Am-241 of Cm-244, Pu-240, and Am-241, which become dominant nuclides, are about 60–70% smaller in case 2 than in case 1. The lowest calculated values of case 4 in Fig. 6.3.3 for the high- burnup sample are caused by the difference in the amount of dominant nuclide Cm-244 formed, in much the same way as in the low-burnup sample.

## REFERENCES

1. Judith F. Biersmeister (ed.), “MCNP™ — A General Monte Carlo Code N — Particle Transport Code Version 4A, “La–12625 (1993).
2. *SCALE4.3: Modular Code for Performing Standardized Computer Analyses for Licensing Evaluation for Workstations and Personal Computers*, NUREG/CR-0200, Rev. 5, Vols. I, II, and III (DRAFT September 1995). Available from Radiation Safety Information Computational Center at Oak Ridge National Laboratory as CCC-545.
3. K. Kosako, et al., “FSLIB-J3R2: A Continuous Energy Cross Section Library for MCNP Based on JENDL-3.2,” JAERI-Data/Code 94-020 (1994).
4. T. Nakagawa, et al., “Japanese Evaluated Nuclear Data Library Version 3, Revision-2: JENDL-3.2,” *Journal of Nuclear Science and Technology* 32[12] (December 1995).
5. Criticality Safety Experimental Data Examination Working Group, Criticality Safety Special Sectional Committee of the Nuclear Fuel Facility Safety Study Committee of the Japan Atomic Energy Research Institute: *Criticality Safety Handbook*, second edition, JAERI, 1999, p. 1,340.

Table 6.3.1. Object nuclides for criticality safety analysis

Object nuclides	Ac	FP
	U-234	(Mo-95)
	U-235	(Tc-99)
	U-236	(Ru-101)
	U-238	(Rh-103)
	Pu-238	(Ag-109)
	Pu-239	(Cs-133)
	Pu-240	Nd-143
	Pu-241	Nd-145
	Pu-242	Sm-147
	Am-241	Sm-149
	Am-243	Sm-150
	Cm-242	Sm-151
	Cm-243	Sm-152
	Cm-244	(Eu-153)
	Cm-245	(Gd-155)
	Cm-246	
	Cm-247	
	Np-237	

Note: Nuclides with no measured data are shown in ( ).

Table 6.3.2. Primary neutron source strength

Sample name	Cooling time	$(\alpha, n)$ Reaction	Spontaneous nuclear fission	Total
SF97-1-1 17950 MWd/MTU	0 year	1.15E+07	6.00E+07	7.15E+07
	0.5 year	5.94E+06	3.24E+07	3.84E+07
	1 year	3.35E+06	1.95E+07	2.29E+07
	2 years	1.67E+06	1.07E+07	1.23E+07
	5 years	1.40E+06	7.58E+06	8.98E+06
	7 years	1.51E+06	7.09E+06	8.60E+06
	10 years	1.66E+06	6.44E+06	8.10E+06
	15 years	1.86E+06	5.51E+06	7.38E+06
	20 years	2.02E+06	4.75E+06	6.77E+06
	30 years	2.22E+06	3.59E+06	5.81E+06
	50 years	2.33E+06	1.46E+06	3.79E+06
SF97-1-5 48220 MWd/MTU	0 year	1.04E+08	1.49E+09	1.59E+09
	0.5 year	5.68E+07	1.24E+09	1.29E+09
	1 year	3.47E+07	1.14E+09	1.18E+09
	2 years	1.98E+07	9.98E+08	1.02E+09
	5 years	1.54E+07	8.73E+08	8.89E+08
	7 years	1.51E+07	8.10E+08	8.25E+08
	10 years	1.48E+07	7.23E+08	7.38E+08
	15 years	1.42E+07	5.99E+08	6.13E+08
	20 years	1.36E+07	4.97E+08	5.10E+08
	30 years	1.27E+07	3.42E+08	3.55E+08
	50 years	9.43E+06	5.99E+07	6.93E+07

Unit : n/sec/IHM-ton

Table 6.3.3. Primary neutron source strength SF97-1-1 17950 MWd/MTU

Nuclide composition		Cooling time										
		Immediately after cooling	0.5 year	1 year	2 years	5 years	7 years	10 years	15 years	20 years	30 years	50 years
Case 1	( $\alpha$ , n) Reaction	1.15E+07	5.94E+06	3.35E+06	1.67E+06	1.40E+06	1.51E+06	1.66E+06	1.86E+06	2.02E+06	2.22E+06	2.33E+06
	Spontaneous nuclear fission	6.00E+07	3.24E+07	1.95E+07	1.07E+07	7.58E+06	7.09E+06	6.44E+06	5.51E+06	4.75E+06	3.59E+06	1.46E+06
	Total	7.15E+07	3.84E+07	2.29E+07	1.23E+07	8.98E+06	8.60E+06	8.10E+06	7.38E+06	6.77E+06	5.81E+06	3.79E+06
Relative ratio		1.00E+00	5.37E-01	3.20E-01	1.72E-01	1.26E-01	1.20E-01	1.13E-01	1.03E-01	9.47E-02	8.13E-02	5.30E-02
Case 2	( $\alpha$ , n) Reaction	1.03E+07	5.23E+06	2.92E+06	1.40E+06	1.13E+06	1.22E+06	1.34E+06	1.49E+06	1.61E+06	1.77E+06	1.84E+06
	Spontaneous nuclear fission	5.26E+07	2.76E+07	1.61E+07	8.24E+06	5.63E+06	5.27E+06	4.81E+06	4.15E+06	3.61E+06	2.78E+06	1.26E+06
	Total	6.29E+07	3.29E+07	1.90E+07	9.63E+06	6.76E+06	6.49E+06	6.15E+06	5.65E+06	5.22E+06	4.55E+06	3.10E+06
Relative ratio		8.79E-01	4.60E-01	2.66E-01	1.35E-01	9.46E-02	9.08E-02	8.60E-02	7.90E-02	7.30E-02	6.36E-02	4.34E-02
Case 3	( $\alpha$ , n) Reaction	1.15E+07	5.90E+06	3.33E+06	1.65E+06	1.38E+06	1.50E+06	1.65E+06	1.85E+06	2.01E+06	2.21E+06	2.31E+06
	Spontaneous nuclear fission	6.00E+07	3.23E+07	1.94E+07	1.06E+07	7.54E+06	7.05E+06	6.40E+06	5.48E+06	4.71E+06	3.56E+06	1.43E+06
	Total	7.15E+07	3.81E+07	2.27E+07	1.23E+07	8.93E+06	8.54E+06	8.05E+06	7.33E+06	6.72E+06	5.76E+06	3.75E+06
Relative ratio		1.00E+00	5.34E-01	3.18E-01	1.71E-01	1.25E-01	1.20E-01	1.13E-01	1.03E-01	9.40E-02	8.06E-02	5.24E-02
Case 4	( $\alpha$ , n) Reaction	1.27E+07	6.47E+06	3.61E+06	1.74E+06	1.42E+06	1.54E+06	1.70E+06	1.91E+06	2.06E+06	2.27E+06	2.38E+06
	Spontaneous nuclear fission	6.59E+07	3.51E+07	2.09E+07	1.11E+07	7.76E+06	7.25E+06	6.59E+06	5.64E+06	4.86E+06	3.68E+06	1.51E+06
	Total	7.86E+07	4.16E+07	2.45E+07	1.28E+07	9.18E+06	8.79E+06	8.28E+06	7.55E+06	6.92E+06	5.95E+06	3.90E+06
Relative ratio		1.10E+00	5.82E-01	3.42E-01	1.79E-01	1.28E-01	1.23E-01	1.16E-01	1.06E-01	9.69E-02	8.32E-02	5.45E-02

Unit = n/sec/IHM-ton

Table 6.3.4. Primary neutron source strength SF97-1-5 48220 MWd/MTU

Nuclide composition		Cooling time										
		Immediately after cooling	0.5 year	1 year	2 years	5 years	7 years	10 years	15 years	20 years	30 years	50 years
Case 1	( $\alpha$ , n) Reaction	1.04E+08	5.68E+07	3.47E+07	1.98E+07	1.54E+07	1.51E+07	1.48E+07	1.42E+07	1.36E+07	1.27E+07	9.43E+06
	Spontaneous nuclear fission	1.49E+09	1.24E+09	1.14E+09	9.98E+08	8.73E+08	8.10E+08	7.23E+08	5.99E+08	4.97E+08	3.42E+08	5.99E+07
	Total	1.59E+09	1.29E+09	1.18E+09	1.02E+09	8.89E+08	8.25E+08	7.38E+08	6.13E+08	5.10E+08	3.55E+08	6.93E+07
Relative ratio		1.00E+00	8.13E-01	7.41E-01	6.40E-01	5.59E-01	5.19E-01	4.64E-01	3.86E-01	3.21E-01	2.23E-01	4.36E-02
Case 2	( $\alpha$ , n) Reaction	9.89E+07	5.34E+07	3.24E+07	1.83E+07	1.43E+07	1.41E+07	1.38E+07	1.34E+07	1.30E+07	1.22E+07	9.37E+06
	Spontaneous nuclear fission	1.40E+09	1.16E+09	1.04E+09	9.39E+08	8.22E+08	7.62E+08	6.81E+08	5.64E+08	4.68E+08	3.23E+08	5.69E+07
	Total	1.50E+09	1.22E+09	1.08E+09	9.57E+08	8.36E+08	7.76E+08	6.94E+08	5.77E+08	4.81E+08	3.35E+08	6.63E+07
Relative ratio		9.45E-01	7.65E-01	6.77E-01	6.02E-01	5.26E-01	4.88E-01	4.37E-01	3.63E-01	3.02E-01	2.11E-01	4.17E-02
Case 3	( $\alpha$ , n) Reaction	1.04E+08	5.65E+07	3.45E+07	1.97E+07	1.54E+07	1.51E+07	1.47E+07	1.41E+07	1.36E+07	1.26E+07	9.37E+06
	Spontaneous nuclear fission	1.48E+09	1.23E+09	1.11E+09	9.97E+08	8.73E+08	8.09E+08	7.23E+08	5.99E+08	4.96E+08	3.42E+08	5.98E+07
	Total	1.59E+09	1.29E+09	1.14E+09	1.02E+09	8.88E+08	8.24E+08	7.37E+08	6.13E+08	5.10E+08	3.55E+08	6.91E+07
Relative ratio		9.99E-01	8.11E-01	7.18E-01	6.40E-01	5.59E-01	5.19E-01	4.64E-01	3.86E-01	3.21E-01	2.23E-01	4.35E-02
Case 4	( $\alpha$ , n) Reaction	1.16E+08	6.03E+07	3.45E+07	1.71E+07	1.24E+07	1.23E+07	1.22E+07	1.19E+07	1.17E+07	1.12E+07	8.94E+06
	Spontaneous nuclear fission	1.32E+09	1.03E+09	8.88E+08	7.75E+08	6.72E+08	6.23E+08	5.56E+08	4.61E+08	3.82E+08	2.64E+08	4.68E+07
	Total	1.43E+09	1.09E+09	9.23E+08	7.92E+08	6.84E+08	6.35E+08	5.69E+08	4.73E+08	3.94E+08	2.75E+08	5.57E+07
Relative ratio		9.02E-01	6.85E-01	5.81E-01	4.98E-01	4.31E-01	4.00E-01	3.58E-01	2.98E-01	2.48E-01	1.73E-01	3.51E-02

Unit = n/sec/IHM-ton

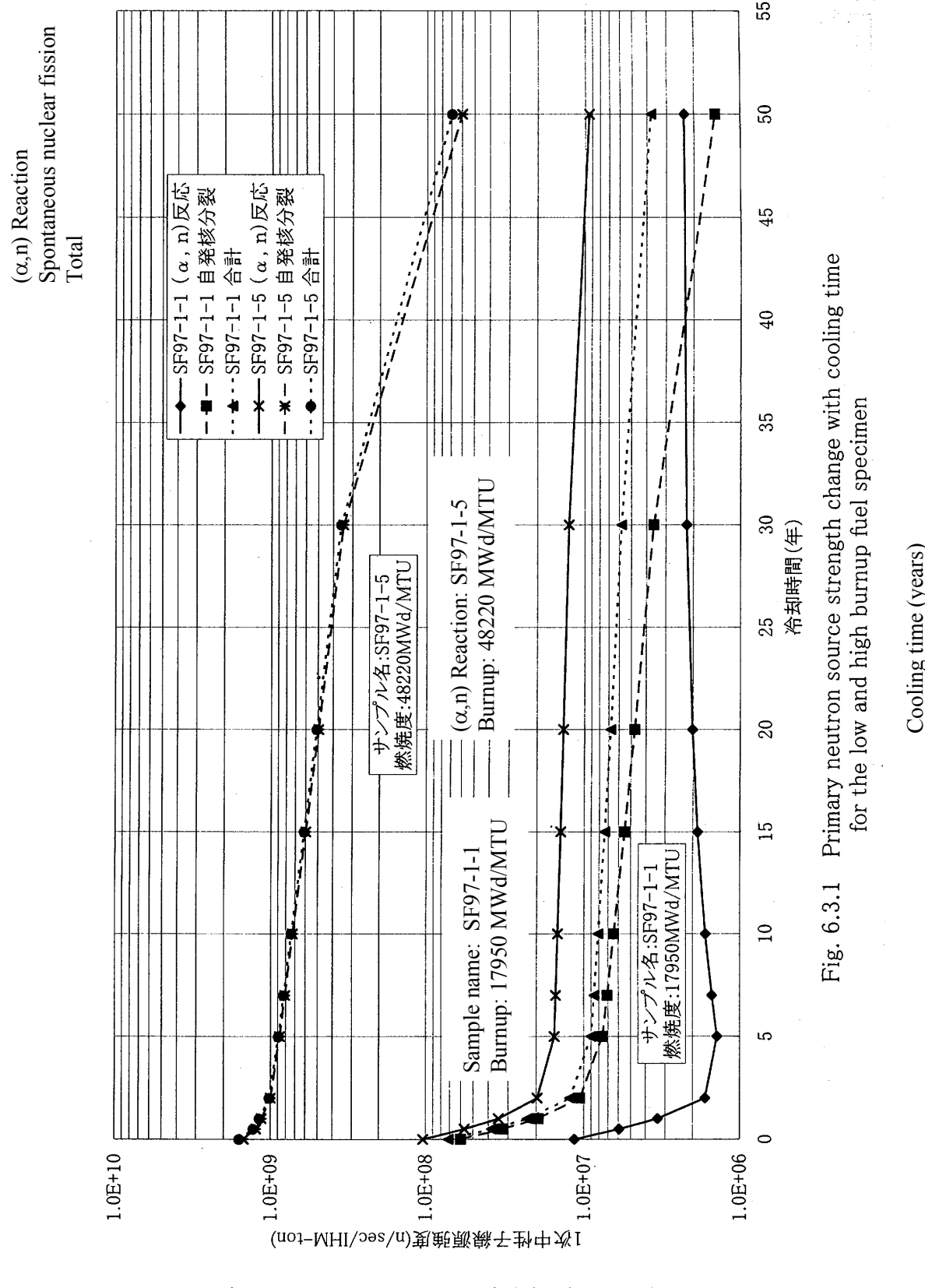


Fig. 6.3.1 Primary neutron source strength change with cooling time  
for the low and high burnup fuel specimen

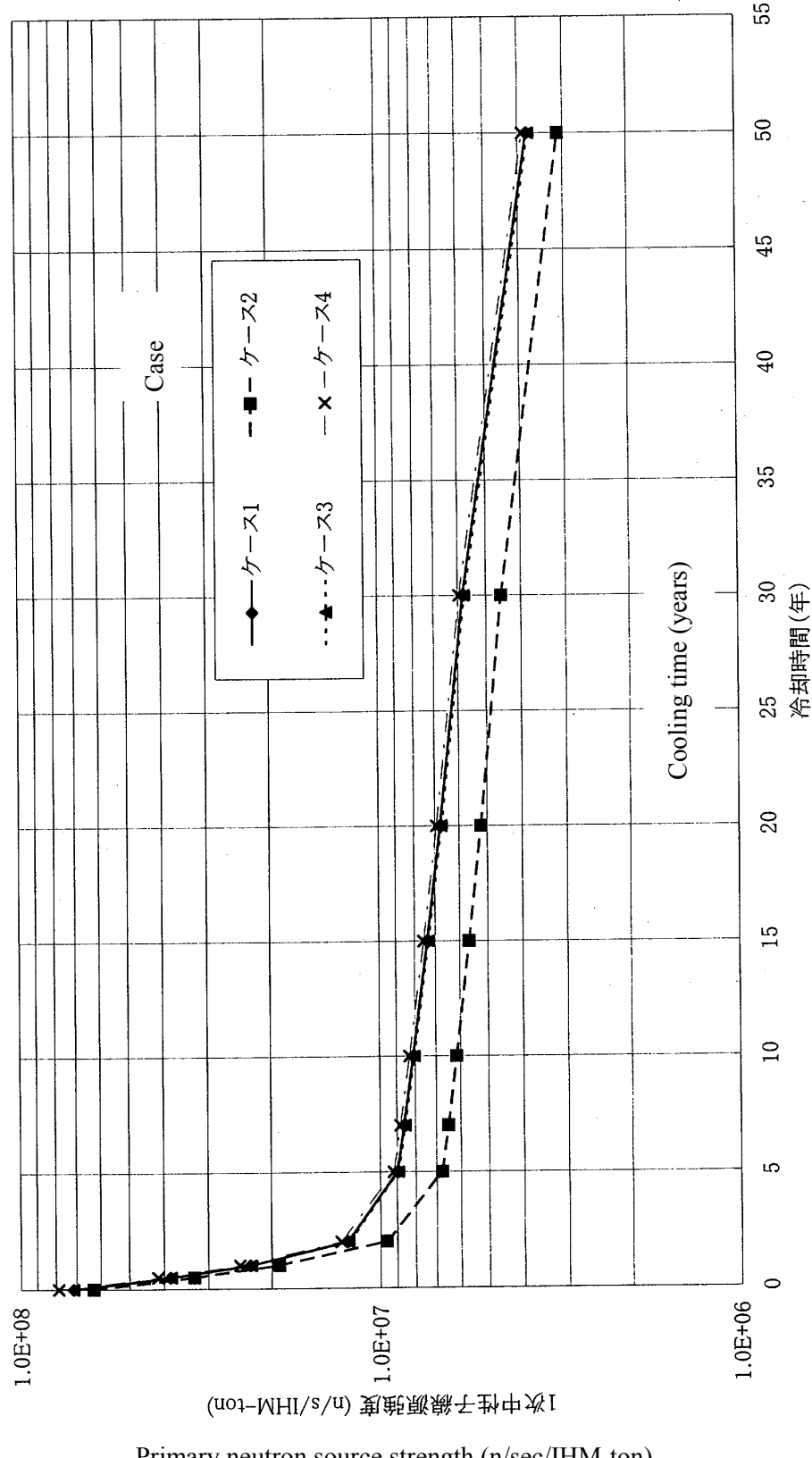


Fig. 6.3.2 Primary neutron source strength change with cooling time  
(SF97-1-1,17950MWd/MTU)

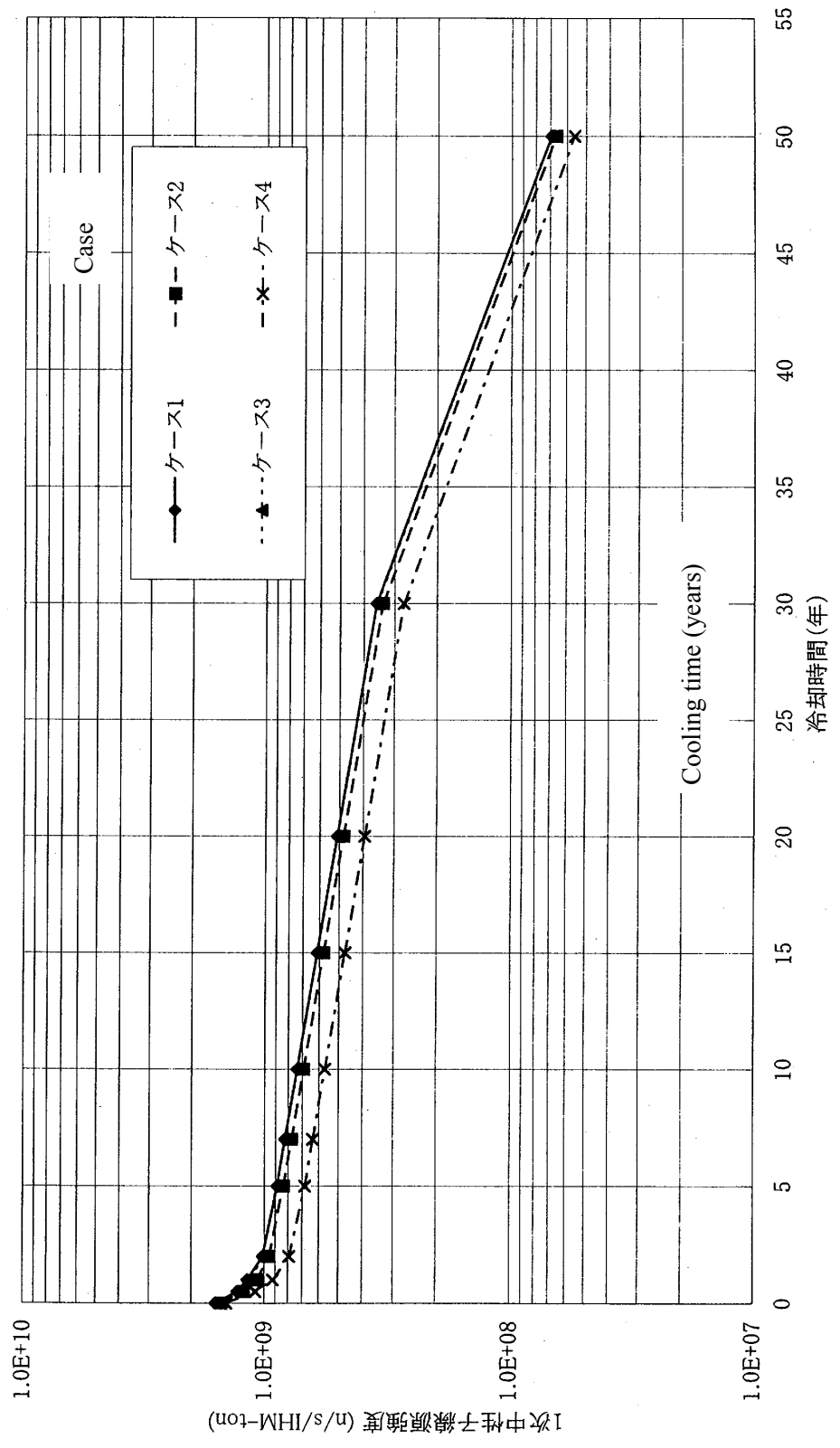


Fig. 6.3.3 Primary neutron source strength change with cooling time  
(SF97-1-5,48220MWd/NMTU)



## 7. CONCLUSION

The IAEA advisory group meeting on the implementation of burnup credit in spent fuel management systems made the following recommendations on the basis of the present status of various countries (Ref. 2 of Sect. 1).

- (1) There is a need for a great variety of data to support burnup credit activities and applications (storage, transport, reprocessing, and disposal) for four fuel types (BWR, PWR, MOX, and WWER). Some data development activities are already underway and these should be continued. These data are needed to support benchmark activities.
- (2) Countries and organizations requiring specific types of data should collaborate with one another as far as possible to share experiments, costs, and experimental results. Countries carrying out data development programs for their own sake should give consideration to making data available to other countries through contracts or joint agreements. Whenever possible, data for burnup credit should be contributed for publication as references open to the public.
- (3) An effort must be made to determine if any data can be exchanged between the respective fuel types and applications. There might be some overlapping of applicable regions.
- (4) Effort should be focused on obtaining well-established standards to validate actinides + FP burnup credit methods. These standards should be compared for the quality of standards given in the OECD/NEA International Handbook of Evaluated Criticality Safety Benchmark Experiments, and eventually should include an FP group of  $^{95}\text{Mo}$ ,  $^{99}\text{Tc}$ ,  $^{101}\text{Ru}$ ,  $^{103}\text{Rh}$ ,  $^{109}\text{Ag}$ ,  $^{113}\text{Cd}$ ,  $^{133}\text{Cs}$ ,  $^{135}\text{Cs}$ ,  $^{143}\text{Nd}$ ,  $^{144}\text{Nd}$ ,  $^{145}\text{Nd}$ ,  $^{146}\text{Nd}$ ,  $^{148}\text{Nd}$ ,  $^{150}\text{Nd}$ ,  $^{147}\text{Sm}$ ,  $^{149}\text{Sm}$ ,  $^{150}\text{Sm}$ ,  $^{152}\text{Sm}$ ,  $^{153}\text{Eu}$ ,  $^{154}\text{Gd}$ ,  $^{155}\text{Gd}$ ,  $^{156}\text{Gd}$ ,  $^{157}\text{Gd}$ ,  $^{158}\text{Gd}$ , and  $^{160}\text{Gd}$ .
- (5) The accuracy of different calculation tools should be evaluated, and a method to manage errors that occur when burnup is used as criticality management should be developed. With regard to this, an interface at a necessary time and place should be developed to compare calculation tools (for burnup and criticality) that differ in the East and the West.
- (6) Errors inherent to currently existing quantitative burnup validation measurement methods should be reduced with significant quantities. Accordingly, a program to improve the burnup validation measurement methods currently in use, and if necessary to develop a new method, should be started.
- (7) The axial burnup profile of an assembly has a large effect on burnup credit for spent fuel management systems. If a quantitative burnup validation method is required, then the effect of the reactivity of the axial burnup profile related to the management system under consideration must be evaluated, otherwise this effect must be assured by including it in advance in loading curves/standards of the system, or by applying safety factors evaluated to be safe for measured burnups. Therefore, the measurement of an axial profile on-line and the evaluation of the reactivity effect of this profile pertaining to the system under consideration should be combined, and a program to develop a method/device to judge whether this reactivity effect is consistent with the loading curves/standards of the system should be started.

(8) The burnup profile in the radial direction of an assembly has little importance. However, we recognize that it is impossible to reach a final conclusion at present as to whether the radial burnup profile is always represented by an average value (constant) in the radial direction with respect to reactivity. Accordingly, systematic studies should be made of the reactivity effect of the radial burnup profile.

Most of the above-mentioned recommendations refer to the need to make accurate measurements and to acquire measured isotopic data to grasp errors of various sorts more accurately, which are induced by the introduction of burnup credit, and emphasize the importance of experiments needed for this purpose.

The work of the present special committee focused just on this aspect and acquired basic measured data essential to the study of burnup credit, such as axial  $\gamma$ -ray activity profile data of spent fuel rods, nuclide composition data of spent fuel samples, and criticality data of spent fuel assemblies, using actual fuels such as commercial PWR/BWR spent fuels.

Furthermore, the adequacy of burnup calculation codes and the adequacy of criticality calculation codes were evaluated; axial burnup profiles were evaluated/examined; and the influence of source terms related to criticality, shielding, and heating was evaluated, all of these being most important issues that must be taken into consideration in introducing burnup credit by using measured data.

Although there are many problems to be overcome before burnup credit can be applied to spent fuels, we are certain that the fruits of the work of the present special committee will be very useful for research/development on burnup credit in the future.

## ACKNOWLEDGMENTS

We would like to express our hearty thanks to all persons at the JAERI Hot Laboratory for their fine cooperation in the experiments related to spent fuels conducted in the present work, and to Kansai Electric Co., Ltd., Tokyo Electric Co., Ltd., and the Atomic Power Technology Development Organization (foundation) for readily providing spent fuels and irradiation history data. This paper is a summary of the work on "Technical Development on Criticality Safety Management for LWR Spent Fuels" undertaken under a contract with the Science and Technology Agency of Japan, and we are very grateful for the support of the Science and Technology Agency of Japan over many years.

## APPENDIX

### A.1. REGULATORY STATUS ON BURN-UP CREDIT

None of the regulations in various countries on the criticality safety of storage and transportation of spent fuels prohibit the use of burn-up credit from the standpoint of improving the safety of workers and that of the public. We do not mean to imply, however, that the use of burn-up credit is flatly approved without restrictions, because some problems do remain on burn-up credit evaluation methods, such as validation of the analysis codes to show criticality safety, and the taking of all the effects of relevant data into consideration. For example, in May of 1995, the NRC approved the use of burn-up credit at a level with actinides alone in the criticality safety design of transportation and storage casks of spent PWR fuels, based on a request from the Department of Energy (DOE). On the other side, the use of burn-up credit at a similar level has been approved for a long time in France.

#### A.1.1. Worldwide Status on Burn-Up Credit Uses

With regard to introducing burn-up credit into the design of transportation and storage facilities for spent fuels by deciding which level of burn-up credit to adopt, assurance of the safety margin must be investigated by considering the current status of burn-up calculation or criticality calculation accuracy. When we look at the status overseas, the way of introducing burn-up credit differs, depending on the specific regulations in each country. It is not the general practice to employ a single criterion for use comprising only decreases in fissionable components; the actual status in various countries as of 1999 is as follows (Ref. 1):

Taking only actinides into consideration has been adopted in France, Germany, Russia, and Switzerland. In France, the formation and decay of  $^{235}\text{U}$ ,  $^{236}\text{U}$ ,  $^{238}\text{Pu}$ ,  $^{239}\text{Pu}$ ,  $^{240}\text{Pu}$ ,  $^{241}\text{Pu}$ , and  $^{242}\text{Pu}$  by assembly averaged burn-up in the range of 50 cm from the bottom of the fuel region are taken into consideration in wet storage, wet and dry transportation, and in the reprocessing (of PWR fuels only) of spent fuels. In Germany, credit of only uranium and plutonium isotopes at the minimum average takeout burn-up of 5 MWd/kgU was approved in the dry transportation of spent BWR fuels by CASTOR V52 casks. In Russia, credit of only uranium and plutonium isotopes at the minimum average takeout burn-up of 25 MWd/kgU was approved in the wet transportation of VVER-440 spent fuels taken out of the Kola nuclear power station. In Switzerland, credit on assembly averaged burn-up in the range of 50 cm from the bottom of the fuel has been approved, as in France, for the dry storage of PWR spent fuels.

A use criterion comprising consideration of the effect of the neutron absorption of actinides and fission products was approved by the authorization for wet storage facilities for PWR spent fuels in the USA, Korea, and Spain, wet storage facilities for RBMK spent fuels from the Smolensk nuclear power station in Russia and the Ignalina nuclear power station in Lithuania, and dry storage facilities in the USA. In a PWR or BWR wet storage pool, a fixed amount of soluble boron is contained in the pool water, and a portion of the amount of this boron may be considered in a criticality safety analysis in the USA and Spain. The use of this boron credit is not allowed in a criticality safety analysis at normal operating conditions of wet storage facilities in the other countries.

The credit level of a combustible neutron absorbing material was approved by the authorization for BWR wet storage facilities in Germany, Spain, and Sweden. Furthermore, in Japan also, there has been one instance of approval in the design of a spent fuel storage pool for BWR fuels.

### A.1.2. Authorization Status of Burn-Up Credit Uses in Each Country

As regards burn-up credit, the regulatory authorities of various countries have approved the effect of the reactivity of certain limited nuclides in accordance with the technical level of each country. Which level of burn-up credit mentioned in the preceding section should be used is determined by the accuracy of the burn-up credit evaluation method to be used and the characteristics of the spent fuel management system under consideration.

In the USA, for example, spent fuels are stored in a wet or dry storage facility at a reactor site until they are accepted in a civilian radioactive waste management system (CRWMS) at a final stratum disposal site. Furthermore, since there are no more plans for civilian reprocessing, spent fuels must be transported to the disposal site once acceptance for a disposal site is decided, but in this case they are transported in the dry mode. In 1997, the NRC approved an application including burn-up credit in a PWR spent fuel storage pool at two sites, Lesko and Newmyer. Here, the boron component in the pool water became the requirement for ensuring criticality safety. Burn-up credit is not adopted in a BWR spent fuel storage pool, because no boron is used in these storage pools. For PWR spent fuel dry storage, the concept of moderator removal is used. That is, it is authorized that, after a spent fuel is loaded in boron-containing pool water into a storage vessel (at this stage the approval of burn-up credit is obtained), the water is removed and the vessel is transferred to a place with no danger of flooding and stored. With respect to this, in 1998, the NRC examined a burn-up credit status report with only the effect of absorption of actinides taken into consideration, presented by the DOE, and approved the DOE report in May of 1999. Usually, once a dry transportation vessel for a PWR spent fuel is approved, it is applied the same way to dry storage as well.<sup>2</sup>

In France, wet storage (La Hague), transportation, and reprocessing are authorized separately at present for PWR spent fuel assemblies of low enriched uranium oxides, and in any stage the ascertaining of burn-up by the facility operator is required for burn-up credit to be approved. In this case, two requirements are imposed based on the results of criticality safety analysis. One requirement is well satisfied by presenting qualitative measurement results which show that the fuel assembly has been actually irradiated in a reactor, when the required burn-up is lower than the minimum burn-up based on one cycle irradiation as ensured by the reactor operator. The other requirement is to make sure the burn-up is subjected to quantitative measurement. This quantitative measurement is performed on the least irradiated lower 50 cm of the effective fuel length. In the evaluation of criticality safety, only principal actinoids ( $^{235}\text{U}$ ,  $^{238}\text{U}$ ,  $^{238}\text{Pu}$ ,  $^{239}\text{Pu}$ ,  $^{240}\text{Pu}$ ,  $^{241}\text{Pu}$ , and  $^{242}\text{Pu}$ ) are considered, and the presence of FP is disregarded. In storage, a similar viewpoint is approved for BWR spent fuels as well.<sup>3</sup>

In the UK, the majority of the reactors being operated at present for power generation are improved gas-cooled reactors (AGRs), and some PWRs are used in Sizewell. BNFL is carrying out the production of fuels for AGRs and PWRs, the transportation, storage, and reprocessing of spent fuels, and moreover the reprocessing of PWR and BWR spent fuels contracted from abroad. Burn-up credit is currently considered for LWR (PWR, BWR) spent fuels in the criticality safety management of the following facilities:

1. Wet storage of spent fuels in Sizewell.
2. Wet transportation of spent fuels mainly from abroad to the Sellafield reprocessing plant.

3. Wet storage of spent fuels in Sellafield.
4. Reprocessing of spent fuels at the Sellafield reprocessing plant.

Furthermore, research and evaluation to incorporate the burn-up credit of MOX spent fuels in particular is underway in the UK (Ref. 4).

Light-water-reactor (PWR and BWR) spent fuels in Germany are stored in the wet mode, and burn-up credit where the presence of combustible neutron poison dispersed in the fuel matrix is taken into consideration is approved for the evaluation of criticality safety, but it is required that the presence of soluble boron in a PWR spent fuel storage pool be disregarded in the evaluation of safety in normal operations. The use of burn-up credit is allowed, but in such a case it is required that the reason for abandoning the assumption of a new fuel be stated. PWR spent fuel wet storage racks manufactured by the Siemens KWU Co. have been exported so far to various countries such as Spain, Korea, South Africa, and Brazil, and in the evaluation of the criticality safety of the design of these, the net reduction in fissionable nuclides and the neutron absorption effect of actinide (U, Np, Pu, Am) isotopes and moreover fissionable material (FP) isotopes are taken into consideration. On the other hand, PWR and BWR spent fuels are transported with the use of dry-mode CASTOR casks, and their criticality safety is evaluated with the assumption of a new fuel for initial enrichments of up to 4.2 wt %. Above this level, burn-up credit that only takes the absorptive effect of actinides into consideration is employed. The use of burn-up credit is not considered at present in the final disposal of spent fuels.<sup>5</sup>

In our country, there are no examples except the use of burn-up credit considering only the absorptive effect of actinides, in the criticality safety design of spent fuel storage pools to be attached to 6 reprocessing plants currently under construction. More and more spent fuels are being accumulated with longer power generation by PWRs and BWRs, and at present most of these spent fuels are stored in storage pools at the power station sites. Some are stored in dry storehouses with the use of metal castors on the premises of the Fukushima No. 1 Nuclear Power Station. In addition, criticality safety design is provided based on the assumption of a new fuel, including the transportation vessels to be used in transportation to reprocessing facilities. International transportation, as specified in IAEA transportation regulation ST-1, is carried out in accordance with the international agreement that transportation can be accepted automatically in a receiving country if the approval of the design of a B(U)F-type transportation vessel is given by the regulatory authorities of the shipping country. Therefore, it follows that the method of adopting burn-up credit in PWR spent fuel transportation with a B(U)F transportation vessel approved by French regulatory authorities is also acceptable to Swiss regulatory authorities for receipt of the transported material.<sup>6</sup>

## A.2. CHARACTERISTICS OF IRRADIATED FUELS

First, the destructive analysis used in the code accuracy evaluation will be summarized. Table A.2.1 shows the major data for the Takahama No. 3 reactor, where the NT3G23 fuel assembly from which SF95 and SF96 destructive analysis data were obtained, and the NT3G24 fuel assembly from which SF97 destructive analysis data were obtained and which was also used in exponential experiments, were irradiated.

Table A.2.2 shows data for the No. 2 reactor of the Fukushima No. 2 Power Station where the 2F2DN23 fuel assembly from which SF98 and SG99 destructive analysis data were obtained, was irradiated.

Tables A.2.3 and A.2.4 show data for the Genkai No. 1 reactor and the Ohi No. 2 reactor from which the commonly called P14 fuel assembly (proper name C11) and P17 fuel assembly (proper name JR2) used in exponential experiments were obtained.

The design parameters for the NT3G23 and NT3G24 fuel assemblies are listed in Table A.2.5, the design parameters for the 2F2DN23 fuel assembly are listed in Table A.2.6, the design parameters for the C33 fuel assembly are listed in Table A.2.7, and the design parameters for the J2R fuel assembly are listed in Table A.2.8.

The positions of the fuel rods in the NT3G23 assembly for SF95 destructive analysis are shown in Fig. A.2.1. The positions of the fuel rods in the NT3G23 assembly for SF96 destructive analysis are shown in Fig. A.2.2. The positions of the fuel rods in the NT3G24 assembly for SF97 destructive analysis are shown in Fig. A.2.3. The positions of the fuel rods in the 2F2DN23 assembly for SF98 destructive analysis are shown in Fig. A.2.4. And the positions of the fuel rods in the 2F2DN23 assembly for SF99 destructive analysis are shown in Fig. A.2.5.

Averaged enrichments of the individual fuel rods that form the 2FDN23 fuel assembly are shown in Fig. A.2.6, axial averaged enrichments are shown in Fig. A.2.7, and the distribution of void ratios are shown in Fig. A.2.8.

The positions of the fuel rods used for  $\gamma$  scanning of the NT3G23 fuel assembly are shown in Fig. A.2.9, the positions of the fuel rods used for  $\gamma$  scanning of the NT3G24 fuel assembly are shown in Fig. A.2.10, and the positions of the fuel rods used for  $\gamma$  scanning of the 2F2DN23 fuel assembly are shown in Fig. A.2.11.

The initial isotopic compositions of various fuels are listed in Tables A.2.9–A.2.12.

The burning histories of various reactor cores are listed in Tables A.2.13–A.2.15.

The sampling positions of SF95 to SF-98 are listed in Tables A.2.16–A.2.20.

Irradiation histories are listed in Tables A.2.21–A.2.26. These data were evaluated so as to give the burn-up degrees of the destructive analysis samples measured by the Nd-148 method, based on the power history data for the fuel assemblies and fuel rods disclosed to JAERI.

Table A.2.1. Data of Takahama 3

Core	
Number of loops	3
MWe	870
MWt	2652
Core diameter (m)	3.04
Uranium weight (ton U)	72
Active height of core (m)	3.66
Input temp. (°C)	284
Output temp. (°C)	321
Fuel assembly	
Type	17 × 17
Number of assembly	157
Total length (m)	4.06
Assembly pitch (mm)	214
Number of fuel rods	264
Uranium weight (kg)	~ 460

Table A.2.2. Data of Fukushima Daini-2

MWt	3293
Number of loop	2
Total flow rate of coolant	$48.3 \times 10^3$ t/h
Sub-cooling at inlet of core	11.4 kcal/kg
Average steam weight ratio at outlet of core	13.2 wt %
Dome pressure in reactor pressure vessel	70.0 kg/cm <sup>2</sup> g
Core	
Active height	3.71 m
Core diameter	4.75 m
Uranium weight	~ 131 t (New 8 × 8)
Flow rate of steam	$6.41 \times 10^3$ t/h
Steam pressure	70.7 kg/cm <sup>2</sup> g
Steam temp.	286°C

Table A.2.3. Data of Genkai 1

Core	
Number of loops	3
MWe	559
MWt	1650
Core diameter (m)	2.46
Uranium weight (ton U)	48
Active height (m)	3.66
Inlet temp. (°C)	288
Outlet temp. (°C)	323
Fuel assembly	
Type	14 × 14
Number of assembly	121
Total length (m)	4.17
Assembly pitch (mm)	197
Number of fuel rods	179
Uranium weight (kg)	~ 400

Table A.2.4. Data of Ohi 2

Core	
Number of loops	4
MWe	1175
MWt	3411
Core diameter (m)	3.37
Uranium weight (ton U)	87
Active height (m)	3.66
Inlet temp. (°C)	289
Outlet temp. (°C)	325
Fuel assembly	
Type	17 × 17
Number of fuel assembly	193
Total length (m)	4.06
Assembly pitch (mm)	214
Number of fuel rods	264
Uranium weight (kg)	~ 460

Table A.2.5. Data of fuel assembly : NT3G23 and NT3G24 from Takahama 3

Item	Assemblies	
	NT3G23(SF95 and SF96)	NT3G24 (SF96)
Pellet	Enrichment	~ 4.1 wt % • $^{235}\text{U}$
	Diam.	~ 8.05 mm
	Height	~ 9.0 mm
	Density	~95% T.D.
	Gd Enrichment	— ~ 6 wt %
Clad	Material	Zr-4
	Outer diam.	~ 9.5 mm
	Inner diam.	~ 8.22 mm
	Thickness	more than 0.59 mm
	Sn Contents	1.4 ~ 1.7 wt %
Fuel rod	Gas press.	~ 33 kg/cm <sup>2</sup> a
	Plenum (Upper)	~ 139 mm
	Plenum (Lower)	~ 36 mm
	Stack length	~ 3648 mm
	Total length	~ 4035.5 mm

Table A.2.6. Data of fuel assembly : 2F2DN23 from Fukushima Daini-2

Item		Assembly
		2F2DN23 (SF98 and SF99)
Pellet	Enrichment	~ 3.0 wt % • $^{235}\text{U}$ *
	Diam.	~ 10.3 mm
	Height	~ 10 mm
	Density	~ 95 % T.D.
	Gd enrichment	Less than 6 wt %
Clad	Material	Zry-2 (Zr lining)
	Outer diam.	~ 12.3 mm
	Thickness	0.86 mm (Zr-lining ~ 0.1 mm)
	Pellet-clad clearance	0.24 mm
Plenum	Plenum volume ratio	0.1
Fuel rod	He pressure	~ 3 a
	Stack length	~ 3710 mm
	Outer diam. of water rod	15.0 mm
Fuel assembly	Total length (including handing mech.)	~ 4470 mm

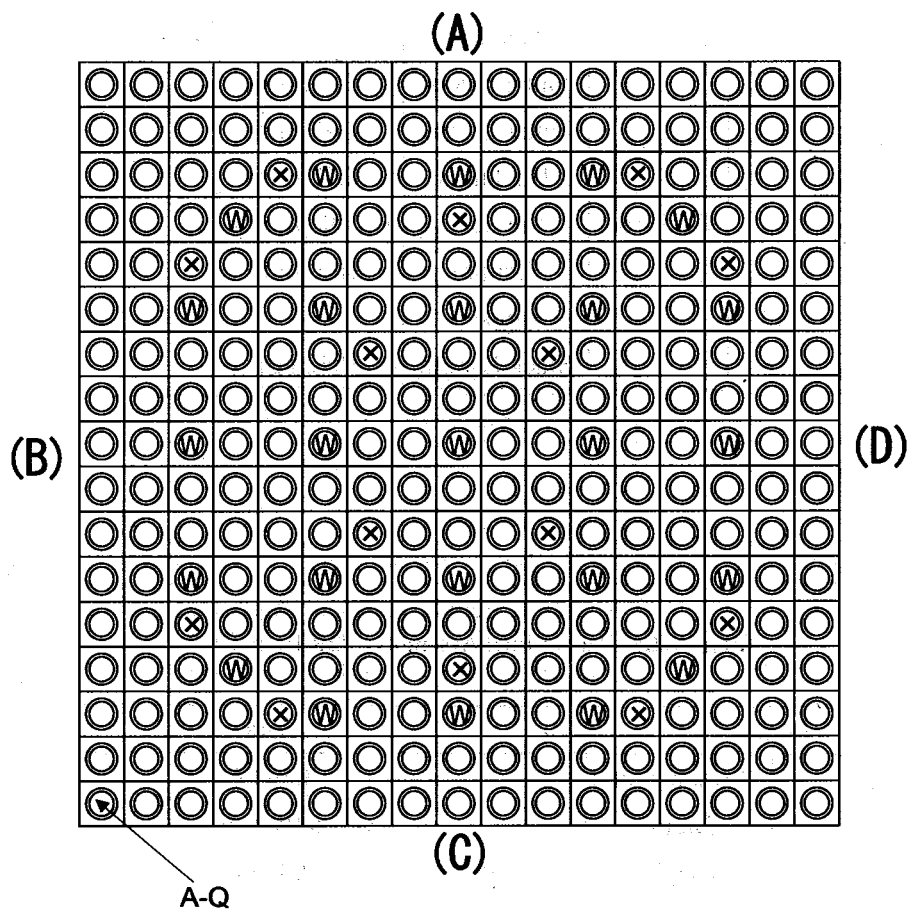
\*  $^{235}\text{U}$  enrichment distribution is shown in Fig. A.2.7.

Table A.2.7. Data of fuel assembly : C33 from Genkai 1

Item		Data
Pellet	Enrichment	3.40 wt %
	Diam.	9.294 mm
	Height	15.2 mm
	Density	95% T.D.
Clad	Material	Zr-4
	Outer diam.	10.72 mm
	Inner diam.	9.48 mm
	Thickness	0.62 mm
Fuel rod	Pressure	$\sim 33 \text{ kg/cm}^2$ a
	Plenum	179 mm
	(upper)	
	Stack length	3642 mm

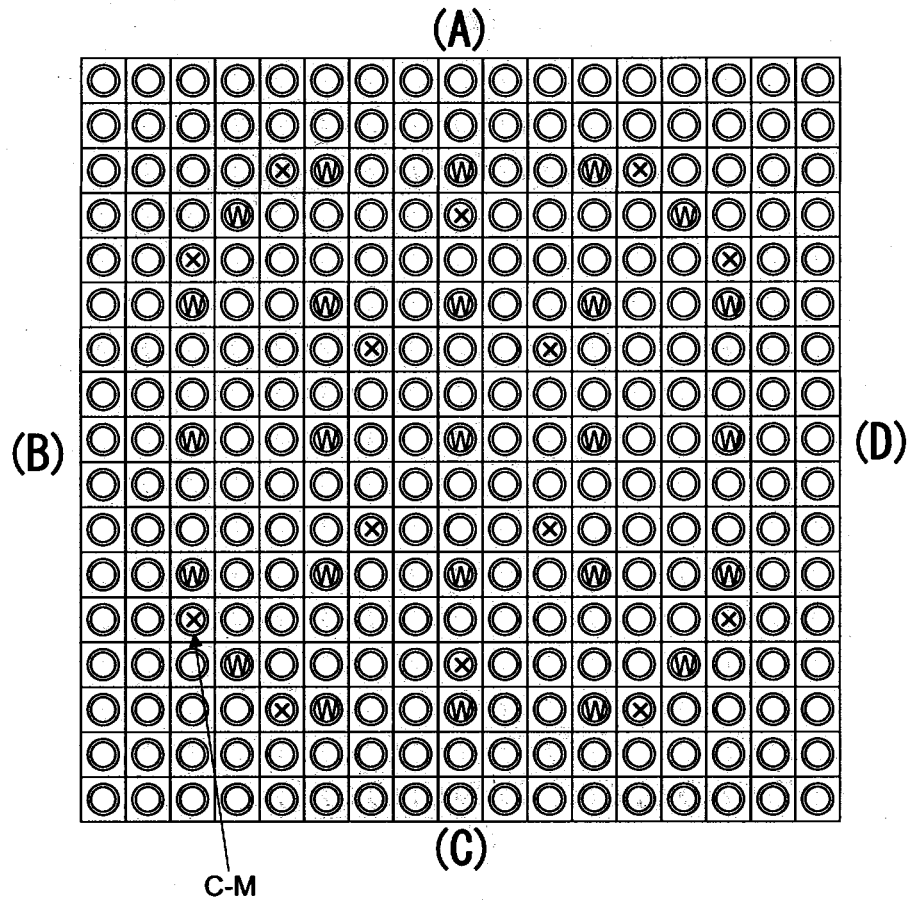
Table A.2.8. Data of fuel assembly : J2R from Ohi 2

Item		Data
Pellet	Enrichment	3.4 wt %
	Diam.	8.05 mm
	Height	9.0 mm
	Density	$\sim 95\%$ T.D.
Clad	Material	Zr-4
	Outer diam.	9.50 mm
	Thickness	0.64 mm
Fuel rod	Stack length	$\sim 3648$ mm
Fuel assembly	Total length	$\sim 4035.5$ mm
Position of Grid		11/482/937/1391/1846/2300/2755/3265/37775 mm



W: Position of Control Rod ( fill with coolant)  
 X : Gd Fuel Rod

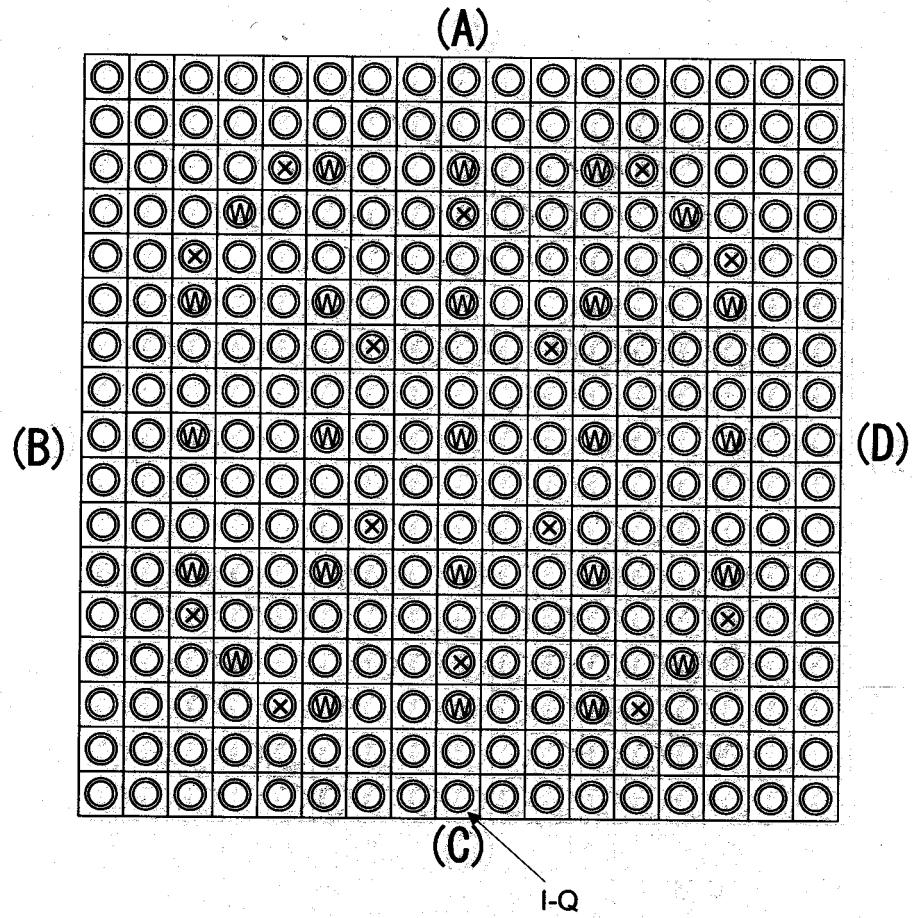
**Fig. A.2.1** Position of Fuel Rod in NT3G23 assembly for SF95 Destructive Analysis



W: Position of Control Rod ( fill with coolant)

X : Gd Fuel Rod

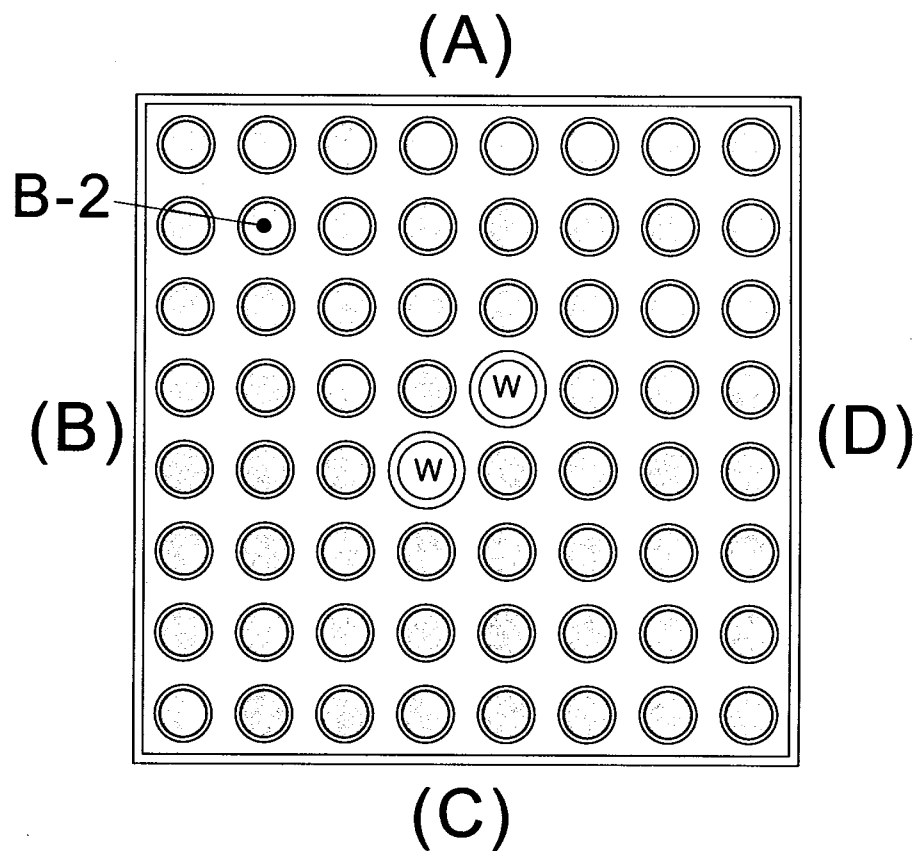
**Fig. A.2.2 Position of Fuel Rod in NT3G23 assembly for SF96 Destructive Analysis**



W: Position of Control Rod ( fill with coolant)

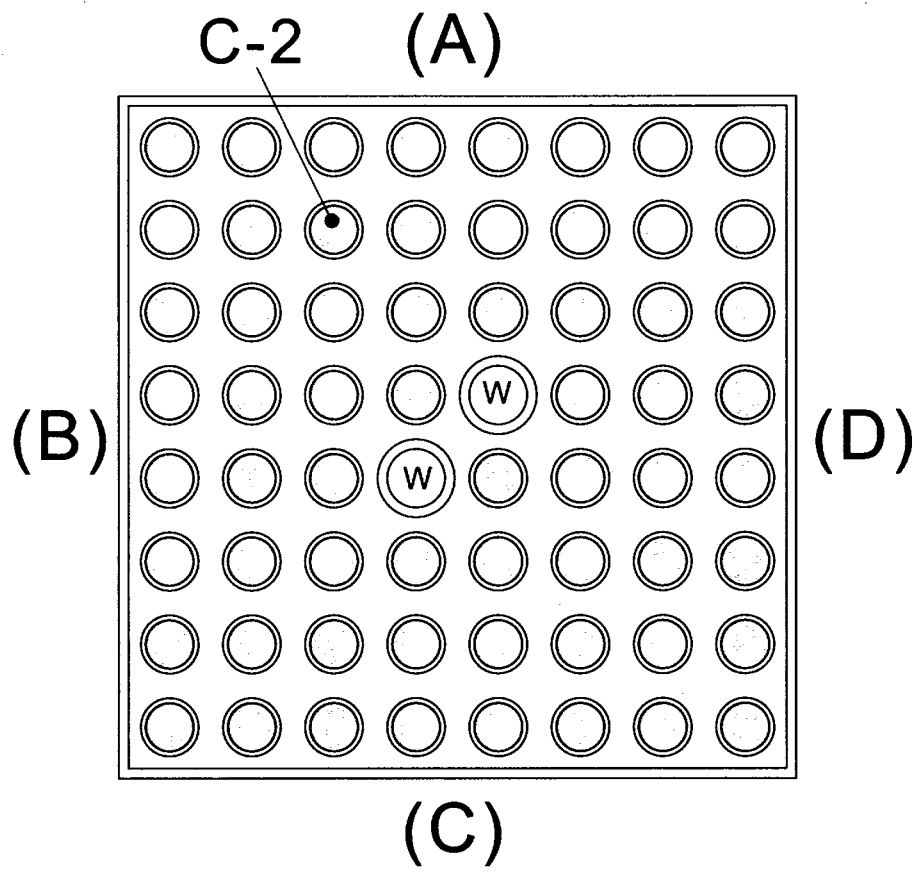
X : Gd Fuel Rod

**Fig. A.2.3 Position of Fuel Rod in NT3G24 assembly for SF97 Destructive Analysis**



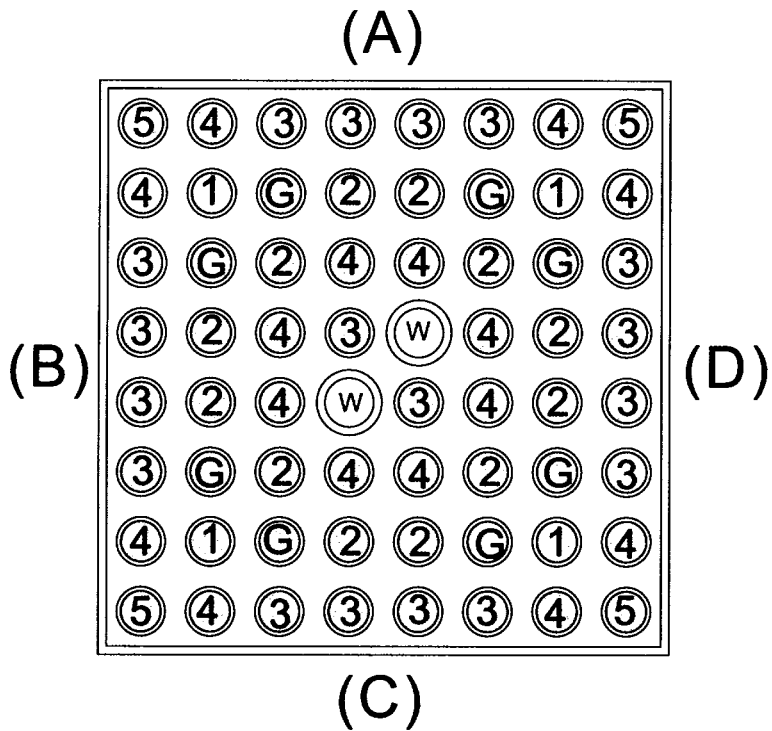
**W: Water Rod**

**Fig. A.2.4** Position of Fuel Rod in 2F2DN23 assembly for SF98 Destructive Analysis



**W: Water Rod**

**Fig. A.2.5 Position of Fuel Rod in 2F2DN23 assembly for SF99 Destructive Analysis**



W: Water Rod G: Gadolinium fuel

Numbers present types of fuel. Averaged enrichments (weight %) of uranium-235 are following,

1: 3.63, 2: 3.22, 3: 3.18, 4: 2.72, 5: 1.89

Averaged uranium-235 enrichment value of this assembly is 3.01 weight %.

**Fig. A.2.6** Radial Distribution of  $^{235}\text{U}$  Enrichment in 2F2DN23 assembly

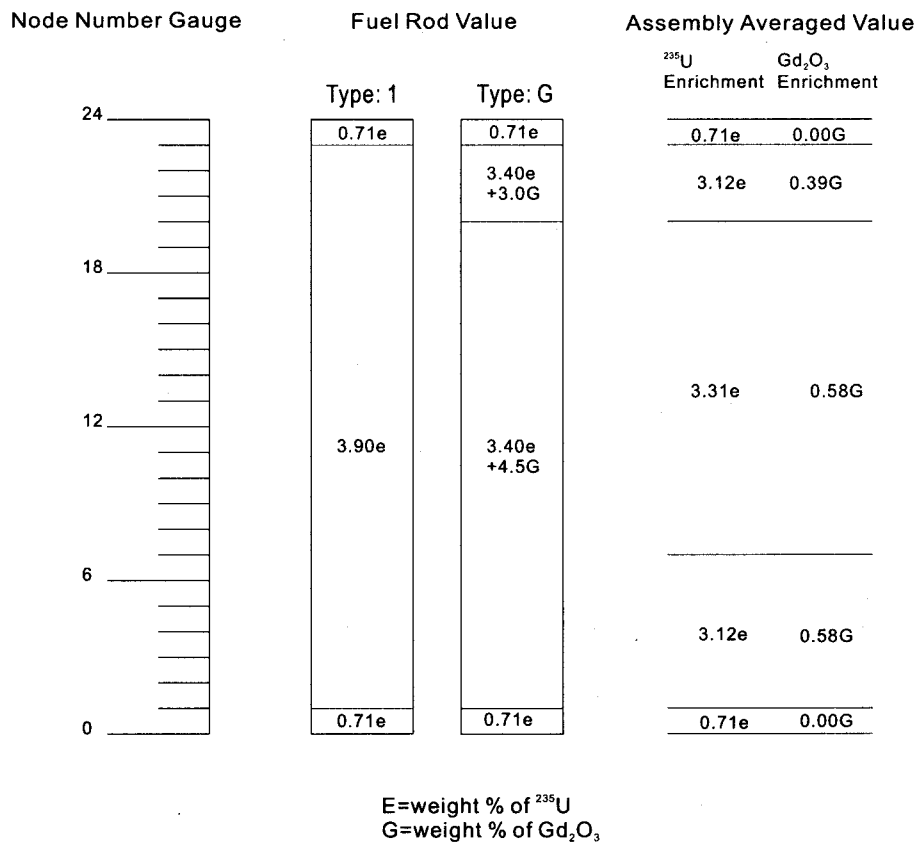


**Fig. A.2.7** Axial Distribution of  $^{235}\text{U}$  Enrichment in 2F2DN23 assembly

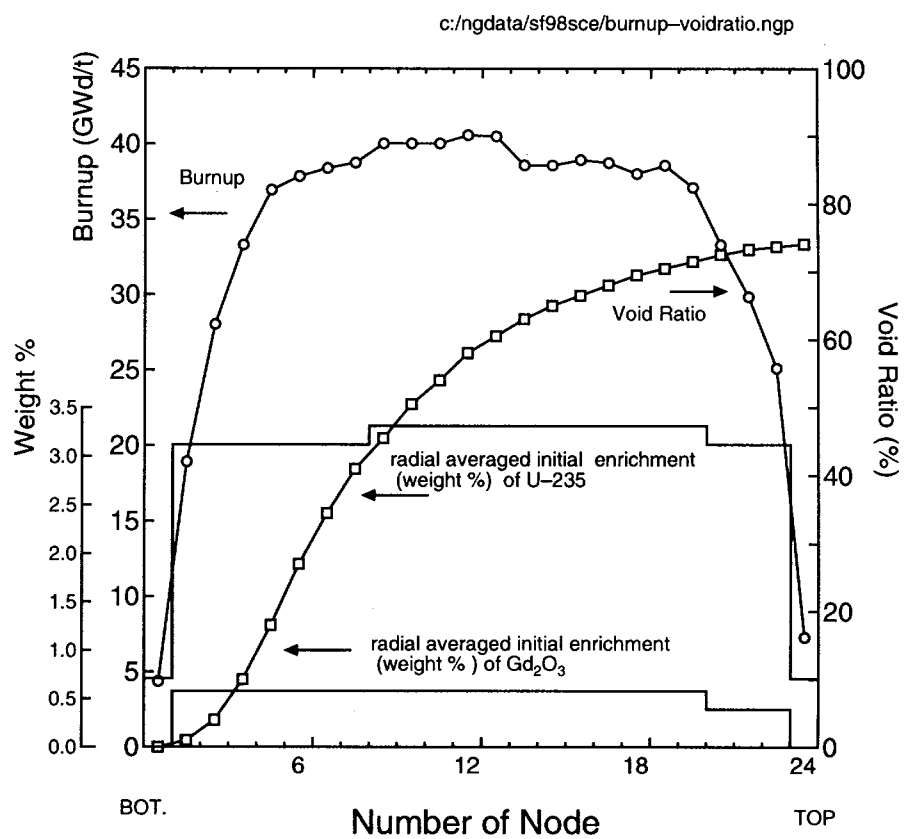
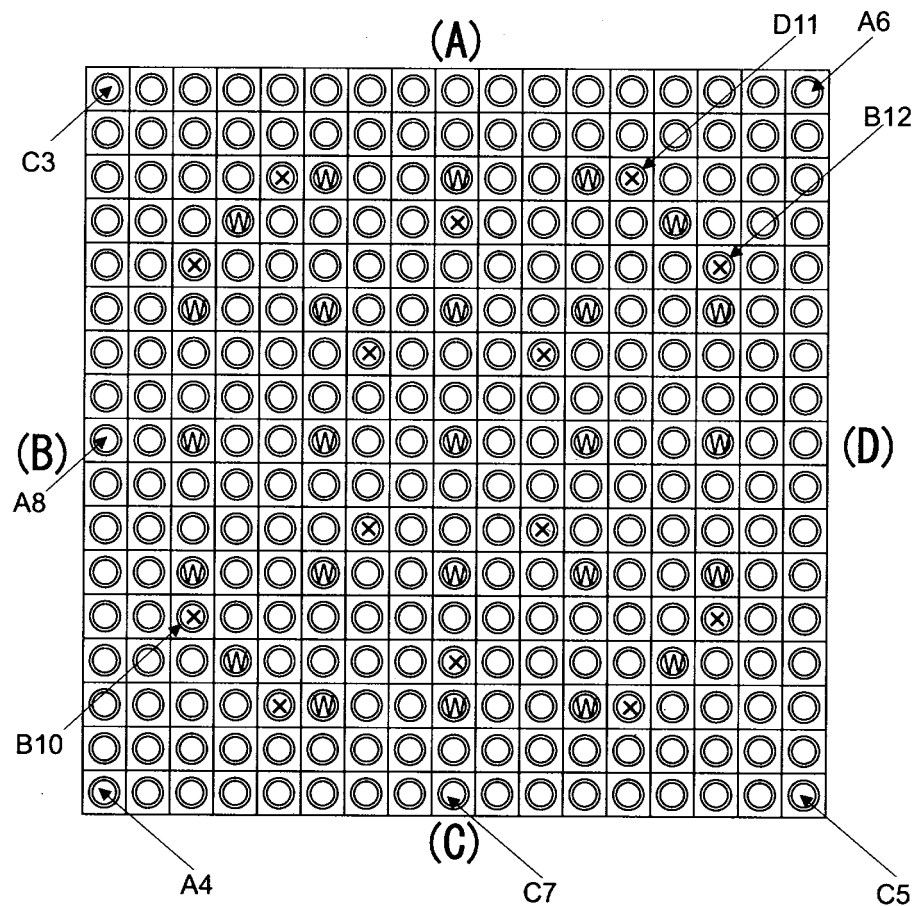
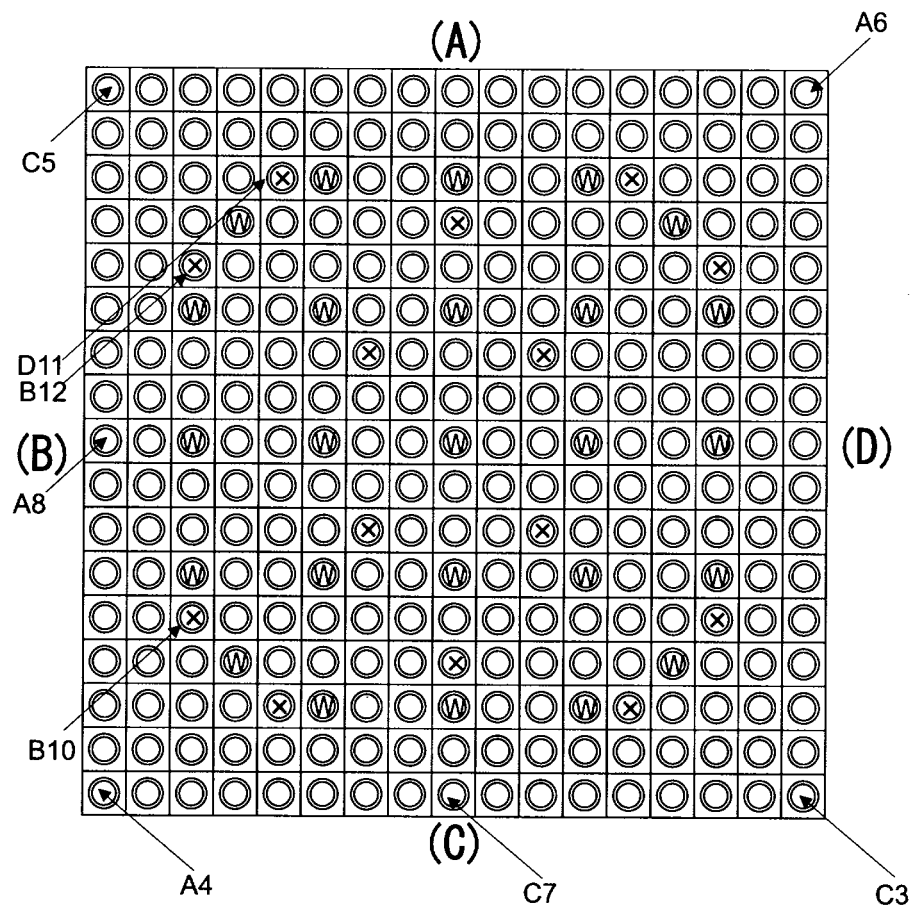


**Fig. A.2.8** Axial Distribution of Burnup, Void Ratio (%),  $^{235}\text{U}$  Enrichment of 2F2DN23 assembly



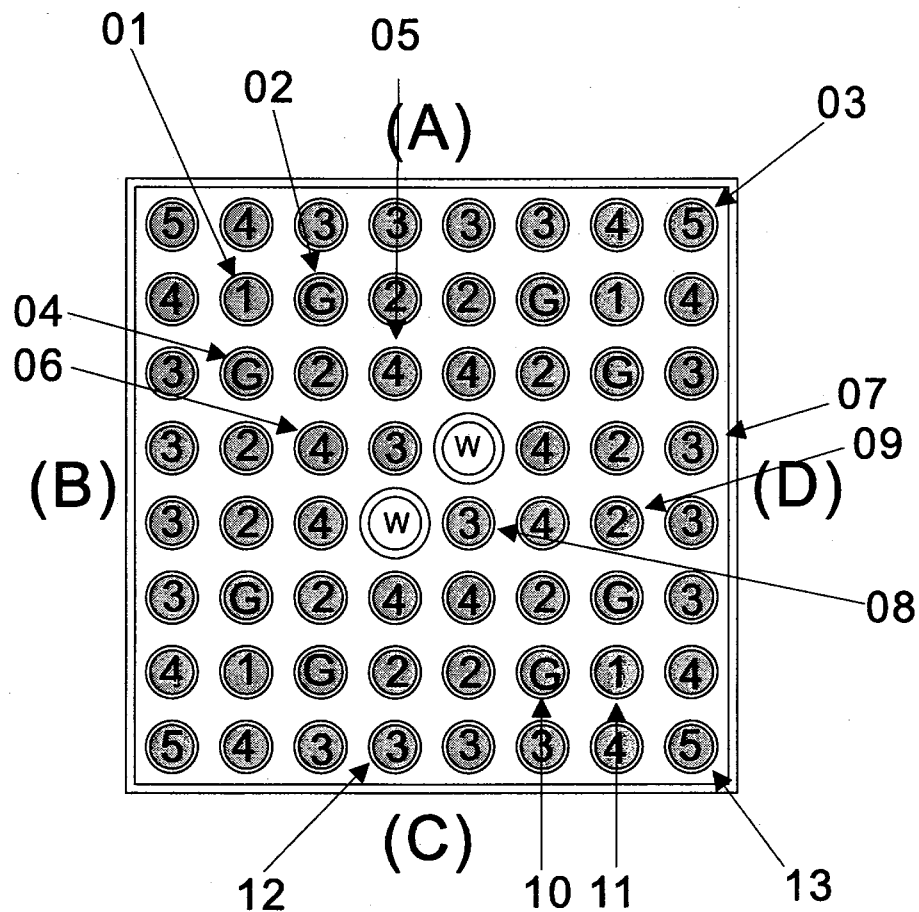
W: Position of Control Rod ( fill with coolant)  
 X : Gd Fuel Rod

**Fig. A.2.9** NT3G23  $\gamma$  Scan Position



W: Position of Control Rod ( fill with coolant)  
 X : Gd Fuel Rod

**Fig. A.2.10** NT3G24  $\gamma$  Scan Position



W: Water Rod G: Gadolinium fuel

Numbers in circle present types of fuel. Averaged enrichments (weight %) of uranium-235 are following,

1: 3.63, 2: 3.22, 3: 3.18, 4: 2.72, 5: 1.89

**Fig. A.2.11 2F2DN23  $\gamma$  Scan Position**

Table A.2.9. SF95 and SF97 : Initial isotopic composition ( Weight (%) )

Isotope	Weight %
U-234	0.04
U-235	4.11
U-238	95.85

Table A.2.10. SF96 : Initial isotopic composition ( Weight (%) )

Isotope	Weight %
U-234	0.02
U-235	2.63
U-238	97.25

Table A.2.11. SF98 : Initial Isotopic Composition ( Weight (%) )

Isotope	Weight %
U-234	0.04
U-235	3.91
U-238	96.05

Table A.2.12. SF99 : Initial isotopic composition ( Weight (%) )

Isotope	Weight %
U-234	0.03
U-235	3.41
U-238	96.56

Table A.2.13. Operation history of Takahama 3 (SF95 and SF96)

Start	Stop	Days	Status
1990/ 1/26	1991/ 2/15	385	Burnup
1991/ 2/15	1991/ 5/14	88	Cool
1991/ 5/14	1992/ 6/19	402	Burnup

Table A.2.14. Operation history of Takahama 3 (SF97)

Start	Stop	Days	Status
1990/ 1/26	1991/ 2/15	385	Burnup
1991/ 2/15	1991/ 5/14	88	Cool
1991/ 5/14	1992/ 6/19	402	Burnup
1992/ 6/19	1992/ 8/20	62	Cool
1992/ 8/20	1993/ 9/30	406	Burnup

Table A.2.15. Operation history of Fukushima Daini-2 (SF98 and SF99 and Sub-critical experiment)

Start	Stop	Days	Status
1989/ 1/14	1989/ 6/ 4	141	Burnup
1989/ 6/ 4	1989/ 6/25	21	Cool
1989/ 6/25	1990/ 3/ 9	257	Burnup
1990/ 3/ 9	1990/ 7/ 4	117	Cool
1990/ 7/ 4	1991/ 5/22	322	Burnup
1991/ 5/22	1991/ 5/31	9	Cool
1991/ 5/31	1991/ 8/25	86	Burnup
1991/ 8/25	1991/11/14	81	Cool
1991/11/14	1992/11/16	368	Burnup

Table A.2.16. SF95 : Sampling position

No.	From bottom of active length (mm)	From top (mm)
SF95-1	3606	201
SF95-2	3446	361
SF95-3	2926	881
SF95-4	1646	2161
SF95-5	246	3561

Table A.2.17. SF96 : Sampling position

No.	From bottom of active length (mm)	From top (mm)
SF96-1	3631	176
SF96-2	3471	336
SF96-3	2951	856
SF96-4	1671	2136
SF96-5	271	3536

Table A.2.18. SF97 : Sampling position

No.	From bottom of active length (mm)	From top (mm)
SF97-1	3644	163
SF97-2	3457	350
SF97-3	3180	627
SF97-4	1968	1839
SF97-5	881	2926
SF97-6	251	3556

Table A.2.19. SF98 : Sampling position

No.	From bottom of active length (mm)	From top (mm)
SF98-1	39	4030
SF98-2	167	3902
SF98-3	423	3646
SF98-4	692	3377
SF98-5	1214	2855
SF98-6	2050	2019
SF98-7	2757	1312
SF98-8	3397	672

Table A.2.20. SF99 : Sampling position

No.	From bottom of active length (mm)	From top (mm)
SF99-1	134	3935
SF99-2	286	3783
SF99-3	502	3567
SF99-4	686	3383
SF99-5	1189	2880
SF99-6	2061	2008
SF99-7	2744	1325
SF99-8	3388	681
SF99-9	3540	529
SF99-10	3676	393

Table A.2.21. Irradiation history SF95 samples

Days	Power (MW/t)				
	SF95-1	SF95-2	SF95-3	SF95-4	SF95-5
0	0.00	0.00	0.00	0.00	0.00
12	5.08	8.65	12.59	13.04	10.80
8	20.32	34.61	50.34	52.15	43.20
27	20.33	34.62	50.36	52.17	43.22
35	20.42	34.78	50.59	52.40	43.42
28	20.22	34.44	50.09	51.89	42.99
21	20.09	34.23	49.78	51.57	42.73
35	20.02	34.10	49.60	51.37	42.56
35	19.71	33.57	48.83	50.58	41.90
28	19.72	33.59	48.85	50.61	41.93
27	19.60	33.39	48.57	50.31	41.68
49	19.33	32.92	47.89	49.60	41.10
15	19.07	32.47	47.23	48.93	40.54
37	18.80	32.03	46.59	48.26	39.98
19	18.61	31.71	46.12	47.77	39.58
9	18.50	31.51	45.84	47.48	39.34
88	0.00	0.00	0.00	0.00	0.00
10	4.36	7.43	10.80	11.19	9.27
11	17.52	29.85	43.42	44.97	37.26
20	17.69	30.14	43.84	45.41	37.62
23	17.78	30.28	44.04	45.62	37.79
28	17.75	30.23	43.97	45.55	37.74
28	17.72	30.17	43.89	45.46	37.67
28	17.68	30.12	43.80	45.37	37.59
35	17.65	30.06	43.72	45.29	37.52
28	17.61	30.00	43.63	45.20	37.45
34	17.57	29.93	43.53	45.09	37.35
43	17.50	29.81	43.36	44.91	37.21
28	17.34	29.53	42.95	44.49	36.86
28	17.17	29.25	42.54	44.06	36.51
35	17.08	29.09	42.31	43.82	36.31
15	17.00	28.96	42.12	43.63	36.15
8	16.97	28.91	42.05	43.56	36.09

Table A.2.22. Irradiation history SF96 samples

Days	Power (MW/t)				
	SF96-1	SF96-2	SF96-3	SF96-4	SF96-5
0	0.00	0.00	0.00	0.00	0.00
12	0.99	2.09	3.59	3.68	3.08
8	3.97	8.37	14.37	14.73	12.32
27	4.21	8.88	15.24	15.62	13.07
35	4.47	9.44	16.19	16.60	13.89
28	5.04	10.64	18.25	18.70	15.65
21	5.64	11.90	20.42	20.93	17.52
35	6.39	13.48	23.13	23.71	19.84
35	7.97	16.82	28.85	29.57	24.75
28	8.90	18.78	32.21	33.02	27.63
27	9.84	20.76	35.61	36.50	30.55
49	10.71	22.59	38.75	39.72	33.24
15	11.42	24.10	41.34	42.37	35.46
37	12.13	25.59	43.90	44.99	37.66
19	12.34	26.04	44.68	45.79	38.32
9	12.61	26.59	45.62	46.76	39.14
88	0.00	0.00	0.00	0.00	0.00
10	5.61	11.84	20.32	20.83	17.43
11	11.30	23.84	40.90	41.92	35.08
20	11.45	24.16	41.45	42.48	35.55
23	11.57	24.41	41.88	42.93	35.93
28	11.64	24.56	42.13	43.18	36.14
28	11.71	24.70	42.37	43.43	36.35
28	11.78	24.86	42.64	43.71	36.58
35	11.86	25.01	42.91	43.99	36.81
28	11.93	25.16	43.16	44.24	37.02
34	11.99	25.29	43.38	44.46	37.21
43	12.06	25.44	43.65	44.74	37.44
28	12.06	25.44	43.65	44.74	37.44
28	12.04	25.40	43.57	44.66	37.38
35	12.07	25.45	43.67	44.76	37.46
15	12.08	25.48	43.72	44.81	37.50
8	12.09	25.50	43.74	44.83	37.52

Table A.2.23. Irradiation history SF97 samples (1/2)

Days	Power (MW/t)					
	SF97-1	SF97-2	SF97-3	SF97-4	SF97-5	SF97-6
0	0.00	0.00	0.00	0.00	0.00	0.00
12	3.54	6.15	8.44	9.42	9.46	8.17
8	14.24	24.74	33.94	37.86	38.04	32.84
27	14.37	24.96	34.24	38.20	38.38	33.13
35	14.57	25.31	34.72	38.73	38.91	33.59
28	14.73	25.59	35.10	39.16	39.34	33.96
21	14.81	25.74	35.31	39.39	39.58	34.17
35	14.93	25.95	35.60	39.71	39.90	34.44
35	15.02	26.09	35.80	39.93	40.12	34.63
28	15.12	26.27	36.04	40.21	40.40	34.87
27	15.43	26.81	36.78	41.03	41.22	35.58
49	15.66	27.21	37.33	41.64	41.84	36.12
15	15.65	27.20	37.31	41.62	41.82	36.10
37	15.64	27.18	37.29	41.60	41.79	36.08
19	15.62	27.14	37.23	41.53	41.72	36.02
9	15.59	27.09	37.17	41.46	41.66	35.96
88	0.00	0.00	0.00	0.00	0.00	0.00
10	8.39	14.58	20.00	22.31	22.42	19.35
11	16.72	29.06	39.87	44.47	44.68	38.57
20	16.61	28.85	39.58	44.16	44.37	38.30
23	16.49	28.65	39.30	43.84	44.05	38.02
28	16.29	28.31	38.84	43.32	43.53	37.57
28	16.12	28.00	38.42	42.86	43.06	37.17
28	16.03	27.85	38.21	42.62	42.82	36.97
35	15.94	27.70	38.00	42.39	42.59	36.76
28	15.93	27.69	37.98	42.37	42.57	36.75
34	15.91	27.64	37.91	42.30	42.49	36.68
43	15.76	27.39	37.58	41.92	42.12	36.36
28	15.58	27.08	37.14	41.44	41.63	35.94
28	15.53	26.99	37.03	41.31	41.50	35.83
35	15.54	27.01	37.05	41.33	41.53	35.85
15	15.47	26.88	36.87	41.13	41.33	35.67
8	15.44	26.83	36.81	41.06	41.25	35.61

Table A.2.24. Irradiation history SF97 samples (2/2)

Days	Power (MW/t)					
	SF97-1	SF97-2	SF97-3	SF97-4	SF97-5	SF97-6
62	0.00	0.00	0.00	0.00	0.00	0.00
12	6.97	12.11	16.62	18.54	18.63	16.08
8	13.96	24.25	33.27	37.11	37.29	32.19
49	14.03	24.39	33.45	37.32	37.49	32.37
28	14.14	24.57	33.70	37.60	37.77	32.61
29	14.22	24.70	33.89	37.80	37.98	32.79
34	14.21	24.69	33.87	37.79	37.96	32.77
28	14.20	24.68	33.86	37.77	37.95	32.76
28	14.27	24.79	34.01	37.94	38.11	32.90
35	14.25	24.75	33.96	37.88	38.06	32.85
27	14.21	24.69	33.87	37.79	37.96	32.77
29	14.22	24.72	33.91	37.82	38.00	32.80
35	14.19	24.66	33.82	37.73	37.91	32.73
28	14.21	24.69	33.88	37.79	37.97	32.77
19	14.25	24.75	33.96	37.88	38.06	32.85
17	14.22	24.72	33.91	37.83	38.00	32.81

REM: Data of Sm Isotopes is as for 3.96 years cooling time.

Table A.2.25. Irradiation history SF98 samples

Days	Power (MW/t)							
	SF98-1	SF98-2	SF98-3	SF98-4	SF98-5	SF98-6	SF98-7	SF98-8
0	0.00	0.00	0.00	0.00	0.00	0.00	0.00	0.00
6	1.27	8.10	11.29	12.95	13.45	12.21	12.05	8.31
3	3.20	20.46	28.50	32.68	33.95	30.81	30.41	20.98
132	3.95	25.22	35.14	40.29	41.84	37.98	37.49	25.86
21	0.00	0.00	0.00	0.00	0.00	0.00	0.00	0.00
5	1.43	9.13	12.73	14.59	15.16	13.76	13.58	9.37
244	3.44	22.00	30.65	35.15	36.51	33.13	32.70	22.56
8	3.99	25.47	35.49	40.70	42.27	38.36	37.87	26.12
117	0.00	0.00	0.00	0.00	0.00	0.00	0.00	0.00
5	1.43	9.13	12.73	14.59	15.16	13.76	13.58	9.37
317	3.44	22.00	30.65	35.15	36.51	33.13	32.70	22.56
9	0.00	0.00	0.00	0.00	0.00	0.00	0.00	0.00
4	1.49	9.52	13.27	15.21	15.80	14.34	14.15	9.76
72	3.50	22.38	31.19	35.76	37.15	33.71	33.28	22.95
10	3.95	25.22	35.14	40.29	41.84	37.98	37.49	25.86
81	0.00	0.00	0.00	0.00	0.00	0.00	0.00	0.00
3	1.63	10.42	14.52	16.65	17.29	15.69	15.49	10.69
365	3.65	23.29	32.45	37.20	38.64	35.07	34.62	23.88

REM: Data of Sm isotopes : SF98-1,2,3 and 4 are as for 5.5 years cooling.

REM: Data of Sm isotopes : SF98-6 is as for 6.2 years cooling.

REM: Data of Sm isotopes : SF98-5,7 and 8 are as for 5.9 years cooling.

Table A.2.26. Irradiation history SF99 samples

Days	Power (MW/t)									
	SF99-1	SF99-2	SF99-3	SF99-4	SF99-5	SF99-6	SF99-7	SF99-8	SF99-9	SF99-10
0	0.00	0.00	0.00	0.00	0.00	0.00	0.00	0.00	0.00	0.00
6	2.30	6.92	9.92	10.83	11.44	9.89	9.82	6.67	5.09	2.20
3	5.81	17.46	25.03	27.33	28.87	24.97	24.79	16.84	12.85	5.55
132	7.16	21.53	30.86	33.69	35.58	30.78	30.56	20.76	15.84	6.84
21	0.00	0.00	0.00	0.00	0.00	0.00	0.00	0.00	0.00	0.00
5	2.59	7.80	11.18	12.21	12.89	11.15	11.07	7.52	5.74	2.48
244	6.25	18.78	26.92	29.40	31.05	26.85	26.66	18.12	13.82	5.97
8	7.23	21.75	31.17	34.04	35.95	31.09	30.87	20.98	16.00	6.91
117	0.00	0.00	0.00	0.00	0.00	0.00	0.00	0.00	0.00	0.00
5	2.59	7.80	11.18	12.21	12.89	11.15	11.07	7.52	5.74	2.48
317	6.25	18.78	26.92	29.40	31.05	26.85	26.66	18.12	13.82	5.97
9	0.00	0.00	0.00	0.00	0.00	0.00	0.00	0.00	0.00	0.00
4	2.70	8.13	11.65	12.72	13.44	11.62	11.54	7.84	5.98	2.58
72	6.35	19.11	27.39	29.91	31.59	27.33	27.13	18.43	14.06	6.08
10	7.16	21.53	30.86	33.69	35.58	30.78	30.56	20.76	15.84	6.84
81	0.00	0.00	0.00	0.00	0.00	0.00	0.00	0.00	0.00	0.00
3	2.96	8.90	12.75	13.92	14.71	12.72	12.63	8.58	6.54	2.83
365	6.61	19.88	28.50	31.11	32.86	28.42	28.22	19.17	14.62	6.32

REM: Data of Sm isotopes : SF98-1,3,5,7 and 9 are as for 6.7 years cooling.

REM: Data of Sm isotopes : SF98-8 is as for 6.5 years cooling.

### A.3. RESULTS OF DESTRUCTIVE ANALYSIS

The results of the destructive analysis are measured as values per uranium atom, and are given as normalized to the number of atoms immediately after irradiation per uranium atom before irradiation, after converting to the value per initial uranium atom based on the evaluation of the number of fissions, and making a correction for the decay. However, it should be noted that the amount of Pu-239 is in effect the sum of Np-239 and Pu-239, since its amount cannot be corrected for the contribution of Np-239 that exists immediately after irradiation (its effect is 1–2%). Furthermore, the data of Sm isotopes are given as the values on the day of measurement, because their amounts could not be corrected for the decay. The burn-up calculation results are often compared in the value per ton of heavy element (uranium in the case of a uranium fuel) before irradiation, and thus the values converted to that unit are listed in Tables A.3.27–A.3.31.

Furthermore, the burn-up values listed in these tables were measured by the Nd-148 method, and the effective fission yield required in that method was determined by evaluating the proportions of fission of U-235, U-238, Pu-239, and Pu-241 by SWAT.

Table A.3.27. Results of destructive analysis (End of irradiation) : SF95

Sample	SF95-1	SF95-2	SF95-3	SF95-4	SF95-5
Burnup (GWd/t)	14.30	24.35	35.42	36.69	30.40
Isotope	Exp (g/TIHM)				
U-234	2.987E+02	2.850E+02	1.873E+02	1.870E+02	2.829E+02
U-235	2.674E+04	1.927E+04	1.326E+04	1.230E+04	1.544E+04
U-236	2.672E+03	4.024E+03	4.911E+03	4.999E+03	4.566E+03
U-238	9.499E+05	9.424E+05	9.338E+05	9.335E+05	9.388E+05
Pu-238	1.718E+01	7.102E+01	1.539E+02	1.588E+02	1.020E+02
Pu-239	4.227E+03	5.655E+03	6.194E+03	6.005E+03	5.635E+03
Pu-240	7.802E+02	1.539E+03	2.186E+03	2.207E+03	1.821E+03
Pu-241	3.690E+02	9.578E+02	1.486E+03	1.466E+03	1.153E+03
Pu-242	3.790E+01	1.844E+02	4.516E+02	4.803E+02	2.976E+02
Am-241	1.378E+01	2.344E+01	3.310E+01	2.351E+01	2.840E+01
Am-242m	1.840E-01	5.201E-01	7.877E-01	7.282E-01	5.687E-01
Am-243	2.682E+00	2.289E+01	8.047E+01	8.472E+01	4.400E+01
Cm-242	1.510E+00	7.672E+00	1.964E+01	2.328E+01	1.006E+01
Cm-243	1.415E-02	1.240E-01	3.720E-01	3.976E-01	2.293E-01
Cm-244	2.712E-01	5.042E+00	2.562E+01	2.837E+01	1.064E+01
Cm-245	5.519E-03	1.962E-01	1.396E+00	1.587E+00	4.839E-01
Cm-246	2.560E-04	1.190E-02	1.049E-01	1.251E-01	1.952E-02
Cs-137	5.405E+02	9.336E+02	1.347E+03	1.400E+03	1.148E+03
Cs-134	2.343E+01	7.012E+01	1.404E+02	1.471E+02	1.014E+02
Eu-154	4.093E+00	1.306E+01	2.525E+01	2.657E+01	1.817E+01
Ce-144	1.937E+02	3.160E+02	4.560E+02	4.301E+02	3.868E+02
Sb-125	1.471E+00	2.900E+00	3.733E+00	3.169E+00	3.262E+00
Ru-106	4.447E+01	8.340E+01	1.360E+02	1.401E+02	1.208E+02
Ag-110m	0.000E+00	0.000E+00	0.000E+00	0.000E+00	0.000E+00
Nd-142	3.429E+00	8.887E+00	2.116E+01	2.222E+01	1.371E+01
Nd-143	4.631E+02	7.149E+02	9.299E+02	9.373E+02	8.303E+02
Nd-144	3.276E+02	6.046E+02	9.347E+02	1.024E+03	7.928E+02
Nd-145	3.328E+02	5.384E+02	7.392E+02	7.598E+02	6.518E+02
Nd-146	2.809E+02	4.925E+02	7.340E+02	7.624E+02	6.185E+02
Nd-148	1.592E+02	2.736E+02	3.979E+02	4.126E+02	3.401E+02
Nd-150	7.200E+01	1.258E+02	1.896E+02	1.959E+02	1.572E+02

Table A.3.28. Results of destructive analysis (End of irradiation) : SF96

Sample	SF96-1	SF96-2	SF96-3	SF96-4	SF96-5
Burnup (GWd/t)	7.79	16.44	28.20	28.91	24.19
Isotope	Exp (g/TIHM)				
U-234	1.805E+02	1.522E+02	1.251E+02	1.250E+02	1.354E+02
U-235	1.944E+04	1.408E+04	8.638E+03	8.064E+03	9.937E+03
U-236	1.421E+03	2.411E+03	3.244E+03	3.302E+03	3.013E+03
U-238	9.660E+05	9.580E+05	9.476E+05	9.475E+05	9.522E+05
Np-237	6.125E+01	1.323E+02	2.168E+02	2.252E+02	1.875E+02
Pu-238	8.536E+00	4.172E+01	1.206E+02	1.248E+02	7.978E+01
Pu-239	3.781E+03	5.459E+03	6.001E+03	5.819E+03	5.519E+03
Pu-240	6.764E+02	1.494E+03	2.303E+03	2.327E+03	1.964E+03
Pu-241	2.622E+02	8.684E+02	1.498E+03	1.480E+03	1.203E+03
Pu-242	2.440E+01	1.615E+02	5.103E+02	5.411E+02	3.551E+02
Am-241	5.985E+00	1.735E+01	2.845E+01	3.094E+01	2.149E+01
Am-242m	1.218E-01	4.579E-01	6.413E-01	6.793E-01	5.647E-01
Am-243	1.147E+00	1.728E+01	8.872E+01	9.598E+01	5.078E+01
Cm-242	8.502E-01	5.781E+00	1.628E+01	1.679E+01	1.115E+01
Cm-244	9.560E-02	3.092E+00	2.862E+01	3.128E+01	1.280E+01
Nd-143	2.521E+02	4.778E+02	7.158E+02	7.184E+02	6.433E+02
Nd-144	1.536E+02	3.588E+02	7.292E+02	7.513E+02	5.927E+02
Nd-145	1.800E+02	3.575E+02	5.766E+02	5.880E+02	5.095E+02
Nd-146	1.536E+02	3.266E+02	5.795E+02	5.948E+02	4.910E+02
Nd-148	8.770E+01	1.851E+02	3.201E+02	3.280E+02	2.733E+02
Nd-150	4.130E+01	8.972E+01	1.591E+02	1.628E+02	1.331E+02
Cs-137	2.813E+02	5.983E+02	1.018E+03	1.053E+03	8.572E+02
Cs-134	8.609E+00	3.759E+01	1.002E+02	1.047E+02	7.146E+01
Eu-154	2.309E+00	8.538E+00	1.973E+01	1.992E+01	1.423E+01
Ce-144	1.179E+02	2.250E+02	3.362E+02	3.453E+02	3.145E+02
Sb-125	1.433E+00	2.829E+00	3.658E+00	4.645E+00	3.690E+00
Ru-106	2.830E+01	6.053E+01	1.402E+02	1.291E+02	1.344E+02

Table A.3.29. Results of destructive analysis (End of irradiation) : SF97

Sample	SF97-1	SF97-2	SF97-3	SF97-4	SF97-5	SF97-6
Burnup (GWd/t)	17.69	30.73	42.16	47.03	47.25	40.79
Isotope	Exp (g/TIHM)					
U-234	2.939E+02	2.348E+02	2.010E+02	1.872E+02	1.865E+02	2.057E+02
U-235	2.347E+04	1.571E+04	1.030E+04	8.179E+03	7.932E+03	1.016E+04
U-236	3.115E+03	4.560E+03	5.312E+03	5.528E+03	5.532E+03	5.272E+03
U-238	9.493E+05	9.377E+05	9.282E+05	9.246E+05	9.247E+05	9.310E+05
Np-237	1.521E+02	4.034E+02	5.845E+02	6.604E+02	6.701E+02	5.570E+02
Pu-238	2.370E+01	1.250E+02	2.581E+02	3.199E+02	3.188E+02	2.175E+02
Pu-239	3.844E+03	5.928E+03	6.217E+03	6.037E+03	5.976E+03	5.677E+03
Pu-240	9.347E+02	1.871E+03	2.471E+03	2.668E+03	2.648E+03	2.326E+03
Pu-241	4.237E+02	1.235E+03	1.689E+03	1.770E+03	1.754E+03	1.494E+03
Pu-242	6.185E+01	3.152E+02	6.517E+02	8.246E+02	8.341E+02	5.977E+02
Am-241	1.492E+01	4.017E+01	4.909E+01	5.311E+01	5.327E+01	4.297E+01
Am-242m	2.270E-01	8.838E-01	1.179E+00	1.233E+00	1.200E+00	9.756E-01
Am-243	4.448E+00	5.132E+01	1.410E+02	1.924E+02	1.935E+02	1.170E+02
Cm-242	2.134E+00	1.049E+01	1.839E+01	2.044E+01	1.903E+01	1.616E+01
Cm-243	2.483E-02	2.773E-01	6.921E-01	8.721E-01	8.670E-01	5.600E-01
Cm-244	4.981E-01	1.384E+01	5.696E+01	8.810E+01	8.823E+01	4.221E+01
Cm-245	1.087E-02	6.848E-01	3.735E+00	6.042E+00	5.915E+00	2.363E+00
Cm-246	3.866E-04	4.222E-02	3.648E-01	7.440E-01	7.549E-01	2.481E-01
Cm-247	No Data	4.043E-04	4.974E-03	1.098E-02	1.075E-02	3.139E-03
Nd-143	5.450E+02	8.307E+02	1.008E+03	1.048E+03	1.049E+03	9.736E+02
Nd-144	4.661E+02	8.843E+02	1.331E+03	1.567E+03	1.599E+03	1.311E+03
Nd-145	4.045E+02	6.480E+02	8.387E+02	9.118E+02	9.179E+02	8.247E+02
Nd-146	3.502E+02	6.304E+02	8.929E+02	1.008E+03	1.014E+03	8.586E+02
Nd-148	1.945E+02	3.389E+02	4.662E+02	5.204E+02	5.226E+02	4.504E+02
Nd-150	8.570E+01	1.582E+02	2.234E+02	2.516E+02	2.518E+02	2.130E+02
Cs-137	6.617E+02	1.151E+03	1.582E+03	1.749E+03	1.761E+03	1.531E+03
Cs-134	2.983E+01	1.030E+02	1.829E+02	2.139E+02	2.144E+02	1.632E+02
Eu-154	5.253E+00	1.973E+01	3.293E+01	3.739E+01	3.707E+01	2.859E+01
Ce-144	2.026E+02	3.061E+02	3.720E+02	3.756E+02	3.750E+02	3.714E+02
Sb-125	2.462E+00	5.118E+00	4.966E+00	6.090E+00	7.507E+00	4.546E+00
Ru-106	5.163E+01	1.162E+02	1.829E+02	1.936E+02	1.162E+02	1.959E+02
Sm-147	1.529E+02	2.050E+02	2.355E+02	2.468E+02	2.479E+02	2.371E+02
Sm-148	4.092E+01	1.194E+02	1.978E+02	2.338E+02	2.357E+02	1.809E+02
Sm-149	2.935E+00	3.976E+00	4.259E+00	3.943E+00	3.799E+00	3.843E+00
Sm-150	1.323E+02	2.499E+02	3.599E+02	4.074E+02	4.113E+02	3.409E+02
Sm-151	9.324E+00	1.351E+01	1.503E+01	1.491E+01	1.465E+01	1.294E+01
Sm-152	6.526E+01	9.546E+01	1.191E+02	1.298E+02	1.319E+02	1.207E+02
Sm-154	1.425E+01	2.977E+01	4.536E+01	5.252E+01	5.298E+01	4.231E+01

Data of Sm isotopes : As for 3.96 years cooling time.

Table A.3.30. Results of destructive analysis (End of irradiation) : SF98

Sample	SF98-1	SF98-2	SF98-3	SF98-4	SF98-5	SF98-6	SF98-7	SF98-8
Burnup (GWd/t)	4.15	26.51	36.94	42.35	43.99	39.92	39.41	27.18
Void ratio (%)	0.0	0.0	3.0	11.0	32.0	54.5	68.0	73.0
Isotope	Exp (g/TIHM)							
U-234	4.880E+01	2.677E+02	2.178E+02	1.976E+02	1.903E+02	1.860E+02	1.962E+02	2.354E+02
U-235	4.128E+03	1.743E+04	8.142E+03	5.966E+03	6.315E+03	9.062E+03	9.357E+03	1.545E+04
U-236	4.858E+02	3.551E+03	4.994E+03	5.284E+03	5.307E+03	5.140E+03	5.140E+03	4.291E+03
U-238	9.884E+05	9.460E+05	9.406E+05	9.358E+05	9.328E+05	9.334E+05	9.332E+05	9.431E+05
Np-237	2.379E+01	1.479E+02	3.346E+02	4.318E+02	3.862E+02	5.157E+02	4.573E+02	2.918E+02
Pu-238	3.135E+00	2.827E+01	1.167E+02	1.678E+02	1.936E+02	1.692E+02	2.083E+02	9.544E+01
Pu-239	2.297E+03	3.372E+03	3.694E+03	3.792E+03	4.265E+03	5.305E+03	5.628E+03	5.341E+03
Pu-240	5.474E+02	1.121E+03	2.135E+03	2.458E+03	2.613E+03	2.630E+03	2.668E+03	1.816E+03
Pu-241	1.332E+02	4.308E+02	8.949E+02	1.032E+03	1.172E+03	1.292E+03	1.355E+03	9.079E+02
Pu-242	1.688E+01	9.292E+01	4.623E+02	6.622E+02	6.939E+02	5.431E+02	5.439E+02	2.220E+02
Am-241	1.028E+01	2.300E+01	3.271E+01	3.417E+01	3.734E+01	4.091E+01	4.388E+01	3.295E+01
Am-242m	7.984E-02	2.967E-01	4.999E-01	5.298E-01	6.417E-01	8.623E-01	8.975E-01	7.074E-01
Am-243	5.839E-01	6.991E+00	6.678E+01	1.138E+02	1.273E+02	1.116E+02	1.087E+02	3.259E+01
Cm-242	5.309E-01	3.581E+00	1.696E+01	2.263E+01	3.460E+01	5.925E+01	2.892E+01	1.153E+01
Cm-243	No Data	3.710E-02	3.135E-01	4.247E-01	4.946E-01	5.347E-01	5.932E-01	2.073E-01
Cm-244	3.094E-02	8.003E-01	1.696E+01	3.635E+01	4.999E+01	4.299E+01	4.484E+01	8.687E+00
Cm-245	No Data	1.646E-02	5.485E-01	1.338E+00	2.322E+00	2.480E+00	2.734E+00	3.928E-01
Cm-246	No Data	No Data	7.666E-02	2.311E-01	3.850E-01	2.935E-01	3.007E-01	1.635E-02
Cm-247	No Data	No Data	No Data	No Data	No Data	No Data	No Data	No Data
Nd-143	1.208E+02	7.567E+02	8.234E+02	8.486E+02	9.039E+02	9.199E+02	9.183E+02	7.358E+02
Nd-144	1.153E+02	8.511E+02	1.275E+03	1.492E+03	1.476E+03	1.284E+03	1.207E+03	7.478E+02
Nd-145	9.192E+01	5.974E+02	7.648E+02	8.423E+02	8.667E+02	7.950E+02	7.845E+02	5.770E+02
Nd-146	7.769E+01	5.278E+02	7.629E+02	8.916E+02	9.320E+02	8.427E+02	8.330E+02	5.550E+02
Nd-148	4.560E+01	2.905E+02	4.058E+02	4.662E+02	4.850E+02	4.407E+02	4.356E+02	2.997E+02
Nd-150	2.187E+01	1.279E+02	1.867E+02	2.193E+02	2.294E+02	2.098E+02	2.080E+02	1.389E+02
Cs-137	1.634E+02	8.286E+02	1.329E+03	1.577E+03	1.588E+03	1.508E+03	1.559E+03	9.494E+02
Cs-134	3.579E+00	3.214E+01	1.010E+02	1.407E+02	1.553E+02	1.514E+02	1.621E+02	6.979E+01
Eu-154	8.151E-01	6.857E+00	1.818E+01	2.413E+01	2.601E+01	2.931E+01	2.924E+01	1.708E+01
Ce-144	2.782E+01	1.833E+02	2.996E+02	3.538E+02	4.107E+02	3.520E+02	3.786E+02	2.867E+02
Sb-125	No Data	No Data	No Data	No Data	No Data	5.223E+00	No Data	No Data
Ru-106	1.749E+01	4.985E+01	1.091E+02	1.237E+02	1.326E+02	1.113E+02	1.309E+02	7.522E+01
Sm-147	4.777E+01	2.303E+02	3.091E+02	3.207E+02	3.025E+02	2.891E+02	2.800E+02	2.454E+02
Sm-148	5.983E+00	5.771E+01	1.531E+02	1.971E+02	2.022E+02	1.855E+02	1.852E+02	1.079E+02
Sm-149	6.367E-01	2.201E+00	2.553E+00	2.502E+00	3.701E+00	3.374E+00	4.199E+00	4.082E+00
Sm-150	3.343E+01	1.790E+02	3.309E+02	3.865E+02	3.808E+02	3.536E+02	3.505E+02	2.408E+02
Sm-151	2.554E+00	8.203E+00	9.192E+00	9.738E+00	1.039E+01	1.272E+01	1.310E+01	1.245E+01
Sm-152	2.230E+01	9.016E+01	1.425E+02	1.555E+02	1.432E+02	1.233E+02	1.222E+02	9.771E+01
Sm-154	4.561E+00	1.874E+01	3.950E+01	4.828E+01	4.912E+01	4.377E+01	4.472E+01	2.933E+01

Data of Sm isotopes : SF98-1,2,3 and 4 : As for 5.5 years cooling.

Data of Sm isotopes : SF98-6 : As for 6.2 years cooling.

Data of Sm isotopes : SF98-5,7 and 8 : As for 5.9 years cooling.

**Table A.3.31. Results of destructive analysis (End of irradiation) : SF99**

Sample	SF99-1	SF99-2	SF99-3	SF99-4	SF99-5	SF99-6	SF99-7	SF99-8	SF99-9	SF99-10
Burnup (MW/u)	7.53	22.63	32.44	35.42	37.41	32.36	32.13	21.83	16.65	7.19
Void ratio (%)	0	1.4	5.8	10.8	27.7	54.7	66.5	71.7	72.9	74.3
Isotope										
U-234	3.898E+01	2.006E+02	1.782E+02	1.666E+02	1.602E+02	1.649E+02	1.643E+02	1.960E+02	2.184E+02	4.094E+01
U-235	2.913E+03	1.398E+04	8.657E+03	6.981E+03	7.381E+03	1.046E+04	1.092E+04	1.575E+04	1.906E+04	3.041E+03
U-236	6.863E+02	3.467E+03	4.522E+03	4.522E+03	4.295E+03	9.423E+03	3.458E+03	9.403E+05	9.538E+03	6.743E+02
U-238	9.839E+05	9.522E+05	9.452E+05	9.452E+05	9.394E+05	9.406E+05	9.403E+05	9.493E+05	9.538E+05	9.841E+05
U-237	5.674E+01	2.177E+02	3.632E+02	3.666E+02	4.617E+02	4.146E+02	2.758E+02	1.975E+02	5.493E+01	5.493E+01
Np-237	1.130E+01	3.961E+01	9.696E+01	1.145E+02	1.234E+02	1.374E+02	1.377E+02	6.476E+01	3.427E+01	1.098E+01
Pu-238	3.010E+03	3.907E+03	3.980E+03	3.865E+03	4.549E+03	5.635E+03	6.036E+03	5.448E+03	4.731E+03	3.011E+03
Pu-239	1.064E+03	1.519E+03	2.131E+03	2.293E+03	2.535E+03	2.445E+03	2.487E+03	1.647E+03	1.182E+03	1.052E+03
Pu-240	3.598E+02	6.763E+02	9.452E+02	1.010E+03	1.196E+03	1.263E+03	1.313E+03	8.332E+02	5.372E+02	3.359E+02
Pu-241	8.237E+01	1.896E+02	4.374E+02	5.573E+02	6.073E+02	4.334E+02	4.215E+02	1.723E+02	8.334E+01	7.328E+01
Pu-242	2.698E+01	2.110E+01	3.950E+01	3.410E+01	4.363E+01	4.558E+01	4.848E+01	3.619E+01	2.885E+01	1.612E+01
Am-241	2.469E-01	4.239E-01	5.444E-01	5.418E-01	6.917E-01	9.306E-01	9.240E-01	6.812E-01	4.078E-01	2.138E-01
Am-242m	5.780E+00	1.895E+01	6.496E+01	9.037E+01	1.128E+02	8.514E+01	8.453E+01	2.574E+01	9.255E+00	5.620E+00
Am-243	2.848E+00	1.624E+01	2.270E+01	3.477E+01	6.130E+01	3.844E+01	4.067E+01	1.593E+01	5.534E+00	3.583E+00
Cm-242	2.999E-02	9.310E-02	2.759E-01	3.692E-01	4.750E-01	4.413E-01	4.762E-01	1.629E-01	7.257E-02	3.279E-02
Cm-243	5.891E-01	3.180E+00	1.645E+01	2.692E+01	3.871E+01	3.008E+01	3.000E+01	6.152E+00	1.515E+00	6.833E-01
Cm-244	1.006E-02	8.762E-02	5.699E-01	1.014E+00	1.767E+00	1.735E+00	1.793E+00	2.702E+01	8.183E-02	1.319E-02
Cm-245	9.574E-04	No Data	6.949E-02	1.495E-01	2.412E-01	1.603E-01	1.631E-01	1.441E-02	1.217E-02	No Data
Cm-246	3.945E-04	No Data	1.427E-03	No Data	2.809E-03	No Data	3.881E-03	3.881E-03	No Data	No Data
Cm-247	1.948E+02	6.136E+02	7.627E+02	7.808E+02	8.397E+02	7.984E+02	8.089E+02	6.143E+02	5.007E+02	1.895E+02
Nd-143	4.177E+01	6.537E+02	1.321E+03	1.203E+03	1.166E+03	9.321E+02	8.171E+02	5.531E+02	4.406E+02	2.509E+02
Nd-144	2.629E+02	4.917E+02	6.728E+02	7.198E+02	7.511E+02	6.519E+02	6.509E+02	4.671E+02	3.705E+02	1.517E+02
Nd-145	1.579E+02	4.476E+02	6.610E+02	7.314E+02	7.774E+02	6.671E+02	6.645E+02	4.397E+02	3.307E+02	1.366E+02
Nd-146	1.410E+02	4.476E+02	3.570E+02	3.903E+02	4.130E+02	3.575E+02	3.556E+02	2.411E+02	1.837E+02	1.970E+01
Nd-148	8.284E+01	2.486E+02	1.674E+02	1.142E+02	1.979E+02	1.735E+02	1.724E+02	1.136E+02	8.436E+01	8.436E+01
Nd-150	4.177E+01	8.515E+02	1.231E+03	1.346E+03	1.427E+03	1.249E+03	1.262E+03	1.262E+03	2.772E+02	2.772E+02
Cs-137	2.859E+02	8.588E+00	4.205E+00	4.588E+00	4.667E+00	5.071E+00	5.837E+00	2.430E+00	1.234E+00	8.973E-01
Ru-106	2.661E+01	3.280E+01	8.056E+01	7.833E+01	6.988E+01	6.898E+01	4.985E+01	4.366E+01	5.029E+01	3.862E+01
Cs-134	1.041E+01	4.643E+01	9.117E+01	1.126E+02	1.306E+02	1.137E+02	1.193E+02	5.684E+01	3.213E+01	1.091E+01
Eu-154	2.664E+00	1.022E+01	1.792E+01	1.992E+01	2.465E+01	2.549E+01	2.659E+01	1.404E+01	8.215E+00	2.755E+00
Ce-144	No Data	2.153E+02	No Data	2.915E+02	3.847E+02	3.169E+02	4.240E+02	2.540E+02	1.657E+02	No Data
Sb-125	9.655E-01	3.674E+00	1.220E+01	8.973E-01						
Sm-147	7.780E+01	No Data	2.609E+02	No Data	1.579E+02	No Data	1.579E+02	1.404E+01	8.215E+00	No Data
Sm-148	1.649E+01	1.022E+01	No Data	1.167E+02	No Data	1.545E+01	1.343E+02	7.545E+01	4.483E+01	No Data
Sm-149	8.841E-01	No Data	2.469E+00	No Data	2.723E+00	No Data	3.426E+00	2.959E+00	2.600E+00	No Data
Sm-150	6.174E+01	No Data	2.676E+02	No Data	3.246E+02	No Data	2.778E+02	1.830E+02	1.313E+02	No Data
Sm-151	3.408E+00	No Data	8.490E+00	No Data	1.025E+01	No Data	1.294E+01	1.155E+01	9.999E+00	No Data
Sm-152	3.946E+01	No Data	1.179E+02	No Data	1.272E+02	No Data	1.024E+02	7.730E+01	6.172E+01	No Data
Sm-154	9.380E+00	No Data	3.355E+01	No Data	4.215E+01	No Data	3.579E+01	2.211E+01	1.540E+01	No Data

Data of Sm isotopes : SF98-1,3,5,7 and 9 : As for 6.7 years cooling.

Data of Sm isotopes : SF98-8 : As for 6.5 years cooling.

## REFERENCES

1. International Atomic Energy Agency, "Implementation of Burnup Credit in Spent Fuel Management Systems," *IAEA-TECDOC-1013*, April 1998. (Proceedings of an Advisory Group Meeting held in Vienna, 20–24 October 1997 ).
2. W. Lake, "Burnup Credit Activity being Conducted in the United States," in *Proceedings of an Advisory Group Meeting, Implementation of Burnup Credit in Spent Fuel Management Systems*, p. 109, Vienna, April 1998. International Atomic Energy Agency (as IAEA-TECDOC-1013).
3. Y. Chanzy and E. Guillou, "COGEMA/TRANSNUCLEAIRE's Experience with Burnup Credit," in *Proceedings of an Advisory Group Meeting, Implementation of Burnup Credit in Spent Fuel Management Systems*, p. 33, Vienna, April 1998. International Atomic Energy Agency (as IAEA-TECDOC-1013).
4. Russel Bowden, "The Application of Burnup Credit for Spent Fuel Operations in the United Kingdom," in *Proceedings of an Advisory Group Meeting, Implementation of Burnup Credit in Spent Fuel Management Systems*, p. 97, Vienna, April 1998. International Atomic Energy Agency (as IAEA-TECDOC-1013).
5. J. C. Neuber, "Present Status and Future Developments of the Implementation of Burnup Credit in Spent Fuel Management Systems in Germany," in *Proceedings of an Advisory Group Meeting, Implementation of Burnup Credit in Spent Fuel Management Systems*, p. 39, Vienna, April 1998. International Atomic Energy Agency (as IAEA-TECDOC-1013).
6. P. Grimm, "Status of Burnup Credit Implementation in Switzerland," in *Proceedings of an Advisory Group Meeting, Implementation of Burnup Credit in Spent Fuel Management Systems*, p. 93, Vienna, April 1998. International Atomic Energy Agency (as IAEA-TECDOC-1013).



## 国際単位系(SI)と換算表

表1 SI基本単位および補助単位

量	名称	記号
長さ	メートル	m
質量	キログラム	kg
時間	秒	s
電流	アンペア	A
熱力学温度	ケルビン	K
物質量	モル	mol
光度	カンデラ	cd
平面角	ラジアン	rad
立体角	ステラジアン	sr

表3 固有の名称をもつSI組立単位

量	名称	記号	他のSI単位による表現
周波数	ヘルツ	Hz	$s^{-1}$
力	ニュートン	N	$m \cdot kg/s^2$
圧力、応力	パスカル	Pa	$N/m^2$
エネルギー、仕事、熱量	ジュール	J	$N \cdot m$
工率、放射束	ワット	W	$J/s$
電気量、電荷	クーロン	C	$A \cdot s$
電位、電圧、起電力	ボルト	V	$W/A$
静電容量	ファラード	F	$C/V$
電気抵抗	オーム	$\Omega$	$V/A$
コンダクタンス	ジーメンス	S	$A/V$
磁束密度	ウェーバー	Wb	$V \cdot s$
磁束密度	テスラ	T	$Wb/m^2$
インダクタンス	ヘンリー	H	$Wb/A$
セルシウス温度	セルシウス度	°C	
光束度	ルーメン	lm	$cd \cdot sr$
照度	ルクス	lx	$lm/m^2$
放射能	ベクレル	Bq	$s^{-1}$
吸収線量	グレイ	Gy	$J/kg$
線量当量	シーベルト	Sv	$J/kg$

表2 SIと併用される単位

名 称	記 号
分、時、日	min, h, d
度、分、秒	°, ', "
リットル	L
トントン	t
電子ボルト	eV
原子質量単位	u

$$1 \text{ eV} = 1.60218 \times 10^{-19} \text{ J}$$

$$1 \text{ u} = 1.66054 \times 10^{-27} \text{ kg}$$

表5 SI接頭語

倍数	接頭語	記号
$10^{18}$	エクサ	E
$10^{15}$	ペタ	P
$10^{12}$	テラ	T
$10^9$	ギガ	G
$10^6$	メガ	M
$10^3$	キロ	k
$10^2$	ヘクト	h
$10^1$	デカ	da
$10^{-1}$	デシ	d
$10^{-2}$	センチ	c
$10^{-3}$	ミリ	m
$10^{-6}$	マイクロ	μ
$10^{-9}$	ナノ	n
$10^{-12}$	ピコ	p
$10^{-15}$	フェムト	f
$10^{-18}$	アト	a

(注)

1. 表1～5は「国際単位系」第5版、国際度量衡局1985年刊行による。ただし、1eVおよび1uの値はCODATAの1986年推奨値によった。

2. 表4には海里、ノット、アール、ヘクタールも含まれているが日常の単位なのでここでは省略した。

3. barは、JISでは流体の圧力を表わす場合に限り表2のカテゴリーに分類されている。

4. EC開発理事会指令ではbar、barnおよび「血圧の単位」mmHgを表2のカテゴリーに入れている。

### 換 算 表

圧 力	MPa(=10 bar)	kgf/cm <sup>2</sup>	atm	mmHg(Torr)	lbf/in <sup>2</sup> (psi)
1	0.101972	0.224809			
9.80665	1	2.20462			
4.44822	0.453592	1			
粘度 1 Pa·s(N·s/m <sup>2</sup> )	= 10 P(ポアズ)(g/(cm·s))				
動粘度 1 m <sup>2</sup> /s	= 10 <sup>4</sup> St(ストークス)(cm <sup>2</sup> /s)				

エネルギー・仕事・熱量	J(=10 <sup>7</sup> erg)	kgf·m	kW·h	cal(計量法)	Btu	ft · lbf	eV	1 cal = 4.18605 J(計量法)
1	0.101972	2.77778 × 10 <sup>-7</sup>	0.238889	9.47813 × 10 <sup>-4</sup>	0.737562	6.24150 × 10 <sup>18</sup>		= 4.184 J(熱化学)
9.80665	1	2.72407 × 10 <sup>-6</sup>	2.34270	9.29487 × 10 <sup>-3</sup>	7.23301	6.12082 × 10 <sup>19</sup>		= 4.1855 J(15 °C)
3.6 × 10 <sup>6</sup>	3.67098 × 10 <sup>5</sup>	1	8.59999 × 10 <sup>3</sup>	3412.13	2.65522 × 10 <sup>6</sup>	2.24694 × 10 <sup>25</sup>		= 4.1868 J(国際蒸気表)
4.18605	0.426858	1.16279 × 10 <sup>-6</sup>	1	3.96759 × 10 <sup>-3</sup>	3.08747	2.61272 × 10 <sup>19</sup>	仕事率 1 PS(仏馬力)	
1055.06	107.586	2.93072 × 10 <sup>-4</sup>	252.042	1	778.172	6.58515 × 10 <sup>21</sup>	= 75 kgf·m/s	
1.35582	0.138255	3.76616 × 10 <sup>-7</sup>	0.323890	1.28506 × 10 <sup>-3</sup>	1	8.46233 × 10 <sup>18</sup>	= 735.499 W	
1.60218 × 10 <sup>-19</sup>	1.63377 × 10 <sup>-20</sup>	4.45050 × 10 <sup>-26</sup>	3.82743 × 10 <sup>-20</sup>	1.51857 × 10 <sup>-22</sup>	1.18171 × 10 <sup>-19</sup>	1		

放射能	Bq	Ci	吸収線量	Gy	rad	照射線量	C/kg	R	線量当量	Sv	rem
1	2.70270 × 10 <sup>-11</sup>	1	100	1		1	3876		1	100	
3.7 × 10 <sup>10</sup>		1	0.01	1		2.58 × 10 <sup>-4</sup>	1		0.01	1	

(86年12月26日現在)

# INTERNATIONAL SYSTEM OF UNITS (SI) AND CONVERSION TABLES

TABLE 1. SI BASE SI UNITS AND AUXILIARY UNITS. KEY: (a) quantity; (b) name; (c) symbol; (d) length; (e) meter; (f) mass; (g) kilogram; (h) time; (i) second; (j) electric current; (k) ampere; (l) thermodynamic temperature; (m) Kelvin; (n) amount of substance; (o) mole; (p) luminous intensity; (q) candela; (r) plane angle; (s) radian; (t) solid angle; and (u) steradian.

(a) 量	(b) 名 称	(c) 記 号
(d) 長さ	メートル	(e) m
(f) 質量	キログラム	(g) kg
(h) 時間	秒	(i) s
(j) 電流	アンペア	(k) A
(l) 热力学温度	ケルビン	(m) K
(n) 物質量	モル	(o) mol
(p) 光度	カンデラ	(q) cd
(r) 平面角	ラジアン	(s) rad
(t) 立体角	ステラジアン	(u) sr

TABLE 2. UNITS USED TOGETHER WITH THE SI. KEY: (a) name; (b) symbol; (c) minute, hour, day; (d) degree, minute, second; (e) liter; (f) ton; (g) electronvolt; and (h) atomic mass unit.

(a) 名 称	記 号 (b)
(c) 分, 時, 日	min. h. d
(d) 度, 分, 秒	°, ' , ''
(e) リットル	L
(f) トン	t
(g) 電子ボルト	eV
(h) 原子質量単位	u

$$1 \text{ eV} = 1.60218 \times 10^{-19} \text{ J}$$

$$1 \text{ u} = 1.66054 \times 10^{-27} \text{ kg}$$

TABLE 3. SI DERIVED UNITS WITH SPECIAL NAMES. KEY: (a) quantity; (b) name; (c) symbol; (d) expression in terms of other SI units; (e) frequency; (f) hertz; (g) force; (h) newton; (i) pressure, stress; (j) pascal; (k) energy, work, quantity of heat; (l) joule; (m) work, radiant flux; (n) watt; (o) quantity of electricity, electric charge; (p) coulomb; (q) electric potential difference, voltage, electromotive force; (r) volt; (s) electrostatic capacity; (t) farad; (u) electric resistance; (v) ohm; (w) conductance; (x) siemens; (y) magnetic flux; (z) weber; (A) magnetic flux density; (B) tesla; (C) inductance; (D) henry; (E) Celsius temperature; (F) degrees Celsius; (G) luminous flux; (H) lumen; (I) illuminance; (J) lux; (K) radioactivity; (L) becquerel; (M) absorbed dose; (N) gray; (O) dose equivalent; and (P) sievert.

(a) 量	(b) 名 称	(c) 記号	他のSI単位による表現(d)
(e) 周 波 数	ヘルツ	Hz	$s^{-1}$
(g) 力	ニュートン	N	$kg\cdot m/s^2$
(i) 圧 力、応 力	パスカル	Pa	$N/m^2$
(k) エネルギー、仕事、熱量	ジュール	J	$N\cdot m$
(m) 工率、放射束	ワット	W	$J/s$
(o) 電気量、電荷	クーロン	C	$A\cdot s$
(q) 電位、電圧、起電力	ボルト	V	$W/A$
(s) 静電容量	ファラード	F	$C/V$
(u) 電気抵抗	オーム	Ω	$V/A$
(w) コンダクタンス	ジーケンス	S	$A/V$
(y) 磁束	ウェーバ	Wb	$V\cdot s$
(A) 磁束密度	テスラ	T	$Wb/m^2$
(C) インダクタンス	ヘンリイ	H	$Wb/A$
(E) セルシウス温度	セルシウス度	°C	
(G) 光束	ルーメン	lm	$cd\cdot sr$
(I) 照度	ルクス	Jx	$lm/m^2$
(K) 放射能	ベクレル	Bq	$s^{-1}$
(M) 吸收線量	グレイ	Gy	$J/kg$
(O) 練量当量	シーベルト	Sv	$J/kg$

TABLE 4. UNITS TENTATIVELY KEPT WITH THE SI. KEY: (a) name; (b) symbol; (c) angstrom; (d) barn; (e) bar; (f) gal; (g) curie; (h) roentgen; (i) rad; and (j) rem.

(a) 名 称	記 号(b)
(c) オングストローム	Å
(d) バーン	b
(e) バル	bar
(f) ガル	Gal
(g) キュリ	Ci
(h) レントゲン	R
(i) ラド	rad
(j) レム	rem

$$\begin{aligned}
 1 \text{ Å} &= 0.1 \text{ nm} = 10^{-10} \text{ m} \\
 1 \text{ b} &= 100 \text{ fm}^2 = 10^{-40} \text{ m}^2 \\
 1 \text{ bar} &= 0.1 \text{ MPa} = 10^5 \text{ Pa} \\
 1 \text{ Gal} &= 1 \text{ cm/s}^2 = 10^{-2} \text{ m/s}^2 \\
 1 \text{ Ci} &= 3.7 \times 10^{10} \text{ Bq} \\
 1 \text{ R} &= 2.58 \times 10^{-4} \text{ C/kg} \\
 1 \text{ rad} &= 1 \text{ cGy} = 10^{-1} \text{ Gy} \\
 1 \text{ rem} &= 1 \text{ cSv} = 10^{-1} \text{ Sv}
 \end{aligned}$$

TABLE 5. SI PREFIXES. KEY: (a) factor; (b) prefix; (c) symbol; (d) exa; (e) peta; (f) tera; (g) giga; (h) mega; (i) kilo; (j) hecto; (k) deka; (l) deci; (m) centi; (n) milli; (o) micro; (p) nano; (q) pico; (r) femto; and (s) atto.

(a)倍数	(b)接頭語	記号(c)
$10^{18}$	エクサ	(d) E
$10^{15}$	ペタ	(e) P
$10^{12}$	テラ	(f) T
$10^9$	ギガ	(g) G
$10^6$	メガ	(h) M
$10^3$	キロ	(i) k
$10^2$	ヘクト	(j) h
$10^1$	デカ	(k) da
$10^{-1}$	ヒー	(l) d
$10^{-2}$	セント	(m) c
$10^{-3}$	ミリ	(n) m
$10^{-6}$	マイクロ	(o) μ
$10^{-9}$	ナノ	(p) n
$10^{-12}$	ピコ	(q) p
$10^{-15}$	フェムト	(r) f
$10^{-18}$	アト	(s) a

## NOTES

1. Tables 1–5 are based on the "International System of Units", 5th edition; International Bureau of Weights and Measures, 1985. The values of 1 eV and 1 u were taken from the 1986 recommended values of CODATA.
2. Nautical mile, knot, are, and hectare are also included in Table 4, but are omitted here because they are not specialized units.
3. Bar is classified in the category of Table 2 in JIS only when expressing the pressure of a fluid.
4. Bar, barn, and the unit of blood pressure, mm Hg, were placed in the category of Table 2 according to instructions from the EC Board of Directors of Cabinet Ministers.

**CONVERSION TABLES.** KEY: (a) force; (b) viscosity; (c) (poise); (d) kinematic viscosity; (e) (stokes); (f) pressure; (g) energy, work, quantity of heat; (h) (Weights and Measures Act); (i) radioactivity; (j) absorbed dose; (k) irradiated dose; (l) dose equivalent; (m) (thermochemistry); (n) (International Vapor Table); (o) work; (p) (French horsepower); and (q) as of December 26, 1986.

力 (a)	N (=10 <sup>3</sup> dyn)	kgf	lbf	(f) 壓 力	MPa (=10 bar)	kgf/cm <sup>2</sup>	atm	mmHg (Torr)	lbf/in <sup>2</sup> (psi)
	1	0.101972	0.224809		1	10.1972	9.86923	7.50062 × 10 <sup>3</sup>	145.038
	9.80665	1	2.20462	力	0.0980665	1	0.967841	735.559	14.2233
	4.44822	0.453592	1		0.101325	1.03323	1	760	14.6959

(b) 粘度  $1 \text{ Pa}\cdot\text{s} (\text{N}\cdot\text{s}/\text{m}^2) = 10 \text{ P} (\text{ボアズ}) (\text{g}/(\text{cm}\cdot\text{s}))$  (c)  
(d) 効粘度  $1 \text{ m}^2/\text{s} = 10^4 \text{ St} (\text{ストークス}) (\text{cm}^2/\text{s})$  (e)

(f)  $1.33322 \times 10^{-1}$   $1.35951 \times 10^{-1}$   $1.31579 \times 10^{-1}$   $1$   $1.93368 \times 10^{-1}$

(g)  $6.89476 \times 10^{-1}$   $7.03070 \times 10^{-1}$   $6.80460 \times 10^{-1}$   $51.7149$   $1$

エネルギー (g)	J (=10 <sup>3</sup> erg)	kgf·m	kW·h	cal (計量法)	(h) Btu	ft · lbf	eV	1 cal = 4.18605 J (計量法) (h) = 4.184 J (熱化学) (m)	
	1	0.101972	$2.77778 \times 10^{-1}$	0.238889	$9.47813 \times 10^{-1}$	0.737562	$6.24150 \times 10^{14}$		
	9.80665	1	$2.72407 \times 10^{-1}$	2.34270	$9.29487 \times 10^{-1}$	7.23301	$6.12082 \times 10^{14}$	= 4.1855 J (15 °C)	
	$3.6 \times 10^4$	$3.67098 \times 10^3$	1	$8.59999 \times 10^4$	3412.13	$2.65522 \times 10^4$	$2.24694 \times 10^{14}$	= 4.1868 J (国際蒸気表) (n)	
	4.18605	0.426858	$1.16279 \times 10^{-1}$	1	$3.96759 \times 10^{-1}$	3.08747	$2.61272 \times 10^4$	(o) 仕事率 1 PS (仏馬力) (p)	
	1055.06	107.586	$2.93072 \times 10^{-1}$	252.042	1	778.172	$6.58515 \times 10^{11}$	= 75 kgf·m/s	
	1.35582	0.138255	$3.76616 \times 10^{-1}$	0.323890	$1.28506 \times 10^{-1}$	1	$8.46233 \times 10^{14}$	= 735.499 W	
	$1.60218 \times 10^{19}$	$1.63377 \times 10^{-19}$	$4.45050 \times 10^{-16}$	$3.82743 \times 10^{-16}$	$1.51857 \times 10^{-11}$	$1.18171 \times 10^{-11}$	1		

放射能 (i)	Bq	Ci	(j) 吸收 線量	Gy	rad	(k) 毒 物 質	C/kg	R	(l) 放 射 性 質	Sv	rem
	1	$2.70270 \times 10^{-11}$		1	100		1	3876		1	100
	$3.7 \times 10^{10}$	1		0.01	1		$2.58 \times 10^{-4}$	1		0.01	1

(q) (86年12月26日現在)



**INTERNAL DISTRIBUTION**

1. S. M. Bowman, 6011, MS-6370
2. M. D. DeHart, 6011, MS-6370
3. I. C. Gauld, 6011, MS-6370
4. J. N. Herndon, 6011, MS-6370
5. C. V. Parks, 6011, MS-6370
6. ORNL Laboratory Records - RC  
4500N, MS-6254
7. ORNL Central Research Library  
4500N, MS-6191

**EXTERNAL DISTRIBUTION**

8. W. H. Lake, Office of Civilian Radioactive Waste Management, U.S. Department of Energy, RW-46, Washington, DC 20585
- 9–10. R. Y. Lee, U.S. Nuclear Regulatory Commission, RES/DSARE/SMSAB, MS O10 B3, Washington, DC 20555-0001
11. Y. Nomura, Japan Atomic Energy Research Institute, Tokai-mura, Naka-gun, Ibaraki-ken, 319-1195, JAPAN
12. A. Nouri, OECD Nuclear Energy Agency, 12, Bd des Iles, 92130 Issy-les-Moulineaux, FRANCE
13. Heesung Shin, Spent Fuel Management Technology Research Team, Korea Atomic Energy Research Institute, PO Box 105, Yusong, Daejon, KOREA, 305-600
14. K. Suyama, OECD Nuclear Energy Agency, 12, Bd des Iles, 92130 Issy-les-Moulineaux, FRANCE
15. B. H. White IV, U.S. Nuclear Regulatory Commission, NMSS/SFPO, MS O13 D13, Washington, DC 20555-0001
- 16–17. C. J. Withee, U.S. Nuclear Regulatory Commission, NMSS/SFPO, MS O13 D13, Washington, DC 20555-0001

